ORGANIZED BY:

NATIONAL RESERCH & DEVELOPMENT
INSTITUTE FOR TEXTILE
AND LEATHER (INCDTP) - DIVISION
LEATHER AND FOOTWEAR
RESEARCH INSTITUTE (ICPI)

INCDTP

ICPI

SUPPORTED BY:

ANCS
Autoritatea Nationala pentru Cercetare Stiintifica

ICAMS 2012

ADVANCED MATERIALS AND SYSTEMS

Proceedings of the 4th International Conference

September 27th - 29th, 2012

Bucharest, ROMANIA

ORGANIZED BY:

NATIONAL RESEARCH &
DEVELOPMENT INSTITUTE FOR
TEXTILE AND LEATHER (INCDTP),
BUCHAREST, ROMANIA

DIVISION LEATHER & FOOTWEAR
RESEARCH INSTITUTE (ICPI)
BUCHAREST, ROMANIA

NATIONAL AUTHORITY FOR
SCIENTIFIC RESEARCH,
BUCHAREST, ROMANIA

PARTNERS

UNIVERSITY OF
BUCHAREST,
ROMANIA

LEATHER ENGINEERING
DEPARTMENT
EGE UNIVERSITY,
TURKEY

"GH. ASACHI" TECHNICAL
UNIVERSITY OF IASI,
ROMANIA

"POLITEHNICA"
UNIVERSITY
BUCHAREST,
ROMANIA

"ITA TEXCONF "
ROMANIAN ENTITY
WITHIN
INNOVATION &
LEATHER
TECHNOLOGICAL
TRANSFER

CONFEDERATION OF NATIONAL ASSOCIATIONS OF
TANNERS AND DRESSERS OF THE EUROPEAN COMMUNITY

ROMANIAN LEATHER & FUR PRODUCERS
ASSOCIATION

Luminita ALBU
Viorica DESELNICU
EDITORS

Proceedings of

THE 4th INTERNATIONAL CONFERENCE ON ADVANCED MATERIALS AND SYSTEMS

Bucharest, ROMANIA
September 27 – 29, 2012
INCDTP - ICPI
ROMANIA

FOREWORD

ICAMS 2012 offers the framework for presenting the latest results in research, focusing on a field of Materials science, which records an impressive dynamics and is recognized as a current national and European priority.

The conference will provide the opportunity for exchanging ideas and experience with researchers, scientists and experts at international level, and for developing new scientific contributions.

The conference topics include, but are not limited to:

1. **Materials**
    - *Intelligent and Functional Materials*
    - *Product Development and Design*
    - *Nano-Stuctured Materials*
    - *Computer simulations of advanced materials*
    - *Composite and polymeric materials*
    - *Structural characterization*
2. **Biomaterials**
    - *Polymeric Biomaterials: Theory, Experiments and Computational Modeling*
    - *Progresses in Biomaterials Engineering Biomechanics*
    - *Biomimethics*
    - *Biosensors*
3. **Systems and Technologies**
    - *Biotechnologies*
    - *Nanotechnologies/ Nanoengineering*
    - *Clean and sustainable technologies*
    - *New technologies and methods for managing complexity*
4. **Environment**
    - *Environment preservation*
    - *Wastes Recycling and Management*
    - *Pollution impact on health*
    - *New technologies for energy and resources conservation*
    - *Environment Engineering and Management*
5. **Cultural Heritage**
    - *Cultural Heritage*
    - *Conservation of historical monuments*
    - *Measuring and evaluation techniques for damage assessment*
    - *New methods for protection, conservation and restoration*
6. **Innovation**
    - *Product Innovation, development and Marketing*
    - *Innovative Materials and products*
    - *Eco-Innovation*
    - *New research opportunities and challenges*
7. **Quality Management and Competitiveness**
    - *National / International Standards*
    - *Management and control*
    - *International Competitiveness on the global market*
    - *Policies and Procedures (on a global, national, regional scale)*

We would like to thank all the participants, the International Scientific Committee, and all the sponsors that made possible this scientific event.

We hope that the Conference will become a tradition in the future, contributing to the advancement of Materials science in academic, social and business environments worldwide.

EDITORS,
Dr. Luminiţa Albu
Director, INCDTP – Division: Leather and Footwear Research Institute (ICPI), RO

Coordinator: **Dana Corina DESELNICU**
Cover: **Nicolae MITOI**
Word-processing: **Dana GURAU, Ciprian CHELARU, Daniela STELESCU, Sergiu GUTA, Mihai GEORGESCU**

Luminita ALBU
Viorica DESELNICU

EDITORS

Proceedings of

THE 4th INTERNATIONAL CONFERENCE ON ADVANCED MATERIALS AND SYSTEMS

Bucharest, ROMANIA
September 27th -29th, 2012

INCDTP-ICPI
ROMANIA

Editura CERTEX
certex@ns.certex.ro
Bucureşti, str. Lucreţiu Patrascanu nr. 16, sector 3
Tel/ fax: 021 3405515

Descrierea CIP a Bibliotecii Naţionale a României
Luminita ALBU
Viorica DESELNICU
The 4TH INTERNATIONAL CONFERENCE ON ADVANCED MATERIALS AND SYSTEMS
Luminita ALBU, Viorica DESELNICU
Bucureşti: CERTEX, 2012
ISSN: 2068 – 0783

Şef redacţie:
Marius Iordănescu

Coperta:
Nicolae Mitoi

Editat cu sprijinul Ministerului Educaţiei, Cercetării, Tineretului şi Sportului
Autoritatea Naţională pentru Cercetare Ştiinţifică

CONFERENCE COMMITTEE

Luminita ALBU, INCDTP-ICPI, RO
Carmen GHITULEASA, INCDTP, RO
Lucretia MIU, INCDTP, RO
Viorica DESELNICU, INCDTP-ICPI, RO
Laurentia ALEXANDRESCU, INCDTP-ICPI, RO
Altan AFSAR, Ege University, Bornova, TR
Emin ARCA, Marmara University, TR
Huseyin ATA KARAVANA, Ege University, TR
Philip AZARIADIS, University of the Aegean, GR
Emil-Stefan BARNA, University of Bucharest, RO
Viacheslav BARSUKOV, Kiev National University of Technology and Design, UA
Gheorghe BERIJAN, INCDTP-ICPI, RO
Gheorghe COARA, INCDTP-ICPI, RO
Carmen GAIDAU, INCDTP-ICPI, RO
Mihaela GHICA, "Carol Davila" University of Medicine and Pharmacy, RO
Gustavo GONZALEZ-QUIJANO, Secretary General, COTANCE, BE
Gurbuz GULUMSER, Ege University, Bornova, TR
Ioannis IOANNIDIS, INCDTP-ICPI, RO
Valeriu JINESCU, Politehnica University, Bucharest, RO
Alpaslan KAYA, Mustafa Kemal University, Antakya, TR
Minodora LECA, University of Bucharest, RO
Giovani LOMBARDI, ENEA, IT
Stelian MAIER,"Gheorghe Asachi"Technical University of Iasi, RO
Alcino MARTINHO, CTIC, PT
Aurelia MEGHEA, Politehnica University Bucharest, RO
Aura MIHAI, "Gheorghe Asachi" Technical University of Iasi, RO
Mehmet METE MUTLU, Ege University, TR
Georgios PANAGIARIS, Technological Education Institute, GR
Victoriya PLAVAN, Kiev National University of Technology and Design, UA
John A. SWIGER, OLLU University, San Antonio, USA
Irina TITORENCU, N. Simionescu I.C.B.P., RO
Emilia VISILEANU, INCDTP, RO
Gabriel ZAINESCU, INCDTP-ICPI, RO
Ding ZHIWEN, Leather & Footwear Industry Research Institute, CH

ORGANIZING COMMITTEE

Dr. Luminita Albu, Chair, Director
INCDTP - Leather and Footwear Research Institute Division (ICPI), RO
Dr. Carmen Ghituleasa, Co-Chair, General Director
National Research and Development Institute for Textile and Leather, RO
Dr. Viorica Deselnicu, Co-Chair, Scientific Secretary, INCDTP - Leather and Footwear Research Institute Division, RO
Ioana Pivniceru, INCDTP – ICPI , RO
Dr. Dana Deselnicu, INCDTP – ICPI, RO
Eng. Ciprian Chelaru, INCDTP - ICPI, RO
Dana Gurau, INCDTP - ICPI, RO
Elena Ninciuleanu, INCDTP - ICPI, RO
Ramona Florea, INCDTP - ICPI, RO
Daniela Stelescu, INCDTP - ICPI, RO
PhD student Sergiu-Adrian Guta, INCDTP - ICPI, RO

The 4th International Conference on Advanced Materials and Systems,
27th –29th of September, 2012, Bucharest, Romania

We would like to present our appreciation and sincere thanks for financial support to:

MINISTRY OF EDUCATION, RESEARCH, YOUTH AND SPORT

NATIONAL AUTHORITY FOR SCIENTIFIC RESEARCH
(MECTS - ANCS)

and our sponsors:

S.C. PIELOREX S.A.
33A Prelungirea Soseaua Giurgiului
Str., Jilava, Ilfov
Acsinte Dorel, Director

S.C. TARO INDUSTRY S.A.
6 Ana Davila Str.,
sector 5, Bucharest
Tonea Stoica, Director

S.C. CLASS SHOE S.R.L.
12-14 Martin-Opitz Str., 400272,
Cluj-Napoca, Romania
Lena Bejan, Director

S.C. A&A VESA S.R.L.
14 Banatului Str., Sebis, Arad
Gheorghe Vasile Vesa, Director

S.C. MANUFACTURA MAGURA SRL
44/A Magurei Str., Sebis, Arad
Gheorghe Hera, General Manager

S.C. PICOMA S.A.
6 Stefan O. Iosif Str., Satu-Mare
Dorel Berende, Director

S.C. PRODSTEFANO S.R.L.
3-5 Sfredelului Str.,
Fundeni, Ilfov
Batagoi Natalia, Director

PRO COMOD SHOES SRL
8 Sos. Berceni,
sector 4, Bucharest
Angela V. Pache, Administrator

MUSETTE EXIM SRL
2 Alexandru Donici Str.,
sector 2, Bucharest
Adrian Roberto Bitlan,
Administrator

S.C. HOFIGAL EXPORT-IMPORT S.A.
2 Intrarea Serelor Str., 042124,
Sector 4, Bucharest
Manea Dumitru, Director

HIGH HEELS DESIGN
5 Moinesti Str., Bucharest
Cornelia Sarghe, Administrator

CONTENTS

SOCIAL AND ENVIRONMENTAL REPORTING - WORKSHOP COTANCE

INNOVA-LEATHER INTERNATIONAL WORKSHOP

PLENARY LECTURE

I. MATERIALS

II. BIOMATERIALS

III. SYSTEMS AND TECHNOLOGIES

IV. ENVIRONMENT

V. CULTURAL HERITAGE

VI. INNOVATION

VII. QUALITY MANAGEMENT AND COMPETITIVENESS

SOCIAL AND ENVIRONMENTAL REPORTING - WORKSHOP COTANCE

THE FIRST SOCIAL & ENVIRONMENTAL REPORT OF THE EUROPEAN LEATHER INDUSTRY

FEDERICO BRUGNOLI, GUSTAVO GONZALEZ-QUIJANO

COTANCE -3, Rue Belliard, B-1040 Brussels, Belgium, brugnoli@spin360.biz; cotance@euroleather.com

The paper represents a novel approach for the social and environmental reporting (SER) of the European leather industry that goes beyond the simple description of legal requirements. It is the follow-up of a series of social and environmental reports of the tanning industry in a number of EU member States produced in a previous Social Dialogue project. No other sector involved in the leather value chain, in fact, has ever prepared such a comprehensive analysis of the environmental and social factors of relevance in the economic growth of the industry. The social and environmental report takes into consideration the main elements that are linked with the sustainable development of European tanneries. It presents the structure of the European sector and, thanks to the cooperation of several national industrial associations it provides specific environmental and social indicators related to the industrial activity. Organised in 6 sections, the paper presents the Socio-Environmental principles of the EU Tanning sector according to the COTANCE-ETUF:TCL Framework Agreement, the European Tanning sector, the Social and Environmental indicators and data, Social and Environmental certifications in the leather industry and the main Priorities for sustainable development of the EU tanning industry. On September 27th 2012, the first Social & Environmental Report of the European Leather Industry, elaborated within the context of the SER III Social Dialogue Project, will be presented in Bucharest during ICAMS 2012, the 4th INTERNATIONAL CONFERENCE ON ADVANCED MATERIALS & SYSTEMS.

Keywords: social report; environmental reporting; sustainable development

INTRODUCTION

The introduction describes the aim of the document, provides a description of the social and environmental values of leather production in Europe and introductory comments on main data and indicators. The introduction also focuses on the need of European tanners to see the international market recognising social and environmental values as drivers for a fair international trade.

SOCIO-ENVIRONMENTAL PRINCIPLES OF THE EU TANNING SECTOR

The Socio-Environmental principles of the EU tanning sector are enshrined in so called Framework Agreements and Joint Statements, done by COTANCE and IndustriAll, defining the Socio environmental mission of the sector, its medium term strategic objectives in terms of market, sustainability and compliance with EU strategic objectives. The section also describes the role of Social partners in the evolution of environmental and social policies of the sector.

THE EUROPEAN TANNING SECTOR

The roots of European tanning industry can be found in very ancient times. Pre-historic tanning activities have left little archeological remains apart of certain flaying tools, some products and certain references and ilustrative drawings. Quite a big well preserved tannery was discovered in the ruins of Pompei city (Italy), destroyed by the Vesuvio volcano more than two thousand years ago (August 24th 79 b.c.). Moreover, the importance of the industry has always been prominent for the European economy as, even at the beginning of the XX^th^ century, the tanning sector still was the one of the biggest industries of the whole area. Even if its incidence at global level has been declining in recent decades due to the growth of the sector in some emerging economies, the European tanning sector is still the global leader both in terms of:

(a) turnover, covering 26,7% on world total (after China, accounting for 29,5%);

(b) overall quality level reached by the industry through product and process innovation, as referred to technology (through a constant research on the processing cycle and product performance modernization), environmental performance (chemicals, water, solid waste and air emissions consequent to the tanning process are all treated and recycled), social commitment (relationships with workers and social dialogue with related trade unions have led to improved education and training and a constant reduction of injuries), design and style innovation (a very big importance is given to the research, the creation and the development of new fashion trends).

According to last annual data available (2011), at present the sector is composed by nearly 1.800 companies and 34.500 workers. As outlined in the following graph, the trend in the last decade, following the production volume results, has been on the decrease for both elements: -25% for the number of companies, -36% for employees.

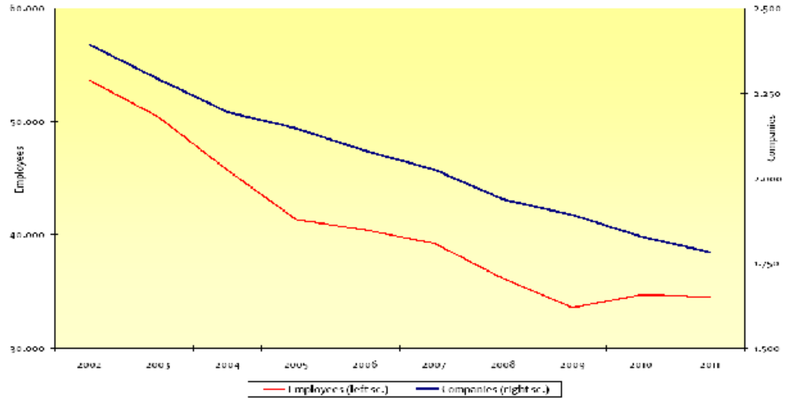

Figure 1. The European Tanning Industry - Number of companies and employees - Source: Eurostat, Entrepreneurial Associations

The tanning sector has traditionally been mainly composed by small and medium sized enterprises, but big companies have not been missing. At present, the average size of an EU tanning company is 18 person per enterprise and it is important to notice that in 2000 it was 24 with a continuous decline in the following years. This tendency seems to reveal that the resilience of the sector in the last decade can be illustrated by the topical sentence ”Small is Beautiful”. In other words, it appears that small and medium sized companies have been giving a better response to the big changes characterizing the world leather market in the first ten years of the new century. From this point of view, the European national industries present different characteristics, mostly depending on their productive specialization. The most important tanning sectors of Southern Europe (Italy, Spain, Portugal, France) are mainly composed by smaller undertakings. These countries are mostly specialized in the production of leather for fashion sectors, that often need a craftmanship approach that big companies are not able to provide. Conversely, the most important tanning sectors of Central and Northern Europe, focused on the upholstery destinations, present higher average dimensions of companies as economies of scale play a key role in these particular marketplaces.

In 2011, the total turnover of the EU tanning industry was 7,8 billion Euro, corresponding to a production of 224 millions sq.m. of finished leathers and about 44 thousands tons of sole leather.

Italy traditionally represents also the main tanning country in the European Union. Its share on total production is around 62% in terms of total EU tanning turnover and 60% in terms of volume. There has been just a little increase as compared to 2002, as in that year the country accounted for 60% in turnover and 57% in volume.

Spain ranks 2nd, covering 10/11% (in volume and value) but registering a fall during the last decade (when its incidence was 12/13%).

Austria, France, Germany and United Kingdom are actually around 3% to 6% on the EU total. There were no very big changes for them if compared to ten years ago although their product mix in terms of market destination may have changed. With the exceptions of Denmark, Luxembourg and Malta, all the others EU members still record the presence of tanners in their own territories.

The European leather production has always been very flexible, processing hides and skins from all the main animal origins and serving all the main client manufacturing utilizations.

The analysis of the production in terms of animal typology reveals that the main origin processed by the industry has always been hides of large bovines (71% on total), followed by sheepskins (14%), then goat skins (8%) and calf skins (6%). The remaining animal raw materials processed (principally hides and skins from reptiles, pigs, deers…) cover a very small part of the industry (less than 1%) and can be considered as niches. This segmentation, that is strictly linked to the meat industry, has never shown very big modifications.

The principal destination use of leather, not only in Europe, has traditionally been the production of leather for uppers for the footwear sector. That is still the first manufacturing client of the EU leather industry (41% on total). In spite of the big fall suffered by the market destination in the furniture sector during the recent years, the second most important utilization of EU leather is for upholstery; divided into furniture (17%) and car interiors (13%). Leather goods covers 19%, while garments presently absorbs 8% (2% for the remaining niche segments).

SOCIAL AND ENVIRONMENTAL INDICATORS AND DATA

The active cooperation of 7 national associations (Italy, Spain, France, Germany, UK, Sweden, Romania), has allowed collecting first hand data from a highly significant sample that represents 90,9% of EU companies, 76,6% of the workforce, 87,8% of the turnover.

Social and environmental indicators have been collected and elaborated by the associations at national level and aggregated at European level. The document provides a detailed description of the indicators and their relevance both from a social and an environmental point of view for the years 2010 and 2011.

Social Indicators (Extract)

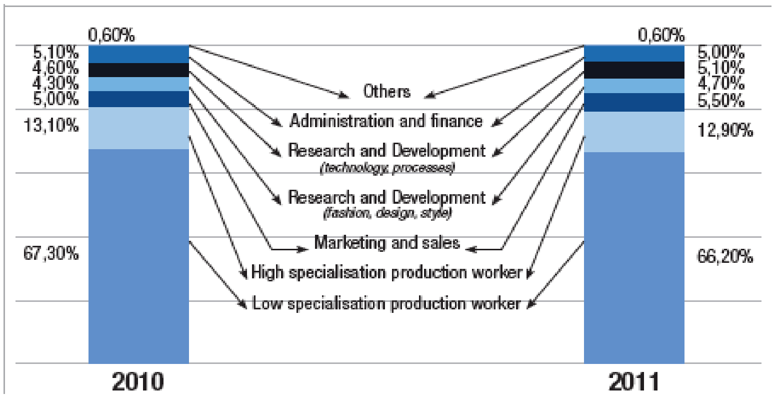

Figure 2. Specialisation of the workforce (%)

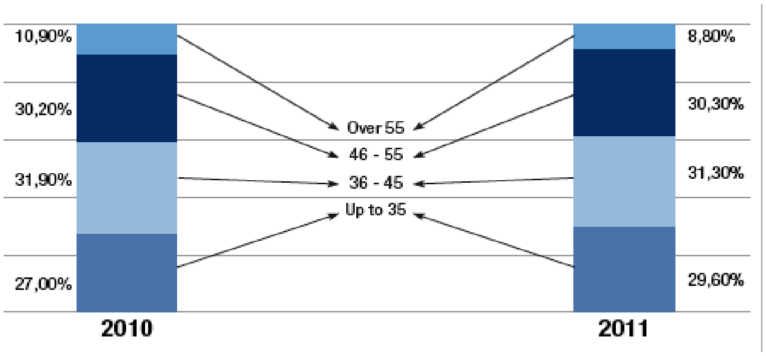

Figure 3. Age brackets (%)

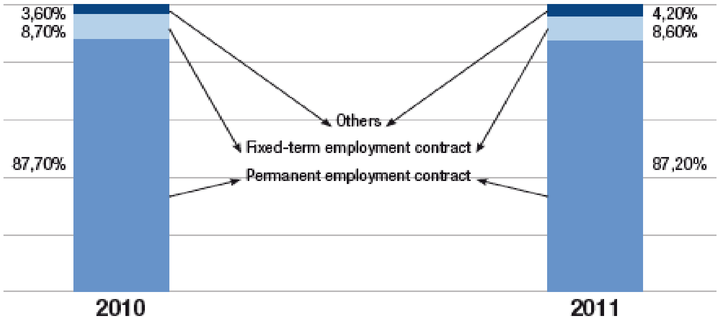

Figure 4. Contractual types (%)

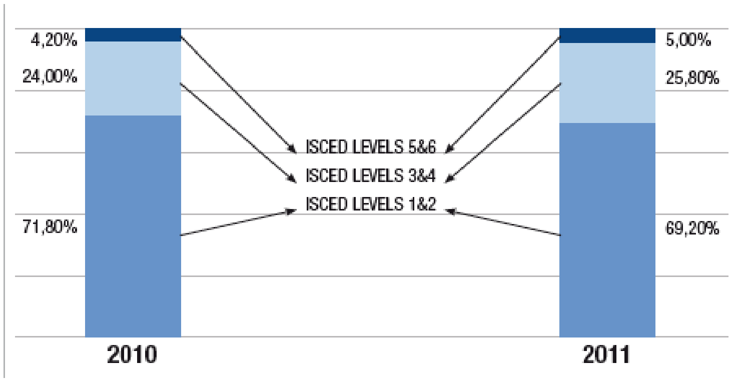

Figure 5. Education (%)

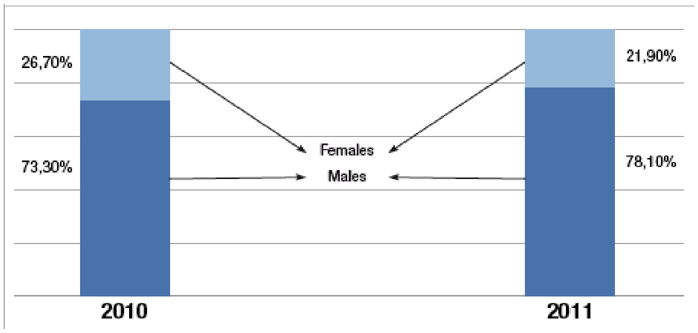

Figure 6. Gender information (%)

Environmental Indicators (Extract)

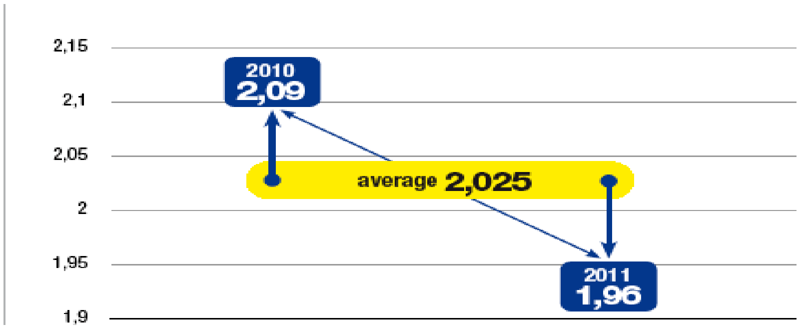

Figure 7. Chemicals consumption (kg/m^2)

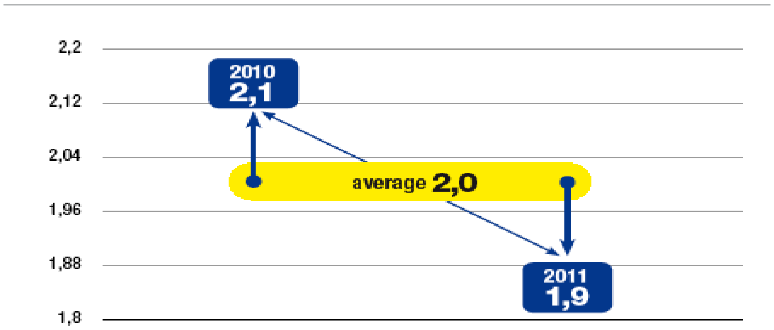

Figure 8. Energy consumption (TOE/ 1000 m^2)

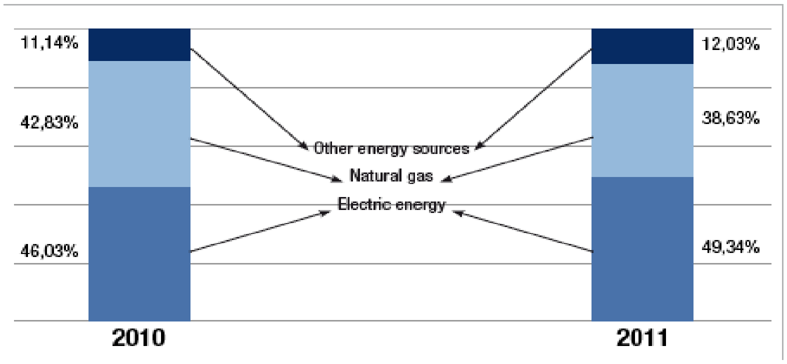

Figure 9. Energy sources (%)

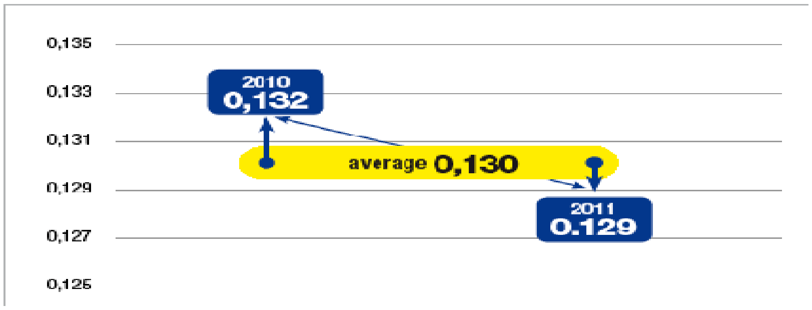

Figure 10. Water consumption (m^3/m^2)

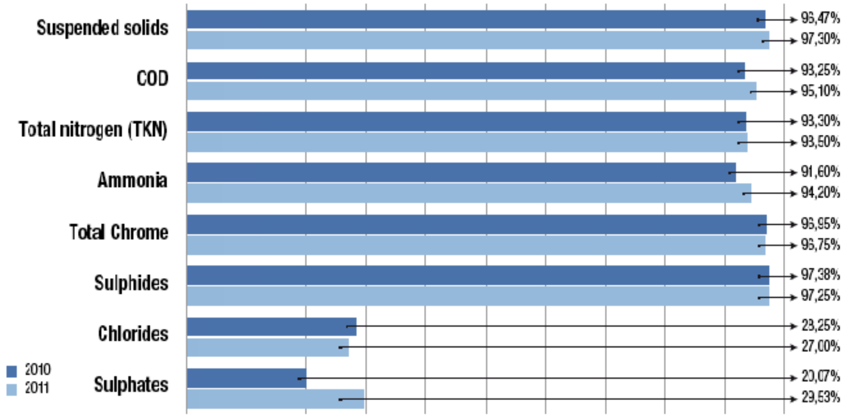

Figure 11. Wastewater purification (%)

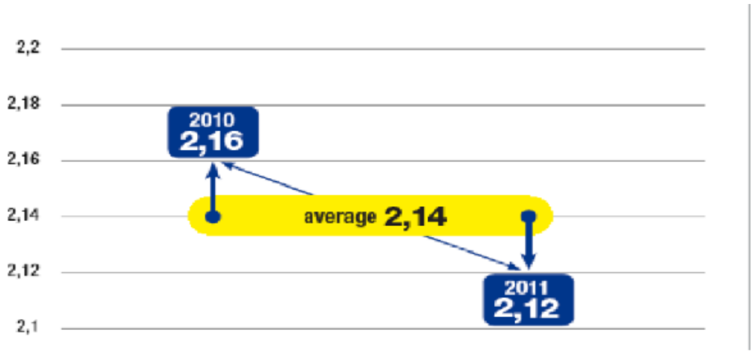

Figure 12. Waste generation (kg/m^2)

These social and environmental indicators of the European Tanning Industry evidence an industrial sector that strives for excellence and that holds collectively a leading position at global level.

SOCIAL AND ENVIRONMENTAL CERTIFICATIONS IN THE LEATHER INDUSTRY

The document also provides a description of the main system and product certifications (EMAS, 14001, 18001, SA8000, EPD, product certification), which are adopted in European tanneries. Data are elaborated per type and per country.

PRIORITIES FOR SOCIO - ENVIRONMENTAL IMPROVEMENT ON THE EU TANNING INDUSTRY

This section provides a description of the more relevant needs of the EU tanning industry in terms of trade environment, organisation, technology, products, skills and other actors for the competitive development of of a sustainable European tanning industry.

Acknowledgements

COTANCE would like to thank ETUF:TCL / IndustriAll European Trade Union, its Social Partner and partner in this EU sponsored projects for the excellent cooperation throughout the initiative.

The Social partners of this project express their gratitude in particular to all European Leather Associations, companies and worker representatives that have offered their support and contribution to the development of all activities.

Finally, COTANCE and IndustriAll European Trade Union thank the European Commission and in particular the Directorate General for Social Affairs for the financial support received for the development of these 3 projects.

REFERENCES

COTANCE – Social Project (VS/2008/0478) and Follow-up Projects (VS/2009/0473 & VS/2011/0407) "*Social & Environmental Reporting in the European Leather Industry*", 2009 - 2012, Brussels.

This paper has been elaborated with the support of the European Union. The content is the sole responsibility of the authors and does not necessarily reflect the position of the European Union.

INNOVA-LEATHER INTERNATIONAL WORKSHOP

PROTEIC INGREDIENTS FOR COSMETIC PRODUCTS

MADALINA GEORGIANA ALBU[1], IOANNIS IOANIDIS[1], MIHAELA VIOLETA GHICA[2],
VIORICA DESELNICU[1], CIPRIAN CHELARU[1], GHEORGHE COARA[1]

[1] *INCDTP - Division: Leather and Footwear Research Institute, Collagen Department, 93 Ion Minulescu Str, 031215, Bucharest, Romania, albu_mada@yahoo.com*

[2] *"Carol Davila" University of Medicine and Pharmacy, Faculty of Pharmacy, Physical and Colloidal Chemistry Department, 6 Traian Vuia Str, 020956, Bucharest, Romania, mihaelaghica@yahoo.com*

Hydrolyzed collagen is a natural protein which is successfully used for cosmetic formulation purposes. The aim of this study was to obtain collagen hydrolysate from wet white leather wastes which were pre-tanned with organic (oxazolidine and oxazolidine-resorcinol) and mineral (Titanium-aluminium complex) tanning agents. Solutions of 10% collagen hydrolysates named A, B and C were characterized by dry substance, amide nitrogen, ash, primary amino groups, fatty, pH, FT-IR spectroscopy and rheological analyses. The results demonstrated that the collagen hydrolysate characteristics are influenced by the raw materials (wet white leather) and the properties allow them to be used in manufacture of cosmetic products.

Keywords: wet white, leather wastes, hydrolysates

INTRODUCTION

The cosmetic industry is a field destined to grow rapidly owing to its universal appeal for improving the quality of life (Kligman, 2000). According to Secchi (Secchi, 2008) the protein materials for cosmetic purposes are available from ancient time but the first rational use of proteins in cosmetics dates back to the 1950s. In order to use proteins in water-based cosmetics, they need to be converted into a soluble form, which is easier to manipulate and is more practical for formulating purposes.

Hydrolyzed collagen is a natural protein derived from the collagen found in animal tissue, especially in skins and bones (Trandafir et al., 2007).

Hydrolysates of non-tanned collagen waste can be advantageously used without further modification as hydration substances in cosmetic preparations (Langmaier et al., 2005).

Leather industry produces a large amount of solid waste containing proteins from skin. In this paper we have investigated the possibilities of using these wastes as a source of protein for the cosmetic industry. As raw material we used two types of wet white leather: mineral and organic tanned leather and the obtained hydrolysates were characterized by dry substance, amide nitrogen, ash, primary amino groups, fatty, pH, FT-IR spectroscopy and rheological analyses.

MATERIALS AND METHODS

Collagen Hydrolysate Preparation

Collagen hydrolysates were prepared by acidic hydrolysis of wet white leather wastes at 125°C during 8 hours according to the technology previously described (Trandafir et al., 2007). The wet white leather wastes were pre-tanned previously with oxazolidine, tinanium-aluminium complex and oxazolidine-resorcinol and liquid hydrolysates were obtained, named hydrolysate A, B and C respectively. They were dried by freeze-drying using the lyophilization program previously described (Albu, 2011).

Rheological Analysis

The rheological behaviour of the hydrolysates was evaluated using a rotational viscometer Multi-visc Rheometer-Fungilab. For the determination of the dynamic viscosity, the shear rate and the shear stress the LCP low viscosities adaptor was used. The rheological experiments were performed at 25°C±0.5°C.

FT-IR Analysis

The FT-IR for collagen hydrolysates were recorded using a FT-IR 6000 spectrofotometer with ATR reflection system MK II Golden Gate Single (Jasco). The spectra were scanned in absorption mode at 4 cm^{-1} resolution.

RESULTS AND DISCUSSION

The collagen hydrolysate obtained as previously described in materials and methods section were based on wet white wastes pre-tanned with oxazolidine (hydrolisate A), Ti-Al complex (hydrolysate B) and oxazolidine-resorcinol (hydrolysate C).

Oxazolidine is a heterocyclic compound obtained by the reaction of aminohydroxy compounds with aldehydes which has the shrinkage temperature of about 85°C. The combination of resorcinol and oxazolidine together as tanning agents increase the shrinkage temperature of above 100°C (Chen and Shana, 2010). Moreover, resorcinol has low toxicity and is cheap, being used in hair dye intermediates and other cosmetic products (Nohynek et al., 2010).

The obtained hydrolysates showed the characteristics presented in the Table 1.

Table 1. Basic characteristics of collagen hydrolysates

Characteristics	Hydrolysate A	Hydrolysate B	Hydrolysate C
Dry substance, %	9.48	9.74	8.76
Amide nitrogen in dry substance, %	1.67 / 17.62	1.31 / 17.81	1.55 / 17.69
Proteic substance, %	9.39 / 99.05	9.74 / 100.00	8.71 / 99.43
Primary amino groups in dry substance, %	0.05 / 0.53	0.01 / 0.57	0.06 / 0.66
Fat in dry substance, %	free	free	free
pH for 5% solution	3.92	3.17	3.42

All the obtained hydrolysates contained high amount of collagen. The amide nitrogen in dry substance is between 17.62 and 17.81, the hydrolysate having very close value of molecular weight. Although, the free content of fat allows them to be used in cosmetics and medicine.

The rheological analyses of the studied hydrolysates were performed to determine their flow behaviour and their viscosity (Ortan et al., 2011; Dinu-Pîrvu et al., 2012) as the Figure 1 a-c showed.

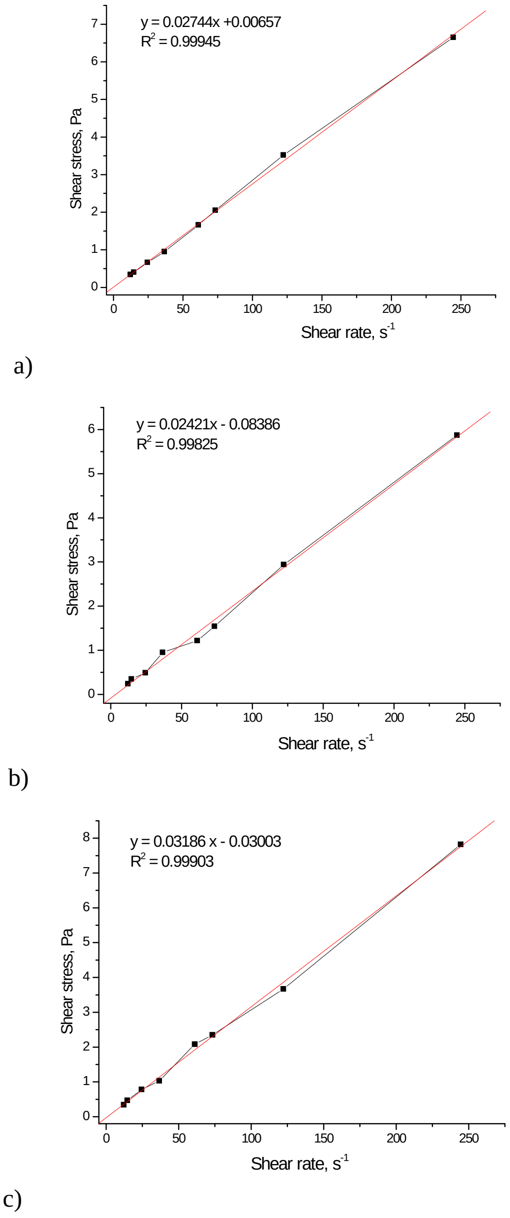

Figure 1. Rheological behaviour of collagen hydrolysates: a) A hydrolysate; b) B hydrolysate; c) C hydrolysate

The viscosity is approximately constant for a certain type of hydrolysate, the rheogram shear stress as function of shear rate being consequently linear. From the line slope (Figure 1 a-c) the dynamic viscosity was determined, namely: 0.0275 Pa·s (2.75cP) for hydrolysate A, 0.0241 Pa·s (2.41cP) for hydrolysate B, and 0.0318Pa·s (3.18cP) for hydrolysate C respectively. We can remark that the determination coefficient R^2 has values superior to 0.9960.

The modifications of collagen structure can be appreciated by the following semiquantitative relations from the FT-IR spectra:

- A_{III}/A_{1450} ratio, correlated with maintaining of integrity of triple helical structure – values higher or equal to unity indicate preservation of conformation (Albu et al., 2009);
- A_I/A_{II} ratio, correlated with the hydrolysis degree;

The values of A_{III}/A_{1450} and A_I/A_{II} ratios and the Amide A of all studied hydrolysates are presented in the Table 2 and Figure 2 respectively.

Table 2. Spectral characteristics of collagen hydrolysates

Sample	A_{III} / A_{1450}	A_I / A_{II}
Hydrolysate A	0.712	1.454
Hydrolysate B	0.708	1.551
Hydrolysate C	0.713	1.374

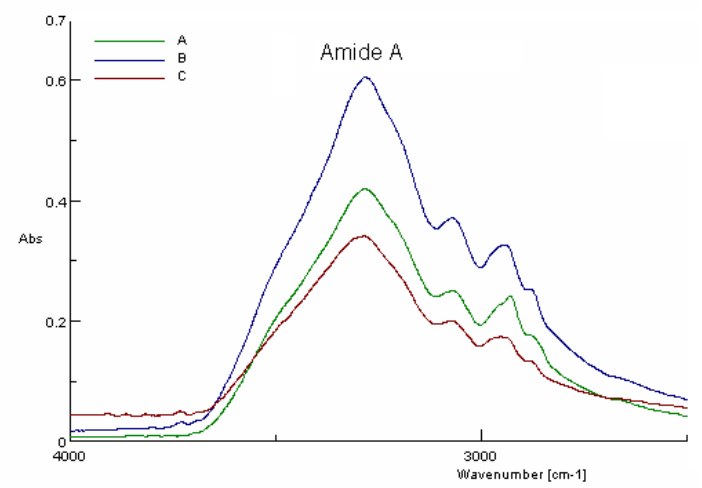

Figure 2. Amide A of hydrolysates A, B and C determined by FT-IR spectra

From the Table 2 and Figure 2 we can conclude that the integrity of triple helix was over about 70% destroyed and highest degree of hydrolysis was for B hydrolysate. This could be explained due to the strongest cross-linking of pre-tanned leather with organic tannins. The FT-IR results are in agreement with rheological ones, B hydrolysate having also the smallest viscosity, of 2.41cP.

CONCLUSIONS

Three types of collagen hydrolysates were obtained by acidic hydrolysis from wet white leather wastes tanned with oxazolidine, titanium-aluminium complex and oxazolidine-resorcinol. All the obtained hydrolysates contained high amount of collagen and the amide nitrogen in dry substance is between 17.62 and 17.81, the hydrolysate having very close value of molecular weight. The dynamic viscosity was 2.75cP for hydrolysate A, 2.41cP for hydrolysate B, and 3.18cP for hydrolysate C respectively, with a determination coefficient R^2 higher than 0.9960. The FT-IR results are in accordance with rheology behavior, the properties of hydrolysates allowing them to be used in manufacture of cosmetic products.

Acknowledgements

This work has been financed by the European Fund for Regional Development and the Romanian Government in the framework of Sectoral Operational Programme under the project INNOVA-LEATHER: «Innovative technologies for leather sector increasing technological competitiveness by RDI, quality of life and environmental protection» – contract POS CCE-AXA 2-O 2.1.2 nr. 242/20.09.2010 ID 638 COD SMIS – CSNR 12579.

REFERENCES

Albu, M.G. (2011), “Collagen Gels and Matrices for Biomedical Applications”, *Lambert Academic Publishing, Saarbrücken*, 23-24.

Albu, M.G., Ghica, M.V., Giurginca M. et al. (2009), “Spectral characteristics and antioxidant properties of tannic acid immobiliyed in drug delivery systems”, *Revista de Chimie*, 60, 666-672.

Chen, H., Shana, Z.H. (2010), “Stabilization of collagen by cross-linking with oxazolidine E-resorcinol”, *Journal of Biological Macromolecules*, 46(5), 535-539.

Dinu-Pîrvu, C., Ghica, M.V., Ivana, S. et al. (2012), “Formulation and physico-chemical characterization of piroxicam-based carbomer-hydrogels”, *AMHB*, 1(1), 7-16.

Kligman, A.K. (2000), “A dermatologist looks to the future: promises and problems”, *Dermatologic Clinics*, 18(4), 699-709.

Langmaier, F., Mokrejs, P., Karnas, R. et al. (2005), “Modification of chrome-tanned leather waste hydrolysate with epichlorhydrin”, *Journal of the Society of Leather Technologists and Chemists,* 90, 29-34.

Nohynek, G.J., Antignac, E., Re, T. et al. (2010), “Safety assessment of personal care products/cosmetics and their ingredients”, *Toxicology and Applied Pharmacology*, 243, 239–259.

Ortan, A., Dinu-Pîrvu, C., Ghica, M.V. et. al. (2011), “Rheological study of a liposomal hydrogel based on carbopol”, *Romanian Biotechnological Letter*, 16 (1 Suppl.), 47-54.

Secchi, G. (2000), “Role of protein in cosmetics”, *Clinics in Dermatology*, 26, 321–325.

Trandafir, V., Popescu, G., Albu, M.G. et al. (2007), *Collagen-based Bioproducts* (in Romanian), Ars Docendi, Bucharest, 111-112.

NEW WET WHITE TANNING AGENTS AND TECHNOLOGY

MARIAN CRUDU, VIORICA DESELNICU, IOANNIS IOANNIDIS, LUMINITA ALBU, ANDRA CRUDU

INCDTP - Division: Leather and Footwear Research Institute, 93 Ion Minulescu, Bucharest, Romania, email: icpi@icpi.ro

Leather industry has to cope nowadays with major environmental problems because of the polluting processes (a World Bank report has placed the leather industry in the ninth place when considering the environmental impact).Therefore, increasing the environmental efficiency in the leather sector is the major aim of leather, auxiliary materials and equipment manufacturers. The development of new tanning agents and new technologies is required to cope with the increasingly higher environmental pressure on the current tanning materials and processes such as tanning with chromium salts. The original contribution of this work in solving the above problems has involved the use of solid titanium wastes (cuttings) resulting from the process of obtaining highly pure titanium (ingots) in the preparation of new tanning compounds intended to increase the environmental efficiency of the leather sector.

Keywords: Ti-Al tanning agents, wet white, clean technology

INTRODUCTION

Hitherto, the mineral tanning agents most frequently used throughout the world are salts of chromium (III) (ca. 85% of total world finished leather output), which remain unsurpassed in the qualities offered to leather; these, in turn, include high hydrothermal, thermal and light stability and versatility with regard to the variety of leather articles, which can be made from the intermediate, chromium (III)-tanned leather, «wet-blue» (Covington A.D., 2008).

In general, chromium (III) tanning agents uptake under typical technological conditions is of the order of 60 – 80 % of the offered quantities (typical offer: 80-90 kg Cr-tanning salts/t of pelt weight), with 3-7 kg $Cr^{3+/}$t of raw hides /skins (2-7g Cr(III)/Lt of exhaust tanning liquor) discharged with the process effluent. Even though there is no legislation or norm that requires that chromium (III) should be absent from leathers, maximum allowable concentrations have been stipulated for the total chromium or chromium (III) content in leather digests or extracts, whereas an even stricter concurrent legislative requirement has been imposed for chromium (VI) absence (non detectable) in most finished leathers. In particular, Chromium (VI) and its salts are classified as known carcinogens not used for tanning and normally absent from chromium (III) tanning salts. However, apart from its potential presence in pigments, colouring additives and fixatives, commercial chromium tanned leathers can be tested positive for the presence of chromium (VI) in quantities exceeding the stipulated legal or normative limits. De-facto chromium (VI) does not exist in finished chrome-tanned leather, and apart from the frequently never told truth of test method inefficacy or non-appropriateness, intelligent tentative interpretations of the observed chromium (VI) formation agree that can be the product of oxidative conversion of chromium (III) under specific leather manufacturing or storage conditions e.g. high leather pH or use of specific fat liquoring agents. Along the same lines, several eco-certification schemes stipulate limits in Cr (III) content: (i) in aqueous extracts of leathers and leathers products with water, artificial sweat or in some cases in their digest and (ii) in the effluent after depuration (0,2-3 ppm) that are impossible to match, if leathers continue to be tanned or/and re tanned with Chromium (III) tanning agents.

These practical and operational constraints have stimulated research efforts to find an alternative to chromium (III) tanning (German H.P., 2010) for the production of **F**ree-**O**f-**C**hrome (FOC) and in some cases also Metal-Free leathers, whilst retaining the often expected by the consumer mineral character in leather articles, with some profound examples of succeeding in replacing fully chrome-tanning lines in Industrial upper leather production (Carvalhos OAK Leather). Accordingly, Al (III) (Waldo W, 1983; R. A. Hancock, 1980), Zr (III), Ti (III & IV) (Bi Yu Peng, 2007), Fe –salts (Te-Pang Hu,1921, Kleban, M.), their mixed salts (Covington A.D.), and most recently nano-silicates (Liu, Y. et al,2010) and sodium water glass (EU-funded 2001-2003) were tested as effective partial or total replacement mineral tanning agents for the production of a reversibly or irreversibly – most recently - tanned new intermediate semi-processed product and commodity: “wet-white” or “wet-stabilised” leather. Overall metal ion complexes have some affinity for protein, however, the mechanism of their binding to collagen – if taking place – is far from being resolved with several hypotheses and models often postulated and used, but seldom proven for this purpose. Moreover, when applying the criteria of adequate reactivity, colour, availability, cost and toxicity, and most recently LCIA, nearly all of the commercially available agents were rendered redundant as viable options. A good example is Aluminum salts that have long been associated with stabilising animal origin pelts and have the advantage of being abundant and cheap. However, Aluminum is only loosely bound and fixed to collagen, so that the reaction is readily reversed, when the leather is wetted and found in acidic environments; for this reason, this process is regarded as a pseudo-tannage and called tawing, rather than tanning. However, as shown byone of the co-authors in earlier studies (Ioannidis, I.A 1990) the effectiveness of a tanning molecule depends on its ability to provide high molecular weight cross-linked moieties within the collagen molecule and was possible to propose reactive Aluminium tanning agents preparations that match this requirement (Ioannidis, I.A.,1989), which, on the other hand, were never taken up by the Industry, due to emerging renewed toxicity considerations, but primarily as a result of the undoubtedly superior versatility, cost effectiveness and reliability of Cr (III)-tanning systems.

Within this framework of industrial needs high levels of excess Cr(III)-tanning products remain a potential threat and hazard to the environment or contribute significantly to the amount of recalcitrant pollutants. Consequently, there is mounting pressure on tanners to reduce levels of Cr(III)- tanning agents employed during leather manufacture and their discharge with the outflow of tannery ETPs.

Along these lines, new Ti (III)-based, Cr(III)-free, precursor tanning agents have been produced from metallurgic Industry end waste, aiming at the development of new tailored sustainable wet-white tanning chemistry that enables for the first time the in-situ generation of reactive Ti(IV)-tanning species, as a viable alternative to Cr(III), vegetable and syntan (pre)tanning agents. Hence, the principal axes of our synthetic approach, from product design phase to its industrial eventual application, have been: recovery and recycling of waste metals, simplicity and cost-effectiveness of the new tanning agent application, as well as closed loop processing, in order to protect the environment and improve the quality of life. Major challenges to match in our efforts remain commercial viability and consumer acceptability of the finished leather article.

The new tanning agents, in fact, will act as a prelude towards new eco-friendly leather manufacture, in which no potentially toxic, noxious and harmful chemicals have been used and discharged – currently and according to the Environmental Reports of the

Tanning Sector 30-40 % of chemicals used during leather manufacture are characterised as potentially toxic or hazardous.

MATERIALS AND METHODS

Raw and Auxiliary Materials

Solid Titanium waste (filings); aluminum sulphate, (SR EN 878/2004); sodium citrate (STF 116/2000); sodium tartrate (STF 34/199); ammonium sulfate (STAS 450-1975) Magnesium oxide (STAS 4995-1980); sulphuric acid (95-97% -STAS 97-1980).

Bovine Pelts

For all tanning trials bovine pickled pelts of Romanian origin, with mean weights ranging from 20-25 kg were used (pH ca. 3.0).

Ti-based Agents Synthesis

For the solubilisation of Titanium waste and in order to obtain tanning compounds was used a glass reaction vessel equipped with a VELP SCIENTIFIC mechanical stirrer. In-house design laboratory equipment with vacuum ILMVAC type was used for the filtration of Titanium solution resulted by dissolving wastes. The pH of the tanning bath was determined using a calibrated for this purpose WTW- INOLAB pH LEVEL 2 -digital pH-meter.

Metal Content in Ti-end Waste

Metals' content was determined using plasma emission spectroscopy device (ICP-SPECTRO) and an in-house protocol for this purpose.

Hydrothermal Stability Measurements of Prototype Leathers

Wet-white and control prototype leathers thermal analysis was carried out using (i) a Differential scanning calorimeter (204 F1 PHONIX-NETZSCH. To determine the curves of heat of enthalpy change as a function of the temperature a Perkin-Elmer DSC 7 calorimeter was used. Each sample was weighed (3-6 mg) and placed in an Aluminum crucible. Thermal effects were measured against a similar empty crucible in the calorimeter at room temperature while nitrogen was purged, and heated in the temperature range 50-260°C. On the other hand, shrinkage temperature measurements were recorded within the range 22-to-100°C at a heating rate of 2 degree/min.

RESULTS AND DISCUSSION

Synthesis of New Mixed Ti-Al Tanning Agents from Metallurgic End Waste

The main classification criterion for titanium wastes was their contaminant level (Buzatu M., 1994). The highest contaminant level in titanium wastes and titanium alloys is in cuttings resulting from the mechanical processing of ingots and cast articles (Figure 1).

a) Titanium ingot

b) Cutting and shaping the ingots

c) Unrecyclable cuttings

Figure 1. Titanium wastes

Basic metal composition of the Titanium wastes (filings) used as raw materials for the production of the new Ti (III) tanning agents is given in Table 1.

Table 1. Heavy Metal composition of the Titanium wastes

Metal	Ti	Al	V	Fe
%	89-95	1-6	0,1-4	0,0001-0,0005

The Aluminum salt used was $Al_2(SO_4)_3 . 18 H_2O$ (15.3% Al_2O_3, 8.55% Al). The schematic outline of the synthetic pathway designed and applied for the generation of the mixed new tanning agents based on Titanium and Aluminum is shown in Figure 2 (Crudu M. et al., 2008, 2009). The results of chemical analysis carried out for the novel tanning agents' solution and powder form are reported in Table 2.

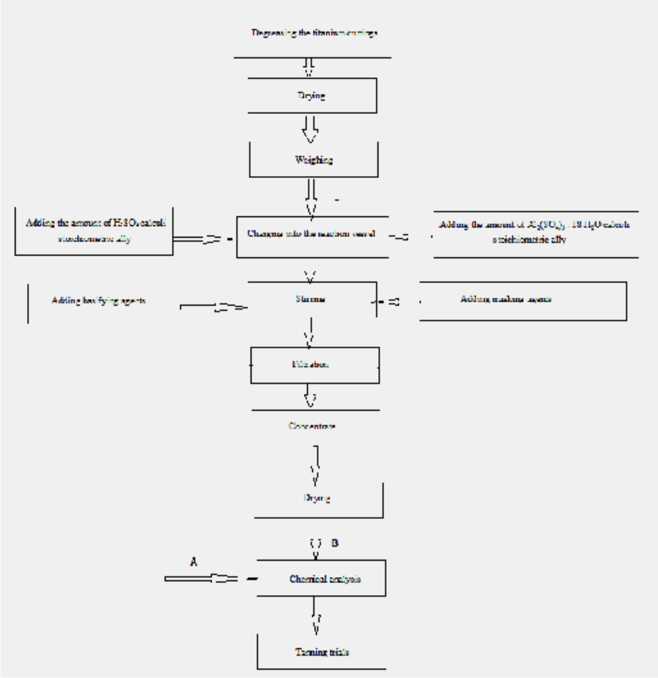

Figure 2. Chemical synthesis pathway for obtaining the new tanning agents based on Ti and Al

Table 2. Chemical analysis of the Tanning agents

Characteristics	Solution	Powder
Density (g/cm^3)	1.25 – 1.45	
pH	1.8 – 2.3	
Total ash (g/dm^{-3})	75 – 140	
Total metal oxides content (g/dm^{-3})	65-130	
Total metal oxides, %	-	13-18
pH (1:10)	-	1.8 – 2.3

The evaluation new tanning agents', and in particular topographic distribution – mapping - of the metal species, was obtained by means of scanning electron microscopic (SEM) and energy dispersive X-ray (EDAX) analyses (Figure 3).

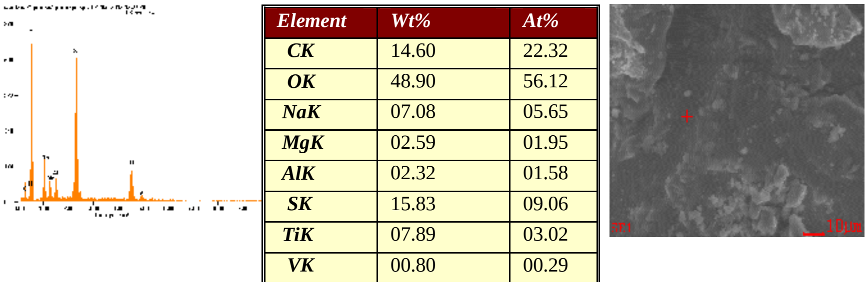

Element	Wt%	At%
CK	14.60	22.32
OK	48.90	56.12
NaK	07.08	05.65
MgK	02.59	01.95
AlK	02.32	01.58
SK	15.83	09.06
TiK	07.89	03.02
VK	00.80	00.29

Figure 3. SEM-EDAX analysis

New Wet-White Leathers Characterization and Evaluation

Full thickness semi-processed tanned leathers resulting from application of the new Titanium-Aluminum tanning agents as described here is white, with a smooth grain full and supple, as shown with the photographic image in Figure 4.

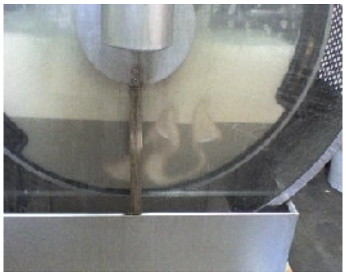

Figure 4. Wet-white leathers tanned with the new agent

Figure 5. Wet-white split and shaved

Shrinkage temperature values determined for the different new tanning agent variants ranged from 68-82°C, whereas wet white leathers were successfully processed through the subsequent mechanical operations of splitting – easily grain, middle and bottom split were obtained, as well as shaving, as demonstrated with the photographic image of Figure 5.

Good hydrothermal stability of the prototype leathers was confirmed with measurements undertaken using the Micro-Hot table device, with Ts=70-80°C, as shown in Figure 6.

T_{in}	**A1**	**B1**	**C**	**B2**	**A2**	**T_{fin}**
°C						
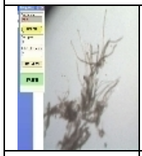	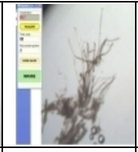	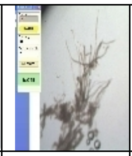	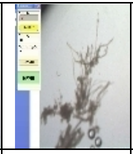	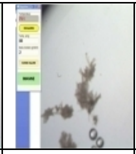	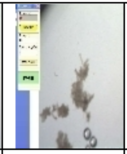	
27.5	69.7	72.7	**76.1**	79.1	80.0	83.4

Figure 6. Determination of shrinkage temperature by MHT method

Another confirmation of the thermal behavior of the new semi-wet type of leather tanned with white pre-tanning agents was obtained by using DSC analysis (differential scanning calorimetric dynamic analysis). A typical example of the thermographs recorded for samples taken from the prototype wet-white leathers tanned with the new Ti-Al based tanning agents is shown in the Figure 7.

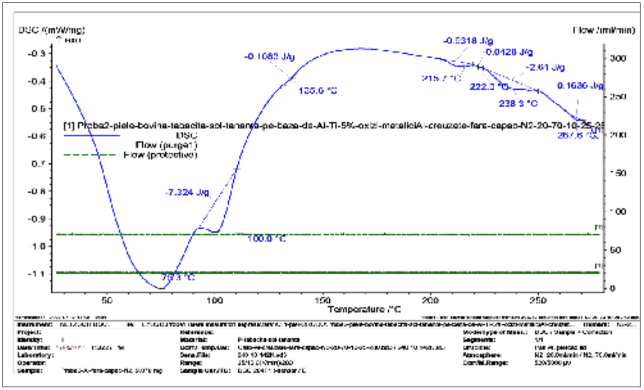

Figure 7. DSC-thermograph for wet-white tanned with the new Ti-Al tanning agents

The endothermic transitions recorded for the new wet white leathers consists of at least three (3) peaks, indicative of consecutive denaturation processes. The first transition is recorded for temperatures within the range 50°C and 125°C. A second set of peaks is registered for temperature values between 130° and 250°C, strongly linked to the processing history of the material (in particular the degree of tanning); the denaturation process occurring can be tentatively explained by the crystalline-amorphous two-phase model of collagenic materials. According to this model the super-coiled triple-α helix is partially crystalline and embedded in an amorphous matrix. Consequently, the minimum of endotherm II is associated with uncoiling / melting of the crystalline region. In turn, the tanning process by inducing the formation of synthetic crosslinks, can result in increased stiffness of the matrix, and, thus, is responsible for the observed shift of the melting process to higher temperature values. Monitoring the temperatures at which process II occurs may, therefore, reveals the degree and effectiveness of tanning, whereαs for leathers tanned with Cr(III) –salts the second peak is not visible as it overlaps with the pyrolytic transition. Hence, DSC thermographs, as those recorded for wet-white prototype leathers and shown in Figure 5 are specific to each material and can be used as material –specific and unique «fingerprints» (Budrugeac, P. 2004).

In order to characterize the new wet-white leather and prove the tanning potential of tanning potential of the newly synthesised compounds, chemical analyses has been carried out both on the split and grain layers of the product leathers and the results obtained are shown in Table 3.

Table 3. Wet-white grain and split leather chemical analyses

No.	Characteristics	Layer	
		Grain	Split
1.	Volatile matters, (%)	53.1	51.2
2.	Extractible, (%)	1.58	2.35
3.	Ash, (%)	10.4	10.9
4.	Metal Oxides, (%)	8.2	8.3
5.	Shrinkage temperature, (°C)	77	75
6.	Shrinkage temperature, (°C-MHT method)	76.1	73.9
7.	pH of water extract	3.98	4.0

Similar analytical values obtained for both layers tested have led to the conclusion that the penetration of the new tanning agents was not only complete but also uniform, assuring sufficient stabilization of the wet-white for further mechanical or other chemical processing. The evaluation of the modification of collagen by new tanning agents', and in particular topographic distribution – mapping - of the metal species in the prototype leathers, was obtained by means of scanning electron microscopy (SEM) and energy dispersive X-ray analysis (EDAX). (Figure 8).

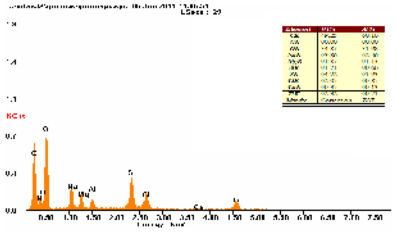

Figure 8. Mineral species topographic mapping

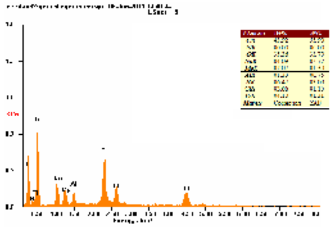

Figure 9. EDAX mapping of split

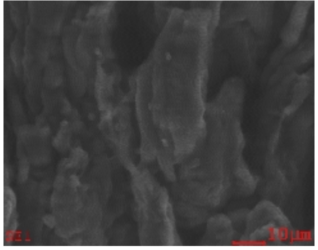

Figure 10. SEM – image of grain split of wet white leathers

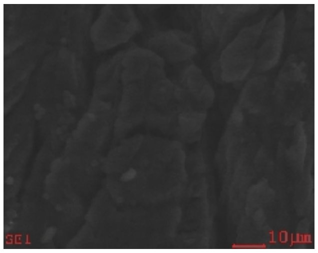

Figure 11. SEM – image of the bottom split of wet white leathers

CONCLUSIONS

Exploring the valorisation of solid Titanium metallurgic end wastes, as a low cost raw material has yielded new tanning agents for the replacement of Cr(III) tanning salts, a hitherto unthinkable or non technically feasible mission. In turn, as demonstrated here it is plausible to:

- increase of eco-efficiency in the leather manufacturing sector by making use of solid wastes, which cannot be recycled in the industry that generated them;
- total or partial replacement of chromium salts in the tanning process with cheap to produce and easy to apply in rapid full substance bovine leather manufacture, that, in turn required minimum process rationalisation or modification; moreover, the new mineral tanning agents are free of restricted or regulated metals Cr, Pb, Cd, Hg and Ni;
- increase in articles diversity.

The experimental results obtained so far in pretanning trials, are a clear witness that it is now possible at pilot scale to produce full substance bovine wet white with the desired smooth grain, that possesses the minimum hydrothermal stability for subsequent mechanical processing and further R&D ought to be carried out aiming at:

- improving the methods of waste processing to make them more efficient;
- a complete survey of environmental impact and LCIA of the products, effluent and waste generated;
- obtaining quantitative yield and costing data from large scale lots;
- the diversification and rendering more efficient the tanning materials, application processes, and wet-white leather semi-processed commodity products.

Acknowledgements

This work has been financed by the European Fund for Regional Development and the Romanian Government in the framework of Sectoral Operational Programme under the project INNOVA-LEATHER: «Innovative technologies for leather sector increasing technological competitiveness by RDI, quality of life and environmental protection» – contract POS CCE-AXA 2-O 2.1.2 nr. 242/20.09.2010 ID 638 COD SMIS – CSNR 12579.

REFERENCES

Budrugeac, P., Miu, L., Popescu, C., Wortmann, F.J. (2004), "Identification of collagen-based materials that are supports of cultural and historical objects", *Journal Therm Anal.Cal*, 77(3), 975.

Buzatu, M., Moldovan, P. (2008), "Reacting and Light Alloys–Part I: Alloys Based on Titanium", Lecture, 1994.

Covington, A.D. (2008), "Quo vadit chromium? The future direction of tannage", *JALCA*, 103.

Crudu, M., Deselnicu, V., Mutlu, M.M., Gulumser, G., Bitlisli, B.O., Basaran, B., Zengin, A.C.A. (2010), "New tanning agents based on titanium and zirconium", *Proceedings of ICAMS 2010*, 27-32, 16-18 September 2010, Bucharest, RO, ISSN: 2068-0783, CERTEX.

Crudu, M., Niculescu, M., Deselnicu, V., Sutiman, D., Sibiescu, D., Cailean, A., Boca, N., Patent RO 126300/2011.

Crudu, M., Boca, N., Sutiman, D., Ioanid, A., Caileanu, A., Sibiescu, D. (2009), *Compounds with tanning capacity obtained from Ti-end unrecyclable waste of the Ti-metalurgic industry* (in Romanian, CERTEX, ISBN 978-973-1716-54-1.

Crudu, M., Deselnicu, V., Albu, L., Niculescu, M., Roşca, I., Sutiman, D., Sibiescu, D., Cailean, A. (2008), "Eco-friendly tanning agents to be used in leather manufacture", *10th International Chemical and Biological Engineering Conference*, Portugal, ISBN 978.972.97810.3.2.

German, H.P. (LGR) (2010), "Sustainable Leather Manufacture: A realistic target or Wishful thinking?", BM DAS Memorial Lecture, LERIG Congress India.

Peng, B.Y. et al. (2007), "Novel titanium (IV) tanning for leathers with superior hydrothermal stability II. The influence of organic ligands on stability and tanning power of titanium sulfate solutions", *JALCA*, 102(9), 261.

EMERGING MARKET FOR FOC-LEATHER ARTICLES: A REAL NEED OR JUST MARKETING EDGE

DANA CORINA DESELNICU, IOANNIS IOANNIDIS

INCDTP - Division: Leather and Footwear Research Institute, Bucharest, Romania, email: d_deselnicu@icpi.ro

The purpose of this paper is to examine relevant aspects of quality of ecological leather used in footwear manufacture in Romania, from the clients' perspective. The main method used in the study is the survey employing questionnaire application to a non-probabilistic sample of Romanian footwear clients. The paper examines conceptual models proposed in relevant quality literature and advances a conceptual and applied framework for quality and ecological aspects for leather-made footwear, from a customer's perspective. This framework can provide a valuable basis for the development of new ecological products in the leather and footwear sector, and also guide their introduction to the market based on assessed consumer preferences in Romania. In the future, a larger empirical study can be employed to investigate the validity of the framework.

Keywords: quality, ecological, leather, footwear, clients

INTRODUCTION AND PURPOSE

Much emphasis is put on the quality of products. The customer concern over quality provides a great reason for industries to see product quality as being essential to the survival of business. Nowadays, the rapid development of intelligent production and manufacture, and increasing consumption, have given rise to a growing public and government concern over environmental aspects, in almost all areas of activity. Concepts as bio-degradable, bio-sustainable, good to the environment, ecological, organic, green and so on are only a few to demonstrate the emergent global movement which pushes the change to an eco-friendlier economy and lifestyle. There are concentrated activities in Europe towards implementation of the Eco-label and its Flower symbol for all products and services meeting environmental-friendly standards.

These new concepts are becoming prominent in recent years and they are influencing the traditional approach to conception, production and marketing of mainly goods, but also services. Also, there is increasing evidence of their inclusion in consecrated management practices such as Quality Assurance or Corporate Social Responsibility (Deselnicu, D.C., 2005).

PRODUCT QUALITY

Quality management was initially developed in the manufacturing industry. In the first part of the last century, the most prominent development took place in the USA, later followed by its significant evolution in Japan (Parasuraman, 1985).

Garvin (1987) proposed the following eight dimensions for quality that, as he stated, can define both product and service quality: performance (concerned with the primary operating characteristics of a product), features (characteristics that supplement the basic performance functions), reliability (the probability of a product working fault-free within a specified time period), conformance (the extent to which a product meets established standards/specifications), durability (a measure of a product life), serviceability (concerned with repairs, field services), aesthetics, and perceived quality (the reputation factors influencing the customers' image of the corporation - Langrosen, 2001). These subjective dimensions of quality are important (Grönroos, 1982).

ECOLOGICAL ASPECTS IN LEATHER AND FOOTWEAR INDUSTRY

Leather industry is one of the traditional and very old known industries in Romania and throughout the world. In the present global scenario towards "cleaner production", the leather industry is facing severe environmental challenges. Pollution caused by the leather industry is due to the use of numerous organic and inorganic chemicals in the production process, and their subsequent discharge. Besides the effect of wastes discharged during processing from skin to leather, a number of chemicals may also have a toxic effect because of their residues in finished products, such as footwear.

Chrome tanning is a popular tanning method practiced worldwide. Almost all tanneries use chromium (III) as a tanning agent. Approximately 90% of the leather manufactured around the word is tanned using chromium (III). Due to the toxicity of chromium, tanners are often placed under pressure to reduce its content of the effluent discharges and sludge (the uptake of chromium in tanning is around 60-65%).

RESEARCH METHODOLOGY

The current study was conducted as an exploratory survey employing quantitative methodology, for investigating ecological and quality aspects related to the leather footwear items in Romania, from clients' (consumers') perception.

Research Design

The research method was the exploratory survey. The research instrument consisted in a self-administered questionnaire containing 20 items investigating: ecological leather (4 items), quality of leather footwear (5 items), comfort of leather footwear (6 items), and buying behavior of clients of footwear (5 items), followed by 3 questions concerning age, gender and education level of the respondent. Likert close-ended answer scales were used, ranging from "1 – To a very limited extent/ Not at all important" to "5 – To a very large extent/ Very important".

The sample consisted in the clients visiting a footwear store in a big Mall in Bucharest. The customers were asked to participate in the study and to fill in the questionnaires. Therefore, the non-probabilistic method was used for sampling, as the configuration of the researched population (clients of footwear items) and its availability was not adequate for probabilistic sampling, neither from a dimensional, nor from a structural point of view. Consequently, a mixture of Henry's (cited by Hutu, 2001) sample types were used: convenience, typical cases, critical cases and "snowball". The sample consisted in 30 individuals as follows (Figure 1, 2, 3):

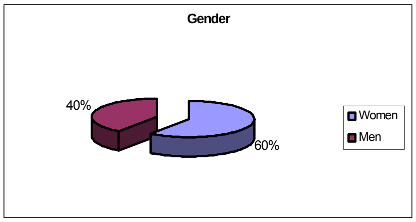

Figure 1. Sample structure by gender

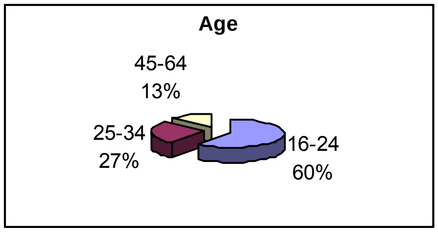

Figure 2. Sample structure by age

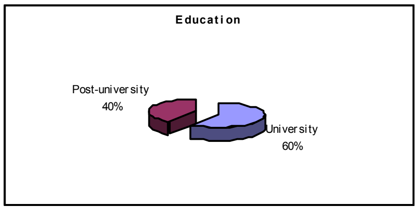

Figure 3. Sample structure by education level

DATA ANALYSIS AND INTERPRETATION

The data was analyzed using the SPSS for Windows 17.0 statistical program, and consisted in the statistical summary of the data, correlation and contingency analysis.

Ecological Aspects of Leather-Footwear

The first part of the questionnaire aimed to investigate the extent to which the clients of footwear articles were interested in different ecological aspects of the leather and leather making process. These aspects, health and environment protection, and the certification and corresponding labeling of the ecological products, were derived from the official EU website on Eco label.

All thirty respondents declared that they would prefer for their shoes leather which is guaranteed not to contain substances harmful to health. However, regarding the preference towards a leather whose production process does not pollute, thus protecting the environment, only 80% of the respondents declared their preference to the higher extent, 7% to a medium extent, while 13% declared that they were not interested.

When asked if they would like that footwear items made from such ecological leather be labeled accordingly, in order to be easily recognized by the consumers, the opinions of the respondents were also diverse (standard deviation - S.D. of 0.579), with 95% of the respondents being interested in medium to high extent (mean of 4.79), and 5% of them being not at all interested in the matter. Concerning the availability to pay more for footwear manufactured from ecological leather, the respondents' opinions were even more diverse (S.D. 1.014), but the majority of the clients would however pay more for this special ecological feature (mean of 4.20, where max. value is 5).

This analysis of the perception and preference of the clients versus ecological aspects of leather and footwear indicate that for the investigated sample, the interest is high, and also the clients are willing to pay more for this type of products.

Quality Aspects of Leather Footwear

The second part of the questionnaire enquired on the importance to the clients of some quality aspects of the leather footwear: style/ design of footwear, durability, special finishing, and easy maintenance. Descriptive statistic indicators for these variables (Table 1) reveal that the most important quality aspects for footwear clients are style / design of shoes (mean =4.93), and also easy care and maintenance of footwear (mean =4.40). Most respondents agree to these aspects. On the contrary, quality aspects concerning durability of footwear and special finishing are more controversial, illustrating the variety of clients' preferences.

Table 1. Descriptive statistics for quality of footwear variables

	N	Minimum	Maximum	Mean	Standard Deviation
Style	30	4	5	4.93	.258
Durability	30	1	5	3.93	1.280
Special finishing	30	2	5	3.60	1.056
Maintenance	30	3	5	4.40	.737

Comfort Aspects of Leather Footwear

The division of the questionnaire concerning comfort of footwear comprised 6 items referring to: comfort (the footwear is soft, flexible and light), temperature isolation of footwear (protects against overheating of the feet in summertime and freezing in wintertime), antifungal treatment of the shoes, vapor evaporation (the feet do not perspire excessively), the footwear does not develop an unpleasant smell inside, the color inside the footwear does not migrate on the socks.

Table 2. Statistic indicators for Comfort aspects of leather footwear

		Comfort	Isolation	Antifungal treatment	Vapour evaporation	Smell	Colour migration
N	Valid	30	30	30	30	30	30
	Mean	4.87	4.87	4.33	4.67	5.00	5.00
	Median	5.00	5.00	5.00	5.00	5.00	5.00
	Mode	5	5	5	5	5	5
	Std. Deviation	.352	.352	1.175	.724	.000	.000
	Variance	.124	.124	1.381	.524	.000	.000

As it can be seen from Table 2, all respondents agree that inside unpleasant smell development and color migration are very important comfort issues for their footwear. General comfort of shoes and temperature isolation are also important aspects (mean of 4.87), and so is feet perspiration (mean of 4.67), while antifungal treatment of the shoes seems to be the least important for the investigated sample (mean of 4.33).

Buying Behavior of Leather Footwear

In order to investigate the clients preferences when buying footwear, respondents were asked to evaluate the importance of several aspects which influence their buying behavior: the footwear brand, the store from which they buy from and its reputation, the footwear advertising from TV, newspapers, magazines, Internet and outdoor publicity, the trend and fashion, and also the price (Table 3).

Table 3. Statistic indicators for buying behavior of clients of leather footwear

		Brand	Store	Advertising	Trend	Price
N	Valid	30	30	30	30	30
	Mean	3.33	3.07	2.47	3.60	3.73
	Median	4.00	3.00	2.00	4.00	4.00
	Mode	4	3	1	4	5
	Std. Deviation	1.291	1.223	1.356	1.242	1.486
	Variance	1.667	1.495	1.838	1.543	2.210

As seen from the statistic analysis in Table 4, the most influent aspect when buying footwear is the price (mean of 3.73). This is also the most controversial aspect among the respondents (standard deviation of 1.486). Other important issues that the clients take into account when buying are the fashion / trend (mean of 3.60), the brand (mean of 3.33), and also the store (mean of 3.07). Surprisingly, the advertisements have the smallest impact on the buying behavior for footwear items for the investigated sample, some possible explanations being the scarcity of such advertisements in the media in Romania, the abundant footwear market, and the subjective nature of the purchase.

Correlations Analysis

Because a very large correlations table was obtained, only significant correlations between the investigated variables will be presented briefly.

The ecological aspects of leather footwear covariate with other quality and comfort aspects, indicating that these three concepts are highly inter-correlated and belong to similar fields. The usage of ecological leathers which contain no harmful substances for human health is positively correlated with comfort (Pearson correlation coefficient r = 0.677, significant at the 0.05 level). The labeling of footwear made of ecological leather is positively correlated to the style / design (r = 0.888) significant at the 0.05 level, price (r = 0.572), durability of footwear (r = 0.573), significant at the 0.01 level, and negatively correlated to age of the respondents (r = -0.623, significant at the 0.05 level), showing that younger people are more willing to have the ecological footwear products labeled accordingly.

Concerning quality aspects, style is correlated with gender (Pearson r = -0.599), showing that women are more interested in footwear design that men are, and also with age of the respondents (r = -0.619), indicating that style is more important to younger people (both correlations significant at the 0.05 level). Durability of footwear is positively correlated with price of the footwear (r = 0.616) and with the labeling of ecological leather footwear (r = 0.573), both correlations significant at the 0.05 level.

Special finishing of the footwear, another quality defining characteristic, is correlated to the antifungal treatment of footwear (r = 0.518) and to trend (r = 632), both correlations significant at the 0.05 level.

Also comfort of shoes is correlated with the antifungal treatment (r = 0.633, significant at the 0.05 level), and with vapor evaporation characteristic of the footwear (r = 0.654, significant at the 0.001 level). Isolation from heat and cold presents high correlations to the same variables, namely antifungal treatment (r = 0.633) and vapor evaporation (0.935, significant at the 0.01 level), indicating the close connection between these concepts and properties of footwear.

Regarding buying behavior variables, brand is negatively correlated with price willing to be paid by the respondents (r = - 0.620, significant at the 0.05 level) showing that, for the investigated sample, people who are attracted to brand footwear are also the ones willing to pay less for their shoes. This relationship can be possibly explained by the Romanian national high-context culture, which promotes fine dressing and footwear even in scarce financial and economical conditions. Similarly, buying from a recognized store is inversely correlated to durability of the footwear (r = - 0.545, significant at the 0.05 level), proving that people who buy from such stores do not expect their shoes to last very long, and positively correlated to advertising (r = 0.669, significant at the 0.05 level). Advertising itself is correlated to store reputation, as mentioned above, and to respondents' education level (r = - 0.549, significant at the 0.05 level), revealing that more educated people are more sensitive to footwear publicity and buy their shoes influenced in some extent by it. The price willing to be paid by respondents for their shoes is also positively correlated to education level (r = 0.540, significant at the 0.05 level), and to their age (r = 0.540, significant at the 0.05 level). More educated people, and also older ones are would pay more for their footwear.

By adding all individual aspects of comfort into one variable which designates overall comfort, it could be observed that it is positively correlated to overall quality of shoes (r = 0.640, significant at the 0.05 level), demonstrating that the two concepts are highly associated.

CONCLUSIONS

This paper offers a conceptual and applied framework for quality and ecological aspects for leather-made footwear, from a clients' perspective. Based on statistical analysis of the gathered data, it has been demonstrated that quality, comfort and ecological aspects are highly associated, indicating their similarity and their belonging to the same conceptual areas. Aspects concerning ecological leather and footwear produced from such leather are not yet very popular and familiar to Romanian respondents, some of them being not interested of the matter and not willing to pay more for such products, although a positive reaction to these concepts does exist.

Comfort and quality aspects of the footwear items are important for the consumers, and they are correlated with each other. The buying behavior of the investigated Romanian clients is mostly guided by price of footwear items, by trend and fashion.

This framework can provide a valuable practical basis for the development of new ecological products in the leather and footwear areas, and also guide their introduction to the market based on assessed consumer preferences in Romania. In the future, a larger empirical study can be employed to further investigate the validity of the framework.

Acknowledgements

This work has been financed by the European Fund for Regional Development and the Romanian Government in the framework of Sectoral Operational Programme under the project INNOVA-LEATHER: "Innovative technologies for leather sector increasing technological competitiveness by RDI, quality of life and environmental protection" – contract no. 242/20.09.2010.

REFERENCES

Deselnicu, D.C. (2005), "Practical tools for change: A Software support for self-assessment of the business excellence implementation process in Romanian enterprises", in *Proceedings of the 4th International Conference on Management of Technological Changes*, Book 2, Chania, 17-23.

Garvin, D.A. (1987), "Competing on the eight dimensions of quality", *Harvard Business Review*, 65(6),101-109.

Grönroos, C. (1982), *Strategic Management and Marketing in the Service Sector*, Swedish School of Economics and Business Administration, Helsingfors.

Hutu, C.A. (2002), *Organizational culture and leadership – Textbook*, Venus Publishing House, Iasi.

Lagrosen, S. (2001), "Strengthening the weakest link of TQM - from customer focus to customer understanding", *The TQM Magazine*, 13 (5), 348-354.

Parasuraman, A., Zeithaml, V.A. and Berry, L.L. (1985), "A conceptual model of service quality and its implications for future research", *Journal of Marketing*, 49(Fall), 41-50.

***, www.ecolabel.eu

SYNTHETIC ORGANIC TANNING SYSTEM

VIORICA DESELNICU, MARIAN CRUDU, IOANNIS IOANNIDIS, DANA CORINA DESELNICU

INCDTP - Division: Leather and Footwear Research Institute, 93 Ion Minulescu, Bucharest, Romania, v_deselnicu@yahoo.com

Even the optimization of common chromium tannage, and combined tannage with chromium and other tanning materials have led to outstanding results related to the lowered pollution level in effluents and sludge, the problem has not been solved wholly. The single solution for this problem is finding out an environmentally friendly alternative to chromium tannage. This work also is within the above line, aiming to obtain wet-white leather by an organic tanning process in order to reduce chromium in tannery effluent.

Keywords: organic tannage, wet white, synthetic tannage.

INTRODUCTION

Chrome tanning is the most common type of tanning in the world. Chrome tanned leathers are characterised by top handling quality, high hydro-thermal stability and excellent user properties. Chrome waste from leather processing poses a significant disposal problem. It occurs in three forms: liquid waste, solid tanned waste and sludge. In most countries, regulations governing chrome discharge from tanneries are stringent. Today, all tanneries must thoroughly check their waste streams. Chrome discharge into those streams is one of the components that has to be strictly controlled.

The environmental impact of chrome waste from tanneries has been a subject of extensive scientific and technical dispute. Statutory limits have since been set for chrome discharge and disposal, and relevant guidelines have been drawn up throughout the world. Given the close correlation between chrome tanning and the environmental impact of leather processing, auditing the efficiency of processing operations takes on prime importance.

Conventional chroming process generally involves in pickling, chroming and basifying, and there are several defects existing in the process (Sykes 1981, Germann 1995): i) 8-10% salt and 1.0-1.2% sulfuric acid were used in pickling, which results in higher contents of chlorides, sulfates and chemical oxygen demand (COD) in the effluent. ii) The uptake of chromium in conventional chroming is lower (70-80%), a considerable amount of chromium left in the effluent may result in environmental problems(Ludvik 1997). iii) A great deal of chrome containing solid wastes such as splittings and shavings are produced, which is certainly difficult to be degraded and harmful on the environment if discharged directly (Tao Zhang et al., 2009).

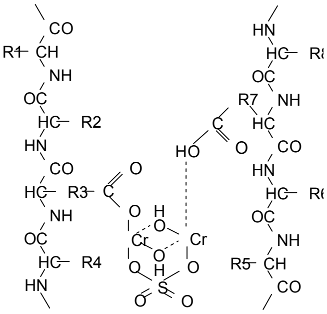

Figure 1. Collagen-chromium (III) compounds – crosslinked

Much criticism has been directed towards the use of chromium salts in leather tanning, but it has to be borne in mind that chromium can occur in different oxidation states and its compounds behave differently. Most chromium(VI) compounds are highly toxic and classified as MAK III A 2 carcinogens, but chromium(III) is an important trace element in man and animals.

Chromium compounds are, or at least used to be, one of the most common causes of occupational skin disorders. Chromium(III) is not regarded as being sensitizing, because it does not readily penetrate the skin, but water-soluble chromium(VI) compounds penetrate the skin very easily. Chromium(VI) is then reduced intracutaneously to trivalent chromium, which enables it to react with the proteins in the skin and trigger an allergic reaction.

The issue of chrome is perhaps one of the most debated issues between authorities and the tanning industry because of the difference in opinion about the toxicity of chromium (III) salts used in the tanning industry. The tanning industry has the view that the chromium (III) tanning agent is not toxic and can be compared with table salt. Authorities opinion is that chromium (III) should be considered toxic, especially for aquatic life. What is agreed is that chromium (VI) is much more toxic than chromium (III). The toxic mechanism of action differs for hexavalent versus trivalent chromium. Hexavalent chromium causes cellular damage via its role as a strong oxidising agent, whereas trivalent chromium can inhibit various enzyme systems or react with organic molecules. Chromium (III), the naturally occurring form, has low toxicity because it is non-corrosive and passes poorly through membranes, but chromium (VI) is highly toxic because it has strong oxidation characteristics and passes readily through membranes.

Chrome is mentioned in list 2 of the Annex to Council Directive 76/464/EEC of 4 May 1976 on pollution caused by certain dangerous substances discharged into the aquatic environment of the Community. Tannery wastes containing chromium are not included in the European Hazardous Waste List on the basis that the wastes do not possess the characteristics necessary for classification as a hazardous waste (COTANCE, 2002).

Despite the fact that chromium has been under pressure from some regulatory authorities, the extent of substitution of chromium tanning agents has been limited. The main reason for this is that chromium is the most efficient and versatile tanning agent available, and it is relatively cheap.

These practical and operational constraints have resulted in attempts to find an alternative to chromium (III) tanning (German H.P., 2010) for the production of free-of-chrome (FOC) leather, whilst retaining the mineral character in leather. Accordingly, Al (III) (Hernandez J.H., 1983; Hancock R. A. et al., 1980), Zr (III), Ti (III & IV) (Bi Yu Peng et al., 2007), Kleban, M., US Pat, Appl. No. 200601151738, their mixed salts (Covington A.D., US Patents 4563156, 4731089) and most recently nano-silicates (Liu, Y, et al 2010) and sodium waterglass were tested as effective partial or total replacement tanning agents or for the production of a reversibly tanned new intermediate semi-processed product and commodity: “wet-white” or “wet-stabilised” leather. Overall metal ion complexes have some affinity for protein, but when applying the criteria of adequate reactivity colour, availability, cost and toxicity eliminates nearly all of the commercially available agents as viable options.

Syntans, Resins, and Polyacrylates are agents used alternatively or in addition to chrome and vegetable tannins.

Previous research studies demonstrated that using oxazolidine (Roig et al., 2011) (Figure 2) or resorcinol tanning agents (Hiu et al., 2009) (Figure 3) combined with other (vegetable or synthetic agents) allows for the obtaining of quality leathers that can be used by footwear and upholstery industries.

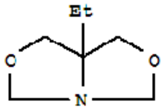

Figure 2. Oxazolidine E

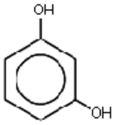

Figure 3. Resorcinol

Oxazolidines

Oxazolidines (Angus Chem. GmbH) are saturated heterocyclic compounds prepared by reacting primary amino alcohols with formaldehyde. Monocyclic or bicyclic oxazolidine ring structures are formed depending on the choice of starting chemicals, it is therefore possible to synthesize a variety of oxazolidines from different amino alcohols. Oxazolidines are highly useful chemicals for a wide variety of applications: corrosion inhibitors, emulsifiers, diluents or tanning agents. The oxazolidine marketed for use as tanning agents are water soluble compounds, compatible with most chemicals normally used in tanning operations and can be introduced at several points in the tanning process.

The capacity of the Oxazolidine E for tanning leather is based on the formation of a reaction intermediate due to:

- the protonation of oxygen of each ring in acid medium, which weakens the C-O bond or,

- the oxazolidine rings opening caused by hydrolysis in an acid medium to provide an intermediate with two N-(hydroxymethyl) groups, and the subsequent nucleophilic attack of the collagen amino groups to this intermediate specie (Figure 4).

Leathers tanned with chromium salts have a high stability, determined by a shrinkage temperature (Tg) over 100°C, while the leathers tanned with oxazolidine alone reach shrinkage temperatures of below 75°C. It is therefore necessary to carry out the oxazolidine tanning in combination with synthetic or vegetable tanning agents to achieve higher shrinkage temperatures and obtain leather of comparable quality to the chrome tanned leather.

Resorcinol

Resorcinol is a diphenol which can be transformed into a prepolymer by Manich reaction with formaldehyde.

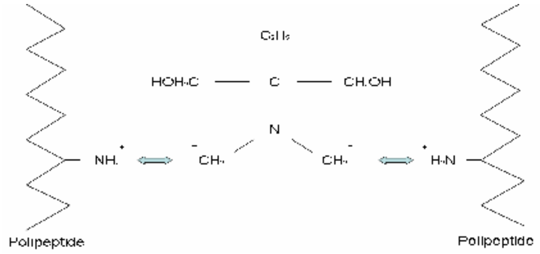

Figure 4. Collagen-oxazolidine crosslinked (Roig M. et al. 2011)

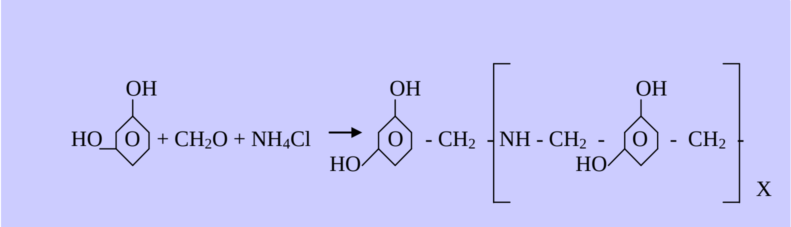

Figure 4. Tanning agent based on resorcinol pre-polymer

Resorcinol – Oxazolidine E

Recent studies demonstrated that resorcinol-oxazolidine E treated collagen is more stable system than that with sequential combination tannages with the same materials. The study has demonstrated that oxazolidine E underwent ring opening to form the N-methylol intermediate and reacted with the hydrogen bonds of resorcinol to form Tanning Matrix. The Tanning Matrix then penetrated into the collagen fibres and by aggregation prevented the denaturation of collagen fibres of heating. The next reaction is the involvement of hydrogen bonds and hydrophobic interactions, and the aldehyde groups of oxazolidine E in reaction with basic amino acid side chains of collagen as the major force involved in stabilization of collagen. In this way, a multiple point combination tanning occurs with the Tanning Matrix creating a high level stabilization of collagen and high hydrothermal stability (Hui et al., 2009).

This model of reticulation of resorcinol-oxazolidine E with collagen is shown in Figure 6.

This paper present the results obtained from different tanning tests on cowhides, at a pilot scale, using oxazolidine, resorcinol prepolymer or oxazolidine-resorcinol combination as an alternative to traditional chrome tanning. It is presented the procedures followed, physical characterization of obtained leathers, as well as the impact of this technology on waste water and solid waste generated.

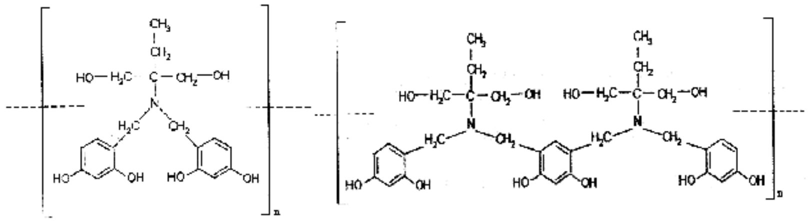

Figure 6. Reticulation model of resorcinol-oxazolidine E with collagen

MATERIALS AND METHODS

Salted cowhides were chosen as raw material for the chromium-free leather production for determining the effects of the newly synthesized leather tanning products. These newly synthesized organic tanning agents based on pre-polymers shown in Figures 2 and 3 were used as pre-tanning agents for this study (Platon et al., 2010).

The Figure 7 presents the Flow Chart for conventional and experimental processes and the Figure 8 presents the equipment for experiments at pilot scale.

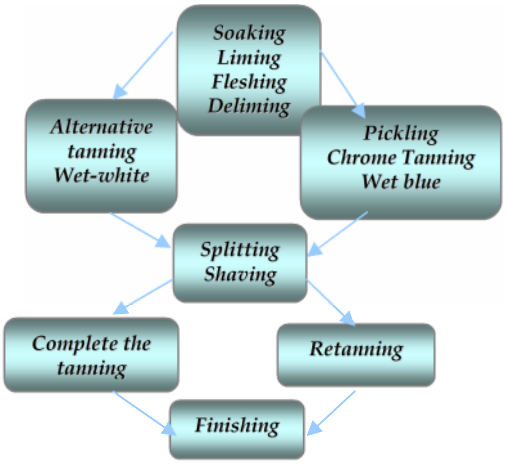

Figure 7. Flow Chart for conventional and experimental processes

EXPERIMENTAL

Wet salted cowhides were treated from soaking to bating as usual. The bated pelts were cut along the backbone line, left parts for conventional process, and right parts for the experimental ones. The chemicals employed in the experiments are of commercial grade, the chemicals used for analytical technique are of reagent grade.

Figure 8. Tanning drum used in pre-tanning tests on pilot scale

Experimental and conventional processes are provided as Table 1. As Table 1 showing, bated pelts were directly pre-tanned with oxazolidine E (Experiment E3). The bated pelts were of high pH value (6.8-7.0) and most active groups of collagen were exposed. Control sample was made using Chromium salts (Experiment C) on pickled pelts. The other experiments were conducted also on pickled pelts at 2.8-3.0 pH. Then the pre-tanned pelts were split and shaved.

Table 1. Conventional and experimental pre-tanning

Exp code	Process	Chemical	Time	$pH_{initial}$ /pH_{final}
C	Conventional chrome tanning on pickled pelts	8% Chromium salts (25% Cr_2O_3) + 10% sodium bicarbonate	8 hours	3.0-4.0
E 1	Pre-tanning with Oxazolidine E on pickled pelts	2 % Oxazolidine E	5 hours	3.0-4.8
E 2	Pre-tanning with Resorcinol and Oxazolidine E on pickled pelts	4% Resorcinol pre-polymer + 2% Oxazolidine E + 1% sodium bicarbonate	10 hours	2.8-4.8
E 3	Pre-tanning with Oxazolidine E on bated pelts	2 % Oxazolidine E	5 hours	6.8-8.5

The pre-tanned leathers were analysed for shrinkage temperature presented in the Table 2.

Table 2. Shrinkage temperature (Ts) of the pre-tanned leathers

No.	Experiment code	Shrinkage temperature, Ts, °C
1.	C (conventional)	102
2.	E1	70
3.	E2	72
4.	E3	68

In the Table 3 the characteristics of tanning effluents are presented.

Table 3. Characteristics of Tanning Effluents

No.	Characteristics	Conventional chrome tanning	Organic tannings experiments		
		C	E1	E2	E3
1.	Sulfates, mg/dm ^{3}	31669	265	30000	3374
2.	Chlorides, mg/dm ^{3}	34602	-	30005	5744
3.	Chrome oxie, g/dm ^{3}	4377	-	-	-

RESULTS AND DISCUSSION

Results indicated that the highest Ts of combination tanning leathers is resorcinol pre-polymer-oxazolidine E in sequence. In course of resorcinol pre-polymer tanning first the tanning parameters were pH 3.0 and 4% dosage (based on weight of caw pelts), and the tanning parameters were pH 3.5 and 2% dosage when oxazolidine E as tanning agent. The Ts of pre-tanned leather with resorcinol-oxazolidine combination was 72°C (Experiments E2).

Pickling is a preliminary process for preparing hides for tanning, largely by adjusting the pH with acid and controlling the swelling with salt. Higher salt concentrations in the tannery effluent resulting from the conventional pickling process have been an environmental concern, leading to a trend in developing a salt-free pickling process. Additionally, failure to control the swelling of hides during this step would lead to damage or defects in the fibre. This not only impacts the subsequent tanning process, but also the final quality of the tanned leather. In this study of salt-free pickling process oxazolidine E was used and compared to a conventional acid/salt pickling process (Experiments E1 and E3).

The penetration of the new tanning agents reflected by Shrinkage temperature (Ts) was not only complete, but also uniform, assuring stabilization of the wet-white leathers for further mechanical or other chemical processing.

All characteristics of Chrome Tanning Effluent (experiment C) are higher than those of experimental organic tanning.

The benefits of the novel tanning system using oxazolidine or/and resorcinol as the pre-tanning agents are:

- no chromium in organic tanning effluents which make it easier and cheaper to treat;
- residual salt could be significantly reduced;
- because the system eliminates a pickle step, there is a reduction in strong mineral and organic acids use;
- the tanning process could be reduced by up to five hours;
- the shrinkage temperatures ranged from 68-72°C, depending on the substrate.

CONCLUSIONS

Oxazolidines and resorcinol can be used as tanning agents in several different ways as illustrated in this paper.

Combinations of oxazolidines with resorcinol can replace chrome tanning without sacrificing the physical and thermal properties of the tanned leather. Finally, with the use of oxazolidine, a more effective salt-free pickling process can be achieved and the environmental impact within leather manufacturing can be further reduced.

Since there was no chromium existed in the splittings and shavings, the wastes could be treated and reused more easily.

Acknowledgements

This work has been financed by the European Fund for Regional Development and the Romanian Government in the framework of Sectoral Operational Programme under the project INNOVA-LEATHER: «Innovative technologies for leather sector increasing technological competitiveness by RDI, quality of life and environmental protection» – contract POS CCE-AXA 2-O 2.1.2 nr. 242/20.09.2010 ID 638 COD SMIS – CSNR 12579.

REFERENCES

Buljan, J., Reich, G., Ludvik, J. (1998), *Leder u. Häutemarkt*, 4, 30.

Buljan, J., Reich, G., Ludvik, J. (1998), *Leder u. Häutemarkt*, 5, 25.

Chen, W.Y., Li, G.Y. (2005), *Tanning Chemistry*, Beijing, Light Industry Press, 209-220.

COTANCE (2002), *The European Tanning Industry Sustainability Review*, World Summit on Sustainable Development.

Covington, A.D., US Patent 4563156.

Covington, A.D., US Patent 4731089, *Synektan TAL*, ICI.

Germann, H.P. (1995), *JSLTC*, 79(3), 82-85.

Germann, H.P. (2010), “Sustainable Leather Manufacture: A realistic target or Wishful thinking?”**,** LERIG Congress India.

Hancock, R.A., Orszulik, S.T., Sykes, R.L. (1980), “Tannage with Aluminum salts. Part 2. Chemical basis of the reactions with polyphenols”, *J. Soc. Leather Technol. Chem*, 64(2), 32.

Hernandez, J.H. (1983), *JALCA*, 78(8), 217.

Kleban, M., *Chrome-free Waterproof Leather*, US Pat, Appl. No. 200601151738.

Liu, Y. et al. (2010), “An Environmentally Friendly Leather-Making Process Based on Silica Chemistry”, *JALCA*, 105.

Ludvik, J. (1997), UNIDO Report US/RAS/92/120, 15.

Peng, B.Y. et al. (2007), “Novel titanium (IV) tanning for leathers with superior hydrothermal stability II. The influence of organic ligands on stability and tanning power of titanium sulfate solutions”, *JALCA*, 102(9), 261.

Platon, F., Deselnicu, V., Crudu, M., Albu, F.L., (2010), *Process for treating animal raw hides*, Patent RO 123001 B1.

Roig, M., Segarra, V., Bertazzo, M., Martinez, M.A., Ferrer, J., Raspi, C. (2011), “Chrome-free leather, tanned with oxazolidine”, Proceedings of XXXI IULTCS Congress, Valencia.

Saravanabhavan, S., Thanikaivelan, P., Rao, J.R. (2006), *Environ. Sci. Technol*, 40(3), 1069 -1075.

Sykes, R.L., Coning, S.B., Earl, N.J. (1981), *JALCA*, 76(3), 102-125.

INNOVA LEATHER: A KNOWLEDGE BASED PLATFORM FOR SUSTAINABLE LEATHER MANUFACTURE

SERGIU-ADRIAN GUTA[1], GHEORGHE BOSTACA[1], GABRIELA MACOVESCU[1], IOANNIS IOANNIDIS[1,2]

[1] *INCDTP - Division Leather and Footwear Research Institute, 93 Ion Minulescu St., Bucharest, Romania, email: icpi@icpi.ro*

[2] *Me-Med Consultants for Leather Industry, 23 Aristodimou St, Athens, Greece, email: ioannidisioa@gmail.com*

This paper presents a knowledge based platform which has been developed to underpin sustainable leather manufacturing. The platform comprises three independent databases that share roughly the same architecture. These databases are: Environmental Legislation Database for The Leather and Footwear Industry, Database for Clean Technologies in The Leather Industry and Analysis and Tests for Leather, Research Centres and Laboratories. These databases contain information regarding clean technologies such as ecological chemicals, leather processing machines and also about restricted chemicals for leather, environmental legislation and research centres. The platform is intended to be an useful tool for companies, students, technicians, engineers and researchers whose activity is related to the leather and footwear industry. It's aim is to promote technological progress, economic efficiency and research through the valuable information gathered from experts and accredited sources. Moreover due to legal measure of reducing pollution in form of treaties, conventions, directives, regulations, laws, players in the leather industry will find this platform useful in controlling the impact of the activities that they perform on the environment by taking into account environmental legislation stored in the platform. Aspects of the platform such as: the architecture, access, records, search, administration are investigated. Issued relating to environmental pollution generated by leather and footwear industry, Romanian and European legislation on environmental regulation, clean technologies in the leather industry are considered.

Keywords: knowledge based platform, leather manufacture, clean technologies.

INTRODUCTION

Leather and fur production is a pollution-generating process. In the current context, its reduction, for the purpose of sustainable development, is a major target of the industry. Thus during the technological process, raw materials are processed using appropriate chemicals and machines and the resulting assortments are based on operations and technological processes which induce variable degrees of pollution.

The leather industry, generating pollutant emissions in waters, soils and in the atmosphere faces current environmental regulations at both national and European scale. Therefore it was necessary to develop a database regarding national and European legislation on environmental regulations, their harmonization, as well as the degree of legislation implementation in the leather industry, database that will be presented in this paper (Macovescu & Guta, 2012).

Leather and fur articles have restrictions regarding the content of certain chemical compounds considered toxic, according to regulations stipulated in products standards or various technical specifications. Consequently a database with clean technologies for leather industry has been developed.

Although science and technology provide to some extent efficient solution to environmental issues, these are incomplete unless political decisions at international level, through concerted action on mitigating environmental pollution, are done.

The paper is organized as follows. Firstly are presented the three databases that form the platform for sustainable leather manufacture. Secondly it is outlined the platform architecture, technologies used for developing it, minimal technical requirements and also the access to the platform. Finally conclusions and further work are summarized.

CLEAN TECHNOLOGIES DATABASE

The raw hide is a by-product of the meat industry and from this raw material the leather manufacturing industry converts 25-30% by weight into leather. Leather manufacturing processes imply numerous chemical and mechanical operations which require intensive use of water and of hazardous chemicals. Consequently leather industry generates considerable amounts of solid, liquid and gaseous wastes (Page, 2004; Deselnicu & Albu, 2007). Clean technology can significantly reduce the costs of environmental compliance by reducing effluent loadings and chemical costs in leather manufacture (BLC Leather Technology Centre). The imperative and desideratum at the same time of selecting the most adequate chemicals, operations, technologies, machines, in relation to the state of the art and leading to the best performance in terms of ecology, in the context of a diversified and rich offer of producers in the field, is of paramount importance and requires careful and exhaustive documentation (Bostaca & Guta, 2004). To tackle the above mentioned issues a database dedicated to clean technologies and ecologic aspects has been developed and it will be presented in the following section. The structure of the database which is integrated part of the knowledge based platform for clean technologies is depicted in Table 1.

Table 1. Clean technologies database structure

Ordering and access criterion	Processing chemicals	Operations	Technological processes	Assortments	Restricted chemicals for leather	Leather processing machines
Selection option within the criterion	Liming	Liming	Footwear uppers	Footwear uppers	-	Liming
	Tanning	Tanning	Upholstery	Upholstery		Tanning
	Dyeing	Dyeing	Clothing	Clothing		Dyeing
	Surface finishing	Surface finishing	-	-		Surface finishing

The database for clean technologies in leather industry is divided in six sections namely: Processing Chemicals, Operations, Technological Processes, Assortments, Restricted Chemicals for Leather, Leather Processing Machines. Below are presented summarily some of these sections.

Section Processing Chemicals presents ecological products that are used for leather manufacturing and which comply with European legislation. Regarding these ecological products the following information are stored into the database: name of the product, the producer, contact details of the producer, description, usage, effects. One important section is restricted chemicals for leather where a list of chemicals that are forbidden is shown. In leather processing machines section information regarding machines used for dying, tanning, liming, surface finishing are presented. A Screen shot of the database for clean technologies is illustrated in Figure 1.

Figure 1. Screen shot for the database for clean technologies

ENVIRONMENTAL LEGISLATION DATABASE

Leather and fur manufacturing generate pollutant emission in soil, atmosphere and also in water. Consequently these production activities face environmental regulation at both national and European level. Hence it was necessary to develop a knowledge based platform (database) regarding Romanian and European legislation on environmental regulation. The platform, designed for leather industry, comprises information on Romanian and European legislation in the following areas of interests:

- Integrated pollution prevention and control (IPPC);
- Environmental Management Systems (EMS);
- Air quality;
- Water quality;
- Waste management;
- Eco label;
- Registration, Evaluation, Authorisation and Restriction of Chemical substances (REACH).

The environmental legislation database can be accessed by typing the following in any browsers address bar: http://legislatie.innovaleather.ro. At the time this database was developed, access to existing information is free to all users. A screen capture of the main page is presented below in Figure 2.

Legislatie nationala/europeana, sectorul de pielarie -incaltamine

Baza de date cuprinde legislatia nationala si europeana din sectorul de pielarie-incaltamine. In ceea ce priveste structura, aceasta este organizata in urmatoarele sectiuni: Legislatie (cu urmatoarele subsectiuni: Apa, Aer, Sol, Deseuri Solide, Namol), Monitorizare, Substante interzise, REACH, Eco-etichetare, Management de mediu. In sectiunea "Monitorizare", sunt prezentate firmele din domeniu care se ocupa cu monitorizarea aerului, apei, solului, zgomotului precum si Institutul National de Cercetare Dezvoltare pentru Ecologie Industriala.

Contact

INCDTP- Sucursala INSTITUTUL DE CERCETARE PIELARIE INCALTAMINTE (ICPI)

Adresa: Str. Ion Minulescu nr. 93, Sector 3
Bucuresti, 031215, Romania

Email: icpi@icpi.ro
Telefon: 021-323.50.60
Mobil: 021 323.52.80
http://www.innovaleather.ro

Informatii proiect

Baza de date actuala a fost realizata in cadrul proiectului "TEHNOLOGII INOVATIVE PENTRU SECTORUL DE PIELARIE CARE SA ASIGURE CRESTEREA COMPETITIVITATII PRIN CDI, CALITATII VIETII SI PROTECTIA MEDIULUI"

InnovaLeather
Copyright InnovaLeather © 2011. All Rights Reserved.

Figure 2. Environmental legislation database for the leather industry

The database offers a user-friendly and intuitive interface which is structured on categories and subcategories as follows:

- Legislation for: water, air, soil, solid wastes, sludge;
- Pollutant monitoring;
- Restricted substances;
- REACH;
- Eco-labelling;
- Environmental management.

ANALYSIS AND TESTS FOR LEATHER, RESEARCH CENTRES AND LABORATORIES DATABASE

Analysis and Tests for Leather, Research Centres and Laboratories Database is accessible via http://Innovaleather.ro/analize-piei. A screen shoot is shown in Figure 3.

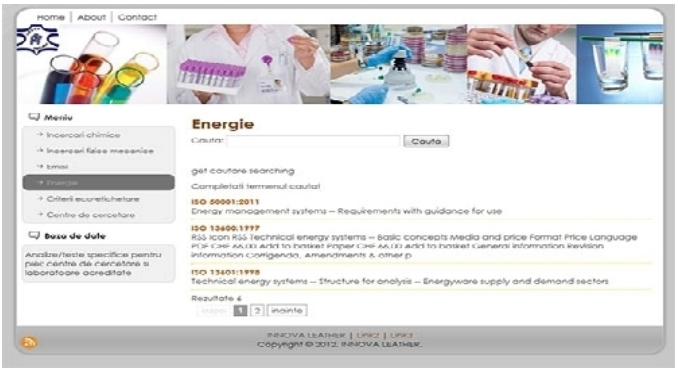

Analize/teste specifice pentru piei; centre de cercetare si laboratoare acreditate

Energie

get cautare searching

Completati termenul cautat

ISO 50001:2011
Energy management systems -- Requirements with guidance for use

ISO 13600:1997
RSS Icon RSS Technical energy systems -- Basic concepts Media and price Format Price Language PDF CHF 66,00 Add to basket Paper CHF 66,00 Add to basket General information Revision information Corrigenda, Amendments & other p

ISO 13601:1998
Technical energy systems -- Structure for analysis -- Energyware supply and demand sectors

Rezultate 6

Copyright © 2012, INNOVA LEATHER.

Figure 3. Analysis and Tests for Leather, Research Centres and Laboratories Database

This database has six sections namely leather chemical tests, physical test methods for leather, emission, energy, eco-labelling and research centres for leather industry.

This database allow user to search information within all sections. Users can search either the name or the description of the records Annexes. A download link is provided so users can download files and annexes of the tests for leather.

PLATFORM ARCHITECTURE

Technologies used to develop the platform that host all three databases mentioned in this paper are:

- PHP - a powerful tool for creating dynamic and interactive web pages; PHP is widely used, it is free and it is an efficient alternative for its competitor, ASP from Microsoft;
- MySQL - a relational database management system; the most popular open-source RDBMS to date.

Access to the MySQL is made using the PhpMyAdmin application, an open-source and popular database management application. This application enables creating, deleting, changing, importing and exporting MySQL tables. Through the PhpMyAdmin interface MySQL queries can be run, and existing database tables can be optimised, repaired and checked.

Other facilities offered by PhpMyAdmin (PhpMyAdmin Tutorial):

- friendly graphic interface;
- data import from CSV and SQL files;
- data export in various formats: CSV, SQL, XML, PDF, ISO/IEC 26300 - OpenDocument Text and Spreadsheet, Word, Excel, LATEX;
- global search in the entire database or in a specified section.

Minimal Technical Requirements

In order to host the platform, a web server was necessary, which would run:

- PHP programming language, version 5.2.17 or later;
- MySQL database server version 5.1.56-log or later.

In order to install each of the three databases on the server, the following steps were undertaken:

- Archived files were uploaded to the server;
- A MySQL 5.1.56-log database and a user account were created;
- The MySQL 5.1.56-log script and required queries were executed;
- The configuration file was edited (previously run on a local computer, localhost) and the database name, the user name and the password were changed to run on a server.

Platform Access

In order to access the platform for the leather industry, browse http://innovaleather.ro/ web page and subsequently access Results section and choose Databases. At the time this database was developed, access to existing information is free to all users. A screen capture of the main page is presented below.

PLATFORM ADMINISTRATION

Platform administration is done by an administrator who is in charge of updating existing information and deleting outdated data. Access to the administration area of platform is done by means of a user name and password.

To protect the platform from hardware and software failure, a back-up system has been devised which allow database restoration as soon as the failure has been fixed with minimal loss of information.

CONCLUSIONS

The knowledge based platform is intended as a useful tool for companies, students, technicians, engineers and researchers whose activity is related to the leather and footwear industry. Although the platform could be an effective instrument for all people interested in leather and footwear industry, it has been built having the success of companies in mind. More precisely managers are provided with the opportunity of picking the right technology, product, machine for their business. The platform offers good protection and reliability of data, since access to control panel is limited to user accounts, allowing access to software only after logging in with a user name and password. Also, the database was designed considering the possibility to easily update or delete existing information. Future work will be focused on improving the existing functionalities of the platform, providing information in accordance with visitors needs and on keeping the information available on the platform accurate.

Acknowledgements

This paper has been financed by the European Fund for Regional Development and the Romanian Government in the framework of Sectoral Operational Programme CCE-AXIS 2, Operation 2.1.2, through the INNOVA-LEATHER project: «Innovative technologies for leather sector increasing technological competitiveness by RDI, quality of life and environmental protection» – contract no. 242/20.09.2010 ID 638 COD SMIS – CSNR 12579.

REFERENCES

BLC Leather Technology Centre, Clean Technology in Leather Processing, http://www.blcleathertech.com/leather-technology/clean-technology.htm (accessed 05.07.2012).

Bostaca, G. and Guta, S.A. (2012), "Database for Clean Technologies in The Leather Industry", *Revista de Pelărie Încălţăminte* (*Leather and Footwear Journal*), 11(4), 319-326.

Deselnicu V., Albu, L. (2007), *Modern Leather and Fur Processing Technologies* (in Romanian), Certex, ISBN 13 978-973-1716-25-1, Bucharest, Romania.

Macovescu, G. and Guta, S.A. (2012), "Environmental Legislation Database for The Leather and Footwear Industry", *Revista de Pelărie Încălţăminte* (*Leather and Footwear Journal*) 12(1), 19-26.

Page, C. (2004), Understanding Clean Technology, http://www.tfl.com/web/files/cleantechnologybrochure.pdf (accessed 02.06.2012).

***, PhpMyAdmin Tutorial, http://www.siteground.com/tutorials/phpmyadmin/phpmyadmin-features.htm (accessed 13 05, 2012).

INNOVA-LEATHER PROJECT: TWO YEARS OF RTD AIMING AT INCREASING CAPACITIES & COMPETITIVENESS OF THE ROMANIAN LEATHER SECTOR THROUGH KNOWLEDGE BASED CLEAN TECHNOLOGIES - PART I

IOANNIS IOANNIDIS, MARIAN CRUDU, GABRIEL ZAINESCU, MADALINA ALBU, VIORICA DESELNICU, DANA CORINA DESELNICU, SERGIU GUTA, LUMINITA ALBU

INCDTP - Division: Leather and Footwear Research Institute, 93 Ion Minulescu, sector 3, Bucharest, RO- 031215, Phone: +40-21 323 50 60, Fax: +40-21 323 52 80, e-mail: icpi@icpi.ro

In the last three decades concerted RTD efforts world wide focused explicitly upon innovation in leather manufacturing chemical and mechanical operations aiming at the development of clean technologies and a significant reduction of the environmental impact of the complete production cycle for the transformation of hides and skins, a by-product of the meat industry, to leather, an added value luxurious unique for its natural intrinsic characteristics, properties and performance. In the light of the emerging and growing need for such a holistic RTD and cost-effective approach, Innova-Leather project commenced on 20th of September 2010 and aimed in inventing and developing ready for take up at industrial scale cost effective clean wet end knowledge based technologies, valorising waste and renewable resources in Romania, in conjunction to solid waste valorising technologies to added value by-products. The new tanning agents, in fact, will act as a prelude towards new eco-friendly leather manufacture, in which no potentially toxic, noxious and harmful chemicals have been used and discharged. Waste valorisation and management was also taken into consideration from the start in order to propose to the Tanners world wide a holistic solution that will be ready for industrial application.

Keywords: knowledge-based tanning agents, knowledge-based technology, wet-white leather.

WHY INNOVA-LEATHER PROJECT?

Innova-Leather project commenced in September 2010, starting point was the development of high-tech instrumental analytical tools and bench testing models for deriving knowledge at the molecular level of the reactivity of the collagenic matrix, which, in turn stirred the design of novel knowledge based chrome-free mineral and synthetic organic tanning agents (KTA-tanning agents) and technologies (KTA-technologies).

The S&T objectives of the project can be outlined as follows:

- New tanning agents modeling, design & Synthesis (Knowledge based Tanning Agents / KTA);
- Development of new eco-technologies for leather pretanning/ tanning;
- Sustainable production of commodity semi-finished leathers free-of-chrome ("wet white");
- Valorisation of "wet-white" leather wastes into added-value by-products;
- New biodegradable auxiliaries generation from KTA-process waste;
- Design of comprehensive strategies regarding collection and conversion of waste;
- LCIA - Life Cycle Impact Assessment Studies for the newly developed processes and products.

NEW TI-AL BASED KTA-M TANNING AGENTS AND KTA-M TANNING TECHNOLOGIES

Along these lines, new Ti (III)-based, Cr(III)-free, precursor tanning agents have been produced from metallurgic Industry end waste, aiming at the development of new tailored sustainable wet-white tanning chemistry that enables for the first time the in-situ generation of reactive Ti(IV)-tanning species, as a viable alternative to Cr(III), vegetable and syntan (pre)tanning agents.

Hence, the principal axes of our synthetic approach, from product design phase to its industrial eventual application, have been: recovery and recycling of Ti-rich waste, simplicity and cost-effectiveness of the new tanning agent application, as well as closed loop processing, in order to protect the environment and improve the quality of life.

Major challenges to match in our efforts remain commercial viability and consumer acceptability of the finished leather article.

Synthesis of New Mixed Ti-Al Tanning Agents from Metallurgic End Waste

Basic metal composition of the Titanium wastes (filings) used as raw materials for the production of the new Ti(III) tanning agents is given in Table 1.

Table 1. Heavy Metal composition of the Titanium wastes

Metal	Ti	Al	V	Fe
%	89 - 95	1- 6	0.1- 4	0.0001-0.0005

The Aluminum salt used was $Al_2(SO_4)_3 \cdot 18\ H_2O$ (15.3% Al_2O_3, 8.55% Al).

A schematic outline of the synthetic pathway designed and applied for the generation of the mixed new tanning agents based on Titanium and Aluminum or Zirconium is shown in Scheme 1 (Crudu et al., 2009a, 2009b; Crudu, 2008; Crudu et al., 2008).

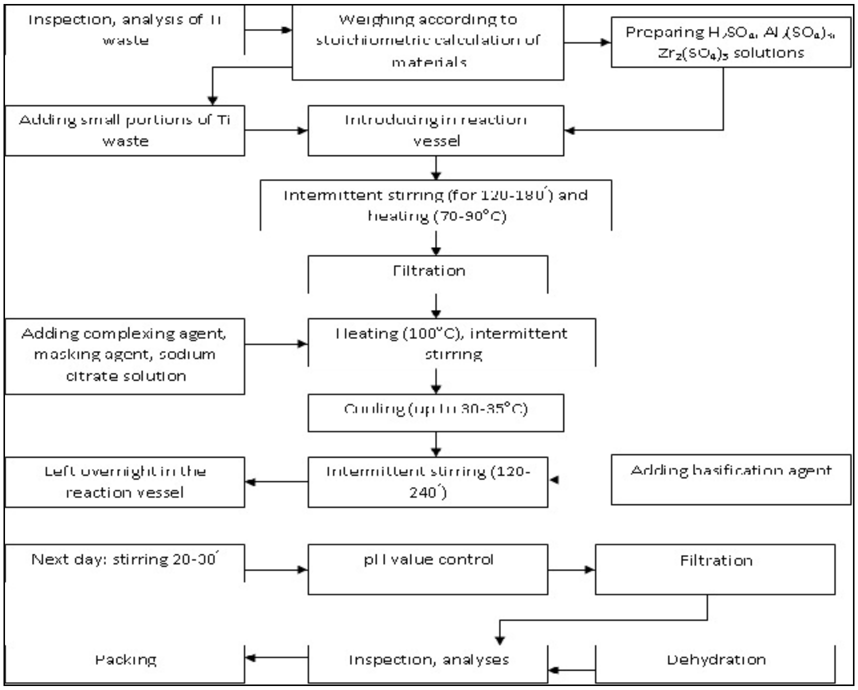

Scheme 1. Ti-based KTA-M Tanning Agents Synthetic Pathway

The results of chemical analysis carried for the novel tanning agents' solution are reported in Table 2.

Table 2. Chemical analysis of tanning agent solution

Parameter	Content
Density (g/cm^3)	1.25 – 1.45
pH	1.8 – 2.3
Total ash (g/dm^{-3})	75 – 140
Total metal oxides content (g/dm^{-3})	65-130

On the other hand, some compositional analytical data of the dry Titanium-Aluminum tanning agent powders derived thereof are shown in Table 3.

Table 3. New Titanium-Aluminum tanning agents (powder form) metal content and pH

Parameter	Content
Total metal oxides, %	15 – 20
pH (1:10)	1.8 – 2.3

Moreover, ICP-MS analysis (plasma emission spectroscopy, ICP-type SPECTRO) of one of the newly prepared tanning agents based on Ti-Al was carried out and the following results were obtained (Table 4). Most significant is the absence of Cr, Cd, Pb, Hg, Ni and As – non detectable.

Table 4. New Titanium-Aluminum tanning agents (powder form) metal contents (ICP-AES)

Element	Content
Ti-Al (%)	99.6
V (%)	0.13
Mg (%)	0.33
Fe (%)	0.03
Zr (%)	0.23

New KTA-M Wet-White Leathers Characterisation and Evaluation

Full thickness semi-processed tanned leathers resulting from application of the new Titanium-Aluminum tanning agents as described here is white, with a smooth grain full and supple.

Shrinkage temperature values determined for the different new tanning agent variants ranged from 68-82°C, whereas wet white leathers were successfully processed through the subsequent mechanical operations of splitting – easily grain, middle and bottom split were obtained, as well as shaving.

Good hydrothermal stability of the prototype leathers was confirmed with measurements undertaken using the Micro-Hot table device, with Ts=70-80°C.

Another confirmation of the thermal behavior of the new semi-wet type of leather tanned with white pre-tanning agents was obtained by using DSC analysis (differential scanning calorimetric dynamic analysis). A typical example of the thermographs recorded for samples taken from the prototype wet-white leathers tanned with the new Ti-Al based tanning agents is shown in Figure 1.

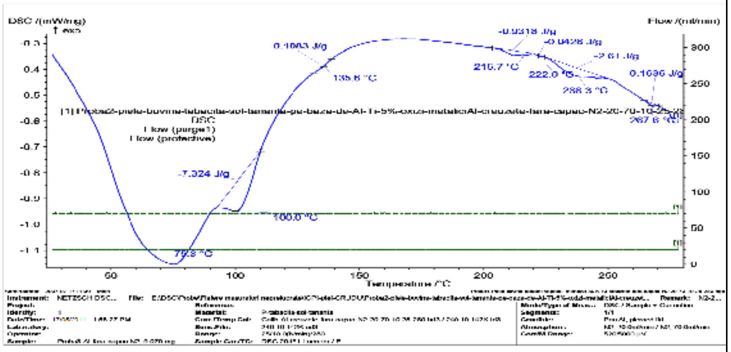

Figure 1. DSC-thermograph obtained for wet-white tanned with the new Ti-Al tanning agents

The endothermic transitions recorded for the new wet white leathers consists of at least three (3) peaks, indicative of consecutive denaturation processes. The first transition is recorded for temperatures within the range 50°C and 125°C. A second set of peaks is registered for temperature values between 130° and 250°C, strongly linked to the processing history of the material (in particular the degree of tanning); the denaturation process occurring can be tentatively explained by the crystalline-amorphous two-phase model of collagenic materials. According to this model the super-coiled triple-α helix is partially crystalline and embedded in an amorphous matrix. Consequently, the minimum of endotherm II is associated with uncoiling / melting of the crystalline region. In turn, the tanning process by inducing the formation of synthetic crosslinks, can result in increased stiffness of the matrix, and, thus, is responsible for the observed shift of the melting process to higher temperature values. Monitoring the temperatures at which process II occurs may, therefore, reveals the degree and effectiveness of tanning, whereαs for leathers tanned with Cr(III) –salts the second peak is not visible as it overlaps with the pyrolytic transition. Hence, DSC thermographs, as those recorded for wet-white prototype leathers are specific to each material and can be used as material-specific and unique «fingerprints» (Budrugeac et al., 2004).

In order to characterize the new wet-white leather and prove the tanning potential of the newly synthesised compounds, chemical analyses have been carried out both on the split and grain layers of the product leathers and the results obtained are shown in Table 5.

Table 5. Wet-white grain and split leather chemical analyses

No.	Parameter	Layer	
		Grain	Split
1.	Volatile matters (%)	53.1	51.2
2.	Extractible (%)	1.58	2.35
3.	Ash (%)	10.4	10.9
4.	Metal Oxides (%)	8.2	8.3
5.	Shrinkage temperature (°C)	77	75
6.	Shrinkage temperature (°C -MHT)	76.1	73.9
7.	pH extract	3.98	4.0

Similar analytical values obtained for both layers tested have led to the conclusion that the penetration of the new tanning agents was not only complete but also uniform, assuring sufficient stabilisation of the wet-white for further mechanical or other chemical processing.

The evaluation of the modification of collagen by new tanning agents', and in particular topographic distribution – mapping - of the metal species in the prototype leathers, was obtained by means of scanning electron microscopic (SEM) and energy dispersive X-ray analysis (EDAX). These are most appropriate methods for the characterisation of surfaces and the results obtained confirm all previous assumptions about metal tanning agents uniform penetration and distribution, as well as provide semi-quantitative data of the mineral species topographic mapping.

Trials were conducted using a newly purchased duplex drum using bovine hides (13-15kg mean weight), ovine and goat pelts in lime or pickled, respectively, whereas a variant model for the pre-tanning operations using Ti-Al new tanning agents is foreseen for ovine pickled skins processing.

Table 6. Shrinkage temperatures measured for leathers pretanned with KTA-M1 &-M2

S/N	Trial Code	Shrinkage temperature value (Ts, °C)
1.	P II	92
2.	P III	74
3.	P VII	74
4.	P VIII	81

In order to appreciate the outcome of the pilot scale trials, which evidently yielded leathers with medium – high shrinkage temperatures and were mechanically processed without any real problems - with a clean and fibrous shaving residue and a good quality grain and flesh and possibly also mid split of uniform thickness without any gelatinization or yellowing of the grain split.

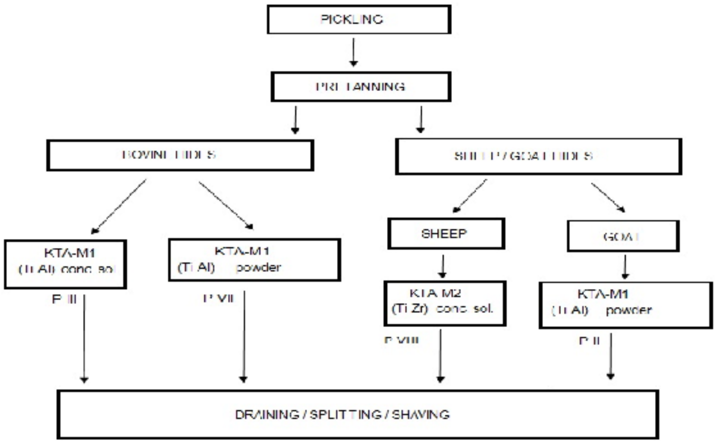

Scheme 2. Pre-tanning and tanning KTA-M pilot scale trials flow diagram

SYNTHETIC ORGANIC TANNING AGENTS (KTA-S)

Oxazolidine is a bifunctional aldehydic type alkylator – formaldehyde replacement - with high reactivity for the collagenic amine groups and phenolic groups of condensed vegetable tannins. Its advantage over glutardialdehyde and glutardialdehyde modified products is that the aldehydic activity is the crosslinking capacity and the relatively low free monomeric formaldehyde release from crust leathers when used in combination organic tanning systems. Solo- and combination oxazolidine tanning with condensed vegetable tannins or THPS has been the subject of numerous experimental surveys (Shi et al., 1996, 1997, 1999) and the synergistic reactions with condensed vegetable tannins have been modeled (Covington, 2009) to explain the increase of the shrinkage temperature achieved (>100°C). However, hitherto, taking up by the industry has been slow, if not limited, most probably due to the pungent and irritating to most odour of oxazolidine E and the relatively high unit price of the product. The determinative physical parameter for inducing crosslinking is pH, but, according to several researchers heat induction is also necessary for maximizing the efficiency of the tanning reaction.

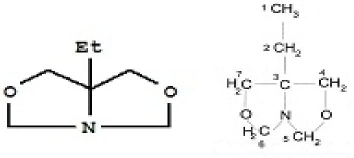

Oxazolidine E / Zoldine ZE

(1H,3H,5H-Oxazolo[3,4-c]oxazole,7a-ethyldihydro-) (4)

Molecular formula: $C_7H_{13}NO_2$

CAS number: 7747-35-5

Molecular mass: 143, 18 g/mol

Figure 2. Oxazolidine E bifunctional crosslinking pretanning agent

Innova-leather has looked into the design and development of a bi-component combination synthetic organic tanning system comprising in oxazolidine and a tailored resorcinol prepolymer. Modeling of the tanning reaction is founded on the hypothesis for the formation of the multi-functional polymeric crosslinking moieties of resorcinol with oxazolidine E in situ, which bears the necessary number of available reactive groups, for multiple weak hydrogen bonding, as well as molecular size (crosslink effective molecular weight) for forming multiple intra- and inter-fibrillar crosslinks; a prerequisite for this synergistic reaction is that the phenolic moieties of resorcinol act as a condensed tannin (replacement syntan) in situ; oxazolidine pre-tanning ensures “switching-on” of the polymerization and crosslinking reaction (“locking”) without compromising the penetration rate through full substance pelts or risking early surface binding and fixation of one or both highly reactive compounds. Several of the resulting crosslinks according to the model must be hydrogen bond breaking resistant, whilst ought to result in a significant increase of the shrinkage temperature and improved fullness of the product leathers. In a nutshell, each of the components of the system is not novel or the reactivity of oxazolidine towards resorcinol (Chen & Szana, 2010), but their combination in synthetic organic tanning with the concomitant replacement of condensed vegetable tannins for this purpose is a significant breakthrough, as it has been possible to optimise in this manner the tanning reaction rate and tanning agents’ penetration uniformity (“linking”) and scavenge free monomeric formaldehyde generated. The selection of oxazolidine E was due to its moderate reactivity when compared to oxazolidine A.

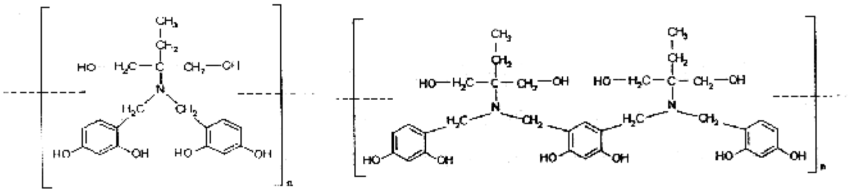

Figure 3. Polymeric crosslinker formed in situ from resorcinol and oxazolidine E

Along these lines the pre-tanning organic tanning formulations applied were optimised by using selected oxazolidine based tanning agents (DOLATAN VA50 and ZOLDINE ZE), pickled and depickled pelts, as graphically demonstrated with Scheme 3.

The aim of the project was not to attain high hydrothermal stability tannages, but a versatile and stable wet white, "Free-of-Chrome" and using the minimum quantities of chemicals for this purpose; this is the reason for obtaining wet white with moderate hydrothermal stability, as the offers of both oxazolidine and resorcinol pre-polymers were kept to the absolute minimum (Table 7).

Table 7. Prototype KTA-S wet white leathers shrinkage temperature

S/N	Trial Code	Shrinkage temperature value (Ts, °C)
1.	P I	72
2.	P IV	70
3.	P V	68
4.	P VI	68

Hydrothermal stability of prototypes is just at threshold minimum value for an acceptable wet white.

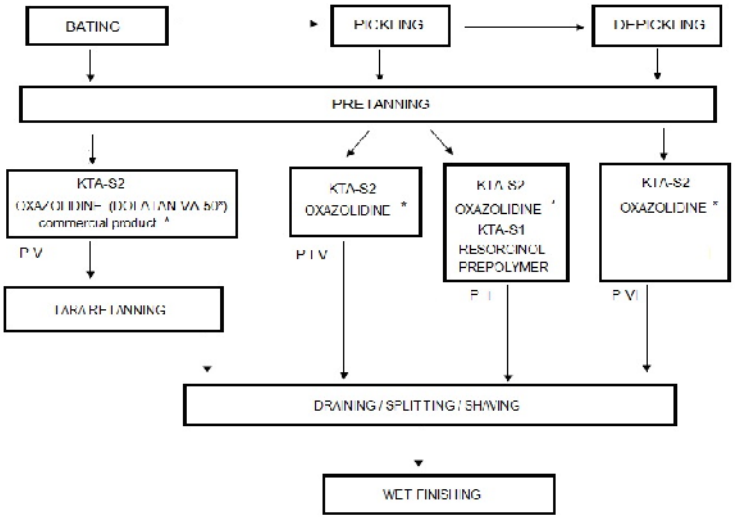

Scheme 3. KTA-S synthetic organic tanning trials flow diagram

Scale up of the formulations at pilot scale was then carried out, as the results obtained at small scale experiments regarding the rate and uniformity of the FOC tanning reactions, as well softness of the prototype wet-white leathers were most promising.

On the other hand, most recently a new list of candidate SVHC have appeared, which included resorcinol amongst the enlisted substances for classification, currently evaluated for REACh Directive purposes. The regulation will be enacted as from the year 2014. This development has been crucial for the development strategies set as early as 2010 when the project has been presented and eventually approved for financing or even at the start of the project execution phase, which, in turn will have inevitably to be revised and adjusted providing the Romanian Tanners with viable clean technology alternatives in the short – but also in the long-term.

PILOT SCALE PRODUCTION OF FOC LEATHERS (UPPER, GARMENT, UPHOLSTERY)

The most crucial factor recognized early during the implementation of tasks of this activity was setting the criteria for the design of the processes and the selection of retanning agents, dyestuffs and fatliquors, as well of finishing agents tailored for their post-tanning application for finishing wet white prototypes, products of pilot scale trials carried out in this reporting period.

The excessively cationic charge of Ti+Al tanned KTA-M wet-white and the anionic charge of the hybrid synthetic organic tanned KTA-S wet-white, as well as the significantly reduced hydrothermal stability of all known wet white hitherto, respectively, necessitated targeted design of the functional models developed and tested so far (Scheme 4).

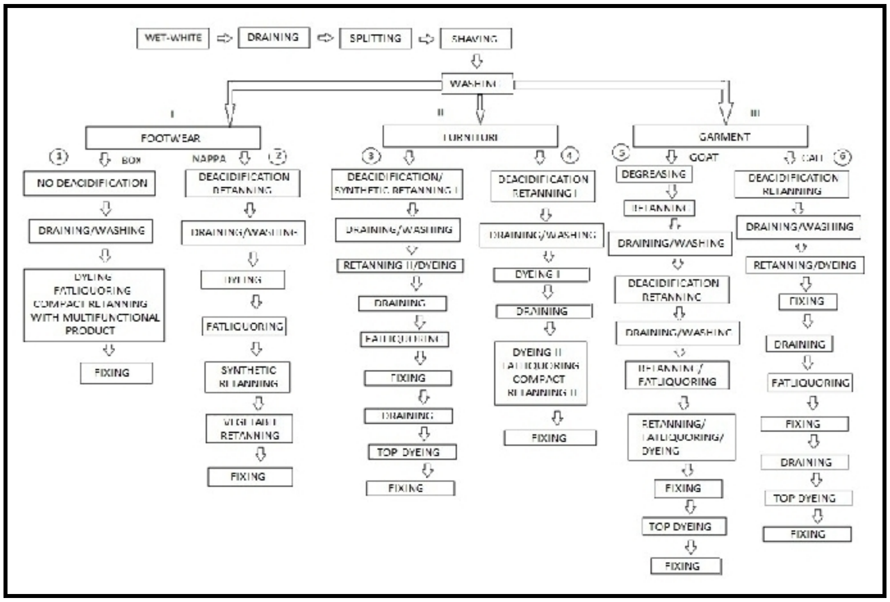

Scheme 4. Six (6) functional wet finishing models of KTA- wet white for the production of FOC leathers

The availability of auxiliaries suitable for anionic charged wet- semi processed leathers is relatively limited, as demonstrated also by the lack of products which can be used for retanning, dyeing, hydrophobising and finishing full vegetable tanned leathers, with the exception of several new auxiliaries commercially available for the growing market of FOC automotive leathers.

In a nutshell, wet-finishing trials were successfully carried out by employing similar methods to those routinely applied in commercial chrome leathers production were applied, where adjustments were made to satisfy the additional requirements outlined above, stemming from the charge and stability of the wet white prototypes.

The wet finishing systems validated hitherto comprise:

- step by step operations application, in separate baths and with intermediate discharging of exhaust liquors and wasteful washing / rinsing of leathers
- compact (successive administration in the same float) – all in one bath;
- ultra-compact, with the use of multifunctional, compound products

Crust leathers (FOC type) obtained so far were comparable with crust chrome-tanned leathers, in terms of their haptic properties, performance under stress (mechanical strength) and chemical composition (with the exception of chromium).

Experiments in the pilot stage of bovine leathers surface dry finishing: The approach adapted for targeted surface dry-finishing of prototype crust FOC leathers generated in wet finishing pilot scale trials is schematically outlined with Scheme 5.

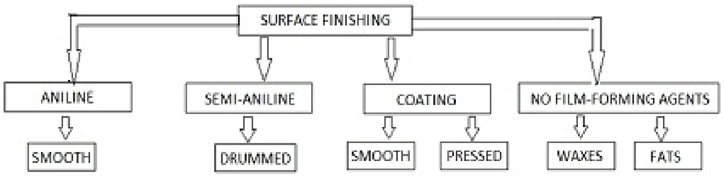

Scheme 5. Six (6) functional models for surface dry-finishing of FOC crust leathers

No particular problems were encountered during surface dry-finishing of FOC crust prototype leathers apart from operations like hot-ironing which require the employment of high contact temperature.

CONCLUSIONS

Exploring the valorisation of solid Titanium metallurgic end wastes, as a low cost raw material, as well as knowledge based combination synthetic organic tanning using a bifunctional aldehydic crosslinker (oxazolidine E) in conjunction with a resorcinol pre-polymer, have yielded new tanning agents for the replacement of Cr(III) tanning salts.

In turn, as demonstrated here it is plausible to:

- increase of eco-efficiency in the leather manufacturing sector by making use of solid wastes, which cannot be recycled in the industry that generated them;
- total replacement of chromium salts in the tanning process with cheap to produce and easy to apply in rapid full substance bovine and ovicaprine leather manufacture, that, in turn required minimum process rationalisation or modification; moreover, the new mineral tanning agents are free of restricted or regulated metals Cr, Pb, Cd, Hg and Ni;

- two (2) new wet white semi-processed intermediate products easily processed with available chemicals at the dye yard and the finishing department of any tannery;
- increase in assortments diversity.

Scaling up of the production of the Ti-based new tanning agents is now plausible as an agreement was formalised and production initiated with a Romanian metallurgic company, assuring availability and consistent auxiliary composition.

Post-tanning processing of the new wet white was possible for three (3) types of finished leather products: upper, garment and upholstery, with at least six (6) functional models defined and successfully tested for this purpose, using low end chemical auxiliaries available at any tannery in Romania, ensuring take up regardless of several limitations in supply of specialty chemicals, as those already experienced and expected to hinder take up of cutting edge or new tanning agents as Granofin F90 ®and X-Tan®. The selection of chemicals, operations and machines will be facilitated by the knowledge based platform created at ICPI for this purpose comprising already 3 Databases and soon an LCA S/W tool and databases service.

The new tanning agents, in fact, will act as a prelude towards new eco-friendly leather manufacture, in which no potentially toxic, noxious and harmful chemicals have been used and discharged – currently and according to the Environmental Reports of the Tanning Sector 30-40 % of chemicals used during leather manufacture are characterised as potentially toxic or hazardous.

Acknowledgements

This work has been financed by the European Fund for Regional Development and the Romanian Government in the framework of Sectoral Operational Programme under the project INNOVA-LEATHER: «Innovative technologies for leather sector increasing technological competitiveness by RDI, quality of life and environmental protection» – contract POS CCE-AXA 2-O 2.1.2 nr. 242/20.09.2010 ID 638 COD SMIS – CSNR 12579.

REFERENCES

Budrugeac, P., Miu, L., Popescu, C., Wortmann, F.J. (2004), “Identification of collagen-based materials that are supports of cultural and historical objects”, *Journal Therm Anal.Cal*, 77(3), 975.

Chen, H. and Szana, Z.H. (2010), “Stabilisation of collagen with Oxazolidine E-resorcinol”, *J. Biol. Macromol*, 46(5), 535-9.

Covington, A.D. (2009), *Tanning Chemistry: The Science of Leather*, RSC Publishing.

Crudu, M. (2008), “Study regarding the use of inorganic compounds in natural leather processing in view of preventing environmental pollution” (in Romanian), Ph.D. Thesis, “Gh.Asachi” University, Iasi.

Crudu, M., Deselnicu, V., Albu, L., Niculescu, M., Roşca, I., Sutiman, D., Sibiescu, D., Cailean, A. (2008), “Eco-friendly tanning agents to be used in leather manufacture”, 10th International Chemical and Biological Engeneering Conference Braga-Portugal.

Crudu, M., Boca, N., Sutiman, D., Ioanid, A., Caileanu, A., Sibiescu, D. (2009a), *Compounds with tanning capacity obtained from Ti-end unrecyclable waste of the Ti-metalurgic industry* (in Romanian), CERTEX.

Crudu, M., Niculescu, M., Deselnicu, V., Sutiman, D., Sibiescu, D., Cailean, A., Boca, N. (2009b), Romanian Patent App. A/00941/17.11.2009.

Shi, B., Covington, A.D. and Attenburrow, G.E. (1996), “Studies of High Hydrothermal Stability Organic Tannages”, Proceeding of 3rd Asian International Conference of Leather Science and Technology, Japan, 51-59.

Shi, B., He, Y., Fan, H., Zeng, S., Covington, A.D. and Attenburrow, G.E. (1997), “Mechanism of Vegetable Tannin-Oxazolidine II Combination Tannage”, International Union of Leather Technologist and Chemists Societies Congress, September, 279-283.

Shi, B., He, Y., Fan, H., Zeng, S., Covington, A.D. and Attenburrow, G.E. (1999), “High Stability Organic Tanning Using Plant Polyphenols, Part 2, The Mechanism of the Vegetable Tannin-Oxazolidine Tannage”, *J. Soc. Leather Technol. Chem.*, 83, 8-19, 199.

INNOVA-LEATHER PROJECT: TWO YEARS OF RTD AIMING AT INCREASING CAPACITIES & COMPETITIVENESS OF THE ROMANIAN LEATHER SECTOR THROUGH KNOWLEDGE BASED CLEAN TECHNOLOGIES - PART II

IOANNIS IOANNIDIS, MARIAN CRUDU, GABRIEL ZAINESCU, MADALINA ALBU,
VIORICA DESELNICU, DANA CORINA DESELNICU, SERGIU GUTA, LUMINITA ALBU

*INCDTP - Division: Leather and Footwear Research Institute, 93 Ion Minulescu, sector 3,
Bucharest, RO- 031215, Phone: +40-21 323 50 60, Fax: +40-21 323 52 80, e-mail: icpi@icpi.ro*

In the last three decades concerted RTD efforts world wide focused explicitly upon innovation in leather manufacturing chemical and mechanical operations aiming at the development of clean technologies and a significant reduction of the environmental impact of the complete production cycle for the transformation of hides and skins, a by-product of the meat industry, to leather, an added value luxurious unique for its natural intrinsic characteristics, properties and performance. In the light of the emerging and growing need for such a holistic RTD and cost-effective approach, Innova-Leather project commenced on 20th of September 2010 and aimed in inventing and developing ready for take up at industrial scale cost effective clean wet end knowledge based technologies, valorising waste and renewable resources in Romania, in conjunction to solid waste valorising technologies to added value by-products. The new tanning agents, in fact, will act as a prelude towards new eco-friendly leather manufacture, in which no potentially toxic, noxious and harmful chemicals have been used and discharged. Waste valorisation and management was also taken into consideration from the start in order to propose to the Tanners world wide a holistic solution that will be ready for industrial application.

Keywords: waste valorisation, added-value by-products, LCIA.

WET WHITE WASTE VALORISATION

Experiments on Obtaining Useful Components from Wet White Leather Waste

Preliminary hydrolysis trials of leather waste tanned with resorcinol using di-potassium phosphate has not yielded satisfactory results, as total hydrolysis did not take place.

On the other hand, the results of screening single enzymes and their combinations revealed the questionable applicability of routinely and commercially available enzymes for the production of by-products from organic and mineral tanned wet white leather waste. Although the enzymatic treatments were proved to be efficient for triple helical collagen extraction from untanned skin, for processing of wet-white leather the yield are very low and the results are insignificant.

Thus, it soon became apparent that the hydrolysis of tanned wet white leather wastes had to be further investigated designing and developing targeted hydrolytic regimes, not applicable or tested hitherto.

Design, development and testing of novel chemical and physical wet white hydrolytic methods for the production of hydrolysates suitable as cosmetics components

Consequently further hydrolysis trials of wet-white leather waste using suitably developed for this purpose combinations of physical and chemical methods, respectively:

1. Alkaline hydrolytic trials

Wet white waste tanned with oxazolidine did not show any significant degree of conversion during a 48 hour long alkaline hydrolytic treatment. For this reason the samples were washed and then subjected to further acidic treatment.

2. Combined Alkaline + Acidic Hydrolysis

On the other hand wet-white tanned with Ti + Al leather was subjected to both acidic and alkaline treatments.

3. Combined Alkaline +Acidic Hydrolysis followed by Thermal Induction

Following chemical treatment specimens received a thermal post-hydrolytic processing at 100°C for 24 hours.

4. Hydrolysates from the three (3) physico-chemical hydrolytic protocols

The proteic hydrolysates obtained so far were filtrated and lyophilized with a program established for this purpose at ICPI. The yield of the process was high with 30.50% reported as active substance.

At this point the various proteic hydrolysates generated as above were characterised. The conclusions that can be drawn based on all available analytical results are the following:

- The best yield in terms of protein substance was measured for the products of acid hydrolysis (97.8% protein content, whilst the yield for the alkaline hydrolysis products was far lower (87-88%).
- Fat content determined for all hydrolysates was very low (approx. 0.2%) or indeed absent.
- Ash content measured for the extracts obtained with alkaline hydrolysis was found quite high, namely equal to 8.27 and 10.13% respectively (both for the hydrolysate and hydrolytic residue). This is a particularly significant result, as Ti+Al wet white waste acid hydrolysate total ash content was very low (0.61%).

At this point it can be safely concluded that there is a clear advantage in obtaining proteic hydrolysates for cosmetics end-use from KTA- wet white waste by a tailored combination process, namely acid hydrolysis followed by a thermal treatment at 100°C. Moreover, as demonstrated at lab scale the filtrate of the hydrolysate can be easily lyophilised using a program developed for this purpose over 48 hours.

The results obtained so far for both types of wet white waste were most promising and comparable to those obtained for pure collagenic substrates alkaline or enzymatic routine hydrolysis.

Design, development and testing of novel combination chemical and enzymatic KTA-M wet white hydrolytic methods for the production of hydrolysates suitable as agricultural and industrial end use

In parallel to the investigation of physico-chemical hydrolytic regimes of KTA-M and KTA-S wet white waste successfully completed, a novel approach was devised and tested for the chemical and enzymatic hydrolysis of KTA-M wet white waste. The experimental survey undertaken along these lines aimed at defining alternatives to enzymatic solo hydrolysis, which evidently failed to yield satisfactory results for the production of hydrolysates suitable for their conversion to useful by products for agricultural / industrial use.

The selection of Ti+Al tanned wet white waste was due to their favourable content of Ti and Al metals for their eventual end use as a construction material or in agricultural use.

Moreover, a zero waste research approach was adapted aiming at the production of the desired recyclable products, rendering redundant tasks projected at start for the reduction of the organic charge of secondary waste possibly generated in the conversion process.

I. Chemical analyses of wet white waste

First step towards the attainment of that goal was the chemical analysis of Titanium-containing wet white leather wastes obtained from ICPI, kept at room temperature, to determine the following parameters using standard or in house routinely applied methods: pH, humidity content, total ash, total Kjeldahl nitrogen (TKN), titanium, and fat content.

II. Alkaline hydrolysis

The first set of experimental trials aimed at testing the applicability of alkaline hydrolysis of wet white waste for the production of the proteic hydrolysates precursors of the desired end added value products.

For this purpose 1000g titanium containing wet white leather wastes were weighed in 5l water, and were subjected to a pre-treatment by adding 10% CaO or 10% MgO for 4-6 h.

The actual hydrolysis followed in a 50l double jacket autoclave adding 3-7% K_2HPO_4 at 90-98°C for 2.5-5 hours.

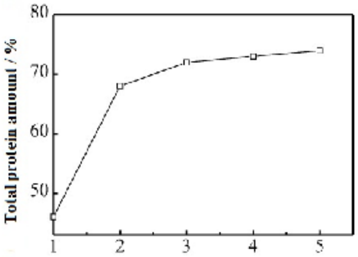

Figure 1. Hydrolysis reaction kinetics chart

The hydrolysate biosolid containing titanium was kept at room temperature for analyses and acid or enzymatic treatment.

III. Enzymatic hydrolysis

For advancing hydrolysis three (3) commercial enzyme products were used. 500g of wet white leather waste hydrolysate (containing titanium) were weighed and were subjected to pre-treatment in 1-1.5 l water and 1.5-3% MgO, at room temperature for 4 - 6 hours. This pre-treatment step is required to obtain optimum pH for enzymatic digestion. Then 0.5-1% enzymatic commercial product D or K was added and maintained for 1.5-2.5 hours at 35-40°C.

Protein hydrolysate solutions obtained thereof were analysed for their chemical composition.

IV. Selection of alkaline basification agent

CaO and MgO were used as basification agents, as they are more effective and easier to filter than enzymes upon titanium containing leather waste hydrolysis.

CaO as alkaline agent had three significant advantages compared to MgO:

- Coagulation properties of calcium sulphate (the sulfuric acid group resulted from the tanning process) appeared to lead to precipitation of titanium hydroxide, and co-precipitation of the two compounds helped to separate the titanium hydroxide from the hydrolysis liquid.
- Total ash content of resulting hydrolysate was minimal when using lime, and can be maintained consistently below 10%.
- Using MgO in titanium containing leather waste treatment can lead to a rapid increase of alkaline strength in the initial stage, thus resulting in an excessive digestion of collagen.

It clearly appears that using $Ca(OH)_2$ has led to a consistent hydrolysis due to its buffering capacity.

The results obtained so far led to the definition of a novel conversion technology of KTA-M tanned wet white waste to useful byproducts for at least six (6) industrial and agricultural end uses.

One (1) technology, for converting Ti-containing wet white leather waste has been established, which, through hydrolysis and mixing with 10-20% protein biopolymers from limed leather wastes, can be used as fertilizers in agriculture. However, remains to be proven with specific dedicated testing final product appropriateness as fertiliser. For this purpose specific analyses will be performed at specialized institutes, as well as experiments on soils and a patent application will be submitted.

It must be mentioned here that as a result of experiments carried out so far for wet white leather waste hydrolysis NO effluents or other wastes result.

CONCLUSIONS AND FURTHER WORK

Experiments for the establishment of three (3) physico-chemical hydrolytic methods of KTA-M and KTA-S wet white for the separation of added value proteic phase were successfully completed and remained to be further processed for the conversion of wet white KTA-waste to cosmetics components.

The expected deliverable technology for the acid hydrolysis and thermal-mechanical processing of the obtained hydrolysates of both synthetic organic tanned and mineral tanned wet white waste was therefore in place, however remains to be optimised and its applicability validated for cosmetics components production.

In parallel, a new two-step chemical-enzymatic hydrolytic regime for the conversion of Ti-Al wet white waste (KTA-M) to useful for agricultural and industrial end use was developed.

In this manner waste valorisation and management was taken into consideration from the start in order to propose to the Tanners world wide a holistic solution that will be ready for industrialisation in the 3rd year of the project execution phase. For this purpose, however, it is necessary to evaluate cost efficacy and demand trade conditions

In a nutshell, the results obtained so far at pilot scale for the production of upper, garment and upholstery finished FOC leathers and solid waste valorisation are clear witnesses that it is now possible at pilot scale to produce full substance bovine wet white with the desired smooth grain, that possesses the minimum hydrothermal stability for subsequent mechanical processing.

The IPRs of the results were protected with three (3) National Patent Applications, filed in 2011 and, therefore, technological transfer was possible. Moreover, numerous scientific communications and ISI scientific articles have been generated aiming at results and potential benefits of the products of the project dissemination at national and world wide level. Towards that end two (2) workshops were held open to the Authorities, the Leather Sector and the scientific community, whilst publications and announcements were presented at regional and National Press targeted at the wider public in Romania.

Further R&D ought to be carried out aiming at:

- a complete survey of environmental impact and LCA of the products, effluent and waste generated;
- obtaining quantitative yield and costing data from large scale lots;
- the diversification and rendering more efficient the tanning materials, application processes, and wet-white leather semi-processed commodity products.

Acknowledgements

This work has been financed by the European Fund for Regional Development and the Romanian Government in the framework of Sectoral Operational Programme under the project INNOVA-LEATHER: «Innovative technologies for leather sector increasing technological competitiveness by RDI, quality of life and environmental protection» – contract POS CCE-AXA 2-O 2.1.2 nr. 242/20.09.2010 ID 638 COD SMIS – CSNR 12579.

REFERENCES

Zainescu, G., Ioannidis, I., Deselnicu, D.C., Crudu, M. (2012), Romanian Patent application no. A 00617/ 23.08.2012.

NEW VERSATILE CONVERSION TECHNOLOGY FOR WET WHITE WASTE TRANSFORMATION TO BIOFERTILISERS

GABRIEL ZAINESCU[1], DANA CORINA DESELNICU[1], IOANNIS IOANNIDIS[1], MARIAN CRUDU[1], PETRE VOICU[2]

[1] *National R&D Institute for Textile and Leather – Division: Leather and Footwear Research Institute, 93 Ion Minulescu str., 031215, Bucharest, Romania, email: icpi@icpi.ro*

[2] *Research Institute for Soil Science and Agrochemistry, 61 Marasti Blvd., 71331, Bucharest, Romania*

A large number of tanneries and leather product manufacturers are facing serious problems regarding waste disposal, the more so as their storage in landfills leads to negative effects on the ecosystem. Using tanned waste is of particular interest because it offers the opportunity to eliminate all wastes from tanning, while obtaining qualitatively and economically valuable products. Organic biopolymers represent a source of raw material for agriculture, because the composition of protean wastes provides enough elements to improve composition and rehabilitation of degraded soils, and plants can capitalize some elements: nitrogen, calcium, magnesium, sodium, potassium, titanium etc. The wastes used for this innovative procedure for obtaining biopolymers, are obtained from wet white tanned leather through a new technique based on Ti-Al tanning agents. The work presents a new pilot technology for biochemical decay of the tannery protein wastes and use of the resulted products as fertilizers.

Keywords: leather wastes, technology, biofertilizers.

INTRODUCTION

The production of leather industry solid wastes has increased and the use of such wastes as fertilizers represents an interesting alternative for their disposal, with less potential impact to the environment (Oliveira et al., 2004). A new method was suggested for wet white tanned leather waste treatment. Organic biopolymers represent a source of raw material for agriculture, because the protein waste composition provides adequate elements that will improve composition and rehabilitation of weathered soils. Protean waste capitalization represents a necessity of clean, ecological technologies, because only 25% raw hide becomes finished product.

The novelty of this work is based primarily on the fact that the applied research it promotes has as a starting point developing new complex products – multicomponent polymers - by processing organic wastes with application in remediating and/or conditioning degraded or contaminated soils (the combination of organic biopolymers in tanneries and synthetic polymers with applications in pedology.

Reducing the effects of degradation / contamination / pollution involves the application of remediation methods, to improve characteristics of the soil affected by degradation processes or limiting factors, in order to recover its original state of fertility and productivity, higher, or at least to a state close to the original.

EXPERIMENTAL DATA AND DISCUSSIONS

Due to the fact that protein matters resulted from biochemical treatments of tannery wastes can be obtained from small and medium industry specialized in processing natural hides, the possible beneficiaries of the studied technology are mainly tanneries, which contribute to environmental protection policy as well as expand their product range and make their business cost-effective; the possible users of the resulted products are leather and agriculture industry enterprises (Gammoun et al., 2007; Rosentreter et al., 1998; Compassi, 1992).

All treatments applied to wastes aim at substantially reducing environmental pollution. Complex characteristics of protein wastes from leather industry are approached by establishing with precision the chemical composition of hide wastes and the various possibilities of recovery and recycle using biotechnologies (Brown et al., 1996; Cabeza et al., 1999; Rangel Serrano et al., 2003; Zainescu et al., 2010).

In this study, we established an adequate hydrolysis method for wet white leather waste, in order to obtain the desired recyclable products and fully use titanium containing leather waste with zero waste.

Figure 1. Wet white waste

Analysis of Ti-containing wet white wastes In order to characterize the new wet-white leather and prove the tanning potential of tanning potential of the newly synthesized compounds, chemical analyses has been carried out both on the split and grain layers of the product leathers and the results obtained are shown in Table 1.

Table 1. Wet-white grain and split leather wastes chemical analyses

No.	Parameter	Layer	
		Grain	Split
1.	Volatile matters (%)	53.1	51.2
2.	Extractible (%)	1.58	2.35
3.	Ash (%)	10.4	10.9
4.	Metal Oxides (%)	8.2	8.3
5.	Dermal substance	35,1	34,8
6.	pH extract	3.98	4.0

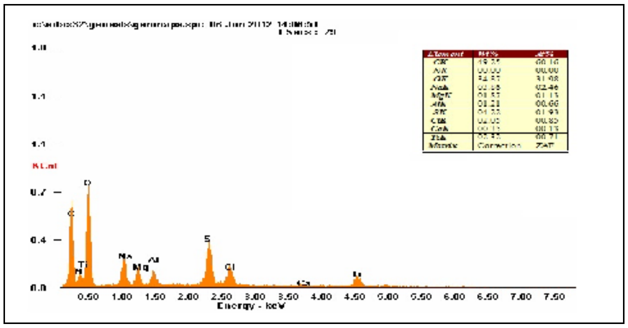

Figure 2. SEM-EDAX mapping of grain layer

A new method of treating wet white wastes was suggested, namely by wet white wastes hydrolysis in 2 steps, obtaining a protean biopolymer which, in combination with other polymers (polyacrylamide, acrylic, maleic, cellulose, starch etc.) will be used in agriculture.

Figure 3. Facility for processing wet white wastes

These leather wastes were treated by chemical-enzymatic hydrolysis. Thus, a quantity of wet white leather wastes containing titanium was weighed, then mixed with water (200-500%) and subjected to a pretreatment by adding CaO or 2- MgO for 4-6 h The mixture is hydrolysed in a 50 l autoclave with double jacket and stirrer, adding K_2HPO_4 at a temperature of 90-98°C for 2.5-5 hours. Then, the titanium containing hydrolysate is passed through a sieve with a mesh of about 0.5-1 mm^2. Two parts are thus obtained, a liquid part that has passed through the sieve and an unhydrolysed solid part called “titanium containing sludge”, about 4-9% of the original waste subjected to hydrolysis. The liquid hydrolysate is dried and used as a fertilizer in agriculture.

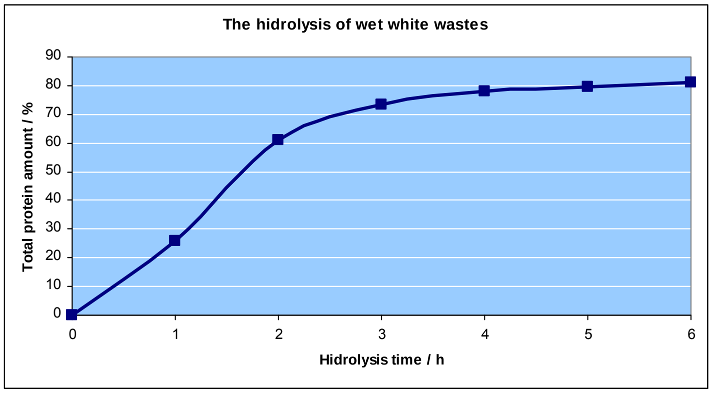

Figure 4. The hydrolysis of wet white wastes

The second stage can be carried out, weighing wet white leather waste (containing titanium) and “titanium containing sludge” in proportion of 1:1 and subjecting it to a pretreatment in water (200-500%) and 1:2 MgO with NaOH at room temperature for 4-6 hours. This pretreatment step is required to obtain optimum pH for enzymatic digestion. Then 0.5-1% Swiss commercial enzymatic product K or D containing 30,000 MWU lipase, 900 units/g cellulase, 1.200 unit/g amylase and 10,000 units/g protease are added. The mixture is maintained for 1.5-2.5 hours at 35-40°C.

The technological process of obtaining protean biopolymer - biofertiliser (from Ti-containing wet white wastes) is presented below:

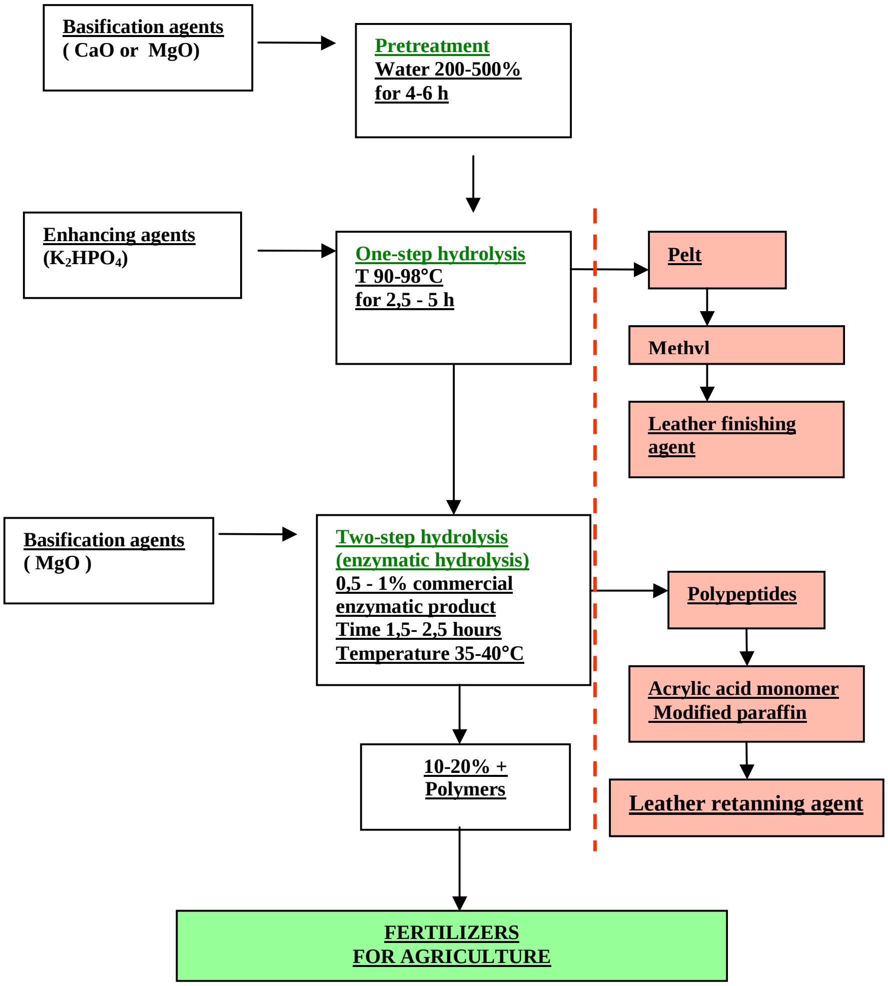

Figure 5. Technological process of obtaining protean biopolymer – biofertiliser from Ti-containing wet white wastes

The process of biochemical combination of synthetic polymers with organic biopolymers from tanneries has innovative applications in pedology. The study involved treating by chemical and enzymatic process the wet white wastes from bovine hide.

Soil conditioning consists in improving the physical properties by means of substances with varied origins, known in literature as “soil conditioners”. Soil contamination represents a moderate increase in the concentration of certain substances which are not harmful for plant growth and development, but can represent the initial phase in the pollution process. Decreasing the effects of soil weathering/ contamination/

pollution involves the use of certain methods which lower the negative consequences of the soil fertility degradation and contamination or pollution.

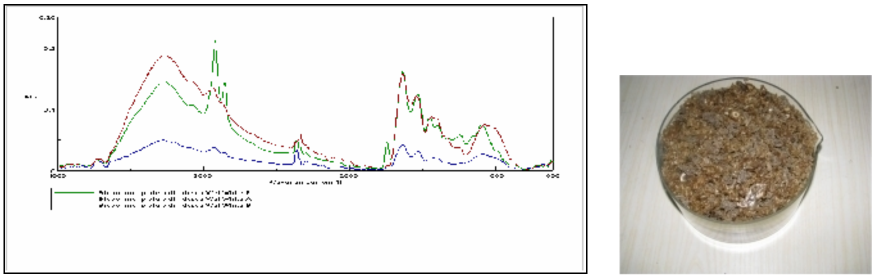

Figure 6. FT/IR-ATR spectra of biofertiliser samples

ICPI together with the National Research & Development Institute for Pedology, Agrochemistry and Environment Protection Bucharest have recently tested protein biopolymer systems for use on degraded soils and for greenhouse and field plant growth. Usually, polyelectrolytes and other polymer classes contribute to the improvement of soil properties, through one or more of the following effects: an increase in the aggregation of soil structural elements in weathered soils; prevention of crust formation in the period between sowing and spring, especially for plants with small seeds, which are very vulnerable; an increase in resistance to water and wind erosion of soils located on slopes and coarse grained soils (less than 12% clay).

Micromorphology analyses were conducted on a glazed, loamy-clayish chernozem, on leossoide deposits in the north area of Bucharest, where the protein biopolymer was applied. Micromorphology analyses for thin sections on the distribution behaviour of the soil biofertiliser and its relationship with different components of soils was made possible by using a new technique (marking the conditioner with three types of dyes - hematoxylin, fluorescein, isothiocyanate).

The biofertiliser was experimented on a culture of peas for improving the land with biologically fixed nitrogen and to allow the early release of land. The land was then prepared for sowing barley. Beside the nutrients in the soil, it has been shown that peas need nitrogenous fertilizers, especially during the first stages of development. Subsequently, it grows at the expense of the fixed nitrogen in the air by bacteria that form nodosities on the roots. The most suitable soil type for pea cultivation is neutral or slightly alkaline, which can be amended with limestone, but only by predecessor plants (not directly). In the blooming phenophase, the nodosities on the pea roots were considered from the treatment before sowing with biofertiliser (0.25 kg/m^2).

The biofertiliser (0.25-0.5 kg/m^2) soil treatment significantly influenced the number of nodules developed on the plant roots. Roots and organic remainders gathered in the soil by the pea plants are an important source of nutrients and energy for soil microorganisms. Additionally, their decomposition results in a significant amount of necessary elements (especially nitrogen) for the nutrition of superior plants.

These studies contribute both to the recovery of poor and degraded soils in agriculture and to the reduction of environmental pollution by exploiting protein wastes.

CONCLUSIONS

In conclusion, a Ti-containing wet white leather waste conversion technology can be established, which, through hydrolysis and mixed with 10-20 % protein biopolymers from limed leather wastes, can be used as fertilizers in agriculture. We must mention that as a result of experiments carried out for wet white leather waste hydrolysis no effluents or other wastes result. Biopolymers have been obtained by an innovative enzymatic procedure of processing wet white waste resulted from leather processing. In combination with other polymers (polyacrylamide, acrylic polymer, maleic polymer, cellulose, starch, etc.) they can be used for improvement of degraded/eroded soils and growth of greenhouse and field plants.

All instrumental analyses (UV-VIS, IR spectroscopy, thermal analyses, X-ray diffraction, microscopy etc.) have highlighted both reticulations between the protein polymer and the synthetic one, and the high order of the polymeric structure, which is due to the enzymatic hydrolysis process. For an efficient crop growth, it is not enough to add only the missing element, but also to satisfy, as much as possible, all the needs of the plants. This implies acting simultaneously on various factors in the complex condition determining agricultural production.

The obtained experimental results demonstrate that the protein biofertilizer materials produced an interesting outcome both in terms of improving the soil quality and growing large-scale crop plants, showing highly potential applications in agriculture and environmental sciences.

Acknowledgements

This work was performed within the framework of the project INNOVA-LEATHER: “Innovative technologies for leather sector increasing technological competitiveness by RDI, quality of life and environmental protection” contract POS CCE-AXA 2-0 2.1.2 no. 242/20.09.2010 ID 638 COD SMIS -CSNR12579, financed by the European Fund for Regional Development and the Romanian Government in the framework of Sectoral Operational Programme Increase of Economic Competitiveness.

REFERENCES

Brown, E.M., Taylor, M.M. and Marmer, W.N. (1996), “Production and potential uses of co-products from solid tannery waste,” *Journal of the American Leather Chemists Association*, 91(10), 270–276.

Cabeza, L.F., Taylor, M.M., Brown, E.M. et al.(1999), “Treatment of sheepskin chrome shavings. Isolation of high value protein products and reuse of chromium in the tanning process,” *Journal of the American Leather Chemists Association*, 94(7), 268–287.

Compassi, M.K. (1992), “Processo de dissolucao termo-quimica de serragem e/ou retalhos e aparas de couros curtidos ao cromo,” Br PI 9202408.

Gammoun, A., Tahiri, S., Albizane, A. et al. (2007), “Separation of motor oils, oily wastes and hydrocarbons from contaminated water by sorption on chrome shavings,” *Journal of Hazardous Materials*, 145(1-2), 148–153.

Oliveira, L.C.A., Dallago, R.M. and Nascimento Filho, I. (2004), “Processo de reciclagem dos resıduos solidos de curtumes por extracao do cromo e recuperacao do couro descontaminado,” Br PI 001538.

Rangel Serrano, A., Maldonado, V.M., Kösters, K. (2003), “Characterization of Waste Materials in Tanneries for Better Ecological Uses”, *Journal of the American Leather Chemists Association*, 98, 43-484.

Rosentreter, H., Klein, H.G., Wehling, B. and Makowka, B. (1998), “Processo de curtimento ao cromo de couros descarnados e depilados piquelados,” Br Pi 8804055.

Zainescu, G. et al. (2010), “Application of tannery organic wastes in degraded soils remediation”, *Journal of Biotechnology* 150 Supp (November 2010), 290, Elsevier Science Publishers.

PLENARY LECTURE

ACTUAL PROBLEMS OF THE LEATHER WORLD AND DISCUSSION ON THE WAYS TO OVERCOME

DR. VOLKAN CANDAR

President of IULTCS, email: acandar@pulcrachem.com

The leather world is facing different problems which can affect its future. Recently the Life Cycle Assessment of leather and leather Carbon Footprint comes up for discussion in different media. Beside this very important issue for the industry SVHC and hazardous chemicals problematic has been taken under spotlight. In this relationship the leather industry faces negative perception and as an evident consequence inaccurate attacks surround the industry. Some brands or leather and leather products' users request unreasonable specification from the material and some laboratories carry out analysis of the material according to non-correct, non-standard methods even if they might have an accreditation. The only way to overcome is certainly to create irrefutable scientific arguments, increasing the awareness of the thirds, research and application of innovative solution in order to increase the value of the leather material. This can be defended then by legitimate global organization of the industry. In this study I will try to put on the table the actual problems of the leather industry and discuss the proposed solutions in different aspects.

Keywords: LCA, leather carbon footprint, Best Available Techniques.

LCA AND CARBON FOOTPRINT OF LEATHER

Mr. Zeitz, the CEO of Puma accused leather material in his interview to the Financial Times last June 2012, while he was commenting the UN Rio +20 meeting. He stated in brief that the leather industry is responsible for the ecologic footprint left by the animal during its life. This was one of the inaccurate accusations for leather material as the CO2 emission of leather was assumed starting from breeding. It was actually an evident consequence of treating hides and skins as co-products of the meat industry. But a scientific approach and a comprehensive methodological study (Brugnoli, 2012) reveals important proofs for the acceptance of leather industry raw materials as by-products. Such a conclusion arises not only by assumptions but also by applying rational methodology. Hence, the system boundary has to be framed accordingly and then a process can be analyzed rationally.

Whatever a product is it should be assessed in relationship with his impact on the environment and the climate. For a given product the whole process can be identified by Key Performance Indicator (KPI's). Carbon and Water Footprints are perceived more and more often as important KPI's for a given article.

For determining Carbon and Water Footprint in case of the leather as an article, its system boundary must be correctly defined. For this aim one must give a correct answer for following questions:

Is leather a co-product of the meat industry? Or a by-product? Or a waste?

According to a work (Brugnoli, 2012; Dietrich, 2012) presented in UNIDO 18th Leather Panel recently held this can be answered considering and analyzing the input and output of a process as well as the process itself. The input of the system consists obviously of water, energy and chemicals. The process can be assumed to start from breed, slaughter and meat production. Then hides/skins will be used in the tanning operations and be transformed to an article like garment, footwear, upholstery or else. Later these articles will be used and finalize their life. According to several works

(Weidema, 1999; Mekonnen & Hoekstra, 2012; EBLEX, 2010) it has been revealed that Water- and Carbon Footprint contribution for Leather of a tannery operation is insignificant small, 1% for Water Footprint and 4% in case of Carbon Footprint. Let's consider a co-product "A" as a product of a determining process "A". Assume that "A" is based on a process originated renewable resources. To enable the production of "A" assume that a product "B" forms inevitably. Assume as well that "A" determines its volume and quality without being affected by the demand of "B" which replaces a certain product "C" used for the production of the product "D". Those assumptions and designations fit perfectly to the case of leather. If A designates Farming and A Milk and Meat, B would designate Leather, C, Textile and D Shoe, Garment, Upholstery, Seat or something similar. Leather doesn't carry any burden of the animal breed as the latter is the origin of meat and milk industry and the demand of milk and meat are not affected from leather demand. This reasonable and rational approach demonstrates the fact that the leather LCA boundary is framed between slaughterhouse and later operations. This scientifically proven methodology was recently agreed from UNIDO very recently. From now on global leather organizations, IULTCS, ICT, ICHSLTA and new formed GLCC will take action to legitimate this proven position. These organizations will definitely inform the public opinion releasing the truth about the industry. Leather LCA and Carbon Footprint have further been researched scientifically and discussed positioning the material with others.

LEATHER INDUSTRY AND CHEMISTRY

Leather processing and chemistry are tightly bounded. Often special requirement are fulfilled only by the use of appropriate chemicals. Hence, the development in leather industry demands always innovations especially in the chemistry and also in other disciplines. On the other hand our responsibility to our environment has droved the leather chemical industry to innovate in a more sophisticated manner in order to care about the environment without compromising the highest requirement of the leather industry.

A general glance to last 20 years of the IULTCS congresses shows up that more than 85% of researches and developments were carried out on this fact. Implementing more severe restrictions and putting into effect new regulations as for instance in the case of REACh brought the leather industry to more challenging position. Leather uses more and more cleaner technologies, substitute's hazardous chemicals, refers to more advanced works as for example Best Available Techniques (BAT, 2012). In different technical and scientific events various works were presented where substitution chemicals are lanced in terms of their application performances (Candar, 2012a).

Most challenging works consist of CrVI elimination and prevention (Candar et al., 2000; Candar et al., 2001), substitution of banned azo-dyes, SVHC substitutes, salinity problems etc. NPEO and NP is already substituted by new generation surfactants with similar, even better performance. Developments continue without break and improvements are often reported (Candar, 2012b). Leather technology needs sustainability and the leather world works continuously on this issue. On the other hand one can observe that the non-leather world has insufficient and in some cases inadequate information about the leather reality. We can observe this for instance facing irrelevant requirements from leather and leather articles. An example can be the end pH value of a deep black nubuck or suede. It has been recorded some requirements forcing pH not less than 7 which is technically impossible to achieve. Another example would be a requirement of CrVI less than 2 ppm which has no sense since the detecting limit of hexavalent Chromium analysis is 3ppm according to EN ISO 17075 method. Less than this value nothing is reliable and doesn't make sense. Unfortunately many laboratories that have accreditations don't follow correct leather analysis methods and report test results according non-accurate methods. They use sometimes another material's standard analysis method and obtain false positive results. Global organizations have the responsibility to create awareness on leather material and avoid such unfair behavior.

CONCLUSION

Nowadays the Leather World tries to position itself under very difficult conditions. Although the leather industry invests for environmental care and improves its conditions all around the world its perception continues to be not it is worth. However R&D investments and improvements should never stop. There are many signs proving this fact. Solely IULTCS events prove that enough. All papers applied to the regional conferences, in South America and in Far East, and then those applied to 32nd Congress in Istanbul are encouraging taking into account interesting topics.

REFERENCES

Brugnoli, F. (2012), 18th Session of the UNIDO Leather and Leather Products Industry Panel Presentation, 1-6 Sept. 2012, Shanghai, China.

Candar, V. (2012a), "Possibilita' di Sostituzione di Alcune Sostanze Chimiche in Campo Conciario, Discussioni", UNIC, Convegno Innovazione Technologica Settore Cuoio, 25th Jan. 2012 Milan.

Candar V. (2012b), "Sostanze Nuove nello Sgrassaggio", UNIC, Convegno Innovazione Technologica Settore Cuoio, 27th June 2012 Milan.

Candar, V., Palma, J.J., Zorluoglu, Y., Reetz, I. (2001), "Many Faces of Aging", 26th IULTCS Congress, 2001, Cape Town, South Africa.

Candar, V., Reetz, I., Ferranti, M. (2000), "How to Avoid CrVI", European Congress, AICC 2000, San Miniato, Italy.

Dietrich, T. (2012), 18th Session of the UNIDO Leather and Leather Products Industry Panel Presentation, 1-6 Sept. 2012, Shanghai, China.

Mekonnen, M., Hoekstra, A. (2012), *Ecosystems*, Jan. 2012.

Weidema, P. (1999), 7th LCA Case Studies Symposium SETAC Europe.

*** (2010), EBLEX, Phase 1 study.

*** (2012), BAT, EU Working Draft June 2012.

I.
MATERIALS

MULTIVARIANT NATURE OF DISPLACIVE TRANSITIONS IN COPPER BASED SHAPE MEMORY ALLOYS

OSMAN ADIGUZEL

Firat University, Department of Physics, 23169 Elazig-Turkey, oadiguzel@firat.edu.tr

Shape memory effect is an unusual property exhibited by certain alloy systems, and based on a displacive transition, martensitic transition. Copper based alloys exhibit this property in metastable β –phase region and bcc-based high temperature parent phase structures martensitically turn into the layered complex structures on cooling from high temperature. Martensitic transformations occur with cooperative movement of atoms by means of lattice invariant shears on a {110} - type plane of austenite matrix which is basal plane of martensite. The lattice invariant shears occurs, in two opposite directions, <110 > -type directions on the {110}-type basal plane. This kind of shear can be called as {110}<110> - type mode, and possible 24 martensite variants occur. This lattice invariant shear gives rise to the formation of layered structure. Product martensitic phase has the unusual layered structures which consist of an array of close-packed planes with complicated stacking sequences called as 3R, 9R or 18R martensites depending on the stacking sequences on {110}- type planes of parent phase. The basal plane of martensite is subjected to the hexagonal distortion with martensite formation on which atom sizes have important effect. It is known that the local stress and composition conditions can play an important role in the final structures of the material.

Keywords: Martensitic transition, shape memory effect, martensite variants, Bain distortion.

INTRODUCTION

Shape-memory alloys are a new class of functional materials with a peculiar property known as shape memory effect. These alloys have an ability to recover a particular shape with changing temperature. These alloys involve the repeated recovery of macroscopic shape of material at certain temperature intervals. The origin of this phenomenon lies in the fact that the material changes its internal crystalline structure with changing temperature. The functional behavior of shape memory alloys, as thermoelastic and pseudoelastic effects, is related to the first-order martensitic transition. Copper based ternary alloys exhibit shape memory effect in metastable β-phase field. These alloys undergo the non-conventional structures on cooling from high temperatures, following two ordered reactions (Adiguzel, 2007; Zhu & Liew, 2003). Inhomogeneous shears, latte invariant shears occur as martensite variants on a {110} - type planes of austenite matrix which is basal plane of martensite. The lattice invariant shears occur, in two opposite directions, <110 > -type directions on the {110}-type planes, and this kind of shear can be called as {110} <110 > - type mode and has 24 variants in self-accommodating manner (Adiguzel, 2007; Sutou et al., 2005). A pair of shears in the $[\bar{1}10]_\beta$ and $[1\bar{1}0]_\beta$ - directions occur as two variants along the $(110)\beta$ plane. This lattice invariant shear causes to the formation of layered structure. These shears cause to the formation of layered structures. The {110} – type planes of parent phase turn into unusual layered structures which consist of an array of close- packed planes with complicated stacking sequences called as 3R, 9R or 18R martensites depending on the stacking sequences on the close-packed planes of the ordered lattice. The periodicity and therefore the unit cell are completed through 18 layers in direction z in 18R case (Zhu & Liew, 2003; Pelegrina & Romero, 2000). The martensitic transformations basically have the diffusionless character and exhibit the order of parent phase structure existing prior to the transformation. The complicated long-period stacking ordered structures can be described by different unit cells. In case the parent phase has a B2 - type superlattice, the stacking sequence is ABCBCACAB (9R) (Zhu & Liew, 2003; Pelegrina & Romero, 2000). The stacking of $(110)_\beta$ - planes in DO_3 – type structure and formation of layered structures are shown in Figure 1. Martensitic transformation is characterized by a change in the crystal structure of the material at the atomic level, and martensite phases have the long-period stacking ordered structures that is the underlying lattice is formed by stacks of close-packed planes. More specifically, microstructural evaluation provides a mechanism by which the transformation from the high temperature austenite phase to the low temperature martensite phase takes place.

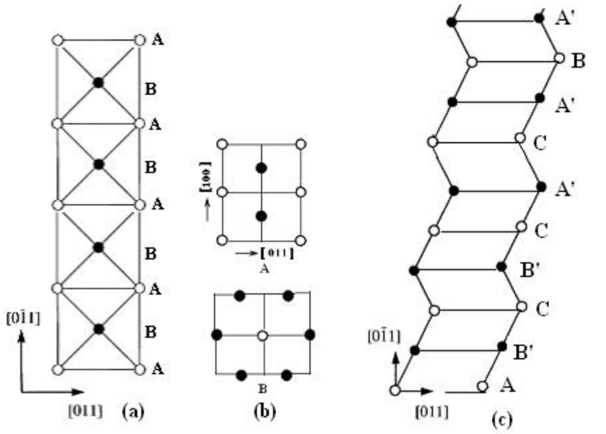

Figure 1. a) Stacking of $(110)_\beta$ planes viewed from $[001]_\beta$ direction, b) Atomic configuration on first and second layers of (110)β plane in DO_3 - type structures, c) inhomogeneous shear and formation of layered structures, stacking sequences of half 18R or M18R unit cell in direction z

EXPERIMENTAL

In the present contribution, two copper based ternary alloys were selected for investigation: a CuZnAl alloy with a nominal composition by weight of 26.1% zinc, 4% aluminium, the balance copper, while the other was a CuAlMn alloy with a nominal composition by weight of 11% aluminium, 6% manganese and the balance copper. Powder specimens for X-ray examination were prepared by filling the alloys. Specimens for TEM examination were also prepared from 3mm diameter discs and thinned down mechanically to 0.3mm thickness, tthese specimens were heated in evacuated quartz tubes in the β-phase field (15 minutes at 830°C for CuZnAl and 20 minutes at 700°C for CuAlMn) for homogenization and quenched in iced-brine. These specimens were also given different post-quench heat treatments and aged at room temperature. TEM and X-ray diffraction studies carried out on these specimens. TEM specimens were examined in a JEOL 200CX electron microscope, and X-ray diffraction profiles were taken from the quenched specimens using Cu-K_α radiation with wavelength 1.5418 Å.

RESULTS AND DISCUSSION

An x-ray powder diffractogram taken from the quenched and long term aged CuAlMn alloy sample is shown in Figure 2.

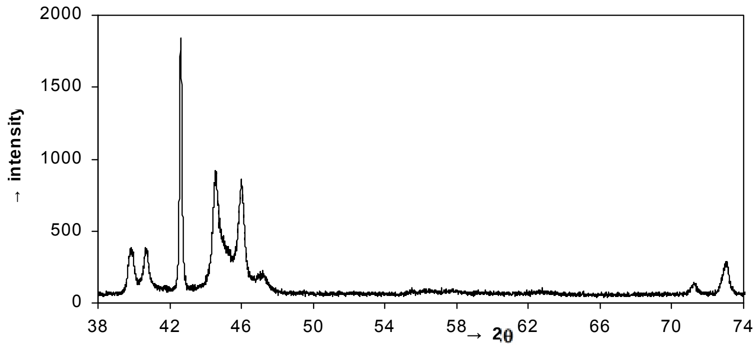

Figure 2. An x-ray diffractogram taken from the long term aged CuAlMn alloy sample

Two electron diffraction patterns taken from CuZnAl and CuAlMn alloy samples are also shown in Figure 3. X-ray powder diffractograms and electron diffraction patterns were taken from CuZnAl and CuAlMn samples. X-ray powder diffractograms and electron diffraction patterns reveal that this alloy has an ordered structure in martensitic condition, and exhibit superlattice reflections. X-ray powder diffractograms and electron diffraction patterns were taken from both CuZnAl and CuAlMn alloy samples in a large time interval and compared with each other. It has been observed that electron diffraction patterns exhibit similar characteristics, but some changes occur at the peak locations and intensities on the x-ray diffractograms with aging duration. These changes occur as rearrangement or redistribution of atoms in the material, and attribute to new transitions in diffusive manner (Adiguzel, 2007; Li et al., 2008). The ordered structure or super lattice structure is essential for the shape memory quality of the material. In the shape memory alloys, homogenization and releasing the external effect is obtained by ageing at β−phase field for adequate duration. Crystallization is essential for shape memory quality, and crystallization and formation of the ordered structure is also obtained by the quenching process in the suitable media. The quenching rate is also important for the formation of homogenous ordered structures and shape memory optimization. The martensitic transformation obtained on cooling is called thermally induced phase transformation. The obtained martensite consists of up to 24 variants, which are regions of the same structure but with different crystallographic orientations (Li et al., 2008; Adiguzel, 2012; Paidar, 2008).

Figure 3. Two x-ray diffractograms taken from the CuZnAl and CuAlMn alloy samples

On the other hand, post-quench ageing and service processes in devices affect the shape memory quality, and give rise shape memory losses. These kinds of results lead to the martensite stabilization in the reordering or disordering manner. In order to make the material satisfactorily ordered and to delay the martensite stabilization, copper-based shape memory alloys are usually treated by step-quenching after homogenization.

Although martensitic transformation has displacive character, martensite stabilization is a diffusion controlled phenomena, and leads to redistribution of atoms on the lattices sites. Stabilization is important factor and causes to memory losses, and changes in main characteristics of the material, such as transformation temperatures, and x-ray diffraction peak location and peak intensities.

It can be concluded from the above results that the copper-based shape memory alloys are very sensitive to the ageing treatments, and heat treatments can change the relative stability and the configurational order of crystal planes. This result attributes to a rearrangement of atoms.

REFERENCES

Adiguzel, O. (2007), “Smart materials and the influence of atom sizes on martensite microstructures in copper-based shape memory alloys”, *Journal of Materials Processing Technology*, 185(1-3), 120-124.

Adiguzel, O. (2012), “Martensitic Transformation And Microstructural Characteristics In Copper Based Shape Memory Alloys”, *Key Engineering Materials*, 510-511, 105-110.

Li, Z., Gong, S. and Wang, M.P. (2008), “Macroscopic shape change of Cu13Zn15Al shape memory alloy on successive heating”, *Journal of Alloys and Compounds*, 452(1), 307-311.

Paidar, V. (2008), “Shuffling in displacive phase transformations”, *Materials Science and Engineering A*, 481–482, 243-246.

Pelegrina, J.L. and Romero, R. (2000), “Calorimetry in Cu–Zn–Al alloys under different structural and microstructural conditions”, *Materials Science and Engineering A*, 282(1-2), 16-22.

Sutou, Y. et al. (2005), “Effect of grain size and texture on pseudoelasticity in Cu–Al–Mn-based shape memory wire”, *Acta Materialia*,, 53(7), 4121-4133.

Zhu, J.J. and Liew, K.M. (2003), “Description of deformation in shape memory alloys from DO_3 austenite to 18R martensite by group theory”, *Acta Materialia*, 51(9), 2443-2456.

CHEMICALLY GRAFTED POLYCHLOROPRENE CONTACT ADHESIVE NANODISPERSIONS. PART I – METHODS OF ASSESSING THE GRAFTING REACTION

LAURENTIA ALEXANDRESCU[1], MIHAI GEORGESCU[1], MARIA SONMEZ[1], MINODORA LECA[2], ZENOVIA MOLDOVAN[2]

[1] *INCDTP – Division: Leather and Footwear Research Institute, 93 Ion Minulescu St., Sect. 3, 031215-Bucharest, Romania, email: icpi@icpi.ro, laura_alexandrescu@yahoo.com*

[2] *University of Bucharest, Faculty of Chemistry, 4-12 Regina Elisabeta Blvd., Sect. 3, 030018-Bucharest, Romania, email: minodora.leca@yahoo.com, z_moldovan@yahoo.com*

Water-based adhesives with increased bonding characteristics were obtained by two methods: chemical grafting of polychloroprene with methyl methacrylate to increase the bonding strength and dispersing of the grafted polymers at nanometric scale to enhance the protruding of dispersed particles into the pores of the supports to be joined. Grafting was done on roll in the presence of benzoyl peroxide as initiator, dodecyl mercaptan as chain interrupter and the usual additives for processing of polychloroprene. The obtained compounds, dissolved in a mixture of methylene chloride/ethyl acetate 30/70 in volume were dispersed in water containing dispersion agent and pH regulator. FT-IR spectra of films obtained by evaporation show that grafting was produced. Particle size distribution demonstrates that a large part of particles are of nanometric size, especially for dispersions obtained from polychloroprene with higher degree of grafting. SEM images of cross sections of films, obtained by cryogenic fracture, show a changing of morphology from lamellar having the fillers finely dispersed into a biphasic one consisting of spherical particles distributed within a matrix with lamellar morphology, their number increasing with the amount of monomer.

Keywords: chemically grafted polychloroprene, nanodispersions, adhesive.

INTRODUCTION

A contact adhesive is an adhesive dry to touch but instantaneously adherent to a surface in contact. The classic example is the chloroprene rubber in organic solvents, Harshorn (1986), Mittal, (1999). Contact adhesives develop and diversify continually in view of obtaining the best preset characteristics for manufacture and application.

Due to its characteristics, the polychloroprene rubber is the raw material of choice for the adhesives based on volatile organic compounds (VOCs), used in the footwear and others manufactures. The initial and final bonding strength characteristics of polychloropren adhesives are not good enough, but they can be improved by polymer grafting. The toxicity of solvent-based adhesives can be reduced and even eliminated by dispersing the modified polymer in water. Dispersion at nanometric scale facilitates the protruding of dispersed particles into the pores of the materials to be joined. Such a class of adhesives represents the most innovative substitution of VOCs adhesives, Clemens (2009), Cheung (2009), Selic (2010).

The chemical grafting method represents an advantageous way of obtaining new products, taking the advantage of the equipment currently used in polymer processing. It is able to transform polychloroprene structure and improve its adhesive properties, Bhattacharya and Misra (2004), Pepenzhik et al. (1969). The grafted polychloroprene has been mainly used as adhesive for vulcanized or cold sealed footwear, Misra et al. (1980, 1984).

Chemical grafting by radical mechanism conducted on roll in monomer-polymer systems with benzoyl peroxide as initiator was used in the present study to improve the adhesive properties. The obtained compounds were dissolved in a mixture of methylene chloride and ethyl acetate and the concentrated solution dispersed in water containing dispersion stabilizer and pH regulator. The obtained dispersions were characterized by particle size distribution as well as FT-IR spectra and SEM of films obtained by evaporation of disperse medium.

EXPERIMENTAL PROCEDURE

Materials

Polychloroprene NEOPRENE AD 20, (DuPont) as polymer, methyl methacrylate (Merck, Germany) as monomer, benzoyl peroxide as initiator and dodecylmercaptan as inhibitor (both Sigma-Aldrich Chemie, Germany), ZnO and MgO as cross-linking agents and to consume the HCl eliminated during the reaction, a diphenylamine derivative as antioxidant (the last three from Bayer, Germany); polyvinyl alcohol and triethanolamine as dispersion agent and pH stabilizer respectively (Merck, Germany), natural resin colophony (Caroco, Bulgaria) as adherence improver, and Desmodur RE – triphenyl methane triisocyanate 27% in ethyl acetate – as cross-linking agent (Bayer, Germany) were used.

Procedure

The technology of obtaining grafted polychloroprene dispersions involves three steps, Arabi et al. (2008), Ma et al. (2001): chemical grafting of polymer, its dissolving in a convenient solvent and dispersion of concentrated solution in water containing dispersion stabilizers and pH regulators.

NEOPRENE AD 20 was grafted with methyl methacrylate on a laboratory roll with water-cooled cylinders in the presence of components presented in Table 1 and the compounds B0-B3 were obtained.

Table 1. Formulations of adhesive compounds obtained by chemical grafting

Components, g	B0	B1	B2	B3
Polychloroprene	200	200	200	200
Benzoyl peroxide	-	1	1	1
Methyl methacrylate	-	20	30	40
Zinc oxide	10	10	10	10
Magnesium oxide	8	8	8	8
Styrenated phenol	4	4	4	4
Dodecyl mercaptan	-	2	2	2
Total	222	245	255	265

The roller mixing regime was the following:
- plasticizing of elastomer - 4 min;
- introducing benzoyl peroxide and grafting agent (MMA) - 30 min;
- introducing zinc and magnesium oxides as well as styrenated phenol - 10 min;
- cooling and adding dodecyl mercaptan - 10 min;
- homogenisation and removing of mixture from the roll as thin sheets - 5 min;
- total time: 59 min;

The danger of polychloroprene cyclization was avoided by a strong cooling of cylinders, using of reduced friction and rotational speed (1:1.5 and 25-30 rpm respectively), as well as by a small gap between the roll's cylinders.

The compounds from Table 1 were dissolved in a mixture of methylene chloride/ ethyl acetate 30/70 in volume. The resulted concentrated solutions were dispersed under stirring (300 rpm) for 1.5-2.0 h in demineralized water containing polyvinyl alcohol as dispersion and stabilizing agent and triethanolamine as pH regulator. The dispersions B0-B3 having the compositions from Table 3 were obtained.

Table 2. Compositions of dispersions B0-B3

Components (mass parts)	B0	B1	B2	B3
Compound	46.25	50.99	53.07	55.17
Solvent mixture	33.75	29.01	26.93	24.83
Polyvinyl alcohol, aqueous solution 10%	50	50	50	50
Triethanolamine	15	15	15	15
Demineralized water	80	80	80	80
KOH, solution 10%	1	1	1	1
Total	226	226	226	226

A first characterization of dispersions were done by the percentages of solids, free monomer and poly(methyl metacrylate), flowing time through Ford cup and pH. The obtained values are given in Table 3.

Table 3. Characteristics of dispersions B0-B3

Characteristic/dispersion	B0	B1	B2	B3
% Solids	48.58	52.06	53.64	57.59
% Free monomer	0.00	0.03	0.06	0.1
% Poly(methyl methacrylate)	0.00	0.10	0.14	0.2
Flowing time Ford cup, s	18	17	19	20
pH	13	13	13	13

Testing Methods

1. FT-IT spectra were recorded using the FT-IR 4200 JASCO, Herschel series, instrument, equipped with ATR having diamond crystal and sapphire head, within the spectrometric range 2000-570 cm^{-1}.
2. Particle size distribution was determined by laser light scattering using the Mastersizer Hydro 2000S Particle Size Analyzer, Malvern Instruments Ltd., equipped with the Malvern soft, which controls the system during the measurements and processes the information based on standard operation procedure (SOP). The three standard points to read the distribution characteristics are D(v, 0.1), D(v, 0.5) and D(v, 0.9), which represent the fractions from the total particle volume having the volume higher than a given value.
3. SEM. Dispersions B0-B3 were transformed into films by evaporating the disperse medium at 105°C. They were cryogenically fractured and their cross sections analyzed by SEM, using an ESEM QUANTA 200 instrument operating in low vacuum, equipped with LFD detector.

RESULTS AND DISCUSSION

The FT-IR spectrum of the film obtained from dispersion B0, given in Figure 1, shows the fundamental bands of trans-1,4-polychloroprene.

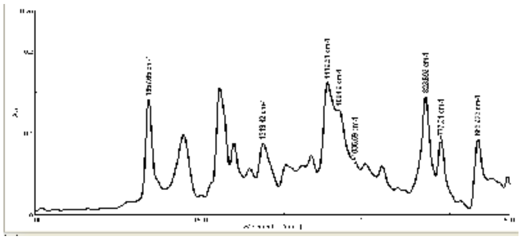

Figure 1. FT-IR spectrum of film obtained from NEOPRENE AD 20

Comparing the spectra of the films obtained for dispersions B1-B3, given in Figure 2a-c, with that of the reference sample from Figure 1, the following differences can be emphasized: decreasing of intensity of some bands from the polychloroprene spectrum, which depends on the amount of methyl methacrylate introduced (1657 cm^{-1} – assigned to C=C stretching, 1313 cm^{-1} – specific to CH_2 wagging, 823 and 777 cm^{-1} – assigned to CH_2 rocking and 666 cm^{-1} – assigned to C-Cl stretching), indicating the decreasing of amount of polychloroprene, and changing of the aspect and broadening of the bands in the region 1150-1015 cm^{-1}, Celina et al. (2000). Thus, the bands from 1119 cm^{-1} (i), 1085cm^{-1} (shoulder) and 1037 cm^{-1} (shoulder) from Figure 1, assigned to C-C, Mas and Haris (2007), Berry et al. (1987), increase in intensity.

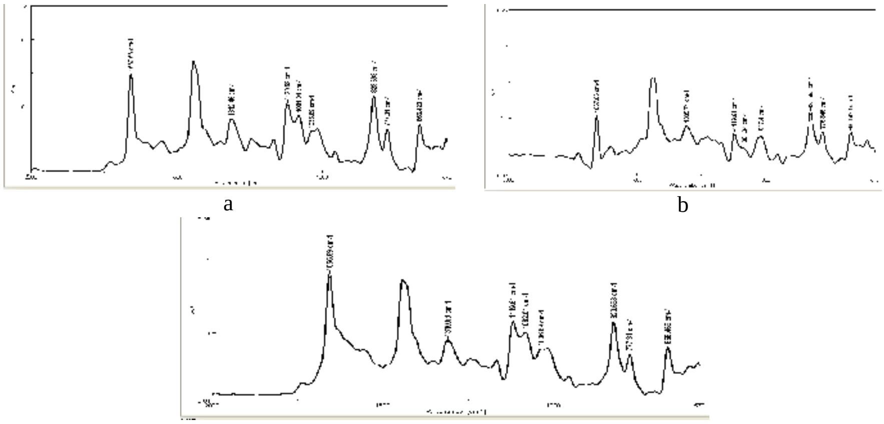

a

b

c

Figure 2. FT-IR spectra of films obtained from dispersions: a – B1; b – B2; c – B3

The particle size distribution curves for the adhesive dispersions from Table 1 are presented superposed in Figure 3.

The Figure shows the effect of grafting with methyl methacrylate on size and size distribution of particles: as the amount of grafted monomer increases the fraction of particles with nanometric size increases while the distribution becomes narrower, the polymodal distribution preserves but it reduces from three to two maxima. Thus, if the curves of particle size distribution start at 0.3 μm, that for the dispersion containing non-grafted polymer (B0) end at about 400 μm and contains three maxima, whilst those containing grafted polychloroprene (B0-B3) end at about 70 μm, the main maximum displaces to lower values, that is the preponderant fraction displaces towards lower size.

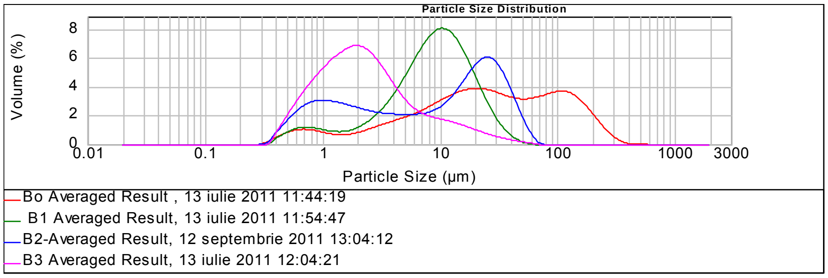

Figure 3. Particle size distribution curves for dispersions B0-B3

The values of standard points to read the distribution characteristics for the dispersions B0-B3 are given in Table 4.

Table 4. Values of standard points to read distribution characteristics for B0-B3

Sample	D(v, 0.1), μm	D(v, 0.5), μm	D(v, 0.9), μm
B0	2.256	24.588	143.293
B1	1.846	8.799	21.168
B2	0.815	9.637	35.430
B3	0.738	2.107	10.104

Therefore, chemical grafting of polychloroprene with methyl methacrylate on roll has two effects on the particle size of dispersions obtained by mechanical dispersion of solutions and on particle size distribution:

- maintaining of the type of polymodal distribution;
- reducing of particle size with the increase of amount of methyl methacrylate used for grafting from 10 to 20 parts related to rubber amount, except for sample B2, grafted with 15 parts monomer, for which the values D(v, 0.5) and D(v, 0.9) are higher.

The SEM image of the cross section of the film obtained from polychloroprene (B0), shown in Figure 4a, emphasizes a lamellar structure, having the elements of the fillers finely dispersed inside.

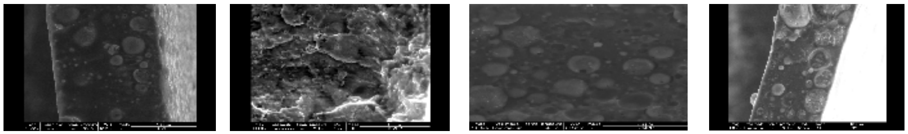

a
B0, 1000X

b
B1, 1000X

c
B2, 10000X

d
B3, 1000X

Figure 4. SEM images of cross sections of films obtained from dispersions:
a – B0, b – B1, c – B2 and d – B3

Instead, the SEM images of cross sections of films obtained from the other three dispersions, in which the polychloropren was chemically grafted, have completely different aspects (Figure 4b-d): they show a biphasic type morphology consisting of spherical particles distributed within a matrix with lamellar morphology, their number increasing with the amount of methyl methacrylate.

CONCLUSIONS

High performance environmentally friendly aqueous adhesive nanodispersions for shoe manufacture were obtained by chemical grafting of polychloroprene on roll using benzoyl peroxide as initiator.

The absence of methyl methacrylate and poly(methyl methacrylate) from the dispersions B1-B3 demonstrates that the grafting of monomer onto the polychloroprene chains took place.

Decreasing of intensity of some bands from the polychloroprene spectrum as well as and changing of the aspect and broadening of the bands in the region 1150-1015 cm^{-1} can be considered as proofs that methyl methacrylate grafted onto polychloroprene.

Particle size decrease and particle size distribution narrows when polychloroprene is grafted with methyl methacrylate, that is the percentage of particles having nanometric size increases with the degree of grafting.

SEM images of the cross section of the film obtained from the dispersions show the changing of morphology from lamellar for the dispersion containing non-grafted polychloroprene to biphasic, consisting of spheroid particles distributed within a matrix with less evident lamellar aspect, for those containing grafted rubber, the number of particles increasing with the amount of monomer.

REFERENCES

Alexandrescu, L. et al. (2010), *Leather and Footwear Journal*, 10(1), 63.
Arabi, H. et al. (2008), *Iranian Polymer J.*, 17, 379.
Berry, R.J. et al. (1987), *J. Chem. Phys.*, 87, 6303.
Bhattacharya, A. and Misra, B.N. (2004), *Prog. Polym. Sci.*, 29, 767.
Celina, M. et al. (2000), *Polym. Degrad. Stab.*, 68, 171.
Cheung, J.T.M. et al. (2009), *Footwear Sci.*, 1, 31.
Clemens, M. et al. (2009), *Footwear Sci.*, 1(5), Canada.
George, W.O. and McIntyre, P.S. (1987), *Infrared Spectroscopy*, Wiley and Sons, Inc., New York.
Harshorn, S.R. (1986), *Structural Adhesives: Chemistry and Technology*, Plenum Press, New York.
Hearn, J. et al.. (2000), *Adv. Colloid Int. Sci.*, 86, 195.
Kuptsov, H. and Zhizhin, G.N. (1998), *Handbook of FTIR Polymers*, Elsevier, Amsterdam.
Ma, Z., Merkus et al. (2001), *Part. Syst. Charact.*, 18, 243.
Mas Haris, M.R.H et al. (2008), *Asian. J. Chem.*, 20, 4511.
Mishra, B.N. et al. (1984), *J. Polym. Sci. Polym. Chem.*, 22, 2767.
Misra, B.N. et al. (1980), *J. Polym. Sci. Polym. Chem.*, 18, 749.
Mittal, R.L. and Pizzi, A. (2003), *Handbook of Adhesives Technology*, 2nd ed., Dekker, New York.
Pepenzhik, M.A., et al. (1969), *Vysokomol. Soedin.*, Ser. B 11, 245.
Schields, J. (1984), *Adhesives Handbook*, 3rd ed., Butterworths, London.

CHEMICALLY GRAFTED POLYCHLOROPRENE CONTACT ADHESIVE NANODISPERSIONS. PART II – ASSESSING ADHERENCE OF ADHESIVE NANODISPERSIONS

LAURENTIA ALEXANDRESCU[1], MIHAI GEORGESCU[1], MARIA SONMEZ[1], MINODORA LECA[2], ZENOVIA MOLDOVAN[2]

[1] *INCDTP – Division: Leather and Footwear Research Institute, 93 Ion Minulescu St., Sect. 3, 031215-Bucharest, Romania, email: icpi@icpi.ro, laura_alexandrescu@yahoo.com*

[2] *University of Bucharest, Faculty of Chemistry, Department of Analytical Chemistry, 4-12 Regina Elisabeta Blvd., Sect. 3, 030018-Bucharest, Romania, email: minodora.leca@yahoo.com, z_moldovan@yahoo.com*

The possibility of obtaining adhesives showing bonding characteristics superior to those of the classic adhesives, a good bonding strength at high temperature and humidity resistance, which could be used for a variety of supports was studied. The chemical grafting technique has been experimented based on the chained radical mechanism of directed transformation of the structure and properties of the elastomer used in the study, namely chloroprene elastomer. The evaluation of adhesiveness of ecologic adhesive nanodispersions based on elastomer grafted on supports with varied structures, specific to the footwear field, is presented. Dispersions obtained were tested rheologically, physically, mechanically, and in terms of peel resistance according to standards in force.

Keywords: chemically grafted polychloroprene, nanodispersions, adhesive.

INTRODUCTION

A contact adhesive is an adhesive dry to touch but instantaneously adherent to a surface at contact. The classic example is the chloroprene rubber in organic solvents (Harshorn, 1986; Mittal, 1999). Such adhesive relies on the auto-adhesive characteristics of the dried polymer, often enhanced by resin modification. This resulted in the enlargement and diversification of adhesive production, allowing the development of adhesives with the best preset characteristics for manufacture and application. But, in addition to their rheological and bonding strength characteristics, adhesives have to show no toxicity, flammability and environmental pollution (Nielsen & Schneberger, 1983; Schields, 1984).

Due to its characteristics, the polychloroprene rubber is the raw material of choice for the adhesives based on volatile organic compounds (VOCs), used also in the footwear manufacture. This has led to a large number of studies to improve the adhesive performances of polychloroprene. Operations such as grafting of the polychloroprene chains to improve the initial and final bonding strength characteristics and dispersing in water at the nanometric scale to decrease toxicity were investigated. Due to the tiny particles such products will penetrate deeply the support and show high solid contents, leading to an outstanding binding to the rough supports. This class of products represents the most innovative substitution of VOCs adhesives (Clemens, 2009; Cheung, 2009, Selic, 2010).

Improving of adhesion strenght of polychloroprene by chemical grafting with methyl methacrylate in the presence of benzoyl peroxide as initiator, characterization of the obtained adhesive dispersions from structural, particle size, particle size distribution and bonding capacity points of view and increasing of adherence by their mixing with colophony resin, Desmodur RE (triphenylmethane triisocyanate solution 27% in ethyl acetate) and their mixture in equal amounts as cross-linking agent are presented into the present paper.

EXPERIMENTAL PROCEDURE

Materials

Polychloroprene NEOPRENE AD 20, (DuPont) as polymer; methyl methacrylate (Merck, Germany) as monomer; benzoil peroxide as initiator and dodecylmercaptan as inhibitor (both Sigma-Aldrich Chemie, Germany), ZnO,MgO, as cross-linking agent and to consume the HCl eliminated during the reaction; diphenylamine derivative as antioxidant (the last three Bayer, Germany); polyvinyl alcohol and triethanolamine as dispersion and pH stabilizer (Merck, Germany); natural resin colophony (Caroco, Bulgaria) as adherence improver, and Desmodur RE – triphenyl methane triisocyanate 27% in ethyl acetate as cross-linking agent (Bayer, Germany) were used.

Procedure

The technology involves three phases: (Knecht et al., 2008; Hearn et al., 2000; Kuptsov et al., 1998) chemical grafting of elastomer with methyl methacrylate on roller using formulations presented in Table 1 followed by dissolving the resulting composition into a convenient solvent and dispersing solutions in water containing steric and electrostatic stabilization agents, as well as pH adjustment agents. The laboratory roll with water-cooled cylinders was used for grafting.

The roller mixing regime was the following:

- plasticizing the elastomer - 4 min;
- introducing benzoil peroxide and grafting agent (MMA), ZnO, MgO - 40 min;
- styrenated phenol, cooling and adding dodecyl mercaptan -10 min;
- homogenisation and removing the mixture from the roll in thin sheets - 5 min;
- total: 54-59 min;

Roller homogenisation time of mixtures was very high, in order to amplify the grafting effect.

The mixing process is difficult because the rolls hinder processing due to friction forces and may cause cyclization of elastomer. These difficulties can be avoided by strongly cooling the rolls, reduced friction and rotational speed (1:1.5 and 25-30 rpm), as well as by a small distance between the rolls.

Given the small amounts tested at laboratory scale, a heating nest fitted with stirrer was used.

Compositions B0-B3 resulting from roller processing were dissolved in a mixture of methylene chloride/ethyl acetate 30/70 in volume, and resulting solutions were dispersed in aqueous medium.

Dissolving was done as follows: the sample was introduced in a glass flask, the solvent mixture was added, the stirrer was adapted to the reaction vessel. Stirring was done with a constant speed of 300 rotations/min. Stirring continued for 1.5-2.0 h.

The formulations from Table 1 were used and the dispersions B0-B3 resulted (Celina et al., 2000; Mas Haris et al., 2008).

Table 1. Formulations for the adhesive dispersions obtained by chemical grafting

Components, g	B0	B1	B2	B3
Polychloroprene rubber	200	200	200	200
Benzoil peroxide	-	1	1	1
Methyl methacrylate	-	20	30	40
Zinc oxide	10	10	10	10
Magnesium oxide	8	8	8	8
Styrenated phenol	4	4	4	4
Dodecyl mercaptan	-	2	2	2
Total	222	245	255	265

Components in Table 1 were introduced drop by drop in the elastomer solution for 1 h, and dispersions are presented in Table 2.

Table 2. Formulations used to obtain adhesive dispersions by dispersing solutions of compounds B0-B3 (mass parts)

Components	B0	B1	B2	B3
Compound	46.25	50.99	53.07	55.17
Solvent mixture	33.75	29.01	26.93	24.83
Polyvinyl alcohol, aqueous solution 10%	50	50	50	50
Triethanolamine	15	15	15	15
Demineralized water	80	80	80	80
KOH, solution 10%	1	1	1	1
Total	226	226	226	226

The dispersions were characterized by the percentage of solids, free monomer and polymethyl-metacrylate, flowing time through Ford cup and pH. The obtained values are given in Table 3.

Table 3. Characteristics of dispersions B0-B3

Characteristic/dispersion	B0	B1	B2	B3
% Solids	48,58	52,06	53,64	57,59
% Free monomer	0,00	0,03	0,06	0,1
% Polymethylmethacrylate	0,00	0,10	0,14	0.2
Flowing time Ford cup, s	18	17	19	20
pH	13	13	13	13

To improve the bonding capacity colophony resin or/and Desmodur RE were introduced into the above dispersions.

The resin was previously pre-reacted with magnesium oxide to transform it into a resin with high melting point (higher than 250°C), which increases the adhesive film resistance to high temperatures. 100g resin was dissolved in toluene (100 g) under stirring (200 rpm) until all the resin was dissolved then 10 g of magnesium oxide and 1 g of demineralized water were added. The solution was conditioned for 24 h at room temperature.

The resin solution, cross-linking agent or their mixture in equal amounts (w/w) were introduced directly into dispersions, the amounts being 5, 10 and 15 g to 100 g.

Testing Methods

The adherence was measured according to SR EN 1392:2006 standard, test known as “peeling test at (23 ± 2)°C”. The following supports were used: (a) mixture of standard rubber, hardness 85°ShA; (b) cotton cloth; (c) linen; (d) leather; (e) split leather; (f) synthetic leather. The steps used were the following: preparing of support by polishing to increase the roughness when standard/standard samples were jointed, application of the adhesive, drying, jointing of test samples, conditioning and peeling measurements.

The adhesives were applied by brushing as monolayer on rubber support and as bilayer on textiles, split and synthetic leather. The drying was done in separated rooms, equipped with devices for vapor absorption. The open time ranged between 15 min and 1-2 h, depending on the absorptive properties of supports. The drying time was reduced by preheating the supports at 70°C.

After drying the supports were joined and pressed down for 30 s at 3.5-4.0 atm, then conditioned according to the European standard EN 1391 (24 and 72 h respectively at the standard temperature of 23 ± 2°C, 3 h at 50°C and 168 h at 70°C, the last two temperatures to produce accelerated aging).

The peeling test was done using a dynamometer after 24 h for the samples conditioned at room temperature, immediately for those heated at 50°C and after 24 h for those heated at 70°C.

RESULTS AND DISCUSSION

Bonding capacities were determined for the dispersions B0-B3, as well as for those containing some additives to optimize the adherence: colophony resin, cross-linking agent Desmodur RE (triphenylmethane triisocyanate solution 27% in ethyl acetate) as well as their mixture in equal amounts in volume.

The resin and cross-linking agent solutions were prepared separately and dozed directly into the adhesive dispersions, the ratio resin/dispersion being 5/100. Increasing of the ratios to 10/100 or 15/100 does not modify practically the peeling resistance. The peeling resistances for the initial and modified dispersions are given in Tables 4-7.

Table 4. Peeling resistance, N/mm, for B0 dispersion and B0 with additives, conditioned at different times

Dispersion/ support	24h						72 h	168 h	72h/3h at 50°C, immediate peel	72h/168hx70°C, peel after 24h
	St/ St	St/ leath	St/ split	St/ len	St/ cotton	St/ synt. leat	Cs/ Cs	Cs/ Cs	Cs/Cs	Cs/Cs
B0	0,3	0,3	0,5	0,6	0,5	0,4	0,5	0,4	0,4	1,0
B0 5% Desmodur RE	0,3	0,4	0,6	0,5	0,6	0,4	0,6	0,5	0,5	1,0
B0+5% resin	0,4	0,5	0,9	0,6	0,6	0,6	0,4	0,4	0,3	0,5
B0+5% Desmodur RE+ 5% resin	0,7	0,4	0,5	0,8	0,5	0,5	0,5	0,5	0,3	0,8

Table 5. Peeling resistance, N/mm, for A1 dispersion and A1 with additives, conditioned at different times

Dispersion/ support	24h						72 h	168 h	72h/3h at 50°C, immediate peel	72h/168h x70°C, peel after 24h
	St/ St	St/ leath	St/ split	St/ len	St/ cotton	St/ synt. leat	Cs/ Cs	Cs/ Cs	Cs/Cs	Cs/Cs
B1	0,6	0,6	0,8	0,7	0,7	0,5	0,6	0,5	0,7	1,3
B1+5% Desmodur RE	0,7	0,8	0,9	0,6	0,6	0,6	0,7	0,5	0,6	1,4
B1+5% resin	0,6	0,8	1,1	0,9	1,0	0,7	0,9	0,5	0,4	0,7
B1+5% Desmodur RE +5% resin	0,9	1,2	0,8	0,9	0,7	0,8	0,5	0,6	0,7	1,1

Table 6. Peeling resistance, N/mm, for A2 dispersion and A2 with additives, conditioned at different times

Substrates	24h						72 h	168 h	72h/3h la 50°C, immediate peel	72h/168h x70°C, peel after 24h
	St/ St	St/ leath	St/ split	St/ len	St/ cotton	St/ synt. leat	Cs/ Cs	Cs/ Cs	Cs/Cs	Cs/Cs
B2	0,8	0,7	0,9	1,2	0,8	0,8	0,9	0,6	1,1	1,5
B2+5% Desmodur RE	0,8	0,4	1,1	1,2	1,0	1,2	0,9	1,3	0,8	2,1
B2+5% resin	0,9	0,5	0,6	0,8	0,7	0,7	0,5	0,5	0,4	0,7
B2+5% Desmodur RE +5% resin	1,2	1,5	1,3	1,7	0,9	1,0	0,5	0,9	1,0	1,8

Table 7. Peeling resistance, N/mm, for A3 dispersion and A3 with additives, conditioned at different times

Substrates	24h						72 h	168 h	72h/3h la 50°C, immediate peel	72h/168hx 70°C, peel after 24h
	St/ St	St/ leath	St/ split	St/ len	St/ cotton	St/ synt. leat	Cs/ Cs	Cs/ Cs	Cs/Cs	Cs/Cs
B3	3,1	0,2	2,4	1,5	3,8	0	3,9	5,1	2,7	5,6
B3+5% Desmodur RE	3,6	0,4	2,2	5,2	3,7	0	5,5	7,2	2,5	6,1
B3+5% resin	2,6	2,0	2,5	2,6	2,7	1,0	3,1	3,9	3,5	5,5
B3+5% Desmodur RE +5% resin	5,9	0,5	3,4	8,3	5,3	0,3	4,3	6,0	2,2	8,0

The four tables emphasize the following influences of grafting and of additives:

- grafting of methyl methacrilate onto polychloroprene chains increases the adherence with 15-40%, depending on support and monomer amount, their peeling resistance being very close or even higher than those of the solvent-based adhesives on support as leather, split leather, linen and cotton cloth (higher than 3 N/mm);
- colophony resin, Desmodur RE and blend resin/Desmodur RE, increases significantly the adherence of all the dispersions on all the supports;
- high values of the adherence were obtained at 50 and 70°C, which suggests that the dispersions in which the polychloropren is grafted with methyl methacrilate give very resistant binding at higher temperature.

CONCLUSIONS

High performance environmentally friendly aqueous adhesive nanodispersions for shoe manufacture were obtained by chemical grafting of polychloroprene using benzoyl peroxide as initiator and colophony resin or/and Desmodur RE as adhesion improvers.

Peeling resistance is higher for dispersions containing grafted polychloroprene with, it increases with monomer amount and depends on the nature of substrate to which the standard rubber is bonded.

The colophony resin increases the adherence, especially for the non-grafted polychloroprene dispersion, the values depending also on the nature of substrate.

The increase of the peeling resistance produced by the cross-linking agent is lower than that given by resin, while the mixture of adherence increasers is effective only in some cases.

Accelerated aging for 3 h at 50°C produces a slight increase of peeling resistance for some dispersions and decreasing for others.

Aging for 168 h at 70°C increases the adherence in all the cases between about 1.2 and 12.3 times, depending on the degree of polychloroprene grafting and the nature of the adhesion improver used. Introduction of resin and Desmodur RE in dispersion B2 gives bond resistances higher than the cohesion of standard rubber.

The dispersions obtained by chemical grafting of polychloropren latex are stable for 30 to 40 days but the technology is time and money consuming.

The obtained adhesives dispersions, and especially B2, are very adequate for manufacturing of footwear resistant to high temperatures.

REFERENCES

Alexandrescu, L., Ficai, M., Leca, M., Moldovan, Z. (2010), *Leather and Footwear Journal*, 10(1), 63.

Celina, M., Clough, R.L., Gillen, K.T., Ottesen, D.K., Wise, J. (2000), *Polym. Degrad. Stab.*, 68, 171.

Cheung, J.., Yu, J., Wong Duo, W. Zhang, M., (2009), *Footwear Science*, 1, 31-46, Plenum Press, New York.

Clemens, M., Heaming, E.M., Thorsten, S. (2009), *Footwear Science*, 1(5), Canada.

Hearn, J., Steward, P.A., Wilkinson, M.C. (2000), *Adv. Colloid Int. Sci.*, 86, 195.

Knecht, R., Mark, A.E., Marrink, S.J., Risselada, H.J. (2008), *J. Col. Int. Sc.*, 318(2), 477.

Kuptsov, H., Zhizhin, G.N. (1998), *Handbook of FTRI Spectra of Polymers*, Elsevier, Amsterdam.

Mas Haris, M.R.H, Kathiresan, S., Mohan, S. (2008), *Asian. J. Chem*., 20, 4511.

Mittal, R.L., Pizzi, A. (1999), *Handbook of Adhesives Technology*.

Nielsen, P.O., Schneberger, G.L. (1983), *Adhesive Manufacturing*, Dekker, New York.

Selic (2010), Technical information, Chemical Company Limited, Thailand.

Schields, J. (1984), *Adhesives Handbook*, Third edition, Butterworths, London.

INFLUENCE OF RETANNING MATERIALS WITH DIFFERENT ROPERTIES ON THE FLAMMABILITY OF LEATHER

FAN CHENG[1,2], LINGYUN JIANG[1], WUYONG CHEN[1,2], CARMEN CORNELIA GAIDAU[3], LUCRETIA MIU[3]

[1] *National Engineering Laboratory and for Clean Technology of Leather Manufacture, Sichuan University, Chengdu 610065, P. R. China, email: ffffcheng2008@163.com*

[2] *The Key Laboratory of the Education Ministry of Leather Science and Engineering, Sichuan University, Chengdu 610065, P. R. China, email: wuyong.chen@163.com*

[3] *INCDTP - Division: Leather and Footwear Research Institute, 93 Ion Minulescu St., sector 3, 031215 Bucharest, Romania, email: carmen_gaidau@hotmail.com*

During leather making, plenty of materials were added to the hide fiber in some treatments including tanning, retanning and fatliquoring. Most of these processes and materials would impact the flammability of leather. In this paper, effects of retanning agents on leather flammability were emphatically discussed. First, six retanning agents were selected, including chromitan, vegetable tannin, glutaraldehyde, syntans and organophosphorus agent, to treat cattle wet blue with routine processes. Then the flammability of the retanned and the control leather was evaluated by vertical flame test, oxygen index test and smoke density test. The surface area of the retanned leather was also measured by nitrogen adsorption method. The results show that the effect of different properties of retanning agents on leather flammability varies greatly. This is mainly due to three aspects, the combining ways between retanning agents and leather fibres, the filling ability of retanning materials to leather and the flame resistant element contained in retanning agents. These results may offer some guidance for the choices of retanning agent for fire-resistant leather.

Keywords: retanning materials, leather, flammability.

INTRODUCTION

To make animal skins into finished and utility leathers, skins have to be treated with many processes including soaking, degreasing, unhairing, liming, pickling, tanning, retanning, fatliquoring and finishing. During these processes, many sorts of materials were added in the leather system and therefore would influence the flammability of leather. Among those treatments, retanning is one of the most important factors that affect fire retardance of leather (Donmez and Kallenberger, 1992). At present the effects of tanning (Chen et al., 2007), retanning (Huang et al., 2005), fatliquoring (Huang et al., 2006) and finishing (Gong et al., 2007) on the flammability of leather were studied in domestic. But the effect of retanning was only studied with different retanning agent dosages and the results obtained were exhibited without analyzing the relation between the properties of retanning material and the fire-resistance of leather. In this experiment, six common kinds of retanning agents with different properties were selected to treat the cattle wet blue. Then the flammability of the retanned leathers and the control samples was measured by vertical flame test (ALCA Method E 50), oxygen index test (OI) (ASTM D 2863-77) and smoke density test (GB/T 8627-1999). During the test, we used precise sampling and extra mechanical treatment to eliminate the influence of region difference of wet blue and mechanical action on the result and to obtain a more accurate consequence.

EXPERIMENTAL

Materials

Cattle Wet-blue, tanned with routine method, was shaved to a thickness of 1.2 mm. The six retanning agents were commercial products and their properties are shown in Table 1 and Table 2.

Table 1. Six retanning agents selected in the experiment

Name	Category	Basic parameter		Manufacturers
		Active ingredients	Content	
Chromitan	Mineral tanning agent	Cr_2O_3	23%	Chemical industry Chongqing, China
Mimosa tannin	Vegetable tannin	Tannin	68%	Fine chemical industry, Sichuan, China
Modified glutaraldehyde	Glutaraldehyde	Glutaraldehyde	≧45%	Organic Limited Corporation, Wuhan, China
Relugan RE	Acrylic resin	Acrylic copolymer	40%	BASF
Basytan AN	Aromatic syntan	Aromatic sulfonic condensate	96%	BASF
Granofin F-60	Organophosphorous	Tetrakis(hydroxyl methyl) phosphonium salt	75%	Clariant

Table 2. Properties of retanning agents

Name	Effective retanning group	Main combining ways to leather fibres	Filling ability*	Fire-resistant element
Chromitan	Chrome complex ion	Coordinate bonds	+	none
Mimosa tannin	Phenol hydroxyl group	Multi-point hydrogen bonds	+++	none
Modified glutaraldehyde	Aldehyde group	Covalent bonds	+	none
Relugan RE	Carboxyl and hydroxyl group	Hydrogen and electrovalent bonds	++	none
Basytan AN	Sulfonic and hydroxyl group	Hydrogen and electrovalent bonds	++	none
Granofin F-60	Hydroxyl group	Hydrogen and covalent bonds	+	phosphorus

*The number of “+” represents the filling ability and the filling ability ranks as: “+++” > “++” > “+”.

Preparation of Retanned Leather Samples

12 sample pieces (35 cm x 40 cm) were symmetrically cut from the part next to the back bone of the cattle wet blue. The six samples from the right part were weighed and

then retanned with 4% different retanning agents based on the weight of the single sample. The final retanned leathers were marked as A_1, B_1, C_1, D_1, E_1, F_1, respectively. Matched pieces from the left part were taken for the control samples and marked with A_0, B_0, C_0, D_0, E_0, F_0, respectively. The control samples were treated with the same operation but without adding retanning agent.

After retanning, all the samples were separately thrown into a drum and treated in a 300% float for 3 h at 30°C to eliminate the effect of mechanical action on the flammability test results. After that they were dried and then stretched flat.

Sampling for Flammability Test

A set of samples, including 5 pieces for the vertical flame test, 5 pieces for oxygen index test and 3 pieces for smoke density test were taken from each retanned and control leather piece. The samples for the vertical flame test were 51 mm by 317.5 mm, and their long axis was perpendicular to the backbone. Oxygen index test samples were 52 mm by 140 mm and samples for smoke density test were 50 mm by 52 mm. The prepared samples were stored in a chamber at 20±1°C and 65±2% relative humidity for 48 h and then the thickness of each sample was measured.

Flammability Test

The vertical flame, the oxygen index and the smoke density of all the samples were tested according to ALCA Method E50, ASTM D 2863-77 and GB/T 8627-1999 respectively.

Determination of Surface Area of Leather

The samples were cut into small particles and 0.3 ~ 0.5 g were taken respectively for the measurement according to GB/T19587-2004.

RESULTS AND DISCUSSIONS

Vertical Flame and Oxygen Index Analyses

The lower the vertical flame test indexes, including after-flame, after-glow, char length and weight loss, the better flame resistance of leather. The oxygen index (OI) indicates the minimum concentration of oxygen needed to keep the sample burning. The greater the oxygen index the more difficult the burning.

The vertical flame test and OI test results are shown in Table 3 and Table 4. According to the early study (Huang Zan et al., 2005) the flame resistance of leather was usually weakened after retanning. However from the results in this experiment, the flammability of leather retanned with chromitan and modified glutaraldehyde was almost unchanged. This is possibly because the combining ways between retanning materials and leather fibres are coordinate bonds and hydrogen bonds respectively, which are very stable. For mimosa tannin retanned leather, the weight loss and char length increased by 14.6% and 22.6% respectively, because of the unfirm hydrogen bonds between tannin extract and leather fibre. However, the OI value increased by 7% too, mainly because the filling ability of tannin to leather was very strong, which prevented the circulation of air in leather. For Relugan RE and Basytan AN retanned leather, the OI values were decreased and the after flame and after glow times were increased, indicating that both of the acrylic resin and the aromatic syntan weakened the fire-resistance of leather. However, the after flame and after glow of leather retanned with Granofin F-60 which containing tetrakis (hydroxymethyl) phosphonium salt (THP) decreased to zero. And the OI value increased to 30.3% which reflected the better flame retardance of organic phosphorus retanned leather. The explanation for this phenomenon is that Granofin F-60 contains THP salt which is always used as a flame retardant in some field.

Table 3. Vertical flame test results

Retanning agent		Thickness (mm)	After flame (s)	After glow (s)	Weight loss (%)	Char length (cm)
Chromitan	0%	0.879	0.91	13.48	4.26	0.81
	4%	0.900	0.50	145.45	4.72	1.23
Mimosa tannin	0%	1.062	1.02	12.49	3.02	0.53
	4%	1.235	1.09	58.22	3.46	0.65
Modified	0%	1.129	0.80	11.73	3.37	0.57
Glutaraldehyde	4%	1.134	0.44	9.20	3.51	0.54
Relugan RE	0%	1.167	0.82	32.66	3.14	0.60
	4%	1.300	2.09	19.56	2.99	0.55
Basytan AN	0%	0.995	0.64	15.19	4.07	0.70
	4%	1.064	0.80	29.47	3.70	0.72
Granofin F-60	0%	1.198	0.33	9.56	3.14	0.42
	4%	1.238	0	0	2.81	0.33

Table 4. Oxygen index test results

Retanning agent		Chromitan	Mimosa tannin	Glutaral-dehyde	Relugan RE	Basytan AN	Granofin F-60
Thickness	0%	1.086	1.125	1.060	1.120	1.020	1.150
(mm)	4%	1.112	1.280	1.085	1.285	1.040	1.220
OI	0%	27.3	27.0	27.1	26.8	27.0	27.9
(%)	4%	28.3	27.5	27.3	26.4	26.3	30.3

Surface Area

According to the test, there is a relation between surface area and flammability of leather. The smaller the surface area, the tighter the leather fibre and the more disadvantageous to leather interior air flow. As it can be seen in Figure 1, surface area of mimosa extract retanned leather is the smallest, 1.9756m^2/g, which indicates the best filling ability of vegetable tannin. Based on this characteristic, permeability of oxygen in this leather sample is prevented and high OI is obtained which is consistent with the oxygen index test results. Following after tannin retanned leather are leathers retanned by acrylic resin and systan, whose surface areas are 2.0815m^2/g and 2.1572m^2/g, respectively. On the contrary, glutaraldehyde and Granofin F-60 retanned leathers have larger surface areas, indicating that the filling abilities of organic phosphorus and glutaraldehyde are not good when they are solely used in retanning process. Besides, the increase of leather thickness after retanning, as detailed in Table 3 and Table 4, reflects the filling ability of retanning agents too.

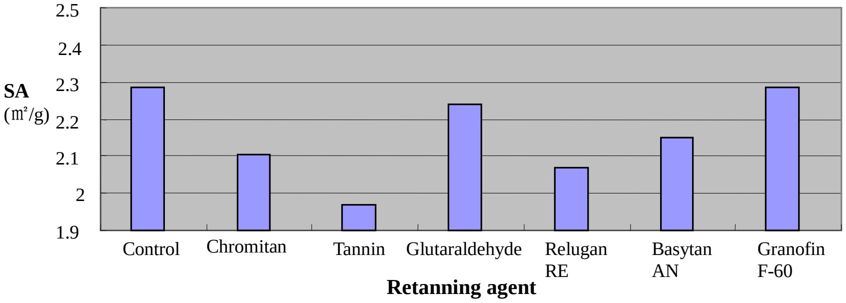

Figure 1. Surface area of retanned samples

Smoke Density

Smoke is one of the most serious risk factors in fire disasters. “Flame retardancy” and “smoke suppression” are equally important requirements to the flame retardant materials. But they often contradict each other. Generally, materials generate less smoke when they can burn easily and completely. Smoke is dangerous in fire disasters which keeps people from evacuating and results in suffocating. The larger the smoke density the shorter the fire fighting time left. So the smoke density is another important factor to investigate the fire-safety of leather.

The smoke density results are shown in Table 5. The smoke density of chrome and glutaraldehyde retanned leather reduced by 12.2% and 9.8%, respectively. Glutaraldehyde is an aliphatic hydrocarbon compound and many oxygen elements exist on its main chain, resulting in completely burning out during a fire with little smoke released. After retanning with mimosa extract or acrylic resin or aromatic syntan, the smoke density of leather increased, especially with acrylic resin which increased by 30%. This is because materials containing many olefins and side chains usually produce much smoke as they can form carbon grains through cyclization and polycondensation in fire (Ou Yuxiang, 2002). It is worth mentioning that, leather retanned with Granofin F-60 obtained good flame retardant results as can be seen from the vertical flame test and OI test. Furthermore, the smoke density of this retanned leather was also small which showed that the organic phosphorus retanning was beneficial for leather in fire disaster prevention.

Table 5. Smoke density results

Retanning agent		Chromitan	Mimosa tannin	Glutaral-dehyde	Relugan RE	Basytan AN	Granofin F-60
Thickness	0%	0.956	1.083	1.082	1.118	0.996	1.176
(mm)	4%	1.036	1.214	1.095	1.253	1.141	1.202
Smoke	0%	49	48	51	50	49	51
Density (%)	4%	43	53	46	65	53	49

CONCLUSIONS

The flammability of leather retanned with different retanning agents is variable, because of the different properties of the retanning materials. The performance of the three properties of retanning agents on the flame resistance of leather can be ranked as: the flame resistant element ﹥ the filling ability﹥ the combining ways. Despite of the smoke density, the fire resistance of various retanned leather can be ranked as: Organophosphorous﹥ tannin extract﹥chromitan﹥ glutaraldehyde﹥ acrylic resin﹥ aromatic syntan. When smoke density is taken into consideration, it may be ranked as: Organophosphorous﹥ chromitan﹥ glutaraldehyde﹥ tannin extract﹥ aromatic syntan ﹥ acrylic resin. So, in order to make leathers with good fire retardancy, it is significant to use the retanning agent with flame resistant element, better filling ability as well as stable combining way to leather fibre.

Ackowledgements

The authors wish to thank Ministry of Science and Technology of China for the project of Co-operation in Science and Technology between Romania and China (item No. 2009DFA42850 and No.40-3).

REFERENCES

Chen, W. et al. (2007), "Influence of Tanning on the Flammability of Leather", *Journal of the Society of Leather Technologist and Chemists*, 91, 159-161.
Donmez, K. and Kallenberger, W. E. (1992), "Flame Resistance of Leather", *Journal of the American Leather Chemists Association*, 87, 1-19.
Gong, Y. et al. (2007), "Influence of Finishing on the Flammability of Leather", *Journal of the Society of Leather Technologist and Chemists*, 91, 208-211.
Huang, Z., Li, L. and Chen, W. (2006), "Influence of Fatliquoring on the Flammability of Leather", *Journal of the Society of Leather Technologist and Chemists*, 90, 155-158.
Huang, Z., Li, L. and Chen, W. (2005), "Influence of Retanning on the Flammability of Leather", *China Leather*, 34(3), 1-4.
Ou, Y. (2002), *Practical Flame Retardant Technology*, Chemical Industry Publishing House, Beijing.

FLOCCULANT MATERIALS BASED ON ACRYLAMIDE AND SODIUM ACRYLATE OBTAINED BY COPOLYMERIZATION WITH ELECTRON BEAM

GABRIELA CRACIUN, ELENA MANAILA

National Institute for Laser, Plasma and Radiation Physics, Electron Accelerators Laboratory, 409 Atomistilor St., 077125 Magurele, Romania, e-mail: gabriela.craciun@inflpr.ro

The goal of the paper is to present some physical and chemical characteristics of polymeric materials obtained by electron beam irradiation. These polymeric flocculants resulting from the copolymerization process of acrylamide and sodium acrylate are environmentally friendly and have the following characteristics: high conversion coefficient $C_c > 90\%$, low residual monomer concentration $M_r < 0.05\%$, high intrinsic viscosity $\eta_{intr} > 6$ dl/g, low linearity coefficient $k_H < 1$ and good water solubility. These characteristics are always associated with a minimal toxicity and a high capacity of advanced coagulation or flocculation. The ability to initiate chemical reactions and therefore material changes at room temperature, brought unique advantages for radiation technology: (1) almost 100% efficiency in the conversion of the raw material into finished materials (the process is practically free of wastes); (2) reduction of the production time by tens to hundreds times; (3) material characteristics that cannot be achieved by the traditional processes; (4) good adaptability to the highest exigencies for the environment quality because of no release of secondary reaction products; (5) adaptability to any automation level (technological line speeds of 500 m/min can be used) and strict process control; (6) energy saving, frequently 20-30 times less energy than in the classical heating and traditional processes.

Keywords: flocculants, copolymerization, acrylamide, sodium acrylate, electron beam.

INTRODUCTION

The fact that water is the most important material used by mankind defines the importance of water purification. Wastewater and industrial effluent treatment require removal of suspended solids for purification and possible re-usage. The removal can be accomplished by gravitation (very slow), by coagulation (dependent on electric charge situation) and by flocculation (not dependent on electric charges and the fastest).

Flocculation is caused by the addition of minute quantities of chemicals known as flocculants. There are two types of flocculants: organic and inorganic. Inorganic flocculants are substances with multivalent cations such as aluminum, iron, calcium or magnesium. Examples of inorganic flocculants are polyaluminium chloride (PAC), which is the most common in use, aluminum sulfate, calcium hydroxide, iron (II) sulfate, iron (III) sulfate etc. Organic flocculants can be divided into two categories: (1) organic polymers (chitosan, gelatin, guar gums and alginates); (2) synthetic polymers: anionic, cationic and non-ionic (polyacrylamide and poly(ethylene oxide), polyelectrolytes derived by introducing quarternary ammonium, polymers containing carboxyl groups and sulfonic acid groups). Both inorganic and organic flocculants are in use. Among the inorganic flocculants, are applied most often - in high concentrations (Brostow et al., 2009). Inorganic flocculants are used in very large quantities, they leave large amounts of sludge and are strongly affected by pH changes. Organic flocculants are typically polymeric in nature; by contrast to inorganic ones, they are effective already in ppm concentrations. Both synthetic and natural water-soluble polymers are used as flocculants.

The goal of the paper is to present some physical and chemical characteristics of polymeric materials (flocculants) obtained by electron beam irradiation. These materials are included in water soluble polyelectrolyte class (organic materials), which are destined to totally or partially replace (in the range of 50% to 75%) classical electrolytes (inorganic materials such as ferric chloride, aluminum sulfate or calcium carbonate). The acrylamide copolymers are used as coagulation aids for wastewater and potable water treatment (polyacrylamides with very low residual monomer contents) (Edzwald, 1993; Fetting et al., 1991; McCormick et al., 1990; Martin et al., 1995). Results obtained both by fundamental studies and in pilot stations and industrial plants, point out the efficiency of the electron beam irradiation as a material processing method, because it is able to induce physical and chemical reactions, in most cases without catalysts and initiators (Martin et al., 1995; Martin et al., 1996; Zuga et al., 2007; Craciun et al., 2011). Mainly, polymerization with ionizing radiation is similar to conventional polymerization, by free radical addition. The initiation step involves, in both cases, the admittance of some external energy that is initiation energy. The subsequent steps of propagation, termination and chain transfer are similar to a chemically catalyzed process. In the radiation-induced polymerization, a completely inert component does not exist and therefore, any substance added to the monomer radiolizes because absorption of ionizing radiation is a purely electronic process and this leads to production of free radicals. Thus, for polymerization in solution, primary radicals are formed from the monomer, but also from the initiator and solvent.

EXPERIMENTAL

Materials

For flocculants obtaining the following materials were used: acrylamide (molar mass 71.08 g mol^{-1}; density 1.13 g/cm^3; solubility in water 2.04 kg/L at 25°C); acrylic acid (molar mass 72.06 g mol^{-1}; density 1.051 g/mL; solubility in water: miscible); sodium hydroxide (molar mass 39.99 g mol^{-1}; density 2.13 g/cm^3; solubility in water 1110 g/dm^3 at 20°C); sodium chloride (molar mass 58.44 g mol^{-1}; density 2.165 g/cm^3; solubility in water 359 g/dm^3 at 20°C); sodium formate (molar mass 68.01 g mol^{-1}; density 1.92 g/cm^3; solubility in water 97 g/100 mL at 20°C) - serves as chain transfer agent in the copolymerization process) and potassium persulfate (molar mass 270.322 g mol^{-1}; density 2.477 g/cm^3; solubility in water 1.75 g/100 mL at 0°C), - serves as initiator in the copolymerization process. All materials were procured from E-Merck, Germany. (Note: Acrylic acid reacts with sodium hydroxide to form sodium acrylate).

Preparation and Irradiation of the Samples

For the preparation of acrylamide-sodium acrylate monomer solution, 360 g of acrylamide, 40 g of acrylic acid, 22.22 g sodium hydroxide and 80 g of sodium chloride were dissolved in 1000 mL distilled water. Initiator, potassium persulfate (0 and 1.5 ml) and chain transfer agent, sodium formate (0.75 ml) are added and then, this mixture is irradiated with electron beams at room temperature.

Experiments were carried out with an experimental installation consisting mainly of the following units: an electron linear accelerator (ALIN-10) of 6.23 MeV energy and 75 mA peak current of the electron beam and an irradiation chamber containing the samples of monomer solution. Electron beam dose rate was fixed at 2.4 kGy/min (for a series of samples) and 1.2 kGy/min (for another series of samples) in order to accumulate doses between 0.4-1.6 kGy. We have established certain irradiation doses (between 0.4 and 1.6 kGy) which were collected at two different irradiation dose rates in order to study also the effect of the irradiation dose rate on the final product properties because it is well known that the electron beam effects are related to the absorbed dose (D) expressed in Gray or J kg^{-1} and absorbed dose rate (D*) expressed in Gy s^{-1} or J kg^{-1} s^{-1}.

Methods for the Physical and Chemical Characteristics Determination

Polyelectrolytes (flocculants) water solubility and flocculation ability are strictly related to their physical and chemical characteristics such as: conversion coefficient (C_c), residual monomer concentration (M_r), intrinsic viscosity (η_{intr}) and linearity coefficient expressed by Huggin's constant (k_H) and our interest was focused on the optimization of these physical-chemical characteristics.

The conversion coefficient (C_C) and the residual monomer concentration (M_r) are determined based on the bromation reaction of the double-bond (Dimonie et al., 1986). The intrinsic viscosity (η_{intr}) and the Huggins' constant (k_H) are determined by the viscosimetry method, using a Hoppler BH-2 (Dimonie et al., 1986). Sodium nitrate was used as a solvent 1N ($NaNO_3$) and the working temperature was 30°C.

RESULTS AND DISCUSSION

Conversion coefficient (C_c), is the first important parameter in desired polyelectrolyte characterization and it is required to be higher than 90%. A high conversion coefficient is equivalent with a high monomer transformation efficiency in polymerization process and a substantial reduction of residual monomer concentration, M_r. This is particularly important because of the well known acrylamide toxicity in the monomer state. For the intrinsic viscosity, η_{intr}, we expected to obtain values over 6 dl/g, which means a linear polymer, without ramifications and with good water solubility. Regarding the linearity constant, k_H, we aim to obtain values below 1, because only in this case is solubility ensured, and a good flocculation of the polymer. Residual monomer concentration, M_r, has to be less than 0.05% for the polyelectrolite to be in accordance with rules established by the IPCS - International Programme in Chemical Safety in the document named "Environmental Health Criteria-49-Acrylamide". Thus, the acrylamide concentration in treated water should not exceed 0.1 μg/L according to the legislation.

In our experiments we have tested two types of monomeric solution: with and without initiator. We did this in order to determine the initiator influence on the flocculant obtaining process by electron beam irradiation. In this case we have also studied the irradiation dose rate effects on the final product properties choosing to accumulate the established irradiation dose of 0.4; 0.6; 0.8; 1; 1.2; 1.4 and 1.6 kGy at two different irradiation dose rates: 2.4 kGy/min and 1.2 kGy/min. The characteristics of the acrylamide-sodium acrylate acid copolymers may be influenced by the following factors: chemical composition of the solutions to be irradiated, absorbed dose level (D = energy quantity per unit mass in Gy or J kg^{-1}) and absorbed dose rate level (D* = energy quantity per unit mass and unit time in Gy/s or J kg^{-1} s^{-1}).

Figures 1-8 show the effect of irradiation dose and irradiation dose rate on the C_c, M_r, $\eta_{intr.}$ and k_H, in the presence and absence of initiator.

For all tested samples the conversion coefficient C_c increases slightly with the electron beam absorbed dose, independent of irradiation dose rate and of the presence or absence of initiator (Figures 1 and 2). We have observed that for the samples without initiator a minimum irradiation dose of 1.2 kGy is necessary in order to obtain values higher than 90%for C_c. Instead, for the samples containing initiator a minimum irradaition dose of 0.8 kGy is necessary in order to obtain values higher than 90% for the same parameter. We have also observed a reduction in irradiation dose necessary for the samples with initiator. Conversion coefficient, C_c is closely related to residual monomer concentration, M_r. Thus, for the samples that show high values of C_c (> 90%), Mr shows very low values < 0.015%, (Figures 3 and 4) and that coincides with the proposed purpose.

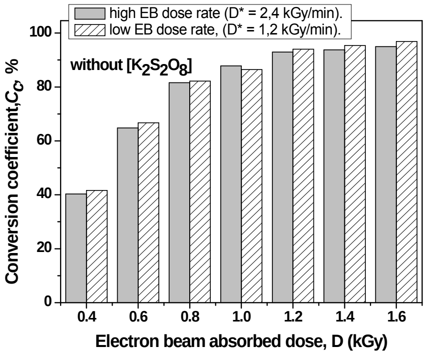

Figure 1. The irradiation dose effect on the conversion coefficient, C_c at high and low irradiation dose rates (2.4 kGy/min and 1.2 kGy/min) for samples without initiator [$K_2S_2O_8$]

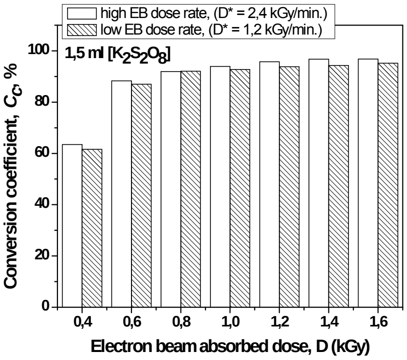

Figure 2. The irradiation dose effect on the conversion coefficient, C_c at high and low irradiation dose rates (2.4 kGy/min and 1.2 kGy/min) for samples with 1.5 ml initiator [$K_2S_2O_8$]

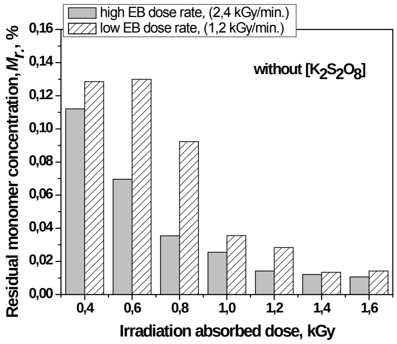

Figure 3. The irradiation dose effect on the residual monomer, M_r at high and low irradiation dose rates (2.4 kGy/min and 1.2 kGy/min) for samples without initiator [$K_2S_2O_8$]

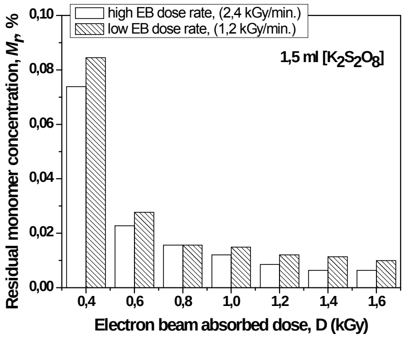

Figure 4. The irradiation dose effect on the residual monomer, M_r at high and low irradiation dose rates (2.4 kGy/min and 1.2 kGy/min) for samples with 1.5 ml initiator [$K_2S_2O_8$]

Unlike C_c and M_r, intrinsic viscosity η_{intr} and Huggin's constant k_H, remain sensitive to the initiator concentration variation for all used irradiation doses.

Usually, the intrinsic viscosity η_{intr} increases rapidly with electron beam absorbed dose increasing for all samples (with and without initiator), reaches a maximum and then decreases rapidly at lower irradiation doses and slower at higher irradiation doses (Figures 5 and 6).

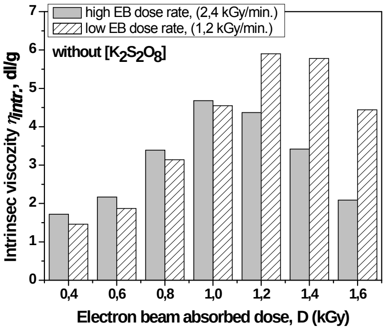

Figure 5. The irradiation dose effect on the intrinsic viscosity, η_{intr} at high and low irradiation dose rates (2.4 kGy/min and 1.2 kGy/min) for samples without initiator [$K_2S_2O_8$]

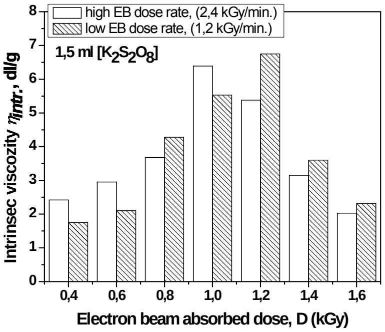

Figure 6. The irradiation dose effect on the intrinsic viscosity, η_{intr} at high and low irradiation dose rate (2.4 kGy/min and 1.2 kGy/min) for samples with 1.5 ml initiator [$K_2S_2O_8$]

For high D* (2.4 kGy/min), η_{intr} exhibits good values for samples obtained at low electron beam absorbed dose: both samples (with and without initiator) present the best values on same electron beam absorbed dose: 1 kGy (η_{intr}=4.69 dl/g and η_{intr}=6.39 dl/g, respectively). For low D* (1.2 kGy/min.), the same is noticed: both samples (with and without initiator) present the best values for η_{intr} on same dose of irradiation: 1.2 kGy (η_{intr}=5.38 dl/g and η_{intr}=6.75 dl/g, respectively). Huggin's constant k_H, follows the variation of intrinsic viscosity (Figures 7 and 8). Thus, it rises and falls with practically the same rate that intrinsic viscosity η_{intr}, falls and rises, depending on the electron beam absorbed dose.

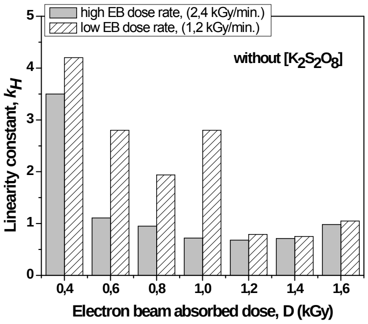

Figure 7. The irradiation dose effect on the linearity constant, k_H at high and low irradiation dose rates (2.4 kGy/min and 1.2 kGy/min) for samples without initiator [$K_2S_2O_8$]

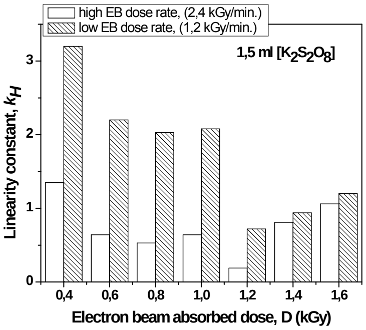

Figure 8. The irradiation dose effect on the linearity constant, k_H at high and low irradiation dose rates (2.4 kGy/min and 1.2 kGy/min) for samples with 1.5 ml initiator [$K_2S_2O_8$]

We can say that, by getting high values for the intrinsic viscosity $\eta_{intr,}$ minimum values are obtained for the linearity constant k_H. For high D* (2.4 kGy/min), k_H exhibits good values for samples obtained at low electron beam absorbed dose: both samples (with and without initiator) present the best values on same electron beam absorbed dose: 1.2 kGy (k_H =0.68 and k_H =0.79 respectively). For low D* (1.2 kGy/min.), the same is noticed: both samples (with and without initiator) present the best values for η_{intr} on same dose of irradiation: 1.2 kGy (k_H =0.19 and k_H =0.72 respectively). The measured values of Huggin's constant k_H are well below 1 and that is a very important result because polyelectrolites' (flocculants) efficiency is assured by their linearity, i.e. by $k_H < 1$. High intrinsic viscosity values are sometimes associated with low solubility of acrylamide-acrylic acid copolymers and k_H >0.5 (the copolymers is not linear), especially for samples irradiated at small dose rates. In this case, the cross-linking effect can be controlled by chain transfer agent concentration. It is very important to mention that the samples irradiated at high dose rates always exhibit small values for k_H (k_H <1), even for an over-irradiation above the proper dose level.

CONCLUSIONS

This study was carried out to illustrate the synthesis of flocculants copolymers based on various compositions of acrylamide and sodium acrylate monomers (in the presence and absence of initiator) under the effect of electron beam irradiation. The characteristics of the flocculant copolymers are influenced by the following factors: chemical composition of the solutions to be irradiated (with or without initiator), electron beam absorbed dose (D), and absorbed dose rate level (D*). For the samples that show high values of C_c (> 90%), Mr shows very low values < 0.015%, but associated with a cross-linked structure (poor water solubility which means Huggins' constant k_H > 0.5) and low intrinsic viscosity η_{intr}.(<6 dl/g).

REFERENCES

Brostow, W. et al. (2009), “Polymeric Flocculants for Wastewater and Industrial Effluent Treatment”, *Journal of Materials Education*, 31(3-4), 157-166.

Craciun, G., Manaila E. and Ighigeanu, D. (2011), “Polymeric Flocculants Based on Acrylamide and Acrylic Acid Obtained by Electron Beam Irradiation”, *Leather and Footwear Journal*, 11(2), 121-132.

Dimonie, M. et al. (1986), *Poliacrylamide* (in Romanian), Technical Press, Bucharest, 36-36, 194-197.

Edzwald, J.K. (1993), “Coagulation in Drinking Water Treatment: Particles, Organics and Coagulants”, *Water Science &Technology*, 27(11), 21-35.

Fetting, J., Ratnaweera, H. and Odegaard, H. (1991), “Synthetic Organic Polymers as Primary Coagulants in Wastewater Treatment”, *Water Supply*, 9, 19-26.

McCormick, C.L. et al. (1990), “Water Soluble Copolymers 30. Effects of Molecular Structure on Drag Reduction Efficiency”, *Macromolecules*, 23(8), 2124-2131.

Martin, D. et al. (1995), “Low Power-high Energy Linacs for Irradiation in Polymeric Systems”, *Radiation Physics and Chemistry*, 45(4), 615-621.

Martin, D. et al. (1996), “IAP Linacs in Applied Research”, *Nuclear Instruments and Methods in Physics Research Section B: Beam Interactions with Materials and Atoms*, 113(1-4), 106-109.

Zuga, M.D. et al. (2007), “Products of Ethylene-Propylene Terpolymer Rubber (EPDM) Obtained by an Environmentally Friendly Process”, *Materials and Technologies*, 23, 333-336.

STUDY OF THE CREEP BEHAVIOUR WITH PRANDTL LAW CONSTITUTIVE EQUATION FOR CD 304L SS

AMIR HOSSEIN DAEI SORKHABI[1], FARID VAKILI TAHAMI[2], VAHIDEH VAHDATPANAHI SHOKOUH[1]

[1] *Islamic Azad University, Tabriz Branch, Department of Mechanical Eng., Tabriz, Iran, email: amirsorkhabi@iaut.ac.ir*

[2] *University of Tabriz, Department of Mechanical Eng., Tabriz, Iran*

In this paper Prandtl law constitutive equation (sine hyperbolic) has been proposed to study the creep behaviour of cold-drawn 304L stainless steel. For this purpose, the material and physical parameters for the creep constitutive equation has been determined using experimental data. The creep behaviour and properties for this material were examined by conducting uni-axial creep tests. Test samples have been obtained from cold-drawn bars and the material conforms to ASTM A276-05a specifications. Constant temperature and constant load of uni-axial creep tests have been carried out at three temperatures of 680,700 and 720°C, subjected to initial stresses of 320, 340 and 360MPa. The experimental data have been used to obtain the creep constitutive parameter for Prandtl law using numerical optimization techniques. The results show that the constitutive equations in the form of Prandtl law provide agreement with experimental data.

Keywords: creep; Prandtl law; constitutive equation.

INTRODUCTION

Creep is a time-dependent plastic deformation under a fixed stress at temperatures of roughly 0.3–0.5T_m, where T_m is the melting temperature of metals.

Engineering parts, which operate at high temperature and under mechanical loads, have many applications in power generation and petrochemical plants. Therefore, it is necessary to study the creep behaviour of the high temperature alloys, which are used in these systems.

Over the past several decades, considerable efforts have been made to gain a fundamental understanding of the creep mechanisms and to develop an efficient engineering design criterion for high temperature components, which operate under multi-axial stress states. However, a realistic creep testing procedure requires tremendous effort and long time tests which are expensive and often unachievable. To overcome this shortcoming, usually, tests have been carried out at uni-axial condition under high temperature and stress levels.

Hald (2008) and also Agamennone et al. (2006) have quantified the microstructural evolution during the creep at 650°C of tempered martensite 9–12% Cr-steel modified with 2%W and 5%Co. Hayhurst et al. (2005) have studied the creep deformation and rupture data of butt-welded pipes associated with 0.5Cr0.5Mo0.25V ferritic steel.

Kimura et al. (2009) have studied long-term creep deformation properties of modified 9Cr–1Mo steel. They have shown that, with decrease in stress level, the magnitude of creep strain at the onset of accelerating creep stage decreases from about 2% in the short-term regime to less than 1% in the long-term region. They have also shown that the time to 1% total strain, that is an important parameter for design of high temperature components, lies in the transient creep stage in the short-term regime; whereas, it shifts to the accelerating creep stage in the long-term regime.

Saucedo-Munoz et al. (2002) have evaluated the creep properties for 316 HTB austenitic stainless steel using the small-punch creep tests at 650°C for loads of 234, 286, 338, 408 and 478N and at 700°C for loads of 199 and 234 N. They have shown that the creep curves, determined by means of the small-punch creep tests, are similar to those obtained from a conventional uni-axial creep test.

Latha et al. (2008) have studied the thermal creep properties of alloy D9 and 316 stainless steel tubes. They have compared their results with the properties of 20% cold worked type 316 stainless steel tubes and showed that alloy D9 has higher creep rupture strength, lower creep rate and lower rupture ductility than 316 stainless steel.

Hayhurst et al. (2003) have obtained constitutive equations for time independent plasticity and creep of 316 stainless steel at 550°C.

In this paper the material and physical parameters for the Prandtl law creep constitutive equations have been calculated using the experimental data obtained by conducting uni-axial creep tests. Test samples have been machined out from cold-drawn 304L stainless steel (CD 304L SS) bars, which conform to ASTM A276-05a specifications (2005). Constant temperature and constant load uni-axial creep tests have been carried out at three temperatures of 680,700 and 720°C, under initial stresses of 320, 340 and 360MPa. Creep constitutive parameters have been calculated for Prandtl Law constitutive equation.

Uniaxial Creep Constitutive Relationship (Prandtl law), Boyle and Spence (1983), Yao et al. (2007)

The deformation of a tensile specimen under constant load depends on stress σ, time t and temperature T. Consequently, the creep strain of materials can be written as:

$$\varepsilon_c = f(\sigma,t,T) \tag{1}$$

where ε_c is creep strain. Equation (1) is usually assumed to be separated into:

$$\varepsilon_c = f_1(\sigma) f_2(t) f_3(T) \tag{2}$$

The stress and time dependence of creep under constant stress has received considerable attention. As a result, there are a number of alternative expressions. One of most commonly used function of stress is Prandtl law:

$$f_1(\sigma) = A\sinh(\alpha\sigma) \tag{3}$$

where A and α are material constants. The function is popular for its simplicity in application to stress analysis. An important time function is the so-called Bailey law

$$f_2(t) = Dt^m \quad \left(usually\ \tfrac{1}{3} \le m \le \tfrac{1}{2}\right) \tag{4}$$

where D and m are material constants. According to Arrhenius's law, the temperature dependence is given as:

$$f_3(T) = B\exp\left(\frac{-\Delta H}{RT}\right) \tag{5}$$

where $-\Delta H$ is activation energy and R is Boltzman's constant. Then the creep strain may be written as:

$$\varepsilon_c = C'\sinh(\alpha\sigma)\exp\left(\frac{-\Delta H}{RT}\right)t^m \tag{6}$$

for isothermal conditions, the creep strain is:

$$\varepsilon_c = C'\sinh(\alpha\sigma)t^m \tag{7}$$

which is known as Prandtl law and used in creep analysis. Equation (7) is developed for the constant stress and can describe the primary, secondary or tertiary creep stages. Also, steady state creep strain rate $(\dot{\varepsilon}_{ss})$ is:

$$\dot{\varepsilon}_{ss} = C\sinh(\alpha\sigma)\exp\left(\frac{-\Delta H}{RT}\right) \tag{8}$$

Material and Creep Test Set up

Type 304 stainless steel is the most widely used alloy of the austenitic group. Type 304L is an extra low-carbon variation of Type 304 with a 0.03% maximum carbon content that eliminates the possibility of carbide precipitation due to the welding. The maximum temperature to which Types 304 and 304L can be exposed continuously without appreciable scaling is about 899°C. Hardness of Type 304L does not increase significantly by heat treatment. It can be annealed by heating to 1038 - 1121°C, and then cooled rapidly. Cold worked parts can be stress relieved at 399°C for 1/2 to 2 hours (2005). Most of the small and medium size seamless tubes, which are widely used in boiler-super-heaters and heat exchangers, are manufactured using cold forming or cold dawning processes and therefore, it is necessary to study the creep behaviour of the cold-drawn form of the 304L SS.

In this research, the samples for creep tests have been obtained directly from new austenitic 304L stainless steel cold-drawn bars which have been solution annealed at 1050°C. The material conforms to ASTM A276-05a specifications. Chemical composition of this material is given in Table 1. In this table, both the standard values (2005) and those which have been obtained from quantometric measurements of the specimens under investigation are given. The test specimens have been machined out from the bars according to the ASTM E8M-04 (2004) with gauge length of 100mm and diameter of 10mm.

Table 1. Chemical composition of 304L SS in percent

	C	Si	Mn	P	S	Cr	Mo	Ni	N
Standard	0.019	0.41	1.75	0.036	0.006	18.28	0.34	8.04	0.04
Tested (CD304LSS)	0.025	0.42	1.80	0.035	0.015	17.80	0.27	8.10	-

Uni-axial creep tests have been carried out using 5000kg, AMSLER creep test machine according to the ASTM E139 (2006) standard. Its lever-arm loading ratio is 25:1 with load accuracy of +/-0.5%. The temperature range of the furnace or chamber of the machine is up to 1000°C with the accuracy of +/-0.5°C. The testing machine also provides displacement-time graphs with the accuracy of +/-0.5μm. The maximum extension of the specimen is 10mm.

Experimental Results and Discussion

Uni-axial creep tests have been carried out at three temperature levels of 680, 700 and 720°C under different loads. During the creep tests, the temperature and load levels remain constant and the variation of the total true strain with time has been obtained for each test condition.

Creep failure in engineering components can be regarded in two ways: when the time to rupture, t_r, has been reached or the time, $t_{\text{Creep Strain=C\%}}$, at which the creep strain reaches a critical level of C%. In most of the engineering components, the latter condition plays a major role; and therefore, it has been used in this study. Since the maximum extension of the specimen is 10mm (total strain of 10%) in the creep-testing-machine, all the tests have been carried out until the true creep strain of 3% has been reached or $t=t_{\text{Creep Strain=3\%}}$. At this amount of deformation, most of engineering components would be regarded as failed. The summary of the creep test results have been given in Table 2. Also, the minimum creep strain rate, $(\dot{\varepsilon}_{ss})$, for each test has been given in this table. The results given in Table 2 show that by increasing the stress or temperature, time to reach 3% creep strain decreases significantly.

Table 2. Uni-axial creep testing results for CD 304L SS

Temperature (°C)	Stress (MPa)	$t_{\text{Creep Strain=3\%}}$ (hr)	Min. Creep Strain Rate (1/hr)
680	320	400	$7.57187*10^{-5}$
680	340	348	$8.59975*10^{-5}$
680	360	236	0.000128547
700	320	224	0.000131228
700	340	180	0.000160666
700	360	106	0.000271897
720	320	98	0.000307829
720	340	72	0.000378703
720	360	55	0.000555202

Due to the nonlinear behaviour of the creep deformation, usually there is a large scatter in creep test data. Also, errors due to the data recording and discrepancy of the test results lead to different values of constitutive parameters for each test. Therefore, the constitutive parameters which fit best with all test data should be obtained using numerical methods. The usual procedure to estimate the constitutive parameters for creep tests is to adopt optimization techniques which provide best fit to the experimental data. Using these methods, the constitutive parameters can be obtained by minimising the difference between the values of experimental data points and the calculated amount.

Different methods of optimization techniques can be used for this purpose, where as, the most viable technique is the Least Square method. Using this method, the summation of total error values can be defined as:

$$Error = \left[\sum_{i=1}^{n} \left(\dot{\varepsilon}^{exp} - \dot{\varepsilon}^{the} \right) \right]^{1/2} \tag{9}$$

in which $\dot{\varepsilon}^{exp}$ and $\dot{\varepsilon}^{the}$ are the experimental and theoretical values for the minimum creep strain rate respectively. The experimental values are given in Table 2; and the theoretical values are obtained using Equations (8) at different stress and temperature levels for each test. A computer code has been developed based on unconstrained nonlinear optimization method to obtain constitutive parameters by minimizing the error function. The calculated constitutive parameters are given in Table 3 for Prandtl law constitutive equation. In calculating the constitutive parameters, the same amount of acceptable error has been used. Also, the amount of activation energy (ΔH) is assumed to be the same. This assumption is justified due to the fact that the governing mechanism for the thermal recovery and distribution of dislocations is the same during the creep of material.

Table 3. Creep constitutive parameters for CD 304L SS

PRANDTL LAW PARAMETERS	C	ΔH	A
	9.8347× 10-10	2.6×105	0.0218

Figure 1 shows the variation of minimum creep strain rate, which have been calculated using Prandtl law constitutive equation, with 1/T for different stress levels. Also in this figure, the results obtained using this constitutive equation has been compared with the experimental data. Figure 1 shows that by increasing temperature or stress, creep strain rate increases significantly. Figure 2 presents the variation of minimum creep strain rate with stress in logarithmic scale. The results have been obtained using Prandtl law constitutive equation. Also in this figure, the calculated minimum creep strain rates have been compared with experimental data obtained for this material. Both figures (Figures 1 and 2) show that there is a good agreement between calculated values and the experimental data in terms of the trend of the variation of minimum creep strain rate with 1/T or stress. Also, Figure 1 and 2 show that the difference between experimental data and calculated values are temperature independent. This is due to the fact that the same formulation (exponential form) has been used in both constitutive equations to model the temperature dependency of the creep deformation.

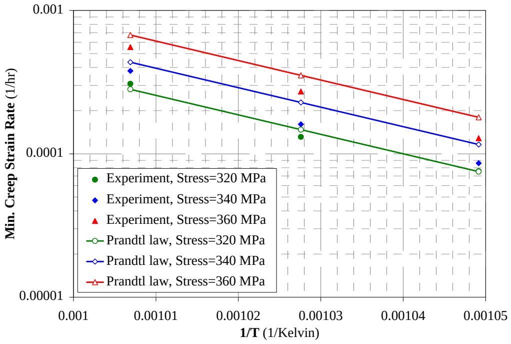

Figure 1. Variation of minimum creep strain rate with 1/T for different stress levels

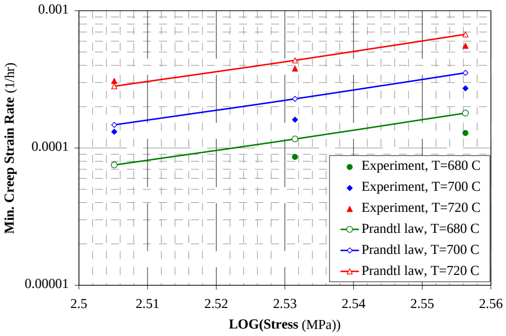

Figure 2. Variation of minimum creep strain rate with stress in logarithmic scale

CONCLUSION

Constant load creep tests have been carried out to predict the creep behavior, constitutive parameters and time to reach 3% creep strain for CD 304L SS.

It has been shown that by using these test data, constitutive parameters can be obtained. These tests have been used to determine the constitutive parameters for Prandtl law equation. This equation can be used to estimate the creep lifetime of the mechanical structures or can be implemented in numerical modeling.

The results show that the constitutive equations in the form of Prandtl law provide agreement with experimental data.

REFERENCES

Agamennone, R., Bluma, W., Guptab, C. and Chakravartty, J. K. (2006), “Evolution of microstructure and deformation resistance in creep of tempered martensitic 9–12%Cr–2%W–5%Co steels”, *Acta Materialia*, 54, 3003-3014.

ASTM A276 - 05a (2005), Standard Specification for Stainless Steel Bars and Shapes Volume: 02.04.

ASTM E139-06 (2006), Standard test methods for conducting creep, creep-rupture, and stress-rupture tests of metallic materials.

ASTM E8M-04 (2004), Standard test methods for tension testing of metallic materials (metric).

Boyle, J.T. and Spence, J. (1983), *Stress analysis for creep*, Butterworth & Co. Ltd.

Hald, J. (2008), “Microstructure and long-term creep properties of 9-12% Cr steels”, *International Journal of Pressure Vessels and Piping*, 85, 30-37.

Hayhurst, D.R., Vakili Tahami, F. and Zhou, J.Q. (2003), “Constitutive equations for time independent plasticity and creep of 316 stainless steel at 550^{o}C”, *International Journal of Pressure Vessels and Piping*, 80, 97-109.

Hayhurst, R.J., Mustata, R. and Hayhurst, D.R. (2005), “Creep constitutive equations for parent, Type IV, R-HAZ, CG-HAZ and weld material in the range 565–640°C for Cr–Mo–V weldments”, *International Journal of Pressure Vessels and Piping*, 82, 137-144.

Kimura, K., Kushima, H. and Sawada, K. (2009), “Long-term creep deformation property of modified 9Cr–1Mo steel”, *Material Science and Engineering A*, 510-511, 58-63.

Latha, S., Mathewa, D., Parameswaran, P., Rao, K. and Mannan, S.L. (2008), “Thermal creep properties of alloy D9 stainless steel and 316 stainless steel fuel clad tubes”, *International Journal of Pressure Vessels and Piping*, 85, 866-870.

Saucedo-Muñoz, M.L. et al. (2002), “Creep property measurement of service-exposed SUS 316 austenitic stainless steel by the small-punch creep-testing technique”, *J. Master Res.*, 17, 1945-1953.

Yao, H.T., Zhen Xuan, F., Wang, Zh. and Tung Tu, Sh. (2007), “A review of creep analysis and design under multi-axial stress states”, *Nuclear engineering and Design*, 237, 1969-1986.

UTILIZATION OF RECYCLED POLYURETHANE GRANULATE FOR THERMAL INSULATING MATERIALS PRODUCTION

JITKA HROUDOVÁ, JIŘÍ ZACH

[1] *Brno University of Technology, Faculty of Civil Engineering, Institute of Technology of Building Materials and Components, Veveří 331/95, 602 00 Brno, Czech Republic,*
hroudova.j@fce.vutbr.cz, zach.j@fce.vutbr.cz

At present, there is a growing demand worldwide demand for new advanced materials that have high performance characteristics, materials which is energetically and material-wise undemanding in production. These materials represent a progressive direction in the field of sustainable development, whereas this category also includes materials (among others) whose production process uses secondary raw materials. This paper describes the initial phase of research activities in the field of development of thermal insulation materials based on waste polyurethane granulation products. The material which is being developed should be useful either alone (in the form of plates) or it should works as an integrated heat-insulating board (e.g. in ceramic masonry shaped pieces).

Keywords: PUR granulate, insulation materials, thermal conductivity.

INTRODUCTION

More and more increasing demand for new advanced building materials, which are affordable in terms of price, environmentally friendly and showing better and better use characteristics, puts pressure on manufacturers who try to develop and produce new materials for production of which they must use more advanced production technologies and for which they also have to look for raw materials resources that are affordable, easily renewable and environmentally friendly.

Regarding the field of thermal insulation materials, there is currently growing popularity of insulators based on polyurethane (PUR and PIR foams), especially for its very good ratio of thermal insulation and mechanical properties. Another advantage of polyurethane is its relative easy manufacture, good workability and possibility of active modification of its properties in the production process by using appropriate selection ratio of input components. In the manufacture process of moulded polyurethane foam elements, there are residues / chips appearing very often, those which can be modified by crunching into the form of PUR granules of defined grain size. In the Brno University of Technology, there have been research works held since 2011. They are aimed to both study of properties of PUR granules and also its use in construction industry. The main emphasis is placed on development of filling insulating material used in cavity ceramic shaped pieces. This paper describes study of basic properties of sorted polyurethane granules (PUR) resulting during production of polyurethane insulation boards (PUR). It also describes the initial phase of development of filling insulation based on polyurethane granules and silicate binders.

POLYURETHANE GRANULES AND THEIR POSSIBLE WAYS OF USE

The current modern world produces a lot of waste materials whose disposal is difficult and non-ecological. These waste materials also include the wastes based on polyurethane which is widely used as packing material. But we may also see it in the construction industry where it is used as thermal insulation of building structures. Due to the large amount of this waste, it is necessary to look for a suitable recycling technology and the subsequent possibilities of using this recycled material, e.g. polyurethane granules, in practice. Regarding very good ratio of thermal insulation and mechanical properties, the polyurethane granules appear to be an interesting secondary raw material for potential production of thermal insulation materials. They could also be used for producing of heat-insulating filling integrated to ceramic masonry shaped-pieces.

During the research activities carried out at Faculty of Civil Engineering at the Brno University of Technology, there is the development of thermal insulation materials based on polyurethane granules which should potentially be applicable for the production of thermal insulation masonry shaped-pieces with integrated insulation fill. Therefore, the main emphasis is - during the research - placed on achieving the best thermal insulating properties of the material while maintaining minimum mechanical properties which would guarantee stability of the insulating material in the cavities of ceramic shaped-pieces.

RESEARCH OF PROPERTIES OF POLYURETHANE GRANULES

The initial phase of research was devoted to studying the properties of polyurethane granules. That was the sorted granulation product supplied by the company called IZOMALT. The product appears by crushing chips generated in the production of PUR sandwich panels and insulation boards. The chips are crushed and then sorted by screens into three fractions: 0-1, 1-3, 3-5 mm. IZOMALT delivered 3 test samples of granulation products: First test sample (fraction 0-1), second test sample (fraction 1-3), third test sample (fraction 3-5).

In the initial phase, the powder density was determined and screen analysis was performed on each test sample.

Figure 1. Mixture of granulation products PUR 0-1

Figure 2. Mixture of granulation products PUR 1-3

Figure 3. Mixture of granulation products PUR 3-5

Measurement results are presented in the Table 1 and graph below.

Table 1. Overview of powder density values of PUR granulation products of different fractions

Sample n.	Weight [kg]	Powder density [kg.m^{-3}]
Sample n. 1 (PUR 0–1)	0,65270	158,4
Sample n. 2 (PUR 1–3)	0,23415	57,1
Sample n. 3 (PUR 3–5)	0,16341	40,2

In the beginning of solving the issue there were screen analyses of all fractions carried out, see Figure 4.

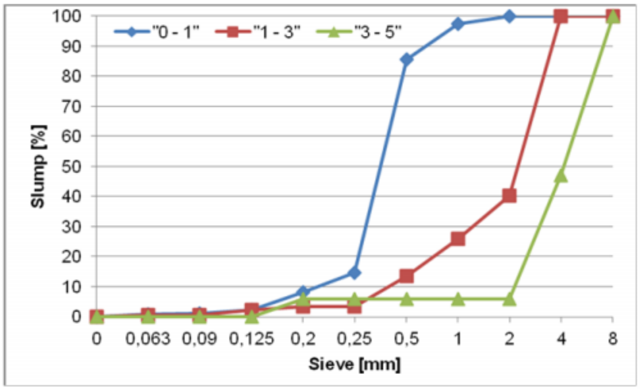

Figure 4. Curves of grain size in individual fractions of PUR granulation product

Furthermore, there was determination of thermal conductivity in steady state. Measurements were performed at a mean temperature of 10°C and temperature gradient of 10 K, according to EN 12667 (ISO 8301) on the device of Lambda 2300 made by Holometrix. The principle is based on the stationary plate method. There was the sample of polyurethane fraction (PUR) of the granulation product poured into the wooden box measuring 290 x 290 mm with the height of 48 mm. This sample was defrayed on the surface, whereas the amount of PUR granulation products was modified in such the way that the samples show a powder density consistent with previously measured values - see Table 1. Measurement results are presented in Table 2.

Table 2. Overview of measured characteristics of PUR granulation products of different fractions

Sample n.	Weight [kg]	Powder density [kg.m^{-3}]	Thermal conductivity [W.m^{-1}.K^{-1}]
Sample n. 1 (PUR 0–1)	0,65270	158,4	0,0431
Sample n. 2 (PUR 1–3)	0,23415	57,1	0,0328
Sample n. 3 (PUR 3–5)	0,16341	40,2	0,0334

Table 3. Overview of measured thermal conductivities of PUR granulation products at different temperatures

Sample n.	Thermal conductivity [W.m^{-1}.K^{-1}]			
	10°C	20°C	23°C	30°C
PUR 0–1	0,0431	0,0417	0,0407	0,0411
PUR 1–3	0,0328	0,0329	0,0330	0,0345
PUR 3–5	0,0334	0,0346	0,0346	0,0357

DEVELOPMENT OF THERMAL INSULATION MATERIALS MADE OF PUR GRANULATION PRODUCTS

Furthermore, there was a proposal of a thermal insulator made of PUR granulation product. Based on the results of measurements of fundamental physical properties, there have been the fractions of 1-3 and 3-5 chosen for the development of thermally insulating material.

In the initial stage of the development of thermal insulation fills, there were two test batches proposed:

- Batch No. 1 where both factions of PUR granulation products (1-3 and 3-5) were used in 1:1.
- Batch No. 2 where only the fraction of 3-5 mm was used.

In both batches there was Portland cement CEM I 42.5 R used as a binder. The cement comes from the factory of Mokrá (Českomoravský Cement a.s.). The amount of cement was determined with regards of the fractions of PUR granulation products used. The recipes are shown in the following table.

Table 4. Overview of testing batches

Component	Batch n. 1	Batch n. 2
PUR granulate [kg]	1,2	0,9
Cement [kg]	1,8	2,1
Water [kg]	3,8	3,5

There were scantling pieces with the size of 40 x 40 x 160 mm prepared for determining the mechanical properties. There were also square boards with the edge of 300 mm and the thickness of 60 mm prepared for determining the thermal conductivity.

Determination of thermal conductivity was performed on 3 test samples in dry condition, using the stationary method of boards at different mean temperatures: +10, +20, +30 °C with temperature gradient at 10 K. The measurement was performed on the device of Lambda 2300. The measurement results are listed in Table 5.

Table 5. Overview of the average measured values of thermal conductivity coefficient in the testing batches, depending on the temperature

Batch	Thickness [mm]	Thermal conductivity $[W.m^{-1}.K^{-1}]$ at different mean temperatures		
		+10°C	+20°C	+30°C
Batch No. 1	60,11	0,0832	0,0869	0,0957
Batch No. 2	59,94	0,0710	0,0729	0,0775

Furthermore, there were mechanical properties determined on test rectangular samples with dimensions of 40 x 40 x 160 mm.

Tensile strength in bending was determined according to the formula:

$$f = 1{,}5 \, . \, F \, . \, l \, / \, (b \, . \, h^2) \ [N.mm^{-2}] \qquad (1)$$

where: F – maximum force [N], l – axial distance of supports [mm], b – width of the cross section of the body [mm], h – height of the cross section of the body [mm].

Compressive strength was determined according to the formula:

$$f_c = F \, / \, A \ [N.mm^{-2}] \qquad (2)$$

where: F – maximum force [N], A – testing area of the body $[mm^2]$.

Measurement results are presented in Table No. 6.

Table 6. Overview of the average measured values of mechanic properties

Batch	m [g]	a [mm]	b [mm]	c [mm]	ρ $[kg.m^{-3}]$	f $[N.mm^{-2}]$	f_c $[N.mm^{-2}]$
Batch No. 1	58,91	158,97	40,13	40,27	229	0,21	0,22
Batch No. 2	61,77	159,72	39,71	40,85	238	0,22	0,41

CONCLUSION

Based on previously obtained results from studies of polyurethane granulation product characteristics (PUR) and development of thermal insulation materials based on polyurethane granulation products, it is possible to say that PUR granulation product is an interesting secondary raw material that can be applied in the development of thermal insulation materials being used in building industry.

Results obtained during measurements of test samples of insulation material made of polyurethane granulation product (PUR) and Portland cement show that materials based on polyurethane granulation product and silicate binder show good thermal insulation characteristics. However, while thinking about use of this material for producing heat-insulation shaped pieces with integrated thermal insulation fills, it is necessary to optimize the curve of granularity of the PUR granulation product used and the ratio of binder and filler in such a ways that a significant reduction in thermal conductivity coefficient value is reached. Furthermore, we can assume that for bonding polyurethane granules are more suitable polymeric binder based on the use of which would be less degrading thermal insulation properties of the resulting insulator. This issue will be discussed in further research work.

Acknowledgements

This paper was elaborated with the financial support of the project MPO FR-TI3/231 and Centre AdMaS (ref. n. CZ.1.05/2.1.00/03.0097).

REFERENCES

Benkreira, H., Khan, A. and Horoshenkov, K.V. (2011), "Sustainable acoustic and thermal insulation materials from elastomeric waste residues", *Chemical Engineering Science,* 66(18), 4157-4171.

Ferreira, L., Brito, J. and Saikia, N. (2012), "Influence of curing conditions on the mechanical performance of concrete containing recycled plastic aggregate", *Construction and Building Materials,* 36, 196-204.

Gadea, J., Rodríguez, A., Campos, P.L., Garabito, J. and Calderón, V. (2010), "Lightweight mortar made with recycled polyurethane foam", *Cement and Conrete Composites,* 32(9), 672-677.

Šťastník, S. and Zach, J. (2002*), Testing of insulating materials,* CERM, Brno.

Zach, J., Hroudová, J. and Sedlmajer, M. (2012), "Utilization of Alternative Insulation Materials for Thermal Insulating Ceramics Blocks Production", *Advanced Materials Research,* 482-484, 1570-1575.

Zach, J. and Hroudová, J. (2012), "The use of recycled polyurethane granulate in building construction", *Juniorstav*, 1, 1-4.

Zia, K.M., Bhatti, H.N. and Bhatti, I.A. (2007), "Methods for polyurethane and polyurethane composites, recycling and recovery", *Reactive and Functional Polymers,* 67(8), 675-692.

ASSESSMENT OF ANTIBACTERIAL ACTIVITY OF SILVER DOPED HYDROXYAPATITE ON LEATHER

MERUYERT KOIZHAIGANOVA[1], İHSAN YAŞA[2], GÜRBÜZ GÜLÜMSER[1]

[1] *Leather Engineering Department, Engineering Faculty, Ege University, Bornova, Izmir 35100, Turkey, email: meruyert_k@hotmail.com*

[2] *Industrial Basic Microbiology Department, Basic Science Faculty, Ege University, Bornova, Izmir 35100, Turkey*

In this study, silver doped hydroxyapatite (Ag-HA) prepared by microwave method was applied as the finishing agent on leather and its antibacterial effect was investigated. By using X-ray Diffraction (XRD) and Fourier Transform Infrared Spectroscopy (FTIR) structural properties of the prepared Ag-HA have been determined. Antibacterial activity of the leather treated with the Ag-HA was revealed by the agar diffusion method and the percentage of bacterial reduction tests. According to the results of the study, the leather treated with Ag-HA containing 2% and above amount of silver (Ag) showed strong antibacterial activity and the usability of the Ag doped hydroxyapatite as an antibacterial agent on lining leathers was decided upon.

Keywords: silver doped hydroxyapatite, antibacterial activity, leather.

INTRODUCTION

Hydroxyapatite (HA) has been widely used as biomaterial in dentistry, orthopedy and bioengineering, because of its good biocompatibility and bioactivity (Tanaka et al., 2003). It possesses similar structure to the major mineral constituent of human hard bone and can also serve as a carrier of antibiotics to reduce the bacterial infections in the bone-implant interface. By taking advantage of the ion-exchange capabilities, HA can be effective in controlling microorganisms with the introduction of transient metal ion such as silver (Oh et al., 2003).

Silver has been known as a disinfectant for many years and has a broad spectrum of antibacterial activity while exhibiting low toxicity towards mammalian cells. Several in vitro studies reported that the silver ions in the HA coatings play an important role in preventing or minimizing initial bacterial adhesion (Stanic et al., 2011). Recently, the antibacterial effects of silver-substituted HA have been studied on different materials, including textile (Lv et al., 2006).

In this study, the silver doped hydroxyapatite was prepared by microwave method and its antibacterial performance as the antibacterial finishing agent on leather was investigated. The prepared 0%-5% Ag-HA powders have been characterized by using X-ray Diffraction (XRD) and Fourier Transform Infrared Spectroscopy (FTIR). Antibacterial activity of the leather treated with the Ag-HA was revealed by the agar diffusion method and the percentage of bacterial reduction tests.

EXPERIMENTAL

Preparation and Characterization of HA and Ag-HA Solutions

Analytical grade calcium hydroxide ($Ca(OH)_2$, Merck), diammonium hydrogen phosphate (DAP, $(NH_4)_2HPO_4$, Merck), and silver nitrate ($Ag(NO)_3$, Fluka) were used for the preparation of the Ag-HA according to the literature (Rameshbabu et al., 2006). $Ag(NO)_3$ was first dissolved in deionized distilled water (0.25M solution), and it was added to 0.3M $Ca(OH)_2$ suspension in deionized distilled water under stirring conditions. The 0.3M DAP solution was added to the silver nitrate dissolved calcium hydroxide aqueous suspension for 5 min by stirring. The silver content was increased in order to prepare 0% Ag-HA to 5% Ag-HA. The precursor solution in an uncovered glass beaker was immediately subjected to the microwave irradiation for about 30 min in a domestic microwave oven. The precipitate was used for the further application. A certain amount of the precipitate was filtered and oven-dried at 90°C for overnight then the flake was powdered by a mortar and pestle. The phase analysis of the 0%-5% Ag-HA powders was characterized by X-ray Diffraction (XRD, Phillips X'Pert Pro, Japan) and the functional groups present in the 0%-5% Ag-HA were ascertained by Fourier Transform Infrared Spectroscopy (FTIR, Perkin Elmer, Spectrum 100, USA).

Antibacterial Assessment

The antibacterial activity was evaluated following two different tests, the qualitative test: Agar Diffusion Method based on the AATCC 147 test method, and the quantitative test: Percentage of Bacterial Reduction, according to the general guides of the AATCC 100 test method (AATCC 147, 1998; AATCC 100, 2004). The procedure of both tests was slightly modified due to its application on leather. The bacteria utilized for the test were *Staphylococcus aureus* ATCC 6538-P as Gram positive bacterium, *Escherichia coli* ATCC 12228, *Salmonella typhimurium* CCM 5445 and *Pseudomonas aeruginosa* ATCC 27853 as Gram negative bacteria.

RESULTS AND DISCUSSION

The phase analysis of the 0%-5% Ag-HA powder samples was done by XRD (Phillips X'Pert Pro, Japan) using a 40 kV current, with a monochromatic CuKα (target) radiation and a scan range from $2\theta = 10$ to 70°. The XRD patterns of pure HA and the as-synthesized 0.5%-5% Ag-HA powders formed is depicted in Figure 1. The d-values correspond to that of calcium hydroxyapatite ($Ca_{10}(PO_4)_6(OH)_2$). From the XRD pattern, the characteristic peak of calcium phosphate clearly shows the development of poorly crystallized apatite phase at $2\theta \sim 25–34.5°$. The HA crystals that were synthesized revealed characteristic peaks in the XRD pattern that were consistent with International Centre for Diffraction Data files for hydroxyapatite (JCPDS, 2003). It is clearly seen from Figure 1 that apatite peaks were generally found at 2θ of 25.40°, 29.00° and 31.50°, corresponding to (002), (102) and (211) orientations for the powder sample. In addition, the low intensity peaks were determined at 2θ of 39.20°, 39.60°, 46.50° and 49.00°.

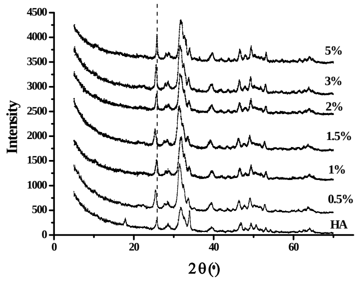

Figure 1. XRD patterns of the 0%-5% Ag-HA

Figure 2 summarizes FTIR spectra of pure HA and of 0.5%-5% Ag-HA, respectively. The presented significant absorbance agreed with HA component in all powders (Chung et al., 2005). Major characteristic HA bands are assigned as: ν_1 PO_4^{3-} band around 962 cm^{-1}; ν_2 PO_4^{3-} band around 471-472 cm^{-1}; ν_3 PO_4^{3-} band around 1023-1025 and 1090 cm^{-1}; ν_4 PO_4^{3-} band around 560-562 and 600-602 cm^{-1}; adsorbed water and hydroxyl groups of broad absorption around 631-633 cm^{-1}. For pure HA the presence of strong O–H vibration peak could be noticed at wave number of 3570 cm^{-1}. However, for Ag-HA samples, the intensity of O–H vibration peak is reduced.

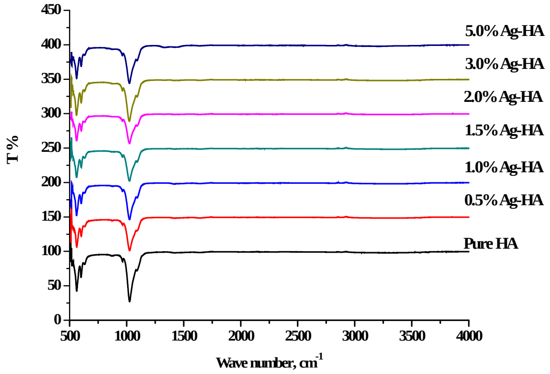

Figure 2. FTIR spectra of the 0%-5% Ag-HA in synthesized condition

Table 1. The functional groups in FTIR spectra of the 0%-5% Ag-HA in synthesized condition

Functional groups	Pure HA	0.5% Ag-HA	1% Ag-HA	1.5% Ag-HA	2% Ag-HA	3% Ag-HA	5% Ag-HA
	Wavenumber (cm^{-1})						
ν_2 PO_4 vibration band*	471	471	471	471	471	471	472
ν_4 PO_4 vibration band	562	563	560	562	562	559	562
ν_4 PO_4 vibration band	600	602	601	601	602	601	601
ν_1 PO_4 vibration band	962	962	962	962	962	962	962
ν_3 PO_4 vibration band	1025	1025	1025	1024	1024	1024	1023
-OH band	632	632	632	633	632	631	632
ν_3 PO_4 vibration band	1090	1090	1090	1090	1090	1090	1090
-OH band	3570						

*not shown in Figure 2

In this study, 0.5%-5% Ag-HA was applied on leather during finishing process and antibacterial activity was revealed by qualitative and quantitative tests. Regarding the antibacterial activity, the agar diffusion method was performed as the qualitative test for all samples. Results showed that the major differences between the coated samples are related with the used Ag concentration in Ag-HA. The sample coated with 1% Ag-HA presented the lowest antibacterial activity, while samples coated with 2% and 3% have shown better inhibition against test bacteria.

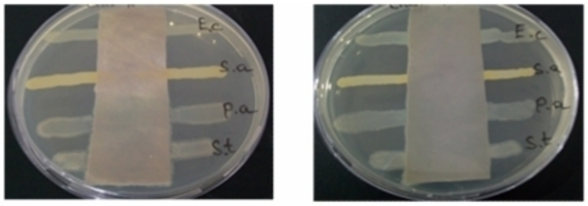

a) control b) 1 % Ag-HAP

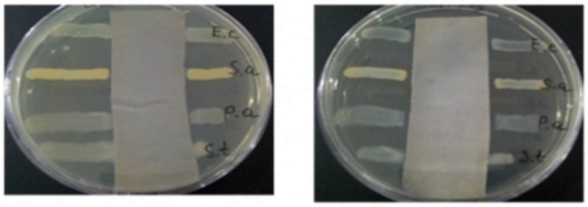

c) 2 % Ag-HAP d) 3 % Ag-HAP

Figure 3. Antibacterial activity test results of the leather

According to the qualitative test results, the leather samples coated with 1% - 5% of Ag-HA were chosen to perform the percentage of bacterial reduction test. This quantitative test was performed at 60 minutes contact time of the sample with the test bacteria inoculate. A non-coated leather sample was used as control and was submitted to a parallel test using an identical inoculate of the tested bacteria. The obtained results showed that the coated leather (with 1%-5% Ag-HA) exhibited considerable antibacterial activity as a significant reduction of CFU/mL was observed after 60 min. Table 2 presents a survey of the obtained results, confirming that the increasing of silver concentration in Ag-HA lead to the increasing of antibacterial activity of the leather coated with Ag-HA.

Table 2. Bacterial reduction on leather samples treated with different concentrations of Ag-HA in 60 min test time

Initial number of bacteria	*Escherichia coli* 35.2 x 10^3		*Staphylococcus aureus* 27.2 x 10^3	
Specimens		Reduction rate (%)		Reduction rate (%)
Control	5.7 x 10^3		1.14 x 10^3	
1.0 % Ag-HA	2.6 x 10^3	54.39 %	0.28 x 10^3	75.44 %
1.5 % Ag-HA	0.1 x 10^3	98.24 %	0.18 x 10^3	84.21 %
2.0 % Ag-HA	0	100 %	0	100 %
3.0 % Ag-HA	0	100 %	0	100 %
5.0 % Ag-HA	0	100 %	0	100 %

CONCLUSIONS

In this research, it was found that the Ag-HA provides effective antibacterial properties to leather material. Its performance was increased by increasing the concentration of Ag. According to the results of the agar diffusion method the minimum level for obtaining antibacterial leather was established at 2% of Ag in Ag-HA. The leather samples treated with 1.5% of Ag-HA demonstrated the highest antibacterial activity in 60 min against *S. aureus* with 84.21% bacterium removal, while the same concentration of Ag-HA applied to leather was enough to exhibit the excellent percentage reduction of *E. coli* of 98.24%. Moreover, concentrations of Ag-HA which were effective against all tested bacteria were 2% and higher of Ag in Ag-HA with 100% of reduction of both tested bacteria. The results are promising for Ag-HA use in applications as antibacterial coating on leather.

Acknowledgements

We would like to thank the Research Foundation of Ege University for the financial support (Project № 09MÜH080).

REFERENCES

American Association of Textile Chemists and Colorists (1998), *Antibacterial Activity Assessment of Textile Materials: Parallel Streak Method*, AATCC 147.

American Association of Textile Chemists and Colorists (2004), *Antibacterial Finishes on Textile Materials: Assessment of*, AATCC 100.

Chung, R.J. et al. (2005), "Anti-Microbial Hydroxyapatite Particles Synthesized by a Sol–Gel Route", *Journal of Sol-Gel Science and Technology*, 33, 229–239.

International Centre for Diffraction Data, and American Society for Testing and Materials (2003), *Joint Committee on Powder Diffraction Standards (JCPDS) Database of Standards: Powder Diffraction (Inorganic and Organic)*, Swarthmore, PA.

Lv, G. et al. (2006), "Preparation and Antibacterial Activity of Silver Ions-substituted Hydroxyapatite/Titania", *Materials Science Forum*, 510-511, 78-81.

Oh, K.S. et al. (2003), "Effect of Fabrication Processes on the Antimicrobial Properties of Silver Doped Nano-sized Hap", *Key Engineering Materials*, 240-242, 583-586.

Rameshbabu, N. et al. (2006), "Antibacterial Nanosized Silver Substituted Hydroxyapatite: Synthesis and Characterization", *Journal of Biomedical Materials Research* Part A, 80(3), 581-591.

Stanic, V. et al. (2011), "Synthesis of Antimicrobial Monophase Silver-doped Hydroxyapatite Nanopowders for Bone Tissue Engineering", *Applied Surface Science*, 257, 4510-4518.

Tanaka, Y., Hirata, Y. and Yoshinaka, R. (2003), "Synthesis and Characteristics of Ultrafine Hydroxyapatite Particles", *Journal of Ceramic Processing Research*, 4(4), 197-201.

THE ISSUE OF NEW HIGHLY HEAT-RESISTANT ADHESIVE COMPOSITIONS

OKSANA PETRIVNA KOZAR[1], VALENTINA VASYLIVNA OLIYNIKOVA[2], VICTOR PAVLOVYCH KONOVAL[2], YURIY VIKENTIYOVYCH MYHALYNA[1]

[1] *Mukachevo State University, Mukachevo, Ukraine, email: kop@msu.edu.ua*

[2] *Kyiv National University of Technology and Design, Kyiv, Ukraine, email: kktvsh@gmail.ua*

The important question is the improvement of thermal performance of polyurethane adhesives used by domestic industries through research of existing and development of new adhesive compositions. The purpose of this study is to examine the development of new adhesive compositions that could be used for making shoes that will be used under elevated temperature conditions. Currently there are about a hundred brands of domestic synthetic adhesives that are based on the ability to withstand more or less heat load can be divided into three groups: adhesives that can withstand prolonged exposure to temperatures around 60°C; heat-resistant adhesives that can withstand long or short-term effect of temperatures of 100°C; highly heat-resistant adhesives that can withstand short-term effect of temperature to 300°C. Firms “Bayer”, “Tivolli”, “Henkel”, “Loctite”, “Teroson” (Germany) are the worldwide leaders in adhesives and materials for their production. Lately, foreign companies produce new highly heat-resistant adhesive compositions that can withstand the heat load of about 300-500°C. However, these adhesive compositions have low flexural properties and therefore not recommended for products that are exposed to irregular separation and shock loads, i.e. for the production of shoes. Thus, there is a need to explore the creation of new adhesive compositions which would contain non-toxic natural ingredients as a modifier and at the same time increase heat resistance and would be economically beneficial and allow to reduce the shoe manufacturing process technology that would withstand high temperature stress.

Keywords: shoe, adhesive composition, thermal stability.

INTRODUCTION

Along with the growth of footwear production of glued method of fastening requirements for its quality and range also increase. The use of new artificial and synthetic materials of different chemical composition for the top and bottom of shoes, a large range of special shoes, and increased atmospheric temperature parameters during usage lead to an increase in temperature of asphalt, thus worsening the reliability of glued joints. It requires a variety of heat-resistant adhesives with a wide range of properties.

Requirements for glued attaching of synthetic materials best meet polyurethane adhesives. These adhesives should provide not only high strength adhesive-bonded joints in the initial state, but also preservation of strength parameters during usage at elevated temperatures, have the ability to harden at low temperatures and pressures, do not emit volatile products during solidification and have high physical and mechanical properties.

Many certificates have been devoted to improvement of properties and development of new polyurethane compositions (Багалова К.М. и соавторы, 1987).

THE PURPOSE OF THE GIVEN WORK

With increasing demands for quality footwear and high competitiveness of manufacturers in our market imported expensive heat-resistant compositions that require high culture of production and related equipment are used.

Domestic footwear production enterprises are not equipped with advanced technologies and conditions of ventilation are inadequate, which is the main cause of failure to use certain components to enhance the heat resistance of adhesive composition.

Thus, the issue of improving thermal performance of adhesives that are used by domestic industries through research of existing and developing new ones is urgent.

In the domestic footwear industry glues-solvents based on polyurethane rubber are mostly used. The aim of this study is to explore the possibility of modifying domestic polyurethane adhesive compositions that could be applied for making shoes, used at elevated temperature conditions and, accordingly, the development of optimum compositions for further study of physical and mechanical properties of heat resistance.

RESULTS AND DISCUSSIONS

By rational selection of urethane elastomer with doping agents that promotes adhesion, it is possible to obtain materials with good adhesive properties, and also change the physical and mechanical parameters depending on the required properties of the adhesive connection.

There are different classes of heat-resistant adhesives such as epoxy and phenol formaldehyde, element and inorganic (phosphate, ceramic, metal), adhesives based on aromatic polymers containing heterocycles, which have different applications. The term "heat-resistant adhesive" is relative and can be interpreted differently depending on the purpose of its use. For the shoe industry the term "heat-resistant adhesive" means the ability to withstand thermal loads within 100°C.

Expansion of the use of adhesive joints in various industries and increasing demands to adhesive joints led recently to a large number of brands of adhesives based on synthetic resins of different types modified with fillers and other additives.

Now there are about a hundred brands of domestic synthetic adhesives, which have different physical, mechanical and technological properties. Depending on the ability to withstand more or less thermal load adhesives can be divided into three groups (Петрова А.П., 1977):

- Adhesives that can withstand prolonged exposure to temperatures around 60°C;
- Heat-resistant adhesives that can withstand long or short-term effect of temperatures of 100°C;
- Highly heat-resistant adhesives that can withstand short-term effect of temperature up to 300°C.

The most famous flameproofing initiator, which is recommended for the manufacturing of shoe adhesive compositions to give flameproofing or ability to self extinguish is pentabromftorbenzol. It is used alone or in combination with other compounds, o,o-di(2,3-dibromopropyl)methyl-phosphonic acid of general formula $CH_3R(O)(OCH_2CHBrCH_2Br)_2$, quaternary amine chelate complexes with metals $[Co(NH_3)_6]C1$, $[Co(NH_3)_5C1]C1_2$; $Co(NH_3)_6Br_3$; $[Cr(NH_3)C1]C1_2$; $Zn(NH_3)_4(BF_4)_2$; $Ni(NH_3)_6(BF_4)_2$. Zinc borate type 2335, antimony trioxide Sb_2O_3 (Лисицина И.И. и соавторы, 1978 is nontoxic, fire retardant.

The most well-known companies abroad that produce adhesive compositions and their components are “Bayer”, “Tivolli”, “Henkel”, “Loctite”, “Teroson” (Germany).

Firms Henkel, Loctite, Teroson are the worldwide leaders in production of adhesives and raw materials. Leading experts of group Henkel have developed such brands of industrial adhesives as SHEMOSIL, CUVERTIN, FLOCKIL, MELONIL, TEROSTAT.

The firm "Bayer" produces adhesives that are used in the domestic market, a mixture of polyurethane rubber type Desmokol and isocyanates containing vulcanizing mixture Desmodur. However, the adhesive includes scarce and toxic components and does not provide high strength adhesive connection.

To improve the initial strength and heat resistance of one-component shoe adhesives firm "Bayer" has developed special grade of urethane rubber - Desmokol 530 and Desmokol 540 (Багалова К.М. и соавторы, 1987). Adhesives based on Desmokol 530, 540 possess more strength and crystallization communications, better adhesion to many materials and higher hydrolytic stability than urethane rubber Desmokol 400 which is widely used in shoe industry. Comparative performance characteristics of the original strength and softening temperature is shown in Figures 1 and 2.

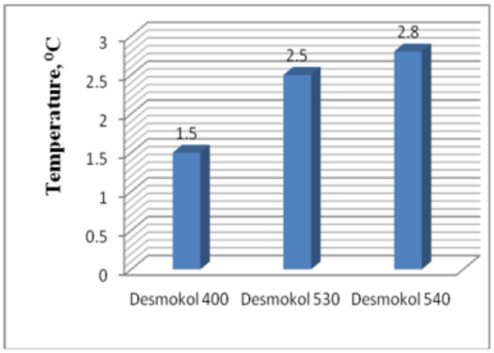

Figure 1. Softening temperature of polyurethane rubber type Desmokol marks 400, 530, 540 (0.18 MPa shear force)

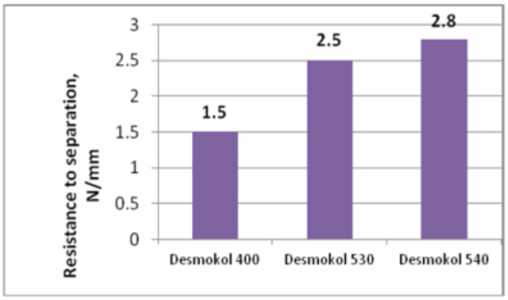

Figure 2. Comparative performance characteristics of the initial strength of urethane rubber type Desmokol 400, 530, 540

Foreign companies develop new highly heat resistant adhesive compositions that can withstand the heat load of about 300-500°C. They are:

- phenolic epoxy adhesives and their modifications, adhesives FPL-878 and FPL-881;
- nitrile-phenolic adhesives AF-31, Metlbond 4021 and Metlbond 304;
- polyamide-phenolic adhesives Hidaks 967 and Hidaks 1033;
- polyurethane Desmokol 530, modified with trioxide antimony Sb_2O_3 (Kiev National University of Technology and Design, Ukraine).

According to information from the foreign press (Techn. Informationsblatter, 1998), ceramic and inorganic adhesives based on boron hydroxide, fluoride phosphate, oxychloride, silicon dioxide and other oxides of elements of group VI are used for gluing highly heat resistant materials.

However, these adhesive compositions are not flexible enough and therefore not recommended for compounds that are affected by the uneven separation and shock, for products that have contact with the human body, i.e. for the production of shoes.

CONCLUSION

Thus, there is a need to explore the creation of new adhesive compositions which would as modifiers contain natural, environmentally friendly components to increase thermal stability and make them economically profitable and allow to reduce the duration of the technological process. The authors consider that it is appropriate to continue developing heat-resistant materials that are used and the possible modifiers polyurethane adhesive compositions to produce special footwear that would withstand high temperature stresses.

The development of technological manufacturing process of a special fire resistant boots using new modified adhesive compositions requires additional studies.

REFERENCES

Багалова К.М. и соавторы (1987), «Полиуретановый клей с улучшенными свойствами», Кожевенно-обувная промышленность, № 12, с.39-40. свидетельство №1348363, кл. С 09 J 175/06, 1987.

Лисицина И.И. и соавторы (1978), «Оптимизация рецептов обувных клеев». Кожевенно-обувная промышленность, № 4, с.49-51.

Петрова А.П. (1977), Термостойкие клеи, Москва, Издательство «Химия», 200с.

*** (1998), *Techn. Informationsblatter*, 32с.

HYPERBRANCHED POLYMERIC ANTIFUNGAL AGENT OF LEATHER

XIAOXING LI, JIE CHEN, JIZHANG JIA

China Leather and Footwear Industry Research Institute, Beijing 100016, China,
omaluya@hotmail.com, chenjie@163.com, jiajizhang2008@163.com

This paper studies a new antifungal agent of leather, hyperbranched polymer leather bactericide. Many of the traditional leather fungicides are disabled because they are believed to be harmful to the human body, so the study of new safety antifungal agent of leather is very necessary. This article through the synthesis of terminal having hydroxyl terminated hyperbranched polymer, and the hydroxyl modified by the quaternary ammonium salt, eventually synthesize glycine salt type hyperbranched polymer. The hyperbranched polymer was characterized by Fourier transform infrared spectroscopy (FTIR). This hyperbranched polymer can be used as a kind of Novel Fungicide for leather.

Keywords: leather; antifungal agent; hyperbranched polymeric.

INTRODUCTION

Many of the traditional leather fungicides are disabled because they are believed to be harmful to the human body, so the study of new safety antifungal agent of leather is very necessary. Hyperbranched polymers can have multiple functional groups. And these functional groups can be used to modified to obtain a new fungicide. This paper studies a new antifungal agent of leather, hyperbranched polymer leather bactericide.

EXPERIMENTAL

Materials

Cyanuric chloride, industrial product, Hebei Chengxin Co. Ltd; 1,3,5-trihydroxybenzene, AR, Sinopharm Chemical Reagent Co. Ltd; hydrobromic acid, AR, Sinopharm Chemical Reagent Co. Ltd; chloroacetic acid, AR, Tianjin fuchen Chemical Reagent Co. Ltd; acetone, AR, Beijing Chemical Reagent Co. Ltd; potassium carbonate, AR, Sinopharm Chemical Reagent Co. Ltd; diethylenetriamine, AR, Sinopharm Chemical Reagent Co. Ltd.

Preparation

Cyanuric chloride, potassium carbonate and acetone were mixed in a 250ml round-bottomed, dried and three-necked separable flask with a mechanical stirrer and a thermometer. The flask was covered with ice. Then the 1,3,5-trihydroxybenzene which was solubled in acetone was dropped into the flask when the temperature at 0°C. The temperature raised to room temperature naturally after the 1,3,5-trihydroxybenzene was dropped into the flask completely. The reaction continued for twenty-four hours. It can get the light yellow liquid after filtration and drying. This product is the hyperbranched polymer which contain many hydroxyl terminated.We called it as R-OH.

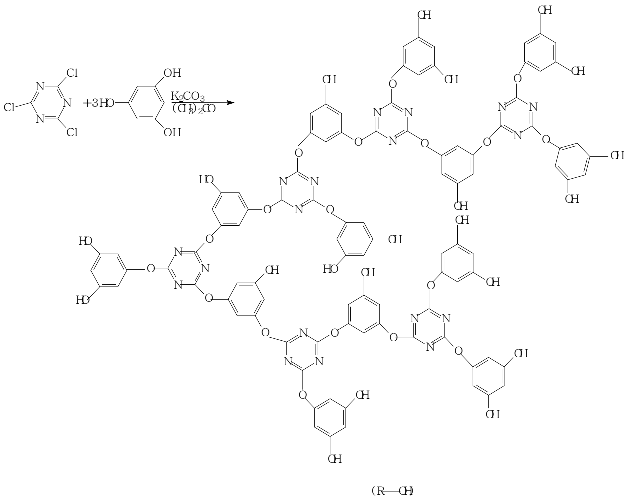

Figure 1. Synthesis of hyperbranched polymers diagram

In the second step, the hyperbranched polymers R-OH were put into a three-necked separable flask which was covered with ice. Then the concentrated sulfuric acid was added slowly, stirring for 1 hour. Then hydrobromic acid (40%) was added, gradually warming up to 90 ~ 95°C, stirred for 8 hours. This flask was put aside for cooling when the reaction was completed. The acid layer was ceded. And the organic layer was washed with a small amount of concentrated sulfuric acid. Then saturated sodium bicarbonate aqueous solution, washed to neutral. The organic layer was dried with Anhydrous calcium chloride and was vacuum distillation.

Then this bromide hyperbranched polymer was reacted with diethylenetriamine, sodium hydroxide (powder), anhydrous magnesium sulfate under 180℃ for 4 hours. The product was filtered and then distilled. The product was added into the flask which contained chloroacetic acid and the amount of deionized water slowly by stirring. Warming to 65 ~ 75°C, the reaction of 3 hours to get the final product, glycine salt hyperbranched polymer.

Application Experiment

We used paper zone of inhibition method to study the antifungal properties of the hyperbranched polymers. The four kinds of fungal was selected for this application experiment, aspergillus (CICC 40374), the aflatoxin (CICC 40375), rope penicillium (CICC 40279), aspergillus versicolor (CICC 2481). All kinds of mold were dubbed a 0.5 McFarland concentration with sterile saline and mixer make the mold suspension uniform. Fungicides with acetone as the solvent dubbed a 0.2% concentration. Medical sterile cotton swab dipped into the mold suspension after coating Cha fungal culture plate, uniform coating three times, each coating a tablet to rotate 60°, and finally the cotton swab around the flat edge of the smear one week. Tweezers to take a sterile blank filter paper, immersed in acetone solution with certain concentration of fungicide, slightly drained, such as acetone after evaporation, attached to the culture plate coated with mold. Fungal culture flat-panel set the mold incubator, 28°C for training, observation, measurement of the size of the zone of inhibition.

RESULTS AND DISCUSSION

Figure 2 shows the infrared spectrum of hyperbranched polymer "R-OH", characteristic peaks of hydroxyl groups occurred at 3226.00cm^{-1} which indicates that the product has generated many hydroxyl groups.

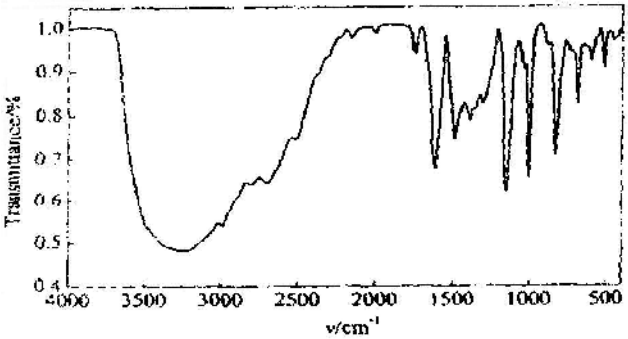

Figure 2. IR absorption spectrogram of hyperbranched polymer"R-OH"

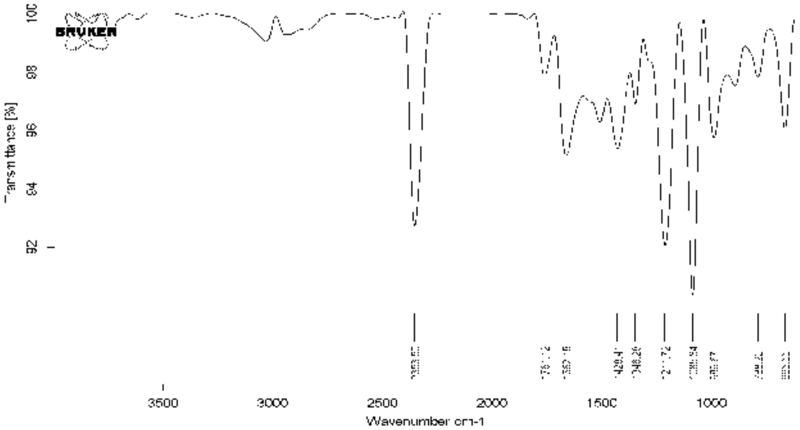

Figure 3. IR absorption spectrogram of glycine salt hyperbranched polymer

Figure 3 shows the infrared spectrum of glycine salt hyperbranched polymer, characteristic peaks of ammonium groups occurred at 2353.50cm^{-1} which indicates that the product has generated ammonium groups; 665.55 cm^{-1} is for the -Cl stretching vibration absorption peak, 3226 cm^{-1} region peaks disappeared which indicated -OH group has been reacted completely.

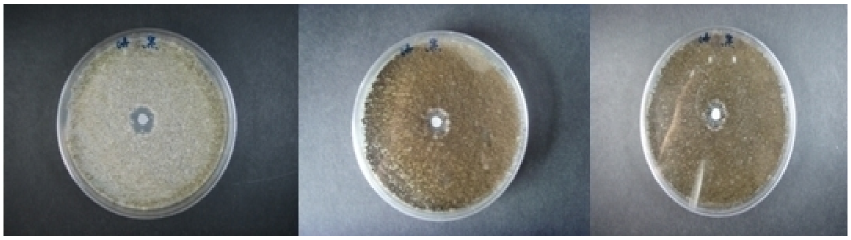

Figure 4. The result of antibacterial circle with aspergillus (2D, 4D, 6D)

Figure 5. The result of antibacterial circle with aflatoxin (2D, 4D, 6D)

Figure 6. The result of antibacterial circle with rope penicillium (2D, 4D, 6D)

Figure 7 the result of antibacterial circle with aspergillus versicolor (2D, 4D,6D)

Table 1. The diameter of antibacterial circle (mm)

	2D	4D	6D
aspergillus	14	12	12
aflatoxin	14	8	8
rope penicillium	6	6	6
aspergillus versicolor	10	7	7

From Figure 4, Figure 5, Figure 6, Figure 7, and Table 1 we can find out that this glycine salt hyperbranched polymer had good inhibitory effect on mold performance to aspergillus. And this hyperbranched polymer also have inhibitory effect on mold performance to aflatoxin and aspergillus versicolor. It did not have good inhibitory effect on mold performance to rope penicillium.

CONCLUSIONS

This paper developed a new type of hyperbranched polymers which can be used as leather antifungal agent. It had good inhibitory effect on mold performance to aspergillus. And this hyperbranched polymer also have inhibitory effect on mold performance to aflatoxin and aspergillus versicolor. It did not have good inhibitory effect on mold performance to rope penicillium.

Acknowledgements

The authors wish to thank National Natural Science Foundation of Republic of China (Project number: 20976188) for the financial support.

REFERENCES

Adminis, U., Huynh, C. and Money, A.C. (2002), “The need for improved fungicides for wet-blue”, *JSLTC*, 86, 118-121.

Gu, H. and Chen, W. (2005), “Mould proof for the leather and the development of fungicides used in leather industry”, *China Leather*, 34(1), 12-15.

PREPARATION OF A COLORED B-CYCLODEXTRIN FRAGRANCE AGENT FOR LEATHER FINISHING

XIAOLING LIU[1,2], XIAOYAN ZHANG[1], WUYONG CHEN[1,2], CARMEN CORNELIA GAIDAU [3], LUCRETIA MIU[3]

[1] *National Engineering Laboratory for Clean Technology of Leather Manufacture, Sichuan University, Chengdu 610065, P. R. China, email: LXLing0@163.com*

[2] *The Key Laboratory of the Education Ministry of Leather Science and Engineering, Sichuan University, Chengdu 610065, P. R. China, email: wuyong.chen@163.com*

[3] *INCDTP - Division: Leather and Footwear Research Institute, 93 Ion Minulescu St., sector 3, 031215, Bucharest, Romania, email: carmen_gaidau@hotmail.com*

Perfume β-cyclodextrin inclusion (P-β-CD) used for leather finishing has been reported already. However when P-β-CD was directly applied in leather finishing, white spots would appear on the leather surface because of the white colour of inclusion compound, which limited its application ultimately. In order to solve the problem, a colored β-cyclodextrin fragrance agent (C-P-β-CD) was prepared through P-β-CD dyed with a reactive dye. Firstly, the P-β-CD was prepared with rose oil and β-cyclodextrin by a saturated solution stirring method, and then the obtained P-β-CD was reacted with a reactive dye to get a colored inclusion. The optimal dyeing conditions of P-β-CD are as follows: the dosage of NaCl is 40g/L, the dye 3.0%, the Na2CO3 15g/L, and the dyeing temperature at 60°C. In addition, the C-P-β-CD was applied in finishing process for fragrant leather and the flavor concentration volatilized from treated leather was evaluated by sensory test. The results demonstrated that the C-P-β-CD could well solve the problem of white spot on the surface of dark color leather with P-β-CD, and the lifetime of leather fragrance was still up to 10 days when the leather with C-P-β-CD was stored under higher temperature and UV intensity conditions.

Keywords: leather, β-cyclodextrin, dyeing.

INTRODUCTION

Recently, there have been several publications about microcapsule technology in the leather fragrance finishing. In 2002, Bayer Company reported the results about fragrance microcapsule used in leather finishing firstly (Kleban et al., 2006). Our group prepared a new perfume β-cyclodextrin inclusion (P-β-CD) by a saturated solution stirring method in 2010 (Xiaoyan et al., 2010). This method can solve the problem of rapid fragrance reducing, however when the P-β-CD was directly applied in leather finishing, white spots appeared on the leather surface due to white color of inclusion material. Thus further application is problematic.

In order to resolve these problems, a colored β-cyclodextrin fragrance (C-P-β-CD) was prepared through P-β-CD dyed with a reactive dye. Firstly, the P-β-CD was prepared with rose oil and β-cyclodextrin by a saturated solution stirring method, and then the obtained P-β-CD was reacted with a reactive coffee dye to get a colored inclusion. The optimal dyeing conditions of P-β-CD were determined by orthogonal experiment. Also, the prepared C-P-β-CD was applied in leather finishing process and the flavor concentration volatilized from treated leather was evaluated by sensory test in the experiment.

EXPERIMENTAL

Materials

The rose oil was purchased from CARBONNEL S.A Company, Spain; the reactive coffee JM-4R dye was bought from Ruihua Chemical Company, Zhenjiang, China; other reagents were purchased from Kelon Chemical Company, Chengdu, China.

Preparation of Perfume β-cyclodextrin Inclusion (P-β-CD)

A β-CD was completely dissolved in water (the ratio of β-CD and water is 1:12) in a round flask to get a saturated solution, and the solution was kept a constant temperature at 50°C. A rose oil (the mass ratio of rose and β-CD is 1:8) previously diluted using ethanol was dropped into the β-CD saturated solution and stirred for 3 hours to get a perfume β-cyclodextrin inclusion (P-β-CD).

Dyeing of P-β-CD

The reactive coffee JM-4R dye is a vinylsulfone dye, whose general formula is D-$SO_2CH_2CH_2OSO_3Na$. The van der Waals forces (VDW) and hydrogen bonding between this kind of dye and inclusion compound are weaker, and the affinity of the dye for inclusion compound is smaller. To improve the uptake rate of dye, an appropriate amount of promoting agent should be added. And this kind of dye is very stable in acidic and neutral solution, while the dye-fiber bonding would be easily hydrolyzed under alkaline conditions. Because the dye should be reacted with inclusion compound in alkaline condition, a specific fixing agent needs to be added to make the dye fix on inclusion compound.

Based on the above discussion, the dyeing processes are as follows. A promoting agent (NaCl) was completely dissolved in the obtained solution of P-β-CD. A reactive coffee JM-4R dye was added and dyed for 30 minutes. A fixing agent (Na_2CO_3) was added and reacted for 1 hour, and then transferred to refrigerator (below 4°C) to store for above 12 hours. After filtrating, the sediment was dried in a 40°C oven to get a colored β-cyclodextrin fragrance (C-P-β-CD). Dried samples were sealed in plastic bags to protect them against changes in humidity.

In order to optimize the dyeing conditions, a series of orthogonal experiments were designed. The uptake rate of dye was as an index, and the main factors selected were the dosage of NaCl (A), the dosage of dye (B), the dosage of Na_2CO_3 (C) and the dyeing temperature (D). Details of four factors in the experiments are described in Table 1.

Table 1. Levels and factors of orthogonal experiment L_{16} (4^4)

Level / Factor*	1	2	3	4
A (g L^{-1})	20	30	40	50
B (%)	1	3	5	7
C (g L^{-1})	5	10	15	20
D (°C)	50	55	60	65

*A is the dosage of NaCl, B is the dosage of dye, C is the dosage of Na_2CO_3, D is the dyeing temperature.

Evaluation of Uptake Rate for Dye

The standard solution of reactive coffee JM-4R dye containing 100μg mL^{-1} was scanned in the UV-visible spectra (350-700 nm) (Lingling et al., 2009). The spectrum absorption curves were drawn, and the maximum absorption wavelength (421.3nm) was determined and used as a standard in determination of the uptake rate of dye.

The dyeing waste (2ml) was exactly absorbed in 50ml volumetric flask and water was added to make the volume up to exactly 50ml. The absorbance (A_x) of dyeing waste and the absorbance (A_0) of blank sample were determined at maximum absorption wavelength, and the uptake rate of dye was calculated using the following formula:

$$\text{uptake rate} = \frac{A_0 - A_x}{A_0} \times 100\% \qquad (1)$$

Application of C-P-β-CD on Leather Finishing

The 8% (w/w) of the C-P-β-CD was mixed with top coating materials and coated on the sofa leather. The coating performance of leather with C-P-β-CD and P-β-CD respectively was evaluated.

Also, the leather samples with C-P-β-CD and rose oil alone were all aged some time in a weathering tester (UV: 0.68W cm^{-2}, 45°C). The flavor concentration volatilized from treated leather was assessed by sensory test every 12 hours. The flavor degree was divided into six levels (see Table 2).

Table 2. Degree of the odor preservation

Level	fragrance
0	odorless
1	easy to find (initial concentration)
2	obvious fragrance (identifiable concentration)
3	easily perceived
4	stronger
5	very strong

RESULTS AND DISCUSSIONS

Dyeing Mechanism of P-β-CD

The hydrophobic perfume was introduced to the β-CD cavity to form inclusion complexes. When the P-β-CD is dyed, the reactive dyes with polar groups are not easily into the cavity in β-CD and bond with the hydroxyls on the lateral of β-CD (Linhui, 2001). Then the P-β-CD was reacted with a reactive dye to get a colored inclusion. All kinds of colored P-β-CD could be prepared with the different colors of reactive dyes and the diagram is shown in Figure 1.

Optimization of the Dyeing Condition for P-β-CD

The orthogonal experiment results and their range analysis are shown in Table 3, using uptake rate of dye as indexes.

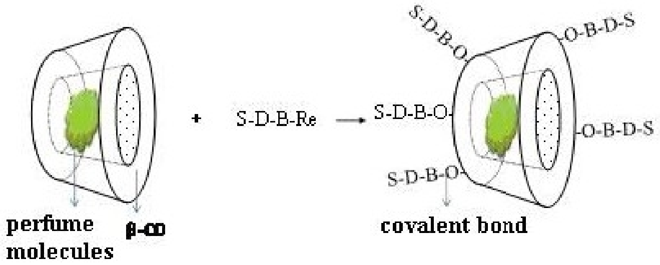

Figure 1. Diagram of the dyeing mechanism for P-β-CD (S-D-B-Re: a chemical structure of reactive dye, S for a water-soluble group, D for a chromophore of dye, B for a joint and Re for an active group)

Table 3. Design of experiments and interpretation of results

Number	A	B	C	D	Uptake rate (%)
1	1	1	1	1	10.59
2	1	2	2	2	25.73
3	1	3	3	3	14.04
4	1	4	4	4	0.77
5	2	1	2	3	22.02
6	2	2	1	4	21.57
7	2	3	4	1	3.47
8	2	4	3	2	9.23
9	3	1	3	4	26.00
10	3	2	4	3	29.47
11	3	3	1	2	4.68
12	3	4	2	1	1.3
13	4	1	4	2	19.48
14	4	2	3	1	28.92
15	4	3	2	4	7.1
16	4	4	1	3	1.19
K1	12.78	19.52	9.51	11.07	-
K2	14.07	26.42	14.04	14.78	-
K3	15.36	7.32	19.55	16.68	-
K4	14.17	3.12	13.30	13.86	-
Range	2.58	23.3	10.04	5.61	-

From the results of Table 4, we can see that the optimal levels of factors A, B, C, D to obtain the highest uptake rate of dye are A3, B2, C3, D3 respectively. So the optimal dyeing conditions of P-β-CD are as follows: the dosage of promoting agent (NaCl) is 40g/L, the dye 3.0%, the fixing agent (Na_2CO_3) 15g/L, and the dyeing temperature at 60°C.

From the range analysis we can see that factor B (dosage of dye) which had the maximum range had the greatest influence on dyeing of P-β-CD. Similarly, the sequences of the four main factors (according to the contribution to the uptake rate of dye) are B (dosage of dye) > C (dosage of Na_2CO_3) > D (dyeing temperature) > A (dosage of NaCl).

Although the dyeing processes can solve the problem of P-β-CD coloring, the uptake rate of dye was lower because of coagulating of dye and weaker affinity for inclusion compound at low temperature. These problems will need to be resolved in subsequent work.

Effect of C-P-β-CD on the Surface of Coated Leather

a b

Figure 2. The effect of C-P-β-CD and P-β-CD on the surface of coated leather (a: C-P-β-CD, b: P-β-CD)

The coating performance of leather with C-P-β-CD and P-β-CD is shown in Figure 2. Some white spots appeared on the leather surface with P-β-CD, which has a greater influence on colored leather (Figure 1b). The coating uniformity of leather with C-P-β-CD was much better (Figure 1a), showing that the C-P-β-CD could well solve the problem of white spot on the surface of dark color leather.

Effect of UV Aging on Odor Retention of Fragrance Leather

To evaluate the effect of C-P-β-CD on odor retention of leather, the odor retention of fragrance leather with C-P-β-CD and rose oil respectively were assessed by sensory test in different aging times (Figure 2).

Figure 3 shows that the lifetime of leather fragrance was only one day when the leather with rose oil was stored under the condition of higher temperature as well as UV intensity. But for the leather with C-P-β-CD, the lifetime of leather fragrance was still up to 10 days. So the odor retention of leather with C-P-β-CD is significantly better than that of rose oil alone, which indicates that C-P-β-CD is a material that can control the flavor release and make the odor preservation time longer. So we might speculate that the lifetime of leather fragrance could be as long as a few years when the leather with C-P-β-CD is stored under natural conditions.

Also, Figure 3 shows that the rank of flavor concentration volatilized from treated leather was reduced as the aging time increasing, because the fixation of coating film to C-P-β-CD would be reduced and the embedding capacity of β-cyclodextrin to perfume could be affected in the condition of high UV intensity.

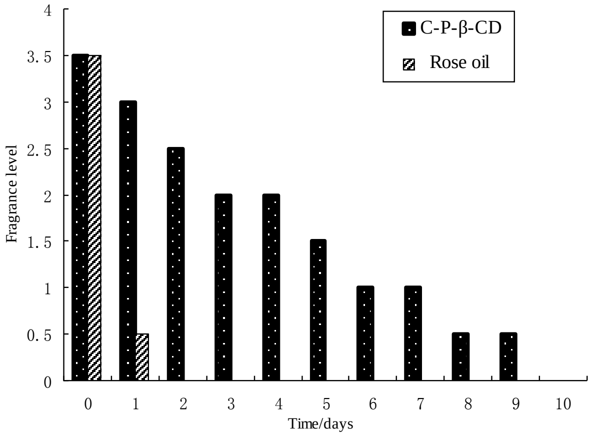

Figure 3. The effect of UV aging on odor retention of fragrance leather

CONCLUSIONS

This study presented a way to prepare a colored fragrant inclusion. The prepared C-P-β-CD could well solve the problem of white spot of P-β-CD in a colored leather finishing. Also, the lifetime of the leather fragrance was still up to 10 days when leather with C-P-β-CD stored under the condition of higher temperature and UV intensity. These results indicate the prepared C-P-β-CD could be used in colored leather with longer odor preservation time.

Acknowledgements

The authors wish to thank the Ministry of Science and Technology of China for financial support of the cooperation project (No.2009DFA42850 and No. 40-3).

REFERENCES

Kleban, M., Weisser, J., Koch, F. et al. (2006), "Leather Finished with Scent-containing Microcapsules", US: 2006216509, 2006-09-28.

Lingling, H., Yunfeng, J. and Meng, Z. (2009), "Alkaline Dyeing of Disperse Dyes for PTT Fabrics", *Printing and Dyeing*, (20), 19-22.

Linhui, T. (2001), *Cyclodextrins Chemical - Basic Application*, Science Press, 10-60.

Xiaoyan, Z., Chen, W., Xiaoling, L. et al. (2010), "Preparation of β-cyclodextrin/Jasmine Oil Inclusion Compounds for Durable Fragrant Leather", *Leather and Footwear*, 39(11), 11-14.

PROPERTIES OF LEATHERS TANNED WITH TI-AL BASED TANNING MATERIALS OBTAINED FROM THE WASTES OF METAL INDUSTRY

MEHMET METE MUTLU[1], ARIFE CANDAS ADIGUZEL ZENGIN[1], MARIAN CRUDU[2], STELIAN SERGIU MAIER[3], VIORICA DESELNICU[2], LUMINITA ALBU[2], GURBUZ GULUMSER[1], BEHZAT ORAL BITLISLI[1], BAHRI BAŞARAN[1], CEMILE CEREN TOSUN[1]

[1] *Ege University, Engineering Faculty, Leather Engineering Department, Bornova, İzmir, Turkiye, mete.mutlu@ege.edu.tr*

[2] *National Research and Development Institute for Textile and Leather, Leather and Footwear Research Institute, Bucharest, Romania*

[3] *"Gheorghe Asachi" Techical University of Iaşi, Faculty of Textiles, Leather and Industrial Management, Iaşi, Romania*

Although chromium tanning is the most popular tanning system worldwide, it is held under the microscope due to increasing requirements on disposal of chromium tanning effluents, by-products and sludge. For this reason; in last decades, researches on alternative tanning materials which will decrease or replace chromium usage take a great share among the main topics in the area of leather researches. In this research, a newly produced titanium based tanning agent, obtained from processing wastes from the industry of nonferrous metals was used as an alternative to chromium tanning agent. The new titanium tanning agent was experimented with 1%, 2.5%, 5%, 7.5 and 10% dosages. Physical tests and chemical analysis of the produced chromium-free leathers gave comparable results to leathers tanned with basic chromium sulphate. 5% usage of titanium tanning agent was found to be optimal.

Keywords: chromium-free leathers, titanium, tanning.

INTRODUCTION

When we talk about tanning today, the topic is usually raised in connection with environmental compatibility. Due to the increasingly stringent requirements governing tannery effluents as regards their chrome content, and due to a variety of problems involved in the disposal or utilization of by-products containing chrome, chrome tannage in particular has recently come under criticism (Germann, 1994).

The chromium salt tanning system, which is still the most popular leather tanning procedure is under continuous pressure from environmental groups and international regulations due to pollution and toxicology reasons unfairly associating the Chromium (III) commonly used with hazardous Chromium (VI) (Adiguzel Zengin et al., 2011)

The environmental regulatory agencies in many countries have come out with stringent stipulations for permissible levels of chromium in wastewater which are in the range of 0.3–2.0 ppm. In recent years, there has been a growing social awareness to contain chromium discharge in wastewaters. Conventional treatment systems adopted for the removal of chromium from waste streams produce large quantities of chrome-containing sludge, which has been listed among the hazardous wastes. Further, the cost escalation in leather processing on the one hand, and the increasing price of the chrome-tanning salts on the other, have rendered the better management of chromium in tanneries a vital economic priority (Sundar et al., 2002).

Under these circumstances, quest for new alternative tanning materials which will decrease or replace chromium use is inevitable. In this research, a newly produced titanium based tanning agent, obtained from processing wastes from the industry of nonferrous metals was used as an alternative to chromium tanning agent. Physical tests and chemical analysis of the produced chromium-free leathers are compared with the leathers tanned with basic chromium sulphate.

MATERIAL AND METHOD

Six pickled sheep skins were used as material. The leathers were cut into four pieces from backbone line and a perpendicular line to the backbone, to increase the repetition of trials. Each leather sample was coded and processed in a different tanning drum. Each trial was made with 4 repetitions. The leather samples were processed with a standard clothing leather production recipe except the Titanium-Aluminum containing tanning material TMW/2 which was a product produced by using the wastes from the industry of nonferrous metals (Crudu, 2010). Various amounts of tanning materials were used in tanning process according to the Table 1.

Table 1. Experimental design for various amounts of tanning material

Trial Name	Parameter
T0	Blank (Chromium tanned leather)
T1	% 1 Titanium tanning material
T2	% 2.5 Titanium tanning material
T3	% 5 Titanium tanning material
T4	% 7.5 Titanium tanning material
T5	% 10 Titanium tanning material

Physical tests and chemical analysis were carried out in the laboratories of Department of Leather Engineering in Ege University, Izmir by using the following equipment: tensile tests with Shimadzu AG-IS, color measurements with Minolta CM-3600d, formaldehyde analysis with Agilent Technologies 1200 Series HPLC, titanium amounts in leather with Perkin Elmer Optima 2100 DV ICP-OES.

Leather samples were prepared in accordance with “sampling location” and conditioned according to “sample preparation and conditioning” standards TS EN ISO 2418 and TS EN ISO 2419 (Anon. 2006b and 2006c).

For determination of the chemical and physical properties of the chromium-free leathers, TS 4119 EN ISO 3376: tensile strength (Anon. 2006a), TS 4119 EN ISO 3376: elongation at break (Anon. 2006a), TS 4118-2 EN ISO 3377-2: tear strength (Anon. 2005a), color measurement of surface with spherical spectrophotometer, TS EN ISO 17226-1: formaldehyde determination with HPLC (Anon. 2009d), TS 4120 EN ISO 3380: shrinkage temperature (Anon. 2005b), TS EN ISO 4045 pH value (Anon. 2009b), TS 4125 EN ISO 4047: ash content % (Anon. 2009a), TS EN ISO 4048 determination of matter soluble in dichloromethane (%) (Anon. 2009c), and TS 4126 chromium oxide (%) (Anon. 1985) tests were performed.

RESULTS AND DISCUSSION

The amount of tanning material as titanium content in leather samples are given in Table 2. It should be expected that there should be a change in Titanium content because of changing amounts of offered tanning material; however there is not a straight correlation. The titanium content of leathers increases proportionally with 1%, 2.5% and 5% tanning material offers. But this increase slows down for 7.5% and 10% tanning material offers. This shows that, we cannot bind all of the tanning material to collagen after 5% metal oxide offer.

The shrinkage temperatures of leathers tanned with varying amounts of tanning materials can be seen in Figure 2. The average shrinkage temperatures of leathers are 75.5, 79.8, 80.4, 80.3 and 81 for tanning material offers of 1%, 2.5%, 5%, 7.5% and 10% respectively. It is seen that there is not a considerable difference for 5% and more amounts. High shrinkage temperatures, like 90°C, can be achieved with Titanium solo tanning, however, this requires large quantities and this causes the leather to be overfilled, and yet remain soft (Covington 2006). Peng et al. (2007) have tanned goat skins with a 7.5% TiO_2 offer and the ending shrinkage temperature was 84°C after tannage. Galiana et al. (2011) have obtained 85°C shrinkage temperature with SANOTAN, a new type of titanium-based tannage.

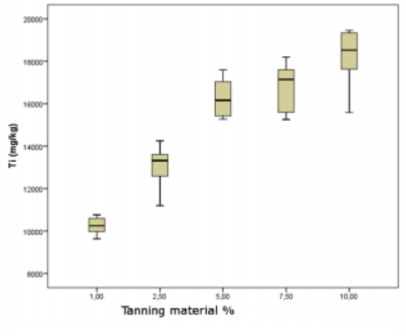

Figure 1. Titanium content of leathers tanned with various amounts of tanning materials

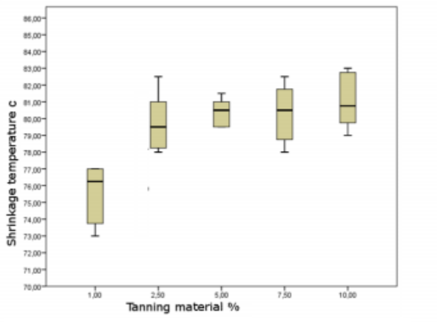

Figure 2. Shrinkage temperatures of leathers tanned with various amounts of titanium tanning agents

When the results of titanium content in leathers and shrinkage temperatures are considered together, it can be claimed that increasing the titanium content up to 5%, also increases the shrinkage temperature proportionally, but this increase loses its importance over 5% titanium content. Shrinkage temperature is one of the key indicators of tannage, however it is not enough alone. The physical and chemical changes of leathers also should be considered.

Table 2 shows the results of physical tests applied to the leathers tanned with chromium and varying amounts of titanium tanning agents. The average of tensile strengths of leathers tanned with titanium tannin is 21 N/mm^2 which is equal to the tensile strength of chromium tanned leather sample. However the elongations of titanium tanned leathers at break are considerably below than the chromium tanned sample. It can be concluded that titanium solo tannage causes low elongations, a pretanning is recommended. When the tear strength values of titanium tanned leathers are considered, their average is 70 N/mm, which is 3.3 times higher than the chromium tanned leathers. UNIDO offers a minimum of $10N/mm^2$, 15 N/mm^2, and 20 N/mm^2 of tensile strength for chromium tanned garment leathers, linings, and shoe upper leathers respectively. Also, UNIDO offers a minimum of 15N/mm, 25 N/mm, and 30 N/mm of tear strength for chromium tanned garment leathers, linings, and shoe upper leathers respectively. The mechanical properties of leather tanned with titanium are compatible with the acceptable quality standards advised by UNIDO (1996).

Table 2. Physical properties of leathers tanned with varying amounts of titanium tanning agents

Trial	Tensile Strength (N/mm^2)	S.D.	Elongation at Break (%)	S.D.	Tear Strength N/mm	S.D.
T0	21	6	77	16	21	3
T1	29	5	28	3	81	6
T2	21	5	30	7	71	14
T3	19	5	31	3	67	13
T4	21	3	30	5	69	10
T5	17	2	29	4	61	7

Another effect of a tanning material to the leather is the color. Tanning materials give their natural color to leather. Covington (2009) stated that the leathers tanned with titanium (IV) salts were initially colorless although it tended to go pale yellow with aging. In Table 3, colors of leathers tanned with chromium and changing amounts of titanium tanning agents and their color differences to white color (ΔE) are given. The pseudo colors are generated by the color measurement software. The color difference of 1% titanium containing leather to white color is similar to the chromium tanned leather as ΔE values. However the colors are different, which can be seen from pseudo colors and L, a, b values. As it is seen in Δb values there is an increase in yellow tones in titanium tanned leathers. But neither color difference nor yellowness increase proportionally with the increase in tanning agent amount.

Table 3. Color measurement values of leathers tanned with chromium and varying amounts of titanium tanning agents

Trial	L	a	b	ΔL	Δa	Δb	ΔE	Pseudo Color
White	98.92	-0.11	-0.36					□
T0	78.92	-2.98	3.90	-20.00	-2.87	4.25	20.65	■
T1	84.46	-2.29	13.72	-15.05	-2.27	14.66	21.14	■
T2	83.27	-1.21	19.66	-15.64	-1.10	20.01	25.58	■
T3	82.77	-1.52	18.10	-16.14	-1.41	18.45	24.78	■
T4	84.54	-1.52	17.76	-14.37	-1.41	18.11	23.31	■
T5	80.82	-1.61	18.45	-18.09	-1.50	18.80	26.43	■

Chemical analysis results of leathers tanned with chromium and varying amounts of titanium tanning agents are given in Table 4. The average fat content of titanium tanned leathers is19.97%, which is very similar to chromium tanned leather. When we consider this data with the physical properties in Table 3, we can say that the strength values are due to the tanning agent change; because strength properties of leathers are a result of behavior of collagen fibers which are mainly affected by tanning and fatliquoring agents. Although the tanning takes place in a very acidic medium, the pH values of titanium tanned leathers are around 4.2 because of the basification process. The ash contents of leathers are indication of inorganic materials in leather and these increases with the inorganic tanning material offer. The free formaldehyde content of leathers are approximately 12.15ppm which is below the limits. It is not recommended that the products for general applications, products in contact with skin, and baby leather products contain formaldehyde higher than 200, 75, and 20 ppm respectively (Anon. 2008).

Table 4. Chemical properties of leathers tanned with varying amounts of titanium tanning agents

Trial	Fat (%)	S.D.	pH	S.D.	% Ash	S.D.	Formaldehyde ppm	S.D.
T0	22.19		4.21		4.14		5.88	
T1	16.98	0.98	4.34	0.19	3.82	0.13	9.48	0.55
T2	20.36	1.30	4.06	0.18	5.18	0.64	13.69	1.89
T3	19.63	1.08	4.10	0.04	5.11	0.12	10.46	1.30
T4	20.16	3.75	4.12	0.07	5.40	0.16	13.82	0.90
T5	19.74	3.93	4.34	0.03	5.95	0.21	13.28	1.87
Mean (T1, T2, T3, T4, T5)	19.97	2.74	4.19	0.17	5.09	0.77	12.15	2.27

CONCLUSION

In this research, it was demonstrated that a material obtained from wastes of metal industry could be used as a tanning material in leather industry. Although the shrinkage temperature was around 80°C, physical and chemical properties of titanium tanned leathers gave comparable results to chromium tanned leathers, but with more yellowish color and less elongation. Although the tensile strength values of titanium tanned leathers are same with the chromium tanned samples, the tear strength values are considerably higher. So these leathers can be used in production of articles where high strength values and form stabilization are required, such as shoe uppers, leather crafts or upholstery leathers.

Titanium containing tanning materials in concentration of 1%, 2.5%, 5%, 7.5% and 10% were offered to leathers. The properties of leathers increased did not increase proportionally with the tanning material offer after 5%. So, a tanning material usage containing 5% titanium can be advised for tanning to get optimal results.

The project has two outcomes: First, a waste of metal industry is evaluated in another industry. Second, environmental load of leather wastes are decreased by using an alternative tanning agent rather than highly discussed chromium.

The chromium free leathers produced under this project have many application advantages as:

- No chromium in effluents;
- Shavings and cuttings can be recycled;
- Leathers are light colored and can be dyed to fashion colors easily;
- Leather have high strength values;
- An efficient quality assort can be made at wet-white stage.

Acknowledgements

The authors would like to thank Tübitak and ANCS for their financial support to this project (Project Number: 109M393) and the State Planning Organization (DPT) along with the Ege University Scientific Research Projects Office (BAP) for their instrumental support (Project number 2007-DPT-001 and 2010-MUH-009).

REFERENCES

Adiguzel Zengin, A.C. et al. (2012), “Eco-leather: Chromium-free Leather Production Using Titanium, Oligomeric Melamine-Formaldehyde Resin, and Resorcinol Tanning Agents and the Properties of the Resulting Leathers”, *Ekoloji*, 21(82), 17-25.

Covington, A. (2006), “The Chemistry of Tanning Materials”. In: Kite M, Thomson R (eds), *Conservation of Leather and Related Materials*, Elsevier, Oxford, UK, 29-30.

Covington, A. (2009), *Tanning Chemistry-The Science of Leather*, The Royal Society of Chemistry, Cambridge.

Crudu M. et al. (2010), “New Tanning Agents Based on Titanium and Zirconium”, *Proceedings of the 3rd Advanced Materials and Systems Conference ICAMS 2010*, 27-32.

Galiana, M.V. et al. (2011), “New Type of Titanium-based Tannage”, XXXI IULTCS Congress, Valencia, Spain.

Germann, H.P. (1994), “Chrome Tannage From The Viewpoint Of Ecology”, *JSLTC*, 79, 82-85.

Peng, B.Y. et al. (2007), “Novel Titanium(IV) Tanning for Leathers with Superior Hydrothermal Stability Part III Study on Factors Affecting Titanium Tanning and an Eco-Friendly Titanium Tanning Method”, *Journal of the American Leather Chemists Association* 102, 297-305.

Sundar, V.J., Raghava Rao, J. and Muralidharan, C. (2002), “Cleaner chrome tanning — emerging options”, *Journal of Cleaner Production*, 10(1), 69-74.

*** (1985), TS 4126 Determination of Chromic Oxide (Cr_2O_3). Turkish Standard (TSE), Ankara, Turkey.

*** (1996), UNIDO Acceptable quality standards in the leather and footwear industry, ISBN: 92-1-106301-9, Vienna.

*** (2005a), TS 4118-2 EN ISO 3377-2 Physical and mechanical tests; Determination of tear load - Part 2: Double edge tear. Turkish Standard (TSE), Ankara, Turkey.

*** (2005b), TS 4120 EN ISO 3380 Physical and mechanical tests - Determination of shrinkage temperature up to 100 C. Turkish Standard (TSE), Ankara, Turkey.

*** (2006a), TS 4119 EN ISO 3376 Physical and mechanical tests - Determination of tensile strength and percentage extention. Turkish Standard (TSE), Ankara, Turkey.

*** (2006b), TS EN ISO 2418 Chemical, physical and mechanical and fastness tests - Sampling location. Turkish Standard (TSE), Ankara, Turkey.

*** (2006c), TS EN ISO 2419 Physical and mechanical tests- Sample preparation and conditioning. Turkish Standard (TSE), Ankara, Turkey.

*** (2008), Restricted substances-formaldehyde. Leather International Magazine 7, 44-45.

*** (2009a), TS 4125 EN ISO 4047 Determination of sulphated total ash and sulphated water- Insoluble ash. Turkish Standard (TSE), Ankara, Turkey.

*** (2009b), TS EN ISO 4045 Chemical tests - Determination of pH, Turkish Standard (TSE). Ankara, Turkey.

*** (2009c), TS EN ISO 4048 Chemical tests - Determination of matter soluble in dichloromethane and free fatty acid content. Turkish Standard (TSE), Ankara, Turkey.

*** (2009d), TS EN ISO 17226-1 Chemical determination of formaldehyde content - Part 1: Method using high performance liquid chromatography. Turkish Standard (TSE), Ankara, Turkey.

FORMALDEHYDE IN CLOTHING AND INTERIOR TEXTILES

MARILENA NICULESCU, CARMEN GHITULEASA, ANA MARIA MOCIOIU,
GHEORGHE NICULA, LILIOARA SURDU

The National R&D Institute for Textiles and Leather Bucharest (INCDTP), 16 Lucretiu Patrascanu st., 030508 Bucharest, Romania, email: certex@ns.certex.ro

In recent years, extensive efforts for competitiveness on the global market have been made to create technologies and new textile products with low environmental impact. This paper presents the legal restrictions for formaldehyde in clothes and interior textiles and discusses the amount of formaldehyde present in textiles on the Romanian market. When human skin is exposed repeatedly to formaldehyde it may occur irritations and in some cases allergies. At high levels of exposure to formaldehyde may even tumors. There were investigated 161 textile products intended to come into contact with the skin (clothing for children, women, men, linen), primarily concern being cotton and its blends. The quantitative formaldehyde assays in clothes for children's textiles and interior textiles are discussed here.

Keywords: textiles, formaldehyde, interior textiles.

INTRODUCTION

Competition advantages required for textile products on the market relate to quality and design, innovation and technology, high added value. And this is not enough, the products have to be officially recognized by certification, ecolabels, etc. These may require additional verification effort or a slight increase in costs.

Present trends for the textile sector include also the marketing of textile products with low environmental impact and human health protection. In this respect one of the monitored substances is the formaldehyde.

Formaldehyde is one of the most widely used chemicals in the world.

Formaldehyde is present in very small quantities, usually less than 0.06 ppm, both within a room and outdoors (Occupational Safety and Health Standards).

When the air reaches the formaldehyde levels 0.1 ppm may appear as health effects: watery eyes, burning sensations in the eyes, nose, and throat, cough, difficulty of breathing, irritation of the skin (De Groot et al., 2010). Similar effects to those produced by formaldehyde appear in case of allergies, cold, flu.

People react differently to formaldehyde: the sensitive one react at a concentration of 0.1 ppm. The World Health Organization recommends no more than 0.05 ppm exposure.

In June 2004, the toxicity of this substance has been revalued upwards by the International Center for research on cancer (CIRC) and thus from "likely" carcinogen (Group 2A) it became "carcinogenic to humans" secure (Group 1). This has led to the multiplication of studies for assessment of formaldehyde emissions on different products and environments.

FORMALDEHYDE IN TEXTILE INDUSTRY

In the textile industry, formaldehyde is present in textile finishing processes to impart to products easy-care properties and other properties such as:

- resistance to wrinkling;
- good dimensional stability;

- compatibility with other agents finishing (waterproofing agents, emulsifiers, whitening);
- color resistance;
- the maintenance of white fabric;
- low emission of formaldehyde;
- protection of the environment in the process of the application of resins and other finishing operations for the final product;

These formaldehyde resins can chemically degrade under certain conditions of heat and humidity, with the release of formaldehyde. For this reason, many countries have introduced by law restrictions on formaldehyde contained in products, including textiles.

EUROPEAN REGULATIOSN ON FORMALDEHYDE AND TEXTILES

Harmonised European legislation does not contain rules on the restriction of free formaldehyde in textiles. But some countries have legal limits on the content of formaldehyde in textile products in order to reduce the risk of allergy and appearance of other adverse health effects on the population. Such laws have been adopted by:

- Germany-Bedarfsgegenständeverordnung, April 1992.
- Austria-194/Ordinance 1990.
- Finland-Decree 210/1988.
- Netherlands-Decree of 22 March 2001.
- Norwegian Government-Regulation nr. 922/June 1, 2004.

EU Eco-Label

In the European legislation has been introduced (1993) by the European Commission the EU eco-label for advertising of products with a high level of environmental performance.

Through the Regulation (EC) no. 66/2010 were established rules for the establishment and implementation of the EU voluntary ecolabelling system.

The EU ecolabel has as symbol a flower whose petals are 12 stars (Regulation (EC) No 66/2010).

Figure 1. EU ecolabel symbol

The EU eco-label is awarded to 23 product groups including those connected with the textile sector which are textiles and bed mattresses.

Commission decision 2009/567/EC establishing the ecological criteria for the award of the Community eco-label to textile products, the following specific criteria (Commission decision 2009/567/EC):

- Formaldehyde shall not be used for stripping or depigmentation (art. 12);
- The amount of free and partly hydrolysable formaldehyde in the final fabric shall not exceed 20 ppm in products for babies and young children under 3 years old, 30 ppm for products that come into direct contact with the skin, and 75 ppm for all other products.

Formaldehyde testing is to be carried out in accordance with the method laid down in the standard SR EN ISO 14184-1.

- Filling materials consisting of fibrous material shall comply the requirements for the formaldehyde in textile products listed in article 26 (art. 31.2).

By comparison, in EU GPP (Green Public Procurement) criteria for textiles (Textile Industry, 2012), (http://ec.europe.eu/environment/gpp/pdf/criteria/textiles.pdf), the admissible amount of free and partially hydrolysable in the final product is much greater.

There are some studies presenting results for the evaluation of free formaldehyde on textiles (Piccinini et al., 2007; GAO, 2010), but they focus on a specific market and are not so ample as to predict the market level. But they give valuable data related to human exposure to chemicals/formaldehyde for consumers of textile products, for market surveillance organizations and organizations that make decisions on public health.

EXPERIMENTS

In order to evaluate the free formaldehyde emissions in textile products, in this paper we tested 161 textile products from the Romanian market, originated in 12 countries, most of them being produced in Romania (see Table 1 and Figure 2).

Table 1. Country of origin for the testing products

Producing country	No of products	Share per country (%)
Bangladesh	3	2
China	8	5
India	1	0,6
Italiy	3	2
Poland	2	1,2
Portugal	1	0,6
Romania	122	76
Spain	3	2
USA	1	0,6
Sweden	2	1,2
Thailand	1	0,6
Turkey	2	1,2
Unknown	12	7,5

The fibrous composition of tested textile products, the percentage of raw materials used is as follows (Figure 2): 57% of the samples are made up of cotton, 21% have the composition of cotton mixed with other fibres, 8% means products of wool and blended wool, 8% viscose, 12% other fibers.

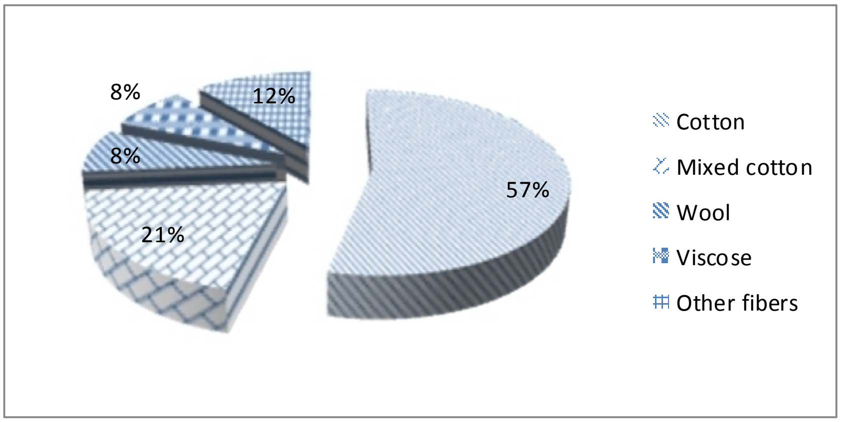

Figure 2. Fibrous composition of tested products

As for the intended user, the tested textile products include the following (Figure 3):

- ✓ textile products for children -16%
- ✓ textile products for women -12%
- ✓ textile products for men -30%
- ✓ various -12%
- ✓ linen -27%

In this paper we present the results for children's textiles and interior textiles.

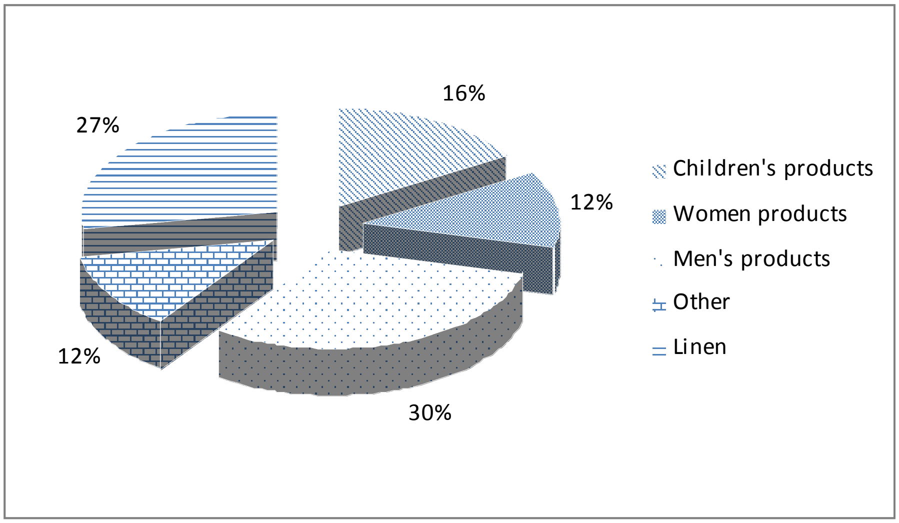

Figure 3. Tested products per user category

Free Formaldehyde Testing on Children's Textiles

When selecting products, particular importance has been given to testing of textiles for children which included products as: thick diaper, shirt, blouse, shirt, socks, stockings, panty, panty, dress, plush toys.

For these products, selection was made in order to have different linings and dyes, and printed motifs.

The products being tested were mostly printed textiles (72%).

Results of testing formaldehyde content in textiles intended for children are shown in Figure 4.

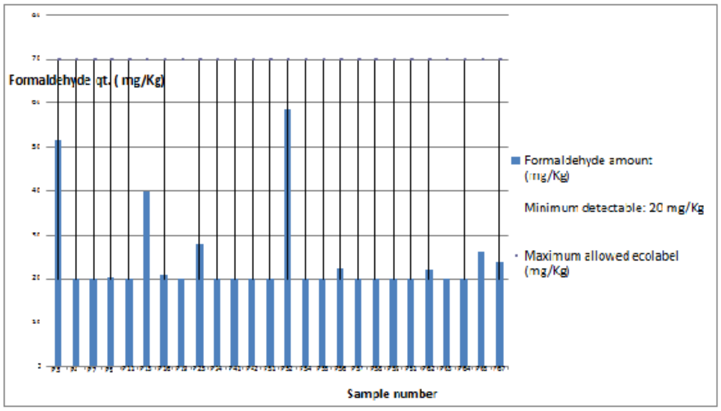

Figure 4. Formaldehyde emissions in children's clothes

The results indicate normal values for the 22 samples representing 78% of the total samples, 3 samples that exceed the limit imposed that is a minimum of 20 mg/Kg (P56-t-shirt, 67-plush bear, P67- dress) and 2 samples with high values for formaldehyde when compared with the limit of 30 mg/Kg (8%):

- P13- printed cotton, underside, 39.8 mg/Kg compare to 30 mg/Kg allowed;
- P52- printed shirt, phosphorescent 58.5 mg/Kg (allowed only 30 mg/Kg).

Free Formaldehyde Testing on Interior Textiles

In this category of samples has been included bed linen, tablecloths type samples, and bath and kitchen towel type.

For the category of linens (29 samples) the majority being printed (representing 18% of all samples), the determined values for existing formaldehyde have a bigger spreading. A very high percentage of samples, 72% have levels that are not permitted by the provisions of the European eco-label.

A high value for formaldehyde content was determined for the pillow (P9), 153 mg/Kg, with the label “non-iron”. For this sample has tested the formaldehyde after washing. The new determination of the formaldehyde gave undetectable levels, in concordance with literature data that indicate a decrease in the formaldehyde levels after washing.

Taking into consideration that the tested samples represent a very small part of the market, the conclusion for tests would be that the consumers should be more cautious especially with linen textiles.

Summary

Statistics on non-compliance values determined in samples submitted for testing to evaluate the free formaldehyde content must have the following:

- 1.2 % of the total samples are over the acceptable limits in case of textile products for children;
- 2.5 % of the total samples are over the acceptable limits for women textiles;
- 1.9 % of all samples are over the acceptable limits for men textile products;
- 13 % of the total samples are over the acceptable limits from textiles bedding.

CONCLUSIONS

In today's society, the population is subject to a significant increase in the number of chemicals that the body comes into contact with. Among these is the formaldehyde, considered carcinogenic for the human being.

In this context, this paper aimed to assess the emissions of formaldehyde of textile products which are distributed on the Romanian market, to establish their impact on children and adults by wearing them or living near them.

The selection of 161 products was planned so as to cover as many types of textile fibres and products as was expected to present free formaldehyde.

We could conclude that textile products for children had adequate treatments so that they are within the limits of the strict requirements set out by the EU eco-label (probably due to the adoption of European ecolabelling legislation and to the more frequent checks of products on the market).

The interior textile products present values for the free formaldehyde that exceeds the allowed limits, but a valid conclusion will require a more large investigation that the present one.

REFERENCES

De Groot, A.C., Le Coz, Ch., Lensen, G.J., Flyvholm, M., Maibach, H.I. and Coenraads, P.-J. (2010), "Formaldehyde-releasers: relationship to formaldehyde contact allergy. Formaldehyde-releasers in clothes: durablepress chemical finishes. Part 1", *Contact Dermatitis*, 62, 259-271.

Occupational Safety and Health Standards, Regulations (Standards - 29 CFR), Toxic and Hazardous Substances1910.1048 App C, Medical surveillance - Formaldehyde.

Piccinini, P., Senaldi, C. and Summa C. (2007), "European Survey on the Release of Formaldehyde from Textiles", Office for Official Publications of European Communities, EUR 22710 EN, Luxemburg.

Regulation (EC) No 66/2010 of the European Parliament and of the Council of 25 November 2009 on the EU Ecolabel, (2010), *Official Journal of the European Union*, L 27, 1-19.

United States Government Accountability Office (GAO) (2010), "Formaldehyde in textiles".

*** (2009), "Commission Decision establishing the Ecological Criteria for the Award of the Community Ecolabel for textile products" (2009/567/EC), *Official Journal of the European Union*, L197, 70-86.

*** (2012), "Workshop on public ecologic acquisitions" (in Romanian), *Industria Textila*, 63(2), 109.

EVALUATING RISKS OF ALLERGY TO CHROMIUM RELEASED FROM FOOTWEAR

MIRELA PANTAZI [1], GABRIELA MACOVESCU[1], SIMINA STEFAN[2] , ANA MARIA VASILESCU[1]

[1]*INCDTP – Division: Leather and Footwear Research Institute, 93 Ion Minulescu St., Bucharest, Romania, email: icpi@icpi.ro*

[2]*Faculty of Applied Chemistry and Material Science, University Politehnica of Bucharest, No 1-7, Polizu Street, Sector 1, 011061, Bucharest, Romania*

Chromium tanning of leather is the most important tanning method and is used in over 80% of tanneries in the world. Several studies have indicated that leather products, when worn, can release chromium as Cr(VI) or Cr(III), compounds which can cause allergic reactions and severe foot eczema. Development of allergy to chromium, among patients with eczema, was investigated in different EU countries (Denmark, Germany, Italy, etc.). The main purpose of this study is to clarify whether the compounds of Cr(VI) and Cr(III) are released from leather shoes in a quantity leading to a risk of causing allergic reactions. In order to highlight chromium content in leather, footwear samples were analyzed according to SR EN ISO 5398/1-2008 to determine total chromium and according to SR EN ISO 17075:2010 for the detection and quantification of soluble chromium VI with a detection limit of 3 mg/kg Cr(VI). The results are a measure of the total potential exposure to Cr(VI) and were used to identify shoes that may present a risk of allergy.

Keywords: leather footwear, chromium, allergy to chromium.

INTRODUCTION

Leather must be tanned in order to get durability, softness and flexibility, properties that make it usable for shoes. Chromium tanning is the most important tanning method and it is over 80% used in the leather industry worldwide. The chemical used in the tanning process is alkaline chromium(III) sulphate. This chemical reacts with the hide and stabilizes certain proteins, making it more resistant to degradation. Hexavalent chromium (Cr(VI)) is not used in the tanning industry and has no effect in the tanning process (Rydin, 2002). Chromium(III) salts can, under certain conditions, be converted into compounds of Cr(VI). It is known that light, UV radiation and heat, combined with the presence of oxidized fatty acids, can cause the conversion of Cr(III) to Cr(VI), in certain types of hides. Also, it is known that the pH value significantly influences the state of chromium. Trivalent chromium oxidation in air may be favoured by elevated pH during neutralization or dyeing processes.

Studies have shown that, under certain conditions, chemicals in leather may release compounds of Cr(VI). Previously, this was not thought possible, because Cr(VI), under the influence of many organic compounds at a low pH value was expected to be reduced to compounds of Cr(III) (Hauber & Germann, 1999). However, it is now known that chemicals in leather are capable of releasing compounds of Cr(VI) due to aging and UV radiation, which is a big problem, because hexavalent chromium compounds are contact allergens. Cr(VI) is considered one of the best known allergens.

Contact allergy develops when reactive substances, with low molecular weight, such as Cr(VI), penetrate human skin and activate the immune system. Activating the immune system means that it is able to recognize and respond to the specific substance when exposed to it again.

Most studies have focused on allergies caused by Cr(VI). However, exposure to chromium, through chromium-tanned leather may also include exposure to trivalent chromium compounds. After tanning, most Cr(III) compounds are bound to the collagen fibres in the leather, but it was proved that an excess of trivalent chromium compounds may be released from leather during the use of footwear.

In 2006 Hansen et al. studied the connection between foot eczema and exposure to Cr(III). It was found that patients with contact allergy, both to Cr(III) and Cr(VI) presented a higher risk of developing foot eczema than patients who responded positively only to Cr(VI). This indicated that Cr(III) plays a role in the development of foot eczema. However, Cr(VI) is considered a more potent allergen than Cr(III).

The main purpose of this study is to clarify whether Cr(VI) and Cr(III) compounds are released from leather shoes made in Romania, in amounts which may lead to risks that could cause allergic reactions.

METHODS

Determining Soluble Cr(VI) in Leather

International Standard SR EN ISO 17075:2008 establishes the method used to determine Cr(VI) in solutions obtained by washing leather under certain conditions.

Soluble Cr(VI) is extracted from the sample in phosphate buffer at 7.5-8.0 pH and if necessary, substances that influence detection are eliminated by solid phase extraction. Cr(VI) in solution oxidizes 1,5-diphenylcarbazide to 1,5-diphenylcarbazone to form a red/purple complex, with chromium, which can be measured photometrically at 540 nm. The results obtained by the method described are strictly dependent on extraction conditions. The results obtained using other extraction procedures (extraction solution, pH, extraction time, etc.) cannot be compared with results obtained using the procedure described in this standard.

This method is recommended in order to quantify Cr(VI) content in leather; according to the method, the detection limit is 3 mg/kg. This method is applied to leather from any animal tanned using chromium salts.

Determining Cr(III) Content in Leather

Total chromium content, expressed as chromium oxide (Cr_2O_3), was determined according to SR EN ISO 5398/1:2008.

SR EN ISO 5398/1:2008 describes a method for the determination of chromium in aqueous solution obtained from leather. This is an analysis for total chromium in leather; it is not compound specific or specific to its oxidation state. This method describes the determination of chrome by iodometric titration and is to be applicable to chromium-tanned leathers which are expected to have chromic oxide contents in excess of 0.3 %. Cr(III) content was determined by subtracting Cr(VI) content from the total chromium content. This is possible due to the generally accepted assumption that chromium is present in the leather only as Cr(III) and Cr(VI). The result is expressed in mg Cr(III)/kg leather.

EXPERIMENTAL

Experiments were carried out on 10 pairs of leather shoes, made in Romania, as follows:

- 4 pairs of children's footwear;

- 3 pairs of women's footwear;
- 3 pairs of men's footwear.

Analysis of hexavalent chromium migration from leather samples was carried out according to SR EN ISO 17075:2008 Leather - Chemical Tests - Determination of Chromium(VI) Content, and determination of total chromium in leather was done according to SR EN ISO 5398/1:2008 Leather - Chemical Determination of Chromic Oxide Content - Part 1: Quantification by Titration.

Results of evaluating hexavalent and trivalent chromium content in leather footwear studied are presented in Table 1.

Table 1. Test results for Cr(VI) and total Cr

Footwear type	Volatile matter %	Chromium oxide %	Total chromium mg/kg	Cr(VI) mg/kg
Children's shoes n.1 	9.83	3.26/3.62*	24768	< 1
Children's shoes n.2 	11.56	2.72/3.08*	21073	< 1
Children's shoes n.3 	11.65	3.98/4.50*	30789	< 1
Children's shoes n.4 	8.89	3.28/3.60*	24631	< 1
Women's shoes n.5 	14.45	4.27/4.77*	32636	< 1
Women's shoes n.6 	10.23	3.96/4.41*	30173	< 1
Women's shoes n.7 	12.05	4.07/4.63*	31679	< 1
Men's shoes n.8 	13	4.73/5.44*	37221	< 1
Men's shoes n.9 	10.31	2.52/2.81*	19215	< 1
Men's shoes n.10 	11.69	3.53/4.00*	27368	< 1

* Values related to chromium oxide are reported to leather free of volatile matter.

Since Cr(VI) concentrations were always under the detection limit of 3 mg/kg (showing values well below 1 mg/kg), values of Cr(III) content can be approximated with the values of total chromium.

The content of chromium (III) has been analysed as the total chromium content in the leather samples. Eventual hexavalent chromium in the products will also be included in these figures, but the content of hexavalent chrome is negligible in relation to the content of chromium (III).

The concentration is expressed as % Cr_2O_3, which is the normal unit in the leather industry. The content of chromium in leather depends on the product, but will normally be between 3 - 5% of Cr_2O_3. The chromium content should generally not be below 2.5% Cr_2O_3 for chrome tanned leather in order to receive a good quality of the leather (UNIDO, 1994).

Health Evaluation – Allergy to Chromium

Contact allergy develops when the reagents, low molecular weight substances such as chromium, penetrate human skin and stimulate the immune system. This stimulation means that the immune system is able to recognize and react to a specific substance. Contact allergy is also called type IV allergy and consists of two phases. The first phase is called induction or sensitization phase, where changes in the immune system are induced. This phase is without symptoms. At subsequent exposure to sufficient amounts of allergens, the immune system will react to the substance and the symptoms will appear. This phase is called elicitation and its symptoms are eczema.

Chromium is a transition metal, which exhibits different oxidation states ranging from + 2 to + 6. However, only trivalent Cr(III) and hexavalent chromium Cr(VI) have stable enough oxidation states to act as contact allergens. To become an allergen, a substance with low molecular weight, should be able to bind to proteins in human skin.

Studies show that Cr(VI) does not react with proteins. It is believed that Cr(VI) penetrates the skin and is reduced to Cr(III) to act as an allergen.

Studies on Threshold Values for Allergy to Chromium

In risk assessment, existing data on people take precedence over the results of animal studies. A typical way of expressing threshold values regarding the effects of allergens is MET10% (minimal elicitation threshold) - which represents the estimated dose causing a reaction in 10% of sensitized individuals. MET10% derives from exposure to an allergen dose over an area of 0.5 cm^2 for 48 hours.

In similar exposure scenarios regarding chromium from cement and wood, nickel in jewellery and dimethyl fumarate, a shoe fungicide, elicitation data such as MET10% were used directly in risk assessment. It is not possible to predict precisely the level of induction for a sensitizing substance, based on knowledge of threshold values such as MET10% elicitation values. But thresholds are sufficiently low to protect against the induction of sensitized individuals (Basketter et al., 2001) and this is the primary and secondary preventive measure.

Threshold Value for Cr(VI)

There are data from several studies conducted on humans, regarding the elicitation threshold for Cr(VI). At a single 48 hour closed exposure MET10% was estimated to be between 0.02-0.9 $\mu g/cm^2$, data given in Table 2.

The latest study was done in Denmark and it estimates that MET10% is 0.03 $\mu g/cm^2$, which corresponds to 1 mg/kg Cr(VI) (Hansen et al., 2003). This is in accordance with the results of the largest published study, where MET10% was 3 mg/kg for a 2 day period (Nethercott, 1994). However, there are variations with both smaller values and 10 times higher than MET10% (Hansen et al., 2002).

The American Environmental Protection Agency has based its risk assessment of allergy to chromium in wood on the study of Nethercott et al. (1994), which was the largest study.

Table 2. Estimated Minimal Elicitation Threshold for 10% of sensitized individuals (MET10%)

MET10%	Number of test subjects	References
0.09 µg Cr(VI)/cm^2/2 days = 3 mg/kg	54	Nethercott et al., 1994
0.35 µg Cr(VI)/cm^2/2 days = 11,67 mg/kg	14	Allenby & Goodwin, 1983
0.90 µg Cr(VI)/cm^2/2 days = 30 mg/kg	17	Kosann et al., 1998
0.02 µg Cr(VI)/cm^2/2 days = 0,67 mg/kg	5	Wass & Wahlberg, 1991
0.03 µg Cr(VI)/cm^2/2 days = 1 mg/kg	18	Hansen MB et al., 2003

Threshold Value for Cr(III)

There are few studies on Cr(III). Identified threshold levels for Cr(III) are much higher than for Cr(VI).

In the study by Nethercott et al. (1994), only 1 of 54 patients responded to Cr(III), which corresponds to a threshold concentration of 33 µg/cm^2, while MET10% for Cr(III) estimated in the study by Hansen et al. (2003) was 0.18 µg/cm^2, at least 6 times higher than for Cr(VI).

DISCUSSIONS

We analyzed the amount of chromium in leather uppers, because the upper comes most often in contact with skin and because there seems to be a slight tendency for allergic reactions that occur on the foot in this area. Moreover, the skin of the foot is thinner than the skin on the sole, thus being more likely to develop allergic reactions.

Low levels of Cr(VI) can cause allergic contact dermatitis. Patients allergic to Cr(VI) may react to a single exposure of 1 mg/kg-3 mg/kg Cr(VI).

SR EN ISO 17075 is the international standard method for detection and quantification of Cr(VI) and has a detection limit of 3 mg/kg.

The results are a measure of total potential exposure to Cr(VI) and were used to identify shoes having a risk of allergy to Cr(VI).

For quantitative analysis, using SR EN ISO 17075, it was found that the content of Cr(VI) did not exceed 3 mg/kg in any of the ten pairs of shoes analyzed.

CONCLUSIONS

The risk of using shoes that release chromium can be influenced by wearability conditions such as humidity, pH, micro-biological contamination and pre-existing skin diseases. This means that, under certain conditions, shoes with low levels of Cr(VI) may present a risk of allergy to chromium. However, in general, the higher the dose of allergen, the greater the risk of allergy. People who have already developed an allergy to Cr(VI) can be so sensitive that they react to levels of Cr (VI) below the limit. In all pairs of shoes analyzed low levels of both Cr(VI) and Cr(III) were found, which demonstrates that, technically, it is possible to produce high quality tanned leather, which falls within the product standard limits, without the risk of allergy to chromium.

The results of this study suggest that there are no problems related to a high content of chromium in leather shoes made in Romania.

REFERENCES

Basketter, D. et al. (2001), “Investigation of the Threshold for Allergic Reactivity to Chromium”, *Contact Dermatitis*, 44(2), 70-4.

Fischer, L.A. et al. (2009), “The Dosis-Response Relationship between Patch Test and ROAT and the Potential Use for Regulatory Purposes”, *Contact Dermatitis*, 614, 201-8.

Hansen, M.B. et al. (2002), “Quantitative Aspects of Contact Allergy to Chromium and Exposure to Chrome-tanned Leather”, *Contact Dermatitis*, 47, 127-134.

Hansen, M.B., Johansen, J.D. and Menné, T. (2003), “Chromium Allergy: Significance of both Cr(III) and Cr(IV)”, *Contact Dermatitis*, 4, 206-214.

Hansen, M.B., Menné, T. and Johansen, J.D. (2006), “Cr(III) Reactivity and Foot Dermatitis in Cr(VI) Positive Patients”, *Contact Dermatitis*, 54(3), 140-4.

Hansen, M.B., Menné, T. and Johansen, J.D. (2006), “Cr(III) and Cr(VI) in Leather and Elicitation of Eczema”, *Contact Dermatitis*, 54(5), 278-82.

Hauber, C. and Germann, H-P., (1999), “Untersuchen zur Entstehung und Vermeidung von Chromat in Leder”, *Leder & Haüte Markt*, 9, 25.

Johansen, J.D., Strandesen, M. and Poulsen, P.B. (2011), “Survey and Health Assessment (Sensitisation only) of Chromium in Leather Shoes”, *Study of the Danish Environmental Protection Agency*, No. 112.

Nethercott, J. et al. (1994), “A Study of Chromium Induced Allergic Contact Dermatitis with 54 Volunteers: Implications for Environmental Risk Assessment”, *Occupational and Environmental Medicine*, 51, 371-380.

Rydin, S. (2002), “Undersøgelse af indholdet af Cr(VI) og Cr(III) i lædervarer på det danske marked”, Kortlægning af kemiske stoffer i forbrugerprodukter. Kortlægning nr. 3, Teknologisk Institut, Miljø.

SR EN ISO 17075:2010 Leather - Chemical Tests - Determination of Chromium(VI) Content.

SR EN ISO 5398/1:2008 Leather - Chemical Tests - Determination of Chromic Oxide Content – Part 1: Quantification by Titration.

UNIDO, Acceptable Quality Standards in the Leather and Footwear Industry, 1994.

PREPARATION OF INSULATING MATERIAL FROM RICE HUSK AND SAW DUST

KHADIJA QURESHI[1], INAMULLAH BHATTI[1], MOHAMMED SALEH[2], ZULFIQAR SOLANGI[1]

[1] *Chemical Engineering Department Mehran UET, Pakistan, qureshi.khadija@yahoo.com*

[2] *Oil and Gas Development Limited Pakistan*

Pakistan is facing lot of energy crisis nowadays. Buildings consume a considerable quantity of energy in all countries. In regions that are tropically hot, a considerable quantity is utilized in cooling and heating buildings. As the summer season goes up to seven months and similarly winter seasons in certain parts of our country. The energy crisis can be reduced by good design, selection of construction material and also the insulating material. The selection of the insulating material plays a vital role in the overall cost and conservation of energy. In the present study a new lightweight insulating material was prepared by the agricultural wastes saw dust and rice husk.

Keywords: insulating material, thermal conductivity, resistance.

INTRODUCTION

Thermal insulation is a material or combination of materials, that, when properly applied, it retards the rate of heat flow by conduction, convection, and radiation. It retards heat flow into or out of a building due to its high thermal resistance. Different researchers have worked on preparing insulating material from coconut peels (Khedari, 2003), fly ash (Krishnaiah, 2006), quary dust (Nataraja & Nalanda, 2008), coconut husk (Olorunnisola, 2009), rice straw (Yang, 2004), coal fly ash (Bhatti et al., 2009), cotton stalk fiber (Zhou, 2010), Palm fiber (Karade, 2010), and Wheat straw (Khedari, 2005).

Pakistan being an agricultural country is a rich producer of rice. Rice is found in abundant quantity, the husk obtained is the upper covering of the rice after processing or polishing. This is the byproduct and can be valuable used as insulating material in the construction and building purposes. Saw dust is the material obtained after the sawing of wood. It has many applications in the manufacturing of chip boards, furniture etc.

The scope of this research is wide because the material prepared from rice husk and saw dust will be light in weight. In the first phase of the research work insulating material was prepared by using different compositions of rice husk and saw dust and mixed with the binder. The second phase of the work comprised of the thermal (thermal conductivity and thermal resistance), Physical (bulk density and shape) and mechanical (compressive strength) analysis of the insulating material.

MATERIALS AND METHOD

Fiber Preparation

Fiber was prepared from both materials i.e. rice husk and saw dust. The raw materials collected were dried in oven at 60°C for 20 hours, crushed and screened, particles of size 352 μm was selected. The fiber was soaked in water for 24 hours filtered and dried at 60°C in the oven for 18 hours.

Preparation of Insulating Material

Five insulating materials of different compositions were prepared from rice husk (R) and saw dust (S). The ratio of the material used was rice husk/saw dust: cement: white glue: sand (5:1:5:1). The ratio of rice husk/saw dust varied from 5 to 25 gm, whereas other materials were kept constant. The fiber was mixed with the binding material (cement) in the proper ratio. Sand was sieved and less than 0.17 mm was used. 5 gm of fiber, 1 gm of cement, 5 gm of white glue and 1 gm of sand were mixed by the agitator at 100 rpms for about 5 minutes. The homogenized sample was compressed at 5000 psi on Buehler Simpllmet-II Press Mold. Pellets of size about 1 inch diameter were prepared.

Analysis of Insulating Material

The thermal conductivity analysis was carried on heat conduction apparatus HT1 Armfield U.K reported in Table 1. Compressive strength of the insulating material was carried out in Universal testing machine Model LT-0950-DN Forney.

RESULTS AND DISCUSSION

Effect of Size of Sand on Thermal Conductivity

Two sizes of sand were taken <0.71mm and 1 mm and the effect of size of sand on thermal conductivity is shown in Figure 1. It was analyzed that the thermal conductivity of both specimen (rice husk and saw dust) was less with the <0.71 mm size of sand. With sand size 1 mm the thermal conductivity of the samples is greater it is due to that fine sand can insert into matrix between fibers. The result is that fibers are aligned to be distant from each other. Therefore, it creates voids and has low density and low thermal conductivity. Similarly the opposite is true for other size of sand. The results calculated for thermal conductivity analysis with sand size <0.71 mm of rice husk samples are in the range of 0.6366-0.584 W/m-K and for saw dust samples reported are 0.6287-0.5894W/m-K. For further experiments size of sand <0.71 mm was kept constant.

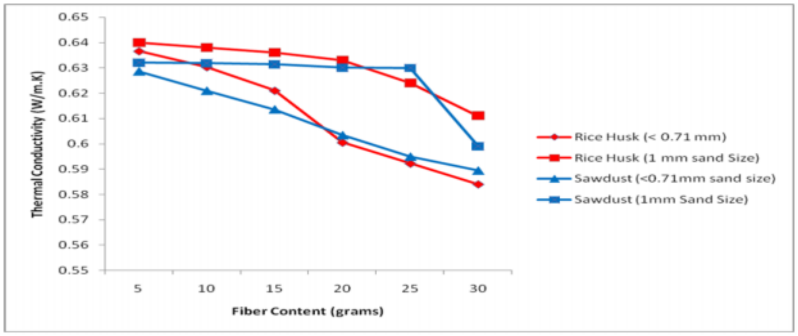

Figure 1. Effect of size of sand on thermal

Effect of Size of Fiber on Thermal Conductivity

Two sizes of fiber were taken 4mm and < 2mm. The effect of size of fiber on thermal conductivity is shown in Figure 2. The thermal conductivity of the samples decreased with < 2mm size of fiber. While it increased with 4mm size of fiber. The thermal conductivity of porous medium is inversely proportional to the voids in the specimen. These voids are occurring from the packing of fibers. In general, the short fibers are more difficult to align than the longer ones. Therefore, makes a lot of voids leading to low thermal conductivity. In further experiments < 2mm size of fiber was kept constant.

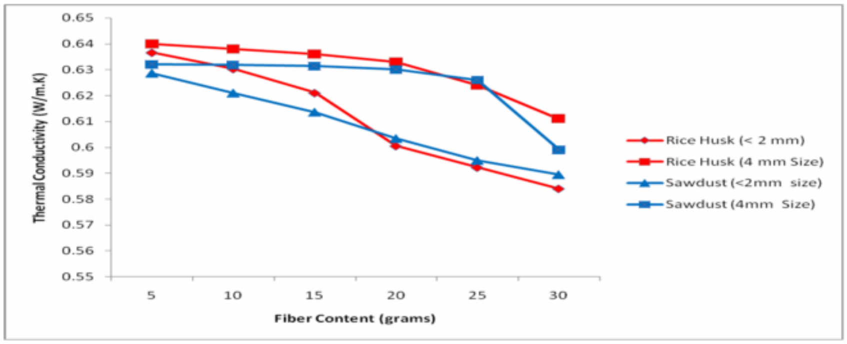

Figure 2. Effect of size of fibre on thermal conductivity

Effect of Fiber Content on Thermal Conductivity

The effect of fiber content on thermal conductivity is shown in Figure 3. The thermal conductivity decreased when the fiber content increased. The quantity of fiber taken was increased from 5 gm to 30 gm. This decrease in thermal conductivity is due to the voids occurring from the packing of the fibers, fiber-fiber matrix ratio. The samples that had low density yielded low values of thermal conductivity. As the density decreased the voids present in between the fibers increased resulting lower thermal conductivity. Thus thermal conductivity is a measure of effectiveness of a material in conducting heat. In general, the more voids present in the specimen the lighter the specimen and lower its thermal conductivity. It can be assumed that heat insulating efficiency of a material is opposite to its density. The results of thermal conductivity for rice husk samples are in the range of 0.6366-0.584 W/m-K and for saw dust samples 0.6287-0.5894 W/m-K are found to be satisfactory when compared with the thermal conductivity of coconut fiber 0.2543 W/m-K and durian peel 0.3506 W/m-K (Khedari, 2005).

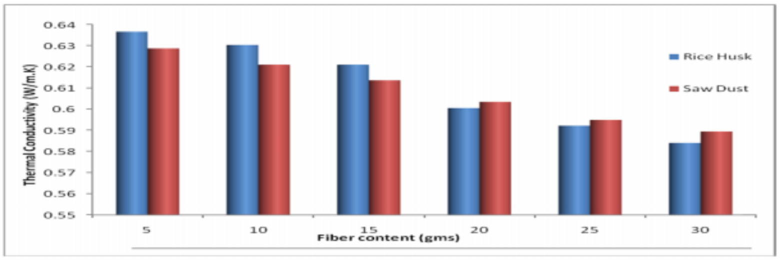

Figure 3. Effect of fiber content on thermal conductivity

Effect of Fiber Content on Compressive Strength

The effect of fiber content on the compressive strength is given in Figure 4. The compressive strength decreased as the fiber quantity was increased. This decrease can be explained as the development of strength properties mostly depends on the formation of fiber matrix, fiber bonds which are affected by dimensions, surface conditions and number of fibers present in a given volume of the material. Therefore, the increase in fiber content resulted in a decrease in bond strength of the specimens, leading to a lower compressive strength. During the mixing of the composites, the rheological properties of mix will naturally depend on how close the fibers get to each other. The voids leads to decrease density as a result the compressive strength decreased accordingly.

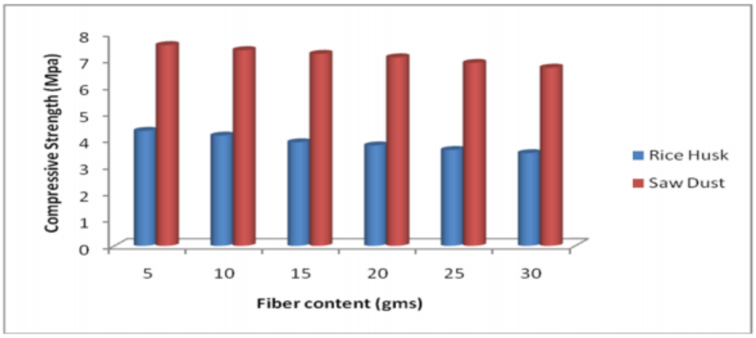

Figure 4. Effect of fibre contents on compressive

The results achieved for rice husk are in the range of 3.49-4.33Mpa and for saw dust are 6.71-7.56Mpa, which are found to be satisfactory when compared with the compressive strength of coconut fiber and durian peel 2.46Mpa and 3.29Mpa (Khedari, 2005).

Effect of Fiber Content (Rice Husk) and Thermal Conductivity on Bulk Density

The effect of fiber content on thermal conductivity and bulk density for rice husk samples is shown in Figure 5. It is clear from the graph that the thermal conductivity increases when the bulk density of the insulating material is increased. Similarly, with decrease in bulk density thermal conductivity is also lowered. The bulk density reported for rice husk samples are in the range of 670-864 kg/m^3 which is found to be satisfactory when compared with the bulk density of coconut fiber 959 kg/m^3 (Khedari, 2005).

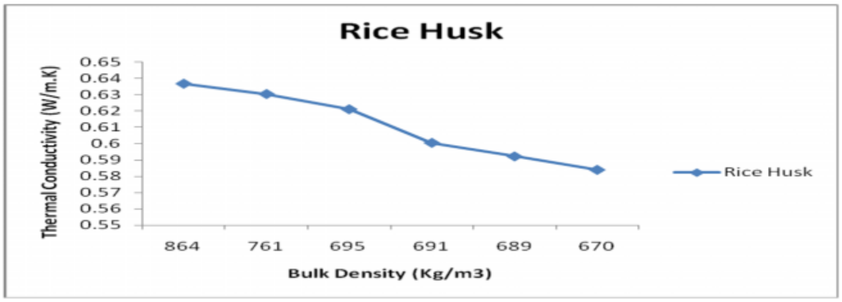

Figure 5. Effect of thermal conductivity on bulk density

Effect of Fiber Content (Saw Dust) and Thermal Conductivity on Bulk Density

The effect of fiber content and thermal conductivity on bulk density for saw dust samples is shown in Figure 6. The results reported are in the range of 660-812 kg/m^3. The results are compared with the bulk density of durian peel 1456 kg/m^3 and coconut fiber 959 kg/m^3 (Khedari, 2005).

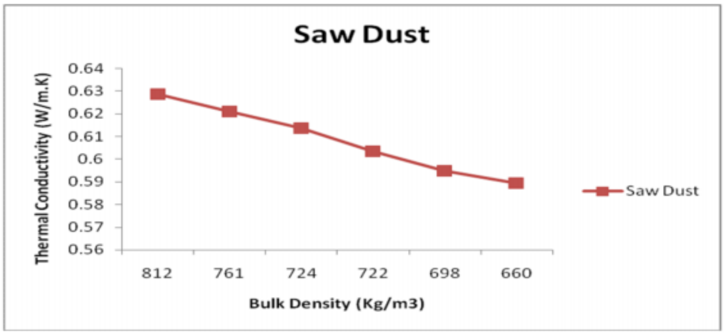

Figure 6. Effect of thermal conductivity on bulk density

CONCLUSION

Insulating materials were prepared from rice husk and saw dust to utilize this material to conserve energy. Different parameters such as size of sand and size of fibers were optimized. It was found that size of sand < 0.71 mm and size of fiber < 2mm showed better results. Rice husk reported the lowest thermal conductivity as 0.584 W/m-K and the thermal conductivity of saw dust was reported as 0.589 W/m-K.The thermal resistance of rice husk was calculated and found to be 36 (m^2-K/W) which shows that rice husk is a better insulating material as compared to saw dust.It was also observed that the compressive strength of saw dust was 7.56 Mpa which was better than other materials found in literature such as Coconut fiber and Durian Peel. This will also solve disposal problems of agricultural wastes and reclaiming of the fill fields that are expensive and difficult.

REFERENCES

Bhatti, I., Qureshi, K. and Memon, A.R. (2009), "Thermal Properties of insulating material prepared from coal fly ash and asphalt", *Mehran University Research Journal of Engineering & Technology*, 28(2).

Karade, S.R. (2010), "Cement-bonded composites from lignocellulosic wastes", C*onstruction and Building Materials*, 24(8), 1323-1330.

Khedari, J. et al. (2003), "New insulating particle boards from durian peel and coconut coir", *Building and Environment*, 38, 435-441.

Khedari, J. et al. (2005), "Development of fibre-based soil-cement block with low thermal conductivity", *Cement & Concrete Composites*, 27, 111-116.

Krishnaiah, S. et al (2006), "Determination of thermal properties of some supplementary cementing materials used in cement and concrete", *Construction and Building Materials*, 20, 193-198.

Nataraja, M.C. and Nalanda, Y. (2008), "Performance of industrial by-products in controlled low-strength materials (CLSM)", *Waste Management*, 28, 1168-1181.

Olorunnisola, A.O. (2009), "Effects of husk particle size and calcium chloride on strength and sorption properties of coconut husk-cement composites", *Industrial Crops and Products*, 29, 495-501.

Yang, H.S. et al. (2004), "Possibility of using waste tire composites reinforced with rice straw as construction material", *Bioresource Technology*, 95, 61-65.

Zhou, X.Y. et al. (2010), "An environmental-friendly thermal insulation material from cotton stalk fibers", *Energy and Buildings*, 42(7), 1070-1074.

NANOSTRUCTURES IN MEMBRANES AND MEMBRANE TECHNIQUES FOR SEPARATION OF SOLUTES

DEMETRA SIMION[1], GEORGETA POPESCU[2], CARMEN GAIDĂU[1], MARGARITA KOLEVA[3], BUJOR-GABRIEL ALBU[2]

[1] *INCDTP - Division: Leather and Footwear Research Institute, 93 Ion Minulescu st., sector 3, postal code: 031215, Bucharest, Romania, demetra.simion@yahoo.com*

[2] *Research Center for Macromolecular Materials and Membranes, Spl. Independentei 206, sector 6, 79611 Bucharest, P.O. Box 15-143, Romania*

[3] *University of Chemical Technology and Metallurgy, Textile and Leather Department, 8 Kliment Ohridski Blvd., Sofia, 1756, Bulgaria*

Specific separation at molecular level implies the development of new materials and nanostructures. The paper deals with the preparation of new materials and nanostructures for nanotechnology application. Three directions are studied namely, preparation of complexant nanoparticles by grafting of carriers onto the surface of nanoparticles, micellar enhanced ultrafiltration and obtaining of ceramic nanostructures. Membrane technology is a relatively new separation process, which fulfils these criteria. It can be applied in process integrated systems and in this way waste problems are drastically reduced while valuable products are recovered. A specific separation process at molecular levels implies the development of new materials and nanostructure correlated with the physical and chemical properties of the compounds that must be removed or separated. The research directions studied in the paper showed that modifications at the level of nanostructures leads to new materials that can be applied in technologies related to separation using ultrafiltration (UF) or micellar-enhanced ultrafiltration (MEUF) of: orange III, methyl red, fenoftalein, phenol, Cu^{2+}. In the literature this process is known as nanotechnology. In conclusion we can point out that the new materials described in the paper have specific properties for separation at molecular level with great impact in the development of the nanotechnology.

Keywords: nanoparticles, micellar enhanced ultrafiltration, ceramic nanostructures membranes.

INTRODUCTION

Physics gives the specific tool for characterization of the materials used as base of the nonporous media and of the systems. Specific separation processes are used more frequently for the purification or removal of biological entities. In this respect the biology knowledge is needed in understandings of the separation mechanism and the behavior of the biological molecules. A great interest is shown to the chemical modification of a nanoporous media with the purpose of linking biological molecules to a support, for: sensors, catalysis, specific identifications and specific biological reactions (Mulder, 1996; Wolde, 1998). Chemistry is giving the insight of the molecular behavior. The membrane science is using polymers, ceramics, modified surfaces, and colloidal chemistry. The last is actually the tool in handling the separation processes it self. From all the branches of chemistry, colloidal chemistry has the greatest impact on membrane technology. The colloidal particles with a size from nanometer to microns are used as a support for separation, as materials in order to obtain the nanoporous media-membranes and they are an integrated part in the fluids subjected to separation. All the knowledge from colloidal chemistry is implied in the development and removal of the colloidal particles. To the same basic principles the nanoparticles are subjected. In fact, in the scientific literature, a very clear distinction it can not be done between nanoparticles and colloidal particles. Colloidal chemistry is vaster and overlapping in important directions with nanoscience and nanotechnology (Philipse, 1996). All the processes implied in membrane and membrane processes can be described and therefore predicted using mathematical simulation (Rautenbach & Albrecht, 1989).

EXPERIMENTAL PART AND RESULTS

In this work we analized different systems in which nanoparticles and nanostructure are implied. The membrane is a system which contains porous varying from a few nanometer to sub-micron.

When a selective separation is required affinity cross flow filtration can be applied. This concept is a combination of an organic specific complexant with colloidal chemistry and membrane science (Figure 1).

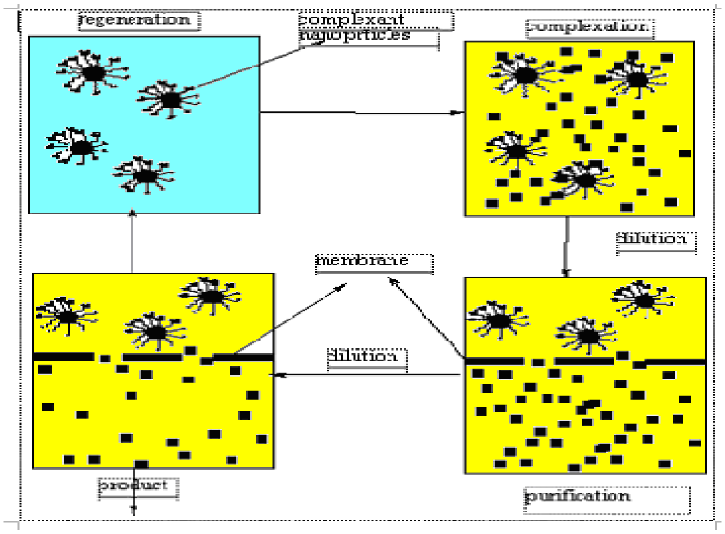

Figure 1. Affinity cross flow filtration principle

The carrier is chemically linked to nanoparticles (organic or inorganic) and then dispersed in wastewater. Micro and ultrafiltration can remove nanoparticles rather easily. In addition, it is included between the nanoparticles and carrier a spacer which was in our study depending on the nature of the solvent in which the particles are going to be dispersed, an aliphatic chain $(CH_2)_n$ or an $(CH_2\text{-}CH_2\text{-}O)_n$ with $6<n<15$. Small particles (organic or inorganic) are in general more difficult to handle. Also, the use of very small particles in wastewater purification procedures can lead easily to flocculate. The re-dispersion of such flocculates is difficult. For technological purposes one must find the compromise between and easily manipulating system and one with a high affinity surface area.

In a number of industrial operations (including coal refining, textiles, dyes and synfuel processing), wastewater contains unacceptable concentrations of both dissolved organic and multivalent ions (e.g., heavy metals). Taking account of the fact that ultrafiltration methods are ineffective in removing organic solutes having molecular weights less than 300 Dalton (as in the case of the most pesticides), hybrid technologies were devised. One such technology, named micellar-enhanced ultrafiltration, consists of adding water – soluble colloids to aqueous streams and subsequently using ultrafiltration to remove target ions and molecules that could not be effectively removed by ultrafiltration. In MEUF solutes are bound at or near the surface of the added colloids, so that species which would ordinarily pass freely through the UF membrane are forced to remain in the retentate solution. The ions are present in the permeate stream at much higher concentrations than in the retentate, and almost all of the colloid remain in the retentate. Such techniques are combining colloid chemistry and membrane science. We used the MEUF process for the removal of dyes (Orange III, Methyl red; organic solutes (Fenoftalein and Phenol) and Cu^{2+}) by the use of the anionic and cationic surfactants (cetyl benzyl dimethyl ammonium chloride, tertiary amines: dodecylamine, hexadecylamine).

Using micellar-enhanced ultrafiltration the following process efficiency was obtained (Table 1).

Table 1. Data results with MEUF and UF

System	Retention (%)	
	UF	MEUF
Orange III	71	98
Methyl red	29	76
Fenoftalein	38	99
Phenol	12	88
Cu^{2+}	57	92

In all cases the surfactant concentration is ranged between bellow critical micelle concentration (CMC) and the CMC. The maximum retention was observed at CMC.

There are situations when the two processes described above can not perform the removal of a solute. Membranes with special characteristics have been developed in order to remove molecule and small sized species. The separation processes in such cases are nanofiltration. Recently ceramic nanofiltration membranes were recommended for the separation of solutes in hard situations where polymeric membranes can not be applied.

A ceramic support with the thickens of 10-50 µm was obtained on which a thin inorganic layer and deposed with the thickness of about 35 µm. The microfiltration membranes show pores of 0.1 – 10 µm. The microfiltration membranes are the bases for the preparation of ultrafiltration membranes and then further for a nanofiltration membrane.

CONCLUSIONS

The research directions studied in the paper showed that modifications at the level of nanostructures leads to new materials that can be applied in technologies related to separation at molecular level. In the literature all the processes that are dealing with reactions and/or separation at nano dimensions is known as nanotechnology. The new materials described in the paper have specific properties for separation at molecular level with great impact in the development of the nanotechnology.

REFERENCES

Mulder, M.H.V. (1996), *Basic principles of membrane technology*, Kluwer Publishing Company, Dordrecht, The Netherlands.

Philipse, A.P. (1996), *Dancing on a Delta peak*, Utrecht, The Netherlands.

Rautenbach, R. and Albrecht, R. (1989), *Membrane processes*, John Wiley and Sons, New York.

Wolde, A.T. (ed.) (1998), *Nanotechnology*, The Netherlands.

THE INFLUENCE OF POLYFUNCTIONAL MONOMER TRIALLYLCYANURATE ON THE MECHANICAL PROPERTIES OF THE SILICONIC RUBBER CROSSLINKED BY ELECTRON BEAM IRRADIATION

MARIA DANIELA STELESCU[1], ELENA MANAILA[2], GABRIELA CRACIUN[2], NICULINA ZUGA[3], MIHAI GEORGESCU[1]

[1] *INCDTP – Division: Leather and Footwear Research Institute, 93 Ion Minulescu St., Bucharest, Romania, email: dmstelescu@yahoo.com*

[2] *National Institute for Laser, Plasma and Radiation Physics, Electron Accelerators Laboratory, 409 Atomistilor St., 077125, Magurele, Romania*

[3] *Constantin Cantacuzino National College, 3 George Cair St., Targoviste, Romania*

Silicone elastomers are a type of polymers with remarkable characteristics, due to the wide range of temperatures at which they can be used, to which are added high resistance to petroleum products with high aniline point, to solvents and weather, as well as easiness of their development for various industrial purposes. The most important stage in the rubber processing technology is crosslinking. During crosslinking, rubber molecules with chain configuration are linked by chemical bridges, and the rubber mass turns from its plastic mass into an elastic one. This paper presents the effect of the polyfunctional monomer triallylcyanurate (TAC) on the mechanical properties of the siliconic rubber crosslinked by electron beam. Silicone rubber was irradiated by electron beam over a dose range of 50–200 kGy. The control samples were obtained by cross-linking with peroxide in a hydraulic press at 160°C. Comparing physical-mechanical parameters of the blends obtained by EB vulcanization with those vulcanized with dibenzoyl peroxide, it is easy to observe higher efficiency first of all, as it leads to a more efficient crosslinking in the whole mass of the elastomer and to obtaining better physical-mechanical characteristics. The optimum values of physical-mechanical rubber parameters present a strong dependence on TAC concentration and irradiation dose.

Keywords: siliconic rubber, electron beam, triallylcyanurate, physical-mechanical properties.

INTRODUCTION

Polysiloxane or silicone productions have increased drastically since their discovery in the late 1940s because of their unique properties (Techno-Nathan; 1988) as, e.g. thermal stability, electric insulation capacity, hydrophobic nature. Typically they are produced as linear macromolecules, which are later crosslinked to get elastomeric materials (Baquey et al., 2005). Cross-linking can be introduced into polysiloxanes structure by a range of methods, including: (i) the use of a tri- or tetrafunctional siloxane comonomer during polymerization, (ii) the incorporation of a thermal initiator which would abstract hydrogen atoms from PDMS and so result in cross-linking or (iii) the exposure of PDMS to high energy irradiation (Hill et al., 2001). The radiation cross-linking of PDMS is still interesting to many radiation chemists. The complete control of cross-link density, the formation of cross-links in the solid state, no need for catalysts or other additives and no heat treatment are all advantages of the radiation technique (Tabata, 1979).

In any polymer exposed to radiation, cross-linking and scission occur simultaneously, with different probabilities. PDMS can be regarded as a cross-linked polymer since the probability of cross-linking is much higher than the probability of chain scission. It may be concluded from the literature data that for PDMS the degree of cross-linking is proportional to the irradiation dose (Delides and Shepherd, 1977).

In order to decrease the irradiation dose required for cross-linking, polyfunctional monomers or curing co-agents can be added. In a research study (Stelescu et al., 2012) we have analyzed the effect of the polyfunctional monomers triallylcyanurate, triallylisocyanurate, trimethylopropane trimethacrylate and zinc diacrylate on the mechanical properties of the siliconic rubber cross-linked by electron beam or peroxide. It was concluded that PFMs can be used in peroxide or EB cured systems by increasing the efficiency of productive radical reactions. These have led to the improvement of physical-mechanical properties of siliconic rubber, and the most efficient PFM for siliconic rubber have been TAC.

This paper presents the effect of the polyfunctional monomer triallylcyanurate (TAC) on the mechanical properties of the siliconic rubber crosslinked by electron beam.

EXPERIMENTAL

The following materials were used in the study: (1) silicone elastomer Elastosil R 701/70 OH (from Wacker-Chemie), (2) Polyfunctional monomer: triallyl cyanurate (TAC) Luvomaxx TAC DL 70 (26% percentage of ash, density 1.34 g/cm^3, 30% active synthetic silica), (3) Di(tert-butylperoxyisopropyl)benzene Perkadox 14-40B-GB (from Akzo Nobel) (1.60 g/cm^3 density, 3.8% active oxygen content, 40% peroxide content) as vulcanizing agent for vulcanization of control samples.

Blends have been made by means of blending technique, on a laboratory roll, total blend time of 5’, friction of 1:1.1. The blend constituents were added in the following sequence and amounts: 100 phr siliconic rubber and 3, 6, 9, respectively 12 phr TAC polyfunctional monomer plates required for physical-mechanical tests have been made by compression molded, using an electrically heated hydraulic press, pressure of 150 MPa and time of 3 min. to obtain sheets of 11.5 x 11.5 x 0.2 cm^3.

Control samples were prepared similarly to those presented with the following specifications: 8 phr of Perkadox 14-40B-GB as vulcanizing agent was added and the blend vulcanization was achieved in a hydraulic press at 160°C; the vulcanization time was measured by means of Monsanto Rheometer (see Table 1).

The resulted plates were subjected to EB vulcanization with ILU-6M accelerator of 1.8 MeV and 10.8 kW output power. The ILU-6M is a resonator-type accelerator, operating at 115±5 MHz. This accelerator generates electron beam pulses of 0.375 ms duration, up to 0.32 A current peak intensity and up to 6 mA mean current intensity. The cross-sectional size of the scanned EB at the ILU-6M vacuum window exit is 1100 mm x 65 mm. The EB effects are related to the absorbed dose (D), expressed in Gray or J kg^{-1}. The single pass dose with conveyor under the ILU-6M scanner is adjustable from 12.5 kGy to 50 kGy. For EB treatments the rubber samples were cut as compressed sheets 2 mm thick in the polyethylene foils to minimize oxidation. The layers of three sandwiched sheets were irradiated by repeatedly passing on a conveyor under the ILU-6M scanner.

The tensile testing of samples was carried out with the testing speed of 460 mm/min at room temperature with a Schoppler strength tester machine. The tensile strength was measured on dumb-bell shaped specimen according to ISO 37/2005. Tear strength test was performed according to SR EN 12771/2003 using angular test pieces (type II). Hardness of samples in terms of Shore A was measured according to ISO 7619-1/2004 using 6 mm thick samples. Elasticity was evaluated with a Schob test machine using 6 mm thick samples, according to ISO 46662/1986. All measurements were taken several times and the resulting values were averaged. Curing characteristics were determined by an oscillating disk rheometer (Monsanto), at 160°C for 30 minutes, according to the SR ISO 3417/1997. Delta torque or extent of crosslinking is the maximum torque (MH) minus the minimum torque (ML). Optimum cure time (t_{90}) is the time to reach 90% of the delta torque above minimum. The cure rate index (CRI) is a measure of the rate of vulcanization based on the difference between optimum vulcanization time (t_{90}) and incipient scorch time (t_{s2}). It was calculated according to the following formula:

$$CRI = 100/(t_{90} - t_{s2}) \quad (1)$$

RESULTS AND DISCUSSIONS

The physical-mechanical and rheological properties of the siliconic rubber samples with different amounts of TAC polyfunctional monomer crosslinking with peroxide are presented in Table 1. It can be seen that both the maximum torque and the delta torque increase with increasing TAC concentration. The delta torque values are a measure of the dynamic shear modulus and related to the crosslink density of the blends. Also the cure rate index (CRI) is higher at blends with the TAC amount introduced. This increase in cure rate may be due to the fact that an increasing concentration of TAC caused the vulcanization reaction to increase and create more active cross-link sites in the rubber compound.

Table 1. Rheological and physical-mechanical characteristics of samples crosslinked with peroxide

Characteristics /The amount of TAC	Free	3phr	6 phr	9 phr	12phr
Rheological characteristics					
M min (dNm)	1	1	1	3.3	6.1
Mmax (dNm)	46.8	64.2	72.7	77.8	82
ΔM, (dNm)	45.8	63.2	71.7	74.5	75.9
T90 (minutes)	7’30”	7’00"	6’36’’	6’48’’	7’12’’
CRI	0.850	0.868	0.872	0.873	0.874
Physical-mechanical characteristics					
Hardness, °ShA	63	77	80	75	81
Elasticity, %	20	22	22	14	16
Tensile strength, N/mm^2	5	4	2.8	2.7	3
Elongation at break, %	180	93	10	10	10
Residual elongation, %	3	4	6	7	4
Tear strength, N/mm	32	22.5	18.5	18.5	21.5

TAC is indeed improving the crosslinking efficiency of peroxide in the present system. From the analysis of physical-mechanical of blends cross-linked with peroxide, the following can be noted:

- hardness increases with the increase of TAC amount up to 6 phr, then shows irregular variation;
- elasticity tends to increase upon increasing TAC amount up to a concentration of 6 phr; it has high values, specific to silicone rubber;
- tensile strength, elongation at break and tear strength decrease with the increase of TAC amount up to a concentration of 6 phr, then shows irregular and insignificant variation.

Physical-mechanical characteristics of the blends with different amounts of TAC vulcanized by EB are presented in Figures 1-6.

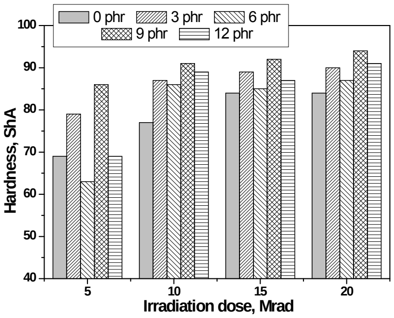

Figure 1. Hardness versus electron beam (EB) irradiation dose and TAC concentration

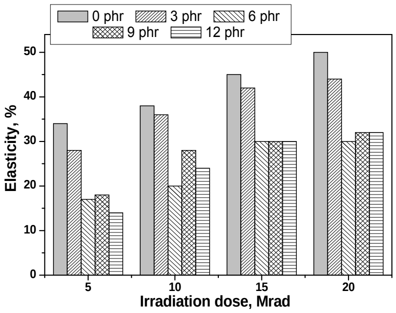

Figure 2. Elasticity versus electron beam (EB) irradiation dose and TAC concentration

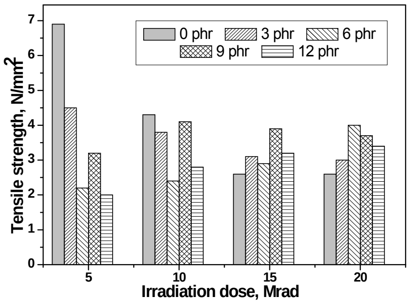

Figure 3. Tensile strength versus electron beam (EB) irradiation dose and TAC concentration

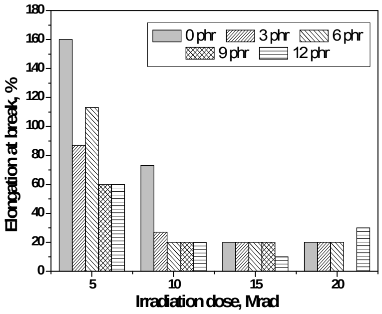

Figure 4. Elongation at break versus electron beam (EB) irradiation dose and TAC concentration

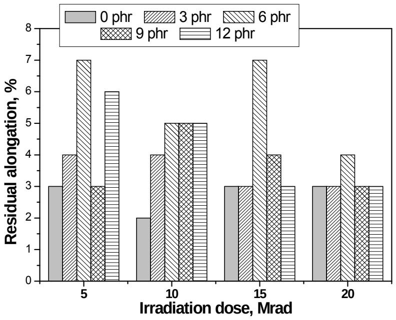

Figure 5. Residual elongation versus electron beam (EB) irradiation dose and TAC concentration

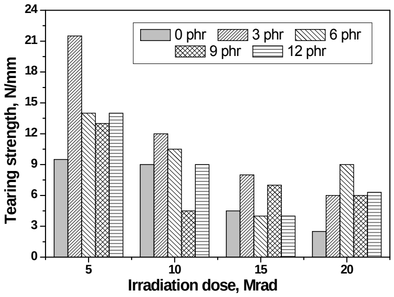

Figure 6. Tearing strength versus electron beam (EB) irradiation dose and TAC concentration

Upon analysis of obtained results, the following can be noted:

- hardness increases with the increase of TAC amount and with the increase of irradiation dose, peaking at an amount of 9 phr TAC, then decreases;
- elasticity increases as the irradiation increases and decreases as the TAC amount increases;
- tensile strength shows insignificant increase upon increasing irradiation dose;
- elongation at break shows significant decrease upon increasing irradiation dose from 5 to 10 Mrad, then the variation is insignificant;
- residual elongation has low values and does not show regular variation; obtained values indicate that at a dose higher than 5 Mrad, all blends are cross-linked;
- tear strength decreases as the irradiation dose increases; the best values have been obtained for an amount of 3 phr TAC at an EA dose of 5 Mrad.

CONCLUSIONS

Comparing physical-mechanical parameters of the blends obtained by EB vulcanization with those vulcanized with dibenzoyl peroxide, it is easy to observe higher efficiency first of all, as it leads to a more efficient crosslinking in the whole mass of the elastomer and to obtaining better physical-mechanical characteristics. The optimum values of physical-mechanical rubber parameters present a strong dependence on TAC concentration and irradiation dose. The optimal irradiation dose is of 5 Mrad and TAC optimal concentration is of 9 phr. Electron beam crosslinking of rubbers has a number of technical advantages over thermal curing such as absence of various noxious chemical additives, high speed of curing process, effective penetration of beam inside the sample and uniformity and ease of curing (Bik et al., 2003; Oproiu et al., 2000; Yasin et al., 2005; Ratnam et al., 2000; Martin et al., 2002). Silicone rubber or poly(dimethyl siloxane) is well-known for low and high-temperature applications and also has bio-compatible properties (Mark et al., 1992). Radiation curing of silicone rubber without using chemical curing agents is of enormous interest, particularly for medical applications.

REFERENCES

Baquey, G. et al. (2005), “Model Study of the Crosslinking of Polydimethylsiloxanes by Peroxides”, *Polymer*, 46, 6283–6292.

Bik, J. et al. (2003), “EB Radiation Crosslinking of Elastomers”, *Radiation Physics and Chemistry*, 67, 421.

Delides, C.G. and Shepherd, I.W. (1977), “Dose Effects in the Crosslinking of Irradiated Polysiloxane”, *Radiation Physics and Chemistry*, 10, 379–385.

Hill, D.J.T. et al. (2001), “Molecular Weight Changes and Scission and Crosslinking in Polydimethylsiloxane on Gamma Radiolysis”, *Radiation Physics and Chemistry*, 62, 11–17.

Mark, J.E., Allcock, H.R. and West, R. (1992), *Inorganic Polymers*, Prentice-Hall.

Martin, D. et al. (2002), “Vulcanization of Rubber Mixtures by Simultaneous Electron Beam and Microwave Irradiation”, *Radiation Physics and Chemistry*, 65, 63.

Oproiu, C. et al. (2000), “Transitory and Permanent Effects of Electron Beam Irradiation on Insulating Materials”, *Nuclear Instruments and Methods B*, 166–167, 669.

Ratnam, C.T. et al. (2000), “Electron Beam Irradiation of Epoxidized Natural Rubber”, *Nuclear Instruments and Methods B*, 171, 455.

Rhone-Poulenc Departement Silicones (1988), *Les Silicones, Production et Application*, Techno-Nathan.

Stelescu, M.D. et al. (2012), “The Influence of Polyfunctional Monomers on the Mechanical Properties of the Siliconic Rubber Cross-linked by Irradiation with Electron Beam”, *Journal of International Scientific*

Publication: Ecology & Safety, Vol. 4, The Ecology & Safety Symposium, June 8–12, Sunny Beach, Bulgaria.

Tabata, Y. (1979), “Radiation-induced cross-linking”, *Radiation Physics and Chemistry*, 14, 235–24.

Yasin, T. et al. (2005), “Effect of Concentration of Polyfunctional Monomers on Physical Properties of Acrylonitrile–butadiene Rubber under Electron-beam Irradiation”, *Radiation Physics and Chemistry*, 73, 155.

TENSILE BEHAVIOR OF GLASS FIBER REINFORCED CEMENT COMPOSITE

GEORGE TARANU, IONUT OVIDIU TOMA, RALUCA PLESU, MIHAI BUDESCU

"Gheorghe Asachi" Technical University of Iasi, Faculty of Civil Engineering and Building Services, email: gtaranu@tuiasi.ro

It is well known that one of the major problems of a cement-based material is the brittle type of failure owing to low tensile strength and poor fracture toughness that impose constraints in structural design and long-term durability of structures. In order to satisfy the performance of cement-based matrices, incorporation of glass fibers is getting growing interest to increase the toughness, energy absorption capacity as well as tensile properties of the basic matrix. In this work, cement matrices reinforced with different types of glass fiber reinforcement mesh were investigated. The influence of type and percentage of glass fiber reinforcement was observed on test results in terms of tensile strengths and tensile elastic modulus.

Keywords: tensile strength, glass fiber, cement composites.

INTRODUCTION

Principal materials for building systems remain concrete, masonry, steel or wood. The reasons are multiple: accessibility, price, their production may be relatively simple, their applications cover many types of buildings and civil infrastructure works. All of these materials have their advantages but also disadvantages (Andrzej, 2008). Founding a new material with mechanical and physical performance similar to those well known is important for the building industry. Glass fibers reinforced mineral matrix can be used to conceive different structural elements (Majumdar and Laws, 1979; Andrzej, 1987). The basic ingredient for obtaining an optimum mineral matrix with an increased workability and capable to be reinforced over glass fiber reinforcement mesh is a mix between sand, ordinary Portland cement and calcium sulphate. High workability of the mix is given by the calcium sulphate in the β anhydride III' form (Baux, 2010). The latter is obtained from phosphogypsum, lactogypsum or citrogipsum and can be used as partial or total replacement of the Portland cement (Aranda et al., 2011).

First tests results showed that the mineral matrix can be cast over a glass fiber reinforcement mesh and can lead to different elements (Toma et al., 2011; Taranu et al., 2011). A structural system can be made from modular panels in vertical and horizontal positions. Details of the composition and final aspect of the shear wall panels are presented in Figure 1 and Figure 2. The fluid mix can be poured in narrow spaces, having a width of at least 5 mm, embedding the glass fiber reinforcement that may be present. However, before using this high workability mineral matrix in structural elements, one needs to follow a two-step procedure.

The first step would be the setting of the formwork in the desired shape of the structural element (Figure 1). This can be done by joining polystyrene sheets to one another. In this way, the formwork also plays the role of thermal insulation. The second step of the procedure is the positioning of the glass fiber net as reinforcement before pouring the fluid composite mix into the formwork. After the fluid mix is cast in the formwork panels a structural element is obtained (Figure 2).

The aim of the paper is to present the mechanical results of the mineral composite material both for un-reinforced matrix and glass fiber reinforced matrix and to discuss main directions of their application in case of structural systems. The attention is concentrated on tensile behavior of the material and its components.

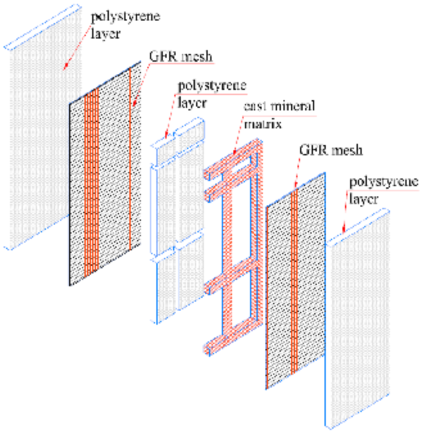

Figure 1. The composition of the shear wall panels made of glass fiber reinforced mineral matrix

Figure 2. Prototype of the wall panels made of glass fiber reinforced mineral matrix

MATERIALS

The materials used in this research are readily available on the market. The sand which occupied 50% of the entire volume of the mineral matrix is rich in quartz and has a maximum grain size of 0.2 mm and was used in dry state.

The Portland cement used in this research was type CEM II/A-S 32.5 R, with high early strength and represents 35% from the total volume of the mineral matrix. The third component of the composite mineral matrix, set to occupy 15% of the total volume, was the calcium sulphate in its β-anhydride III' form, also known as Kerysten. This is a hydraulic sulphatic binder obtained from industrial by-products such as phosphogypsum, lactogypsum, citrogypsum, a.s.o. The product was derived from a hemihydrate ($CaSO_4$ 0,5 H_2O) and anhydride III $CaSO_4$. The combination of the two constituents proved to be a very stable one. The glass fiber reinforcement is a mesh type made of glass fibers arranged along two orthogonal directions. The characteristics of the materials, as given by the manufacturer are shown in Table 1.

Table 1. Characteristics of manufacturer glass fiber reinforcement mesh

Material	Compressive strength [MPa]	Tensile strength [MPa]	Elastic modulus	
			in compression [MPa]	in tension [MPa]
Portland cement CEM II/A-S 32.5 R	32.5	3.5	27500	-
Glass fiber alkali resistant	-	1100	-	72413

Mix Proportions

The constitutive materials of the mineral matrix were weighted in their dry state, by means of a digital scale. The reference mix proportion was established as 50% sand, 35% Portland cement and 15% calcium sulphate. Mix proportions for all of the tested specimens are showed in terms of percentage in Table 2.

After dispensing of the components in dry state, these were placed in the mixer and mixed for 1 minute. The water, representing 40% of the total volume of solid parts, was gradually added within 30 seconds during the second stage of mixing. Following the addition of water, the entire content was mixed for 30 seconds at a speed of 140 rpm and for another 90 seconds at a higher speed of 285 rpm.

Table 2. Mix proportion of the tested materials

Spec. no.	Label	Sand (%)	Portland cement (%)	Calcium sulphate (%)	Water/Total ratio	Glass fiber fabric (%)
1	NCK 50/35/15	50	35	15	0.40	0
2	NCK 1GF 50/35/15	50	35	15	0.40	10
3	NCK 2GF 50/35/15	50	35	15	0.40	20
4	NCK 5GF 50/35/15	50	35	15	0.40	50

Sample Preparation

The obtained fluid mixture was cast in flat specimens (prismatic) with dimensions (length x width x thickness) 400x30x10 mm. The glass fiber mesh was positioned with the weave in the longitudinal direction and the weft along the hoop of the flat specimens. The flat specimens presented in Figure 3 were obtained by pouring the fluid mix in 400x10x30 mm moulds. In case of reinforced samples, the reinforcing mesh was placed in the middle of the mould and the highly fluid mix was cast afterwards. The specimens were reinforced using 1, 2 and 5 layers of glass fiber mesh with the weft positioned along the longitudinal direction. The considered reinforcement ratios were 10%, 20% and 50%. The end sections of the prismatic bars were additionally reinforced using 5 layers of glass fiber mesh on both sides over a length of 100 mm. This was a measure to prevent local crushing of the specimen in the testing equipment. Five samples were made for each investigated case.

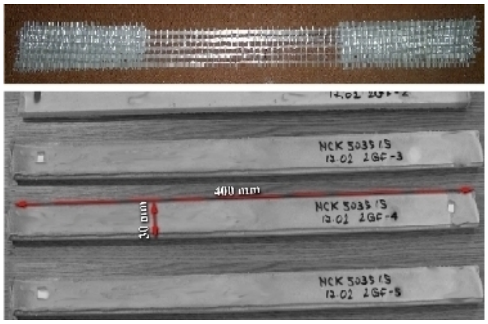

Figure 3. Aspects of the flat specimens 400x30x10 mm

EXPERIMENTAL SET UP

The tensile strength of mineral matrix was measured by means of uniaxial tensile test conducted on flat specimens both for un-reinforced and glass fiber reinforced mineral matrix. The equipment was calibrated before any experiment could be conducted. The age of the specimens was 21 days for the flat specimens. The longitudinal modulus of elasticity was determined both for un-reinforced and glass fiber reinforced specimens in tensile tests. The testing equipment is a Universal Materials Testing Machine ZWICK/ROELL model MTM SP 1000 force controlled. The loading rate was 0.255 MPa/s in compression and 0.1 MPa/s in tension. The extensometer used meets the requirements of Accuracy Class 0.5 to EN ISO 9513 with long sensor arms. The accuracy of macro extensometer is from 20µm and is given by the calibration report. The Elastic Modulus in tension was evaluated as secant for flat specimens with the formula (1).

$$E_t = \frac{L_0\left(X_H - X_L\right)}{ab\left(L_H - L_L\right)} \tag{1}$$

where:
E_c: Compression modulus in N/mm² or MPa
E_t: Tensile modulus in N/mm² or MPa
L_0: Initial gage length in mm = 50 mm
X_H: End of compression modulus determination in N (40% of maximum compressive strength)
X_L: Begin of compression modulus determination in N (at 0)
d: Diameter in mm
a=thickness of the flat specimen
b: width of the flat specimen
L_H: Strain in mm at X_H
L_L: Strain in mm at X_L

RESULTS AND DISCUSSION

The flat specimens both unreinforced and reinforced where tested and stress-strain curves where recorded. Figure 4 presents the comparative compressive stress strain curves of the flat specimens tested in tension.

The uniaxial tensile strength of the unreinforced specimen was determined to be 1.4 MPa. From the analysis of the graph shown in Figure 4, it can be observed that there is a 82% increase in this value for the specimens reinforced with one layer of glass fiber mesh, reaching 2.6 MPa. Both strength and deformability exhibit a significant increase from the un-reinforced specimens to the reinforced ones. Adding an extra layer of reinforcement, leads to an increase of 135% in the value of the tensile strength and the corresponding maximum longitudinal strain.

When 5 layers of glass fiber mesh reinforcement are used, the recorded tensile strength was 5.2 MPa, almost 371% times increase compared to the un-reinforced specimen. At the same time, the maximum corresponding strain decreased to 1.65 times lower. Figure 4 presents the comparative stress-strain curves of the specimens tested. Figure 5 shows the aspect of the specimen tested where the glass fibers are broken.

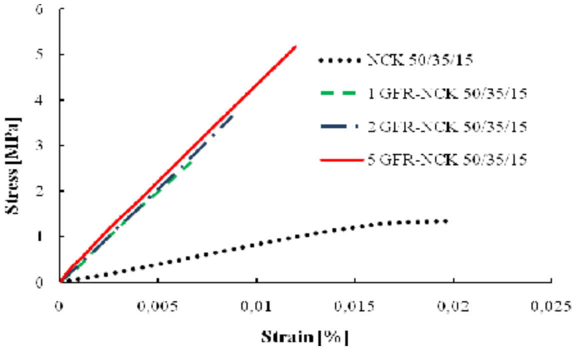

Figure 4. Comparative compressive stress-strain curves of the unreinforced and reinforced flat specimens at 21 days

Values of the Tensile Elastic modulus obtained from these results are presented in Table 3. The difference from unreinforced specimens and glass fiber reinforced ones are significant. There is an increase of 5 times of the elastic modulus in tension.

Table 3. Tensile elastic modulus

Specimen	Elastic modulus in tension (N/mm^2)
NCK 50/35/15	8182
NCK 1GF 50/35/15	41085
NCK 2GF 50/35/15	41896
NCK 5GF 50/35/15	42690

When the glass fiber percentage is greater, there is no significant increase of the elastic modulus between 10% and 50% of reinforcement, but these values are smaller than the glass fiber tensile elastic modulus.

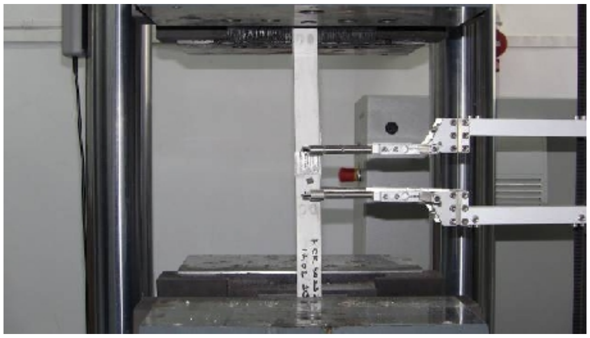

Figure 5. Failure of the reinforced flat specimen in one tensile test

CONCLUSIONS

Tensile behavior and the effectiveness of glass fiber reinforced cement composites have been studied in this research work.

The results obtained and the observations made clearly revealed that the existence of glass fiber reinforcement of maximum 50% not only increased the compressive and tensile capacity of mineral matrix composites but also significantly improved the ductility and Young's moduli of mineral matrix.

It can be concluded that, in the case of uniaxial tensile tests, the glass fiber mesh reinforcement is more effective than in compression tests. Building low cost, light, durable and stiff structures may seem a difficult task. The extensive knowledge obtained from researching composite materials makes it possible to identify a material able to fulfill the durability, strength and economic requirements. Such a composite material is made of a mineral matrix reinforced with glass fiber mesh.

Successful use of various high performance materials based on cement matrix has a considerable positive influence on production of ordinary matrix. The addition of calcium sulphate in its β-anhydride III' form, obtained from industrial by-products such as phosphogypsum, lactogypsum, citrogypsum makes possible to obtain an optimum mineral matrix with an increased workability which can be cast in small spaces. This capability leads in obtaining structural elements made of mineral matrix composites with a low weight and enough load capacity for a structural monolithic system.

Various experimental and theoretical methods that are successfully applied will certainly be used in further research and development. The importance of determining the strength and the elastic modulus in compression and tension consist in use of these parameters in future FEM design of structural elements.

REFERENCES

Andrzej, M.B. (2008), "Fibre Reinforced Cement-based (FRC) Composites after over 40 Years of Development in Building and Civil Engineering", *Composite Structures*, 86(1–3), 3-9.

Andrzej, M.B. (1987), "Present Trends in the Mechanics of Cement Based Fibre Reinforced Composites", *Construction and Building Materials*, 1(1), 28-39.

Aranda, B. et al. (2011), "Synthese d'un Liant Vert Capable de Concurrencer le Ciment Portland", Journée des doctorants, Comunication orale: Université de Rennes, France.

Baux, C. (2010), "Process for the Industrial Manufacture of Compositions Based on Anhydrous Calcium Sulphate In The β-Anhydrite iii' Form, and Corresponding Compositions and Binders", FR Patent WO/2010/003827 A1/14.01.2010.

Majumdar, A.J. and Laws, V. (1979), "Fibre Cement Composites: Research at BRE", *Composites*, 10(1), 17-27.

Taranu, G. et al. (2011), "Experimental Evaluation of Elastic Modulus of Unreinforced and Glass Fibre Reinforced Mineral Matrix Composite", in *ICEUBI 2011-International Conference on Engineering. Universidade da Beira Interior*, Covilhã – Portugal.

Taranu, G. et al. (2011), "Evaluation of Mechanical Properties of Cement and Calcium Sulphate Mineral Matrix", *Bulletin of the Polytechnic Institute of Iasi, Construction and Architecture Section*, LVII (LXI)(2), 131-140.

Toma, I.O. et al. (2011), "Influence of Cement and Sand Type on the Strength Characteristics of Mortars with Various Contents of Green Binder", *Procedia Engineering*, 21(0), 196-203.

TRANSVERSE STIFFNESS OF UNIDIRECTIONAL FIBROUS POLYMERIC COMPOSITES

NICOLAE TARANU, LILIANA BEJAN, RALUCA HOHAN

Technical University "Gheorghe Asachi" Iasi, B-dul Mangeron 67, Iasi, Romania,
taranu@ce.tuiasi.ro, lilbejan@yahoo.com, hohan.raluca@yahoo.com

The transverse modulus of fibre reinforced polymer (FRP) composites is a matrix dominated property that cannot be conveniently evaluated with micromechanics approach. The model based on the micromechanics assumptions is not mathematically rigorous and underestimates the transverse modulus values. Therefore the authors attempt to choose alternative models that enable a more precise calculation of this important design property. Comparative results determined on the selected models are presented, discussed and finally recommended for the evaluation of unidirectional reinforced FRP composites transverse stiffness.

Keywords: fibrous composites, Young modulus, transverse stiffness.

INTRODUCTION

Fibre reinforced polymer (FRP) composites represent a class of materials that has attracted attention of engineers in many industrial areas. The reinforcing fibres constitute the backbone of the material and they determine its strength and stiffness in the direction of fibres, although some "lateral contributions" are not excluded. The unidirectional lamina, Figure 1, is the basic building block in a laminated FRP composite material. The composite properties can be determined by experimental measurements, but this approach is very expensive and time consuming, (Agarwal et al., 2006, Daniel et al., 2006); therefore any theoretical tool that enables evaluation of composite characteristics is more than welcome. Consequently, the experimental procedures are mostly utilised to verify the theoretical results.

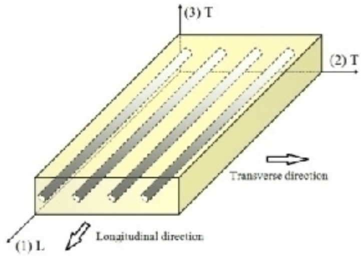

Figure 1. A unidirectional fibre reinforced composite lamina and its principal material axes

The unidirectional composite shows different properties in the material axes directions. The stiffness characteristics of unidirectional fibre reinforced composites, E_1 (longitudinal modulus) and E_2 (transverse modulus) are required in the design process of composite structures. In contrast to the longitudinal modulus E_1, which is a fibre dominated property, the transverse modulus E_2 is a matrix dominated one.

TRANSVERSE MODULUS AND ANALITICAL MODELS

The Inverse Rule of Mixture Model

Consider the simple model shown in Figure 2a, in which the fibres are assumed to be uniform in properties and diameter, continuous and parallel throughout the composite. Since it is assumed that the fibres remain parallel and that the dimensions do not change along the length of the element, the area fractions must equal the volume fractions, (Taranu et al, 2005). The composite is represented by a *series model* of matrix and fibre elements, Figure 2b, and the main assumption is that the stress is the same in the fibre and matrix. (Halpin, 1992; Jones, 1999; Agarwal et al., 2006).

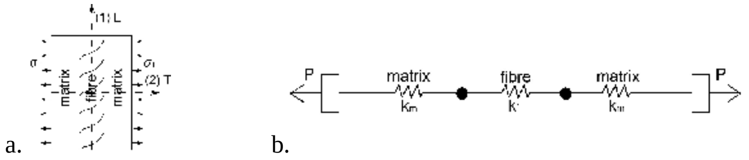

Figure 2. The series model for transverse modulus

The formula for E_2 based on this model, is termed “the inverse rule of mixtures”, Eq.1:

$$E_2 = \frac{E_f E_m}{E_m V_f + E_f V_m} \tag{1}$$

where E_f and E_m are the elastic modulus of fibre and matrix, respectively, and V_f,V_m the fibre and matrix volume fractions. The model utilised to determine the transverse modulus, Eq.1, is not mathematically precise and it leads to underestimation of this property. The isotropic fibres, analysed in this paper are made of glass (*E*-glass, *S*-glass and ECR-glass) and basalt embedded in epoxy matrix. The transverse modulus of a unidirectional composite as predicted by Eq.1 is plotted in Figure.3 as a function of fibre volume fraction, for isotropic fibres and epoxy matrix.

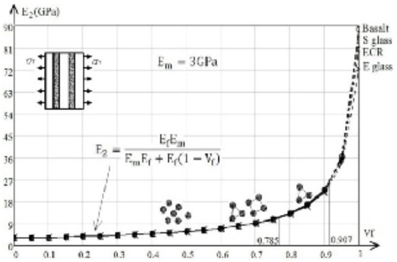

Figure 3. Transverse modulus according to the inverse rule of mixture

Halpin-Tsai Formulas for Transverse Modulus

Halpin and Tsai developed semiempirical equations (Halpin, 1992) to match the results of more exact mechanics analyses. These equations include some parameters that are influenced by the geometry of the reinforcing fibres, their distribution in the composite and the loading condition.

$$E_2 = E_m \frac{1 + \xi\eta V_f}{1 - \eta V_f} \tag{2}$$

where: $$\eta = \frac{\frac{E_f}{E_m} - 1}{\frac{E_f}{E_m} + \xi} \tag{3}$$

in which ξ is a factor depending of the fibre geometry, packing geometry and loading condition. A value of ξ = 2 has been suggested by Halpin and Tsai for fibres with circular cross section. Experimental results indicate the adequacy of Halpin-Tsai equations to predict the transverse composite modulus for practical requirements.

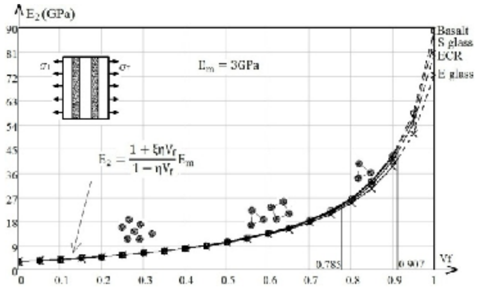

Figure 4. Transverse modulus predicted through Halpin-Tsai equations

The Contiguity Model

The reinforcing fibres on the cross section of unidirectional composite materials are most of the times randomly arranged instead of being distributed in a regular array. Considering C as the degree of contiguity, C=0 corresponds to isolated fibres and C=1 corresponds to all contiguous fibres, Figure 5.

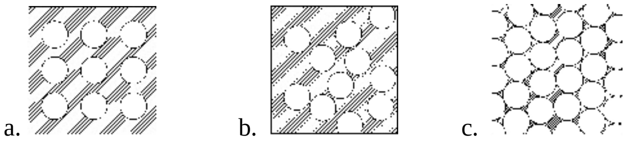

Figure 5. Various schemes of fibre contiguity: a. isolated fibres (C=0); b. actual random fibre (0<C<1); c. isolated matrix (C=1)

This approach that considers the contiguity has been analyzed by Tsai (Jones, 1999):

$$E_2 = A\left[(1-C)\frac{K_f(2K_m + G_m) - G_m(K_f - K_m)V_m}{(2K_m + G_m) + 2(K_f - K_m)V_m} + C\frac{K_f(2K_m + G_f) + G_f(K_m - K_f)V_m}{(2K_m - G_f) - 2(K_m - K_f)V_m}\right] \tag{4}$$

where: $$A = 2[1 - \nu_f + (\nu_f - \nu_m)V_m] \tag{5}$$

$$K_f = \frac{E_f}{2(1-\nu_f)}\,;\; K_m = \frac{E_m}{2(1-\nu_m)}\,;\; G_f = \frac{E_f}{2(1+\nu_f)}\,;\; G_m = \frac{E_m}{2(1+\nu_m)} \tag{6}$$

in which ν_f, ν_m are the Poisson's ratio for fibre and matrix, respectively, and G_f, G_m are the shear moduli of the constituents. In Figure 6 the variation of the transverse modulus, E_2, including the contiguity influence is illustrated.

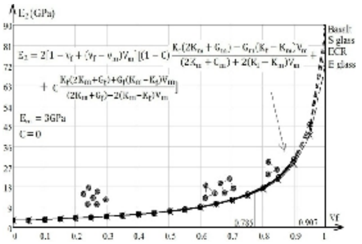

Figure 6. Variation of transverse modulus including the influence of fibres contiguity

The Composite Cylinder Assemblage (CCA) Model

This model enables the exact analytical evaluation of the effective elastic moduli (Jones, 1999). The model consists of an assemblage of composite cylinders, Figure. 7a, each made of a circular fibre core and a concentric matrix shell (ASM, 2001, Zweben, C. 1995). In each cylinder the fibre volume fraction is kept constant (also meaning that the ratio r^2/R^2 is the same); each composite cylinder behaves as an equivalent homogeneous cylinder. The volume of the material is progressively filled out with composite cylinders with different radii. Consequently, the properties of the assemblage approach the properties of one composite cylinder.

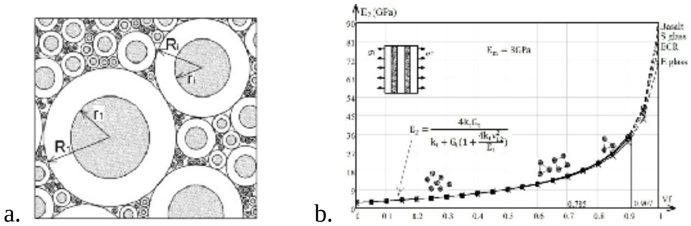

Figure 7. Composite cylinder assemblage (CCA): a. the constituents assemblage; b. variation of transverse modulus with fibre content

The following formula has been elaborated by Hashin and Rosen (Chou, 2005; ASM, 2001):

$$E_2 = \frac{4k_tG_t}{k_t + G_t\left(1 + \dfrac{4k_t\nu_{12}^2}{E_1}\right)} \tag{7}$$

$$k_t = \frac{k_mk_f + \left(V_fk_f + V_mk_m\right)G_m}{V_mk_f + V_fk_m + G_m}\;,\quad k_f = \frac{E_f}{2(1-\nu_f-\nu_f^2)}\quad k_m = \frac{E_m}{2(1-\nu_m-\nu_m^2)} \tag{8}$$

$$G_t = G_m \frac{\left(1+\alpha V_f^3\right)\left(\rho+\beta_m V_f\right)-3V_f V_m^2\beta_m^2}{\left(1+\alpha V_f^3\right)\left(\rho-V_f\right)-3V_f V_m^2\beta_m^2} \tag{9}$$

$$\nu_{12} = \nu_f V_f + \nu_m V_m + \frac{V_f V_m(\nu_f-\nu_m)\left(\frac{1}{k_m}-\frac{1}{k_f}\right)}{\frac{V_m}{k_f}+\frac{V_f}{k_m}+\frac{1}{G_m}} \tag{10}$$

$$\alpha=\frac{\gamma+\beta_m}{\gamma-1}\ ;\ \rho=\frac{\beta_m-\gamma\beta_f}{1+\gamma\beta_f}\ ;\ \gamma=\frac{G_f}{G_m}\ ;\ \beta_m=\frac{1}{3-4\nu_m}\ ;\ \beta_f=\frac{1}{3-4\nu_f} \tag{11}$$

The Self-Consistent Model

The model gives one of the most exact solutions and it is described in engineering terms by Whitney and Riley in 1966 (Halpin, 1992, Chamis at al, 1968). This model has a single fibre embedded in a concentric cylinder of matrix material, Figure 8, (Genta, 1982). The volume fraction of the fibre embedded in the composite cylinder is the same as that given by all fibres in the composite material. The values calculated with Eq. (12) are slightly larger than those evaluated with the rule of mixture.

$$E_2=\frac{\frac{4G_m}{V_f}}{\frac{\alpha_1}{\gamma_1}+\frac{\delta_1}{\beta_1}+\frac{2-2\nu_m}{V_f}} \tag{12}$$

where:

$$\alpha_1=(1-2\nu_f)G_m-(1-2\nu_m)G_f\ ;\quad \beta_1=G_m+(3-4\nu_m)G_f \tag{13}$$

$$\gamma_1=\alpha_1+2G_f(1-\nu_m)\ ;\quad \delta_1=(G_f-G_m)(V_f-4+4\nu_m) \tag{14}$$

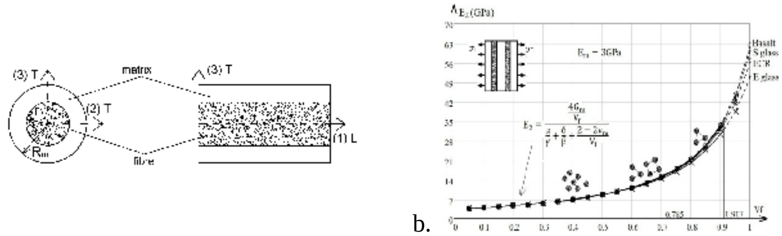

a. b.

Figure 8. Self-consistent model: a. the constituents assemblage; b. variation of transverse modulus with fibre content

RESULTS AND CONCLUSIONS

A synthesis of all results for the transverse modulus in presented in Figure 9. It can be seen from transverse modulus curve, Figure 3, that the fibres have a small contribution to the composite modulus in the transverse direction for low and medium fibre fractions.

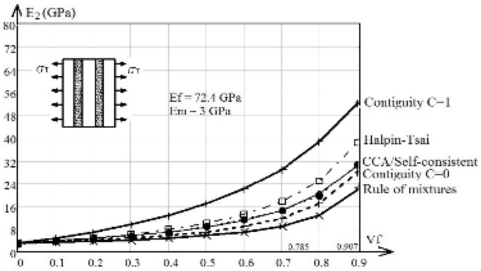

Figure 9. Synthesis of all results for the transverse modulus

To double the transverse modulus values, Figure 3, the fibre volume fractions should exceed 50%. A large increase of the transverse modulus is obtained for fibre volume fractions impractically high. Experimental verification of the theoretical results provided by the inverse rule of mixture reveals the disagreement in moduli values. This mismatch can be explained by the series model, Figure 2b, that does not accurately simulate the behaviour of unidirectional composites loaded in the transverse direction (Agarwal et al., 2006). In real unidirectional composites the long parallel fibres are distributed in the polymeric matrix in a non regular array, Figure 5b. The transverse load is shared between the reinforcing fibres and the polymeric matrix therefore the stresses in the fibre and the matrix have different values. New models have been proposed and applied to match the experimental results with the theoretical ones utilizing more refined micromechanics analyses. The family of graphical curves indicated very closed values for low fibre volume fractions (up to $V_f = 0.3$); the differences can be noticed for medium to high fibre contents. The Halpin–Tsai equations give results that are much closer to the experimental measurements and it has been suggested that these equations are satisfying the practical needs for the transverse composite modulus predictions.

REFERENCES

Agarwal, B.D., Broutman, L.J. and Chandrashekhara K. (2006), *Analysis and Performance of Fibre Composites*, Third edition, Wiley-Interscience, New-York.

Chamis, C.C. and Sendeckyj, G.P. (1968), “Critique on Theories Predicting Thermoelastic Properties of Fibrous Composites”, *Journal of Composite Materials*, 2(3), 332.

Chou, T.W. (2005), *Microstructural Design of Fiber Composites*, Cambridge Solid State Science Series, Cambridge University Press, Cambridge.

Daniel, I. and Ishai, O. (2006), *Engineering Mechanics of Composite Materials*, Oxford University Press, Oxford.

Gay, D. and Hoa, S.V. (2007), *Composite Materials. Design and Applications*, CRC Press, Boca Raton.

Genta, G. (1982), *Progettazione Calcolo Strutturale con i Materiali Compositi*, Tecniche Nuove, Milano.

Halpin, J.C. (1992), Revised *Primer on Composite Materials Analysis*, Technomic, Lancaster.

Jones, R.M. (1999), *Mechanics of Composite Materials*, Taylor & Francis Inc., Philadelphia.

Miracle, D.B. and Donaldson, S.L. (eds.) (2001), *ASM Handbook, Composites*, volume 21, ASM International, The Materials Information Society, Material Park, Ohio.

Şerbescu, A., Pilakoutas, K. and Ţăranu, N. (2006), “The Efficiency of Basalt Fibres in Strengthening the Reinforced Concrete Beams”, *Bul. Inst. Politehnic Iaşi*, s. Constr. Archit., LII (LVI), 3-4, 47-57.

Tsai, S.W. and Hahn, H.T. (1980), *Introduction to Composite Materials*, Technomic, Lancaster.

Ţăranu, N. and Bejan, L. (2005), *Mechanics of fiber reinforced composites*, Cermi Press, Iaşi.

Zweben, C. (1995), “Fibrous Composites: Thermomechanical Properties”, in: A. Kelly (ed.), *Concise Encyclopedia of Composite Materials*, Revised edition, Pergamon Press, Advances in Materials Science and Engineering, Oxford.

THE STIFFNESS MATRIX FOR THICK LAMINATES WITH FIBROUS REINFORCEMENT

NICOLAE TARANU, RALUCA HOHAN, LILIANA BEJAN

Technical University "Gheorghe Asachi" Iasi, B-dul Mangeron 67, Iasi, Romania,
taranu@ce.tuiasi.ro, hohan.raluca@yahoo.com, lilbejan@yahoo.com

Fibre reinforced composite materials are nowadays utilized in many areas of engineering. Most of composite structures made of fibrous composites consist of several distinct unidirectional or bi-directional laminas. Since a single lamina is too thin to be directly used in engineering applications several laminas are bonded together to form a structure termed a laminate.Thin laminates are extensively used in the aerospace structures with loads that will usually lie in their plane. In construction there are many applications with thick laminas that require a particular analysis and an adequate design considering the effect of transverse shear stresses and shear strains. The main objective of this paper is to analytically model the mechanical behaviour of thick reinforced laminas and laminates considering out-of-plane shear. The constitutive relations of a generally thin and thick orthotropic laminas and of laminates built-up from an even and uneven numer of plies are developed and presented. An analysis can be then conducted to obtain the stresses and strains in a lamina or on all laminas making a specific laminated structure with thick layers.

Keywords: fibre reinforced composites, thick lamina, stiffness matrix, stresses and strains, shear effect.

INTRODUCTION

The terms "thick lamina" and "thick laminate" respectively are used to describe the composites with a thickness that influences the response of the material. Experimental results (Chou, 1992) have shown that lamination theory predictions are not applicable for thick laminates. These differences are explained due to the negligible presence of the out-of-plane shear deformation and transverse normal strains. The inclusion of transverse shear deformation in the thin plate theory is attained considering the transverse shear strains, γ_{xz} and γ_{yz}, to be non-zero (Chou, 1992). Assuming a perfect bonding between the plies of a laminate the stresses remain constant across at the interface between them, thus τ_{xz} and τ_{yz} remain continuous along the height of the section (Ashbee, 1989). A laminate laid up from laminas with fibre directions at right angles to one another can be considered orthotropic and the reinforcement as bidirectional (Figure 1).

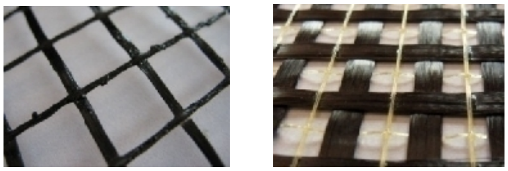

Figure 1. Bidirectional reinforcement

ANALYTICAL MODEL

The Figure 2 depicts the coordinate system of axes of a generally orthotropic lamina in the two-dimensional and three-dimensional case respectively.

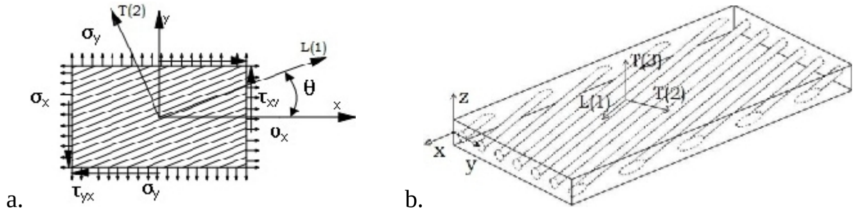

Figure 2. Coordinate system of axes for orthotropic lamina: a. thin; b. thick

The stress-strain relation for a three-dimensional anisotropic element is given by the material constitutive equation: $\{\sigma x\} = [C]\{\varepsilon_x\}$, where [C] is the stiffness matrix, $\{\sigma_x\}$ and $\{\varepsilon_x\}$ are the stress and strain vectors in the global coordinate system (x,y,z).

The developed matrix form (Kaw, 2006; Taranu, 2005) is:

$$\begin{Bmatrix} \sigma_x \\ \sigma_y \\ \sigma_z \\ \tau_{yz} \\ \tau_{zx} \\ \tau_{xy} \end{Bmatrix} = \begin{bmatrix} C_{11} & C_{12} & C_{13} & C_{14} & C_{15} & C_{16} \\ C_{21} & C_{22} & C_{23} & C_{24} & C_{25} & C_{26} \\ C_{31} & C_{32} & C_{33} & C_{34} & C_{35} & C_{36} \\ C_{41} & C_{42} & C_{43} & C_{44} & C_{45} & C_{46} \\ C_{51} & C_{52} & C_{53} & C_{54} & C_{55} & C_{56} \\ C_{61} & C_{62} & C_{63} & C_{64} & C_{65} & C_{66} \end{bmatrix} \begin{Bmatrix} \varepsilon_x \\ \varepsilon_y \\ \varepsilon_z \\ \gamma_{yz} \\ \gamma_{zx} \\ \gamma_{xy} \end{Bmatrix} = \begin{bmatrix} [C_1] & [C_2] \\ [C_3] & [C_4] \end{bmatrix} \begin{Bmatrix} \varepsilon_x \\ \varepsilon_y \\ \varepsilon_z \\ \gamma_{yz} \\ \gamma_{zx} \\ \gamma_{xy} \end{Bmatrix} \qquad (1)$$

in which C_{ij} are the 36 components of the stiffness matrix.

For anisotropic material, due to the symmetry, only 21 terms are distinct and they adequately describe the elastic stress-strain relation. Some of these constants become null and equal in case of orthotropic (9 constants), transversely isotropic (5 constants) or isotropic (2 constants) materials (Kaw, 2006).

Lamina

Thin Lamina

For a thin lamina the constitutive equation has the following condensed form: $\{\sigma_x\} = [Q]\{\varepsilon_x\}$, where [Q] is the reduced stiffness matrix, with Q_{ij} the reduced stiffness terms related to the engineering constants with the developed matrix form (Kaw, 2006):

$$\begin{Bmatrix} \sigma_x \\ \sigma_y \\ \tau_{xy} \end{Bmatrix} = \begin{bmatrix} Q_{11} & Q_{12} & Q_{16} \\ Q_{21} & Q_{22} & Q_{26} \\ Q_{61} & Q_{62} & Q_{66} \end{bmatrix} \begin{Bmatrix} \varepsilon_x \\ \varepsilon_y \\ \gamma_{xy} \end{Bmatrix} \qquad (2)$$

Thick Lamina

Plane stress assumption in the Mindlin-Reissner theory gives: $\{\sigma_x\} = [R]\{\varepsilon_x\}$, where [R] is the reduced stiffness matrix considering out-of-plane shear force (Barros, 1989).

$$\begin{Bmatrix} \sigma_x \\ \sigma_y \\ \tau_{xy} \\ \tau_{yz} \\ \tau_{zx} \end{Bmatrix} = \begin{bmatrix} R_{11} & R_{12} & R_{13} & R_{14} & R_{15} \\ R_{21} & R_{22} & R_{23} & R_{24} & R_{25} \\ R_{31} & R_{32} & R_{33} & R_{34} & R_{35} \\ R_{41} & R_{42} & R_{43} & R_{44} & R_{45} \\ R_{51} & R_{52} & R_{53} & R_{54} & R_{55} \end{bmatrix} \begin{Bmatrix} \varepsilon_x \\ \varepsilon_y \\ \gamma_{xy} \\ \gamma_{yz} \\ \gamma_{zx} \end{Bmatrix} = \begin{bmatrix} \overset{3x3}{[R_1]} & \overset{2x3}{[R_2]} \\ \underset{3x2}{[R_3]} & \underset{2x2}{[R_4]} \end{bmatrix} \begin{Bmatrix} \varepsilon_x \\ \varepsilon_y \\ \gamma_{xy} \\ \gamma_{yz} \\ \gamma_{zx} \end{Bmatrix} \tag{3}$$

The R_{ij} constants for orthotropic laminas are expressed in terms of elastic constants as:

$$R_{11} = \frac{E_x}{1 - \nu_{xy}\nu_{yx}};\ R_{22} = \frac{E_y}{1 - \nu_{xy}\nu_{yx}};\ R_{12} = \frac{\nu_{xy}E_y}{1 - \nu_{xy}\nu_{yx}};\ R_{21} = \frac{\nu_{yx}E_x}{1 - \nu_{xy}\nu_{yx}} \tag{4}$$

$$R_{33} = G_{xy};\ R_{44} = k_{23}G_{yz};\ R_{55} = k_{13}G_{xz} \tag{5}$$

where k_{23} and k_{13} are the corrective factors for shear, considered to match the approximate solution with the exact elasticity solution. All the other constants are zero.

Laminate

Thin Laminate

The constitutive equations according to Kirchhoff hypothesis in the matrix developed form (Chou, 1992; Kaw, 2006) are presented below:

$$\begin{Bmatrix} N_x \\ N_y \\ N_{xy} \end{Bmatrix} = \begin{bmatrix} A_{11} & A_{12} & A_{13} \\ A_{21} & A_{22} & A_{23} \\ A_{31} & A_{32} & A_{33} \end{bmatrix} \overline{\varepsilon^a} + \begin{bmatrix} B_{11} & B_{12} & B_{13} \\ B_{21} & B_{22} & B_{23} \\ B_{31} & B_{32} & B_{33} \end{bmatrix} \overline{\varepsilon^b} \tag{6}$$

$$\begin{Bmatrix} M_x \\ M_y \\ M_{xy} \end{Bmatrix} = \begin{bmatrix} B_{11} & B_{12} & B_{13} \\ B_{21} & B_{22} & B_{23} \\ B_{31} & B_{32} & B_{33} \end{bmatrix} \overline{\varepsilon^a} + \begin{bmatrix} D_{11} & D_{12} & D_{13} \\ D_{21} & D_{22} & D_{23} \\ D_{31} & D_{32} & D_{33} \end{bmatrix} \overline{\varepsilon^b} \tag{7}$$

where N_x, N_y, N_{xy}, M_x, M_y, M_{xy} are the membrane force resultants and moment resultants, respectively, Figure 3a

h_k is the coordinate of the layer k with respect to the midplane, Figure 3b.

[A] – extensional stiffness matrix: $A_{ij} = \sum_{k=1}^{n} (Q_{ij})_k (h_k - h_{k-1})$ (8)

[B] – extension – bending coupling stiffness matrix: $B_{ij} = \frac{1}{2}\sum_{k=1}^{n} (Q_{ij})_k (h_k^2 - h_{k-1}^2)$ (9)

[D] – bending stiffness matrix: $D_{ij} = \frac{1}{3}\sum_{k=1}^{n} (Q_{ij})_k (h_k^3 - h_{k-1}^3)$ (10)

$\overline{\varepsilon^a} = \begin{Bmatrix} \varepsilon_x^0 \\ \varepsilon_y^0 \\ \gamma_{xy}^0 \end{Bmatrix}$ – axial strains at the geometric midplane and $\overline{\varepsilon^b} = \begin{Bmatrix} k_x \\ k_y \\ k_{xy} \end{Bmatrix}$ – bending strains

The stiffness matrix for thin laminates is: $\begin{bmatrix} A & B \\ B & D \end{bmatrix}$ (11)

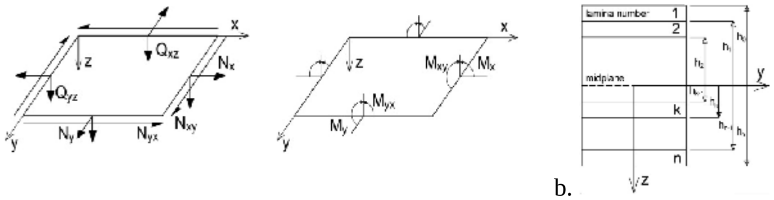

a.

b.

Figure 3a. Resultant forces and moments; b. Multilayered laminate geometry

Thick laminate

The constitutive relations in the developed matrix form of a laminate (Barros, 1989) with anisotropic layers considering out-of-plane shear (Gay, 2007; Chou, 1992) are:

$$\begin{Bmatrix} N_x \\ N_y \\ N_{xy} \end{Bmatrix} = \begin{bmatrix} A_{11} & A_{12} & A_{13} \\ A_{21} & A_{22} & A_{23} \\ A_{31} & A_{32} & A_{33} \end{bmatrix} \overline{\varepsilon}^a + \begin{bmatrix} B_{11} & B_{12} & B_{13} \\ B_{21} & B_{22} & B_{23} \\ B_{31} & B_{32} & B_{33} \end{bmatrix} \overline{\varepsilon}^b + \begin{bmatrix} C_{11} & C_{12} \\ C_{12} & C_{22} \\ C_{13} & C_{23} \end{bmatrix} \overline{\varepsilon}^s \tag{12}$$

$$\begin{Bmatrix} M_x \\ M_y \\ M_{xy} \end{Bmatrix} = \begin{bmatrix} B_{11} & B_{12} & B_{13} \\ B_{21} & B_{22} & B_{23} \\ B_{31} & B_{32} & B_{33} \end{bmatrix} \overline{\varepsilon}^a + \begin{bmatrix} D_{11} & D_{12} & D_{13} \\ D_{21} & D_{22} & D_{23} \\ D_{31} & D_{32} & D_{33} \end{bmatrix} \overline{\varepsilon}^b + \begin{bmatrix} E_{11} & E_{12} \\ E_{12} & E_{22} \\ E_{13} & E_{23} \end{bmatrix} \overline{\varepsilon}^s \tag{13}$$

$$\begin{Bmatrix} Q_{xz} \\ Q_{yz} \end{Bmatrix} = \begin{bmatrix} C_{11} & C_{12} & C_{13} \\ C_{12} & C_{22} & C_{23} \end{bmatrix} \overline{\varepsilon}^a + \begin{bmatrix} E_{11} & E_{12} & E_{13} \\ E_{12} & E_{22} & E_{23} \end{bmatrix} \overline{\varepsilon}^b + \begin{bmatrix} F_{11} & F_{12} \\ F_{12} & F_{22} \end{bmatrix} \overline{\varepsilon}^s \tag{14}$$

where N_x, N_y, N_{xy}, M_x, M_y, M_{xy}, Q_{xz}, Q_{yz} are the membrane force resultants, moment resultants and transverse shear resultants

[A] – extensional stiffness matrix: $A_{ij} = \sum_{k=1}^{n} (R_1)_{ij}^{k} (h_k - h_{k-1})$ (15)

[B] – extension – bending coupling stiffness matrix: $B_{ij} = \frac{1}{2} \sum_{k=1}^{n} (R_1)_{ij}^{k} (h_k^2 - h_{k-1}^2)$ (16)

[C] – shear – extension coupling stiffness matrix: $C_{ij} = \sum_{k=1}^{n} (R_2)_{ij}^{k} (h_k - h_{k-1})$ (17)

[D] – bending stiffness matrix: $D_{ij} = \frac{1}{3} \sum_{k=1}^{n} (R_{ij})_k (h_k^3 - h_{k-1}^3)$ (18)

[E] – bending – shear coupling stiffness matrix: $E_{ij} = \frac{1}{2} \sum_{k=1}^{n} (R_2)_{ij}^{k} (h_k^2 - h_{k-1}^2)$ (19)

[F] – shear stiffness matrix: $F_{ij} = \sum_{k=1}^{n} (R_4)_{ij}^{k} (h_k - h_{k-1})$ (20)

$\overline{\varepsilon}^s = \begin{Bmatrix} \gamma_{yz} \\ \gamma_{xz} \end{Bmatrix}$ – shear strains

The stiffness matrix for thick laminates is: $\begin{bmatrix} A & B & C \\ B & D & E \\ C & E & F \end{bmatrix}$ (21)

For symmetric laminates the matrix [B] and [E] are null. For materials that are not anisotropic the matrix [C] is also null.

CONSTITUTIVE EQUATIONS FOR ORTHOTROPIC LAMINATES

Bidirectional reinforcement can be generated by overlapping unidirectional reinforcement. Overlapping laminas with unidirectional reinforcement only at angles θ = 0^0 or 90^0, with respect to the global coordinate system, forms a specially orthotropic laminate called cross-ply laminate. Overlapping laminas at angles θ ≠ 0^0 or 90^0, but with a 90^0 angle between the layers, develops a generally-orthotropic laminate called angle-ply laminate (Barros, 1989; Ashbee, 1989).

Equations from (2) and (3) are valid for specially orthotropic laminas where the fibres axes are matching the principal axes of the laminas. For a generally orthotropic lamina that is deviated with an angle θ with respect to the global axes the transformation equation (Barbero, 2011) is presented below:

$$[\sigma_x] = \begin{bmatrix} [T_1] & 0 \\ 0 & [T_4] \end{bmatrix} [\sigma_1] \text{ and } [\varepsilon_x] = \begin{bmatrix} [T_1] & 0 \\ 0 & [T_4] \end{bmatrix} [\varepsilon_1] \qquad (22)$$

with

$$[T_1] = \begin{bmatrix} \cos^2\theta & \sin^2\theta & 2\sin\theta\cos\theta \\ \sin^2\theta & \cos^2\theta & -2\sin\theta\cos\theta \\ -\sin\theta\cos\theta & \sin\theta\cos\theta & \cos^2\theta - \sin^2\theta \end{bmatrix} \text{ and } [T_4] = \begin{bmatrix} \cos\theta & \sin\theta \\ -\sin\theta & \cos\theta \end{bmatrix} \qquad (23)$$

where $[T_1]$ and $[T_4]$ are the transformation matrices, $[\sigma_1]$ and $[\varepsilon_1]$ are the stress and strain vector in the local coordinate system, as presented in Figure. 2

RESULTS AND DISCUSSIONS

In-plane, flexural and shear elastic constants of the laminate (Kaw, 2006), can be obtained from the stiffness matrix using Table 1.

Table 1. Elastic constants

Elastic constants	Longitudinal elasticity modulus, E_x	Transverse elasticity modulus, E_y=E_z	Major Poisson`s ratio, ν_{xy}	Shear elasticity modulus, G	Minor Poisson`s ratio, ν_{yx}
Axial	$\frac{1}{hA_{11}^*}$	$\frac{1}{hA_{22}^*}$	$-\frac{A_{12}^*}{A_{11}^*}$	$G_{xy} = \frac{1}{hA_{66}^*}$	$-\frac{A_{12}^*}{A_{22}^*}$
Flexural	$\frac{12}{h^3D_{11}^*}$	$\frac{12}{h^3D_{22}^*}$	$-\frac{D_{12}^*}{D_{11}^*}$	$G_{xy} = \frac{12}{h^3D_{66}^*}$	$-\frac{D_{12}^*}{D_{22}^*}$
Shear	-	-	-	$G_{yz} = G_{xz} = \frac{1}{hkF_{11}^*}$	-

where h is the thickness of the laminate
$[A]^* = [A]^{-1}$ –inverted extensional stiffness matrix
$[D]^* = [D]^{-1}$ – inverted flexural stiffness matrix
$[F]^* = [F]^{-1}$ – inverted shear stiffness matrix

In the case of uneven number of plies in the laminate, when the force and moment resultants acting on the laminate are specified, one can easily obtain (Kaw, 2006; Barros, 1989):

$$\text{-midplane strains: } \begin{Bmatrix} \varepsilon_x^0 \\ \varepsilon_y^0 \\ \gamma_{xy}^0 \end{Bmatrix} = [A]^* \begin{Bmatrix} N_x \\ N_y \\ N_{xy} \end{Bmatrix} \text{ and midplane curvature: } \begin{Bmatrix} k_x^0 \\ k_y^0 \\ k_{xy}^0 \end{Bmatrix} = [D]^* \begin{Bmatrix} M_x \\ M_y \\ M_{xy} \end{Bmatrix} \quad (24)$$

$$\text{- global strains: } \begin{Bmatrix} \varepsilon_x \\ \varepsilon_y \\ \gamma_{xy} \end{Bmatrix} = \begin{Bmatrix} k_x^0 \\ k_y^0 \\ k_{xy}^0 \end{Bmatrix} z \text{ and stresses: } \begin{Bmatrix} \sigma_x \\ \sigma_y \\ \tau_{xy} \end{Bmatrix} = [R_1]_k \begin{Bmatrix} \varepsilon_x \\ \varepsilon_y \\ \gamma_{xy} \end{Bmatrix}; \ \begin{Bmatrix} \tau_{xz} \\ \tau_{yz} \end{Bmatrix} = [F]^* \begin{Bmatrix} \gamma_{xz} \\ \gamma_{yz} \end{Bmatrix} \quad (25)$$

$$\text{where: } \begin{Bmatrix} \gamma_{xz} \\ \gamma_{yz} \end{Bmatrix} = [F]^* \begin{Bmatrix} Q_{xz} \\ Q_{yz} \end{Bmatrix} \quad (26)$$

in which z is the distance from the neutral axis to the required point
$[R_1]_k$, $[R_4]_k$ are the reduced stiffness matrices of the layer k considering shear force

CONCLUSIONS

Thin laminates are extensively used in the aerospace construction with loads that will usually lie in their plane. In construction many times the practical applications are with thick laminates and they require a proper design approach.

The structural response of a laminate requires knowledge on the stresses and strains along the fiber and at an angle with respect to the principal material directions.

The reduced solutions of the classical lamination theory adopted for the thin laminates are not valid in the case of the thick laminates because it does not consider the effect of transverse shear stress and shear strain. When the transverse shear stresses exist they can have an influence on the bending deformation and on the interlaminar adhesion of a laminate.

The effect of stacking sequence and ply orientation on the mechanical behaviour can now be controlled and designed with models that combine the principles of the classical laminate theory and fracture mechanics.

Since the thick plates computation involves more complexity than the classical thin plate approach, an extra effort is needed for an appropriate description of their elastic behaviour.

REFERENCES

Ashbee, K. (1989), *Fundamental principles of fiber reinforced composites*, Technomic Publishing Company Inc.

Barbero, E.J. (2011), *Introduction to composite materials design*, CRC Press.

Barros, J.A.O. (1989), *Modelo de analise de estruturas laminares e de compositos lamindos*, Faculdade de Engenharia, Universidade do Porto.

Chou, T.-W. (1992), *Microstructural design of fiber composites*, Cambridge University Press.

Gay, D., and Hoa, S.V. (2007), *Composite materials – Design and applications*, CRC Press.

Kaw, A.K. (2006), *Mechanics of composite materials*, CRC Press LLC.

Taranu, N. and Bejan, L. (2005), *Mechanics of fiber reinforced composites* (in Romanian), Cermi Press, Iași.

INFLUENCE OF CURING CONDITIONS ON THE SELF WEIGHT AND STRENGTH CHARACTERISTICS OF ECO-MORTARS

IONUŢ-OVIDIU TOMA, IOANA OLTEANU, ANA-MARIA TOMA, MIHAI BUDESCU

"Gheorghe Asachi" Technical University of Iasi, Faculty of Civil Engineering and Building Services, 43 Prof. D. Mangeron Blvd., Iaşi, Romania, 700050, emails: iotoma@ce.tuiasi.ro, ioanaolteanu@ce.tuiasi.ro, anamtoma@ce.tuiasi.ro, mbudescu@tuiasi.ro

The paper presents some preliminary results concerning the influence of curing conditions on the self weight and strength characteristics of an eco-mortar. The binder is considered to be made of eco-cement and ordinary Portland cement. The eco-cement is set to replace the ordinary Portland cement in the mix proportion. It is made from industrial wastes and can be entirely recycled after its expiration date. The curing conditions consisted in air curing for 28 days or various time intervals for curing in water until the day of testing. The strength properties at the age of 28 days are investigated in terms of bending tensile strength and compressive strength. The bending tensile strength is determined on standard size prisms by means of a three-point loading test. The resulting half prisms are inspected for visible cracks and then subjected to an uniaxial compression test in order to determine the compressive strength of the eco-mortar. The obtained results show that the curing conditions play an important role both on the self weight and on the strength characteristics.

Keywords: eco-mortar, curing conditions, strength characteristics.

INTRODUCTION

Concrete made with hydraulic binders, the vast majority of which are based on Portland cement, is by far the most widely employed construction material worldwide in terms of volume.

Being produced using readily available raw materials, easy to use, while in plastic state, and possessing good strength and durability, concrete is indispensable for meeting the needs of modern society for housing (Damtoft et al., 2008). Taking into account that the cement content in normal strength concrete ranges from 10% to 15% by weight and that the concrete industry is the largest consumer of natural resources in the world, roughly 11.5 billion tons a year (Mehta and Monteiro, 2005), one could only imagine the environmental burden the construction industry creates (Arikan, 2004; Koroneos and Dompros, 2007).

However, perhaps the biggest advantage of modern concrete is the possibility of including other industrial by-products into the concrete mix as shown in the work by Meyer (Meyer, 2009). Taking into account that demolition waste generates around 300 million tons of debris per year in the United States alone (Meyer, 2009) it becomes clear that storing these solid wastes in landfills is no longer a viable option. The use of waste materials becomes more and more attractive as an alternative in the construction industry mainly due to the increasing cost of raw materials and the continuous reduction of natural resources.

Since the cement industry itself, is responsible for almost 7% of world's CO_2 emissions (Mehta, 1999), attention needs to be paid by the construction industry to solve the problem. One of the effective ways to reduce the environmental impact is to use mineral admixtures (Lothenbach et al., 2011) as partial or even total replacement of the ordinary Portland cement (Yang et al., 2007). This strategy has the potential to reduce costs, conserve energy and minimize waste. The concept very much fits into the era of sustainable development (Hall et al., 2010).

The present paper brings its contribution to the investigation on the use of a new binder, the anhydrous calcium sulphate in its β anhydrite III' form (WO 2010/003827), also known as Kerysten, a new Cementitious material, as partial replacement of the ordinary Portland cement in concrete. The Kerysten based binder is obtained exclusively from industrial wastes and can be entirely recycled after its expiration date.

MATERIALS AND EXPERIMENTAL SET-UP

The anhydrous calcium sulphate was used as a replacement mineral binder for the cement. The opportunity for using such industrial unrecyclable wastes in construction industry, especially the phosphogypsum, has recently been recognized by researchers (Degirmenci, 2008; Yang et al., 2009) as having net benefits for the environment (Garg et al., 2011). The percentages used in this research were: 20%, 25%, and 30% of the total volume. Together with the cement, the ACS is used to obtain a more eco-friendly binder for mineral matrices. The grain size ranges from 5 μm to 100 μm and the surface area is larger than 10 m^2/g (WO 2010/003827).

The mechanical properties of concrete should be fully understood and correctly addressed if failure of concrete elements was to be avoided. Since the aggregates do not change their mechanical properties during the life-time of concrete, it follows that a closer look should be paid to the characteristics of the mortar paste, be it at the early age (Voigt et al., 2006) or during the entire life-cycle of the structure. The strength characteristics of the mortar depend not only on the mix proportion but also on the curing conditions. It is known that the hydration of cement can continue for years, at a decreased rate provided that there is enough water present and the temperature is favourable (Sajedi and Razak, 2011).

The objective is to assess the influence of the curing conditions on the mechanical properties of eco-mortars. The same sand type, with a maximum grain size of 0.3 mm, was used for all mix proportions. The binder consisted either of OPC, the reference sample, or a mixture of OPC and Kerysten. The considered percentages were fractions of the entire volume.

The two main parameters considered were the percentage of eco-binder in the mix proportion, shown in Table 1, and the curing conditions.

Table 1. Mix Proportions Considered in the Research

Specimen Designation	Binder CEM I [%]	ACS [%]	Sand [%]	Water / Binder [%]
C1K0	50	0	50	40
C1K20	30	20		
C1K25	25	25		
C1K30	20	30		

The specimens were cast in standard size moulds having the dimension 40 × 40 × 160 mm. After 24 hours the specimens were demolded and stored until the day of testing. All specimens made of different mix proportions, including the reference specimens, were cured in water for various lengths of time. Additionally, one set of samples from each mix was cured at room temperature without being submerged in water.

There were 6 specimens cast for each considered case leading to a total number of 180 prisms. At the age of 28 days the specimens were subjected to three point bending test with a constant loading rate of 50 N/s in order to determine the flexural tensile strength (SR-EN 196-1, 2006). The compressive strength was determined on the two resulting halves of the prism with a loading rate of 2400 N/s for the uniaxial compression test.

RESULTS AND DISCUSSIONS

Self Weight

The influence of the added mineral binder to the mix proportion of mortar is firstly investigated in terms of the self weight. Each specimen was measured using a digital calliper in order to check the compliance with the code specifications. The variation of the prisms dimensions, due to shrinkage or expansion, was within the limits imposed by codes. The specimens were also weighted by means of a digital balance with a 0.01g precision.

The obtained results are shown in Figure 1 in terms of the mix proportion and their curing conditions. The first conclusion that can be drawn is that the curing conditions play an important role when it comes to the self weight. The gain is between 5%, for the C1K25 case, and 13%, for the reference mix.

Additionally, a closer look at Figure 1 reveals the fact that the mix proportions for which the ordinary Portland cement was replaced by eco-binder the self weight is smaller. This observation is valid for every mix proportion and for every curing condition chosen at this stage of the research.

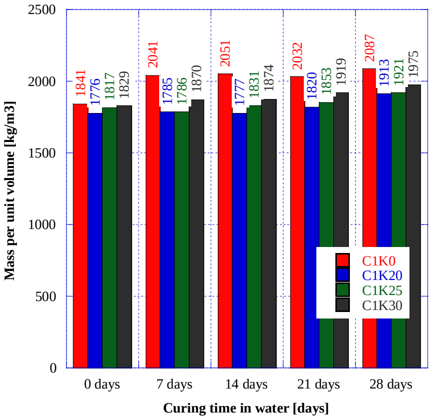

Figure 1. Variation of mass per unit volume

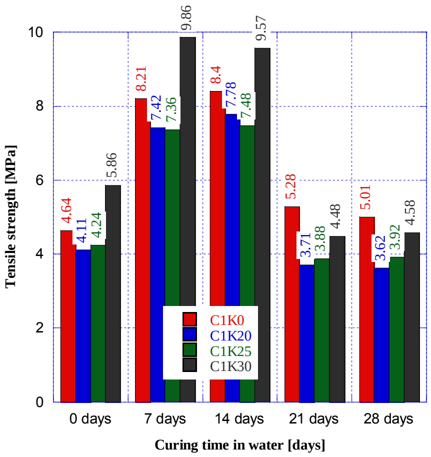

Figure 2. Flexural tensile strength

The most suitable combination, from the point of view of the self weight, would be the C1K20 and C1K25 mixes cured for either 7 days or 14 days in water. Moreover, it can be observed that the 7 days and 14 days water curing time intervals lead to the lowest values in terms of the self weight for the mix proportions made with Cementitious supplementary material.

It can be therefore concluded that, in terms of the self weight, a water curing period of 7 days or 14 days leads to better values. Of course, air curing conditions would lead to even lower values for the self weight but it would be quite detrimental in terms of shrinkage cracking (Aly and Sanjayan, 2008). The question is still pending: how would the curing conditions and the amount of eco-binder influence the mechanical properties of mortars?

Tensile Strength

The tensile strength of mineral matrices is very important from the point of view of the first crack initiation. The higher the tensile strength is, the better a structural element behaves when subjected to tensile stresses. This is of particular importance during seismic events when structural members are subjected to alternating tensile and compressive stresses that may lead to the formation and propagation of cracks.

Figure 2 shows the variation of the tensile strength of mortar depending on the percentage of eco-binder and on the curing conditions. It can be observed that the mix proportions containing large amounts of anhydrous calcium sulphate, e.g. C1K30, exhibited high values for the tensile strength. The values were higher than the control specimen for air curing conditions as well as for 7 days and 14 days water curing. If the specimens were cured in water for longer periods of time, e.g. 21 days or 28 days, their tensile strength dropped significantly. This was valid for all mix proportions. It can be seen that the C1K20 and C1K25 mixes exhibited lower values for the tensile strength compared to the reference mix.

The very high tensile strength of mixes with large percentages of anhydrous calcium sulphate could be explained by the high surface area, ~ 10000 m^2/kg, compared to that of cement, 450 – 650 m^2/kg. In a previous work (Toma et al., 2011), it was concluded that even though the early age tensile strength of mortars with low percentages of eco-binder was slightly lower than the reference mix, at the age of 14 days it became significantly higher.

Compressive Strength

The compressive strength of the eco-mortar was measured on the resulting half prisms from the three point bending test used to determine the flexural tensile strength. The resulting half prisms were examined for the presence of cracks before being submitted to the uniaxial compression test. The results presented in Figure 3 are the average values of 12 tests conducted for each mix proportion and for each curing conditions.

With the sole exception of the air curing conditions, when the compressive strength of the reference mix was lower than the C1K30 case, the reference mix exhibited considerably larger values than the mixes made with eco-binder.

A similar trend is also observed in the case of the compressive strength as with the self weight and the flexural tensile strength. The highest values were registered for the water curing intervals of 7 days and 14 days.

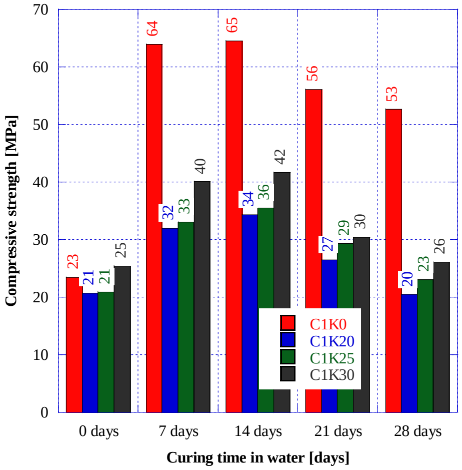

Figure 3. Compressive strength

Longer water curing periods of time, e.g. 21 days and 28 days, led to a decrease in the values of the compressive strength. The results are following the same pattern shown in the work by Itim et al. (2011).

CONCLUSIONS

The present paper brings its contribution at understanding the influence of curing conditions on the strength characteristics of eco-mortars. The investigation was conducted in terms of flexural tensile strength as well as the compressive strength. The obtained results lead to the conclusion that, in terms of the self weight a water curing period of 7 days or 14 days leads to better values. That means lighter structures and better behavior under seismic excitations.

The tensile strength is strongly influenced by both the curing conditions and the percentage of eco-binder in the mix proportion. The results show that the highest values are obtained for water curing periods of time of 7 days and 14 days.

A similar trend is observed for the compressive strength. Even though the values are lower compared to the reference mix, they are still considered to be very good for civil engineering structures. Taking into account that these values were obtained for mix proportions made with different percentages of anhydrous calcium sulphate, an eco-material made entirely from industrial wastes, replacing the Portland cement as mineral binder, the outcome is very encouraging.

However, the authors deem necessary that further researches should be conducted in this field, especially in the direction of long term influence of anhydrous calcium sulphate and ordinary Portland cement on the mechanical properties of mortars. The research should be also extended to the interaction between the mineral matrix and various types of reinforcement. All these should be coupled with an in-depth investigation at the material level to better understand the chemical processes that take place during hardening process of the mineral matrix.

Acknowledgements

This paper was supported by the project "Develop and support multidisciplinary postdoctoral programs in primordial technical areas of national strategy of the research - development - innovation" 4D-POSTDOC, contract no. POSDRU/89/1.5/S/52603, project co-funded from European Social Fund through Sectorial Operational Program Human Resources 2007-2013.

REFERENCES

Aly, T.K. and Sanjayan, J.G. (2008), "Effect of Gypsum on Free and Restrained Shrinkage Behavior of Slag-Concretes Subjected to Various Curing Conditions", *Materials and Structures*, 41(8), 1393-1403.

Arikan, K. (2004), "Feasibility Analysis of Manufacturing High-Performance-Ecological-Cement in Turkey", *Building and Environment*, 39(9), 1125-1130.

Berndt, M.L. (2009), "Properties of Sustainable Concrete Containing Fly-Ash, Slag and Recycled Concrete Aggregate", *Construction and Building Materials*, 23(7), 2606-2613.

Damtoft, J.S. et al. (2008), "Sustainable Development and Climate Change Initiatives", *Cement and Concrete Research*, 38(2), 115-127.

Degirmenci, N. (2008), "Utilization of Phosphogypsum as Raw and Calcinated Material in Manufacturing of Building Products", *Construction and Building Materials*, 22(8), 1857-1862.

Etxeberria, M. et al. (2007), "Influence of Amount of Recycled Coarse Aggregates and Production Process on Properties of Recycled Aggregate Concrete", *Cement and Concrete Research*, 37(5), 735-742.

Garg, M., Minocha, A.K. and Jain, N. (2011), "Environmental Hazard Mitigation of Waste Gypsum and Chalk: Use in Construction Materials", *Construction and Building Materials*, 25(2), 944-949.

Hall, J.K., Daneke, G.A. and Lenox, M.J. (2010), "Sustainable Development and Entrepreneurship: Past Contributions and Future Directions", *Journal of Business Venturing*, 25(5), 439-448.

Itim, A., Ezziane, K. and Kadri, E.-H. (2011), "Compressive Strength and Shrinkage of Mortar Containing Various Amounts of Mineral Additions", *Construction and Building Materials*, 25(8), 3603-3609.

Koroneos, C. and Dompros, A. (2007), "Environmental Assessment of Brick Production in Greece", *Building and Environment*, 42(5), 2114-2123.

Limbachiya, M., Meddah, M.S. and Ouchagour, Y. (2012), "Use of Recycled Concrete Aggregate in Fly-Ash Concrete", *Construction and Building Materials*, 27(1), 439-449.

Lothenbach, B., Scrivener, K. and Hooton, R.D. (2011), "Supplementary Cementitious Materials", *Cement and Concrete Research*, 41(12), 217-229.

Mehta, P.K. (1999), "Concrete Technology for Sustainable Development", *Concrete International*, 21(11), 47-52.

Mehta, P.K. and Monteiro, P.J.M. (2005), *Concrete: Microstructure, Properties and Materials*, 3rd Edition, Mc-Graw-Hill, ISBN-13: 978-0071462891.

Meyer, C. (2009), "The Greening of the Concrete Industry", *Cement and Concrete Composites*, 39(8), 601-605.

Sajedi, F. and Razak, H.A. (2011), "Effect of Curing Regimes and Cement Fineness on the Compressive Strength of Ordinary Portland Cement Mortars", *Construction and Building Materials*, 25(4), 2036-2045.

SR EN 196-1 (2006), "Methods for Cement Testing. Part I: The Determination of Mechanical Properties", (in Romanian).

Toma, I.O. et al. (2011), "Influence of Cement and Sand Type on the Strength Characteristics of Mortars with Various Contents of Green Binder", *Procedia Engineering*, 21, 196-203.

Voigt, T., Malonn, T. and Shah, S.P. (2006), "Green and Early Age Compressive Strength of Extruded Cement Mortar Monitored with Compression Tests and Ultrasonic Techniques", *Cement and Concrete Research*, 36(5), 858–867.

WO-003827A1 (2010), "Process for the Industrial Manufacture of Compositions Based on Anhydrous Calcium Sulphate in the β-Anhydrite III' Form, and Corresponding Compositions and Binders", WO 2010/003827 A1 (in French).

Yang, J. et al. (2009), "Preparation of Load-Bearing Building Materials from Autoclaved Phosphogypsum", *Construction and Building Materials*, 23(2), 687-693.

Yang, K.-H. et al. (2007), "Development of Cementless Mortar using Hwangtoh Binder", *Building and Environment*, 42(10), 3717-3725.

RESEARCH ON MANUFACTURING CUSTOMIZED FOOTWEAR DESIGNED BY QUANTIFYING FORCES ACTING ON THE LOCOMOTOR APPARATUS

ANA MARIA VASILESCU[1], LAURENTIA ALEXANDRESCU[1], ANTON CONSTANTIN MICU[2]

[1] *INCDTP – Division: Leather and Footwear Research Institute, 93 Ion Minulescu, Bucharest, Romania, email: icpi@icpi.ro*

[2] *Politehnica University, Faculty of Mechanical Engineering and Mechatronics, Bucharest, Romania, email: micuanton@yahoo.com*

This paper presents the results obtained in order to manufacture custom shoes for people with normal gait, without severe pathologies, thus contributing to optimization of preventive medical complications manifested in the foot. Making customized footwear in terms of the ground reaction force aims at improving movement during walking or static position. To achieve its purpose, footwear must fulfill its role of reducing medio-lateral component Fy of the ground reaction force. Research conducted have examined the medio-lateral component Fy and My moment developed on the same direction at the ankle, knee and hip, as well as factors influencing them, such as heel material, heel hardness, contact surface and walking style. Recently, mitigating ground reaction force has been a major concern for footwear design and construction. Ground reaction force measurement is carried out using AMTI's AccuGait System force plate.

Keywords: customized footwear, ground reaction, force plate.

INTRODUCTION

Research shows that ground reaction force causes abnormal bone movement in the support phase of the gait cycle, indicating the need to manufacture customized footwear to ensure the structural integrity of feet and joints.

Making customized footwear in terms of the ground reaction force aims at improving movement during walking or static position. The state of comfort or discomfort given by the ground reaction force solution is quantified by the maximum value of the three components: the vertical component Fz, medio-lateral component Fy and anterior-posterior component Fx. These impact forces are transmitted by shock through the body from heel to head through the skeleton structure. According to research in the last three decades, impact forces are shown to be three times the body weight (Hamill, 1996), thus degenerative joint diseases, back pain, stress fractures etc. may occur, being influenced by the walking style, the types of surfaces, lower shoe design and materials shoes are made of.

The goal of research in this work is to develop customized footwear by mitigating the medio-lateral component Fy of the ground reaction force at the time when the foot comes into contact with the ground during walking.

In order to achieve its purpose, footwear must fulfill its role of reducing medio-lateral component Fy of the ground reaction force and implicitly, the My moment in this direction.

EXPERIMENTAL

Manufacturing Customized Footwear

In order to make customized footwear, the values of forces obtained upon the contact between the heel made of several materials (levicel, polyurethane, leather, thermoplastic rubber, polyvinyl chloride, durocol, dermadur) and the walking surface (metal, carpet, linoleum, parquet, rubber, asphalt, tiles) were analyzed for two subjects with similar weights. Subject 1 weighed 70 kg, and subject 2, 69 kg. Also, α angle made by the vertical component Fz and the resultant F in z0y plane was calculated.

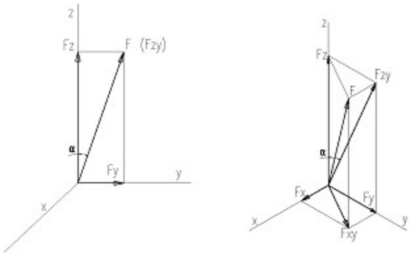

Figure 1. Representation of α angle

Tests conducted on platforms have highlighted that values of ground reaction force components in the three directions (Fz, Fy, Fx), for two subjects with similar weights, wearing the same shoes and walking on the same contact surface are different due to the different ways of walking.

GRF component values are different, depending on the material the shoe sole is made of and the type of ground surface. It was noticed that the angle α is about 2 degrees in both subjects.

The foot and the shoes form an ensemble whose characteristics are specific to each individual, and it is recommended to make custom shoes.

In order to make customized footwear to reduce the medio-lateral component Fy of the ground reaction force, two kinds of shoes were manufactured: shoes and boots with customized heels with height between 17 ÷ 45 mm.

In order to make the customized heel, three rubber formulations were developed, with preset properties for the footwear field, especially for the customized footwear one, with different hardness values. Vulcanized rubber plates were made according to the value of α angle between the vertical component Fz and resultant F in the z0y plane, with an inclination of 2 degrees (Figure 2).

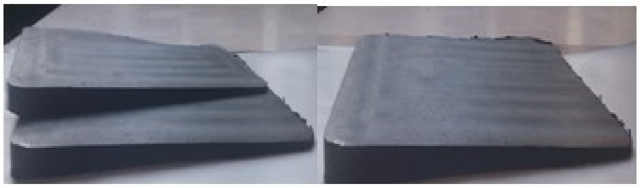

Figure 2. Vulcanized rubber plates

The heel was constructed using a number of top lifts so as to obtain the height corresponding to the last heel height. The top lift on which the heel tip is applied is made of two materials with different hardness values and inclination of 2 degrees, so that, when joined, they form a top lift presented in Figure 3.

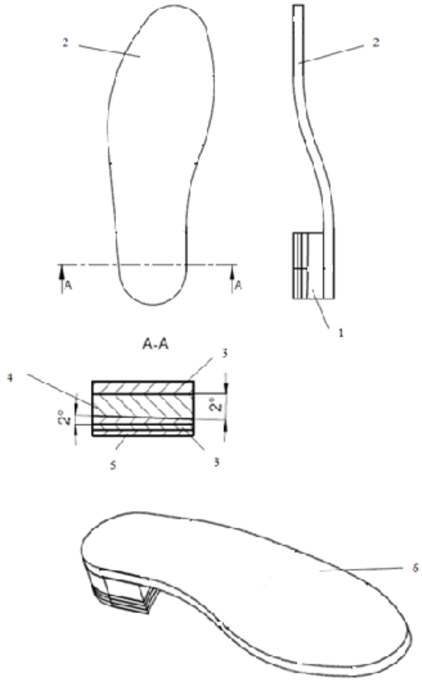

Figure 3. Heel structure: 1 - heel, 2 - sole, 3 - top lift, 4 - layered top lift, 5 - heel tip, 6 - sole-heel ensemble

Shoe models were made on lasts whose sizes correspond to anthropometric foot parameters. The footwear manufacturing system was shoes with glued soles. Following the specific technology for this manufacturing system, shoe models shown in Figure 4 were made.

The heel of each pair of shoes is made of top lifts with different hardness values, ranging between 44 ÷ 93 degrees ShoreA.

Figure 4. Shoe models with customized heel

Experimental Testing of Proposed Solutions

To demonstrate the effectiveness of proposed solutions, the three components of ground reaction force and especially the medio-lateral component Fy were assessed to see their evolution in manufactured shoes. This assessment was performed using AMTI force plate and BioAnalysis software. The subjects involved were those who participated in previous experimental determinations.

The two subjects wore eight models of shoes and walked on four surfaces (parquet, linoleum, carpet, tar board) applied on the force plate. Values were compared to those obtained with the same subjects walking without shoes on the four walking surfaces.

RESULTS AND DISCUSSIONS

Evolution of the medio-lateral component Fy for the eight shoe models on each walking surface separately for the two subjects is depicted in Figure 5.

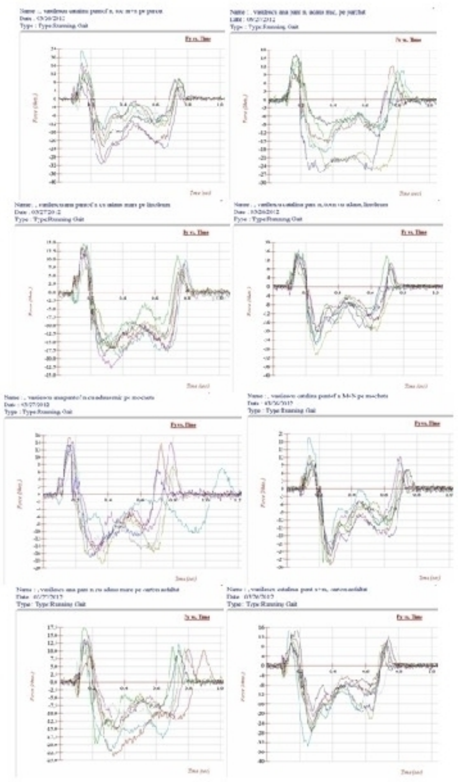

a b

Figure 5. Evolution of the medio-lateral component for the eight shoe models on the four walking surfaces (a - subject 1, b - subject 2)

Figure 6 presents the comparative values of the moment My developed by the medio-lateral component Fy of the eight shoe models at the hip, knee and ankle on the parquet walking surface for both subjects.

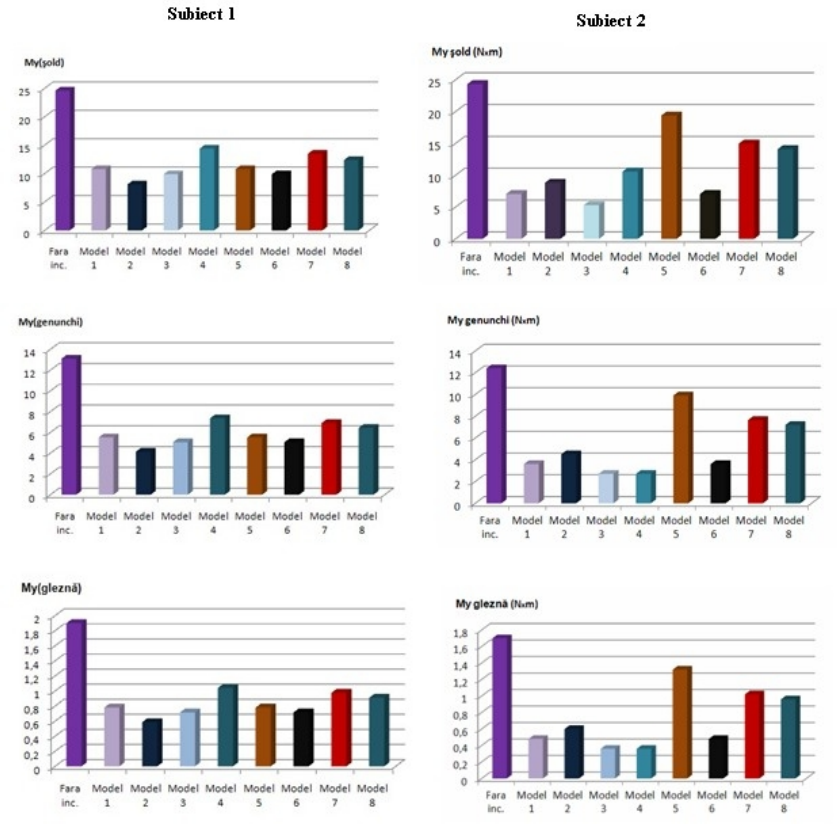

Figure 6. Values of My moment developed by the medio-lateral component Fy

Evolution of the medio-lateral component Fy of the ground reaction force in all eight shoe models in relation to the values obtained depending on the walking surface is as follows:

- on parquet, about 80% lower than walking without shoes,
- on linoleum, about 64% lower than walking without shoes,
- on carpet, about 66% lower than walking without shoes,
- on tar board, about 33% lower than walking without shoes.

Body muscles are responsible for stabilizing the joints, as the body weight acts on the support limb. Alignment of each segment in the limb and their mass influence joint stability. When the mass center of a body segment is not vertically aligned above the joint, its weight generates a rotational force that causes the joint to move. Therefore, the medio-lateral component Fy of the ground reaction force produces moments at the ankle, knee and hip.

The data analysis shows that My moments generated by the medio-lateral force Fy when wearing footwear have reduced considerably compared to the reference, namely walking without shoes.

As a result of conducted tests, it was highlighted that ground reaction force values differ for two subjects with similar weights, wearing the same shoes and walking on the same surface, due to their different walking styles.

CONCLUSIONS

The paper presents the results of a study on manufacturing customized footwear. Thus, customized shoes must meet two basic characteristics:

- they must be made individually for each subject separately,
- they must be a tool for preventing abnormalities.

Recommendation on wearing customized shoes must consider the following aspects: type of footwear, footwear construction method, upper design, sole design, heel height and construction, materials recommended for uppers, linings, soles, etc.

This footwear is designed for wearers who do not have structural or functional abnormalities of the lower limbs, but who value comfort in wear over other issues, such as heel height or shape.

REFERENCES

Aston, J.W. and Carollo, J.J. (1989), “Normal Patterns of Walking and Running”, in Subotnic, S.I. (ed.), *Sport Medicine of the Lower Extremity*, Churchill Livingstone, New York.

Cavanagh, P.R. and Lafortune, M.A. (1979), “Ground Reaction Forces in Distance Running”, *Journal of Biomechanics*, 13, 397-406.

Clarke, T.E., Frederick, E.C. and Cooper, L.B. (1983), “Effects of Shoe Cushioning upon Ground Reaction Forces in Running”, *International Journal of Sports Medicine*, 4(4), 247-251.

Dixon, S.J., Collop, A.C. and Batt, M.E. (2000), “Surface Effects on Ground Reaction Forces and Lower Extremity Kinematics in Running”, *Medicine and Science in Sports and Exercise*, 32(11), 1919-1926.

Hamill, J. (1996), “Evaluating Sport Shoes Using Ground Reaction Force Data”, *ISBS - Conference Proceedings Archive, 14 International Symposium on Biomechanics in Sports*, Biomechanics Laboratory – Department of Exercise Science, University of Massachusetts Amherst, USA, ISSN 1999-4168.

Logan, S. et al. (2010), “Ground Reaction Force Differences between Running Shoes, Racing Flats, and Distance Spikes in Runners”, *Journal of Sports Science and Medicine*, 9, 147-153.

Marasovic, T., Cecic, M. and Zanchi, V. (2010), “Analysis and Interpretation of Ground Reaction Forces in Normal Gait”, Laboratory for Biomechanics and Control System, Faculty of Electrical Engineering, Mechanical Engineering and Naval Architecture, University of Split, Croatia.

Martin, E. and March, A.P. (1992), “Step Length and Effects on Ground Reaction Forces During Walking”, *Journal of Biomechanics*, 25(10), 1237-1239.

Morley, J.B. et al. (2010), “Effects of Varying Amounts of Pronation on the Mediolateral Ground Reaction Forces During Barefoot Versus Shod Running”, *Journal of Applied Biomechanics*, 2, 205-214.

GROUND REACTION FORCE ANALYSIS IN NORMAL GAIT USING FOOTWEAR WITH VARIOUS HEEL HEIGHTS ON DIFFERENT SURFACES

ANA MARIA VASILESCU, MIRELA PANTAZI[1], ANTON CONSTANTIN MICU[2]

[1] *INCDTP – Division: Leather and Footwear Research Institute, 93 Ion Minulescu, Bucharest, Romania, email: icpi@icpi.ro*

[2] *Politehnica University, Faculty of Mechanical Engineering and Mechatronics, Bucharest, Romania, email: micuanton@yahoo.com*

The purpose of this study is to assess ground reaction force in normal gait using shoes with different heel heights and walking without shoes on different surfaces, in order to compare the ground reaction force in terms of characteristics of heel materials on different surfaces. For this purpose, shoes with different heel heights, widths and hardness values were analyzed. In dynamic mode, shoes can cause joint problems, or depending on the type of shoe, the subject makes a greater or lesser effort. By quantifying the ground reaction force using AMTI 's AccuGait System force plate, three components are analyzed: the vertical component Fz, the anterior-posterior component Fx and the medio-lateral component Fy at contact to the ground. The subjects walked on four surfaces: parquet, linoleum, carpet and tar board. This analysis is a case study because a small number of shoe types was examined, to which a single volunteer subject participated.

Keywords: ground reaction, footwear, heel, rolling surface.

INTRODUCTION

Pain experienced in the feet is reported more often in the civilized world. Footwear, created to protect the foot, has turned into an instrument of “torture”. These are the major causes of foot disorders, leading to problems often affecting human health. Women are affected more than men, because they wear shoes with pointed tips (which constricts and deform toes), and high heels which can affect the stability of the pelvis and encourage metatarsalgia (pain in the toes due to compression of metatarsals) etc.

During physical activity, load on the body can be described by measuring ground reaction forces (GRF). Visualizing ground reaction forces helps to understand the effects they have on the body during walking. This force is the resultant of three vector components in the vertical, anteroposterior and medio-transversal directions. Ground reaction force size depends on the body mass size and on the center of gravity acceleration. When body weight shifts to the support foot, vertical, horizontal and rotational forces are generated on the ground. For this reason joint strain and muscle control occur.

The foot and the shoe form an ensemble whose characteristics are specific to each individual, and the recommendation is to make customized shoes in order to meet the role for which footwear was designed, namely: to protect the foot from external agents, to increase the support base for the foot in orthostatic position and during walking, to ensure the biped position of the body, to reduce effort of the muscular and connector system (joints) and to respond to fashion and design factors.

EQUIPMENT AND METHODS

Equipment

In order to conduct the study, the following tools were used: AMTI's AccuGait System force plate; two video cameras with recording speed of 25 frames/second, hard disk data registration and transfer to the computer by USB; video analysis software Kinovea 0.8.7 (Kinovea).

Subjects

One healthy female subject has voluntarily participated in the study, aged 25, weighing 54 kg, having previously agreed to participating in this experiment.

Procedure/Method

The subject walked on the track wearing 13 different types of shoes. Walking took place on four different surfaces applied on the force plate. Only trials in which the right foot landed fully on the plate were considered valid. During quantification of forces, it is important that the analyzed subject spontaneously load the force plate as a natural event during walking on the track where the force plate was placed. It is important that the tested foot fully touch the force plate, while the other foot should remain outside the plate while walking. These tests are repeated several times to have a proper contact of the foot on the force plate.

The shoes had different heel heights, ranging from 0.5 to 7 cm, widths between 2 and 6 cm, made of various materials: polyurethane, rubber, PVC, ABS. Walking surfaces used in the study were: linoleum, parquet, carpet and tar board (Figure 1).

Figure 1. Ground reaction force quantification

EXPERIMENTAL

To analyze the data obtained, experimental conditions were defined, as follows:

- Condition A - walking without shoes;
- Condition B - walking with shoes with heel height ranging from 3÷30 mm, hardness of 35°ShA÷90°ShA and heel width between 40÷70 mm;
- Condition C - walking with shoes with orthopedic soles with heel height between 50÷60 mm, hardness of 50°ShA÷92°ShA and heel width between 23÷30 mm;
- Condition D - walking with shoes with heel height between 45÷80 mm, hardness of 65°ShA÷95°ShA and heel width between 10÷53 mm.

Quantification of values of the three components was done upon the initial heel contact with the ground.

RESULTS AND DISCUSSIONS

Walking without Shoes

Table 1. Values of the three ground reaction force components for the bare foot on various walking surfaces

No.	Walking surface	Fz max (N)	Fx max (N)	Fy max (N)
1	Tar board	520	34	33
2	Carpet	529	21	44
3	Linoleum	549	25	26
4	Parquet	544	27	30

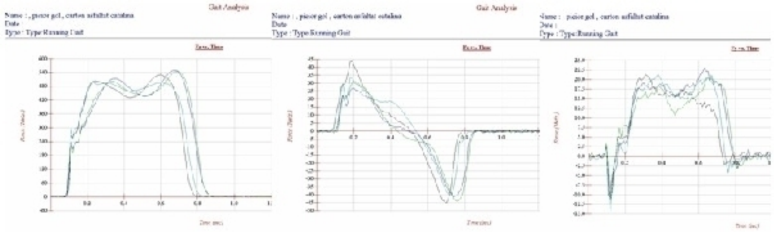

Figure 2. Evolution over time of vertical Fz, antero-posterior Fx and medio-lateral Fy components of ground reaction force in normal gait without footwear

Walking with Shoes with Heel Height Ranging between 3÷30 mm, Hardness of 35°ShA÷90°ShA and Heel Width between 40÷70 mm

Table 2. Values of the three ground reaction force components

No.	Walking surface	Fz max (N)	Fx max (N)	Fy max (N)
1	Tar board	530	31	34
2	Carpet	539	31	49
3	Linoleum	558	25	34
4	Parquet	552	29	27

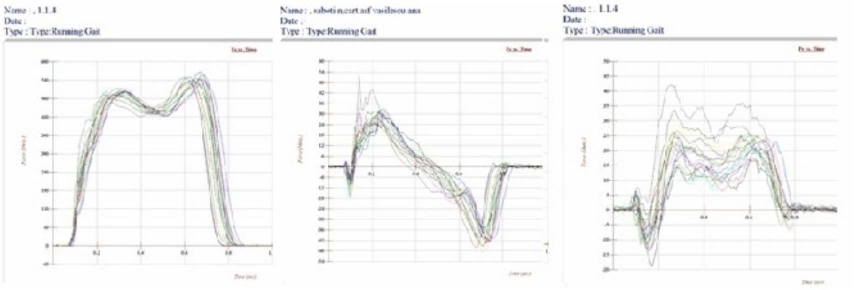

Figure 3. Evolution over time of vertical Fz, antero-posterior Fx and medio-lateral Fy components of ground reaction force in normal gait with low-heeled shoes

Walking with Orthopedic Sole Shoes with Heel Height Ranging between 50÷60mm, Hardness of 50°ShA÷92°ShA and Heel Width between 23÷30 mm

Table 3. Values of the three ground reaction force components

No.	Walking surface	Fz max (N)	Fx max (N)	Fy max (N)
1	Tar board	547	23	32
2	Carpet	563	30	63
3	Linoleum	560	19	35
4	Parquet	550	21	44

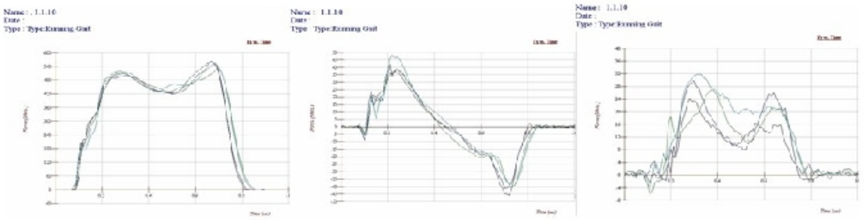

Figure 4. Evolution over time of vertical Fz, antero-posterior Fx and medio-lateral Fy components of ground reaction force in normal gait with orthopedic heel

Walking with Shoes with Heel Height Ranging between 45÷80 mm, Hardness of 65°ShA÷95°ShA and Heel Width between 10÷53 mm

Table 4. Values of the three ground reaction force components

No.	Walking surface	Fz max (N)	Fx max (N)	Fy max (N)
1	Tar board	551	19	45
2	Carpet	559	21	66
3	Linoleum	576	16	38
4	Parquet	545	20	55

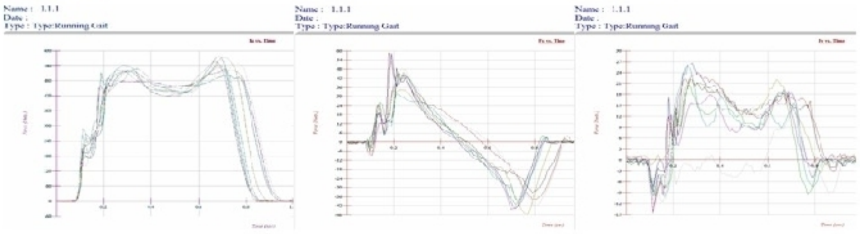

Figure 5. Evolution over time of vertical Fz, antero-posterior Fx and medio-lateral Fy components of ground reaction force in normal gait with high-heeled shoes

Comparative values of the three ground reaction force components are presented in Table 5.

Table 5. Comparative values of the three ground reaction force components

	Walking conditions											
Walking surface	A			B			C			D		
	Fz max (N)	Fx max (N)	Fy max (N)	Fz max (N)	Fx max (N)	Fy max (N)	Fz max (N)	Fx max (N)	Fy max (N)	Fz max (N)	Fx max (N)	Fy max (N)
Tar board	520	34	33	530	31	34	547	23	32	551	19	45
Carpet	529	21	44	539	31	49	563	30	63	559	21	66
Linoleum	549	25	26	558	25	34	560	19	35	576	16	38
Parquet	544	27	30	552	29	27	550	21	44	545	20	55

Results of ground reaction force analysis under the four gait conditions shown in Table 5 allow an objective analysis of the influence of footwear on gait biomechanics compared with the condition in which the subject walked without shoes, on four different surfaces.

Comparative analysis of ground reaction force parameters (Table 5) shows that when the same subject walks under four different conditions on the same walking surface, different values are obtained.

CONCLUSIONS

Tests conducted on the force platform have revealed a variation of the three components of ground reaction (Fy, Fz, Fx) that are dependent on:

- contact pressure between the heel and the ground,
- the nature of the contact surface between the heel and the ground (carpet, tar board, linoleum, parquet),
- duration of contact,
- ground roughness,
- ground wetting degree,
- heel profile,
- the nature of polymers the heel is made of,
- heel material hardness,

- top lift edge processing (rounded, square)
- heel height,
- top lift cover.

The human body has to deal with external forces in one way or another, therefore a higher ground reaction force plays an important role in causing damage, resulting in a potential increase in injury risk. Thus, ground reaction force have an ample effect on body load upon impact and then on the occurrence of the lower extremities injuries.

REFERENCES

Cavanagh, P.R. and Lafortune, M.A. (1979), "Ground Reaction Forces in Distance Running", *Journal of Biomechanics*, 13, 397-406.

Claeys, R. (1983), "The Analysis of Ground Reaction Forces in Pathological Gait Secondary to Disorders of the Foot", *Orthop*, 7(2), 113-9.

Clarke, T.E., Frederick, E.C. and Cooper, L.B. (1983), "Effects of Shoe Cushioning upon Ground Reaction Forces in Running", *International Journal of Sports Medicine*, 4(4), 247-251.

Divert, C. et al. (2005), "Stiffness Adaptations in Shod Running", *J Appl Biomech.*, 21(4), 311-21.

Dixon, S.J., Collop, A.C. and Batt, M.E. (2000), "Surface Effects on Ground Reaction Forces and Lower Extremity Kinematics in Running", *Medicine and Science in Sports and Exercise*, 32(11), 1919-1926.

Kinovea, http://www.kinovea.org/en/

Logan, S. et al. (2010), "Ground Reaction Force Differences between Running Shoes, Racing Flats, and Distance Spikes in Runners", *Journal of Sports Science and Medicine*, 9, 147-153.

Marasovic, T., Cecic, M. and Zanchi, V. (2010), "Analysis and Interpretation of Ground Reaction Forces in Normal Gait", Laboratory for Biomechanics and Control System, Faculty of Electrical Engineering, Mechanical Engineering and Naval Architecture, University of Split, Croatia.

Morley, J.B. et al. (2010), "Effects of Varying Amounts of Pronation on the Mediolateral Ground Reaction Forces During Barefoot Versus Shod Running", *Journal of Applied Biomechanics*, 2, 205-214.

Müler, W. (1977), "Components of Resultant Forces in the Human Sole During Walking", *Das Leder*, 12, W. Diesbschlab.

Nigg, B.M. (1983), "External Force Measurements with Sport and Playing Surfaces", in *Biomechanical Aspects of Sport Shoes and Playing Surfaces*, University Printing, Calgary.

Nigg, B.M. (1986), "Biomechanical Aspects of Running", in: Nigg, B.M. (ed.), *Biomechanics of Running Shoes*, Champaign, Human Kinetics, 1-25.

Snijders, C.J. (1987), "Biomechanics of Footwear", *Clin Podiat Med. Surg.*, 4(3).

White, S.C., Yack, H.J. et al. (1998), "Comparison of Vertical Ground Reaction Forces During Overground and Treadmill Walking", *Med. Sci Sport Exerc*, 30(10), 1537-42.

PREPARATION OF *β*-CYCLODEXTRIN FRAGRANCE FINISHING AGENT REACTED WITH REACTIVE DYE FOR LEATHER FINISHING

XIAOYAN ZHANG[1], WUYONG CHEN[1], XIAOLING LIU[1], YAN XIA[1], CARMEN GAIDAU[2]

[1] *National Engineering Laboratory for Clean Technology of Leather Manufacture, Sichuan University, Chengdu 610065, Sichuan, P.R. China*

[2] *INCDTP - Division: Leather and Footwear Research Institute, 93 Ion Minulescu St, sector 3, 031215, Bucharest, Romania*

In this research, inclusion compounds of Jasmine oil and β-cyclodextrin (β-CD) were prepared by saturated solution stirring method and applied in fragrance finishing of leather. The influencing factors of efficiency and yield in inclusion process were studied by orthogonal experiment. The best conditions to obtain the highest inclusion efficiency and yield are as follows: the mass ratio of jasmine and β-CD is 1:8, the sintering temperature is 50°C,and the inclusion time is 3hs.The formation of inclusion compounds were investigated by Fourier transform-infrared(FT-IR), X-ray diffraction (X-RD), with the mechanical mixture of jasmine and β-CD as a control. The results show that the Jasmine could be successfully wrapped with β-CD. The thermodynamic property of inclusion compounds was tested by Thermal gravimetry (TG). It shows that the inclusion could enhance the thermal stability of Jasmine oil. In addition, the inclusion compounds were used in finishing process for fragrant leather and the flavor concentration volatilized from treated leather were ranked by sensory test. The results indicate the odor retention of leather treated with inclusion compounds is significantly better than that treated by jasmine oil alone.

Keywords: leather, fragrance, β-cyclodextrin.

INTRODUCTION

With the improvement of life quality, consumers are more and more interested in fragrance leather products which have lasting pleasant odor. Recently, as a non-toxic and flavour additive, β-cyclodextrin inclusion complex has been extensively studied. the release rate of perfume covered by β-cyclodextrin can be controlled and turn slow. Therefore, the flavor last time could be longer compared with perfume alone. Perfume β-cyclodextrin inclusion has been widely applied in textile, Chen et al. (2009), food, Zong et al. (2009), tobacco, Li et al. (2009), cosmetics, Valerian et al. (1998) and etc. However, there has not yet found the research about perfume β-cyclodextrin inclusion for leather fragrance finishing.

In this research, the leather fragrance finishing agent will be prepared by inclusion compounds of jasmine oil and β-cyclodextrin. The formation of inclusion compounds were investigated by Fourier transform-infrared (FT-IR), X-ray diffraction (X-RD), with the mixture of Jasmine and β-CD as a control. The thermodynamic property of inclusion compounds was tested by Thermal gravimetry (TG). Then the application effect of jasmine and β-cyclodextrin inclusion in leather finishing was evaluated.

EXPERIMENTAL

Materials

The jasmine perfume was purchased from CARBONNEL S.A Company, Spain; Ethanol (GR) and beta-cyclodextrins (CP) were purchased Kelon Chemical Company, Chengdu, China.

Preparation of Inclusion Complexes

The inclusion was preparation by saturated solution stirring method. In the first series of experiments, β-CD was completely dissolved in water (form saturated solution) in a round flask keep constantly. Jasmine previously diluted using ethanol was then dropped into the β-CD saturated solution and stirred for some hours, and then transferred to refrigerator (below 4°C) to store for above 12 hours. Finally, after filtrating, the sediment was washed with little deionized water and ethanol, and dried at a 40°C oven. Dried sample were sealed in a .plastic bags to protect them against changes in humidity.

In order to optimize the process condition, a series of orthogonal experiments were designed. The efficiency and yield of inclusion were as indexes, and the main factors selected were the stirred time (A), the ratio of jasmine oil and β-CD (B), the dropped rate of the jasmine ethanol solution (C) and the system temperature (D). Details of four factors in the experiments are described in Table 1.

Table 1. Levels and factors of orthogonal experiment $L_{16}(4^4)$

Level Factor	1	2	3	4
A (hr)	1.0	1.5	2.0	3.0
B (Jasmine/β-CD mass ratio)	1：10	1：8	1：6	1：4
C (s/drop)	1	3	5	7
D (°C)	30	40	50	60

Evaluation of Jasmine Inclusion Efficiency and Yield by GC-MS

The efficiency of inclusion (%) is defined as the degree of jasmine wrapped by β-CD in the method, and calculated using the following formula:

$$\mathrm{E}（\% = \frac{m_{\mathrm{total}}}{m_{\mathrm{added}}} \times 100\% \qquad (1)$$

Where m_{total} is the total amount of jasmine on the inclusion, m_{added} is the amount of jasmine added.

The yield of inclusion (%) refers to the mass ratio of the dried inclusion (m_{inclu}) to the β-CD and jasmine before used ($m_{\beta\text{-CD}}+m_{jas}$).

$$\mathrm{Y}（\% = \frac{\mathrm{m}_{inclu}}{\mathrm{m}_{\beta-CD}+\mathrm{m}_{jas}} \times 100\% \qquad (2)$$

Standard Curve of Jasmine Oil by GC-MS

Standard solution containing 0, 10, 20, 40, 80, 120 μg mL-1 jasmine oil were prepared. 1μL of Standard solutions were respectively injected Trace GC/DSQ (Thermo Electron Company, USA). gas chromatograph interfaced to a mass spectrometer (GC-MS). The acetic acid benzyl ester (which is the main component of jasmine oil) was isolated and then identified with XcaliburTM software, combining NIST2005 spectrum database. The integrated peak area of acetic acid benzyl ester in gas chromatogram was in linear relationship with the concentration of jasmine oil solution.

Determination of the Total Amount of Jasmine Oil in Inclusion

Jasmine inclusion (1.0 g) was extracted in 50 mL ethanol for 2 hours and then filtered. The filtrate was collected in 100 ml graduated flask and ethanol was added to make the volume up to exactly 100 ml. the jasmine oil content could then be determined according to the acetic acid benzyl ester GC-MS standard curve.

Identification of Jasmine Inclusion

The formation of inclusion compounds were investigated by Fourier transform-infrared (FT-IR), X-ray diffraction (X-RD), with the mixture of Jasmine and β-CD as a control. The thermodynamic property of inclusion compounds was tested by Thermal gravimetry (TG).

A mechanical mixture was prepared by addition of jasmine oil to β-CD. The jasmine/β-CD mass ratio was maintained as described for inclusion complex preparation.

Application of Jasmine Inclusion on Leather Finishing

Jasmine inclusion was applied ground, middle and top coating of automotive leather. And then the leather treated with jasmine inclusion and jasmine oil were roasted in oven at 50°C for 4 hr. The leather samples were smelled directly, and the leather odor was evaluated by using sensory test.

RESULTS AND DISCUSSION

Optimization of the Condition for Inclusion

The orthogonal experiment results and their range analysis are shown in Table 2, respectively using efficiency and yield of inclusion as index.

Table 2. Design of experiments and interpretation of results

Number	A	B	C	D	Yield (%)	Efficiency (%)
1	1	1	1	1	45.21	13.83
2	1	2	2	2	48.93	27.99
3	1	3	3	3	56.20	35.32
4	1	4	4	4	47.54	25.22
5	2	1	2	3	68.24	44.11
6	2	2	1	4	54.93	46.14
7	2	3	4	1	46.87	29.34
8	2	4	3	2	49.64	29.80
9	3	1	3	4	50.57	32.22
10	3	2	4	3	71.71	62.64
11	3	3	1	2	51.40	33.82
12	3	4	2	1	55.92	25.23
13	4	1	4	2	63.73	47.47
14	4	2	3	1	80.83	38.12
15	4	3	2	4	56.45	57.63

16	4	4	1	3	70.15	65.91
	K1	49.47	56.93	55.42	57.20	
	K2	54.92	64.09	57.38	53.42	
	K3	57.39	52.72	59.31	66.57	
	K4	67.79	55.81	57.46	52.37	
	Range	18.32	11.37	3.89	14.21	
	k1	25.59	34.41	39.92	26.63	
	k2	37.35	43.73	38.74	34.77	
	k3	38.48	39.03	33.86	51.99	
	k4	52.29	36.54	41.17	40.30	
	Range	26.70	9.32	7.31	25.36	

From the range analysis we can see that the sequence of the four main influencing factors (according to the contribution to the efficiency and yield of inclusion) was A> D> B> C, and the optimal conditions to obtain the highest efficiency and yield of inclusion are as follows: the mass ratio of Jasmine and β-CD is 1:8, the sintering temperature is 50°C,and the inclusion time is 3 hrs.

Identification of Jasmine Inclusion

Fourier Transform-Infrared

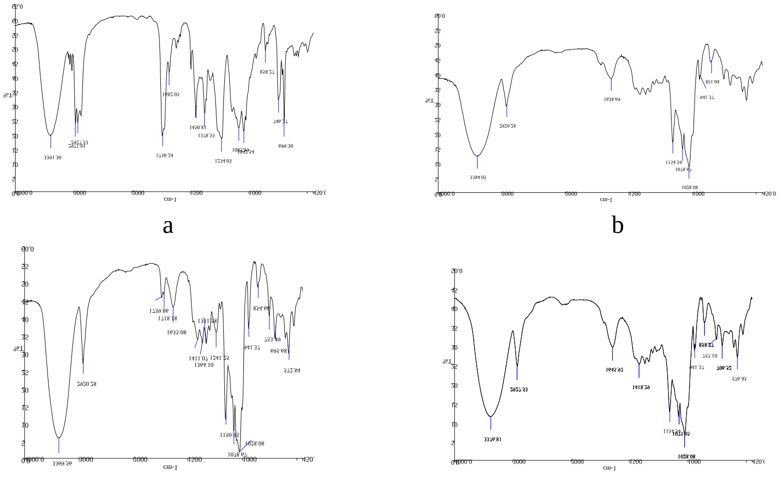

a b

c d

Figure 1. FT-IR spectra of system of β-CD and jasmine oil: a. jasmine oil, b. β-CD, c. jasmine / β-CD inclusion, d. mechanical mixture

The FT-IR spectra of jasmine, β-CD, jasmine inclusion and mixture are shown in Figure 1. There are three characteristics peaks in FT-IR spectra of jasmine oil. One located on 3400cm^{-1}, which occurs because of O-H stretching vibration, and the second one centered on 1736 cm^{-1}, attributing to C=O stretching vibration, the third one existed on 1234cm^{-1}, depending on C-O stretching vibration (Figure 1, a). β-CD present two characteristics peaks depending on O-H stretching vibration at 3384cm^{-1} and cyclodextrin ring vibration at 1638cm^{-1} (Figure 1, b). However, FT-IR spectra of mixture is a superposition of β-CD and jasmine oil, just the peak intensity at 1736 cm^{-1} which is the characteristics peaks of jasmine oil weakened (Figure 1, d). But FT-IR spectra of inclusion is different from the mixture. Particularly，the stretching vibration of C = O at 1736 cm^{-1}, and C-O at 1234cm^{-1} as the characteristics peaks on jasmine oil FT-IR spectra are disappeared. Moreover, the 1638cm^{-1} which is β-CD ring skeleton vibration wavelength shifted toward 1645cm^{-1} (Figure 1, c). These indicate that the molecule of jasmine main compound embedded in the hydrophobic cavity of β-CD, so that the characteristic peaks of jasmine were buried. Also, the above results preliminarily suggested the inclusion action indeed occurred.

X-Ray Diffraction

The X-RD pattern of jasmine inclusion, β-CD and mechanical mixture are shown in Figure 2. It can be seen that no matter from the diffraction peak position, intensity or number, the X-RD pattern of mechanical mixture is almost similar to that of β-CD, but significantly different with that of jasmine inclusion. Further more, the main diffraction peak of β-CD is not existed in inclusion X-RD pattern, or diffraction angle were altered, The results show that the crystal configuration of β-CD changed greatly before and after inclusion. It also indicates that the jasmine inclusion is not a simple mechanical mixture but a new phase which is different from β-CD.

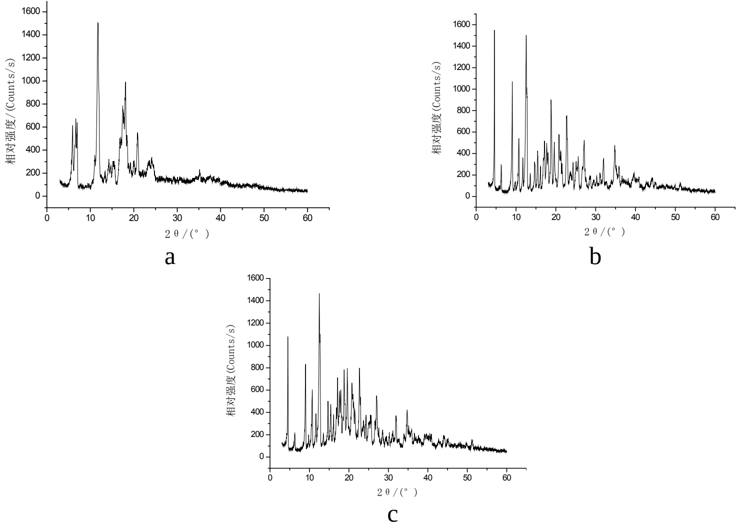

a

b

c

Figure 2. XRD curve of system of β-CD and jasmine oil: a. jasmine inclusion, b. β-CD, c. mechanical mixture of β-CD and jasmine oil

Thermal Analysis

β-CD, jasmine inclusion, mechanical mixture and jasmine oil were subjected to TG. Figure 3 shows the TG curves of the materials. It can be seen that the jasmine oil evaporated slowly from 30°C and exhausted up to 140°C (Figure 3, 4). As to the TG curve of the jasmine β-CD inclusion, a mass loss (18.18%) was recorded before 140°C, there was also no mass change observed in interval from 120 to 240°C, while in interval from 269.6 to 286.6°C, a small mass loss (2.87%) was detected and can be attributed to the release of oil from its inclusion (Figure 3, 2). The curve of mechanical mixture is between guest and host curves, from room temperature to 140°C, 30.12% mass loss was recorded and more than that of inclusion in this interval, which indicates the thermal stability of mechanical mixture is worse than that of inclusion (Figure 3, 3). In a word, the inclusion could enhance the thermal stability of jasmine oil.

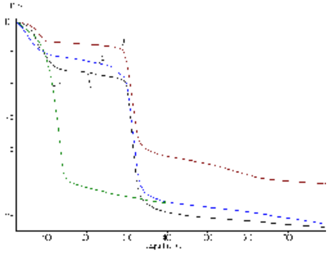

Figure 3. TG curves of the system of β-CD and jasmine oil: 1. β-CD, 2. jasmine inclusion, 3. Mechanical mixture, 4. jasmine oil

Application of Jasmine Inclusion on Leather Finishing

It can be found that whatever jasmine inclusion applied in the group, middle or top coating materials, with the dosage increase, the rank of flavor concentration volatilized from treated leather is raised. Besides, it can be found that the odor retention of leather treated with inclusion compounds is significantly better than that treated by Jasmine oil alone, particularly, this rule of leather samples applied in top coating is more obvious, which indicate the jasmine inclusion is a material that can control flavor release and make the odor reservation time longer.

CONCLUSION

This study presents the preparation of jasmine β-CD inclusion and application in finishing for durable fragrant leather. The optimal condition for the highest inclusion efficiency and yield are obtained. The inclusion was indeed formed and could enhance the thermal stability of jasmine oil. The results indicate the inclusion is an new alternative for manufacture of durable fragrant leather.

Acknowledgements

The authors wish to thank the Ministry of Science and Technology of China for the financial support (Item No. 2009DFA42850).

REFERENCES

Chen, L. and Wang, C. (2009), "Application of Cyclodextrins in textile processing", *Textile Auxiliaries*, 26(3), 6-9.

Li, F. and Liu, Z. (2009), "Michihiko Hygiene. Several Essence and Flavor of Microencapsulation and its Application in Tobacco", *Kunming Institute of Technology*, 31(3), 34-36.

Valerian, T.D. et al. (1998), "Introduction and general overview of cyclodextrin chemistry", *J. Chem. Rev.*, 98(5), 1731.

Zong, W., Miao, R. and Yuan, W. (2009), "Application of cyclodextrin in food industry", *Food Engineering*, (9), 13-14.

REINFORCING OF WOOD PLASTIC COMPOSITES BY CONTINUOUS GLASS FIBERS IN EXTRUSION PROCESS

ABBAS ZOLFAGHARI, AMIR H. BEHRAVESH, ALIREZA ADLI, MAJID TABKHPAZ SARABI

Department of Mechanical Engineering, Tarbiat Modares University, Tehran, Iran, P.O.Box 14115-143, zolfaghari217@gmail.com

The incorporation of wood wastes into the thermoplastics resulted in new class of materials called wood plastic composites (WPCs). These new materials are being mostly used for building applications e.g. decking, roofing and railing. Towards strengthening of WPCs and structural applications of them, this research focused on the continuous reinforcing WPCs by glass roving in extrusion process. For a better compatibility, E-glass roving 2400 tex was impregnated with thermoplastic melt in a melt impregnating die. To introduce the reinforcements into the extruded profiles, a die similar to wire coating concept was designed and manufactured. As a case study a round shape profile with diameter of 14 mm was considered in this research. The implemented tools in the die, balanced the melt flow and hence the improved uniformity of reinforcements. Six melt impregnated glass rovings were embedded into WPCs of 70wt% wood content. The tensile tests were conducted on the un-reinforced and reinforced specimens according to ASTM D3916. Results showed that 510% improvement on the tensile strength was obtained by reinforcing the WPCs. The area under tensile stress-strain curve was measured and indicated that an astonishing increase of toughness was obtained. The locations of glass reinforcements were investigated along the profile. The distance of reinforcements to profile center was generally acceptable.

Keywords: Wood plastic composite (WPC)-Continuous reinforcements-Extrusion

INTRODUCTION

Wood plastic composites (WPCs) are a group of materials where wood components (in the form of particles or flours) are distributed in a polymeric matrix. Recently WPCs have shown an outstanding growth due to their advantages such as light weight, reasonable strength and stiffness. The most usage of WPCs is on the secondary building applications such as decking, roofing, door and window frames where low structural requirement is needed (Smith and Wolcott 2006). Recently, an interest was observed towards structural application of WPCs.

Literature surveys show that research works on the mechanical properties of WPCs are classified to several categories. The compatibilizing of wood flour and polymer surfaces, type and geometry of wood flour, the effect of processing parameters, the type of polymer matrix and using of impact modifier e.g. rubbe (Yang et al. 2007), (Stark and Rowlands 2003), (Yeh and Gupta 2008), (Yuan et al. 2008), (Ruksakulpiwat et al. 2009) and (Kalaprasad et al. 2004). Recently, short reinforcement fibers such as glass fibers were introduced into WPCs (Rizvi and Semeralul 2008) and (Tungjitpornkull and Sombatsompop 2009). The results of these research shows that a little improvement on the mechanical properties were achieved. For introducing WPCs in structural applications it is necessary to further increase the mechanical strength.

It is obvious that long fiber reinforcements increase the mechanical properties better than short fiber ones. This is related to improved stress transfer between fibers and matrix. But in extrusion of hybrid glass fiber/wood flour plastic composites there are limitations for the higher length of fibers. The agglomeration of glass fibers in extrudate due to poor mixing of long fibers may interfere the strengthening mechanism of reinforcement fibers. External reinforcing of WPCs was investigated by some researchers (Jiang et al. 2007), (Naghipour et al. 2011) and (Pulngern et al. 2011). In these methods the process are semi continuous and they can't be applied for various complex profiles.

Embedding of continuous reinforcing fibers into WPCs by extrusion process could be a better and economic way for improving the mechanical properties. In this method the composites will be reinforced on desired direction and locations where major loads are applying on the part. In this research the feasibility and efficiency of this method were investigated experimentally in extrusion process.

MATERIALS AND EQUIPMENTS

E-glass direct roving 2400 tex as reinforcement fibers and HDPE 5620 by Arak Petrochemical Co. as thermoplastic matrix were used. Wood flour of oak species, sieved with a mesh size of 40, was used as filler. For better transferring of stress between the glass roving and WPC matrix, good adhesion between the constituents is necessary. For this purpose, first the rovings were impregnated with HDPE by melt impregnating set up. The nominal diameter of prepreg rod is 2mm.

A laboratory, counter-rotating twin-screw extruder with a screw diameter of 62.5 mm and L-to-D ratio of 22 was utilized in this work. The layout of experiment is shown in Figure 1. The desired profile has a circular cross section with diameter of 14mm which reinforced with six glass rovings as illustrated in Figure 2. Preliminary tests were conducted to find the best configuration of the die. Finally the process similar to wire coating concept was applied for this research. A special die based on the research works (Zolfaghari et al. 2010) and (Soury et al. 2009) for this process is designed and manufactured (Figure 3).

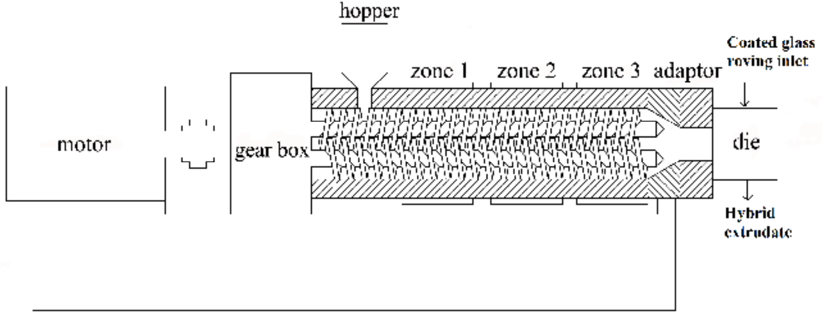

Figure 1. Layout of the experimentations

EXPERIMENTS

HDPE and wood flour of 70% by weight were feed in the hopper of extruder. The temperature zones of 1, 2, 3, 4 and die were set on 170, 170, 170, 168 and 138 degree of Centigrade, respectively. Six impregnated glass rovings were entered into the die from the hole (2) in mandrel (3). The balancing of WPC melt was performed by two deflectors (4). The glass rovings passes through the guide (5) and enters the conical shape created by mandrel and die (7). Regarding that the temperature of guide is same as die, therefore the plastic contained in the roving will be at melt temperature. For finer arranging of rovings over the cross section, fine adjusting ring (6) was located in the die channel. During extrusion via three bolts the melt and hence rovings could be balanced to adjust the positional tolerancses (Figure 2). Also, unreinforced WPC70 was extruded and compared to hybrid WPC706R. Tensile tests with an Instron universal testing machine 5500R were conducted on the specimens. The cross head speed was set on 2mm/min. To prevent the premature failure of reinforced WPC into the jaws of test machine, four aluminum tab grip adaptors were utilized according to ASTM D3916. The length of test specimens was 500mm.

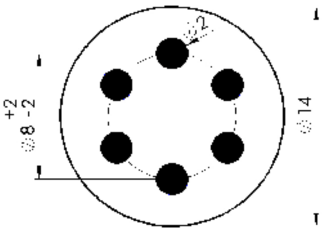

Figure 2. Dimension in mm for continuous reinforced WPC profile (black circles are reinforcing roving)

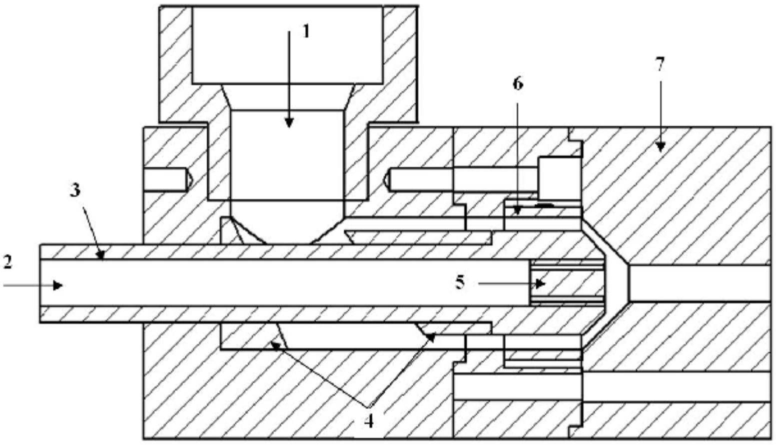

Figure 3. Schematic of the manufactured die; 1) melt inlet from extruder, 2) impregnated glass roving inlet, 3) mandrel, 4) melt balancers, 5) guide of rovings, 6) fine adjusting ring, 7) shaping die.

RESULTS AND DISCUSSIONS

Table 1 shows the tensile properties obtained from the tests. An outstanding increase (about 510%) on the ultimate tensile strength was achieved by embedding six glass rovings. It must be noticed that the tensile strain at break was improved 660%. This indicates the higher toughness of reinforced WPCs. To distinguish the tensile toughness properties of the specimens, the graph of tensile stress versus strain is shown in Figure 4. The area between stress and strain curve is represented as energy absorption or impact resistance. This area was measured and showed an astonishing improvement of 42 times on the impact energy absorption for WPC706R.

Table 1. Mechanical properties of reinforced and un-reinforced samples

WPC code	Tensile strength (MPa)	Tensile strength at break (%)	Tensile modulus(GPa)
WPC70	10.96	0.48%	5.29
WPC706R	66.70	3.65%	5.97

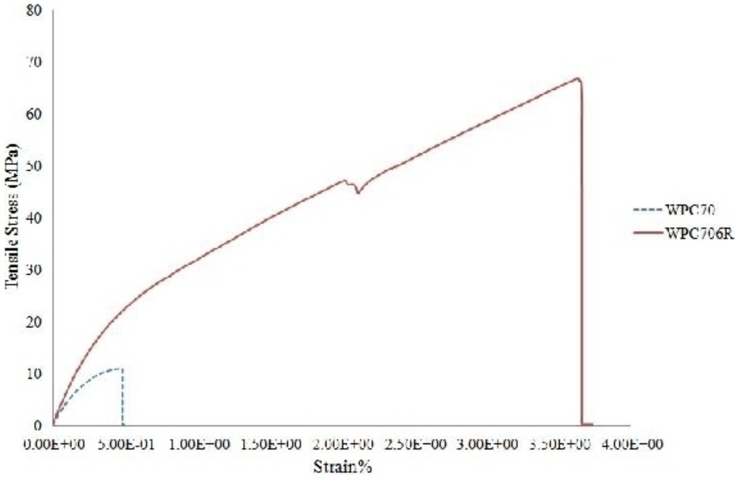

Figure 4. Tensile tests of the specimens

The position of reinforcements into the profile affects the mechanical properties. Figure 5 shows the locations of reinforcing glass fibers (black circles) into the extrudate. The distances of reinforcements to rod center were measured: 3.62, 3.14, 3.27, 2.44, 2.51, and 3.13mm by CAD software. By rewriting in the form of R_{-r}^{+r} where R and r respectively means the nominal distance from center and radial tolerance of all reinforcements, the expression $3.02_{-0.46}^{+0.46}\, mm$ could be used as a parameter in design for structural applications. Comparing to Figure 2, it is obvious a little difference on the positional tolerances was found. More research works are needed to investigate the effect of process parameters on the locations and uniformity of glass roving.

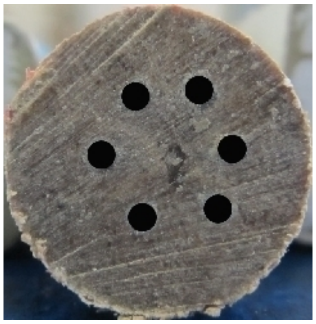

Figure 5. The position of reinforcements (black circles) into the profile

CONCLUSIONS

Continuous glass fiber/wood plastic composites were produced in extrusion process in this study. For this purpose, a special die with similar concept to wire coating process was designed and manufactured. WPC 70wt% reinforced with six glass rovings and un-reinforced were extruded. Tensile strength of WPC70 and WPC706R were measured according to ASTM D3916. The results showed that by addition of six glass rovings into the WPC profile an outstanding increase about 510% on the tensile strength was achieved. The calculated area between stress and strain shows the higher energy absorption of about 42 times was obtained for continuous reinforced WPC. The locations of reinforcing fibers into the profile were measured. The results show that a good positional tolerance was achieved. Also, a design parameter based on the manufacturing process was obtained for the continuous reinforced WPC.

REFERENCES

Jiang, L., Wolcott, M. P., Zhang, J. and Englund, K. (2007) "Flexural properties of surface reinforced wood/plastic deck board", *Polymer Engineering & Science*, 47, 281-288.

Kalaprasad, G. Francis, B. Thomas, S., et al. (2004), "Effect of fibre length and chemical modifications on the tensile properties of intimately mixed short sisal/glass hybrid fibre reinforced low density polyethylene composites", *Polymer International*, 53, 1624-1638.

Naghipour, M., Nematzadeh, M. and Yahyazadeh, Q. (2011), "Analytical and experimental study on flexural performance of WPC–FRP beams", *Construction and Building Materials*, 2011, 25, 829-837.

Pulngern, T., Padyenchean, C., Rosarpitak, V., Prapruit, W. and Sombatsompop, N. (2011), "Flexural and creep strengthening for wood/PVC composite members using flat bar strips", *Materials & Design*, 32, 3431-3439.

Rizvi, G. M. and Semeralul, H. (2008) "Glass-Fiber-Reinforced Wood/Plastic Composites", *Journal of Vinyl & Additive Technology*, 14, 39-42.

Ruksakulpiwat Y, Sridee J, Suppakarn N and Sutapun W. (2009), "Improvement of impact property of natural fiber–polypropylene composite by using natural rubber and EPDM rubber", *Composites Part B: Engineering*, 40, 619-622.

Smith, P.M. and Wolcott, M.P. (2006), "Opportunities for wood/natural fiber-plastic composites in residential and industrial applications", *Forest Products Journal*, 56 (3), 4-11.

Soury, E., Behravesh, A. H., Nasrabadi, H. G. and Zolfaghari, A. (2009), "Design and Manufacture of an Extrusion Die for Wood—Plastic Composite", *Journal of Reinforced Plastics and Composites*, 28, 1433-1439.

Stark, N. M. and Rowlands, R. E. (2003), "Effects of wood fiber characteristics on mechanical properties of wood/polypropylene composites", *Wood and fiber science,* 2003, 35, 167-174.

Tungjitpornkull, S. and Sombatsompop, N. (2009) "Processing technique and fiber orientation angle affecting the mechanical properties of E-glass fiber reinforced wood/PVC composites", *journal of materials processing technology*, 209, 3079-3088.

Yang, H. S., Wolcott, M.P., Kim, H. S., Kim, S. and Kim, H. J. (2007), "Effect of different compatibilizing agents on the mechanical properties of lignocellulosic material filled polyethylene bio-composites", *Composite Structures,* 79, 369–375.

Yeh, S. K. and Gupta, R. K. (2008), "Improved wood–plastic composites through better processing", *Composites Part A: Applied Science and Manufacturing*,39, 1694-16999.

Yuan, Q., Wu, D., Gotama J and Bateman S. (2008), "Wood Fiber Reinforced Polyethylene and Polypropylene Composites with High Modulus and Impact Strength", *Journal of Thermoplastic Composite Materials*, 21, 195-208.

Zolfaghari, A., Behravesh, A. H., Shakouri, E. and Soury, E. (2010), "Flow balancing in die design of wood flour/HDPE composite extrusion profiles with consideration of rheological effect", *Polymer Engineering & Science*, 2010, 50, 543-549.

II.
BIOMATERIALS

FABRICATION OF IRON OXIDE NANOSPHERES USING PYROSOL TECHNIQUE

ECATERINA ANDRONESCU[1], ALEXANDRU GRUMEZESCU[1], ANTON FICAI[1], BOGDAN STEFAN VASILE[1], VALENTINA GRUMEZESCU[2], EUGENIU VASILE[3], DENISA FICAI[1]

[1] *POLITEHNICA University of Bucharest, Faculty of Applied Chemistry and Material Science, Gh Polizu Street 1-7, 011061 Bucharest, Romania, email: manzu_denisa76@yahoo.com*

[2] *National Institute for Lasers, Plasma & Radiation Physics, Lasers Department, P.O. Box MG-36, Bucharest-Magurele, Romania*

[3] *S.C. Metav-CD S.A., 31Rosetti Str., 020015 Bucharest, Romania*

Fabrication of hematite nanoparticles starting from ferric and ferrous salts as precursors via pyrosol process is described. The effect of temperature on the transformation from Fe^{2+} and Fe^{3+} to hematite nanoparticles is investigated. The final product is characterized by XRD and HR-TEM techniques.

Keywords: iron oxide, pyrosol, hematite.

INTRODUCTION

Metal nanoparticles has become an important target for materials science, in biomedical field due to completely new properties as compared to the bulk material (Andronescu et al., 2012; Grumezescu et al., 2012; Kima, Choi, & Park, 2012). Nanomaterials metal-based, such as silver, iron, or zinc, have attracted much attention due to their interesting in biomedical applications (Manzu et al., 2010; Pilloni et al., 2010), especially in biological applications such as cell separation and sorting (Kundu, Chung, Kim, Tae, & Kundu, 2010), drug delivery (Grumezescu, Andronescu et al., 2011; Mihaiescu et al., 2012), antimicrobial properties (Grumezescu, Saviuc et al., 2011; Selvam et al., 2012; Subhasree, Selvakumar, & Kumar, 2012), magnetic resonance imaging (Mantle, 2011), stabilization of essential oils (Saviuc et al., 2011), and inhibition of microbial biofilm development (Mihaiescu, Grumezescu, Balaure, Mogosanu, & Traistaru, 2011). Especially, iron oxide nanopaticles has attracted great interest due to its biomedical applications (Liu et al., 2012).

The iron oxide nanoparticles are important materials in industrial and medical fields (Lind, Berry, Chern, Mathias, & Testardi, 1992). Iron oxide nanoparticles, due to their magnetic properties, can be used as magnetic resonance imaging agents in diagnostic (Cunningham et al., 2005), as heat mediators in hyperthermia treatments (Andronescu, Ficai, Voicu, Manzu, & Ficai, 2010), and additionally as magnetic guidance in drug delivery applications (Mihaiescu et al., 2011).

Pyrosol method is unique because it is applied at atmospheric pressure. The method is based on the pyrolysis of an aerosol. The pyrosol process requires less initial investment and operational expense, because of its atmospheric pressure operation, in comparison with other methods conducted at a high vacuum (Nakasa, Adachi, Usami, Suzuki, & Taniguchi, 2005; Thongsuwan, S., & Singjai, 2007).

The goal of this paper is to investigate the fabrication of iron oxide nanospheres via pyrosol process starting from ferric and ferrous salts solutions. Several structural characteristics using HR-TEM, SAED and XRD are studied and discussed in details.

MATERIALS AND METHODS

Materials

$FeCl_2x4H_2O$ (Merck, ACS reagent~99%), $FeCl_3$ (Sigma, anhydrous powder, ~99,99%) were used as received. The precursor solution (same solution for all three temperatures) was prepared by using distilled water

Fabrication

The nanoparticles were obtained from diluted solution of $FeCl_2$ and $FeCl_3$ (Table 1) via pyrosol process. The pyrosol process consists in the formation of an aerosol from a diluted solution of precursors, using a high-frequency ultrasound generator. The formed aerosol is carried through a furnace, in a quartz tube, by a carrier gas. During the passage of the aerosol through the furnace, some reactions occur such as evaporation, calcination, and densification of powder. At the end of the tube, a high-voltage Mo wire collects the powder (Vasile et al., 2010).

Table 1. Experimental conditions to fabricate iron oxide nanoparticles using pyrosol process

No.	Expected compound	Precursors	Concentration (M)	Temperature (°C)
1	Fe_3O_4	$FeCl_2$+$FeCl_3$	0.005+0.01M	400
2	Fe_3O_4/Fe_2O_3			600
3	Fe_3O_4/Fe_2O_3			800

Characterization

XRD

X-ray diffraction analysis was performed on a Panalytical X'Pert Pro diffractometer at room temperature. In all the cases, Cu Kα radiation from a Cu X-ray tube (run at 15 mA and 30 kV) was used. The samples were scanned in the Bragg angle 2θ range of 10-80.

HR-TEM

The transmission electron microscopy images were obtained on finely powdered samples using a Tecnai^{TM} G2 F30 S-TWIN high resolution transmission electron microscope (HRTEM) from FEI equipped with SAED. The microscope was operated in transmission mode at 300kV with TEM point resolution of 2Å and line resolution of 1Å. The finely MNPs powder was dispersed into pure ethanol and ultrasonicated for 15 minutes. After that diluted sample was put onto a holey carbon coated copper grid and left to dry before it was analyzed through TEM.

RESULTS AND DISCUSSIONS

Hematite, α-Fe_2O_3, is an interesting iron oxide, which has been subject of intensive research for a long time (Sanchez, Arboleda, Saragovi, Zysler, & Barrero, 2007), it is the most stable iron oxide under ambient conditions and has attracted an increasing interest in the fields of nanoscience and nanotechnology because of its industrial and biomedical potential applications (Gupta & Gupta, 2005; Pailhe, Wattiaux, Gaudon, & A., 2008; Wagloehner et al., 2008; Watanabe & Kozuka, 2003). In this paper is reported a simple route to fabricate hematite nanospheres via pyrosol process.

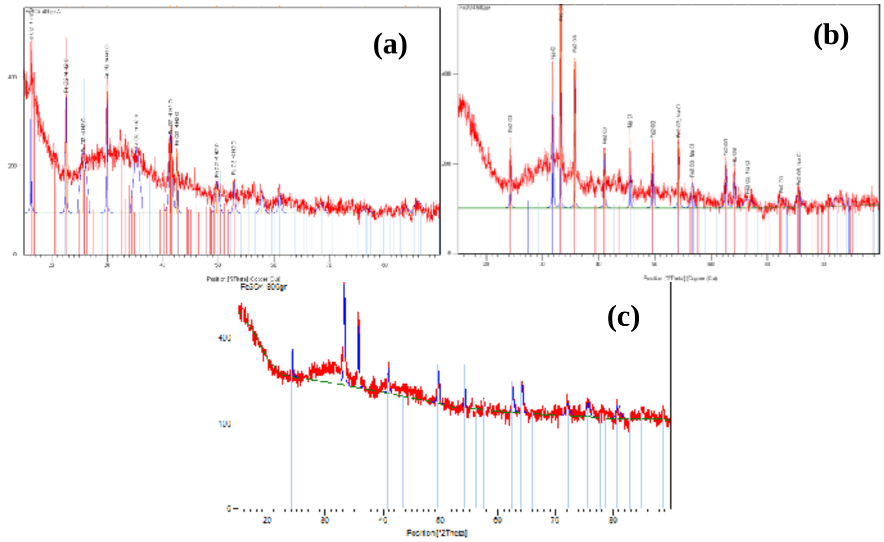

Figure 1. XRD patterns of iron oxide nanoparticles fabricate at different temperature process: (a) 400°C; (b) 600°C; (c) 800°C

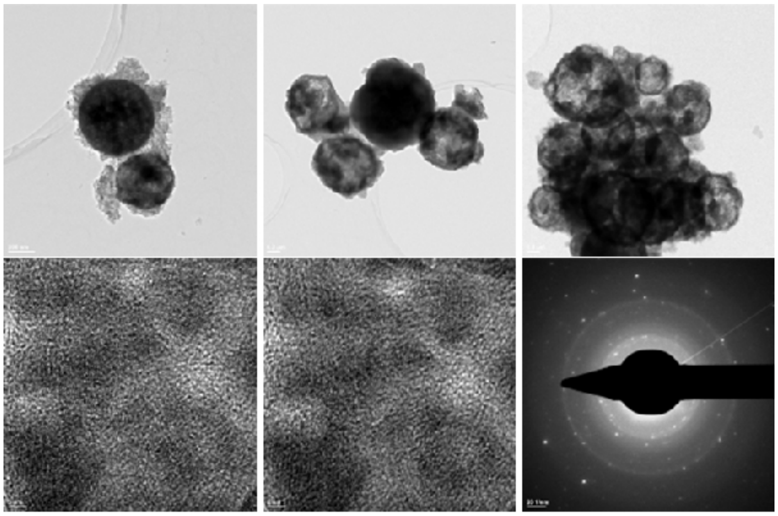

Figure 2. TEM images and SAED pattern of fabricated iron oxide nanoparticles at 600°C

According to XRD patterns it was concluded that the temperature of 400°C is not enough for the transformation of precursors in iron oxide (Figure 1a). In this context the temperature was increased to 600°C and 800°C. At high temperature, over 600°C, the oxidation process leads to obtain exclusively hematite without being able to highlight the formation of magnetite (Figure 1b). Fabrication of pure hematite occurs at 800°C. Arround 600°C the trace of precursors were identified in fabricated nanopowder according to XRD pattern (Figure 1b). In these conditions, fabrication of Fe_3O_4 nanoparticles is not possible from selected precursors. Fig. 1(b) shows the XRD pattern of fabricated nanopowder at 600°C, which reveal α-Fe_2O_3 phase and some traces from precursors as well as NaCl. Fig. 1(c) shows the XRD pattern of fabricated nanopowder at 800°C, which reveal α-Fe_2O_3 phase as single crystalline phase. In Figure 1(a, c) no characteristic peaks for other impurities such as γ-Fe_2O_3, Fe_3O_4 were observed.

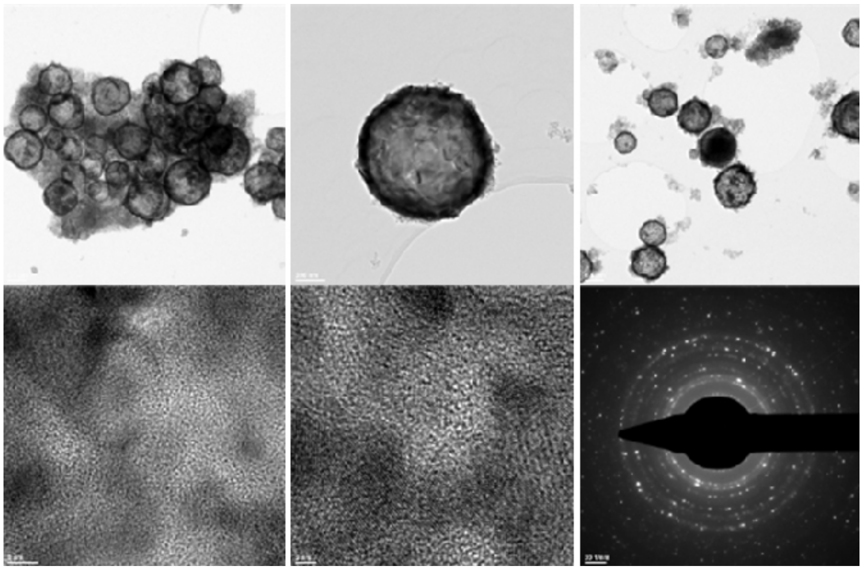

Figure 3. TEM images and SAED pattern of fabricated iron oxide nanoparticles at 800°C

Figure 2 and figure 3 shows the TEM, HR-TEM images and SAED patterns of iron oxides powder obtained via pyrosol process to 600°C and 800°C. At both temperatures it can be identified spherical particles with a rough surface up to 200 nm and particles with few nanometers size, most likely due to the temperature and magnetic attraction forces witch allowed to design these agglomerates. The selected area electron diffraction (SAED) pattern (Figure 3) prove the presence of hematite as the single crystalline phase. SAED pattern (Figure 2) prove the presence of hematite and NaCl as crystalline phases.

CONCLUSIONS

In this paper is reported the synthesis of hematite, a material with broad biomedical and industrial applications, via pyrosol process starting from bulk materials like $FeCl_2$

and $FeCl_3$. The XRD patterns proved that the synthesis of pure hematite is dependent by temperature. At 600°C it was obtained hematite contaminated with NaCl as proved by XRD and SAED patterns. At 800°C it was obtained hematite without any impurities. TEM and HR-TEM images reveals the spherical morfology and nanometric size of hematite agglomerates. As perspective, we intend to produce magnetite via pyrosol method by choosing adequate precursors, with lower temperature of transformation which do not favor magnetite oxidation to hematite.

Acknowledgement

Authors recognize financial support from the European Social Fund through POSDRU/89/1.5/S/ 54785 project: "Postdoctoral Program for Advanced Research in the field of Nanomaterials".

REFERENCES

Andronescu, E., Ficai, M., Voicu, G., Manzu, D., & Ficai, A. (2010), "Synthesis and characterization of collagen/ hydroxyapatite - magnetite composite material for bone cancer treatment", *Journal of Materials Science - Materials in Medicine,* 21(7), 2237-2242.

Andronescu, E., Grumezescu, A.M., Ficai, A., Gheorghe, I., Chifiriuc, C., Mihaiescu, D.E., et al. (2012), "In vitro efficacy of antibiotic magnetic dextran microspheres complexes against Staphylococcus aureus and Pseudomonas aeruginosa strains", *Biointerface Res. Appl. Chem,* 2(3), 332-338.

Cunningham, C.H., Arai, T., Yang, P.C., McConnell, M.V., Pauly, J.M., & Conolly, S.M. (2005), "Positive contrast magnetic resonance imaging of cells labeled with magnetic nanoparticles", *Magnet. Res. Med.*, 53(5), 999-1005.

Grumezescu, A.M., Andronescu, E., Ficai, A., Mihaiescu, D.E., Vasile, B.S., & Bleotu, C. (2012), "Synthesis, characterization and biological evaluation of a Fe3O4/C12 core/shell nanosystem", *Lett.Appl. NanoBioSci*, 1(2), 031-035.

Grumezescu, A. M., Andronescu, E., Ficai, A., Saviuc, C., Mihaiescu, D., & Chifiriuc, C. M. (2011), "Deae-Cellulose/Fe3O4/Cephalosporins Hybrid Materials For Targeted Drug Delivery", *Revista Romana De Materiale-Romanian Journal of Materials,* 41(4), 383-387.

Grumezescu, A. M., Saviuc, S., Holban, A., Hristu, R., Croitoru, C., Stanciu, G., et al. (2011), "Magnetic chitosan for drug targeting and in vitro drug delivery response", *Biointerface Res. Appl. Chem.,* 1(5), 160-165.

Gupta, A. K., & Gupta, M. (2005), "Synthesis and surface engineering of iron oxide nanoparticles for biomedical applications", *Biomaterials,* 26, 3995-4021.

Kima, H. J., Choi, S. H., & Park, H. J. (2012), "Nano-Ag complexes prepared by g-radiolysis and their structures and physical properties", *Rad. Phys. Chem.*, 81, 1612-1620.

Kundu, J., Chung, Y., Kim, Y. H., Tae, G., & Kundu, S. C. (2010), "Silk fibroin nanoparticles for cellular uptake and control release", *Int. J. Pharm.,* 388, 242.

Lind, D. M., Berry, S. M., Chern, G., Mathias, H., & Testardi, L. R. (1992), *Phys. Rev.* B, 45, 1838.

Liu, F., Liu, H., Li, X., Zhao, H., Zhu, D., Zheng, Y., et al. (2012), "Nano-TiO2@Ag/PVC film with enhanced antibacterial activities and photocatalytic properties", *Appl. Surf. Sci.,* 258, 4667-4671.

Mantle, M. D. (2011), "Quantitative magnetic resonance micro-imaging methods for pharmaceutical research", *Int. J. Pharm.*, 417(1-2), 173-195.

Manzu, D., Ficai, A., Voicu, G., Vasile, B. S., Guran, C., & Andronescu, E. (2010), "Polysulfone based membranes with desired pore characteristics", *Mat. Plast.,* 47, 24-37.

Mihaiescu, D. E., Grumezescu, A. M., Balaure, P. C., Mogosanu, D. E., & Traistaru, V. (2011), "Magnetic scaffold for drug targeting: evaluation of cephalosporins controlled release profile", *Biointerface Res. Appl. Chem.*, 1(5), 191-195.

Mihaiescu, D. E., Horja, M., Gheorghe, I., Ficai, A., Grumezescu, A. M., Bleotu, C., et al. (2012), "Water soluble magnetite nanoparticles for antimicrobial drugs delivery", *Lett. Appl. NanoBioSci.,* 1(2), 45-49.

Nakasa, A., Adachi, M., Usami, H., Suzuki, E., & Taniguchi, Y. (2005), "Increase in the conductivity and work function of pyrosol indium tin oxide by infrared irradiation", *Thin Solid Films,* 484, 272 - 277.

Pailhe, N., Wattiaux, A., Gaudon, M., & A., D. (2008), "Impact of structural features on pigment properties of α-Fe2O3 haematite", *J. Solid State Chem.,* 181, 2697-2704.

Pilloni, M., Nicolas, J., Marsaud, V., Bouchemal, K., Frongia, F., Scano, A., et al. (2010), “PEGylation and preliminary biocompatibility evaluation of magnetite-silica nanocomposites obtained by high energy ball milling”, *Int. J. Pharm.*, 401, 103-112.

Sanchez, L. C., Arboleda, J. D., Saragovi, C., Zysler, R. D., & Barrero, C. A. (2007), “Magnetic and structural properties of pure hematite submitted to mechanical milling in air and ethanol”, *Physica B*, 389, 145-149.

Saviuc, C., Grumezescu, A. M., Chifiriuc, M. C., Mihaiescu, D. E., Hristu, R., Stanciu, G., et al. (2011), “Hybrid Nanosystem for Stabilizing Essential Oils in Biomedical Applications”, *Digest J. Nanomat. Biostruct.*, 6(4), 1657-1666.

Selvam, S., Gandhi, R. R., Suresh, J., Gowri, S., Ravikumar, S., & Sundrarajan, M. (2012), “Antibacterial effect of novel synthesized sulfated β-cyclodextrin crosslinked cotton fabric and its improved antibacterial activities with ZnO, TiO2 and Ag nanoparticles coating”, *Int. J. Pharm.*, 434(1-2), 366-374.

Subhasree, R. S., Selvakumar, D., & Kumar, N. S. (2012), “Hydrothermal mediated synthesis of ZnO nanorods and their antibacterial properties’, *Lett. Appl. NanoBioSci.*, 1(1), 2-7.

Thongsuwan, W., S., A., & Singjai, P. (2007), “Preparation of Iron Oxide nanoparticles by a pyrosol technique”, *Key Engineer. Mater.*, 353-358, 2175-2178.

Vasile, B. S., Vasile, O. R., Ghitulica, C., Andronescu, E., Dobranis, R., Dinu, E., et al. (2010), “Yttria totally stabilized zirconia nanoparticles obtained through the pyrosol method”, *Phys. Status Solid. A*, 207(11), 2499-2504.

Wagloehner, S., Reichert, D., Sorzano, D. L., Balle, P., Geiger, B., & Kureti, S. (2008), “Kinetic modeling of the oxidation of CO on Fe2O3 catalyst in excess of O2”, *J. Catal.*, 260, 305-314.

Watanabe, A., & Kozuka, H. (2003), “Photoanodic properties of sol-gel-derived Fe2O3 thin films containing dispersed gold and silver particles”, *J. Phys. Chem. B*, 107, 12713-12720.

STATIONARY AND DYNAMIC RHEOLOGICAL BEHAVIOUR OF SOME COLLAGEN HYDROGELS FOR WOUND MANAGEMENT CONTAINING MIXTURES OF CHLORHEXIDINE DIGLUCONATE AND TANNIC ACID

LAVINIA BRAZDARU[1], MINODORA LECA[1], MARIAN MICUTZ[1], MĂDĂLINA GEORGIANA ALBU[2], TEODORA STAICU[1]

[1] *University of Bucharest, Faculty of Chemistry, 4-12 Regina Elisabeta blvd, 030018 Bucharest, Romania, email: mincan_lavinia@yahoo.com*

[2] *INCDTP - Division: Leather and Footwear Research Institute, 93 Ion Minulescu, 031215 Bucharest, Romania*

Type I collagen hydrogels having a concentration of 1.1% and containing 5, 10 and 15% tannic acid as well as all the combinations between the above amounts of tannic acid and 1.82, 4.55, 9.09% chlorhexidine digluconate were prepared. Intended to be used for wound healing, they were characterized by stationary and dynamic rheological behaviour, to select the most convenient combination from the point of view of application on wound. The hydrogels behave pseudoplastic, start to flow at very low shear stress, destroy under the action of shear rates higher than about 20 s^{-1}, are thixotropic and elasticity prevails on viscosity in their viscoelastic properties. The most convenient concentrations of drugs to be applied as wound dressing is 4.55% CHDG and 10% TA, the hydrogel having the highest elasticity and viscosity. The hydrogel can be applied by spatula or pouring and, being thixotropic, even using a syringe.

Keywords: collagen, tannic acid, chlorhexidine digluconate, hydrogel.

INTRODUCTION

Hydrogels are three-dimensional networks of natural or synthetic hydrophilic polymers having the capacity to hold large amounts of water or biological fluids within their porous structure, Peppas and Mikos (1986), Brannon-Peppas (1990), Pepas et al. (2000). Polymer insolubility is produced by the crosslinking of backbone or their associates by chemical or physical forces or by the entanglement of chains in the case the polymers are linear and flexible, Hoffman (2002). Thus, the hydrogels can be divided in: permanent – cross-linked by covalent forces and physical – formed by physical interactions (hydrogen bonds, ionic interactions or chain entanglement), Campoccia et al. (1998), Hoffman (2002).

The hydrogels have as specific properties soft consistency, permeability for small molecules and low gel-aqueous solution interface tension, Peppas (1986). The content of water and consistency make them similar to natural tissues, Park (1997), making them very useful in medicine and pharmacy, Peppas and Langer (1994). The high water content contributes to biocompatibility and they can be used as membrane for biosensors, materials for artificial leather, matrices for drug delivery, etc., Park (1997), Peppas (1997).

Type I collagen hydrogels are three-dimensional networks consisting of randomly interwoven mesh of fibrils, with poroelastic/biphasic loose lattice structure filled with about 99% fluid, Abou Neel (2006). The remarkable capacity to hold water is mainly due to its hydrophilic groups: amino, carboxyl and hydroxyl, Charulatha and Rajaram (2003) which also allow the formation of physical bonds between fibrils.

Having low percentage of collagen and loose lattice structure their mechanical properties are weak. Their improving can be realized by increasing of crosslinking density.

The oldest and used tanning agent for leather is tannic acid (TA), the hydrolysable tannin having the highest affinity for collagen, Fueaesaku et al. (1972), Meek and Weiss

(1979). It does not induce cytotoxicity, reduce biocompatibility or prevent cell remodeling. Moreover, it has antiviral and antibacterial properties, antimutagenic and antigenic activity, Scalbert (1991), induces apoptosis in animal cells, and has antioxidant action, Khan (2000).

Chlorhexidine digluconate (CHDG) is one of the most widely used antimicrobials in clinical practice for skin antisepsis, Karpanen (2008). It is potent even against mutant streptococci, Emilsm (1994). Its efficacy can be improved using phytochemicals, some of them transforming it *in vivo* from bacteriostatic into bactericide, Şulea (2011).

The objective of the present paper is the preparation and rheological characterization of acid type I collagen hydrogels, pH 3.8, containing some mixtures of CHDG and TA antibacterials, intended to be used for the wound care, in view of predicting the way they can be applied, their behaviour on application site and delivery of active principles.

EXPERIMENTAL

The 1.1% control collagen hydrogels, pH 3.8, extracted from calf hide by the current technology used in INCDTP, Division ICPI, Trandafir et al. (2007), was obtained by diluting the initial 2.54% hydrogel, pH 3.21, with distilled water and 1 M NaOH solution under mechanical stirring. The hydrogels containing 1.82, 4.55 and 9.09% CHDG reported to the amount of collagen were prepared using the same components and CHDG solution under manual stirring. TA was added in concentration of 5, 10 and 15% reported in the same way. TA was supplied by Sigma-Aldrich and CHDG by Fargon (Germany) as 20% aqueous solution (w/w). All the hydrogels were matured at 4°C for 24 h.

Stationary rheological behaviour was determined at 23 ± 0.1°C using a rotational viscometer Hake VT 550 equipped with HV1 sensor system for high viscosities and RheoWin 4 Thermo Fischer Scientific software.

Dynamic (oscillatory) rheological measurements were made at room temperature (23°C) with Micro Fourier Transform Rheometer MRF 2100, GBC-Australia, working under squeezing flow. The angular frequencies were within the 0-1000 rad/s range, 280 discrete frequencies were analyzed simultaneously by a step of 0.5 s^{-1}, 30 spectra acquired for each sample, the gap between the upper and bottom plates was 400 µm and displacement amplitude 0.03 µm, to fall into linear viscoelastic domain. Very small amplitude of pseudorandom squeezing motion allows a continuous monitoring of force transmitted through the viscoelastic sample to the force sensor (bottom plate). By a Fourier transform processing the storage and loss modulus at every individual frequency is obtained.

RESULTS AND DISCUSSION

Various biomedical applications, including controlled delivery systems and wound management, make the rheological characterization of hydrogels a very important task. In the case of the physical hydrogels the rheology can also be used to study the physical interactions between the dispersed phase and the components dissolved into the dispersion medium.

It has been recognized for a long time, Gustavson (1949), that TA interacts with collagen by a variety of forces: hydrogen bonding, hydrophobic and electrostatic, the types of interactions being later confirmed, Heijmen et al. (1997), Cass and Burg (2012). TA interposes between collagen fibrils, by crosslinking the basic side chains groups of polar amino acids of collagen or clustering between, Madhan et al. (2001).

The reaction between collagen and TA is depended on pH: it binds rapidly and quite firmly under acidic conditions – pH 3-4 – and slowly at pH above 6. That is why only hydrogels having an acid pH, of 3.8, were prepared and studied.

Rheological properties of collagen hydrogels are induced especially by the integrity of its fibrils and the fluid movement between the lattice forming collagen fibrils and are governed by the inherent viscoelasticity of the fibrils and their interaction with the fluid, Koob and Hernandez (2002), Park at al. (2002), Elbjeirami at al. (2003), Krishnan (2004).

Giving information on consistency and apparent plasticity, stationary rheological properties are important for predicting the way the hydrogels may be applied (by spatula, pouring, syringe, spray), their behaviour on the application site (entry into intricate spaces versus preventing of flow into critical areas), Moss at all (2006), and delivery of active principles, both properties affecting the kinetics of drug delivery.

The rheograms of the initial collagen hydrogels having the pH 3.8 and of those containing 5, 10 and 15% TA reported to the amount of collagen at increasing of shear rate, γ^*, are given in Figure 1, where τ is the shear stress.

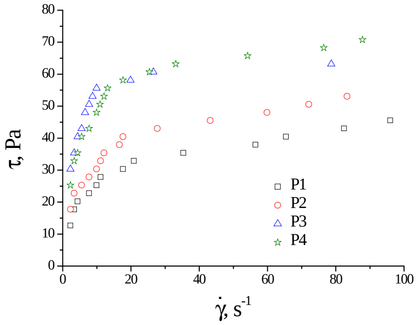

Figure 1. Rheograms of hydrogels crosslinked with: P1 – 0, P2 – 5, P3 – 10, P4 – 15% TA

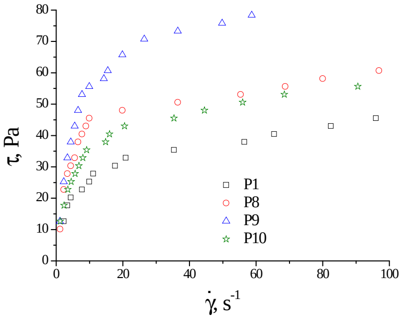

Figure 2. Rheograms of hydrogels with 4.55% CHDG and: P1 – 0, P8 – 5, P9 – 10, P10 – 15% TA

They show that all the hydrogel have pseudoplastic behaviour with practically zero limiting shear stress. The apparent viscosities, η^*, increase with TA amount, excepting 15% TA, for which the values are the same as for 10%, in the limit of experimental errors. This demonstrates that 10% TA is enough to crosslink the collagen. At the same time, the curves show an abrupt decrease of the slopes at γ^* exceeding about 20 s^{-1}, which signify that such a shear stress produces a perceptible destruction of gel structure.

The rheograms obtained at decreasing of shear rates, after the hydrogels were sheared until 1000 s^{-1} (not shown), are placed under those resulted with their increasing for each hydrogel. This indicates that the gel structure does not recover even at low shear rates, which means that the hydrogels have a time-dependent behaviour of thixotropic type.

To estimate the measure of crosslinking and gel destruction as a function of TA content, viscosities at zero shear rate, η_o, for increasing and decreasing of γ^*, are given in Table 1.

The data in Table 1 show that the η_o obtained rising γ^* increase with TA concentration (crosslinking extent), excepting that of hydrogel containing 15%. This can signify that the amount of TA required by crosslinking was surpassed and the excess has detrimental effect on collagen, according to previous findings, Albu (2009). The values obtained when γ^* decreases are much lower: 2.6 times for the reference and 4.0% for the hydrogel with 10% TA, while for 15% it is 19.6%. This supports the detrimental effect of high amounts of TA.

Table 1. Viscosities at zero shear rate obtained with increasing and decreasing of shear rates

Sample	TA , %	CHDG, %	Increasing of γ^*		Decreasing of γ^*	
			η_o, Pas	n	η_o, Pas	N
P1	0	0	9.80	0.43	3.80	0,46
P2	5	0	13.86	0.35	3.73	0,50
P3	10	0	21.55	0.42	5.37	0,44
P4	15	0	19.17	0.41	0.98	0,79
P5	5	1.82	10,14	0,63	7,55	0,40
P6	10	1.82	15,21	0,48	4,45	0,46
P7	15	1.82	20,72	0,30	3,89	0,47
P8	5	4.55	15,51	0,47	8,02	0,39
P9	10	4.55	16,66	0,55	7,91	0,39
P10	15	4.55	11,93	0,49	1,64	0,62
P11	0	9.09	10,10	0,28	6,62	0,41
P12	10	9.09	14,85	0,42	5,07	0,41
P13	15	9.09	9,11	0,70	3,82	0,51

The rheograms of the collagen gels containing 1.82% CHDG and the same amounts of TA (not shown) look very similar with those in Figure 1, but η_o obtained with increasing γ^* have lower values, excepting that for 15% TA. This can be explained by the interaction of the two positive charges of molecule of CHDG, Jones (1997), with collagen and/or TA, reducing probably the excess of TA.

Increasing of CHDG at 4.55% gives the rheograms from Figure 2. They show the most reduced destroying of gel structure for 10% TA, while the other two behave similar.

The hydrogels with 15% TA – P11-P13 – give the lowest η_o values (Table 1) due to some denaturizing of the native collagen conformation produced by the excess TA.

The flowing indices, n, which show the easiness of flowing (the lower the flow index the higher the consistency), calculated with Ostwald-de Vaele equation, are given in Table 1. As can be seen, their values are not in accordance with η_o.

The storage, G’, and loss, G”, moduli give the elastic and viscous contribution to the viscoelastic behaviour of a polymer gel and allow the distinction between uncrosslinked and crosslinked systems: high G’ values indicate the prevalence of elastic properties and high G” values the prevalence of the viscous ones. For hydrogels, which are highly crosslinked polymer networks, both G’ and G” are very high and are nearly parallel to each other, Barth and Pash (2003).

The dependencies of G’ and G” on angular frequency, ω, for collagen hydrogels from Figure 1 are given in Figure 3.

The Figure shows that the storage moduli are about two times higher than the loss ones for all the hydrogels, which means that the elastic components prevail in their viscoelastic behaviour. TA increase more elasticity than viscosity as expected for a crosslinked polymer. The highest values both for G’ and G” were obtained for the hydrogel containing 10% TA, while for 15% G’ is lower and G” has the lowest values, supporting the hypothesis of a slight denaturizing of collagen produced by the excess TA. G’ and G’’ increase practically linear with ω within the entire range and the slopes are pretty close. When 1.82% CHDG is added the curves have the same appearance and placement, but G’ and G” are a little lower over the entire ω range due to the consumption of a part of the crosslinking agent by CHDG.

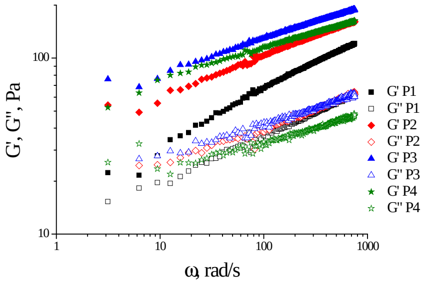

Figure 3. Dependence of G’ and G” on ω for collagen hydrogels from Figure 1

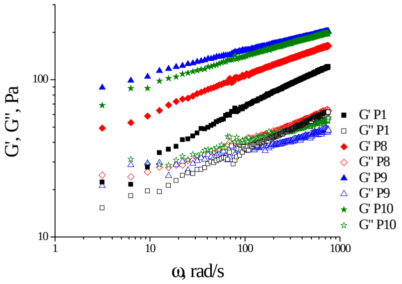

Figure 4. Dependence of G’ and G” on ω for collagen hydrogels from Figure 2

Curves for 4.55% CHDG, presented in Figure 4, show higher values for both moduli, due to the more extended crosslinking. Similar curves are obtained for samples P11-P13.

To make an idea of the values of viscosities at the angular frequency of 1 rad/s (0.16 Hz), the linear fitting of the results were made and the results a given in Table 2.

Table 2. Viscosities of hydrogels at angular frequency of 1 rad/s

Sample	P1	P2	P3	P4	P5	P6	P7	P8	P9	P10	P11	P12	P13
η, Pas	19.1	39.8	56.1	52.8	41.6	43.4	58.2	41.0	81.2	66.7	66.0	76.9	158.6

The viscosities vary with TA and CHDG concentrations in the same way as in Table 1, but all the values are higher than those obtained from stationary measurements, shearing forces, unlike the oscillatory ones, producing the disturbing of gel structure.

The rheological stationary and dynamic measurements show that for a type I collagen hydrogels with concentration 1.1% containing CHDG and TA as antimicrobials, intended to be use as wound dressings, the optimum concentration of CHDG is 4.55% and of TA 10% (sample P9). Such a hydrogel has the highest viscosity and elasticity. Thus, it can be applied both by spatula or pouring, or even using a syringe, given its thixotropic properties.

The drugs delivery measurements, which have to be performed, follows to prove the accuracy of the results given by rheology.

CONCLUSIONS

Type I collagen hydrogels with concentration 1.1% and containing 5, 10 and 15% TA as well as all the combinations between the specified amounts of TA and 1.82, 4.55, 9.09% CHDG, intended to be used for wound treatment, were prepared and characterizes by stationary and dynamic properties.

The hydrogels have pseudoplastic rheological behaviour, start to flow at very low shear stress, destroy under the action of shear rates higher than about 20 s^{-1}, are thixotropic and elasticity prevails over viscosity in their viscoelastic behaviour.

The most convenient concentrations of drugs to be applied as wound dressing is 4.55% CHDG and 10% TA, the hydrogels being both the most viscous and elastic. This hydrogel can be applied by spatula or pouring and, being thixotropic, even by syringe.

REFERENCES

Abou Neel, E.A. et al. (2006), "Use of multiple unconfined compression for control of collagen gel scaffold density and mechanical properties", *Soft Matter.*, 2, 986–992.

Albu, M.G. (2009), "Collagenic gels and matrices with different degrees of hydration and quasi-solid structure for biomedical applications", Ph. D. thesis, University of Bucharest.

Barth, H.G. and Pash, H. (eds.) (2003), *Rheology essentials of Foods and Cosmetics*, Springer Germany, Berlin.

Brannon-Peppas, L. (1990), "Preparation and characterization of crosslinked hydrophilic networks", in L. Brannon-Peppas and R. S. Harland (eds.), *Absorbent Polymer Technology*, Elsevier, Amsterdam.

Campoccia, D. et al. (1998), "Semisynthetic resorbable materials from hyaluronan esterification", *Biomat.*, 2, 2101–2127.

Charulatha, V. and Rajaram, A. (2003), "Influence of different crosslinking treatments on the physical properties of collagen membranes", *Biomaterials*, 24, 759-769.

Cass, C.A.P. and Burg, K.J.L. (2012), "Tannic acid cross-linked collagen scaffolds and their anti-cancer potential in a tissue engineered breast implant", *J. Biomater. Sci*., Polymer Ed., 23, 281-298.

Elbjeirami, W.M. et al. (2003), "Enhancing mechanical properties of tissue-engineered constructs via lysyl oxidase crosslinking activity, *J. Biomed. Mater. Res.*, 66, 513-521.

Emilsm, C.G. (1994), "Potential efficacy of chlorhexidine against mutans streptococci and human dental caries", *J. Dent. Res.*, 73, 682 – 691.

Fueaesaku, Y. et al. (1972), "The new fixation method using tannic acid for electron microscopy and some observations of biological specimens", *Proc. 4th Int. Congr. Histochem. Cytochem.*, T. Takeuchi et al. (eds.), 155.

Gustavson, K.H. (1949), "Some protein-chemical aspects of tanning processes", *Adv. Protein Chem.*, 5, 354-412.

Heijmen, F.H. et al. (1997), "Cross-linking of dermal sheep collagen with tannic acid", *Biomater.*, 18, 749-54.

Hoffman, A.S. (2002), "Hydrogels for biomedical applications", *Adv. Drug Deliv. Rev.*, 54, 3-12.

Jones, C.G. (1997), "Chlorhexidine: Is it still the gold standard?", *Periodontology 2000*, 15, 55–62.

Karpanen, T.J et al. (2008), "Penetration of chlorhexidine into human skin", *J. Antimicrob. Chemotherapy*, 62, 1031–1036.

Khan, N.S. et al. (2000), "Anti-oxidant, pro-oxidant properties of tannic acid and its binding to DNA", *Chem.-Biol. Interact.*, 125, 177-189.

Koob, T.J. and Hernandez, D.J. (2002), "Material properties of polymerized NDGA-collagen composite fibers: development of biologically based tendon constructs, *Biomaterials*, 23, 203-212.

Krishnan, L. et al. (2004), "Design and application of a test system for viscoelastic characterization of collagen gels", *Tissue Eng.*, 10, 241-252.

Madhan, B. et al. (2001), "Molecular mechanics and dynamics studies on the interaction of gallic acid with collagen like peptides", *Chem. Phys. Lett.*, 346, 334-340.

Meek, K.M. and. Weiss J.B. (1979), "Differential fixation of poly(L-arginine) and poly(L-lysine) by tannic acid and its application to the fixation of collagen in electron microscopy", *Biochim. Biophys. Acta.*, 587, 112-120.

Moss, G.P. et al. (2006), "Mechanical characterization and drug permeation properties of tetracaine-loaded bioadhesive films for percutaneous local anesthesia", *Drug Dev. Ind. Pharm.*, 32, 163-174.

Park, K. (1997), *Controlled Release: Challenges and Strategies*, American Chemical Society, Washington.

Park, S-N. et al. (2002), "Characterization of porous collagen/hyaluronic acid scaffold modified by 1-ethyl-3-(3-dimethylamino-propil)carbodiimide cross-linking", *Biomater.*, 23, 1205-1212.

Peppas, N.A. and Mikos, A.G. (1986), "Preparation methods and structure of hydrogels", in *Hydrogels in Medicine and Pharmacy*, N.A. Peppas (ed.), vol. 1, CRC Press, Boca Raton.

Peppas, N.A. (1986), *Hydrogels in Medicine*, CRS Press, Boca Raton.

Peppas, N.A. (1997), "Hydrogels and drug delivery", *Curr. Opin. Coll. Int. Sci.*, 2, 531-537.

Peppas, N.A. et al. (2000), "Hydrogels in pharmaceutical formulations", *Eur. J. Pharm. Biopharm.*, 50, 27-46.

Scalbert, A. (1991), "Antimicrobial Properties of Tannins", *Phytochem.*, 30, 3875-3883.

Şulea, D. et al. (2011), "Collagen-thuja tincture biomaterials for wound treatment 3. Hydrogels containing thuja tincture and chlorhexidine digluconate", *Rev. Roum. Chim.*, 56, 811-817.

Trandafir, V. et al. (2007), *Collagen-based bioproducts* (in Romanian), Ars Docendi, Bucharest.

IN VITRO ANTIVIRAL EFFECT OF THE ESSENTIAL OILS OF THYMBRA SPICATA L. ON HERPES SIMPLEX VIRUS TYPE 2

NIZAMI DURAN, ALPASLAN KAYA, GULAY GULBOL DURAN, NACIYE ERYILMAZ
Mustafa Kemal University, Hatay, Turkey, email: nizamduran@hotmail.com

The essential oils of Thymbra spicata L. has been used for a long time as a folk medicine to treat a lot of diseases. In this study, we aimed to investigate the antiviral effect of The essential oils of Thymbra spicata L. against HSV-2 (Herpes Simplex Virus type 2). Aerial parts of Thymbra spicata L. were used. They harvested at full flowering stage in July 2011 from the botanical gardens, Field Crops Department of Mustafa Kemal University. Chemical analysis of Thymbra spicata L. was performed by GC-MS. In the study, HEp-2 cell line derived from human larynx cancer cells was used. Cultivation of HEp-2 cells was carried out in RPMI 1640 medium with 10% fetal calf serum at an atmosphere of 37°C with 5% CO2. The cell viability was evaluated by a tetrazolium-based colorimetric method using 3-(4,5-dimethylthiazol-2-yl)-2,5-diphenyltetrazolium bromide (MTT). The main components with the highest rates were carvacrol, cymol, gama-terpinene and thymol. While, typical cytopathological changes for HSV-2 on the cells was observed at low Thymbra spicata L., concentrations (10 and 20 µg/ml), no cytopathological changes was observed at high Thymbra spicata L., concentrations (40, 80 and 160 µg/ml). In these concentration, HSV-2 could not affect HEp-2 cells. The present results indicated that Thymbra spicata L., with a minimum concentration value of 40 µg/ml significantly showed antiviral effect against HSV-2 compared to the control group ($p<0.001$). This study shows that the essential oils of Thymbra spicata L. seems to have notable antiviral activity for HSV-2. We think that this antiviral effect of the essential oils of Thymbra spicata L may be attributed the abundant components in the structure such as Carvacrol, cymol, gama-terpinene and thymol. Our results confirmed that the essential oils of Thymbra spicata L. is a potential source of new and selective agent for the treatment of HSV-2 infection. However, further studies are needed to understand its antiviral mechanism and before making a recommendation.

Keywords: HSV-2, Thymbra spicata L., GC-MS, antiviral, HEp-2.

INTRODUCTION

Herpes Simplex Virus Type 2 (HSV-2) is the major agent of genital HSV infection. It can cause severe morbidity and mortality in patients with immune deficiency such as AIDS patients. Acyclovir has been the most effective and widely-used pharmaceutical drug for the treatment of herpes simplex virus (HSV) infections. It is quite effective for treatment of primary and recurrent genital HSV infection. Lately, the resistance to Acyclovir has been reported, especially in patients with immunosuppressive. For this reason, new and alternative antiviral agents are being sought for species that are resistant to Acyclovir (Duran, 2003; Stranska et al., 2005).

For years, plants have provided a rich source of therapeutic agents. Currently 25% of prescribed drugs worldwide are still derived from plant sources, showing that plant species are still an important source of new drugs for diseases that continue to lack a cure, such as cancer (Allahverdiyev et al., 2004; Duran et al., 2008; Duran et al., 2006; Aksoy et al., 2007; Oksuz et al., 2005; Onlen et al., 2007a; Onlen et al., 2007b).

The use of natural products has been one of the most successful strategies for the discovery of new medicines; natural products have been used for folk medicine purposes throughout the world for years. Among these types of natural plants, *Thymbra spicata* L. has attracted increased interest because of its various pharmacological activities (Allahverdiyev et al., 2004; Duran et al., 2008; Duran et al., 2006; Aksoy et al., 2007; Oksuz et al., 2005).

Thymbra spicata L. classified in Lamiaceae family is known as “Kekik or Zahter in

Turkey. It is a kind of herbaceous perennial plant and, it can grow up to 50 cm long with hairy, pink flowers and shrubs appearance. *Thymbra spicata* L. has been used for a long time as a folk medicine to treat a lot of diseases. It is known that *Thymbra spicata* L. is used as herbal tea, condiment. Also, it is reported to be useful for some diseases such as asthma, colic, bronchitis, coughs. Furthermore, *Thymbra spicata* L. is used in food industry for flavoring, aroma and preservative agents (Inan et al., 2011; Daneshvar-Royandezagh et al., 2009).

Due to the many useful properties of *Thymbra spicata* L., it has attracted much attention in recent years as a useful or potential substance used in both medicine and food industry. It has been reported to be the chemical composition of *Thymbra spicata* L. is quite complicated. Carvacrol and thymol are important phenolic compunds that reported to exhibit strong antifungal, antibacterial and antimicrobial activities (Daneshvar-Royandezagh et al., 2009; Shelef, 1983).

Thymbra spicata L.,has various compounds such as thymol, carvacrol and y-terpinene. The components of *Thymbra spicata* L. depend on the collecting location, time and plant source. Consequently, biological activities of *Thymbra spicata* L. gathered from different phytogeographical areas and time periods vary greatly (Cabo, 1982).

As we know, antiviral activity of *Thymbra spicata* L.against HSV-2 (Herpes Simplex Virus Type 2) was not studied before. In this study, we aim to investigate the antiviral activity of *Thymbra spicata* L. gathered from Hatay geographic area against HSV-2 on HEp-2 cell line.

In this study, we aimed to investigate; i) the chemical characterization of *Thymbra spicata* L. samples collected from Hatay geographic area, ii) the antiviral activity of the essential oils of *Thymbra spicata* L. against HSV-2 on HEp-2 cell line.

MATERIALS AND METHODS

Plant Material

Aerial parts of *Thymbra spicata* L. were harvested at full flowering stage in July 2011 from the botanical gardens, Field Crops Department of Mustafa Kemal University.

Isolation of the Essential Oils

The aerial parts of *Thymbra spicata* L. (100 g) were dried to constant weight in an oven at 35°C. Then, they were extracted by hydrodistillation with 1 L distilled water for 3 h using Neo-Clevenger apparatus. The oils were dried over anhydrous sodium sulfate and then stored in dark color (amber) glass bottles, at -4°C ready for GC-MS analysis.

GC-MS Analysis

Analysis of the essential oils carried out by using Thermo Scientific Focus Gas Chromatograph equipped with MS, auto sampler and TR-5MS (5% Phenyl Polysilphenylene-siloxane, 0.25 mm x 30 m i.d, film thickness 0.25). The carrier gas was helium (99.9%) at a flow rate of 1 mL/min; ionization energy was 70 eV. Mass range m/z 50-650 amu. Data acquisition was scan mode. MS transfer line temperature was 250°C, MS Ionization source temperature was 220°C, the injection port temperature was 220°C. The samples were injected with 250 split ratio. The injection volume was 1 µl. Oven temperature was programmed in the range of 50°C to 220°C at

3°C /min. The structure of each compound was identified by comparison with their mass spectrum (Wiley). The data were handled using Xcalibur software program. The retention indices (RIs) were calculated for all volatile constituents using a homologous series of n-alkane standard solutions C_8-C_{20} (Fluka, product no. 04070) and C_{21}-C_{40} (Fluka, product no. 04071).

Cell Culture

Antiviral activity tests were carried out on HEp-2 cell line (human larynx epidermoid carcinoma cells). The HEp-2 cell line was obtained from Ankara University, Veterinary Faculty, Depaertment of Virology. Fort he preparation of the cell culture, RPMI 1640 medium (Sigma) was selected as the culture medium and fetal calf serum (Seromed) was used as the growth factor in the medium at a ratio of 10% (v/v). The culture plates were incubated at 37°C in an atmosphere of 5% CO_2. The culture plates were set to contain $1x10^5$ cell per ml.

Determination of the Viral Titration

To infect HEp-2 cells with HSV-2, the cultured HEp-2 cell monolayers were adsorbed with HSV-2 and incubated at 37°C for 1 h. After this stage, the unbound HSV-2 was removed by gentle washing with phospahate buffered saline. Then, as a maintained medium, fetal calf serum-free medium was added to all wells of plates. And, the microplates were incubated the same conditions. The virus titer was determined as in the previous study (Allahverdiyev, 2004). In the tests, three different viral dilutions were added to 80% confluent HEp-2 cells and incubated at 37°C for 1 h as described above. The cells were evaluated by microscopically for the presence of cytopathological effect after 96 hours of incubation. In the tests, three different viral infection doses (100, 10 and 1 TCID50 (Tissue Culture Infective Dose 50%) were calculated according to the methods of Reed and Muench (Reed & Muench, 1938). The inhibitory concentration of viral proliferation was calculated as in previous study (Allahverdiyev, 2002).

Cytotoxic Activity

The cytotoxicity of the essentiol oils of *Thymbra spicata* L. was evaluated by measuring the cell growth *in vitro*. The monolayered HEp-2 cell were prepared in 24-well flat bottomed tissue culture plates and exposed to various concentrations of the essentiol oils of *Thymbra spicata* L. Microscopic evaluations were made periodically at the incubation of 24., 48., 72. and 96. hours. Morphologically changes such as cell rounding, detachment. The cell viability was evaluated by a tetrazolium-based colorimetric method using 3-(4,5-dimethylthiazol-2-yl)-2,5-diphenyltetrazolium bromide (MTT), as previously described (Mosmann, 1983).

Preparation of Drug Dilutions

Three different concentrations of *Thymbra spicata* L., (10 µl/ml, 20 µl/ml, 40 µl/ml, 80 µl/ml and 160 µl/ml) were prepared in ethyl alcohol. Acyclovir was selected as a standart control dug. The dilutions of Acyclovir (10 µg/ml, 20 µg/ml, 30 µg/ml) was prepared with distilled water.

Determination of Non-toxic Concentration of DMSO against HSV-2

In order to determine the non-toxic concentration of dimethyl sulfoxide (DMSO) against HSV-2, 1x10^5 cell/ml and 100 $TCID_{50}$ of HSV-2 were inoculated into flat bottomed microplates containing RPMI-1640 culture medium. And, they were incubated and HSV-2 were allowed to grow for an additional 72 hours in the presence of decreasing amounts of DMSO (5.12%, 2.56%, 1.28%, 0.64%, 0.32%, 0.16%). The non-toxic concentration was determined up to 2.56%. In the experiments, the essentiol oils of *Thymbra spicata* L. were dissolved in 1% DMSO.

RESULTS AND DISCUSSION

The percentage of identified compounds in *Thymbra spicata* L. was given in Table 1. The main components with the highest rates were carvacrol, cymol, gama-terpinene and thymol (Table 1).

Table 1. The percentage composition of the studied *Thymbra spicata* L. essential oils (% of peak areas) determined by GC-MS

RT	RI	*Thymbra spicata* L. %	Components
3.64	1028	0.56	alpha-pinene
3.71	1033	0.64	alpha-phellandrene
4.36	1073	0.06	camphene
5.16	1113	0.1	beta-pinene
6.1	1155	0.05	delta-3-carene
6.51	1170	1.04	beta-myrcene
6.9	1184	1.48	alpha-terpinene
7.43	1202	0.17	dl-limonene
7.69	1212	0.12	beta-phellandrene
8.86	1252	10.73	gama-terpinene
9.69	1276	12.18	cymol
10.04	1286	0.05	alpha-terpinolene
16.17	1454	0.11	oct-1-en-3-ol
16.59	1465	0.05	trans sabinene hydrate
19.73	1547	0.03	cis sabinene hydrate
19.91	1551	0.03	linalool
21.39	1589	1.28	trans caryophyllene
21.79	1598	0.53	4-terpineol
25.36	1694	0.21	isoborneol
26.55	1728	0.02	d-carvone
30.05	1826	0.04	anethole
34.87	1968	0.65	caryophyllene oxide
39.56	2125	0.15	spathulenol
41.8	2218	2.77	thymol
42.61	2239	66.86	carvacrol
44.26	2281	0.08	Naphthalene, 1,2,3,4,4a,5,6,7-octahydro-4a-methyl-

In new drug researches, cell death and the viability can be measured by cell cytotoxicity and viability assays. The ratio of cell viability in cultures can be measured by quantitative colorimetric assay with MTT (McGahon et al., 1995). The MTT assay is based on metabolic reduction of of 3-(4,5-dimethylthiazol-2-yl)-2,5-diphenyltetrazolium bromide (MTT). It can be measured the metabolic reduction of MTT to the antiviral activity of plant extracts on cells. In our study, we used the MTT assay for cytotoxicity studies.

During the experiment, HSV-2-infected HEp-2 cells were incubated with DMSO alone (without any supplement). Effects of DMSO on the cell viability were compared to the control cells (without DMSO). It was reported that DMSO showed no toxic effect up to 2.56% (v/v) for HSV-2-infected HEp-2 cells. Selected concentration of DMSO (1% DMSO) was not found to show any antiviral effects against HSV-2. At the end of 96 h, there were no statistically significant difference in the number of cell viability between the control and the DMSO-containing groups (p>0.05). Also, there was no comparable cytopathological changes compared with the control group (Figure 1).

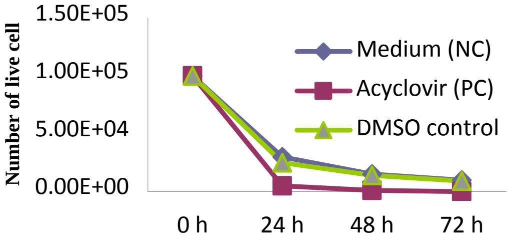

Figure 1. The effects of DMSO in HSV-2 infected HEp-2 cells compared with Acyclovir

To determine the antiviral effects of *Thymbra spicata* L., the morphological changes on HSV-2-infected HEp-2 cells were examined by an inverted microscope. It was determined that typical cytopathological changes for HSV-2 on the cells, such as granulation, detachment, and rounding of the cells were observed. While, typical cytopathological changes for HSV-2 on the cells was observed at low *Thymbra spicata* L., concentrations (10 and 20 μg/ml), no cytopathological changes was observed at high *Thymbra spicata* L., concentrations (40, 80 and 160 μg/ml). In these concentration, HSV-2 could not affect HEp-2 cells (Figure 2). The present results indicated that *Thymbra spicata* L., with a minimum concentration value of 40 μg/ml significantly showed antiviral effect against HSV-2 compared to the control group (p<0.001) (Figure 2).

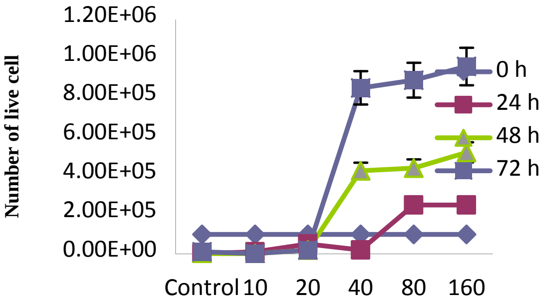

Figure 2. Antiviral activity of the essentiol oils of Thymbra spicata L. in HSV-2 infected HEp-2 cell cultures

CONCLUSIONS

Natural products have been one of the most valuable sources for drug discovery and the development of novel antiviral agents. In this study, it has been demonstrated the efficacy of the essential oils of *Thymbra spicata* L. against HSV-2 *in vitro*. The results of this study, *Thymbra spicata* L. samples collected from Hatay region presents promising antiviral activiyt. This study shows that the essential oils of *Thymbra spicata* L. seems to have notable antiviral activity for HSV-2. We think that this antiviral effect of the essential oils of *Thymbra spicata* L may be attributed the abundant components in the structure such as Carvacrol, cymol, gama-terpinene and thymol. Our results confirmed that the essential oils of *Thymbra spicata* L is a potential source of new and selective agent for the treatment of HSV-2 infection. However, further studies are needed to understand its antiviral mechanism and before making a recommendation.

REFERENCES

Aksoy, A., Duran, N., Toroglu, S., Koksal, F. (2007), “Short-term effect of mastic gum on salivary concentrations of cariogenic bacteria in orthodontic patients”, *Angle Orthod.*, 77, 124-128.

Allahverdiyev, A., Duran, N., Uyanık, O. (2002), “Investigation of the Antiviral Effect of Vepesid on HSV Type 2”, *Turk J Med Sci.*, 32, 7-12.

Allahverdiyev, A., Duran, N., Ozguven, M., Koltas, S. (2004), “Antiviral activity of the volatile oils of Melissa officinalis L. against Herpes simplex virus type-2”, *Phytomedicine*, 11(7-8), 657-661.

Cabo, J., Crespo, M.E., Jimenez, J., Navarro, C., Risco, S. (1982), “Seasonal variation of essential oil yield and composition of Thymus hyemalis”, *Planta Medica*, 380-382.

Daneshvar-Royandezagh, S., Khawar, K.M., Ozcan, S. (2009), “In vitro micropropagation of garden thyme (Thymbra spicata L. var. Spicata L.) collected from Southeastern Turkey using cotyledon node”, *Biotechnol. & Biotechnol. Eq.*, 23(3), 1319-1321.

Duran, G., Duran, N., Culha, G., Ozcan, B., Oztas, H., Ozer, B. (2008), “In vitro antileishmanial activity of Adana propolis samples on Leishmania tropica: a preliminary study”, *Parasitol Res.*, 102, 1217-1225.

Duran, N. (2003), “Genital herpes infections”, *Mikrobiyol Bul.*, 37(2-3), 205-213.

Duran, N., Koc, A., Oksuz, H., Tamer, C., Akaydin, Y., Kozlu, T., Celik, M. (2006), “The protective role of topical propolis on experimental keratitis via nitric oxide levels in rabbits”, *Mol Cell Biochem.*, 281, 153-161.

Inan, K.M, Kaya, A., Kirici, S. (2011), “Effect of harvest time on essential oil composition of Thymbra spicata L. growing in flora of Adıyaman”, *Advances in Environmental Biology*, 5(2), 356-358.

McGahon, A.J., Martin, S.J., Bissonnette, R.P., Mahboubi, A., Shi, Y., Mogil, R.J., Nishioka, W.K., Green, D.R. (1995), “The end of the (cell) line: methods for the study of apoptosis in vitro”, *Methods Cell Biol.*, 46, 153-85.

Mosmann, T. (1983), “Rapid colorimetric assay for cellular growth and survival: application to proliferation and cytotoxicity assays”, *J Immunol Methods*, 65, 55-63.

Oksuz, H., Duran, N., Tamer, C., Cetin, M., Silici, S. (2005), “Effect of propolis in the treatment of experimental Staphylococcus aureus keratitis in rabbits”, *Ophthalmic Res.*, 37, 328-334.

Onlen, Y., Duran, N., Atik, E., Savas, L., Altug, E., Yakan, S., Aslantas, O. (2007a), “Antibacterial activity of propolis against MRSA and synergism with topical mupirocin”, *J Altern Complement Med.*, 13, 713-718.

Onlen, Y., Tamer, C., Oksuz, H., Duran, N., Altug, M.E., Yakan, S. (2007b), “Comparative trial of different anti-bacterial combinations with propolis and ciprofloxacin on Pseudomonas keratitis in rabbits”, *Microbiol Res.*, 162, 62-68.

Putievsky, E., Basker, D. (1977), “Experimental cultivation of marjoram oregano and basil”, *Journal of Horticultural Science*, 52, 181-188.

Reed, L.J., Muench,, H.A. (1938), “A simple method of estimating fifty percent end point”, *Am. J of Hyg.*, 27, 493-497.

Shelef, L.A. (1983), “Antimicrobial effects of spices”, *J.Food Safety*, 6, 29-44.

Stranska, R., Schuurman, R., Nienhuis, E., Goedegebuure, I.W., Polman, M., Weel, J.F., Wertheim-Van Dillen, P.M., Berkhout, R.J., van Loon, A.M. (2005), “Survey of acyclovir-resistant herpes simplex virus in the Netherlands: prevalence and characterization”, *J Clin Virol.*, 32(1), 7-18.

SYNTHESIS AND CHARACTERIZATION OF DENSE COLL/HA COMPOSITE MATERIALS

ANTON FICAI[1], ECATERINA ANDRONESCU[1], MĂDĂLINA GEORGIANA ALBU[2],
ALEXANDRU GRUMEZESCU[1], MARIA SONMEZ[2], DENISA FICAI[1]

[1] *Politehnica University of Bucharest, Faculty of Applied Chemistry and Material Science, Gh Polizu Street 1-7, 011061 Bucharest, Romania, email: anton_ficai81@yahoo.com*
[2] *INCDTP – Division: Leather and Footwear Research Institute, 93 Ion Minulescu st., 031215 Bucharest, Romania*

The synthesis of proper bone graft substitutes is strongly limited by composition and morphology. The current work is intended to surpass the main disadvantages of the previously published controlled drying method. The same or even better results are obtained when, instead of the long drying time necessary for the synthesis of dense COLL/HA composite materials centrifugal force is applied. The use of centrifugal forces reduces dramatically the preparation time up to one thousand times and consequently reduces the degradation of the collagen as results by the FTIR data. For this purpose the ratio between the intensities of the peaks from 1240 and 1450 cm^{-1} are calculated for both method and compared with that corresponding of pure collagen. The purity of the mineral phase was confirmed by XRD, the morphology of the synthesized COLL/HA composite material was analyzed by SEM and the porosity was calculated based on Arthur method.

Keywords: collagen/hydroxyapatite composite materials, microstructure.

INTRODUCTION

The bones have some major functions such as: support of the soft tissue, protection of some organs, movements, mineral storage, blood cell formation, acid-base balance, etc. (Bandyopadhyay-Ghosh, 2008). Bone injuries are frequent and many times require graft materials. This is why, worldwide, the synthesis of bone grafts is of real interest for scientists. The currently applied methods of improvement involve both compositional and morphological aspects. The ceramic properties of the COLL/HA composite materials are influenced by processing route (Andronescu et al., 2011), as well as by composition (Wahl and Czernuszka, 2006; Murugan and Ramakrishna, 2005). In both cases, materials with wide range of ceramic properties were obtained. The porous materials are promising for spongy bones while the compact materials are more suitable for compact bones. From morphological point of view there are some advances such as unidirectional orientation induced by rotating, high magnetic field (Wu, 2007) by electric field, (Ficai et al., 2010a) by self-assembling (Ficai et al., 2010b) or by controlled drying (Ficai et al., 2011). These methods, which lead to the preparation of oriented microstructures, allow the preparation of bone grafts for long bone repairing.

This work relieves the possibility to obtain composite materials with increasing density by using centrifugal forces, the degree of densification being proportional with the rotative speed and time of application. The centrifuged materials have, comparing with the similar materials obtained by "controlled drying", lower degree of denaturation.

EXPERIMENTAL

The collagen gel was provided by the National Research & Development Institute for Textiles and Leather, Collagen Department (M.W.=300 kDa). Calf hide was used in the preparation of collagen gel, through a special chemical process (Albu, 2011), and purified by dialysis against water (Albu et al. 2012). All the hydroxyapatite precursors were used without purification and were acquired from Fluka. The mineralization procedure was similar with the one previously presented in the case of "controlled drying" (Andronescu et al., 2011). Briefly, the mineralization process takes part in alkaline medium (pH=9), hydroxyapatite being precipitated from $Ca(OH)_2$ and NaH_2PO_4. After mineralization the mineralized gel is centrifuged at 10.000 rpm at various time (5-30 min).

X-ray diffraction analysis was recorded on a Shimadzu XRD 6000 diffractometer at room temperature, using Cu Kα radiation. The samples were scanned in the Bragg angle, 2θ range of 10–70, with a scanning rate of 2deg/min.

IR spectroscopic measurements were performed using a Nicolet 6700 FT-IR spectrometer (Thermo Nicolet, Madison, WI). The samples were placed in contact with attenuated total reflectance (ATR) on a multibounce plate of ZnSe crystal at controlled ambient temperature (25^oC). The spectra were recorded over the wavenumber range of 400– 4000 cm^{-1} with a resolution of 4 cm^{-1} for both pure collagen sample and COLL/HA composite materials.

SEM images were recorded on a HITACHI S2600N electron microscope on the composite samples used for assembling as well as on the assembled bone grafts. Prior to analysis all the samples were covered with a thin silver layer.

The porosity was determined by the Arthur method, based on the samples' weight measured in air, before and after immersion in xylene as well as the samples' weight measured by dipping in xylene (using the "pan straddle" system) (ASTM 1992).

RESULTS AND DISCUSSION

X-Ray diffraction pattern (Figure) confirms the formation of HA. All the main diffraction peaks can be attributed to hydroxyapatite, as results from ASTM 03-0747. It is also worth to mention that based on the lack of supplementary peaks it can be affirmed that pure mineral phase was obtained.

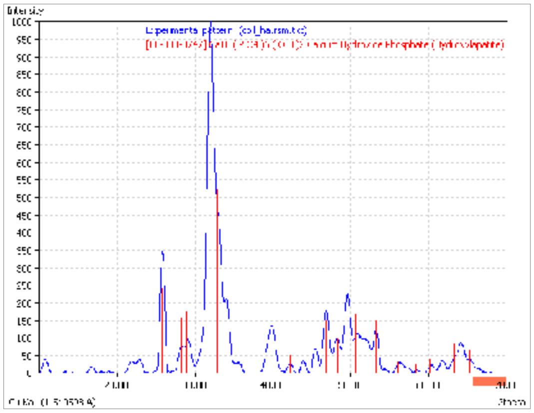

Figure 1. XRD diffraction pattern of COLL/HA composite material obtained by using centrifugal forces

FTIR spectrum of the centrifuged COLL/HA composite material exhibits all the characteristic absorption bands of the collagen and hydroxyapatite. The characteristic collagen peaks have appeared at: 3250–3305cm^{-1} (amide A, N–H stretching), 3072cm^{-1} (amide B, C–H stretching), ~1652cm^{-1} (amide I, C-O stretching), 1552–1561cm^{-1} (amide II, N–H bending and C–N stretching) and 1240cm^{-1} (amide III, C–N stretching and N–H bending). The hydroxyapatite characteristic absorption bands have appeared at: ~ 3300cm^{-1} (OH stretching); 1010, 1041, 1087cm^{-1} (ν_3 antisymmetric P–O stretching threefold degenerated); 962cm^{-1} (ν 1 symmetric P–O stretching, usually inactive in IR); 554, 570, 601cm^{-1} (ν_4 O–P–O bend, threefold degenerated). Based on these bands, the deposited mineral phase can be concluded to be a non-stoichiometric hydroxyapatite. The most visible differences between the two types of materials are the presence of phosphate bands characteristic to the composite materials containing hydroxyapatite.

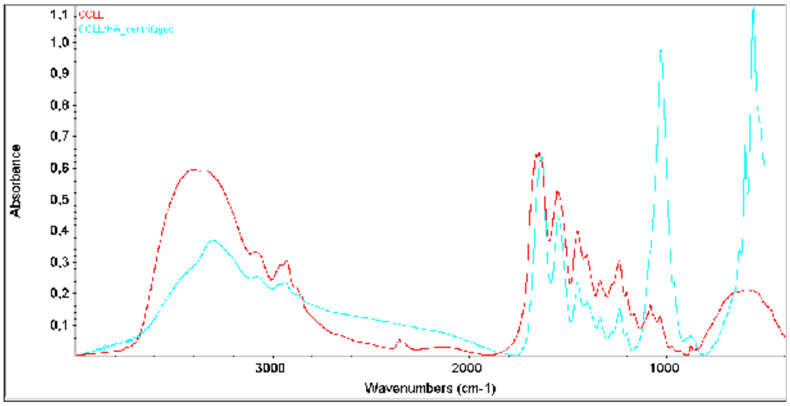

Figure 1. FTIR spectrum of the centrifuged COLL/HA composite material

Table 1. Comparative data regarding the I1240:I1450 ratio associated with the degree of denaturation

	Material	I_{1240}:I_{1450}	Observation
1	Pure collagen	1.13	Native collagen
2	COLL/HA centrifugal forces	1.07	Composite obtained by using centrifugal force
3	COLL/HA 0h	1.08	Composites obtained by “controlled drying” method, based on the FTIR data previously published [2]
4	COLL/HA 10h	1.05	
5	COLL/HA 24h	1.03	
6	COLL/HA 72h	1.01	
7	COLL/HA 168h	0.98	

Based on the FTIR data (Figure 1) recorded for the pure collagen sample the ratio between the intensities of the absorption bands centered at 1240 and 1450cm^{-1} is 1.13. When centrifugal forces are applied, no additional degradation of collagenous structure is observed compared with the synthesized composite material (COLL/HA 0h). When the air drying time increases the I_{1240}:I_{1450} ratio decreases due to a slight degradation of the collagenous structure. From the Table 1 it can be seen that during the long time of “air drying” collagen degradation occurs but, even after complete air drying the degradation is not dramatic (the ratio is 0.98).

The SEM images reveal a denser materials comparing with the materials obtained by “controlled drying”, for instance (Figure 2). It can be observed that compact materials were obtained, the fibrillar forms being associated with unassembled mineralized collagen fibers.

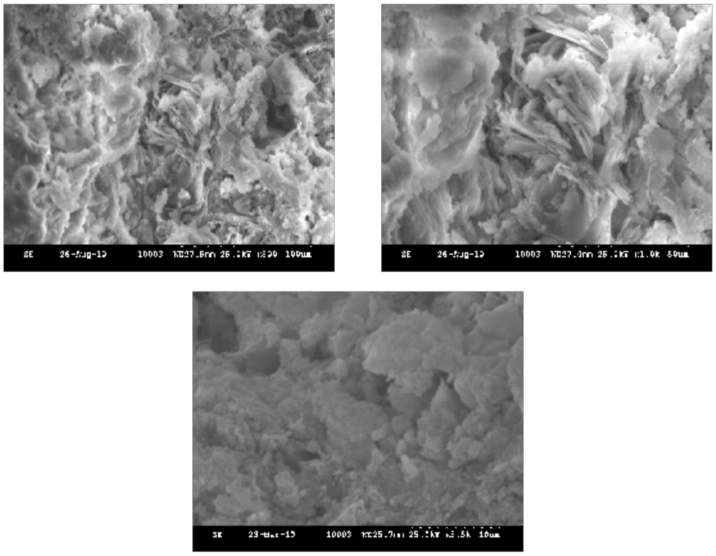

Figure 2. SEM images of COLL/HA composite material obtained by using centrifugal forces

The porosity of the COLL/HA composite materials obtained by centrifugal forces was quantitatively evaluated. Depending on the centrifugation time and (rotative) speed, materials with various porosities were obtained, the most compacted materials having the porosity of ~15%. If compared with the porosity data obtained for the "controlled drying method" (COLL:HA = 1:4 (w)) an important improvement of the densification can be observed.

Table 1. The porosity of the COLL/HA composite materials, comparative data

	Material	Porosity %	Observation
1	COLL/HA centrif	≥15	(9000rpm, 30min)
2	COLL/HA 0-168h	95-37	"controlled drying" method

CONCLUSIONS

The current paper presents the synthesis and characterization of dense COLL/HA composite material by using centrifugal force. The main advantage of this method is the reduced processing time which means same porosity and lower degree of denaturation of collagenous structures. This method can be considered a better way to obtain dense COLL/HA composite materials by replacing the "controlled drying" with this fast and safe method which is based on the centrifugal force. Based on the obtained quantitative data the COLL/HA composite materials obtained by using centrifugal forces is two times denser than the materials obtained by "controlled drying".

Acknowledgements

Authors acknowledge financial support from the European Social Fund through POSDRU/89/1.5/S/ 54785 project: "Postdoctoral Program for Advanced Research in the field of Nanomaterials".

REFERENCES

Albu, M.G. (2011), *Collagen gels and matrices for biomedical applications*, Lambert Academic Publishing, Saarbrücken, Germany.

Albu, M.G., Trandafir, V., Suflet, D.M. et al. (2012), "Biocomposites based on collagen and phosphorylated dextran for bone regeneration", *Journal of Materials Research,* 27(7), 1086-1096.

American Society for Testing and Materials (1992), "F562-84", 150.

Andronescu, E., Voicu, G., Ficai, M. et al. (2011), "Collagen/hydroxyapatite composite materials with desired ceramic properties", *Journal of Electron Microscopy,* 60(3), 253-259.

Bandyopadhyay-Ghosh, S. (2008), "Bone as a Collagen-hydroxyapatite Composite and its Repair", *Trends Biomater Artif Organs,* 22(2), 112-120.

Ficai, A., Andronescu, E., Trandafir, V. et al. (2010a), "Collagen/hydroxyapatite composite obtained by electric field orientation", *Materials Letters,* 64(4), 541-544.

Ficai, A., Andronescu, E., Voicu, G. et al. (2010b), "Self assembled collagen/ hydroxyapatite composite materials", *Chemical Engineering Journal,* 160(2), 794-800.

Ficai, A., Andronescu, E., Voicu, G. et al. (2011), "Collagen/hydroxyapatite composite materials with desired ceramic properties", *Journal of Electron Microscopy,* 60(3), 253-259.

Murugan, R., Ramakrishna, S. (2005), "Development of nanocomposites for bone grafting", *Composites Science and Technology,* 65, 2385–2406.

Wahl, D.A. and Czernuszka, J.T. (2006), "Collagen-hydroxyapatite composites for hard tissue repair", *European Cells & Materials,* 11, 43-56.

Wu, C.Y., Sassa, K., Iwai, K. et al. (2007) "Unidirectionally oriented hydroxyapatite/collagen composite fabricated by using a high magnetic field", *Materials Letters,* 61(7), 1567-1571.

A NOVEL COMPOSITE OF COLLAGEN-HYDROXYAPATITE/GUM ARABIC

WENPO FENG, FANG WANG, KEYONG TANG, JIE LIU

College of Materials and Engineering, Zhengzhou University, Zhengzhou 450052, China, email: keyongtang@yahoo.com.cn

The collagen extracted from rabbit skins was used in combination with $Ca(NO_3)_2$ and $(NH_4)_2HPO_4$ to obtain Col-HA composite in situ. Gum Arabic, a plant-polysaccharide, was also employed to improve the composite's properties. And Fourier transform infrared spectroscope (FT-IR), X-ray diffraction (XRD), scanning electron microscopy (SEM) were applied to study the structure and properties of the Col-HA/Gum A composite. In addition, the properties of the composite, such as mechanical properties, hygroscopicity, degradable properties, and cytotoxicity were tested. FT-IR, XRD, SEM results suggested that the extracted product was type I collagen and the inorganic phases of the composite were mainly hydroxyapatite . The tests on the mechanical properties, hygroscopicity, biodegradability, and cytotoxicity indicated a potential use as bone implant material.

Keywords: collagen, hydroxyapatite, Gum Arabic, artificial bone

INTRODUCTION

Nowadays, autografts, allografts or xenografts are used to address the bone reconstruction. Although they are successful in many operations, limited source of graft materials does exist in autografs. Serious complications including an increased surgery time and donor site pain are also found in autografts. Besides, allografts and xenografts are associated with immunologic barriers, infection and inflammation and have perceived ethical disadvantages. Xenografts also bring the risk of species-to-species transmissible diseases (Wiesmann HP, et. al. 2004, Wahl DA et. al., 2006). Numerous artificial bone substitutes containing metals, ceramics and polymers are introduced to maintain the bone function. However, artificial bone has specific disadvantages, and in current clinical practice, autografts can not perfectly substituted by it.

Indeed, many agree that, by mimicking the structure and characteristics of natural tissue, artificial bone provides a more favorable environment for cellular interactions to improve the symbiosis. As reported, Collagen-hydroxyapatite nanocomposites has an excellent biocompatibility and high osteoconductive activity. However, this composite is still restricted in clinic because of its poor mechanical properties, high swelling, and fast degradation. The addition of some polysaccharide, such as Gum Arabic, may be helpful for the properties of Col-HA composite, with its biological properties unchanged.

In polysaccharide Gum Arabic, there is calcium, magnesium, potassium, iron, and other slightly acidic cations. And owing to its excellent avirulence, good biocompatibility, and easily controlled release, Gum Arabic has been widely used in such fields of chemical engineering, biology, drug, food and etc.

In this paper, the collagen-hydroxyapatite/Gum Arabic(Col-HA/Gum A) composites are prepared in-situ. And the composite are investigated by XRD, FT-IR, SEM and etc to characterize its structure and behaviour, as well the cytotoxicity.

EXPERIMENT

Materials

Rabbit skin was purchased from market. Pepsin and collagenase were from Sigma Company. The standard molecular weight markers were from Takara Biotechnology (Dalian) Co., Ltd. China. DMEM (Dulbecco's minimum essential medium) was from Gibco, USA. Coomassie Brilliant Blue, R-250, was from Sanland Company, USA. Fetal calf serum was from Hangzhou Sijiqing Biological Engineering Materials Co., Ltd, China. MEF-WT cells (wild type mouse embryonic fibroblasts) were preserved in liquid nitrogen at -196°C.

Preparation of Col-HA/Gum A biocomposite in situ

Preparation of Col-HA biocomposite in situ: According to references(Cliche S, et al, 2003, Li D, et al, 2009, Muyonga JH et al, 2004), the Col-HA biocomposite is prepareted in situ.

Preparation of Col-HA/Gum A biocomposite in situ: This procedure was the same above except the addition of 30mL 5wt% Gum Arabic solution to 150mL collagen solution (1wt%). The hydroxyapatite was thus obtained in situ in the mixture.

Tests

Fourier transform infrared spectroscopy (FT-IR): FT-IR spectra of the lyophilized collagen, hydroxyapatite, Col-HA, and Col-HA/Gum A samples were obtained from discs containing 2.0 mg sample in about 100 mg potassium bromide (KBr). All spectra were scanned from 4000 to 500 cm^{-1}.

Scanning electron microscopy (SEM)

X-ray diffraction (XRD)

Mechanical properties

Hygroscopicity: Five experiments were done for each sample and the average values were reported. Water absorption (Wa) was calculated according to the following equation (Zhang L, et al, 2009, Mao JS, et al, 2003):

$$W_a = \frac{W_h - W_d}{W_d} \times 100\% \qquad (1)$$

Collagenase degradation: Degradation rate (Rd) was calculated according to the following equation (Zhang L, et al, 2009, Mao JS, et al, 2003, Liao S, et al, 2007):

$$R_d = \frac{W_o - W_t}{W_0} \times 100\% \qquad (2)$$

Where *Wo* is the original weight, and *Wt* is the weight at time *t*. Each biodegradation experiment was repeated three times and the average values were reported.

Cytotoxicity: The cytotoxicity of composite extracts was evaluated against MEF-WT cells.

Thermogravimetric (TG): Thermogravimetric (TG) of the samples before and after UV irradiation were carried out with a TG209F1 thermal analyzer (NETZSCH, Germany). 6 mg of samples were heated under N_2 atmosphere from 30°C to 800°C at the heating rate of 20°C/min.

RESULTS AND DISCUSSION

FT-IR

As Figure 2a shows, the IR spectrum of the extracted collagen, the characteristic amino acids and high proportion of imino acids of intact collagen molecules are reflected in five major amide peaks in IR spectra (Muyonga JH, et al, 2004, Li D, et al, 2009, Bonnier F, et al, 2002). The bands at 3419cm^{-1}, 2930cm^{-1}, 1640cm^{-1}, 1543cm^{-1}, and 1237 cm^{-1} were denoted as amide A, B, , , and bands respectively. Generally, the amide A and B bands are mainly associated with the stretching vibrations of N–H groups. The amide band, known as the C=O stretching vibration coupled to N–H bending vibration, belongs to the α-helical structure. The amide band was the N-H bending vibration coupled with C-N stretching vibration. The absorption band at 1237 cm^{-1}, due to the C–N bond in-plane vibration (amide), is related to collagen triple helix structure. The absorption band at 1451 cm^{-1} is pyrrolidine ring vibrations of proline and hydroxyproline, indicating the integrity of collagen structure.

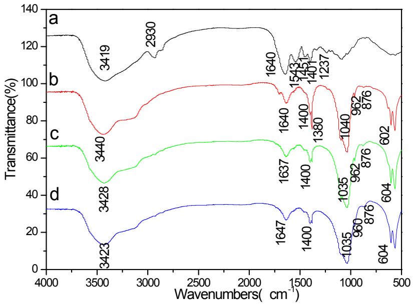

Figure 2. FT-IR spectra of some samples: a-pure collagen; b- HA; c-Col-HA; d-Col-HA/Gum A

Generally, the peaks related to hydroxyapatite are as follows: the peak of hydroxyl groups at 3440cm^{-1}; peaks at 1040 cm^{-1} and 602 cm^{-1} are coincident with phosphate group. CaO bands at 962 cm^{-1} and carbonate compounds at 1450, 1400 and 876 cm^{-1} (Chang MC, et al, 2002, Manso-Silván M, et al, 2003) also appeared (Figure 2b, d).The presence of -CO$_3$ bands indicated that the HA formed here was carbonate-substituted apatite, which was the same as bone apatite (Wahl DA, et al, 2006, Wahl DA, et al, 2007, Fanghanel J, et al, 2008).

From Fig.2c and Fig.2d, we knew that the changes before and after mineralization are mainly in the range of 500 ~ 1700 cm^{-1}. Both peaks of and nearly disappeared, indicating the formation of chemical bonds between between Ca^{2+} on HA and -COO$^-$ on collagen. The peaks at 3428 cm^{-1} and 1637 cm^{-1} moved to 3423 cm^{-1} and 1647 cm^{-1}, respectively, indicating the reaction between gum Arabic and Col-HA. The absorption peak of amide B was weakened or disappeared and the peak of amide A was located at a lower wavenumber of spectra in the Col-HA or the Col-HA/Gum A composites, indicating the formation of chemical bonds between the N-H groups and P-O. From the spectra, it is proved that a complex was formed between hydroxyapatite and collagen.

SEM

As can be seen in Fig.3, granular structure was formed in the Col-HA/Gum A composite, whilst it was smooth in Col-HA matrix.. In the preparation process, the fibrils around the hydroxyapatite microparticles might cover the particle surface. When some HA particles were prepared in the Col-Gum A solution, they might easily deposited in the Col-Gum A matrix and a tight structure was formed.

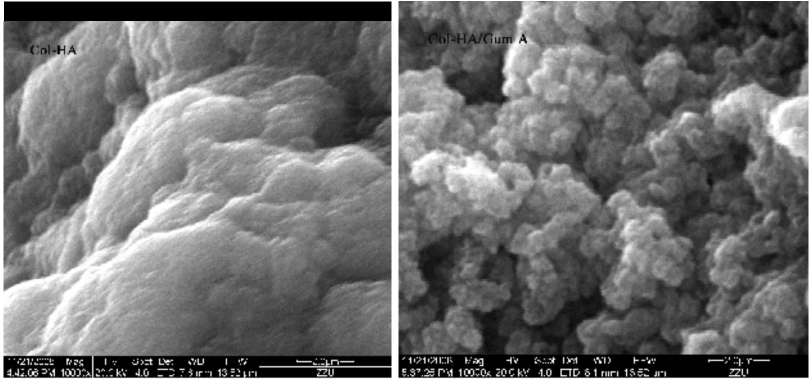

Figure 3. SEM of Col-HA and Col-HA/Gum A composites

X-ray Diffraction (XRD)

Figure 4 shows the XRD spectra of the prepared Col-HA/Gum A composite and a chicken bone. The inorganic phases in the samples were apatite with calcium and phosphate because no peaks of other Ca-P compounds were found.The XRD pattern of the composite (Fig. 4) shows broad peaks with poor crystallinity around the characteristic region near 32° (2*θ*), and the crystallographic structure was more identical with that of natural bone mineral.

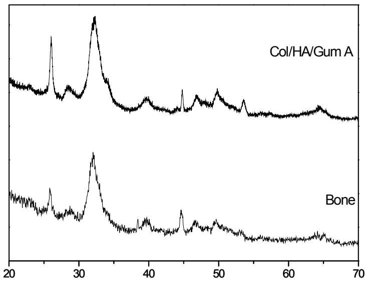

Figure 4. XRD patterns of the composite and natural chicken bone

Mechanical Properties

The Vickers hardness (HV) of the prepared Col-HA/Gum A composites was 82.98±6.94kg/mm, while the cortical HV was 48.84 ± 3.25 kg/mm^2 (Boivin G, et al, 2008). The compression property was shown in Table 1.

Table 1. Compression strength of the samples (n=5)

Samples	Compression modulus (GPa)	Compressive Strength (MPa)
Col-HA/Gum A	0.9674±43.85*	5.768±1.276*
Col-HA	0.8749±11.58	4.053±1.076
Dense Bone (Evans FG., 1969)	7-30	100-230
Spongy Bone (Evans FG., 1969)	0.05-0.5	2-12

* $p<0.05$

The compression modulus and compossive strength of the Col-HA/Gum A were much higher than those of Col-HA materials, indicateing that the Gum A modification improved the mechanical properties.

Hygroscopicity

The water absorption of the Col-HA/Gum A composite was 37% and that of the Col-HA composite was 42%, with a statistical significance ($p < 0.01$).

This property tells us the hydrophilic and hydrophobic of the material. It also reflects the polar groups on the matrix and the 3D structure of the matrix.

And Gum Arabic may react with collagen to reduce the number of polar groups on the matrix surface to decrease the water absorption. It can also be known from the differences between the FT-IR spectra (Fig.2) of Col-HA/Gum A and Col-HA composites: amide A peak moved to 3423 cm^{-1} from the 3428 cm^{-1}, and amide *I* peak moved to 1647 cm^{-1} from the 1637 cm^{-1}, respectively. Besides, the peak of amide B may be observed in the FTIR of Col-HA composite, while it disappeared completely in the Col-HA/Gum A composite.

Enzyme Degradation

As shown in Table 2, the difference in degradation rates is significant difference. By the addition of Gum A and cross-linked with glutaraldehyde, we can control the degradation of composite materials in vivo.

Table 2. Biodegradation degree of the Col-HA/Gum A and Col-HA composites (n=3)

Variable	Mean (%)	SD (%)
Col-HA/Gum A(a)	11.52	0.1815
Col-HA (a)	14.63	0.3905
Col-HA/Gum A(b)	1.596	0.1669
Col-HA (b)	2.319	0.2028

a- non-crosslinked; bcrosslinked with GA; SD-standard deviation;

Cytotoxicity

MEF-WT cells were cultured in the previous prepared extract of composites for 7days, and the morphological characteristics of the cells were observed every day. After cultured 2 days, the number of the cells was lower in the Col-HA/Gum A extract than in that of Col-HA or in the normal control, and it was higher in 50 % composite extraction solution than that of 100%,this phenomenon was also found on the follow days. It indicates that there is some cytotoxicity of Col-HA/Gum A.

The MTT assay revealed that the extracts of the materials in study affected the viability of MEF-WT cells, yet the cell relative growth rates (RGR) are no less than

75%, and the cytotoxicity of the composite is in grade (He Q, et al, 2007). It means that cytotoxicity is slight and the composite has a good cytocompatibility.

CONCLUSIONS

A composite with collagen, hydroxyapatite, and gum Arabic was prepared and characterized. It has good mechanical properties, water absorption, enzyme stability and good cytocompatibility and was expected to be an ideal material for bone repairing.

Acknowledgements

The financial supports from the National Natural Science Foundation Commission of China (No. 50973097, 21076199) and China-Romania Governmental Science & Technology Cooperation Program (No. 40-17) are gratefully acknowledged.

REFERENCES

Boivin, G., Bala, Y., Doublier, A., Farlay, D., Ste-Marie, L.G., Meunier, P.J. et al. (2008), "The role of mineralization and organic matrix in the microhardness of bone tissue from controls and osteoporotic patients", *Bone*, 43(3), 32-538.

Bonnier, F., Rubin, S., Debelle, L., Venteo, L., Pluot, M., Baehrel, B. et al. (2008), "FTIR protein secondary structure analysis of human ascending aortic tissues", *Journal of biophotonics*, 1(3), 204-214.

Chang, M.C., Tanaka, J. (2002), "FT-IR study for hydroxyapatite/collagen nanocomposite cross-linked by glutaraldehyde", *Biomaterials*, 23(24), 4811-4818.

Cliche, S., Amiot, J., Avezard, C., Gariepy, C. (2003), "Extraction and characterization of collagen with or without telopeptides from chicken skin", *Poultry science*, 82(3), 503-509.

Fanghanel, J., Gedrange, T., Proff, P. (2008), "Bone quality, quantity and metabolism in terms of dental implantation", *Biomedizinische, Technik*, 53(5), 215-219.

He, Q., Ao, Q., Wang, A., Gong, Y., Zhao, N., Zhang, X. (2007), "In Vitro Cytotoxicity and Protein Drug Release Properties of Chitosan/Heparin Microspheres", *Tsinghua Science & Technology*, 12(4), 361-365.

Liao, S., Watari, F., Zhu, Y., Uo, M., Akasaka, T., Wang, W. et al. (2007), "The degradation of the three layered nano-carbonated hydroxyapatite/collagen/PLGA composite membrane in vitro", *Dent Mater*, 23(9), 1120-1128.

Li, D., Mu, C., Cai, S., Lin, W. (2009), "Ultrasonic irradiation in the enzymatic extraction of collagen", *Ultrasonics Sonochemistry*, 16(5), 605-609.

Manso-Silván, M., Langlet, M., Jiménez, C., Fernández, M., Martínez-Duart, J.M. (2003), "Calcium phosphate coatings prepared by aerosol-gel", *Journal of the European Ceramic Society*, 23(2), 243-246.

Mao, J.S., Zhao, L.G., Yin, Y.J., Yao, K.D. (2003), "Structure and properties of bilayer chitosan-gelatin scaffolds", *Biomaterials*, 24(6), 1067-1074.

Muyonga, J.H., Cole, C.G.B., Duodu, K.G. (2004), "Fourier transform infrared (FTIR) spectroscopic study of acid soluble collagen and gelatin from skins and bones of young and adult Nile perch (Lates niloticus)", *Food Chemistry*, 86(3), 325-332.

Wahl, D.A., Czernuszka, J.T. (2006), "Collagen-hydroxyapatite composites for hard tissue repair", *European cells & materials*, 11, 43-56.

Wahl, D.A., Sachlos, E., Liu, C., Czernuszka, J.T. (2007), "Controlling the processing of collagen-hydroxyapatite scaffolds for bone tissue engineering", *Journal of materials science*, 18(2), 201-209.

Wiesmann, H.P., Joos, U., Meyer, U. (2004), "Biological and biophysical principles in extracorporal bone tissue engineering: Part II", *International journal of oral and maxillofacial surgery*, 33(6), 523-530.

Zhang, L., Tang, P., Zhang, W., Xu, M., Wang, Y. (2009), "Effect of chitosan as a dispersant on collagen-hydroxyapatite composite matrices", *Tissue engineering*, Apr., 13.

COMPATIBILITY OF BIODEGRADABLE COMPOSITES WITH GELATIN AND POLY(VINYL ALCOHOL)

XIPING GAO[1,2], KEYONG TANG[1], JIE LIU[1], YUQING ZHANG[2]

[1] *College of Materials and Engineering, Zhengzhou University, Zhengzhou 450052, China, email: keyongtang@yahoo.com.cn*

[2] *School of Chemical Engineering and Pharmaceutics, Henan University of Science and Technology, Luoyang 471003, China*

In this paper, the biodegradable composite films with different ratios of gelatin (Gel) and poly(vinyl alcohol) (PVA) were prepared by using a solution blending method. The compatibility between Gel and PVA in the biodegradable composite films was studied. The composite films were characterized by transmittance, infrared spectroscopy (IR), x-ray diffraction(XRD), scanning electron microscopy(SEM). According to the results of optic experiment, the opacity of composite film with the ratio of gelatin to PVA of 20:80 was lower than those of others, indicating a good compatibility between gelatin and PVA at the ratio. The results of IR, XRD, SEM also suggested an intense interaction and good compatibility between them.

Keywords: gelatin, poly(vinyl alcohol), compatibility.

INTRODUCTION

Nowadays, synthetic materials such as polyethylene, polypropylene, polystyrene and so on are widely used for different purposes including plastic packaging. Most of the synthetic materials are made of petroleum and not biodegradable. Petroleum is not renewable. Therefore, it is important and necessary to find alternatives for the traditional non-biodegradable and non-renewable materials. More and more people are paying attention to such environmental problems as "white pollution".

Gelatin is a kind of natural polymer which can be obtained easily with a wide resource. Gelatin is usually obtained by a controlled hydrolysis of the fibrous insoluble collagen, a protein widely found in nature and is the major constituent of skin, bones and connective tissue (A. Bigi, et al, 2001, Rivero, M.A et al, 2009, Pei Y., et al, 2001). Because of its excellent biodegradability, biocompatibility, film-forming ability, and so on (B.S. Chiou, et al, 2008, M. Cheng, et al, 2003, Y.Z. Zhang et al, 2006), it is widely used in many fields such as food, health care, cosmetic, packaging, and medical purpose (Y. Pranoto et al, 2007, S. Rivero, et al, 2010, H. J. Bae et al, 2009). However, pure gelatin film is breakable. It may be easily soluble in water and the mechanical properties are poor. (M. Y. Cheng et al, 2003, Y.Z. Wan, et al, 2001), which limits its applications as packaging materials in food, medicine, biomedicine fields, and so on. Therefore, crosslinking or blending was usually used to improve the properties of pure gelatin film.

Blending is an effective and convenient way to improve the performance of polymer materials (Z. Dong, et al, 2006). Many such natural polymers as chitosan, starch, sodium alginate, silk protein and such synthetic polymers as poly(vinyl alcohol) (PVA), poly lactic acid (PLA), and polyacrylamide have been blended with gelatin. Among these synthetic polymers, PVA is nontoxic and non-irritative. It is good in biodegradability, biocompatibility, film-forming, chemical resistance, and mechanical properties (P.Alexy et al, 2003, A. Sionkowska et al, 2009, A. Sionkowska et al, 2008). The physical properties and water resistant property of pure gelatin film may be greatly improved when PVA is blended with gelatin. The compatibility between gelatin and

PVA should be taken into consideration because gelatin is natural polymer and PVA is synthetic polymer.

In the present study, Gel/PVA composite films with different ratios of Gel and PVA were prepared using a solution blending method, and the compatibility between gelatin and PVA was studied by means of transmittance, infrared spectroscopy (IR), x-ray diffraction (XRD), scanning electron microscopy (SEM), respectively.

MATERIALS AND METHODS

Materials

Gelatin (type B from bovine bone, analytical grade) was purchased from Tianjin Kermel Chemical Reagent Co., Ltd., Tianjin, China. Poly(vinyl alcohol) (PVA) was from Anhui Wanwei High-tech Materials Industry Co., Ltd., Anhui, China.

Preparation of Composite Films

The composite films were produced from a mixture of the solutions (gelatin, solution A; PVA, solution B) using a casting technique. To prepare solution A, 10wt% , the gelatin was vacuum dried for 30 min, weighed, and then dissolved in 55°C water for about 20 min until completely dissolved. For solution B, 10wt%, PVA was homogenized in distilled water and then dissolved at 90°C for 30 min. Solution A and solution B were mixed in 40°C distilled water for about 30 min to yield the film forming solutions with different ratios of gelatin and PVA. The ratios of gelatin to PVA were 0:100, 20:80, 30:70, 40:60, 50:50, 60:40, 80:20, and 100:0, respectively. The resulting film-forming solutions were cast on polypropylene plates (15×15 cm) and dried at room temperature.

Opacity

The absorbency of the films was recorded on an UV-Vis spectrophotometer (7200 Unic, China). The composite films were sampled into rectangle pieces and placed in a spectrophotometer test cell. Air was used as the reference. The areas under the absorption curves from 400 to 800 nm were recorded, and the opacity of the films was calculated according to the following equation:

$$\text{Opacity(T)} = A_{500} \times 500 / L \qquad (1)$$

where A_{500} is the absorption at 500 nm and L is the composite film thickness (um). All the samples were measured three times and the averages were reported.

Fourier-Transform Infrared Spectroscopy (FTIR)

Fourier-transform infrared spectroscopy of composite films was carried out using an infrared spectroscopy instrument (NICOLET, USA) ranging from 4000-500cm^{-1}.

X-ray Diffraction (XRD)

The structure of the Gel/PVA composite films was characterized by XRD. All XRD data was collected using a D8 Advance X-ray diffraction instrument (BRUKER Ltd. Germany). The scanning 2θ range was from 2° to 40°.

Scanning Electron Microscopy (SEM)

Morphology of the cross-section of films was performed using a scanning electron microscope (JSM－5610LV, JEOL Ltd. Japan). Fractured films were then fixed evenly and erectly on stubs using copper conducting adhesive tape to observe the cross-section morphology of the films, respectively. After being coated with gold, the samples were observed under SEM.

RESULTS AND DISCUSSION

FTIR Spectroscopy

In order to investigate the interaction between Gel and PVA, Fourier-transform infrared spectroscopy was used to study the effects of hydrogen bonding on gelatin and PVA in terms of molecular and supermolecular structure. Interaction of hydrogen bonding between gelatin and PVA may reduce the Gibbs free energy of the blending system, providing a good compatibility between the them in the composite films.

Figure 1 showed the FTIR spectra of pure Gel film, pure PVA film and the Gel/PVA composite film with the Gel/PVA ratio of 20:80. In the infrared spectroscopy of pure PVA film, the peak at 3281cm^{-1} was attributed to the stretching band of bounded –OH, the one at 1461cm^{-1} was the bending vibration of CH-OH, and the one at 1091cm^{-1} was associated with the stretching band of C-O. In pure gelatin infrared spectroscopy, the peak at 1633 cm^{-1} was related to the C=O stretching (amide I), the one at 1539cm^{-1} was the stretching (amide II) of N-H and C-N, and the one at 1230cm^{-1} should be the stretching (amide III) of N-H and C-N. In the infrared spectroscopy of Gel/PVA composite film, the changes in the absorption band of amide I, amide II, and amide III of gelatin can be clearly observed. The absorption band of amide I changed from 1633 cm^{-1} to1651 cm^{-1}, that of amide II varied from 1539 cm^{-1} to1557 cm^{-1}, while that of amide III changed from 1230 cm^{-1} to1237 cm^{-1}. From these results, it is suggested that between gelatin and PVA, there exists interactions such as hydrogen bonding to provide a good compatibility between them.

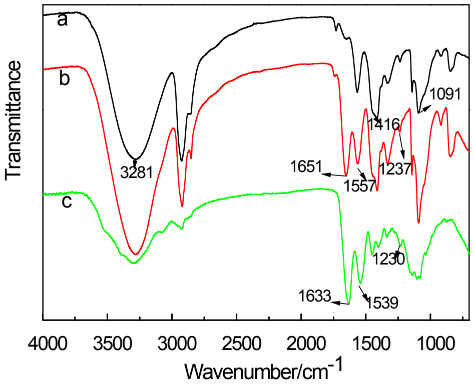

Figure 1. FT-IR spectra of PVA, gelatin and Gel/PVA composite films (a)- PVA film; (b)- Gel/PVA film at ratio of 20:80; (c)- Gel film

Opacity

In order to further study the compatibility between gelatin and PVA, opacity of the composite films was measured. The opacity of the composite films is contrary to transmittance. The lower the opacity of composite films is, the better is the transmittance of the composite films. A lower transmittance indicates a better compatibility between the components in the system.

Table 1. Opacity and absorption of the composite films with different gelatin /PVA ratios

m(Gel):m(PVA)	T
100:0	1.093
80:20	0.826
60:40	0.722
50:50	0.941
40:60	0.695
30:70	0.656
20:80	0.461
0:100	0.423

Table 1 showed that the opacity of the composite films with different Gel/PVA ratios. It should be noted that pure Gel film is lightly yellow and pure PVA film is colorless. The opacity of pure Gel film was the highest and that of pure PVA film was lowest. The opacity of the composite films decreased gradually with increasing the PVA content. In the study, it was observed that the surface of the composite film with the Gel/PVA ratio of 20:80 was smooth and transparent, while the surfaces of the composite films with the Gel/PVA ratios of 40:60, 50:50, and 60:40 were not smooth. According to the opacity results, the opacity of the composite film with the Gel/PVA ratio of 20:80 was the lowest in all composite films. There may be a strong interaction in the composite film with the Gel/PVA ratio of 20:80 to provide a good compatibility between Gel and PVA. The result was accordant with that obtained in the FTIR spectroscopy above.

X-ray Diffraction Analysis

Figure 2 showed the X-ray diffraction patterns of Gel, PVA, and Gel/PVA composite films. In Figure 2, the diffraction pattern of PVA consisted of two obvious crystalline peaks. One is at 2θ= 8.7° for close molecular packing, and the other is at 19.8° for regular crystallization. For gelatin, there is a typically crystalline peak at 2θ = 8.8°, showing that Gel was a low crystalline polymer. In the X-ray diffraction patterns of Gel/PVA composite films (Figure 2), the diffraction peaks at 19.8° of PVA decreased and a new diffraction peak at 29.3° appeared. The strong interaction between Gel and PVA may destroy the close packing of the PVA and regular crystallites can not be formed. A new diffraction peak at 9.7° appeared at the Gel/PVA ratios of 20:80, 40:60, 60:40, and the biggest intensity of diffraction peak at 9.7° was the one at 20:80. This was probably because the stronger interaction between Gel and PVA at the ratio. So it was suggested that the stronger the interaction between Gel and PVA results in a good compatibility between them at the Gel/PVA ratio of 20:80.

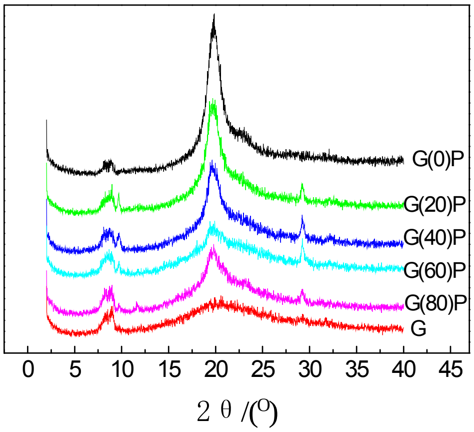

Figure 2. XRD patterns of Gel, PVA and Gel/PVA composite films G-Gel, P-PVA

Scanning Electron Microscopy

The SEM micrographs of cross-section of pure gelatin film, pure PVA film and composite film with the Gel/PVA ratio of 20:80 were shown in Figure 3. In Figure 3(a) and Figure 3(c), the cross-sections of both pure PVA film and pure Gel film were homogeneous. The cross-section of pure gelatin film was smooth, a brittle fracture feature, suggesting that the pure gelatin film is brittle. For pure PVA film, the cross-section was not even with a ductile fracture, indicating that the pure PVA film was flexible. For the cross-section of composite film as shown Figure 2(b), no phase separation can be observed. Therefore, there is an intense interaction between the two components to behave a good compatibility. The cross-section of the composite film is not even and fracture mode of the composite film was flexible. So PVA could improve flexibility of the pure gelatin film.

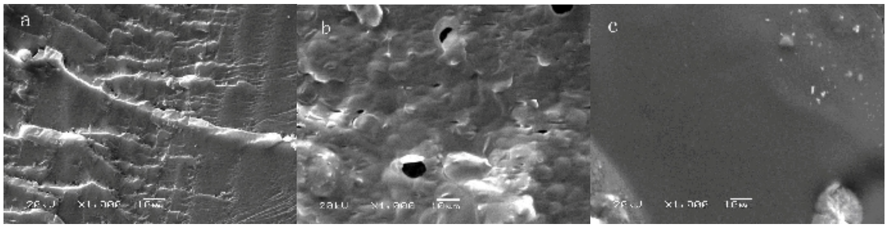

Figure 3. SEM micrographs of fracture surfaces of Gel, PVA and Gel/PVA films (a)-PVA film; (b)-Gel/PVA film at ratio of 20:80; (c)-Gel film

CONCLUSIONS

Gel/PVA composite films were prepared using a solution blending method. The structure of Gel/PVA composite films was characterized by IR, SEM, XRD. It was revealed that there is an intense interaction and good compatibility between gelatin and PVA at the ratio of Gel/ PVA of 20:80.

Acknowledgements

The financial supports from the National Natural Science Foundation Commission of China (No. 50973097, 21076199) and China-Romania Governmental Science & Technology Cooperation Program (No. 40-17) are gratefully acknowledged.

REFERENCES

Alexy, P., Bakos, D., Crkonova, G. et al. (2003), "Poly(vinyl alcohol)–collagen hydrolysate thermoplastic blends: II. Water penetration and biodegradability of melt extruded films", *Polymer Testing*, 22, 811–818.

Bae, H.J., Park, H.J., Hong, S.I. et al. (2009), "Effect of clay content, homogenization RPM, pH, and ultrasonication onmechanical and barrier properties of fish gelatin/montmorillonite nanocomposite films", *LWT - Food Science and Technology*, 42, 1179-1186.

Bigi, A., Cojazzi, G., Panzavolta, S. et al. (2001), "Mechanical and thermal properties of gelatin films at different degrees of glutaraldehyde crosslinking", *Biomaterials*, 22, 763-768.

Cheng, M., Deng, J., Yang, F. (2003), "Study on physical properties and nerve cell affinity of composite films from chitosan and gelatin solutions", *Biomaterials*, 24, 871-2880.

Cheng, M.Y., Deng, J.G. (2003), "Study on physical properties and nerve cell affinity of composite films from chitosan and gelatin solution", *Biomaterials*, 24(17), 2871-2880.

Chiou, B.S., Avena-Bustillos, R.J., Bechtel, P.J. et al. (2008), "Cold water fish gelatin films: Effects of cross-linking on thermal, mechanical, barrier, and biodegradation properties", *European Polymer Journal*, 44, 3748-3753.

Dong, Z., Wang, Q., Du, Y. (2006), "Alginate/gelatin composite films and their properties for drug controlled release", *Journal of Membrane Science*, 280, 37–44.

Moscato, S., Mattii, L., Alessandro, D. et al. (2008), "Interaction of human gingival fibroblasts with PVA/gelatine sponges", *Micron*, 39, 569–579.

Pei, Y., Zheng, X.J., Tang, K.Y. (2001), "Natural Polymer Composites with Collagen and Gelatin as the Matrices: A Review", *Polymer Bulletin*, 58-68.

Pranoto, Y., Lee, C.M., Park, H.J. (2007), "Characterizations of fish gelatin films added with gellan and k-carrageenan", *LWT*, 40, 766–774.

Rivero, S., García, M.A., Pinotti, A. (2010), "Correlations between structural, barrier, thermal and mechanical properties of plasticized gelatin films", *Innovative Food Science and Emerging Technologies*, 11, 369–375.

Rivero, S., García, M.A., Pinotti, A. et al. (2009), "Composite and bi-layer films based on gelatin and chitosan", *Journal of Food Engineering*, 90, 531-539.

Sionkowska, A., P1anecka, A., Koz1owska, J. et al. (2009), "Photochemical stability of poly(vinyl alcohol) in the presence of collagen", *Polymer Degradation and Stability*, 94, 383–388.

Wan, Y.Z., Wang, Y.L., Cheng, G.X. et al. (2001), "Properties of Carbon Fiber Reinforced Gelatin Composites", *Polymer Materials Science and Engineering*, 17(4), 86-89.

Zhang, Y.Z., Venugopal, J., Huang, Z.M. et al. (2006), "Crosslinking of the electrospun gelatin nanofibers", *Polymer*, 47, 2911–2917.

THE INFLUENCE OF CROSSLINKING AGENT ON KINETIC RELEASE AND RHEOLOGICAL BEHAVIOUR OF SOME COLLAGEN-NIFLUMIC ACID HYDROGELS

MIHAELA VIOLETA GHICA[1], MADALINA GEORGIANA ALBU[2], GHEORGHE COARA[2], CRISTINA DINU-PÎRVU[1]

[1] *"Carol Davila" University of Medicine and Pharmacy, Faculty of Pharmacy, Physical and Colloidal Chemistry Department, 6 Traian Vuia Str, 020956, Bucharest, Romania*

[2] *INCDTP - Division: Leather and Footwear Research Institute, 93 Ion Minulescu St., 031215, Bucharest, Romania, email: albu_mada@yahoo.com*

Five different collagen hydrogels were developed and characterized in terms of flow and kinetic properties. The niflumic acid was selected as a non-steroidal anti-inflammatory drug model. The influence of two cross-linking agents (glutaraldehyde and tannic acid) was analyzed. The rheological behaviour was investigated by rotational measurements. The tested hydrogels exhibited non-newtonian pseudoplastic properties, the viscosity decreasing with the shear rate increase. The collagen supports with niflumic acid showed a drug release diffusional mechanism. The kinetic parameters specific to the square root of time model, namely the diffusion coefficient and time-lag, were evaluated. The determined rheological and kinetic parameters were strongly influenced by the nature of the crosslinking agents used for the hydrogels preparation.

Keywords: collagen hydrogels, niflumic acid, kinetic release, rhelogical behaviour.

INTRODUCTION

Cutaneous wound healing is a complex multifactorial dynamic process having as result the wound contraction and closing, and the functional barrier restoration. The wound healing process can be impaired by multiple factors, ranked as local and systemic factors, that affect one or more phase of the process. Thus, the cutaneous wound healing consists of a succession of events, including haemostatis, inflammation, proliferation and remodeling (Menke et al. 2008; Ghica et al. 2011). The healing process event phases have to occur in a precise and regular sequence. If this process is interrupted or prolonged, this can induce delays in the wound healing or even a non-healing chronic wound (Guo and DiPietro 2010; Albu et al. 2012).

Among the drugs facilitating the post-wound inflammatory response and having strong analgesic, anti-inflammatory and antipyretic effects we can mention the non-steroidal anti-inflammatory drugs (NSAIDs). The NSAIDs are used following the soft tissue injuries due to their capacity of reducing the persistent and temporary pain and inflammation near the injuried area by inhibiting the cyclooxygenase activity, without determining a delay in epithelial healing (Krischak et al. 2007; Su et al. 2010).

NSAIDs are however the most frequent cause of the lethal drug toxicity as the gastro-intestinal bleeding, being classified by the Federal Drug Administration as the most frequent cause for the side effects induced by the drugs (responsible for about one quarter of the reported side effects) (Mathy et al. 2005). In order to minimize the side effects of these drugs, an alternative to their oral administration route was searched, that ensures a reduced incidence of the systemic side effects and avoids the factors influencing the gastro-intestinal absorption and also the limitations imposed by the intestinal and hepatic passage effect (Heyneman et al. 2000). Topical drug delivery systems with biodegradable polymeric support represent a suitable vehicle for NSAIDs release. Among these polymers, collagen is an adequate carrier for drug delivery, offering the advantage of a natural biomaterial with haemostatic and wound healing properties (Albu et al. 2011) and also having the capacity to be modeled in various forms, the hydrogels being the vehicles selected for this work.

In order to improve the resistance to biodegradability, the biological stability and the mechanical properties, the collagen gels are subjected to a crosslinking process (Meade and Silver 1990). The crosslinking agents selected in this study were the glutaraldehyde and the tannic acid. The glutaraldehyde is one of the most used cross-linking agents (Lungu et al. 2011), while the tannic acid is a natural cross-linking agent having also antibacterial, antioxidant, astringent and haemostatic properties (Ghica et al. 2009).

Thus, the aim of this study was the developement of some collagen-based topical hydrogels with niflumic acid as a NSAIDs drug model, and the investigation of the influence of different cross-linking agents on their rheological and kinetic properties.

MATERIALS AND METHODS

Materials

Type I fibrillar collagen (C) gel having a concentration of 2.54% (w/w) and pH 2.5 was extracted from calf hide by the currently used technology in Collagen Department of Division Leather and Footwear Research Institute, as previously described (Albu 2011). Niflumic acid (NA) was supplied from ICN Biomedicals Inc. (USA). Glutaraldehyde (GA) and tannic acid (TA) were purchased from Sigma-Aldrich (Germany). Sodium hydroxide, monobasic potassium phosphate and disodium hydrogen phosphate were obtained from Merck (Germany). All the chemicals were of analytical grade and the water was distilled.

Collagen Hydrogels Preparation

Reference hydrogel having the concentration 1.0% and pH 7.4 was prepared from the initial collagen gel under stirring with distilled water and NaOH 1M solution. 0.25% niflumic acid reported to the amount of reference collagen hydrogel was added and some collagen-niflumic acid hydrogels were obtained. The niflumic acid was incorporated after a prior dissolution in NaOH 1M solution. The hydrogels were then cross-linked with glutaraldehyde and tannic acid and stored for 24h at 4°C for maturation and/or cross-linking process. The composition of the collagen formulations is presented in Table 1.

Table 1. Composition of hydrogels

Hydrogel	Collagen C (g%)	Niflumic acid NA (g%)	Glutaraldehyde GA (g%)	Tannic acid TA (g%)
G1	1	0	0	0
G2	1	0.25	0	0
G3	1	0.25	0.005	0
G4	1	0.25	0	0.005
G5	1	0.25	0.005	0.005

*the amounts of C, NA, GA and TA are reported to 100g hydrogel

Rheological Analysis

The rheological behaviour of the tested hydrogels was analyzed using a rotational viscometer Multi-visc Rheometer-Fungilab equipped with standard spindle TR 9 and ultrathermostat ThermoHaake P5. The rheological experiments were performed in triplicate at 23°C±0.5°C and 37°C±0.5°C.

In vitro Niflumic Acid Release Study

Niflumic acid *in vitro* release was evaluated using a modified Franz diffusion cell fitted with a standard cellophane membrane (Autogen Bioclear Ltd) and a peristaltic pump (Masterflex, Cole-Parmer Instrument Company) as previously reported (Ghica et al. 2011). Briefly, about 1 g from each formulation was applied on the artificial membrane surface. Prewarmed phosphate buffer pH 7.4 at 37°C was used as receiving medium and was continuosly stirred by a rotating teflon coated magnet placed inside the cell. The amount of niflumic acid released at predetermined time intervals was spectrophotometrically assayed at 287 nm (Perkin-Elmer spectrophotometer), using the calibration curve, linear for concentrations in the range 0-0.001 g/100mL ($A_{1\%}^{1cm} = 777$, R = 0.9986). Three replicates of each kinetic experiment were performed.

RESULTS AND DISCUSSION

The rheological data recorded for the tested hydrogels at 23°C and 37°C conducted to the rheograms shear stress versus viscosity presented in Figure 1a-b.

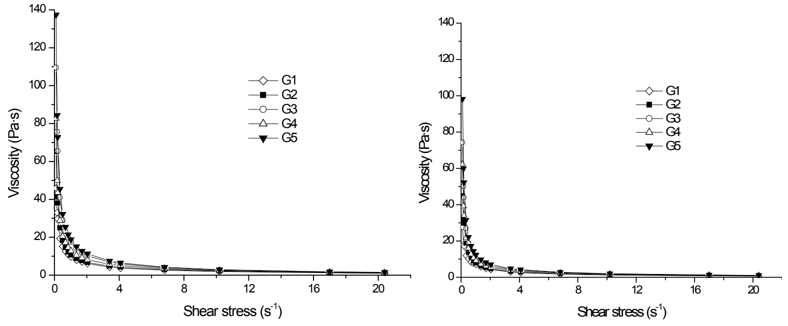

Figure 1. Plots of viscosity as a function of shear stress for the collagen hydrogels evaluated at a) 23°C and b) 37°C

From the rheological profiles illustrated in Figure 1a-b we can notice that the designed hydrogels viscosity (η) decreases for the shear rate increase ($\dot{\gamma}$) at both experimental temperatures. This trend indicates the pseudoplastic behaviour for the collagenic semisolid dosage forms which facilitates the formulations flow (Ortan et al. 2011, Dinu-Pîrvu et al. 2012).

The equation that characterizes the flow behaviour of the designed hydrogels has the following expression (eq. 1):

$$\eta = m \cdot \dot{\gamma}^{-n} \qquad (1)$$

where, m and n are parameters correlated with the analyzed supports formulation factors (Dolz-Planas et al. 1992) and determined through the linearization of equation (1) by double logarithmic method. It can be assessed that m value matches the viscosity obtained for the shear rate of $1\cdot s^{-1}$ (the logarithm for the shear rate equal to one is zero). In all cases the determination coefficient R^2 value was superior to 0.99. The values of the above mentioned constants and of R^2 specific to the model describing the relation between viscosity and shear stress are given in Table 2.

Table 2. The values of the m and n parameters and the determination coefficients specific to the eq. (1) applied to collagen hydrogels

Hydrogel	Temperature					
	23°C			37°C		
	m	n	R^2	m	n	R^2
G1	9.760	0.676	0.9992	6.455	0.618	0.9948
G2	10.867	0.772	0.9991	8.342	0.743	0.9970
G3	17.812	0.795	0.9988	11.212	0.827	0.9984
G4	12.273	0.816	0.9967	9.154	0.828	0.9994
G5	18.258	0.871	0.9991	12.294	0.899	0.9995

From Table 2 we can ascertain that the value of parameter m is lower at 37°C compared to 23°C for all the systems tested, recording a decrease of 1.3 to 1.6 times. This behaviour can be explained by the polymeric chains mobility increase, which leads to the system fluidization.

For the same temperature the influence of the cross-linking agent on flow behaviour can be noticed. Thus, the presence of GA in G3 gel leads to a higher viscosity compared to G4 which is cross-linked with TA, m value being about 1.45 times higher at 23°C and 1.22 times higher at 37°C, and 1.64 times higher at 23°C and 1.34 times higher at 37°C respectively compared to G2 - the uncross-linked hydrogel with NA. It seems that the used GA amount determines a higher cross-linking degree compared to TA. Obviously, the simultaneous presence of the two cross-linking agents from G5 formulation enfaces the highest viscosity to the system. A slight increase of the G2 viscosity can also be noticed for NA addition compared to the reference hydrogel G1.

Further we analyzed the influence of the formulation on the NA release from hydrogels G2÷G5. The kinetic profiles plotted as drug cumulative released percent versus time are illustrated in Figure 2a.

For the determination of the drug release mechanism from collagen hydrogels, the general equation proposed by Peppas was applied:

$$\frac{m_t}{m_\infty} = k \cdot t^n \tag{2}$$

where m_t is the amount of drug released at time t, m_∞ is the total drug contents in the tested collagen hydrogels, m_t/m_∞ is the fractional release of the drug at the time t, k is the kinetic constant, and n is the release exponent, indicating the mechanism of drug release (Ghica et al. 2011). The highest values for the determination coefficient R^2 (Table 3) were obtained for Higuchi model (n=0.5), which means that this model describes best the NA release behaviour. The niflumic acid percentage released varied between 32.92% (G5) and 43.03% (G2) during 180 minutes.

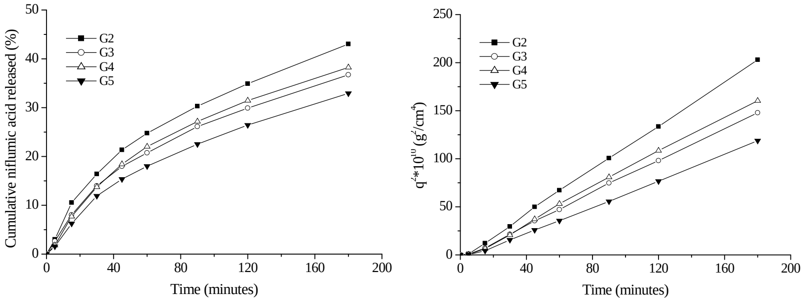

Figure 2. a) Plots of NA cumulative released percent as a function of time; b) Linear plots of q^2 as a function of time

The kinetic parameters specific to Higuchi model, namely the diffusion coefficient (eq. 3) and time-lag are presented in Table 3:

$$D = \frac{q^2 \cdot \pi}{4 \cdot C_0^2 \cdot t} \tag{3}$$

where, q is the drug amount released per membrane unit area, C_0 is the initial drug concentration in the donor medium, D is the drug diffusion coefficient and t is the drug release time. The time-lag is evaluated from the regression line q^2 depending on time. The linear dependence between q^2 and time is shown in Figure 2b.

Table 3. Determination coefficient and kinetic parameters specific for Higuchi model

Hydrogel	Determination coefficient	Diffusion coefficient ($cm^2/s \cdot 10^{+6}$)	Time-lag (min)
G2	0.9993	14.37	2.60
G3	0.9990	10.55	3.36
G4	0.9980	11.57	4.17
G5	0.9981	8.44	5.58

Analyzing the kinetic results given in Table 3 we can observe that the kinetic results are in accordance with the ones obtained from the rheological profiles analysis. Thus, the most viscous hydrogel has the lowest diffusion coefficient value and the highest time-lag value. Smaller D and time-lag values can be noticed for G3 compared to G4. The highest diffusion coefficient value is obtained for the uncross-linked hydrogel G2, noticing an increase of 36.21%, 24.20%, 70.26% in comparison with the G3 hydrogel cross-linked with GA, with the G4 hydrogel cross-linked with TA and with the G5 hydrogel containing both cross-linking agents, respectively. Similarly, the smallest time-lag value is obtained for the same uncross-linked hydrogel G2, of about 22.62% - 53.40% smaller compared to the above mentioned cross-linked hydrogels.

The release kinetic of a drug depends on its chemical nature, but also on the rheological properties of the semisolid support. Therefore it was also necessary to evaluate the kinetically analysed hydrogels from the rheological point of view because the rheological behaviour of the systems analyzed as result of the interactions between the formulation factors influences the medium where the drug release takes place, respectively its diffusion through the hydrogel up to the membrane surface.

CONCLUSIONS

The hydrogels designed in this study showed a non-newtonian pseudoplastic behaviour. The tested collagenic supports with niflumic acid showed a drug release diffusional mechanism. Both the kinetic and rheologic results show the marked influence of the cross-linking agent presence in the formulation. By modulation of the cross-linking agent quantity as well as by combination of the two cross-linking agents in different proportions, the composition can be modeled obtaining hydrogels with a flow behaviour and a kinetic profile suitable to the therapeutic indication and the application site, the cutaneous wound treatment respectively.

Acknowledgements

This work was financially supported by ANCS-UEFISCDI, Capacities Programme PN-2, Module III, Bilateral Cooperation People Republic of China and Romania, project number 502/18.03.2011.

REFERENCES

Albu, M.G. (2011), “Collagen Gels and Matrices for Biomedical Applications”, *Lambert Academic Publishing, Saarbrücken*, 23-24.

Albu, M.G., Titorencu, I. and Ghica, M.V. (2011), “Collagen-based Drug Delivery Systems for Tissue Engineering. In: Pignatello, R. (ed.) Biomaterials Applications for Nanomedicine”, *Intech Open Acces Publisher, Rijeka*, 339.

Albu, M.G., Ferdeş, M., Kaya, D.A. et al. (2012), “Collagen Wound Dressings with Anti-inflammatory Activity”, *Mol. Crys. Liq. Crys.*, 555, 271-279.

Dinu-Pîrvu, C., Ghica, M.V., Ivana, S. et al. (2012), “Formulation and Physico-Chemical Characterization of Piroxicam-based Carbomer-Hydrogels”, *AMHB*, 1(1), 7-16.

Dolz-Planas, M., Gonzalez-Rodriguez, F. and Dominguez Herraez, M. (1992), “The Influence of Neutralizer Concentration on the Rheological Behaviour of 0.1% Carbopol Hydrogels”, *Pharmazie*, 47 (5), 351-355.

Ghica, M.V., Albu, M.G., Popa, L. et al. (2009), “Drug Delivery Systems based on Collagen-Tannic Acid Matrices”, *Rev. Roum. Chim.*, 54(11-12), 1103-1110.

Ghica, M.V., Albu, M.G., Leca, M. et al. (2011), “Design and Optimization of some Collagen-Minocycline based Hydrogels Potentially Applicable for the Treatment of Cutaneous Wound Infections”, *Pharmazie*, 66 (11), 853–861.

Guo, S. and DiPietro, L.A. (2010), “Factors Affecting Wound Healing”, *J. Dent. Res.*, 89 (3), 219-229.

Heyneman, C.A., Lawless-Liday, C. and Wall, G.C. (2000), “Oral versus Topical NSAIDs in Rheumatic Diseases: A Comparison”, *Drugs*, 60 (3), 555-574.

Krischak, G.D., Augat, P., Claes, L. et al. (2007), “The Effects of Non-steroidal Anti-inflammatory Drug Application on Incisional Wound Healing in Rats”, *J. Wound Care*, 16 (2), 76-78.

Lungu, A., Titorencu, I., Albu, M.G. et al. (2011), “The Effect of BMP-4 Loaded in 3D Collagen-hyaluronic Acid Scaffolds on Biocompatibility Assessed with MG 63 Osteoblast-like Cells”, *Dig. J. Nanomater. Bios.*, 6 (4), 1897-1908.

Mathy, F.X., Lombry, C., Verbeeck, R.K. et al. (2005), “Study of the Percutaneous Penetration of Flurbiprofen by Cutaneous and Subcutaneous Microdialysis after Iontophoretic Delivery in Rat”, *J. Pharm. Sci.*, 94 (1), 144-152.

Meade, K.R. and Silver, F.H. (1990), “Immunogenicity of Collagenous Implants”, *Biomaterials*, 11 (3), 176-180.

Menke, M.N., Menke, N.B., Boardman, C.H. et al. (2008), “Biologic Therapeutics and Molecular Profiling to Optimize Wound Healing”, *Gynecol. Oncol.*, 111 (2 Suppl.), S87–S91.

Ortan, A., Dinu-Pîrvu, C., Ghica, M.V. et. al. (2011), “Rheological Study of a Liposomal Hydrogel based on Carbopol”, *Rom. Biotech. Lett.*, 16 (1 Suppl.), 47-54.

Su, W.H., Cheng, M.H., Lee, W.L. et al. (2010), “Nonsteroidal Anti-inflammatory Drugs for Wounds: Pain Relief or Excessive Scar Formation?”, *Mediators of Inflammation*, aticle ID 413238.

CHARACTERIZATION AND APPLICATION OF COLLAGEN-POLYMER BASED COMPOSITE AS WOUND HEALING MATERIAL

DENİZ GÜRLER, EYLEM KILIÇ

Uşak University Department of Leather Engineering, 64200, Uşak, Turkey,
deniz.celik@usak.edu.tr, eylem.kilic@usak.edu.tr

Enzymatically derived collagen hydrolysate powder which is well-known with its good compatibility with skin and mucous membrane and thermoplastic polyurethane based synthetic polymer were used for the preparation of composite films as wound healing material. Prepared composite films were characterized and images of materials were taken using a scanning electron microscope. The wound healing pattern of collagen-polymer grafts were investigated in rabbits and additional preliminary clinical trials were conducted on diabetic foot ulcers to test the applicability of materials.

Key words: collagen hydrolysate, collagen-polymer composites, woundhealing material.

INTRODUCTION

Skin replacement is a procedure to reconstitute dermis in case of extensive damage and loss of skin. The most frequently used methods to replace skin loss include covering the wound site with autografts, homografts and heterografts. Autografts may not be available due of scarcity of donor sites. Homografts and heterografts are very expensive, difficult to obtain, and difficult to store for prolonged periods (Travis et al 1987).These difficulties might be easily avoided by developing inexpensive biological or artificial skin substitutes. For this purpose both artificial and natural polymers such as collagen have been used. Collagen and hydrolyzed collagen which are derived from animal by-products and skin are natural substrates for cellular attachment, growth and differentiation, and promotes cellular proliferation and differentiation which are important parameters for wound dressing materials (Ruszczak 2003).

This study aimed at developing and investigating the applicability of a new collagen based material as wound dressing material. Animal experiments and preliminary clinical experiments were conducted on patients who have diabetic foot ulcers.

MATERIALS AND METHOD

Animal skin derived collagen hydrolysate, Nutrilon Powder-I was obtained from Cognis Chemicals Company. Polyurethane based synthetic polymer at biomedical grade, Pellethane 2363-80 A was purchased from Dow Company. N,N-dimethylformamide is used as solvent.

In order to obtain a proper film, various amounts of collagen hydrolysate 0.5, 1.0, 2 g and 0.5, 1.0, 2.0, 2.5g of polymer were used. Prior to film preparation, polymer was dissolved in N,N-dimethyl diformamide (Pişkin 1987).Mixing ratio of solvent and polymer-collagen is an important parameter, therefore 0.08g polymer and collagen hydrolysate was dissolved in 1 ml of solvent considering the previous studies (Tuncel 1997). The film preparation procedure is presented in Figure 1.

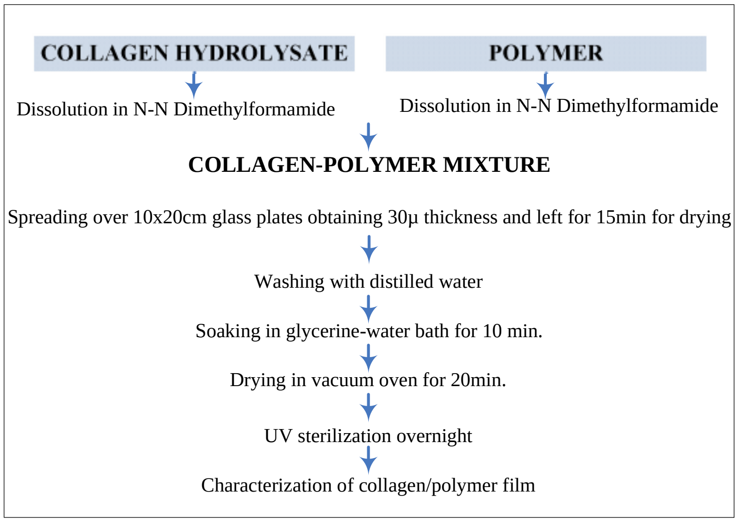

Figure 1. Flow diagram of the collagen-polymer film preparation procedure

RESULTS AND DISCUSSION

The optimum collagen:polymer mixing ratio which enables the best proper film formation was determined as 0.5:1 and 1:1. These materials are called as A type and B type respectively, and further studies were conducted using these two types of collagen-polymer films (Figure 2).

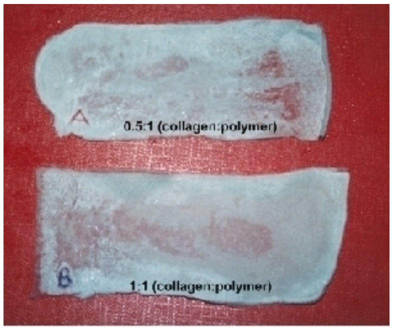

Figure 2. A and B type collagen-polymer films

Characterization of Collagen-Polymer Films

A and B type materials were characterized by determination of pH, thickness, tensile strength and elongation at break, colour and water vapour permeability properties. The experiments were performed in triplicate and the results are presented in Table 1 by the mean values.

Table 1. Properties of collagen-polymer films

	A type	B type
pH	6.4	6.3
Thickness	0.22mm	0.23mm
Tensile strength	8.69 daN/cm^2	6.08 daN/cm^2
Elongation	463%	426%
Colour (L, a, b)	91.68, -0.84, 7.36	93.55, -0.78, 5.56
Water vapour permeability	3153mg/1000mm^2 24h	3013mg/1000mm^2 24h

The thickness of collagen films were measured following the spreading of collagen-polymer mixture over glass plates. Thickness values of collagen films are comparative with the previous studies conducted on collagen based biomaterials (Oran 1999, Lee et al., 2001).Higher tensile strength and elongation properties of A type collagen films reveals that A type has higher mechanical strength and elastic in comparison to B type material..Spectrophotometric colour measurements of collagen-polymer films revealed that increasing collagen amount does not affect the colour of material and both films have white colour. A type material has better water vapour permeability property, mainly due to its higher porosity.

Scanning Electron Microscopy (SEM)

SEM micrographs of A and B type collagen-polymer films were taken at x35, x1000, and x3500 magnifications (Figure 3). B type material had the smallest average pore diameter of 0,62µm and lower porosity. Decrease in polymer concentration increased porosity and resulted in larger pores at A type film, which might provide better attachment of cells during woundhealing and improve recovery time (Vasita 2006).

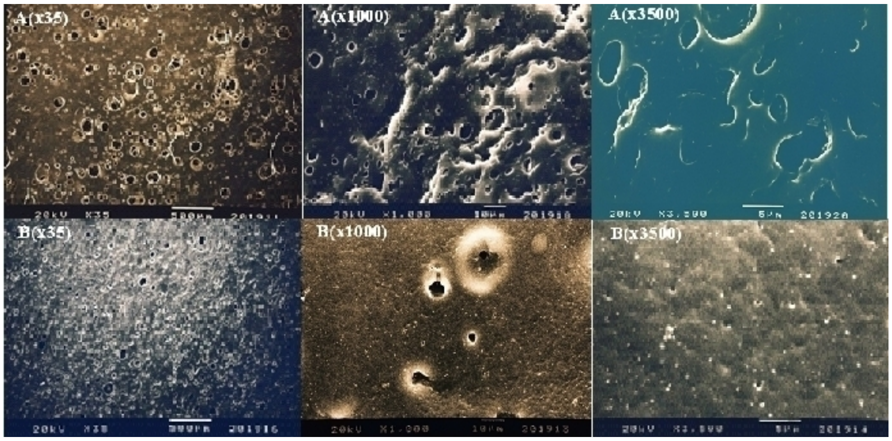

Figure 3. SEM micrographs of A and B material with x35, x1000 and x3500 magnifications

Animal Experiments and Preliminary Clinical Trials

Figure 4 shows the rabbit skin grafting experimental procedures. Eight New Zealand rabbits were selected for the study. Animals were anesthetized and open wounds (1.5x3.0cm) were made under aseptic conditions on lateral chest and abdominal barrier of rabbits (Fig 4a, b). Following the excision of the skin, the grafts cut into the same dimensions were placed on the wound bed (Fig 4c) and sutured to skin by surgical sutures (Fig 4d). The grafted areas were covered with sterile gauze and bandaged. In control group only antibiotic pomade was used.

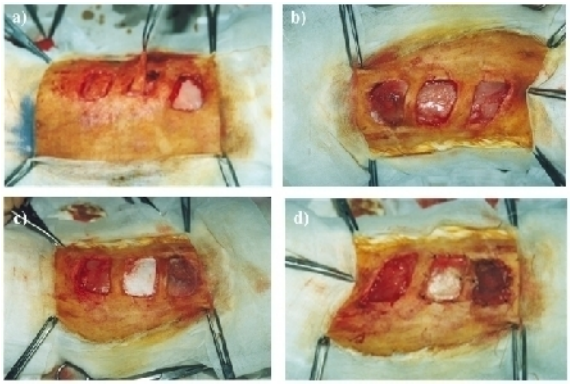

Figure 4. Application of collagen-polymer films on wound defects

Wound healing patterns of implanted A and B type collagen-polymer grafts were investigated at 7th, 14th and 21st days and images are shown in Figure 5.

Figure 5. Progression of wound healing at 7th, 14th and 21st days

With respect to macroscopic observations on wound healing periods of collagen-polymer films, it was found that the wound implanted with collagen-polymer films healed faster than the control wounds. At the end of the 21st day it was observed that the wound coated with A type material was completely recovered, defect covered with B type was almost recovered and the control defect was not recovered and exhibits excessive granulated defect form. Collagen-based substrates induce less wound contraction than occurs in an untreated control wound (Ophof et al. 2003). Because of evidence that prepared collagen grafts can promote wound healing, preliminary clinical trials were undertaken at Department of Endocrinology and Metabolism Diseases of Ege University to evaluate its effectiveness on four patients who have diabetic foot ulcers (Figure 6).

Patient I

Before grafting Week 1 Week 2

Patient II

Before grafting Week 0 Week 3

Patient III

Before grafting Week 1 Week 12

Patient IV

Before grafting Week 2 Week 11

Figure 6. Preliminary clinical trials on diabetic foot ulcers

In clinical trials, it was observed that collagen graft improved the wound healing process. However because of the wound localization and compressive forces applied to the feet, graft of patient II teared up in course of walking. Therefore, further trials should be under taken to modify and to improve the mechanical strength of grafts, and additional clinical studies should be performed with improved collagen-polymer films.

CONCLUSION

In the present study two types of collagen-polymer films were developed. In animal experiments, application of collagen-polymer films on wound sites prevented the wound contraction and deposition of excess granulation tissue and complete recovery was observed at the end of the 21st. Collagen grafts promoted wound healing in preliminary clinical trials, however their mechanical properties should be improved in case of foot wound applications.

REFERENCES

Lee, C. et al. (2001), "Biomedical applications of collagen", *International Journal of Pharmaceutics*, 19, 221(1-2), 1-22.

Lee, C.H. et al. (2001), "Biomedical applications of collagen", *International Journal of Pharmaceutics*, 221, 1–22.

Ophof, R. et al. (2003), "Histologic evaluation of skin-derived and collagen-based substrates implanted in palatal wounds", *Wound Repair and Regeneration*, 12(5), 528-538.

Oran, E. (1999), "Collagen based biomaterials", Hacettepe University, Deparment of Bioengineering, Master thesis, 1-33, Ankara.

Pişkin, E. (1987), *PolimerTeknolojisine Giriş*, İnkilapKitabevi, İstanbul.

Ruszczak, Z. (2003), "Effect of collagen matrices on dermal wound healing", *Adv Drug Deliv Rev.*, 28, 55(12), 1595-611.

Travis, J.H., Harney, J.H. and Thornton, J.W. (1987), "Modified Collagen Membrane as a Skin Substitute: Preliminary Studies", *J.Biomedical. Mer. Res.*, 9, 285-301.

Tuncel, A. et al. (1997), "Nondegradable ve Biyodegradable Yara ve Yanık Örtü Materyalleri", Sağlık Bilimleri AraştırmaGrubu, Ankara.

Vasita, R. and Katti, D.S. (2006), "Nanofibers and their applications in tissue engineering", *Int J Nanomedicine*, 1(1), 15–30.

COLLAGEN-ESSENTIAL OIL SPONGIOUS MATRICES: THERMAL AND ENZYMATIC STABILITY

DURMUŞ ALPASLAN KAYA[1], MĂDĂLINA GEORGIANA ALBU[2], ZINA VULUGA[3], NICOLAE CRISTIAN[3]

[1]*Mustafa Kemal University, Faculty of Agriculture, Department of Field Crops, 31034, Antakya-HATAY, Turkey, dkaya@mku.edu.tr*

[2]*INCDTP – Division: Leather and Footwear Research Institute, 93 Ion Minulescu, 031215, Bucharest, Romania, albu_mada@yahoo.com*

[3]*National Research and Development Institute for Chemistry and Petrochemistry – ICECHIM, 202 Spl. Independentei, 060021, Bucharest, Romania, zvuluga@yahoo.com*

The purpose of the present work was to develop and characterize some spongious matrices based on collagen and essential oils, uncross-linked and cross-linked with glutaraldehyde, obtained by lyophilization. The active components from the obtained matrices were thymbra, lavender and oregano essential oils. The components of studied essential oils were identified by GC-MS. The prepared sponges were analyzed by swelling ability, enzymatic degradation and thermal analyses. The results of this work indicated that the properties of collagen-essential oils depend on the composition of essential oils, the most stable matrix being the collagen-lavender oil one. This property allows its uses as long-term wound dressing in infected skin damages.

Keywords: collagen, sponges, essential oils

INTRODUCTION

Wound infection is a major problem in the medical field because many types of wounds are microbial contaminated leading to infection (Kumar et al. 2011).

Many researchers investigate potential strategies, which could be alternative to antibiotic therapy for treatment of local infections; bacteria have become more and more resistant to antibiotic. Moreover, there is an increasing number of people who reject using synthetic drugs in favour of natural remedies: plant actives and extracts.

In Turkish folk medicine essential oils from several plants – such as lavender, thymbra or oregano oils – have been used for treatment of wounds, abscess and burns (Süntar et al. 2011). Due to their active components such as carvacrol or thymol, the essential oils have been shown to possess potent antibacterial, antifungal and anticandidal activities (Altiok et al., 2010).

On the other hand, the best way to heal a wound is to use natural wound dressing which mimics the extracellular matrix as best as possible (Ruszczak, 2003). The use of collagen as a biomaterial for wound healing is currently undergoing a renaissance in the tissue engineering field (Friess 1988; Albu 2011).

The aim of this study is to obtain and characterize by absorbent properties and by the enzymatic and thermal stability some biomaterials based on collagen as proteic substrate and essential oils as active substance for treatment of wound healing infection.

MATERIALS AND METHODS

Materials

Type I fibrillar collagen gel with an initial concentration of 2.54% (w/w) was extracted from calf hide by chemical treatments as previously described (Albu 2011).

The lavender, oregano and thymbra oils were obtained by steam distillation in neo-clevenger apparatus from dry leaves from wild plants from the province of Hatay in the period when they were blooming. Glutaraldehyde (GA) was purchased from Merck (Germany). Sodium hydroxide, and phosphate buffer solution (PBS), pH, 7.4 were of analytical grade.

GC-MS Analysis

Analyses of the essential oils (lavender, oregano and thymbra) were carried out by using Thermo Scientific ISQ Single Quadrupole Gas Choromatograph equipped with MS, auto sampler and TR-5MS (5% Phenyl Polysilphenylene-siloxane, 0.25 mm x 30 m i.d, film thickness 0.25). The carrier gas was helium (99.9%) at a flow rate of 1 mL/min; ionization energy was 70 eV. Mass range m/z 1.2-1100 amu. Data acquisition was scan mode. MS transfer line temperature was 250^{o}C, MS Ionization source temperature was 220^{o}C, the injection port temperature was 220^{o}C. The samples were injected with 250 split ratio. The injection volume was 1µl. Oven temperature was programmed from 50^{o}C to 220^{o}C at 3^{o}C/min. The structure of each compound was identified by comparison of their mass spectrum (Wiley) data which was handled using Xcalibur software program. The retention indices (RIs) were calculated for all volatile constituents using a homologous series of *n*-alkane standard solutions C_8-C_{20} (Fluka, product no. 04070) and C_{21}-C_{40} (Fluka, product no. 04071).

Collagen Matrices Preparation

Collagen gels based on 1.2% collagen and 4% essential oil (v/v) was adjusted at 7.4 pH with 1 M sodium hydroxide and then they were cross-linked with different 0.25% glutaraldehyde. The obtained gels were freeze-dried using the freeze-dryer Delta 2-24 LSC (Martin Christ, Germany) and the program of lyophilization as we previously described (Lungu et al. 2011). During the freeze-drying process the gels became spongious forms (matrices) coded such as: collagen-lavender oil (Coll-L), collagen-oregano oil (Coll-O), collagen-thymbra oil (Coll-T) and reference sample as collagen matrix (Coll).

Water Uptake

The water uptake capacity was carried out using phosphate buffer pH 7.4 as immersion medium (n= 3), using the method previously described (Lungu et al. 2012).

Enzymatic Degradation

Enzymatic degradation of collagen matrices was investigated by monitoring the weight loss depending on exposure time to collagenase solution by the method previously described (Albu et al. 2012).

Thermal Analyses

Differential scanning calorimetry (DSC) and thermogravimetric analyses (TGA) were performed using a DSC Q2000 from TA Instruments calibrated with sapphire standard, under nitrogen flow (100 mL/min).

RESULTS AND DISCUSSION

The composition of the studied essential oils is very different, being characterized by the following main components:

- Thymbra essential oil (T-EO): 66.86% carvacrol, 12.18% cymol and 10.73% gama-terpinene;
- Lavender essential oil (L-EO): 43.96% lynalyl acetat, 28.00% linalool and 5.94% camphor;
- Oregano essential oil (O-EO): 27.66% thymol, 24.71% carvacrol, 20.01% gama-terpinene and 13.24% cymol.

Groups of chemical compounds participating in chemical compositions of the presented essential oils are presented comparatively in Figure 1.

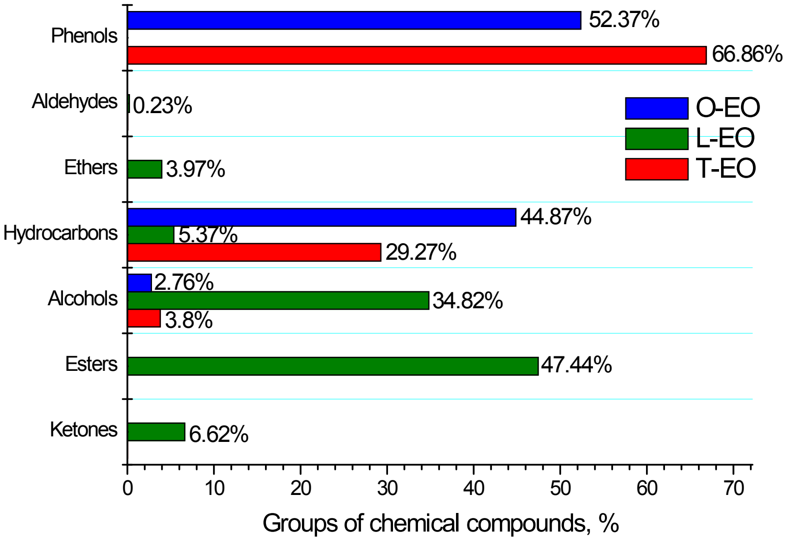

Figure 1. Groups of chemical compounds participating in chemical composition of studied essential oils

As we can see in the Figure 1, the essential oils, which are active components of collagen matrices, are characterized as follows: the O-EO – phenols and hydrocarbons, L-EO – esters and alcohols and T-EO – phenols and hydrocarbons.

In order to determine the influence of essential oils on collagen, the lyophilized matrices (spongious forms) were characterized by water absorption capacity as well as their thermal and enzymatic stability.

Water absorption capacity of spongious forms could be controlled mainly by hydrophilic porous structure and stability in water. In our experiments, all studied matrices absorbed in the fluid in 30 seconds and they reach the equilibrium in 30 minutes. Test results of water up-take of collagen-essential oils matrices are presented in Figure 2.

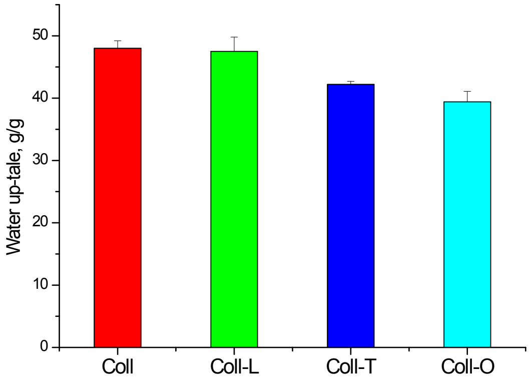

Figure 2. Water up-take for the collagen-essential oils matrices

The most absorbent biomaterial was the reference one (Coll). Water absorption capacity decreased when essential oil was added, making the support more hydrophobic. Comparing the types of studied essential oils it could be observed that the less absorbent is Coll-O, followed by Coll-T and Coll-L. This behavior can be explained by the large amount of phenols (eg carvacrol) from the composition of thymbra and oregano oils.

The control of the degradation rate for collagen-based biomaterials is an important factor because *in vivo* resorption influences the tissue regeneration capacity. Collagen can be completely digested only by collagenase, a distinctive enzyme which cleaves triple-helical regions under physiological conditions of pH and temperature. The degree of crosslinking can be indirectly assessed by degradation, collagenase being able to cleave only main chains and unable to cleave collagen intermolecular bonds.

Experimental data are presented in Figure 3 as the dependence of the percentage of lost weight (%) during 8 hours in all the studied matrices.

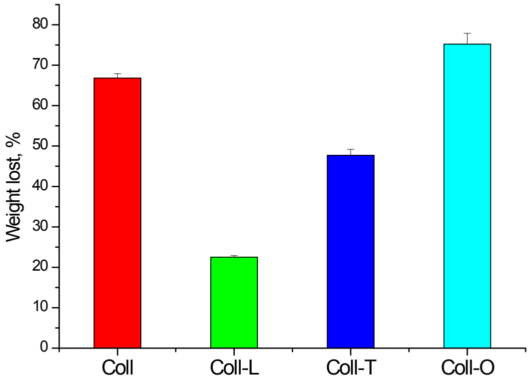

Figure 3. *In vitro* enzymatic degradation for the collagen-essential oils matrices

The results of enzymatic degradation showed that oregano oil samples were digested in a high proportion during the 8 hours. The matrices containing lavender oil are the most resistant to enzymatic degradation.

Table 1 and Figure 4 a÷d present the temperatures of dehydration and degradation as well as the weight loss of biomaterials studied by DSC-TGA.

Table 1. Characteristic parameters of dehydration and thermo-oxidation for studied matrices

Samples	Pick max I (°C)	Pick max II (°C)	Weight lost (%) 25 - 150°C	Weight lost (%) 150 - 600°C	Residue (700°C) (%)
Coll	53.73	316.56	10.12	57.65	30.02
Coll-L	57.37	315.79	7.62	60.12	30.15
Coll-O	39.55	319.60	6.88	65.15	26.28
Coll-T	53.54	320.68	3.47	68.39	25.29

The thermal analysis results presented in Table 1 show that two endothermic processes took place in order to show when temperature increases: the first process (I) consists of collagen dehydration, and takes place in the range 25-125°C and thermal degradation or oxidation between 150-600°C, depending on the environment - inert or air – in which the heating occurs.

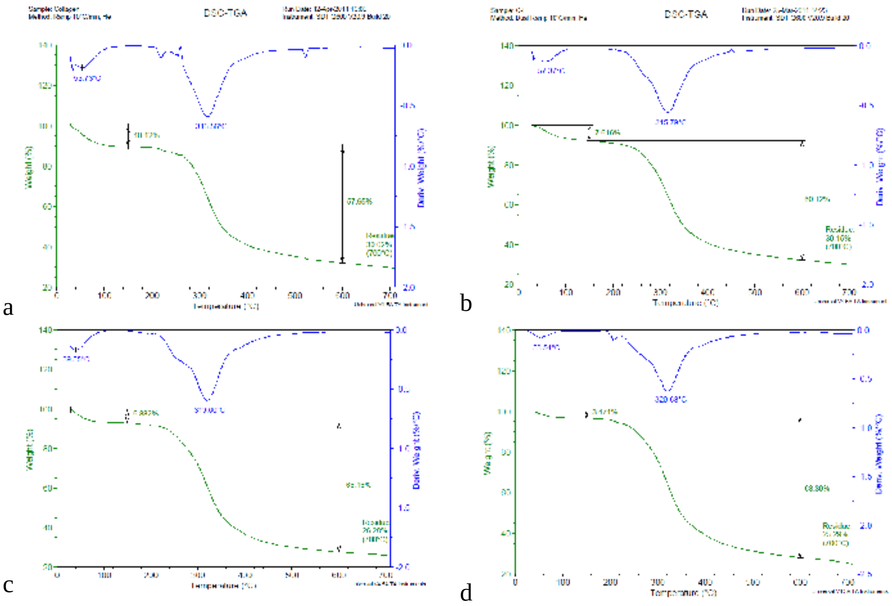

Figure 4. The DSC-TGA curves for the collagen-essential oils matrices: a) Coll; b) Coll-L; c) Coll-O and d) Coll-T

Results obtained by DSC-TGA thermal analyses show that the dehydration temperatures of studied biomaterials are closely correlated with enzymatic degradation. The most stable samples were the ones with lavender oil. This is possible because lavender oil contains high amount of esters and also ketones which produce cross-linking of collagen. Both ketones and esters are not present in Coll-O and Coll-T matrices.

CONCLUSIONS

The results of this study showed that the obtained collagen sponges have different properties depending on the composition of the essential oils which are the active components embedded in the matrices. The essential oils are characterized by different chemical compounds such as: phenols and hydrocarbons in oregano EO, esters and alcohols in lavender EO and phenols and hydrocarbons in thymbra EO, influenced the water absorption and the thermal and enzymatic stability. All the samples had absorbent properties which offer the possibility to be used in wound healing and the enzymatic and thermal stability showed that the collagen-lavender oil matrix was the most stable both by enzymatic and thermal due to the ester and ketone contents which act as crosslinking agent. This property made the spongious form long term wound dressing.

Acknowledgements

The authors gratefully acknowledge for financial support from Romania – Turkey Bilateral research project no: 109T601 founded by The Scientific and Technological Research Council of Turkey (TUBITAK) and project no: 377/2010 founded by National Authority for Scientific Research (ANCS) Romania.

REFERENCES

Albu, M.G. (2011), *Collagen Gels and Matrices for Biomedical Applications*, Lambert Academic Publishing, Saarbrücken, Germany.

Albu, M.G., Ferdes, M., Kaya, D.A. et al. (2012), "Collagen Wound Dressings with Anti-inflamatory Activity", *Molecular Crystal and Liquid Crystal*, 555(1), 271-279.

Altiok, D., Altiok, E., Tihminlioğlu, F. (2010), "Physical, Antibacterial and Antioxidant Properties of Chitosan Films Incorporated with Thyme Oil for Potential Wound Healing Applications", *Journal of Materials Science: Materials in Medicine*, 21, 2227–2236.

Friess, W. (1998), "Collagen – Biomaterial for Drug Delivery", *European Journal of Pharmaceutics and Biopharmaceutics*, 45(2), 113-136.

Kumar, M.S., Kirubanandan, S., Sripriya, R. et al. (2010), "Triphala Incorporated Collagen Sponge: A Smart Biomaterial for Infected Dermal Wound Healing", *Journal of Surgical Research*, 158(1), 162-170.

Lungu, A., Albu, M.G., Stancu, I.C et al. (2012), "Superporous Collagen-Sericin Scaffolds", *Journal of Applied Polymer Science*, DOI: 10.1002/app.37934.

Lungu, A., Titorencu, I., Albu, M.G. et al. (2011), "The Effect of BMP-4 Loaded in 3D Collagen-Hyaluronic Acid Scaffolds on Biocompatibility Assessed with MG 63 Osteoblast-like Cells", *Digest Journal of Nanomaterials and Biostructures*, 6(4), 1897-1908.

Ruszczak, Z. (2003), "Effect of Collagen Matrices on Dermal Wound Healing", *Advanced Drug Delivery Reviews*, 55(11), 1595–1611.

Süntar, I., Akkol, E.K., Keleş, H. et al. (2011), "A Novel Wound Healing Ointment: A Formulation of Hypericum Perforatum Oil and Sage and Oregano Essential Oils Based on Traditional Turkish Knowledge*", Journal of Ethnopharmacology*, 134(1), 89-96.

DEVELOPMENT OF GALLIC ACID ASSISTED EDC/NHS CROSSLINKING OF COLLAGEN MATRIX FOR DESIGN OF SCAFFOLD

GANESAN KRISHNAMOORTHY, THOTAPALLI PARVATHALESWARA SASTRY, ASIT BARAN MANDAL, SAYEED SADULLA

CSIR-Central Leather Research Institute, Adyar, Chennai – 600 020, Tamil Nadu, India, email: sadullams@hotmail.com

The use of collagen matrix in the field of tissue engineering applications is increasing because of its excellent biocompatibility with low antigenicity. To solve undesired stiffness of the collagen matrix, 1-ethyl-3-(3-dimethylaminopropyl)-carbodiimide (EDC) / N-hydroxysuccinimide (NHS) initiated crosslinking of collagen is adapted with Gallic acid (GA). The crosslinked matrix was investigated using Thermo Differential scanning calorimetric (DSC) analysis, water uptake and swelling properties and resistance to collagenase activity and biocompatibility. The results indicate an improved tensile strength (TS, 180±3), % elongation (%E, 32±4) and denaturation temperature (Td, 80.03), structural and biostability (15% biodegradation), and swelling and water uptake properties, resulting in high biocompatibility with greater flexibility. The crosslinked matrix has been produced in highly stable and biocompatible forms that can be further manipulated into functionalized scaffold suitable for biomedical applications.

Keywords: tissue engineering, collagen scaffold, gallic acid.

INTRODUCTION

To devise strategies for using collagen in the development of advanced biomaterials for biomedical engineering, it is necessary to confer mechanical strength, thermal stability and resistance to proteolytic degradation with chemical or physical crosslinking strategies. There are several strategies for crosslinking collagen-based biomaterials. The chemical crosslinking, aldehydes, diphosphorylazide, acyl azides etc, are the most widely used for collagen-based biomaterials (Anderson et al., 2008). However, the above crosslinking agents and the reaction products are associated with cytotoxicity and poor biocompatibility in vivo, because of the presence of crosslinking byproducts and the release of aldehyde-crosslinked collagen peptides during enzymatic degradation. To avoid in vivo cytotoxicity, poor biocompatibility and subsequent calcification of aldehyde treated collagen, several alternative agents have been examined as potential crosslinking such as, carbodiimides and succinimide etc, and physical methods, photo oxidation and gamma or UV-irradiation, etc. While physical methods have no toxicity problems and can provide sufficient stability. Although non-covalent and covalent crosslinks do afford molecular stability, the long-term preservation of collagen matrix has required (Madhavan et al., 2010; Lee et al., 2001; Friess, 1998 and 2003).

A number of polyphenols (PPs) compounds derived from plants have been reported to be interactive or reactive with proteins and resulted in improved properties for collagen-based materials. There are several molecular species of phenolics, which appear to be a promising choice for the stabilization of collagen matrix. These PPs are two types, hydrolysable (polyester of GA and polysaccharides) and condensed (polymerized products of flavan-3-ols and flavan-3, 4-diols, or a mixture of the two), although other PPs occur which are combinations of these two basic structures. The process for crosslinking of Type I collagen fibers with PPs significantly improved the properties. In addition, it has been shown that PPs crosslinked collagen fibers neither elicit a foreign body response nor did they stimulate an immune reaction (Ahmed et al., 2010; Haslam et al., 2007; Tang et al., 2003; Covington et al., 2005).

Gallic acid (GA) is a 3,4,5-trihydroxybenzoic acid, a type of organic phenolic acid, found in gallnuts, sumac, tea leaves, oak bark, and other plants, found both free and as part of tannins, and chemical formula is $C_6H_2(OH)_3COOH$. GA and its derivative are known to form multiple H-bonds with proteins, particularly those rich in proline such as elastin and collagen and used in the manufacture of gelatin product and leather adhesives. Its derivative has been suggested as a potential cross-linking agent and improves the elastin and collagen stability in cardiovascular implants as evidenced by an increased resistance to proteolytic degradation against collagenase activity. The pharmacological properties such as anti-oxidant, anti-inflammatory and antimicrobial activities of GA derivative have been studied (Shahrzad et al., 2001; Punithavathi et al., 2011; Zhang et al., 2008; Jackson et al., 2010). Therefore, it has been considered that GA has a potential possibility as an abundant and natural resource for stabilization of collagen scaffold (Isenburg et al., 2005). An attempt has been made to the process of prepare stable collagen scaffold by GA with presence of EDC/NHS. Achilles tendon which predominantly contains type I collagen has been used in this study.

This study was to develop a collagen scaffold in order to improve the thermal stability, swelling and water uptake properties, resistance to collagenolytic activity, biocompatibility and cell adhesion properties. The molecular level understanding of interaction of collagen with GA was carried out by docking studies.

MATERIALS AND METHODS

Materials

All reagents and chemicals used were analytical grade. Clostridium histolyticum collagenases (Type IA), Gallic acid (GA), 1-ethyl-3-(3-dimethylaminopropyl)-carbodiimide (EDC), N-hydroxy succinimide (NHS) and 2-(N-morpholino) ethanesulfonic acid [MES] were sourced from Fluka and Sigma Chemicals Co., USA. All other reagents and chemicals used for the study were sourced from SRL Ltd., India.

Preparation of Collagen Scaffolds

The collagen scaffolds viz. Coll, Coll-GA, Coll-EDC/NHS and Coll-GA-EDC/NHS were prepared by the described in our earlier method (Krishnamoorthy et al., 2012).

Characterization

The thermal properties of collagen scaffolds were analyzed using by DSC (TA-DSC Q 200) analysis. The water-uptake and swelling ratio were obtained by incubation of the samples in water at room temperature for 2 hrs. The percentage (%) of all scaffolds degradation compared with native scaffold against ChC activity was calculated by the method described in our earlier method (Krishnamoorthy et al., 2012). The MTT assays were performed to assess the % of cell viability and cell adhesion.

Molecular Docking of Collagen-GA and ChC-GA Interaction

The molecular docking studies comprise the determination of the three-dimensional structure of collagen by energy minimization methods and the simulation of the interaction between collagen, GA and ChC active site (Autodock 4.2, Accelrys Discovery Studio 2.5). The collagen like peptide (CLP), ChC and GA structure were obtained from Protein Data Bank (collagen PDB: 3A1H, ChC PDB: 1NQD) and PubChem Database (CID: 370) for this study.

RESULTS AND DISCUSSION

Tensile Strength

The tensile strength (TS) and % elongation (% E) are given in Table 1. TS of the collagen matrix increased with the presence of GA with EDC/NHS. Furthermore, GA-EDC/NHS treated matrix leads to improved TS compared to native, GA and EDC/NHS. The GA-EDC/NHS treated matrix resulted in maximum TS, this is due to the fact that inter and intra molecular crosslinking with hardness lower than that of matrix may well increase thermo mechanical stability.

Table 1. TS, % E, TD, % weight loss of collagen scaffold

Concentration	TS (MPa)	% E	Td (°C)	% Weight Loss
Native scaffold	59±4	8±3	64.11	68.98
EDC/NHS	79±3	19±4	69.09	53.31
GA	120±2	25±6	69.50	52.45
GA-EDC/NHS	180±3	32±4	80.03	31.76

Our data imply that the ratio of -COOH groups to NH_2 groups significantly affects the TS of matrix. According to the molecular structure, the OH and COOH groups of GA and the collagen all provide possibilities for crosslinking. GA-EDC/NHS treated matrix exhibited high TS and high % E where as GA and EDC/NHS treated matrix exhibited low Ts with low % E. By GA-EDC/NHS treatment, the mechanical properties of collagen matrix are improved.

DSC Analysis

The T_D of scaffolds were computed from DSC data and presented in Table 1. The GA-EDC/NHS treated scaffold exhibits an increase in the T_D when compared to native matrix. This may be due to a net increase in the number of inter and intra molecular crosslinks and interactions between the GA-EDC/NHS and collagen. It is known that T_D of matrix is paralleled by destruction of H-bonds and hydrophobic interactions between the protein subunits and helix-coil transformation. Presumably, the combination of high hydrophobicity and capacity to form peptide bonds permits these molecules incorporate in certain areas of collagen fibrils and promote stabilization of their structure. The Ts of matrix depends on stable intermolecular cross-links formed through the GA-EDC/NHS than GA and EDC/NHS.

Water Uptake and Swelling Studies

Water-uptake and swelling ratio of matrix were increased with presence of GA (Figure 1). Although formation of GA-EDC/NHS treated matrix can increase more amount of hydrophilic groups and also presented higher swelling ratio than EDC/NHS. This decrease should be mainly attributed to the partial diminishing of the hydrophilic groups of the scaffold after crosslinking.

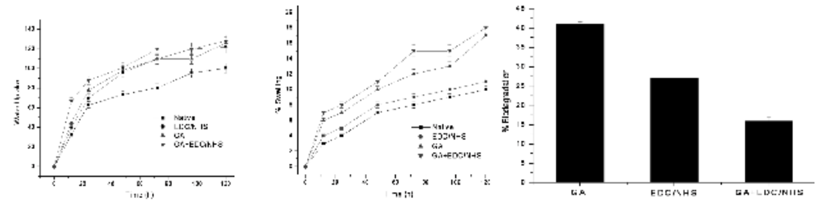

Figure 1. The % of water uptake and swelling ratio and % biodegradation of scaffolds

The swelling ratios of the GA-EDC/NHS treated scaffolds are still big enough to meet the demand of the matrix used in tissue engineering. Consequently, both water uptake and swelling time can be increased by characteristics of GA. Thus, we concluded that the addition of GA-EDC/NHS to collagen scaffold significantly increased the water uptake ability and made them more hydrophilic. Also, it is seen that % swelling of GA-EDC/NHS treated scaffold increased with increase of concentration of GA.

Stability of GA Treated Scaffold Against ChC Activity

% Collagen degradation (based on hydroxyproline released) scaffolds by ChC at various time periods were determined (Figure 1). Significant reduction in the degradation of collagen was observed for the scaffold treated with the GA-EDC/NHS compared to Coll, GA and EDC/NHS. The GA, EDC/NHS and GA-EDC/NHS treated scaffold exhibited 44, 27 and 15 % degradation of collagen as against 93% degradation in the case of Coll at 96 h period of incubation. The GA can interact with collagen through multipoint H-bonding, carboxyamide and hydrophobic interactions. The hydrophobic core of the GA molecule, likely incorporates itself into hydrophobic areas, while OH moieties of GA may establish multiple H-bonds with neighboring collagen molecules, resulting in improved stability of scaffold and prevent the free access of ChC to reactive sites on the collagen chains (Krishnamoorthy et al., 2008, 2011 and 2012).

Molecular Docking of Collagen-GA and ChC-GA Interaction

Figure 2A, B, C and D shows the closest structure to the collagen interlayer region with GA, H-bonding, hydrophobic and closest binding site respectively, where the contact surfaces are colored according to their distance. The best geometries obtained through the docking represent the low interaction energy -5.08 Kcal/mol between collagen-GA, resulting in stronger H-bonds. The interaction of CLP with GA and binding at multiple sites and the predicted H-bonds (dashed yellow lines) are shown (Figure 2B). The light yellow dots represent the possible H-bonds and are involved in hydrophobic interactions. These representations clearly show the possible anchoring points of GA moieties with the collagen interlayer region.

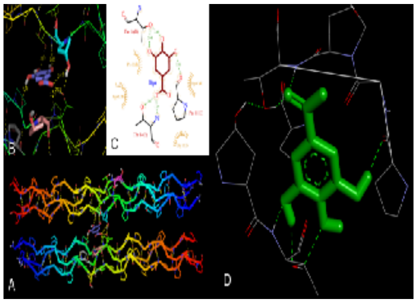

Figure 2. A) GA binding to interlayer region of collagen, B) H-bonding, C) Hydrophobic interaction and D) binding site

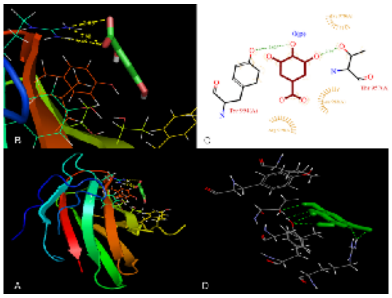

Figure 3. A) GA binding to ChC active site, B) H-bonding, C) hydrophobic interaction and D) binding site

Molecular docking of interaction of GA with ChC active site was carried out. Figure 3A, B, C and D shows the closest structure to the ChC with GA, H-bonding, hydrophobic and closest binding site respectively, where the contact surfaces are colored according to their distance. The best geometries obtained through the docking represent the low interaction energy -4.27 Kcal/mol between ChC-GA, resulting in stronger H-bonds. ChC is represented by its solvent-accessible surface. The yellow dots represent the possible H-bonds and are involved in hydrophobic interactions. This clearly show the possible anchoring points of GA with the ChC active site.

Cell Viability

Fibroblast incubated in the scaffold showed no cytotoxic effect. MTT assay showed more than 85% fibroblast viability (NIH 3T3) after 72 h of culture on scaffold when compared with native scaffold and EDC/NHS (Figure 4). GA-EDC/NHS could improve the cell adhesion to the surface of matrix are shown (Figure 4). After GA-EDC/NHS is introduced into the matrix, the cell-adhesion ratio can be observed to increase significantly.

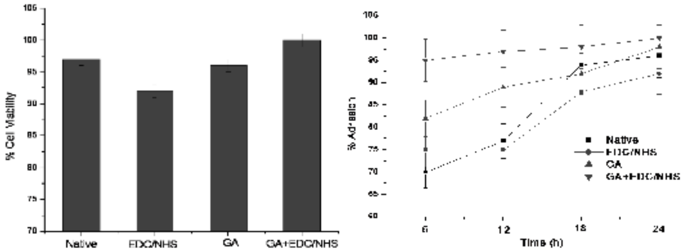

Figure 4. % Cell viability and % Cell adhesion assay of scaffolds

GA-EDC/NHS exhibited more fibroblast adhesion than GA and EDC/NHS treated matrix. It is interesting to note that fibroblast adhesion to EDC/NHS treated matrix demonstrated similar trend to native matrix. It suggests that GA-EDC/NHS may induce the adhesion and spreading of fibroblasts than GA and EDC/NHS.

CONCLUSIONS

The GA with presence of EDC/NHS was shown to improve mechanical strength and thermal stability, swelling and water uptake properties, biocompatibility and cell adhesive properties, effective in the prevention of collagen scaffold degradation. We have shown here that GA interaction with collagen imparts a less binding energy and also shown the possible anchoring points of GA galloyl moieties with the ChC active site. This matrix is more stable and can be effective in the prevention of degradation by collagenase activity and, hence may find use in the preparation of collagenous biomaterials.

REFERENCES

Ahmed, S. (2010), "Green tea polyphenol epigallocatechin 3-gallate in arthritis: progress and promise", *Arthritis Research & Therapy*, 12, 1-9.

Anderson, J.M, Rodriguez, A. and Chang, D.T. (2008), "Foreign body reaction to biomaterials", *Seminars in Immunology*, 20, 86-100.

Covington, A.D., Evans, C.S., Lilley, T.H. and Suparno, O. (2005), "Collagen and polyphenols: new relationships and new outcomes. Part 2. Phenolic reactions for simultaneous tanning and coloring", *Journal of American Leather Chemists Association*, 100, 336-343.

Friess, W. (1998), "Collagen-biomaterial for drug delivery", *European Journal of Pharmaceutics and Biopharmaceutics*, 45, 113-136.

Friess, W. (2003), "Collagen in drug delivery and tissue engineering", *Advanced Drug Delivery Reviews*, 55, 1529-1530.

Haslam, E. (2007), "Vegetable tannins-lesson of phytochemical lifetime", *Phytochemistry*, 68, 2713-2721.

Isenburg, J.C., Simionescu, D.T., Vyavahare, N.R. (2005), "Structural requirements for stabilization of vascular elastin by polyphenolic tannins", *Biomaterials*, 26, 1237-1245.

Jackson, J.K., Zhao, J., Wong, W. and Burt, H.M.J. (2010), "The inhibition of collagenase induced degradation of collagen by the galloyl-containing polyphenols tannic acid, epigallocatechin gallate and epicatechin gallate", *Journal of Materials Science: Materials in Medicine*, 21, 1435-1443.

Krishnamoorthy, G., Sehgal, P.K. Mandal, A.B. and Sadulla, S. (2012), "Novel collagen scaffolds prepared by using unnatural D-amino acids assisted EDC/NHS crosslinking", *Journal of Biomaterial Science: Polymer Edition*.

Krishnamoorthy, G., Madhan, B., Sadulla, S., Raghava Rao, J. and Madhulatha, W. (2008), "Stabilization of collagen by the plant polyphenolics Acacia mollissima and Terminalia chebula", *Journal of Applied Polymer Science*, 108, 199-205.

Krishnamoorthy, G., Sehgal, P.K., Mandal, A.B. and Sadulla, S. (2012), "Studies on collagen-tannic acid-collagenase ternary system: Inhibition of collagenase against collagenolytic degradation of extracellular matrix component of collagen", *Journal of Enzyme Inhibition* and *Medicinal Chemistry*, 27, 451-457.

Krishnamoorthy, G., Sehgal, P.K., Mandal, A.B. and Sadulla, S. (2011), "Protective effect of Withania somnifera and Cardiospermum halicacabum extracts against collagenolytic degradation of collagen", *Applied* Biochemistry and *Biotechnology-Part A*, 165, 1075-1091.

Lee, C.H., Singla, A., Lee, Y. (2001), "Biomedical applications of collagen", *International Journal of Pharmaceutics*, 221, 1-22.

Madhavan, K., Belchenko, D., Motta, A. and Tan, W. (2010), "Evaluation of composition and crosslinking effects on collagen-based composite constructs", *Acta Biomaterialia*, 6, 1413-1422.

Punithavathi, V.R., Stanely Mainzen Prince, P., Kumar, M.R. and Selvakumari, C.J. (2011), "Protective effects of gallic acid on hepatic lipid peroxide metabolism, glycoprotein components and lipids in streptozotocin-induced type II diabetic wistar rats", *Journal of Biochemical and Molecular Toxicology*, 25, 68.

Shahrzad, S., Aoyagi, K., Winter, A., Koyama, A. and Bitsch, I. (2001), "Pharmacokinetics of gallic acid and its relative bioavailability from tea in healthy humans", *Journal of Nutrition*, 131, 1207-1210.

Tang, H.R., Covington, A.D. and Hancock, R.A. (2003), "Structure-activity relationships in the hydrophobic interactions of polyphenols with cellulose and collagen", *Biopolymer*, 70, 403-413.

Zhang, Y., Dong, L., Li, J. and Chen, X. (2008), "Studies on the interaction of gallic acid with human serum albumin in membrane mimetic environments", *Talanta*, 76, 246-253.

YELLOWING OF SKIN COLLAGEN BY UV IRRADIATION

SHUANGWEN LI, FANG WANG, KEYONG TANG, XUEJING ZHENG
College of Materials and Engineering, Zhengzhou University, Zhengzhou 450052, China, email: keyongtang@yahoo.com.cn

Research of the effect of UV radiation on the collagen yellowing is an area of potential interest, owing to the fact that collagen is an important biomaterial finding immense use in various fields. Study on the yellowing of collagen is important to protect leather products or biomaterials, making a contribution to researches on collagen yellowing field. The physical and optical properties of collagen affected by UV irradiation were studied in the present paper. Both studies of UV-Vis spectroscopy and Color Difference Meter indicated the changes in yellowing behavior of the collagen films by UV irradiation. Thermal stability of collagen before and after UV irradiation was determined by Thermogravimetry (TG). Scanning electron microscope (SEM) was employed to study the surface properties of collagen samples before and after UV irradiation. It was shown that UV irradiation may cause yellowing of collagen, while crosslinking or degradation taking place.

Keywords: collagen; UV radiation; yellowing.

INTRODUCTION

Type I collagen, the most abundant extracellular matrix protein in the animal kingdom, provides the basis of tissue structure (Rabotyagova et al., 2008). Collagen fibers in extracellular matrix form a network with different length but isotropy to maintain the stability of tissue (Ottania et al., 2001). As a common fibrous protein, the structural and mechanical properties of many biological systems were determined by collagen, including skin, skeleton, and tendon. The molecular structures of the amino acid sequence have be recognized, requiring the (Gly-X-Y)n repeating sequence for the collagen triple-helix (Beck and Brodsky, 1998).

When being exposed to electromagnetic radiation, synthetic and natural polymers will undergo photo-aging and photo-degradation. One of the main components of the electromagnetic radiation is ultraviolet (UV) radiation (Sionkowska, 2000). UV radiation may caused physical and chemical variations of collagen structure, resulting in the loss of biological activity (Tyana et al., 2002). The collagen structure is sensitive to UV irradiation. By now, most researches are mainly focused on changes in the primary structure, construction, microcosmic structure and properties of collagen (Rabotyagova et al., 2008). It was found that the collagen triple-helix structure is sensitive to UV irradiation, which may accelerate the photodegradation reaction of collagen (Rabotyagova et al., 2008; Tyana et al., 2002; Menter et al., 2001).

In the present paper, changes of pig skin collagen when being ultraviolet irradiated was investigated and it was found that sufficient UV irradiation eventually causes yellowness in pigskin collagen films. The yellowing mechanism was discussed as well.

EXPERIMENTAL

Materials

Type I collagen was obtained in our laboratory from pigskin. The extraction method was described in our previous paper (Feng et al., 2010). The purity and the concentration of collagen (PH 4.6) prepared was studied by SDS-PAGE and UV-Vis spectrophotometer. The concentration of the collagen solution was 3.335 mg/mL.

UV Irradiation

The solution of Type I collagen was casted on a 7×7 cm poly(tetrafluoroethylene) (PTFE) sheet and dried at room temperature (25°C) for 72 h to remove the solvent. Then the collagen films were UV irradiated for different times using a UV Aging Tester (ZN, Linpin, Shanghai, China) with the wavelength of 312 nm. The source of radiation was 25 cm from samples and the samples were located in parallel. All the measurements were performed in the same temperature and the same humidity to avoid any influence on the physico-chemical properties of collagen.

Whiteness Test

The color changes of collagen films were measured with a Colour Difference Meter (SF600X, SPECTRAFLASH) spectrophotometer. The whiteness, denoted as yellowness, was used as an index of the yellowing degree of collagen. The lower the whiteness value is, the higher the yellowness of collagen films is.

UV-Vis

The UV-Vis absorption spectra of the collagen films before and after UV irradiation were recorded with an integrating sphere UV-Vis spectrophotometer (HB902, Zanchen, China).

TG Characterization

Thermogravimetric (TG) of the samples before and after UV irradiation were carried out with a TG209F1 thermal analyzer (NETZSCH, Germany). 6 mg of samples were heated under N_2 atmosphere from 30°C to 800°C at the heating rate of 20°C/min.

SEM Observation

The surfaces of collagen films were examined with a Field Emission Scanning Electron Microscope (JSM-7500F, JEOL Ltd, Tokyo Japan). The surfaces of the samples to be scanned were coated with a thin layer of gold to eliminate the charging effects, particularly at high magnifications.

RESULTS AND DISCUSSION

Color Changes

Figure 1 indicates the color changes of collagen films being UV irradiated for different times.

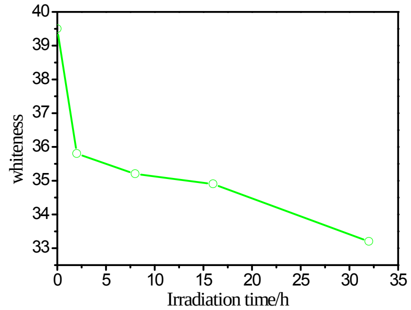

Figure 1. Whiteness of collagen films vs. UV irradiation time

With increasing the UV irradiation time, the whiteness of collagen films decreased obviously. The reason may be explained by the fact that the longer the UV irradiation time is, the more opportunity for collagen structure to be destroyed by UV-light.

UV-Vis

The transmissivity of collagen films before and after being UV irradiated for different times was studied in the range between 280 and 400 nm as shown in Figure 2. It was shown that UV irradiation time affect the transmissivity of collagen. As can be seen, with increase of irradiation time under the same conditions, UV irradiation results in a decrease in overall transmissivity of the collagen films, especially at the UV wavelength range between 280 and 300 nm.

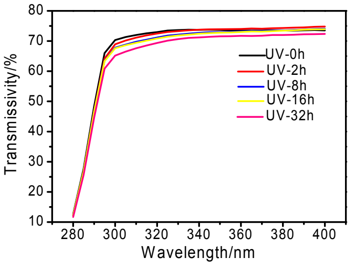

Figure 2. UV-Vis spectra of collagen films before and after UV irradiation

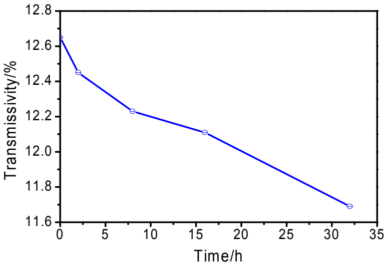

Figure 3. Transmissivity of collagen films at 280 nm after UV irradiation

Figure 3 shows that with the increase of UV irradiation time, the transmissivity of collagen fibers at 280 nm decreased obviously. The change in transmissivity of collagen films at 280 nm was mainly caused by photochemistry of aromatic amino acids. It is generally known that tyrosine and phenylalanine, two aromatic amino acids, are sensitive chromophores absorbing far-ultraviolet (250-280 nm) and may initiate photo-degradation of collagen chains and photodestruction via the cleavage of the side groups (Sionkowska, 2006; He Li et al., 2003).

This may be due to the changing optical properties of the collagen films. We know that artificial UV irradiation causes changes in conformation of the collagen molecule (i.e. helix-coil transition) (Sionkowska et al., 2001; Kaminska and Sionkowska, 1996; Sionkowska and Kaminska, 1999). The increased presence of a coil structure and the progressive loss of the helical character of collagen bring about an overall increase in the scattering level of the sample.

Thermal Stability

In the TG and DTG curves, which characterize the thermal degradation behaviour of collagen before and after UV irradiation, two peaks appeared as shown in Figure 4, suggesting a two-stage destruction.

The first peak appeared at 58.9°C and at 67.8°C for collagen films before and after UV irradiation is accompanied by a weight decrement (Δm^{I}_{max}) of 15.27% and 16.44% respectively (Figure 4, Table 1). The other peak at 313.6°C and 322.0°C is accompanied by a significant weight decrement (Δm^{II}_{max}) of 62.12% and 58.78%, respectively. In the first stage, evaporation of water absorbed in the collagen occurs. In the second one, small molecular products of the thermal degradation of collagen are liberated (Lim and Shannos, 1974).

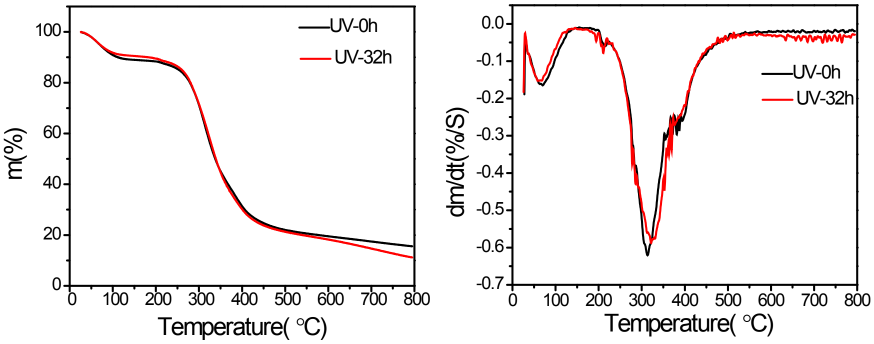

Figure 4. TG and DTG curves of collagen films before and after UV irradiation

The characteristic temperatures of the two processes and the weight losses are listed in Table 1.

Table 1. Parameters of non-isothermal degradation of the samples

Samples	T^{I}_{max} [°C]	T^{II}_{max} [°C]	Δm^{I}_{max} (%)	Δm^{II}_{max} (%)	$m_{redidual\ mass}$(%)
UV-0h	58.9	313.6	15.27	62.12	15.57
UV-32h	67.8	322.0	16.44	58.78	11.19

*: T^{I}_{max}[°C] = the temperature of the first peak in DTG; T^{II}_{max}[°C] = the temperature of the second peak in DTG; Δm^{I}_{max}(%) = the relative weight loss until T^{I}_{max}[°C]; Δm^{II}_{max}(%) = the relative weight loss until T^{II}_{max}[°C]; $m_{redidual\ mass}$ (%) = the relative weight until termination.

After the collagen is UV irradiated, the thermal decomposition occurs at temperature

(T^{II}_{max}) higher than that before irradiation (Table 1). The temperatures with maximum thermal degradation rate were changed only by about a few degrees. This result indicated that UV irradiation may increase the thermal stability of collagen films. UV irradiation may endow the samples with extra crosslinking. Accompanying the process of cross-linking of collagen films, yellowing appeared.

Weight decrements were changed, specifically Δm^{I}_{max} increased obviously, whereas Δm^{II}_{max} and $m_{redidual\ \ mass}$ decreased. This is an evidence that UV radiation may help release of water bound with collagen because of the photolysis of hydrogen bonds between water and collagen (Sionkowska and Kaminska, 1999). It is proved by the less weight loss in the second stage (temperature 313.6°C and 322.0°C). This suggests that some part of the water released in the first stage at the lower temp after breaking up the hydrogen bonds, caused by UV radiation.

SEM

Structural changes on the surface of collagen films by UV irradiation were observed by scanning electron microscope. The SEM images of non-irradiated and irradiated collagen films are shown in Figure 5. Only a little damage of collagen films were observed during UV-irradiation. The surface of collagen film without a UV irradiation history is relatively smooth and flat, while that of the UV irradiated one becomes rougher and ruptured. The wrinkles and micro cracks on the surface of irradiated sample may be directly related to the photochemical transformation.

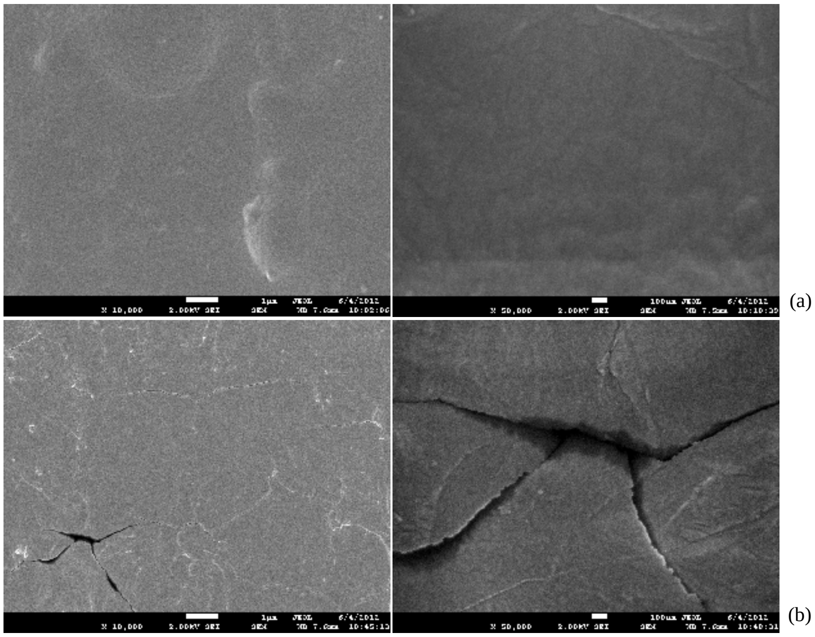

Figure 5. SEM images of collagen films (a) UV-0h; (b) UV-32h

The breakage of inter- and intra-molecular hydrogen bonds in the samples and the release of water may provide fragments that occupy more volume than the original ones. Strain and stress may be caused, which should be responsible for the damage of UV irradiated film (Sionkowska, 2000). Furthermore, the changes in conformation and the cleavage of collagen backbone may also contribute to the damage (Rabotyagova et al., 2008; Sionkowska et al., 2006).

CONCLUSIONS

UV radiation changes the properties of collagen. The yellowness of collagen by UV irradiation results from such photochemical changes as cross-linking and breakup. UV irradiation causes the crosslinking in collagen fibers along with the release of water bound. Besides, UV irradiation causes the formation of wrinkles and micro cracks in the collagen surface. It may be ascribed to that the conformation and backbone of collagen was destroyed by excessive UV irradiation. Accompanying the UV irradiation, yellowing of collagen films will happen.

Acknowledgements

The financial supports from the National Natural Science Foundation Commission of China (No. 50973097, 21076199) and China-Romania Governmental Science & Technology Cooperation Program (No. 40-17) are gratefully acknowledged.

REFERENCES

Beck, K., Brodsky, B. (1998), “Supercoiled Protein Motifs: The Collagen Triple-Helix and the a-Helical Coiled Coil”, *Journal of structural biology*, 122, 17-29.

Feng, W.P., Qi, Y.M., Tang, K.Y. (2010), “Extraction and Characterization Modified of Type I Collagen from Rabbit-Skins”, *Transactions of Beijing Institute of Technology*, 30, 1231-1234.

Kaminska, A., Sionkowska, A. (1996), “Photochemical transformation in collagen in the presence of β-carotene”, *J. Photochem. Photobiol. A*, 96, 123-127.

Li, H., Wang, D.Q., Chen, H.L., Liu, B.L., Gao, L.Z. (2003), “The Shielding Effect of Nano TiO2 on Collagen under UV Radiation”, *Macromol. Biosci*, 3, 351–353.

Lim, J.J., Shannos, M.H. (1974), *Biopolymers*, 13, 1791.

Menter, J.M., Patta, A.M., Sayre, R.M., Dowdy, J., Willis, I. (2001), “Effect of UV irradiation on type I collagen fibril formation in neutral collagen solutions”, *Photodermatol Photoimmunol Photomed*, 17, 114-120.

Ottania, V., Raspanti, M., Ruggeri, A. (2001), “Collagen structure and functional implications”, *Micron*, 32, 251-260.

Rabotyagova, O.S., Cebe, P., Kaplan, D.L. (2008), “Collagen structural hierarchy and susceptibility to degradation by ultraviolet radiation”, Materials Science and Engineering C, 2(8), 1420-1429.

Sionkowska, A. (2000), “The influence of methylene blue on the photochemical stability of collagen”, *Polymer Degradation and Stability*, 67, 79-83.

Sionkowska, A. (2006), “Effects of solar radiation on collagen and chitosan films”, *Journal of Photochemistry and Photobiology B: Biology*, 82, 9-15.

Sionkowska, A., Kaminska, A., Miles, C.A., Bailey, A.J. (2001), “The effect of UV radiation on the structure and properties of collagen”, *Polimery*, 6, 379-389.

Sionkowska, A., Kaminska, A. (1999), “Changes induced by ultraviolet light in fluorescence of collagen in the presence of β-carotene”, *J. Photochem.Photobiol. A*, 120, 207-210.

Sionkowska, A. (2000), “Modification of collagen films by ultraviolet irradiation”, *Polymer Degradation and Stability*, 68, 147-151.

Sionkowska, A., Wiśniewski, M., Skopińska, J., Mantovani, D. (2006), “Effects of Solar Radiation on Collagen-Based Biomaterials”, *International Journal of Photoenergy*, 1–6.

Tyana, Y.C., Liaoa, J.D., Klauserb, R., Wua, I.D., Weng, C.C. (2002), “Assessment and characterization of degradation effect for the varied degrees of ultra-violet radiation onto the collagen-bonded polypropylene non-woven fabric surfaces”, *Biomaterials*, 23, 65–76.

SOLVENT EFFECTS ON THE OPTICAL PROPERTIES OF PHYSICALLY CROSSLINKED POLYVINYL ALCOHOL/GELATIN COMPOSITE HYDROGELS

JIE LIU, XICHAN HE, FANG WANG, KEYONG TANG

College of Materials Science and Engineering, Zhengzhou University, Henan 450052, China,
Phone: 86-371-67763216, email: keyongtang@yahoo.com.cn; liujie@zzu.edu.cn

A series of physically crosslinked composite hydrogels with polyvinyl alcohol (PVA) and gelatin were prepared by a freeze-thawed method, using the mixture of dimethyl sulfoxide (DMSO)/water as a solvent. The PVA/gelatin composite hydrogels behaves various optical properties by changing the solvent being absorbed. The study on the light transmittances of the hydrogels indicated that the optical properties of PVA/gelatin composite hydrogels were sensitive to solvent. The optical property of hydrogels changes periodically when the surrounding solvents changes between water to DMSO. The XRD patterns of PVA and PVA/gelatin hydrogels containing different solvents were similar, indicating that the optical property might be related to the reversible change in homogeneous and heterogeneous structures of PVA/gelatin hydrogels, not the changes in crystalline structure of the hydrogels.

Keywords: polyvinyl alcohol, gelatin, optical.

INTRODUCTION

Nowadays, hydrogels have become increasingly important materials for biomedical and pharmaceutical applications because of their novel mechanical and biomedical properties (Jeeyoung et al., 2007; Hassan and Peppas, 2000; Liu et al., 2010). Gelatin is a natural protein mainly from skins and bones of animals, which is widely used for the development of hydrogels in clinical applications due to its excellent biocompatibility and biodegradability. Polyvinyl alcohol, a nontoxic and biocompatible polymer, is demonstrated a great potential for numerous applications in tissue engineering and drug delivery. Its elasticity and high hydrophilicity makes it appropriate to blend with other polymers including gelatin (Bajpai and Saini, 2005).

In recent years, PVA/gelatin blends have been studied by many researchers (Liu et al., 2010; Bajpai and Saini, 2005; Chiellini et al., 2001). The structure and properties of PVA hydrogels are usually modified because of the incorporation with gelatin (Mendieta-Taboada et al., 2008; Toshihisa et al., 1999). To make the hydrogels more stable in practice, some studies have been done on the synthesis and characterization of PVA hydrogels by freeze-thawing the PVA solutions with liquid nitrogen or in refrigerators (Hassan and Peppas, 2000; Tong et al., 2007).

Both PVA and gelatin can be dissolved in DMSO or DMSO/water mixture (Tong et al., 2007; Hong et al., 1998), however, there only a few attempts have been made to study the preparation of PVA/gelatin hydrogels using DMSO or DMSO/water mixture as a solvent. In this paper, a new preparation of PVA/gelatin composite hydrogels with different composition of solvent via freeze-thawed technique is reported, and the solvent effects on the optical properties of the composite PVA/gelatin hydrogels are investigated.

MATERIALS AND METHODS

Preparation of Hydrogels

PVA was dissolved to obtain a 12.0% (weight percent) solution, and the solution was then cooled to 60°C. A calculated amount of gelatin aqueous solution was added into the PVA solution with agitation for 1 h, and the ratios of PVA to gelatin were kept to 80:20 by weight. The mixture was poured into plastic models for the following freeze and thaw cycles, each cycle including a 20 h freezing at -20°C and 4 h thawing at 25°C. The ratios of water to DMSO were kept at 100:0, 80:20, 60:40, 40:60, and 20:80 by weight, respectively, and the PVA/gelatin samples obtained were denoted as PGD0, PGD20, PGD40, PGD60 and PGD80, respectively. The PVA hydrogels prepared with the same solvent composition were denoted as PVA0, PVA20, PVA40, PVA60, and PVA80, respectively.

Characterization

The hydrogel samples with the thickness of 3 mm were subjected to a UV-Vis spectrometer (UV-2450, Shimadzu, Japan) to obtain the transmittances at the operating wavelength (λ) of 600 nm. The hydrogel samples were subjected to X-ray diffraction (D/MAX-3B, Rigaku, Japan) using CuKα radiation generated at 35 kV and 30 mA, the range of diffraction angle was 5.00 ° - 70.00 ° 2θ.

RESULTS AND DISCUSSION

To remove the DMSO from the biomaterials is usually necessary for the biomedical applications of hydrogels (Jeeyoung et al., 2007). Fig. 1 showed the changes in light transmittances of PVA/gelatin hydrogels in the 7 days of immersion in water. Significant decreases in light transmittances could be observed from the initial transparent composite hydrogels prepared in rich DMSO solutions (PGD60 and PGD80). The two thumb photos in Figure 1 showed the optical differences of PGD80 hydrogel before (top left) and after (bottom right) being immersed in water for 7 days.

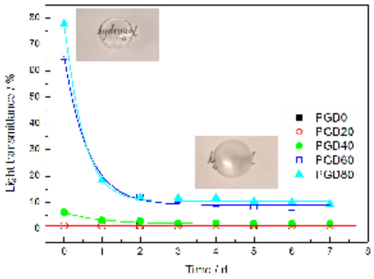

Figure 1. Transmittances and photos of PVA/gelatin hydrogels immersed in water (λ = 600nm)

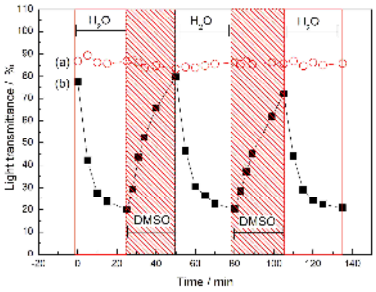

Figure 2. Light transmittances of PVA and PVA/gelatin hydrogels in water and DMSO (λ=600nm). (a): PVA (PVA80); (b): PVA/gelatin (PGD80)

The decrease in light transmittances of PVA/gelatin hydrogels in Figure 1 revealed the possible influences of solvent on the optical properties of PVA/gelatin hydrogels. In order to further evaluate the reason of the change of light transmittances, PVA/gelatin hydrogels were alternately immersed in water and DMSO, and the light transmittances of the hydrogels were recorded at short intervals. Figure 2 showed the light transmittances of PVA80 and PGD80 during the solvent-exchanged process. It was found that the light transmittances of PVA hydrogel (PVA80) were high and constant, which means the hydrogel keeps transparent in water and DMSO. On the other hand, the light transmittances of PVA/gelatin hydrogel (PGD80) changed rapidly in different mediums. Though the transmittance of sample PGD80 decreased to a low level after being immersed in water for 25 minutes, if the PVA/gelatin hydrogel was taken out from water and immersed in DMSO, the transmittance increased up to the same level as that before immersed in water. It was interesting that, if the PVA/gelatin hydrogel was alternately immersed in water and DMSO, the transmittances varied accordingly (Figure 2). The reversible optical properties of PVA/gelatin hydrogels may find applications in sensors and light modulation materials.

The XRD patterns of dried gelatin, dried PVA, and dried PVA/gelatin hydrogels are shown in Figure 3a. PVA is a partially crystalline polymer, and the diffraction peak at the 2θ of 20° corresponds to the (101) plane of PVA, while the peak at the 2θ of 22° is characteristic for the semi-crystalline structure of gelatin (Hong et al., 1998; Wang et al., 2006). With increasing the amount of DMSO used in the PGD hydrogels, nearly all diffraction peaks turn to move to larger angles. The 2θ of peak B increases from 19.31° to 19.75° for PVA/gelatin hydrogels without DMSO and with 80% DMSO. It was indicated that the crystallinity of PVA/gelatin hydrogels was mainly from PVA.

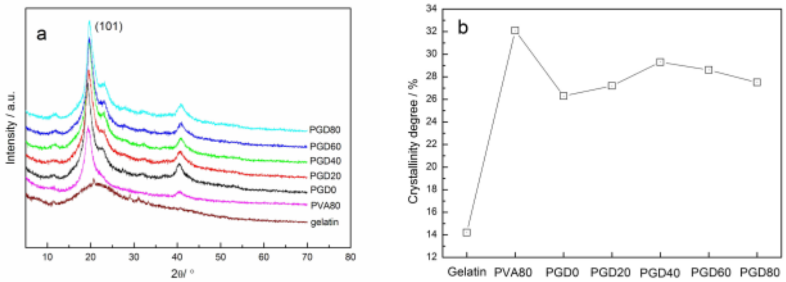

Figure 3. XRD patterns and crystallinity degrees of dried gelatin, dried PVA, and dried PVA/gelatin hydrogels

The crystallinity degrees in Figure 3b indicated that solvent used in the preparation of hydrogels may the crystalline structures of PVA/gelatin hydrogels. It could be observed that the crystallinity degree of PGD80 (27.5%) was lower than that of PVA80 (32.1%). By the wide angle neutron scattering techniques, Kanaya et al. found the crosslinking points of PVA gels were composed of crystallites (Kanaya, 1994), whereas gelatin could hardly form crosslinking points via freeze-thawed method due to its non-crystalline structure. Therefore, gelatin may disperse in the PVA and decrease the of crystallinity degrees of PVA.

The XRD patterns of swollen PVA80 and PGD80 hydrogel samples before and after soaked in water are shown in Fig. 4. Freshly prepared PVA80 and PGD80 hydrogel samples (still containing DMSO) showed similar XRD patterns before water immersion (curves (a) and (b)), and both of them were transparent. After water immersion, however, although changes in light transmittances of PVA and PVA/gelatin hydrogels were different (Figure 2), very similar shapes in the XRD patterns were exhibited as shown in curve (c) and curve (d)), suggesting that the crystalline structure transformation during water immersion may not be the key factor affecting the optical properties. A possible explanation for the solvent sensitivity of optical properties may be the loss of homogeneous structure of PVA/gelatin hydrogels because of the solvent replacement. A complex (Packer and Tomlinso, 1971) may be formed in the mixture of DMSO and water, which reversibly affect the compatibility of gelatin and PVA and partial crosslinking points in hydrogels. Heterogeneous structure hydrogels were formed as a result. It is usually considered that heterogeneous structure is responsible for the optical properties of materials due to light scattering, and further investigation is needed in our future work. In this work, it was proved that the changes in optical properties of PVA/gelatin hydrogels are reversible. The the respondance of PVA/gelatin hydrogels to solvent stimulus is quick.

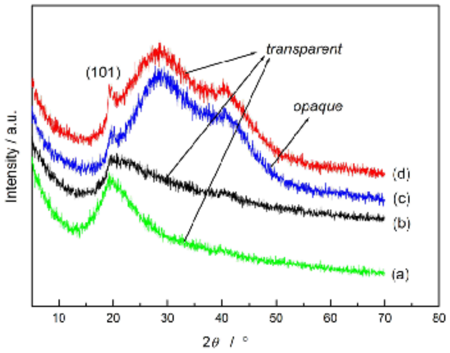

Figure 4. XRD patterns of swollen PVA and PVA/gelatin hydrogels. (a): PGD80-DMSO; (b): PVA80-DMSO; (c): PGD80-water; (d): PVA80-water

CONCLUSIONS

The physically crosslinked PVA/gelatin composite hydrogels using DMSO/water mixture as the solvent behave different optical properties from pure PVA hydrogels. The light transmittances of PVA/gelatin hydrogels were sensitive to solvent, reversibly varying in different kinds of solvents. The mechanism was proved to be not simply related to their crystalline structure transformation.

Acknowledgements

The financial supports from the National Natural Science Foundation Commission of China (No. 50973097, 21076199), China-Romania Governmental Science & Technology Cooperation Program (No. 40-17), and Key Laboratory of Microgravity, Institute of Mechanics, Chinese Academy of Sciences are gratefully acknowledged.

REFERENCES

Bajpai, A.K. and Saini, R. (2005), “Preparation and characterization of biocompatible spongy cryogels of poly(vinyl alcohol)-gelatin and study of water sorption behaviour”, *Polymer International*, 54, 1233-42.

Chiellini, E. et al. (2001), “Gelatin-based blends and composites:morphological and themal mechanical characterization”, *Biomacromolecules*, 2, 806-11.

Hassan, C.M. and Peppas, N.A. (2000), “Cellular PVA hydrogels produced by freeze/thawing”, *Adv Polym Sci*, 153, 37-65.

Hong, P.D. et al. (1998), “Solvebt effect on structural change of poly(vinyl alcohol) physical gels”, *J Appl Polym Sci*, 69, 2477-86.

Jeeyoung, C. et al. (2007), “Effects of solvent dehydration on creep resistance of poly(vinyl alcohol) hydrogel”, *Biomaterials*, 28, 772-80.

Kanaya, T. et al. (1994), “Structure of poly(vinyl alcohol) gels studied by wide- and small-angle neutron scattering”, *Macromolecules*, 27, 5609-15.

Liu, Y.R. et al. (2010), “Thermal behavior and mechanical properties of physically crosslinked PVA/Gelatin hydrogels”, *J Mech Behav Biomed Mater*, 3, 203-9.

Mendieta-Taboada, O. et al. (2008), “Thermomechanical properties of biodegradable films based on blends of gelatin and poly(vinyl alcohol)”, *Food Hydrocolloids*, 22, 1485-1492.

Packer, K.J. and Tomlinso, D.J. (1971), “Nuclear spin relaxation and self-diffusion in the binary system, dimethylsulphoxide(DMSO)+WATER”, *Trans Faraday Soc*, 67, 1302-14.

Tong, X. et al. (2007), “Swelling and mechanical behaviors of carbon nanotube/poly(vinyl alcohol)hybrid hydrogels”, *Materials Letters*, 61, 1704-06.

Toshihisa, T. et al. (1999), “Phase separation in poly(vinyl alcohoi)/gelatin blend systems”, *Polymer International*, 48, 811-18.

Wang, H.Y. et al. (2006), “Preparation and characterization of ZnS:Cu/PVA composite nanofibers via electrospinning”, *Materials Letters*, 60, 2480-84.

PH-SENSITIVE SODIUM ALGINATE/GELATIN HYDROGEL BEADS PREPARED BY DIFFERENT CROSSLINKING METHOD FOR CONTROLLED RELEASE OF SALICYLIC ACID

JIE LIU, YUAN JINGWEN, XUEJING ZHENG, XIANGNAN LIU, XICHAN HE, FANG WANG, KEYONG TANG

College of Materials Science and Engineering, Zhengzhou University, Henan 450052, China, Phone: 86-371-67763216, email: keyongtang@yahoo.com.cn; liujie@zzu.edu.cn

In order to enhance the drug entrapment efficiency and improve the swelling behaviors of drug delivery system, Ca2+ and glutaraldehyde (GTA) crosslinking were used to prepare sodium alginate/gelatin (SA/Gel) hydrogel beads. The mixture solution of SA and gelatin was crosslinked with two different schemes, one step method (OSM) SA/Gel beads were simultaneously crosslinked by Ca2+ and GTA, and two step methods (TSM) SA/Gel beads were firstly crosslinked by Ca2+ and followed with a GTA crosslinking treatment. The chemical structure and morphology of the beads were characterized by Fourier transform infrared spectroscopy (FTIR) and scanning electron microscope (SEM). The swelling and pH-sensitive properties of the beads were investigated, and the drug loading and controlled release properties of the beads were also evaluated using salicylic acid as the model drug. Results indicate that all beads were formed well and the encapsulation efficiency and releasing properties of OSM beads are better than those of TSM beads, and the study provide a facile and effective method to improve the drug delivery system. The kinetic model fitting results showed that release law of OSM beads more accorded with the Ritger-Peppas release model. The mechanism of drug releasing from the prepared drug-loaded hydrogel beads was Fick-diffusion mechanism after the initial burst release.

Keywords: alginate, gelatin, release.

INTRODUCTION

The interest of using natural materials as drug delivery system has long been the subject of great interest in recent years (Saboktakin et al., 2009; Tønesen and Karlsen, 2002). Sodium alginate (SA) is a sodium salt of alginic acid, a naturally occurring polysaccharide found in marine brown algae. Alginate has been widely used as food and pharmaceutical additives, such as a tablet and ice creams. Calcium alginate beads can be produced by dropping a sodium alginate aqueous solution into a calcium chloride solution. Although this is a simple way of obtaining particulate drug carriers, drug loss and high permeability of pure SA hydrogel is considered a major limitation during drug-loaded beads preparation (Torre et al., 1998). Hence, some researchers tried to circumvent this problem by preparing composite hydrogel beads such as SA/pectin (Liu and Krishnan, 1999), SA/chitosan (Anal and Stevens, 2005), SA/gelatin (Shinde and Nagarsenker, 2009) and even SA/PVA (Hua et al., 2010).

Gelatin is a protein with a broad range of functional properties, including film-forming ability, pH sensitivity, biocompatibility, and is obtained by hydrolyzing collagen. Gelatin can be effectively crosslinked by crosslinking agents such as formaldehyde, glutaraldehyde etc, but Ca^{2+} has not crosslinking effect on it (Zheng et al, 2012). The aim of this work was to formulate a dual crosslinked SA/Gel matrix that effectively prolongs drug release, which is obtained by different kind of crosslinking methods. The structure and morphologies were characterized and the swelling properties, pH-sensitivity and their drug release behaviors were studied using salicylic acid as the model drug.

EXPERIMENTAL

Materials

Sodium alginate (SA, a viscosity of 0.035Pa·s in 2% aqueous solution at 25°C) was from Paini Chemical Reagent Factory (Henan, China). Gelatin (type A), calcium chloride, glutaraldehyde and salicylic acid were purchased from Kermel Chemical Co. Ltd. (Tianjin, China). The simulated gastric fluid (SGF, pH 1.2) composed of 0.085M HCl, the simulated intestinal fluid (SIF, pH 7.4) composed of 0.05M potassium phosphate and 0.0395M sodium hydroxide. All the reagents used in this study were of analytical grade and used as received.

Preparation of SA/Gel Beads

One step method SA/Gel beads (OSM beads): Drug-loaded and drug-free SA/Gel beads were prepared by droplet extrusion/precipitation of a sodium alginate/gelatin aqueous mixture solution with or without salicylic acid. All mixture solution contains 1.5% (w/v) sodium alginate and 1.5% (w/v) of gelatin. This solution is prepared by a simple mixing step. Then it is added into a gently stirred (100 rpm) 2.0% (w/v) calcium chloride/0.2% (v/v) GTA aqueous mixture using a syringe with the form of droplets, and the stirring was kept for additional 15min. The dual crosslinked OSM spherical and homogenous SA/Gel beads were obtained, and were washed with distilled water for three times.

Two step method SA/Gel beads (TSM beads): TSM SA/Gel beads were obtained by adding the same mixture solution (1.5% SA and 1.5% gelatin) into 2.0% (w/v) calcium chloride aqueous solution, and the stirring was kept for 15min. After beads preparation, all beads were further crosslinked in a 0.2% (v/v) GTA aqueous solution for additional 15min, excess of crosslinkers is washed out with distilled water for three times.

Characterization

FTIR spectra were obtained at room temperature using a Nicolet Impacta 400 spectrometer (Nicolet iS10, USA) in the range of 4000-400cm^{-1} using KBr pellets. Surface morphology of the dried beads was characterized before release testing, samples of the beads were sputter coated with gold in a vacuum evaporator, and photographed using a scanning electron microscope (JSM-7500F, Japan) using an accelerating voltage of 20 kV.

Swelling Studies

Two aqueous media were used in swelling and drug releasing measurement: HCl buffer solution (SGF, pH 1.2) and phosphate buffer solutions (SIF, pH 7.4). Weighted dry beads were placed at 37.0±0.5°C in conical flasks containing 200mL of buffer solution and magnetically stirred at 50 rpm. Swelling ratio was determined as follows:

$$Swelling\ ratio(\%) = \left(\frac{W_t - W_0}{W_0} \right) \times 100 \qquad (1)$$

where W_t is the weight of the beads at time t; W_0 is the initial weight of beads.

Determination of the Encapsulation Efficiency and *in vitro* Drug Release Profiles

Weighed beads were immersed and dispersed in 200 mL of PBS buffer at pH 7.4 for 24 h, and followed sonicated for 10 min to ensure the complete extraction. Then, the solution was filtered, and the drug content was determined by a UV-spectrophotometer (Shimadzu UV5200, Kyoto, Japan) at wavelength of 290 nm. The ratio of the actual to the theoretical drug contents was termed as entrapment efficiency.

The in vitro drug release tests were carried out using the magnetic mixer, the rotor was rotated at 50 rpm and 37.0±0.5°C. The dissolution media used were PBS buffer at pH 7.4 and HCl buffer at pH 1.2.Weighted beads added to 200 mL dissolution medium. Samples (5 mL) were collected and replaced with the same fresh medium at various time intervals. The amount of drug released was analyzed spectrophotometrically at 290 nm (UV-2450, Shimadzu, Japan). The UV standard absorbance curve for salicylic acid was established in different buffer, and the UV absorbance obeyed the Beer's law in the concentration range from 3.2×10^{-5}-2.9×10^{-4}mol/L.

RESULTS AND DISCUSSIONS

Figure 1 shows the wet beads of drug-free and drug-loaded SA/Gel beads, generally, the drug-free beads are perfectly spherical and have a smooth surface, with a mean diameter of approximately 3.0 mm. As expected, drug incorporation leads to shape change of beads due to the viscosity increase of drug-SA/Gel suspension and its filling effect, the drug-loaded beads show oval shape and the long diameter to short diameter is about 2.8 mm: 2.5 mm. During air drying, the initial spherical and oval shapes are lost and particle shape changes significantly with salicylic acid encapsulation.

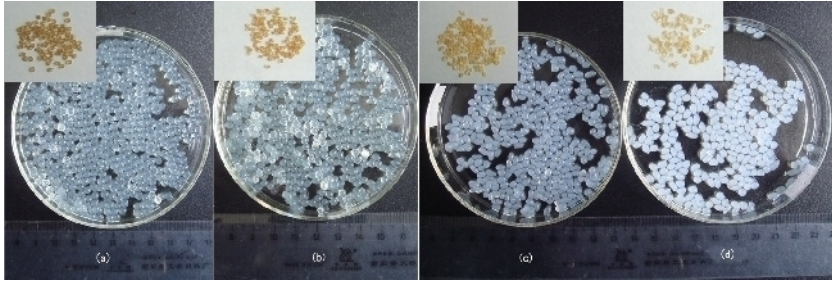

Figure 1. Photographs of wet and dry (upper left corner) sodium alginate/gelatin hydrogel beads (a) drug-free OSM beads; (b) drug-free TSM beads; (c) drug-loaded OSM beads; (d) drug-loaded TSM beads

Figure 2 presents the high-magnified SEM images of drug-free and drug-loaded SA/Gel bead. As can be seen, the surface of drug-loaded TSM bead was smoother than drug-free OSM and TSM bead, while the inclusion of drug in the OSM SA/Gel matrix creates bead with a rough surface adhered with some particles (Figure 2 (c)), the mean diameter of these particles is 0.8 μm. This was due to the inclusion of salicylic acid crystals in SA/Gel suspensions, which could be adhered to the surface of OSM bead with the help of GTA crosslinking. While for TSM bead, salicylic acid crystals can be easily removed from the surface of bead while Ca^{2+} crosslinking provides weaker interaction between drug particles and gel bead compared to the OSM bead. Encapsulation efficiencies of OSM and TSM beads are 88.0% and 51.1% (w/w), respectively. High encapsulation efficiency was achieved for OSM method, the simultaneously crosslinking with Ca^{2+} and GTA led to reduce the drug loss from the beads. In addition, the crosslinking duration of OSM beads in aqueous solution lasted only 15 minutes, while for TSM beads, it extents to 30 minutes (two stages). Salicylic acid presents certain solubility in aqueous solution, when the beads were immersed in crosslinking solution, the loss of drug on the surface of beads are different for OSM and TSM beads.

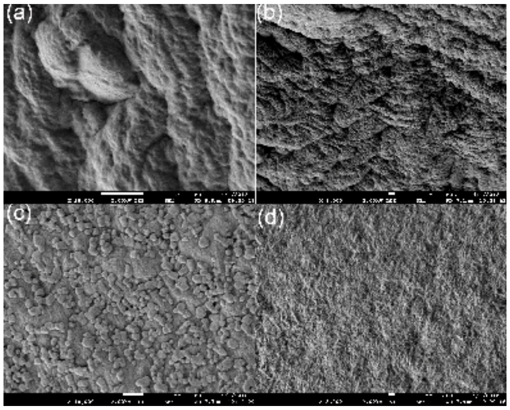

Figure 2. SEM micrographs of sodium alginate/ gelatin hydrogel beads: (a) drug-free beads and (c) drug-loaded OSM beads; (b) drug-free beads and (d) drug-loaded TSM beads

FTIR spectra of crosslinked drug-free and drug-loaded beads were analyzed (Figure 3). FTIR spectrum of drug-free beads showed the bands around 3414, 1653 and 1437 cm^{-1}, which are due to the stretching of −OH, asymmetric and symmetric stretching of −COO−. Drug incorporation caused an obvious shift of -OH stretching bands to higher wavenumber, indicating the possible break of hydrogen bonding between SA and gelatin with the introduction of salicylic acid (Hua et al., 2010). In particular, it can be observed that all bead showed a stretching of C-O at 1027 cm^{-1}, which would be attributed to the reaction between aldehyde group and amino group of gelatin.

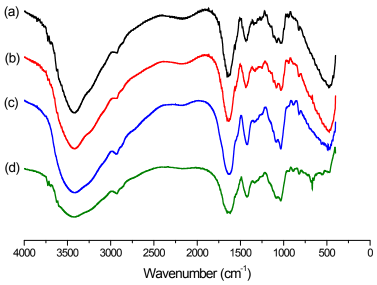

Figure 3. FTIR spectra of (a) drug-free OSM beads; (b) drug-loaded OSM beads; (c) drug-free TSM beads and (d) drug-loaded TSM beads

Plots of dynamic swelling of OSM and TSM beads in SGF (pH 1.2) and the SIF (pH 7.4) buffer are given in Figure 4(a) and 4(b), respectively. It is obvious that in the acidic and neutral environment, maximum swelling for OSM and TSM beads were reached at 15min and 40min, respectively. OSM beads exhibited lower swelling ratio at equilibrium and swelling rate, while TSM beads showed higher swelling ratio at equilibrium and swelling rate. Due to the same component of OSM and TSM beads, the swelling results indicate that the extent of crosslinking of the OSM beads is greater than that of TSM beads. The schematic illustrations of OSM and TSM bead formations with different crosslinking schemes are presented in Figure 5. In OSM beads preparation process, when a drop of SA/Gel mixture aqueous solution was injected into the vial containing Ca^{2+}/GTA mixture, the initially formed soft polymer matrix is favorable to the diffusion of GTA into the inner parts of the gel bead, and it results in a greater restriction of the mobility of polymer chains and thus limits the swelling ratio at equilibrium and swelling rate of beads. For TSM bead, the initially 15min incubation in Ca^{2+} solution after the bead formation harden the walls of the gel beads and reduced the diffusion of GTA molecules into the interior of the bead during the following incubation process in GTA solution.

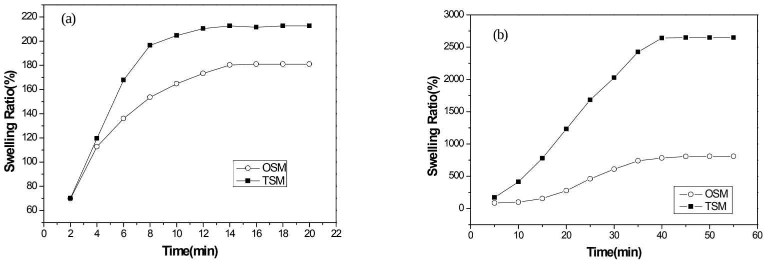

Figure 4. Swelling curves of drug-free OSM and TSM bead in SGF (a) and SIF (b) buffer solution

The salicylic acid release profiles of OSM and TSM beads are shown in Figure 6. In acidic and neutral medium, drug release of TSM beads is rapid and most dissolution is attained within 20-30 min, while OSM beads present a more stable and prolonged release profile. When drug-loaded OSM beads were immersed in a buffer solution, salicylic acid begins to be dissolved and diffuses into the buffer. However, salicylic acid crystal particles with low solubility adhering to the surface of gel beads act as a hard shell around soft gel beads, and then the OSM beads showed quite lower initial burst release compared to TSM beads. Moreover, for TSM beads, loss of surface acrylic acid crystal particles during the incubation process not only reduce the encapsulation efficiency of gel beds, it also leads to a burst release at the initially stage.

The comparison of Figure 6(a) and 6(b) showed that the release properties were associated with the swelling behavior of the beads, and drug-loaded OSM and TSM beads also present significant pH-sensitivity. Under neutral conditions, the gel matrix tends to swell and influencing drug release. The drug releasing process is further enhanced by the presence of phosphate ion, which acts as a calcium sequestrant. This feather was also observed during the swelling tests and probably is the main cause of the high maximum swelling ratio shown in Figure 4(b). Although, since GTA reinforced Ca^{2+} crosslinked SA/Gel network, the dissolution of SA and gelatin did not occur both in acidic and neutral medium.

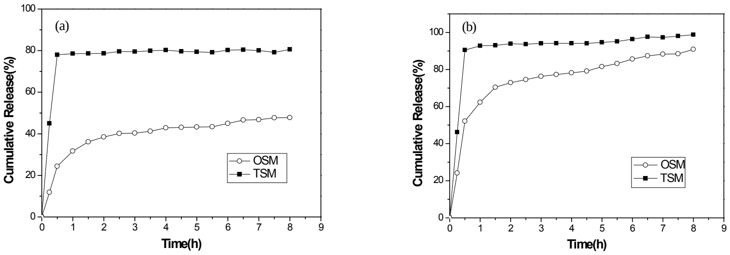

Figure 6. In vitro release of salicylic acid from OSM and TSM beads in SGF (a) and SIF (b) buffer solution

CONCLUSIONS

The results herein presented indicate that regulating crosslinking scheme caused a change of characteristic of salicylic acid-loaded SA/Gel beads, the OSM beads simultaneously crosslinked by GTA and Ca^{2+} provided the higher encapsulation efficiency and prolonged drug releasing profile.

Acknowledgements

The financial supports from the National Natural Science Foundation Commission of China (No. 50973097, 21076199), China-Romania Governmental Science & Technology Cooperation Program (No. 40-17), and Key Laboratory of Microgravity, Institute of Mechanics, Chinese Academy of Sciences are gratefully acknowledged.

REFERENCES

Anal, A.K. and Stevens, W.F. (2005), "Chitosan-alginate multilayer beads for controlled release of ampicillin", *International Journal of Pharmaceutics*, 290, 45-54.

Hua, S.B. et al. (2010), "pH-sensitive sodium alginate/poly(vinyl alcohol) hydrogel beads prepared by combined Ca2+ crosslinking and freeze-thawing cycles for controlled release of diclofenac sodium", *International Journal of Biological Macromolecules*, 46, 517-523.

Liu, P. and Krishnan, T.R. (1999), "Alginate-pectin-poly-L-lysine particulate as a potential controlled release formulation", *J. Pharm. Pharmacol*, 51, 141-149.

Saboktakin, M.R. et al. (2009), "pH-sensitive starch hydrogels via free radical graft copolymerization, synthesis and properties", *Carbohyd. Polym*, 77, 634-638.

Shinde, U.A. and Nagarsenker, M.S. (2009), "Characterization of Gelatin-Sodium Alginate Complex Coacervation System", *Indian J Pharm Sci*, 71(3), 313-317.

Torre, M.L. et al. (1998), "Formulation and characterization of calcium alginate beads containing ampicillin", *Pharm. Dev. Technol*, 3, 193-198.

Tønesen, H.H. and Karlsen, J. (2002), "Alginate in drug delivery systems", *Drug Dev. Ind. Pharm*, 28, 621-630.

Zheng, X.J. et al. (2012), "Preparation and properties of sisal microfibril/gelatin biomass composites", *Composites: Part A*, 43, 45-52.

THE INFLUENCE OF TANNIC ACID AND VALONEA ON COLLAGEN STRUCTURE

CEMILE CEREN TOSUN[1], MĂDĂLINA GEORGIANA ALBU[2], HASAN OZGUNAY[1], CIPRIAN CHELARU[2]

[1] *Ege University Faculty of Engineering Department of Leather Engineering, 35100 Bornova-Izmir-TURKEY, hasan.ozgunay@ege.edu.tr, cctosun@gmail.com*

[2] *INCDTP – Division: Leather and Footwear Research Institute, Collagen Department, 93 Ion Minulescu, 031215, Bucharest, Romania, albu_mada@yahoo.com*

Collagen is one of the most used natural polymers in constructing of scaffolds for tissue engineering. The aim of this study was to investigate the influence of two cross-linking agents on the collagen properties. Type I fibrillar collagen at acidic pH was stabilized with 0.5, 1.0 or 2.0% tannic acid or valonea and then lyophilized in order to obtained 3D spongious form. The physical-chemical properties were assessed using infrared spectroscopy (FTIR), thermal analyses by micro hot table and morphological properties were evaluated by water uptake. The results demonstrated that the collagen scaffolds cross-linked with 1% tannic acid are the most stable.

Keywords: collagen gel, tannic acid, valonea

INTRODUCTION

Collagen, the most abundant protein in the body, is the major constituent of connective tissues. It is readily isolated and purified in large quantities and can be processed into a variety of forms. As such, it has been widely applied in biomaterials applications in form of wound dressing, matrix for controlled release of active agents, or tissue-engineering scaffolds. The advantages of collagen as biomaterial are low toxicity to most tissues, biocompatibility, and well-documented structural, physical, chemical, and immunological properties (Duan and Sheardown, 2005).

However, in its purified form, collagen forms a weakly cross-linked thermo gel with mechanical properties that are not adequate for most *in vitro* and *in vivo* applications, severely limiting its potential as a biomaterial. The formation of covalent intermolecular cross-links between collagen molecules in macromolecular fibrils with appropriate biocompatible molecules is an effective method to improve mechanical integrity and stability. Physical cross-linking (such UV 245 nm or severe dehydrathermal –DHT), although avoiding the introduction of potentially cytotoxic chemical residues, generally does not result in a sufficiently high degree of cross-linking for tissue-engineering applications (Duan and Sheardown, 2005). Since the physical properties of the collagen material are dependent on the cross-linking method adopted, it becomes important to determine the alteration of physical properties that result during cross-linking.

In this study, collagen crosslinking with natural (vegetable) agents was investigated. Vegetable tannins are one of the oldest materials used for tanning hides and skins. Metal – free and natural compositions of vegatable tannins infuse our research. Tannic acid (TA) and Valonea (V) were used as cross-linking agents for collagen gels with possible biomedical applications. Valonea is one of the well-known vegetable tannins used in tanning and re-tanning processes for leather processing. This tannin, obtained from tannin rich fruits of the acorn cups of the *Quercus* species, has been used extensively to tan hide and skin either alone or accompanied by other tanning agents (Ozgunay, Sarı, and Tozan, 2005). Tannic acid is applied as a drug for the treatment of burns and wounds due to its astringent, hemostatic and antibacterial properties. That is why the biomaterials obtained by the combination of collagen with tannic acid and valonea are expected to have enhanced healing benefit properties (Ghica et al. 2009). Both valonea and tannic acid belong to hydrolysable tannins group. These two materials can stabilize the collagen not only by hydrogen bonds but also by ionic bonds which are established between OH groups of collagen and NH_2 groups of tannins.

The aim of our study is to develop and characterize new collagen scaffolds using natural cross-linking agents (TA and V). Therefore, different concentrations of TA and V (0.5, 1.0, 2.0%) were used to obtain hydrogels. After their freeze-drying, natural collagen matrices were obtained and their physical-chemical and morphological properties were characterized.

MATERIALS AND METHODS

Materials

Type I fibrillar collagen gel (Coll) having concentration of 2.56% (w/w) was extracted from calf hide as previously described (Albu, 2011). Tannic acid (TA) was supplied by Sigma-Aldrich (Germany). Valonea (V) was received from Ege University Leather Engineering department, Turkey.

Collagen Scaffolds Preparation

The concentration of collagen gel was adjusted at 1% and pH at 3.5÷3.8. Collagen gels with variable concentration of tannic acid or valonea as the Table 1 shows were cast in dishes and kept at freezer, then they were freeze-dried (lyophilized) using the freeze-dryer Delta 2-24 LSC (Martin Christ, Germany) and the program of lyophilization as we previously described (Lungu et al., 2012).

Table 1. Compositions and codes of cross-linked collagen gels

Codes of samples	Collagen,%	pH	TA, %	V, %
AColl	1	3.5-3.8	0	0
AColl-TA-0.5	1	3.5-3.8	0.5	0
AColl-TA-1.0	1	3.5-3.8	1.0	0
AColl-TA-2.0	1	3.5-3.8	2.0	0
AColl-V-0.5	1	3.5-3.8	0	0.5
AColl-V-1.0	1	3.5-3.8	0	1.0
AColl-V-2.0	1	3.5-3.8	0	2.0

Water Uptake Capacity of Collagen Matrices

The water uptake capacity was measured using distilled water. Pieces of collagen matrices were weighed (W_d) and then introduced in water. At established time intervals, the hydrated matrices were weighed (W_w) and results are calculated using the following formula:

$$Water\ uptake = (W_w - W_d)/W_d\ (g/g) \quad (1)$$

where,

W_w = the weight of wet matrices at immersion time
W_d = the weight of dry scaffolds

FT-IR Spectroscopy

FT-IR spectral measurements were recorded by spectrophotometer Jasco FT/ IR-4200. All the spectra were recorded at the following parameter: 4000-600 cm^{-1}, resolution 0.5-4 cm^{-1} with 30 acquisitions per each sample.

Thermal Analysis

The shrinking temperature measurements were recorded within the range 22 – 100°C with a heating rate of 2°C/min using micro-hot-table technique with a Caloris Micro Hot Table in co-work with a Leica Stereomicroscope.

RESULTS AND DISCUSSION

Tannins are known to readily bind with collagen. The mechanism of bonding of the vegetable tannins to the collagen is shown in Figure 1, respectively.

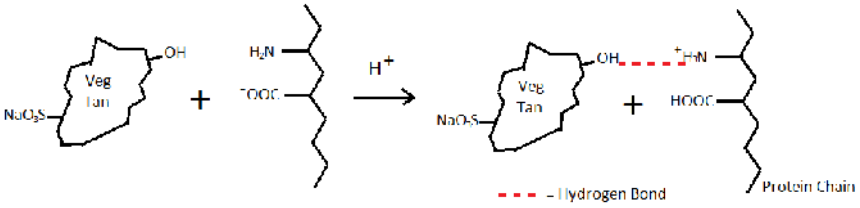

Figure 1. Mechanism of bonding vegetable tannins

As the water up-take analysis shows, the higher cross-linking in collagen matrices means lower water absorption capacity. Table 2 shows water absorption values of samples during 4 hours. All samples disintegrated in less than 4 hours after their immersion into water.

Table 2. Water absorption during time

Time, min	Water absorption, g/g AColl	AColl-TA-0.5	AColl-TA-1.0	AColl-TA-2.0	AColl-V-0.5	AColl-V-1.0	AColl-V-2.0
0	47.10	21.11	23.88	19.49	17.57	18.58	13.09
5	53.34	32.96	35.99	36.68	29.56	27.64	22.93
10	55.03	43.21	44.58	43.09	37.32	39.92	28.98
20	57.01	44.94	48.04	52.14	44.54	47.92	39.88
30	67.20	50.79	56.26	55.80	49.54	55.01	44.46
60	70.36	56.30	62.91	60.84	53.12	67.39	54.15
120	-	63.09	69.88	72.15	54.25	76.69	64.87
180	-	59.30	75.18	77.88	56.09	70.22	69.30
240	-	62.48	78.28	-	-	-	74.07

As it can obviously be seen from Table 2, the water up-take values increase systematicaly in time. Comparing samples with the same concentration of tannin agents we can see differences between collagen tanned with valonea and tannic acid. Although collagen tanned with valonea absorbed higher about of water, as the Figure 2 shows, the samples with tannic acid are more stable in time. In the Figure 2a,b a comparison between A-Coll-TA-1.0 with A-Coll-V-1.0 and A-Coll-TA-2.0 with A-Coll-V-2.0 is given for exemplification.

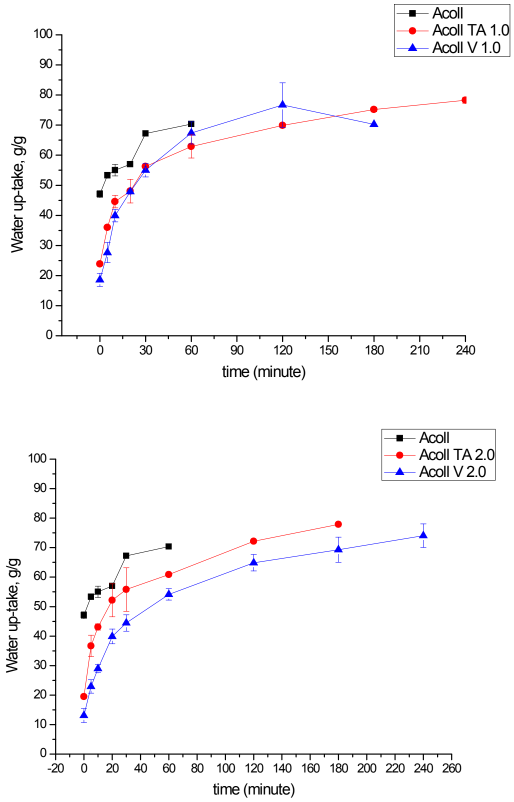

a)

Figure 2. Water up-take of collagen matrices: a) A-Coll-TA-1.0 / A-Coll-V-1.0 and b) A-Coll-TA-2.0 / A-Coll-V-2.0

Collagen has a unique triple helical configuration which is characterized by its amide bands featured in IR spectra (Albu et al. 2011). In the Figure 3, we can observe the typical bands such as N–H stretching ~ 3310 cm^{-1} for the amide A, C–H stretching at ~ 3063 cm^{-1} for the amide B, C=O stretching at 1600–1700 cm^{-1} for the amide I, N–H deformation at 1500–1550 cm^{-1} for the amide II and N–H deformation at 1200–1300 cm^{-1} for the amide III band. Normally, the amide I band is strong, the amide II band is weak and the amide III band is moderate (Chang, Tanaka, 2002).

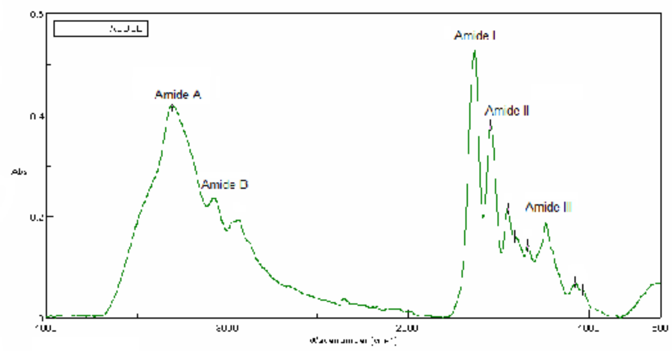

Figure 3. FT-IR spectrum of reference collagen matrix – Acoll

Figure 3 shows the FT-IR spectrum of reference scaffold of acid collagen. The modifications of collagen structure were appreciated through A_I / A_A ratio which is correlated with the cross-linking degree as the Figure 4 shows.

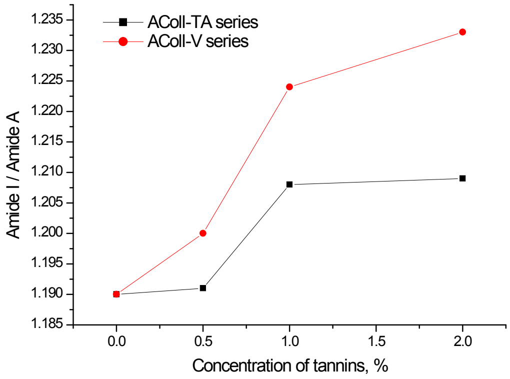

Figure 4. The influence of tannin concentration on A_I / A_A

The cross-linking degrees of the studied samples increase with concentration of tannin increasing. Moreover, the Amide A of ACoII matrix shifts from 3306 cm^{-1} to 3298 cm^{-1} in A-CoII-TA-1.0 and to 3299 cm^{-1} in A-CoII-V-2.0. This happened because of hydrogen bonds formation when the tanning agents were added.

Type I collagen cylindrical molecules ordered laterally by salt links between side chains and take up the shape of pentafibrils. These pentafibrils of diagonal distance 35Å further aggregate to form fibril of dimension 20–100 nm, which in turn leads to the formation of fascicle and fibre. Such highly ordered collagen has a unique temperature at which the fibre shrinks to one third of its original length if heated in a water medium. This temperature is called shrinkage temperature (T_S) or hydrothermal stability (Madhan et al. 2005). In this study, T_S of collagen scaffolds was determined to be 41.2 °C by MHT. Figure 5 presents the graphic for T_S of studied samples.

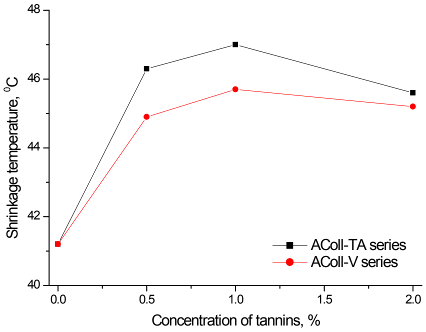

Figure 5. The influence of tannin concentration on T_S

Shrinkage temperature is the most important point which determined the cross-linking degree of collagen. As the results presented in the Figure 5 show, the samples cross-linked with 1.0% of tannin agent had the highest T_S.

CONCLUSIONS

Porous matrices based on collagen cross-linked with tannic acid or valonea were prepared by freeze-drying method. The water uptake test demonstrated that the collagen cross-linked with tannic acid is more stable in time comparing with collagen cross-linked with valonea. The same results were obtained also by FT-IR. The shrinkage temperature showed that 1.0% cross-linking agents on collagen structure gain the best results of thermal stability. This property enables the obtained matrices to be used as scaffold for tissue engineering.

Acknowledgements

This work was supported by Erasmus Student Internship Programme (Placement), Ege University, Turkey.

REFERENCES

Albu, M.G. (2011), *Collagen gels and matrices for biomedical applications*, Lambert Academic Publishing, Saarbrücken, Germany.

Chang, M.C., Tanaka J. (2002), "FT-IR study for hydroxyapatite/collagen nanocomposite cross-linked by glutaraldehyde", *Biomaterials*, 23, 4811-4818.

Duan, X. and Sheardown H. (2005), "Crosslinking of collagen with dendrimers**",** *Journal of Biomedical Materials Research Part A,* 75A(3), 510-518.

Ghica, M.V., Albu, M.G., Popa, L., Leca, M., Brazdaru, L., Cotruţ C. and Trandafir V. (2009), "Drug delivery systems based on collagen-tannic acid matrices", *Revue Roumaine de Chimie*, 54(11-12), 1103–1110.

Lungu, A., Albu, M.G., Stancu, I.C et al. (2012), "Superporous collagen-sericin scaffolds", *Journal of Applied Polymer Science*, DOI: 10.1002/app.37934.

Madhan, B., Subramanian, V., Raghava Rao, J., Nair, B.U., Ramasami, T. (2005), "Stabilization of collagen using plant polyphenol: Role of catechin", *International Journal of Biological Macromolecules*, 37, 47–53.

Ozgunay, H., Sarı, O. and Tozan, M. (2007), "Molecular Investigation of Valonea Tannin", *Journal of the American Leather Chemists Association*, 102(5), 154-157.

ESSENTIAL OILS AS ANTIOXIDANTS FOR FATLIQUORING EMULSION

VIRGILIJUS VALEIKA, JUSTA ŠIRVAITYTĖ, KESTUTIS BELEŠKA, VIOLETA VALEIKIENĖ

Kaunas University of Technology, Radvilenu pl. 19, Kaunas LT-50254, Lithuania

Oxidation can change the properties of fatliquoring emulsion components. For leather fatliquoring are used natural fats or oils, and their recycling products, petrol chemicals products, synthetic fats, oil or soaps. These materials are more or less sensitive to oxidation process. Therefore, for the increase of their stability could be used antioxidants. For sample, polyphenols from plant extracts have been used in different food matrices to improve the oxidative stability of lipids. In the presented material were proposed commercial essential oils of Lavandulae officinalis and Eucalyptus globulus as antioxidants for fatliquoring system assigned to tanned leather. It was established that selected essential oils have different extent of antioxidant activity. The commercial essential oils of Eucalyptus globulus has shown close antioxidant activity comparing with butylated hydroxytoluene. The addition of essential oil into leather fatliquoring emulsion has negligible influence on tanned leather quality indexes.

Keywords: essential oil, antioxidant, fatliquoring

INTRODUCTION

Depending on the storage conditions, two main reactions can affect lipids. Oxidation is a free radical chain process occurring spontaneously or at moderate temperatures in the presence of molecular oxygen. Although the reaction between triplet oxygen and fatty acids is thermodynamically unfavourable (Frankel, 2005), heat, transition metals, and light can accelerate fatty acid free radical formation (Choe et al., 2006). Under light exposure in the presence of sensitizers such as metals or chlorophylls, triplet oxygen can form singlet oxygen, a powerful radical generator that reacts directly with lipids (Choe et al., 2006).

The oxidation can change the fatliquoring emulsion compounds properties. For leather fatliquoring are used natural fats or oil, their recycling products, petrol chemicals products, synthetic fats, oil or soaps. These materials are more or less sensitive to oxidation process (Covington, 2009). Leather fatliquoring process is carried out at 55-60ºC temperature which could also attributed to the lipids oxidation condition. Therefore, for the stop of this process run the antioxidants could be employed. Many sources of antioxidants of a plant have been studied in recent years. Many aromatic plants and spices have been shown to be effective in retarding the process of lipid peroxidation (Kulisic et al., 2004). One component present in aromatic plants and spices, and which may act as a natural antioxidant, is the corresponding essential oil. Polyphenols from plant extracts have been used in different food matrices to improve the oxidative stability of lipids (Boroski et al., 2012).

In this case authors propose natural materials such as Lavandulae officinalis and Eucalyptus globulus essential oils. In previous research was concluded that following essential oils could be used in leather tanning as antimicrobial agents (Sirvaityte et al., 2011). The aim of this research was to investigate antioxidant properties of Lavandulae officinalis and Eucalyptus globulus essential oils.

MATERIALS AND METHODS

For investigation was used rapeseed oil. As control antioxidant was used butylated hydroxytoluene (BHT) and 2,2-diphenyl-1-pikryl-hydrazyl (DPPH) (Sigma Chemicals, USA). Others chemicals were analytical grade.

The essential oils of company “Meta” (Lithuania) were used for experiments. There were commercial essential oils of Eucalyptus globulus (EO) and Lavandulae officinalis (LO).

Cured by salting bovine hides were used in order to obtain chromed leather. The processes were carried out according to the conventional technologies. For the experiments, tanned with chromium leather samples were neutralized and fatliquored under conditions described in Figure 1.

Figure 1. Leather neutralization and fatliquoring conditions (% from wet-blue mass)

Neutralization

a) H_2O 150%; $NaHCO_3$ 1.5%; temperature 35–40ºC; duration 0.5 h; run continuously;
b) HCOONa 2.0%; duration 1.5 h; run continuously; (pH of leather ~ 5.6)
Drain.

Washing

H_2O 100%; temperature 40-45°C; duration 30 min; run continuously.
Drain.

Fatliquoring

a) H_2O 150%; Coripol GF 10.0%; Coripol A 4.0%; Borron SAF 0.2%; **essential oil 1%;**
temperature – 55-60°C; duration – 1.5 h; run – continuously;
b) HCOOH 1%; duration 0.5 h; run continuously; (pH of leather ~ 4.0)
Drain.

Washing

H_2O 100%; temperature 30°C; duration 0.5 h; run continuously.
Drain.

The products of „TFL Holding GmbH” (Germany) were used: Coripol GF is oil based on a combination of selected natural and synthetic fatty substances; Coripol A is viscous oil based on natural phospholipids; Borron SAF – is a clear product, based on sulphated fatty alcohols.

The control samples of leather were tanned according to the conventional technology of Joint-stock company “Kedainiu oda”.

Determination of Radical Scavenging in DPPH• Reaction

The antioxidant activity of essential oils was measured using DPPH• radical scavenging assay method (Brand-Williams et al., 1995). The 5 ml methanol solution of DPPH• was used. The reaction was started by the addition of 25 ml sample and the decrease in absorbance was measured on a Beckman DU-650 spectrophotometer at 515 nm after 16 min and 2 h. Methanol was used as a blank sample. All determinations were performed in triplicate. The antioxidant activity was calculated as the inhibition (%) of the DPPH radical.

Peroxide Value

Primary oxidation products — hydroperoxides — were determined by peroxide value measurements. 1±0.1 g of oil was weighted and subjected to iodometric determination of peroxide value (AOCS, 1990). The induction period was considered as the number of days needed for the peroxide value of the sample to become 20 meq O_2/kg of fat. This is in agreement with a general consideration that oils become rancid at peroxide value higher than 20.

Leather Quality Indexes

The amount of chrome compounds in leather was determined by method described in literature (Standard ISO, 2007). The shrinkage temperature of leather was measured with a special instrument (Golovteeva et al., 1982). The matter soluble in dichloromethane and free fatty acid content were determined according to standard (Standard ISO, 2008).

Statistical Analysis

All data were expressed as the mean ± standard error of triplicate measurements. Confidence limits were set at $P < 0.05$. Standard deviations did not exceed 5% for the majority of the values obtained.

RESULTS AND DISCUSSIONS

The DPPH free radical does not require any special preparation and is considered a simple and very fast method for determining antioxidant activity. So, this method was chosen for estimation of antioxidant activity of commercial essential oils. The obtained data (Table 1) show that antioxidant activity of essential oils increases when increasing their concentration. Also, here could be mentioned that initially LO showed the higher radical scavenging effect comparing with EO. This could be explained by the earlier received results, which had shown that LO contained more phenolic compounds than EO (Sirvaityte et al., 2011). The IC50 of LO was 230 µl/ml (Table 1) and 394 µl/ml in the case of EO (Table 2) (the IC50 is the amount of essential oil needed for 50% inhibition of free radicals.). However, in the course of time the essential oil of Eucalyptus antioxidation capacity increases almost up to 100% during 120 min. LO also has shown the high efficiency, but during storage antioxidative activity reaches only 78%.

Table 1. Antioxidative capacity of the Lavandulae officinalis essential oil

Concentration of essential oil, µl/ml	Time, min 16	30	60	120
166	33.12	34.61	39.00	42.84
200	39.64	39.85	46.48	47.54
230	55.71	59.57	61.14	63.79
286	65.00	68.71	69.29	69.86
333	70.00	70.50	71.64	73.14
375	70.93	71.79	71.86	72.14
412	72.07	73.71	73.79	78.14

Table 2. Antioxidative capacity of the Eucalyptus globulus essential oil

Concentration of essential oil, µl/ml	Time, min 16	30	60	120
333	47.77	58.12	75.80	92.99
355	48.29	55.41	75.13	92.32
375	48.77	56.69	76.40	93.12
394	50.96	61.78	72.61	94.76
412	57.96	71.18	84.87	95.15
474	64.17	75.48	90.13	96.50
500	66.56	76.27	90.29	94.75
524	70.38	79.46	91.88	95.86
545	71.34	81.37	92.34	96.00
565	74.84	83.92	92.56	96.50

To simulate the fatliquoring material the selected essential oil had been mixed with rapeseed oil and peroxide value determined (Table 3). For the experiment were prepared mixtures from rapeseed oil with essential oils or with BHT. The amount of essential oils added into rapeseed oil was 1%. The amount of antioxidant agent BHT was standard and was 0.02% from rapeseed oil mass. As control was used pure rapeseed oil without any additives. As the temperature of fatliquoring usually is 55-60°C, the samples are kept 45 days at 55°C temperature. The results presented in Table 3 show that pure rapeseed oil (control sample) reaches 20 meq O_2/kg during 21 day. In case of LO addition this value was reached during 21 days. EO stops oil oxidation process better and its effect is close to the effect obtained with the use of BHT.

Therefore, LO in mixture with rapeseed oil has shown better antioxidant activity after one hour of storage at 55-60°C temperature, but after 72 hours of storage it becomes less comparing with EO.

So, the obtained results approve the trend obtained measuring the antioxidant activity of the separate essential oils (Tables 1 and 2).

Table 3. Peroxide value (meq O_2/kg) alteration of samples

Used antioxidant agent	Duration, h 1	72	120	168	240	336	504	1080
control	1.21	3.05	4.82	6.9	11.42	17.64	24.24	194.4
BHT	1.60	2.41	3.30	5.14	6.20	9.52	12.75	83.44
LO	1.23	3.55	5.84	7.60	10.41	15.61	29.57	134.72
EO	1.38	2.54	3.81	5.30	7.17	12.94	18.59	134.71

To evaluate the influence of essential oils on leather properties, such indexes as shrinkage temperature, content of Cr_2O_3, matter soluble in dichloromethane and content of moisture were determined. The chromed leather samples were fatliquored (under conditions described in Figure 1) with emulsion, which contains LO (2nd sample) and EO (3rd sample). The received results were compared with leather tanned according to conventional method (1st sample) in manufactory. The data are presented in Table 4.

Table 4. Quality indexes of leather after fatliquoring

Sample No.	Index of chromed leather			
	Shrinkage temperature, ºC	Content of Cr_2O_3, %	Matter soluble in dichloromethane, %	Content of moisture, %
1st (control)	121	4.90	10.0	17.3
2nd	117-119	4.50	13.5	17.5
3rd			16.3	16.7

The shrinkage temperature of leather tanned in manufactory is slightly higher but it can be expected because all processes run better under the industrial conditions. Also, it could be mentioned that higher content of fats was in samples processed using EO (16.3%).

CONCLUSIONS

The result of the present study showed that the commercial essential oil of Eucalyptus globulus and Lavandulae officinalis, which contain high amount of phenolic compounds, exhibited antioxidant activity. Selected essential oils have different extent of antioxidant activity. The commercial essential oil of Eucalyptus globulus has shown close antioxidant activity compared to butylated hydroxytoluene.

The addition of essential oils into leather fatliquoring emulsion has negligible influence on tanned leather quality indexes.

REFERENCES

AOCS (1990). In: Official methods and recommended practices of the American Oil Chemists' Society Method Cd 8-53 and Method Cd 1890. (4th ed.). Champaign: American Oil Chemists' Society.

Boroski M., Giroux H. J., Sabik H., Petit H.V., Visentainer J.V., Matumoto-Pintro P.T., Britten M. (2012), Use of oregano extract and oregano essential oil as antioxidants in functional dairy beverage, Food Science and Technology, 47(1), 167–174.

Brand-Williams, W., Cuvelier, M.E. and Berset, C. (1995), Use of a free radical method to evaluate antioxidant activity, Lebensmittel-Wissenschaft und -Technologie/Food Science and Technology, 28, 25-30.

Choe E, Min D. B. (2006), Mechanisms and factors for edible oil oxidation, *Comprehensive Reviews in Food Science and Food Safety*, 5, 169–86.

Covington A.T. (2009), Tanning Chemistry – The Science of Leather. The Royal Society of Chemistry, Cambridge.

Economou K.D., Oreopoulou V., Thomopoulos C.D. (1991), Antioxidant activity of some plant extracts of the family Labiatae, Journal of American Oil Chemists' Society, 68, 109–113.

Frankel, E.N. 2005. Lipid Oxidation, Second Edition, The Oily Press, Bridgwater, England.

Golovteeva A., Kutsidi D., Sankin L. (1982), Laboratornyj praktikum po khimiyi i tekhnologiyi kozhy i mekha, Legkaiya i Pischevaiya Prom, Moscow (Russ.).

Kulisic, T., Radonic, A., Katalinic, V., Milos, M. (2004). Use of different methods for the testing activity of oregano essential oil. Food Chemistry, 85, 633-640.

Sirvaityte J., Siugzdaite J., Valeika V. (2011), Application of Commercial Essential Oils of Eucalyptus and Lavender as Natural Preservative for Leather Tanning Industry, Revista de Chimie, 62(9), 884-893.

Standard ISO 5398-1:2007. Leather – Chemical determination of chromic oxide content – Part 1: Quantification by titration.

Standard ISO 4048:2008. Leather – Chemical tests – Determination of matter soluble in dichloromethane and free fatty acid content.

POROUS GELATIN HYDROGELS BASED ON CLAY PROMOTED BY CALCIUM MINERALIZATION

TAO ZHANG[1,2], YING GONG[1,3], XIAOLING LIU[1], BO TENG[1], WUYONG CHEN[1]

[1] *National Engineering Laboratory for Clean Technology of Leather Manufacture, Sichuan University, Chengdu, Sichuan, 610065, China, emails: Tao.Zhang@mailbox.tu-dresden.de, wuyong.chen@163.com*

[2] *Department of Chemie, Technische Universität Dresden, Dresden, 01069, Germany*

[3] *College of Chemistry and Chemical Engineering, Yunnan Normal University, 650500, Kunming, China, email: gongying_2004@163.com*

A bioclean method was proposed to prepare porous gelatin-based hydrogels using clay as porogen, water as solvent and calcium as promoter: firstly, laponite clay and gelatin were individually dissolved in deionized water to get aqueous solutions; then the two solutions were blended and exposed to -20°C for 24h to form physically crosslinked hydrogel; finally the hydrogel was soaked in a calcium chloride solution at room temperature for 48h to obtain matrixes with well-defined voids. The gelatin molecules intercalated into the clay slices gained uniform composites, which were confirmed by atomic force microscope, infrared spectrum, X-ray diffractomer and differential scanning calorimetry analyses. As proved by scanning electron microscope study, in the matrix containing 5% gelatin and 2% clay, the voids were interconnecting, and the size of pores focused on a range of 100-200µm. Such matrix might serve as scaffold for tissue engineering because of its typical pore structure and size distribution. Additionally, such material could be used as wound dressings, for it was able to provide a fine moist environment for a surface.

Keywords: hydrogel, gelatin, clay.

INTRODUCTION

In recent years, considerable efforts have been put into natural macromolecule based hydrogels, since such materials hold incomparable biocompatibility, biodegradability and bioactivity which are precisely pre-requisite in a biosystem. Furthermore, the controlled porosity, pore size, degradation rate, as well as tissue matching mechanical properties and appropriate biological response obtained from biocompatible and biodegradable materials are essential for tissue engineering (Barbetta et al., 2010).

Gelatin, as a kind of natural polypeptide obtained from collagen, consists of 18 different amino acids of various active groups such as amino, carboxyl, hydroxyl and phenolic hydroxyl. These side groups endow gelatin with excellent physical and chemical characteristics like film-forming, surface activity, reversible sol-gel transformation, polyampholyte, and high reactivity (Bigi et al., 2004). In this article, two biocompatible materials, gelatin and clay, were proposed to prepare porous hydrogels in an aqueous medium. This technique, avoiding the use of organic solvent, may provide a simple and clean technique to fabricate macroporous scaffolds for tissue engineering applications or other related fields.

MATERIALS AND METHODS

Materials

Gelatin (type B, G9382, isoelectric point 4.7-5.2), derived from bovine hide with an alkaline hydrolysis process, was purchased from Sigma (USA). The clay (laponite, W233) with an average diameter of 25 nm was kindly supplied by Weipu Co. Ltd. (China) and its chemical compositions are: SiO_2 55~57%, MgO 23.5~25.0%, Na_2O 2.8~3.8%, Li_2O 1.2~1.5%, F 5~5.8%. Calcium chloride and other reagents were analytical grade.

Fabrication Process

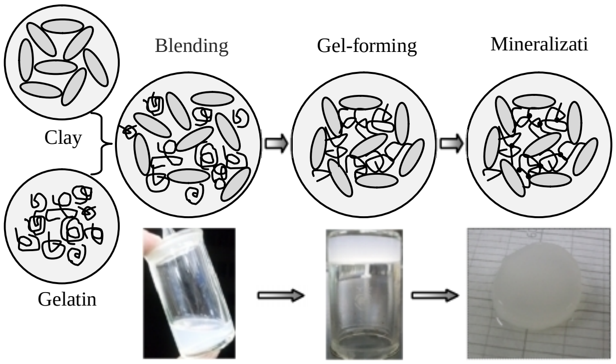

Figure 1. Schematic diagram for fabrication of gelatin-based hydrogels

As schematically illustrated in Figure 1, the preparation for gelatin-based hydrogels consisted of three procedures: blending, gel-forming and mineralization. The operations were as follows. Firstly X g (X=0.2, 0.3, 0.4 and 0.5, respectively) gelatin was dissolved in 5ml deionized water at 50°C for 2h to get solution a, and 0.2g clay was dispersed in another 5ml deionized water at 25°C with rapid agitation to get solution b. Next, the two solutions were blended with agitation, and the blends turned into a translucent sol after high-speed shear-stirring for about 5min. Thereafter, the composite sol was poured into a cylinder mold (Φ3×4cm) and then exposed to a cryogenic environment at -20°C for 24h to obtain hydrogels with physical cross-linking. Finally, the hydrogel was soaked in a 0.5M $CaCl_2$ solution for 48h getting the final product.

Characterization

A SPM-9600 atomic force microscope (Shimadzu, Japan) was used to examine the microstructure change of the hydrogel at each procedure of fabrication. The IR spectra of lyophilized pure gelatin and final products were obtained on KBr pellet and performed on an MAGNA IR560 spectrophotometer (Nicolet, USA). The thermal stability of lyophilized pure gelatin and the hydrogel were assessed with DSC-60 (Shimadzu, Japan) over a temperature range of 30-200°C. X-ray diffraction curves for clay and hydrogels were recorded at 2°/min between 3° and 55° on a X'Pert Pro X-ray diffractometer (Philips, Netherlands) using CuKα radiation (γ=0.154 nm) at a voltage of 40kV and a current of 35mA. The cross-sections in matrixes were observed with a JSM-5900 scanning electron microscope (Philips, Netherlands) to get the microstructure of pores. Then an image analyzer program (Photoshop CS 8.0, Adobe) was used to obtain the top view of the voids in SEM images, in which at least 55 pores were measured to obtain the average diameter. The solvent replacement method was used for porosity measurements (Lai and Li, 2010). The sample was equilibrated in deionized water for 1 h and weighed before being maintained at 37°C and 40% relative humidity in an incubator (MJ-160B-II, Shanghai). The water evaporation rate was measured by weighing the sample at consecutive intervals. The percentage weight remaining (WR) of composite was calculated by $\text{WR (\%)}=\frac{\text{Wr}}{\text{Wi}}\times 100\%$ where Wi is the initial weight of wet gels, and Wr is the weight of material at each interval time.

RESULTS AND DISCUSSION

Fabrication Precision

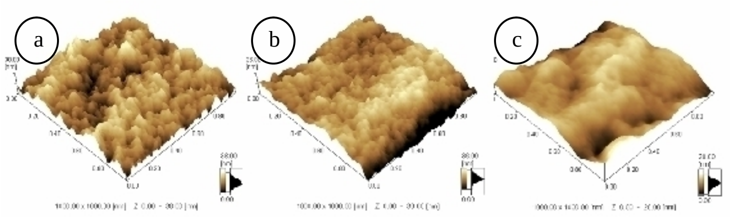

Figure 2. AFM images of the composites during the fabrication process (a, b and c for the composites containing 2% gelatin and 2% clay at the end of each step)

The composite hydrogels were prepared with three procedures including blending, gel-forming and mineralization. The micro-morphology of the composite at the end of each step was observed by AFM and shown in Figure 2. During the blending, gelatin molecules combined with clay molecules to form multi-dispersed amorphous matter (Figure 2a). While in the following two steps, the composite presented a more smoother and homogenous surface (Figures 2b, 2c), which suggested the gelatin molecules may interpenetrate into the interlayer region of clay molecules to obtain uniform composite.

The laponite clay has a layer structure, which, in dispersion in water, is in the form of disc-shaped crystals. The crystals become arranged into stacks which were held together electrostatically by sharing of sodium ions in the interlayer region between adjacent crystals. As indicated in Figure 3, although the 2θ had slight decrease from 28.35° to 23.83°, the XRD curve for the final composite had similar pattern to that for the clay of non-crystal properties. These data demonstrated that the gelatin molecules did not destroy the platelets of the clay except increasing their distance by intercalating into the interlayer space and forming a heterogeneous network.

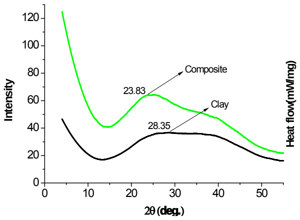

Figure 3. XRD patterns of clay and the composite (both gelatin and clay content as 2%)

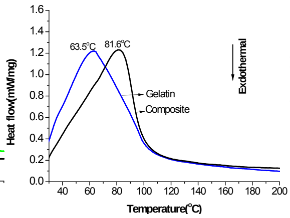

Figure 4. DSC thermographs of gelatin and the composite with 2% gelatin and 2% clay

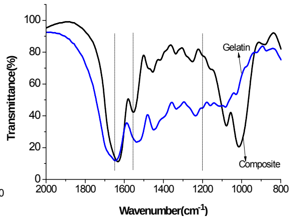

Figure 5. IR spectra of gelatin and the composite (both gelatin and clay content as 2%)

Figure 4 shows the DSC thermographs of the gelatin and hydrogel. The two curves were similar with only one endothermic peak associated to the helix-coil transition of gelatin, which was the denaturation temperature (Td). In theory, crosslinking degree increases the thermal stability of gelatin, as shown by the shift of the Td to higher values. In addition, it is generally accepted that the endothermic process present in the DSC thermogram of collagenous materials involves rupture of hydrogen bonds and a rearrangement of the triple helix into a random configuration. On the other hand, the increased thermal stability exhibited by gelatin has been ascribed to the presence of crosslinking, which breaks exothermically. The Td of the composite rose by 18°C compared with the gelatin, which indicated that there was interaction between the gelatin and clay.

Gelatin is characterized by the amides of protein, IR spectra of which are located on two regions with amide I (anti-symmetric carboxylate absorbance or C=O stretching vibration) and amide II bands (C-N stretching vibration or N-H bending vibration). In this respect, the IR spectra for the hydrogel and gelatin were presented in Figure 5. Compared with gelatin, the amide peak of hydrogels holds a shift to higher wavenumber, specifically, the spectra of δ (NH_2) on 1537 and 1235cm^{-1} disappeared while the spectra of $\delta(NH_3^+)$ on 1553 and 1251 cm^{-1} emerged, indicating that the $-NH^2$ in the gelatin was protonized in the fabrication process. Besides another significant change from 1645 to 1632cm^{-1}, attention was attracted by the 1460-1380cm^{-1} region, since certain differences can be seen in it: characteristic for the gelatin is at 1450cm^{-1} with a shoulder at 1390cm^{-1}; for the hydrogel, a doublet at 1454 and 1417cm^{-1} with a shoulder at 1473cm^{-1}. It is well known that, in the spectral region considered, the bands of the deformation vibrations of –C–H groups and the symmetrical stretching vibrations of –C–O groups of ionized $-COO^-$ groups appeared, the latter of which might be helpful for the formation of coordinate bonding. Otherwise, the characteristic absorption peaks of Si-O tetrahedron at 1013 cm^{-1} were found in the spectra of the composite, indicating the presence of silicate clay in the hydrogels.

As mentioned above, the formation of $-NH_3^+$ and $-COO^-$ was demonstrated by IR analyses. Also, the gelatin molecules interpenetrated into the interlayer region in the laponite clay forming a multiphase network. These results were available to elaborate the fabrication process of the gelatin-based hydrogels. The laponite clay consists of the platelets tightly bound together, which might be exfoliated and dispersed homogenously in a solution by absorbing water into interlayer region. In this study, the clay was firstly dispersed in water with rapid agitation, the interlayer surface of which had a negative charge. After high shear blending, the gelatin in the mixture (pH = 8.5, higher than pI of the gelatin) also had a negative charge, resulting in a polydispersed composite at the end of the first “blending” procedure. Because of small localized positive charges at the edges of the interlayer of the clay generated by absorption of hydroxyl groups, gelatin could interpenetrate into the interlayer region by electrostatic forces in the following cryogenic processing. In the final calcium mineralization step, some $-NH_2$ groups in the gelatin turned into $-NH_3^+$ in the presence of calcium chloride, imparting gelatin partial cationic charge, which may be helpful for the electrostatic bonding between the platelets of the clay and the gelatin. Otherwise, calcium ion may suppress the electric double layer surrounding the platelets of the clay and cause the flocculation of the clay, which led to the strengthened interactions between the clay and the gelatin by shortening their distance. Furthermore, calcium ion could form coordinate or ionic linkage between gelatin and gelatin, as well as gelatin and clay, which ultimately intensified the crosslinking and stability of the whole system.

Effect of the Gelatin Content on the Micro-morphology

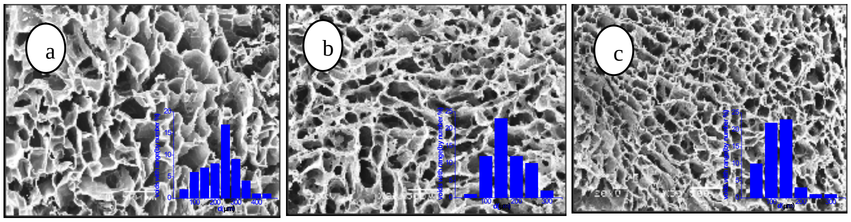

Figure 6. SEM images of the porous hydrogels (gelatin content as a, 3%; b, 4%; c, 5%; clay content as 2%)

Three types of hydrogels with different gelatin content were prepared and their SEM images and the pore size distribution were displayed in Figure 6. The average pore diameter were calculated and shown in Table 1. As indicated, both the porosity and the pore size decreased with an increasing content of gelatin in the hydrogels. There are two possible explanations for the observed findings. First, a higher gelatin concentration could result in an increasing growth rate of nucleation in the composites of gelatin and silicate and thus in a higher amount of pores. Nucleation depends on the instability of the liquor phase as well as the diffusion of atoms into clusters, the former increases with decreasing of temperature, and the latter increases with increasing of temperatures. Higher gelatin content resulted in a decrease of the freezing temperature of the solvent. As a result, the mobility of the atoms to diffuse into clusters was higher, and the nucleation rate increased. Second, by comparison of the gelatin content, the more concentrated materials could possess a decreased heat and protein transfer and thus result in smaller pores. A combination of both is likely the most plausible explanation.

Table 1. The morphological properties of porous gelatin-based hydrogels

Sample	a	b	c
Clay content(w/v)	2%	2%	2%
Gelatin content(w/v)	3%	4%	5%
Porosity	87.21±3.7%	86.24±3.1%	85.23±1.9%
Average pore diameter*	249±16μm	192±21μm	146±10μm

*At least 55 pores were assessed and the values were statistically analyzed and also expressed as the mean ± standard deviation.

Figure 6 also demonstrated the morphology of the pores in the gelatin-based hydrogels. The pores were interconnecting in the four hydrogels, and their average size decreased with the rising gelatin content in the gels. Furthermore, in this material containing 5% gelatin, the pore volume ranged from 50-350μm, focusing on a range of 100-200μm. Such pore size and matrix structure are coincidentally preferred by biomaterials (Vlierberghe et al., 2007), since gradient through this kind of matrix can help oxygen and nutrients diffuse to the cells, and waste products to drain out of the matrix, whereas the pore interconnectivity can promote cell migration and angiogenesis.

Effect of the Gelatin Content on the Solvent Evaporation Rate

The weight of the hydrogels was determined at different time intervals when exposed to a condition of 37°C and 40% relative humidity. The weight of the material decreased linearly in the initial 2.5 h, while gently lowered with the prolonged time (Figure 7). Additionally, the evaporation rate of water slowed with the rising gelatin content. The total volume of the liquid absorbed by gel consists of the solvating solvent bound to polymer network and the capillary solvent filling macropores which can evaporate easier. There was more water absorbed in the large amount of microscopic subunits in the hydrogel with 5% gelatin, resulting in the slowest water evaporation. In addition, the water content in such matrix could be retained higher than 75% even if after 24h in this case. It is reported that a commercially available dressing loses about 50% of its bound water after 12 h and retains about 30% water after 24 h. Therefore the gelatin-based hydrogels could be considered as a potential wound dressing because it could provide a fine moist environment for healing wound surface (Mu et al., 2010).

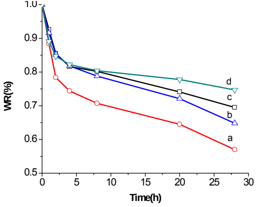

Figure 7. Evaporative water losses from the hydrogels (gelatin content as a, 2%; b, 3%; c, 4%; d, 5%; clay content as 2%)

CONCLUSIONS

An aqueous system was proposed and confirmed for preparing porous hydrogels with gelatin and laponite clay. The fabrication was identified as blending, gel-forming and mineralization three steps. The pore morphology, the pore size and the water evaporation rate could be easily controlled by varying the gelatin content. The hydrogel, consisting of 5% gelatin and 2% clay, had interconnecting pores with size focusing on a range of 100-200μm, which would be available as scaffolds and wound dressings. This approach offers the advantage of fabricating the hierarchical organization of organic/inorganic components without using organic solvents and could be extended to develop new porous materials for a wide range of technological applications.

Acknowledgements

The authors wish to thank the Ministry of Science and Technology of China for financial support of the cooperation project (No.2009DFA42850 and No. 40-3).

REFERENCES

Barbetta, A. et al. (2010), “Porous Gelatin Hydrogels by Gas-in-liquid Foam Templating”, *Soft Matter*, 6(8), 1785-1792.

Bigi, A. et al. (2004), “Relationship between Triple Helix Content and Mechanical Properties of Gelatin Films”, *Biomaterials*, 25(25), 5675-5680.

Lai, J.Y. and Li, Y.T. (2010), “Functional Assessment of Cross-linked Porous Gelatin Hydrogels for Bioengineered Cell Sheet Carriers”, *Biomacromolecules*, 11(5), 1387-1397.

Mu, C.D. et al. (2010), “Collagen Cryogel Cross-linked by Dialdehyde Starch”, *Macromolecular Materials and Engineering*, 295(2), 100-107.

Vlierberghe, S.V. et al. (2007), “Porous Gelatin Hydrogels: 1. Cryogenic Formation and Structure Analysis”, *Biomacromolecules*, 8(2), 331-337.

III.

SYSTEMS AND TECHNOLOGIES

REDUCTION OF ENVIROMENTAL POLLUTION WITH SALTS IN WET LEATHER PROCESSING PHASES

MARIAN CRUDU[1], CARMEN GAIDAU[1], ANDRA CRUDU[1], MARIANA POPESCU[2],
MARCEL IONESCU[3], VIRGILIJUS VALEIKA[4], VIKTORIIA PLAVAN[5]

[1] *INCDTP - Division: Leather and Footwear Research Institute, 93 Ion Minulescu, 031215, Bucharest, Romania, icpi@icpi.ro*

[2] *S.C. PIELOREX SA, Jilava., Romania, office@pielorex.com*

[3] *SC EUROPLASTIC LTD, Bucharest, Romania, euro@europlastic.com*

[4] *Kaunas University of Technology, Radvilenu, Kaunas, Lithuania, virgilijus.valeika@ctf.ktu.lt*

[5] *National University of Technologies and Design, Kiev, Ukraine*

This paper presents the results of testing an innovative material-technology system for reduction of environmental pollution with salts in wet leather processing phases. Deliming and wet finishing experiments on leather were performed using new multifunctional (maleic copolymers) and compact (retanning blends) materials with effects on reduction of ammonium salts and sulphates from wastewaters.

Keywords: wet leather processing, salt reduction, bovine hides.

INTRODUCTION

The term salt in the tanning industry is typically used to refer to the two commonly used salts, namely sodium chloride and sodium sulfate. It is quite typical in the tanning industry to consider both of these inorganic salts together using the simple term salt. These two inorganic salts in the effluent are clearly the most difficult form of pollution to be dealt with in the leather industry. Both are very soluble in water and chemically stable, making it effectively impossible to remove them from a mixed effluent in waste water treatment plants by typical processes such as: sedimentation, oxidation, precipitation or flocculation like most other pollutants.

The salts used in leather processing (inorganic) and the salts formed during this process constitute over 60% of the total chemical substances used in leather processing, which is enough to justify research for rationalization of chemical processes for the purpose of reducing environmental pollution with salts.

This paper presents the results of testing an innovative material-technology system for reduction of environmental pollution with salts in wet finishing leather processing phases.

EXPERIMENTAL

Leather retaining is a key multistep operation in leather processing which requires the use of chemically complex auxiliary materials difficult to biodegrade and which contain large amounts of salts. Most products are wet finishing powders and may contain significant amounts of sodium sulfate as inert salt standards. As an alternative to classical retaining a series of blend type materials with dyeing fatliquoring and retanning function have been developed are used in one dose, after hide neutralization.

Designing new products is based on the latest knowledge on compatible materials with good stability over time, ability to penetrate the porous dermis structure and to interact with functional groups of collagen.

MATERIALS AND METHODS

Materials

- tanned bovine hides (20-25 kg) with basic chromium salts or free of chrome tanned, split, shaved (1.2-1.4 mm) and completely neutralized;
- new wet finishing (black and brown);
- common auxiliaries for leather wet finishing.

Methods

The skins were classified into three groups and retanned (wet finishing) according to the experimental design given in Figure 1 and Table 1.

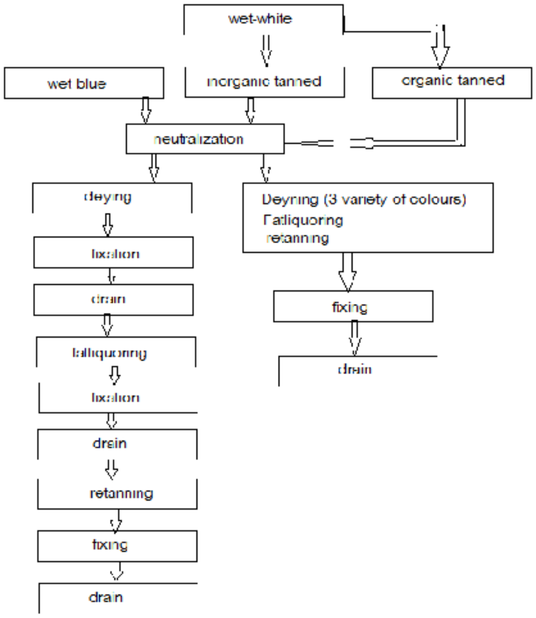

Figure 1. Experimental design of the retanning processes

Table 1. Experimental design of the retanning (wet finishing) processes

Trial no.		Type of treatment
WB	WBM	Wet blue classical retanned
	WBP	Wet blue compact retanned with wet finishing product (black)
WWO	WWOM	Organic wet white classical retanned (oxazolidine)
	WWOP	Organic wet white compact retanned with wet finishing product (black) (oxazolidine)
WWI	WWIM	Inorganic wet white classical retanned (titanium aluminium)
	WWIP	Inorganic wet white classical compact retanned with wet finishing product (black) (titanium aluminium)

The classic multistep retanning chrome bovine hides (or free chrome tanned) were processed according to Table 2.

Table 2. Classic multistep retanning chrome bovine hides

Process	Parameters		
Dyeing	100% water	55^{o}C	
	2% days (black)		20-60'
Fixation	+1% formic acid	(1:10)	15-20'
	control		
Draining			
Fatliquoring	100-150% water	55-60oC	
	8-19% fatliquors compound		40-60'
	control		
Draining			
Retanning	+ 100-150% water	35oC	
	2-3% synthetic resins		20-30'
	5-8% natural tanning (mimosa,		40-50'
	quebracho	control	
Fixation	0.5-1% formic acid	1:10	15-20'
		Control	
			pH=3.8-4.2
Draining			

The new compact retanning hides with new composite blends were processed according to Table 3.

Table 3. Compact retanning with new composite products

Process	Parameters		
Compact retanning	8-100% water	35-38^{o}C	
(dyeing, fatliquoring,	11-13% compact		40-60'
retanning)		control	
Fixing	+ 0.5-1% formic acid	1:10	10-15'
		control	
		pH=3.8-4.2	
Draining			

RESULTS AND DISCUSSION

Physical test results of the leather samples after retanning processes are given in Table 4.

Results of chemical analysis performed on retanned samples are given in Table 5.

Results of salt content in the leather wet finishing effluents are given in Table 6.

Balance of salts in effluents from compact retanning of bovine hides chrome tanned compared to the classical multistep process is presented in Figure2.

Reduction of 60% chloride and 45% sulphates was achieved. Chromium salts from effluents are completely reduced in the case of compact retanning of free of chrome leather.

Balance of salts in effluents from compact retanning of bovine hides free of chrome tanned (organic and inorganic) compared to the classical multistep process is presented in Figure 3.

Table 4. Physical test results of leather after compact retanning process

Trial no.	Tensile strength (N/mm^2)	Amounts required under the standard	Elongation at (break %)	Amounts required under the standard	Tear strength (N/mm)	Amounts required under the standard
WBM	19.20	Min.16	61.50	Max.79	52.10	Min.27
WBP	22.31		67.20		53.20	
WWOM	19.05		51.30		31.04	
WWOP	21.15		56.20		35.21	
WWIM	23.10		53.40		30.05	
WWIP	28.80		58.00		29.40	

Table 5. Results of chemical analysis

Trial no.	Fat %	pH	Ash %	Cr_2O_3 %	Shrinkage temperature °C
WB_M	7.3	3.95	5.9	3.8	101
WB_P	7.5	4.16	5.8	3.5	98
WWO_M	7.4	4.21	2.8	-	84
WWO_P	4.3	2.5	7.6	-	85
WWI_M	3.62	7.9	7.4	-	89
WWI_P	4.01	6.9	7.9	-	92

Table 6. Salt content in the effluent

Trial	Salt content mg/dm^3			
no.	Chloride	Sulphates	Cr_2O_3	Ash
WB_M	1418	11324	607	6900
WB_P	567	6151	580	2800
WWO_M	920	4020	-	950
WWO_P	405	1005	-	502
WWI_M	1030	12500	-	6500
WWI_P	460	5800	-	2600

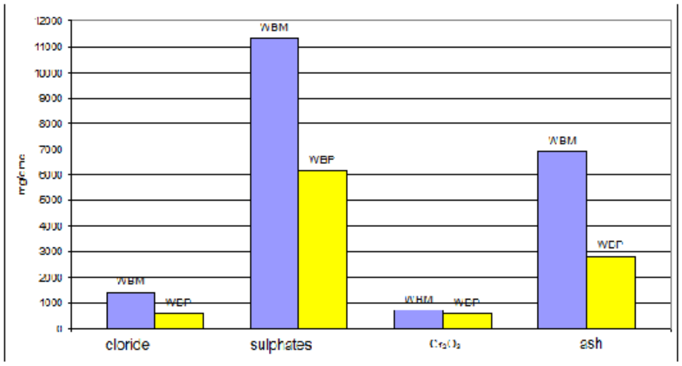

Figure 2. Reduction of salts and chromium content in retanning effluents from bovine hide chrome tanned

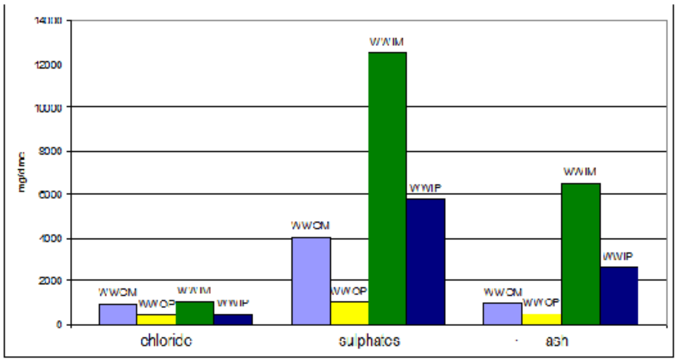

Figure 3. Balance of salts in effluents from compact retanning of bovine hides free of chrome tanned

Salts content from retanning effluents of free chrome tanned bovine hides are reduced by 47% - 60%.

CONCLUSIONS

- Wet multifunctional materials were obtained and tested for wet finishing of hides with retanning, fatliquoring and dyeing properties;
- Reduction of sulphates in the effluents from compact retanning was 45%-75% and reduction of chloride 55%-60%;
- Chromium salts from effluents are completely reduced in the case of compact FOC (free of chrome) leather;
- Reduction of ash content in the effluents from compact retanning was 47%-60%;
- The leather wet finishing with newly multifunctional materials gave comparable physical properties to classical retanning.
- The economic effects to applying compact materials and technologies of bovine leather wet finishing are significant and refer to reducing processing time by 45%, water consumption by 30%, labour by 40%, auxiliary materials by 30%.

Acknowledgements

This work was supported by a grant of the Romanian National Authority for Scientific Research, CNDI–UEFISCDI, EUREKA project number 307/2011.

REFERENCES

Csnaka, H. (1995), UNIDO, Ljubljana.
Munz, K.H. (1993), XXII IULTCS Congress, Brasil, 363.
Papa Konstantinau, D. (2001), “Salt Free High Stability Organic Tanning for the Production of High-Tech Upperleather”, Tecnologie Conciane, March-April, 83-85.
Rajamani, S. and Ramasami, T. (2007), “Salinity-related Issues in India”, World Leather, May, 37-39.
TFL Eco Guidelines (2011), Salt & Nitrogen Reduction in the Leather Making Process, ecology@tfl.com.
*** (2007), “A Compendium of Salinity Related Information”, Word Leather, May, 33-35.

MULTI-AGENT BASED SYSTEM ARCHITECTURE FOR INDUSTRIAL APPICATIONS: LEATHER PROCESSING MONITORING AND DIAGNOSING CASE STUDY

SERGIU-ADRIAN GUTA[1,2], MARIUS AVRAMESCU[1], ADRIAN-BOGDAN HANCHEVICI[1]

[1] *"Politehnica" University of Bucharest, Faculty of Automatic Control and Computers, Romania, emails: guta.sergiu@icpi.ro, avramescu.marius@gmail.com, adrian.hanchevici@upb.ro*

[2] *INCDTP – Division: Leather and Footwear Research Institute, 93 Ion Minulescu, Bucharest, Romania, email: guta.sergiu@icpi.ro*

This paper presents a general agent-based architecture for industrial applications. Subsequently the paper proposes a multi-agent architecture for leather processing monitoring and diagnosing. The architecture is modular and flexible and aims to monitor and diagnose production processes. The capability and the flexibility of the architecture is attained by agent technology that is used to detect anomalies, aware human operators of the occurred problems and suggest corrective mechanisms for keeping up production processes. Agents within the proposed architecture have a heterarchical organization. The autonomic computing vision and the perspective of an ideal tannery that automatically and dynamically responds to customer needs are presented. These aspects are inspired from the functioning of human nervous system that controls vital functions within the body such as heart rate, body temperature and respiratory rhythm without the intervention of our conscious mind. Similar capabilities can be transferred to tanneries, namely self-healing and adaptability to changing circumstances through the use of agent technology. The notions of autonomous agent and multi-agent system are introduced and analyzed, their potential applications in leather manufacturing is outlined. It is shown that agent technology can be beneficial in dynamically changing industrial environments, being a robust and adaptable solution that surpasses other traditional approaches.

Keywords: agent based architecture, multi-agent systems, leather processing.

INTRODUCTION

This paper presents a specific type of architecture that can be used for process and quality monitoring and diagnosis in leather industry. The architecture aims to mitigate subjective examination of leather quality and empirical process monitoring.

The perspective of an ideal tannery that automatically and dynamically responds to customer needs, achieves maximum production, efficiency and profit and also complies with national and international environmental legislation is undoubtedly very attractive to every tannery proprietor.

Tanneries are spatially distributed manufacturing systems of high complexity. In a tannery numerous equipments such as motors, valves and pumps are located in places where they cannot be seen or heard by human operators. Consequently malfunctions and problems can occur without early detection. The raw material, leather, that is processed in drums can be ruined or expensive machines may suffer severe damage before the fault is detected and fixed (Hanchevici & Guta, 2012; TanWare, 2012). Despite the wealth of technological advancements, the vast majority of tanneries relies on stale technologies that cannot offer fool-proof solutions to the errors and failures that may occur in every day functioning.

The autonomic computing vision expressed in 2001 by Paul Horn, IBM senior researcher envisages systems that manage themselves (Kepart et al., 2003). The idea behind this vision is inspired from the functioning of nervous system that controls the body by extracting information from the environment using sensory receptors, processing the information to determine an appropriate action, and sending output signals to muscle or glands to generate an action (Nervous System, 2012). Thus our heart rate, respiratory rhythm and body temperature are controlled by our nervous system freeing our conscious mind from the burden of dealing with these complex and vital functions. Agents, autonomous entities with the capability of sensing and acting upon an environment, have the potential of making a system manage itself according to the owner's goal (Sterritt, 2005). Systems that have a self-healing mechanism and adapt autonomously to changing circumstances undoubtedly have the characteristic of agent systems (Wooldridge, 2009).

AGENTS AND MULTI-AGENT SYSTEMS IN INDUSTRIAL APPLICATIONS

The word agent comes from Latin *agere*, and means *to act.* From the software engineering perspective, an agent is a software component that is immersed in an environment and is capable of flexible autonomous actions. For Bordini, an agent is a reactive system that manifests a certain degree of autonomy in the way that we delegate some tasks to it and this determines the best way of achieving them (Bordini et al., 2007). The difference between a software and an agent is given by the fact that the latter enjoys some properties that make it intelligent. These properties are autonomy, reactivity, social abilities, mobility, proactive behavior, adaptability, to name only a few. Agents can operate in complex environments that are only partly observable, predictable and known. Also the environment in which an agent operates is clearly separated from the agent and from its behavior.

Although expert systems seem similar to agents, there are obvious differences. The differences between agents and expert systems were clearly stated by Wooldridge (Wooldridge, 2009):

- expert systems are not connected to the environment in which they operate;
- expert systems are not capable of proactive or reactive behavior;
- expert systems are not social, in the sense of cooperation, coordination, and negotiation.

Due to the fact that individual agents have control and access to only a part of the environment in which they operate they need to interact with other agents in order to solve or support the solution for complex problems. Two different agents that share the same environment may have different knowledge, diverging interests and also a different perspective of the problems that need to be solved. Consequently, individual agents have limited capabilities and competences in solving complex problems.

When these autonomous entities, agents, interact with one another they form a multi-agent system that has emergent capability that surpasses the sum of capabilities of all individual agents. A multi-agent system is a network of computational agents that work together to find answers to problems that are beyond the individual competence of each agent (Verstraete et al., 2006).

The need for flexible production systems that adapt and reconfigure brought to life *holons* and holonic manufacturing systems (HMS). In essence, holons are autonomous cooperative entities (agents) that are in charge of specific, identifiable parts of a manufacturing system (Paolucci et al., 2004). A multi-agent system can have either holonic or heterachical architecture. In this paper the latter is presented.

REFERENCE ARCHITECTURE FOR INTELLIGENT AGENTS

Agents can be seen as intelligent systems where intelligence is given by a specific architecture that organizes joint functioning of some elements that separately are unintelligent. Generally speaking, agents are composed of two parts: internal (computational) and external (physical), however there are agents that are immersed in software environments and instead of physical part they have virtual sensors and actuators. The reference model architecture for intelligent agents is presented in Figure 1.

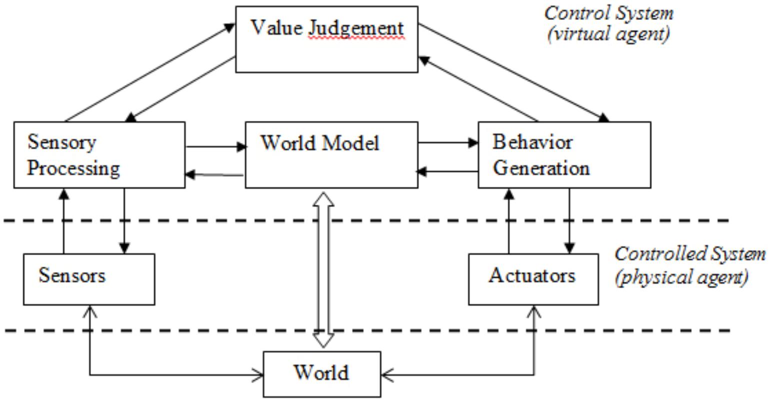

Figure 1. Reference Model Architecture for Intelligent Agents (Meystel et al., 2002)

The internal part of the agent illustrated in Figure 1, above the top dashed line, represents a control system and is a virtual representation of the real world. The Sensory Processing subsystem operates on data collected from sensors to build and maintain a virtual representation of the real world which is stored in the World Model subsystem. The process of behavior generations is improved by continuous development and update of World Model subsystem through the information received from Sensory Processing subsystem. Value Judgement subsystem determines what is good, bad, important, trivial, certain, uncertain etc. and is the basis for decision making or for choosing an action instead of another.

MULTI-AGENT ARCHITECTURES FOR INDUSTRIAL PROCESS MONITORING

The following section presents a general multi-agent architecture for industrial process monitoring. The structure of architecture is presented in Figure 2. The main characteristics and interactions between the elements of the architecture are illustrated below:

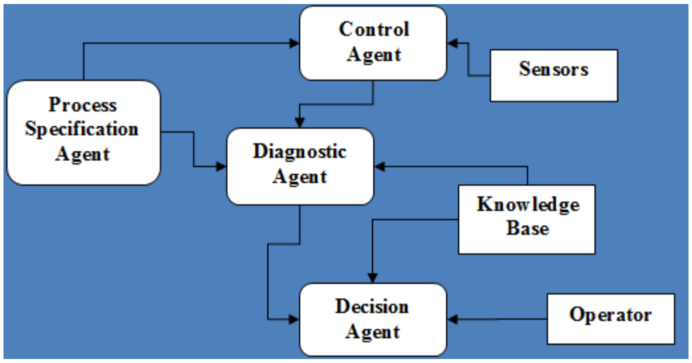

Figure 2. Multi-agent system architecture for industrial process monitoring

Control Agent

- Data acquisition from sensors;
- Communicates with Process Specification Agent regarding technical data (limits, sensor values, etc.);
- Interprets data and sends the results to Diagnostic Agent.

Diagnostic Agent

- Receives analysis from at least one Control Agent;
- Communicates with Process Specification Agent regarding technical data (intermediary process results, etc.);
- Uses the Knowledge Base to discover flaws in the process;
- Gives a diagnosis to the Decision Agent.

Decision Agent

- Receives diagnosis from at least one Diagnosis Agent;
- Solves contradictory results;
- Uses Knowledge Base and even the Operator to give a final decision.

MULTI-AGENT ARCHITECTURE FOR LEATHER PROCESSING MONITORING AND DIAGNOSING

Further the paper presents a multi-agent architecture for leather processing monitoring and diagnosing which is shown in figure 3. Other multi-agent architectures for industrial process monitoring and diagnosing were introduced by Wörn et al., 2002 and Monostori et al., 2006. The architecture is organized in seven levels, the first level is the one represented by production processes and by the system engineer. The system engineer specifies the parameters that need to be monitored and also the accepted tolerance of the parameter values. The last level is represented by the human operator.

Process Specification Agent is in charge of getting the information about the monitored process from the system engineer and from the knowledge base. It has similar capabilities to Control Agent from the architecture shown in Figure 2. The functions of both Diagnostic Agent and Monitoring and Decision Agent (which corresponds to Decision Agent) are similar with those of their analogues from Figure 2. The Diagnostic Agent can use artificial intelligence techniques such as genetic algorithms, fuzzy logic, neural networks to deal with various problems. Initial sorting of hides and skins can be realized by video monitoring using neural networks.

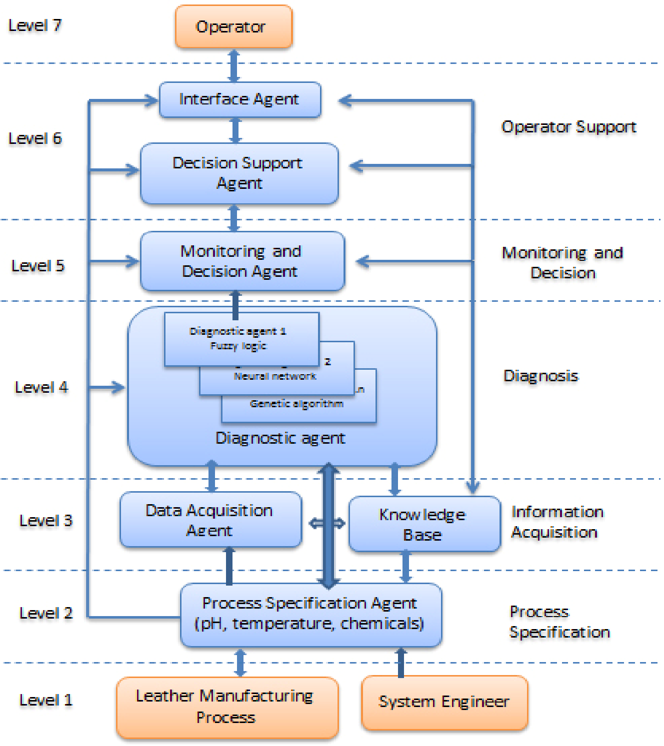

Figure 3. Multi-agent architecture for leather processing monitoring and diagnosing

The presentation of the diagnostic mechanisms to identify faults and the methodologies employed for suggesting corrective actions is out of scope of this paper.

CONCLUSION

Agent technology represents a heuristic approach suited for leather manufactures, among the advantages are effective and efficient real-time fault diagnosis, production monitoring and management. In the proposed architecture, agents do not intervene directly in process control activities, they monitor production processes, detect faults and make a diagnostic of the anomalies occurred. Subsequently, the system devises a clearly defined action plan aimed to solve disturbances and is presented to the human operator.

Early detection of anomalies, process parameters threshold that are not in range (pH, temperature, process duration, chemical ratio) is necessary to ensure consistent quality of the final product. Real-time process monitoring aims at raw material and energy consumption reduction and also at pollution monitoring and prevention. Monitoring and registration of the whole productive process cycles from skin/hide to finished leather for all types and origins of leather will optimize the future production of finished leather. Further work will focus on controlling leather manufacturing processes by using agent technology.

Acknowledgements

The work has been funded by: the Sectoral Operational Programme Human Resources Development 2007-2013 of the Romanian Ministry of Labour, Family and Social Protection through the Financial Agreements POSDRU/107/1.5/S/76909 and POSDRU/88/1.5/S/61178.

REFERENCES

Bordini, R.H., Hübner, J.F. and Wooldridge, M. (2007), *Programming Multi-Agent Systems in Agent Speak using Jason*, Wiley.

Hanchevici, A.B. and Guta, S. (2012), “Supervised Multi-Agent Control of Leather Manufacturing Processes by Using the Fuzzy Logic”, *Revista de Pelărie Încălţăminte* (*Leather and Footwear Journal*), 12(2), 101-112.

Kepart, J.O. and Chess, M.D. (2003), “The Vision of Autonomic Computing”, *The IEEE Computer Society*, 31(1), 41-55.

Meystel, A.M. and Albus, J.S. (2002), *Intelligent Systems: Architecture, Design, and Control*, Wiley Interscience, New York.

Monostori, L., Váncza J. and Kumara, S.R.T. (2006), “Agent-Based Systems for Manufacturing”, *CIRP Annals - Manufacturing Technology*, 55(2), 697–720.

Paolucci, M. and Sacile, R. (2004), *Agent-Based Manufacturing and Control Systems: New Agile Manufacturing Solutions for Achieving Peak Performance*, CRC Press, Florida, USA.

Sterritt, R. (2005), “Autonomic Computing”, *Springer*, 1(1)79-88.

Verstraete, P. et al. (2006), “On Applying the PROSA Reference Architecture in Multiagent Manufacturing Control Applications”, *Proceedings of the Multi-Agent Systems and Software Architecture Special Track at Net.ObjectDays*, Erfurt, Germany, 31-47.

Wooldridge, M. (2009), *An Introduction to Multi Agent Systems*, Wiley, Glasgow, UK.

Wörn, H., Längle, T. and Albert, M. (2002), “Multi-Agent Architecture for Monitoring and Diagnosing Complex Systems”, *Proceedings of the 4th International Workshop on Computer Science and Information Technologies CSIT’2002*, Patras, Greece.

***, Nervous System, available from: http://www.wikipedia.com (accessed 27.07.2012).

***, TanWare Solutions for the Leather Industry, available from: http://www.tanware.com/en/wetprocesses/guardware.html (accessed 02.03.2012).

DETERMINATION OF THE CHANGES IN THE MILITARY BOOTS USED UNDER ACIDIC AND ALKALINE CONDITIONS

HÜSEYİN ATA KARAVANA, CANER GÜLEN, SİNAN CAN GÜZEL, FATİH YALÇIN

Ege University, Engineering Faculty, Leather Engineering Department, 35100, Bornova-Izmir/Turkey, email: huseyin.ata.karavana@ege.edu.tr

In this research, physico-mechanical changes in the military boots used in acidic and alkaline mud solutions were investigated. Nine pairs of defect- and fault-free military boots were used as material. Three pairs of boots were selected for control group, acidic and alkaline mud solutions, randomly. Then, the military boots put on by the mechanical legs of the dynamic footwear water resistance tester were submerged into acidic and alkaline mud solutions and forced to take 200000 steps mechanically. After that, some of the physical tests conducted on the upper leathers and soles of the military boots were examined. It was found that differences of the tensile strength, tear load and stitch tear resistance values of the military boots' upper leathers between the trials were statistically significant ($P<0.05$). A decrease was detected in the tensile strength, tear load and stitch tear resistance values of the upper leathers exposed to acidic and alkaline mud solutions. It was found that an upper/sole adhesion strength value of the military boots soles in the alkaline mud solution trial was higher than that in the acidic mud solution trial. On the other hand, an abrasion resistance value of these soles in the alkaline mud solution was found to be lower than that in the acidic mud solution trial. Differences of the upper/sole adhesion strength and abrasion resistance values between the trials were also found statistically significant ($p<0.05$).

Keywords: Military boots, acidic mud solution, alkaline mud solution, dynamic footwear water resistance test

INTRODUCTION

Being an essential part of daily life, footwear is a type of garment, which not only completes clothes but also protects the feet from external environmental conditions and improves the ability to move. It is a special garment increasing performance depending on working areas of people. Nowadays, several types of shoes have been developed by taking different living and working conditions into consideration.

There are some key points to consider in footwear production such as gathering a great number of different materials, providing hygiene and comfort for the feet, giving the desired fastness and aesthetics, obtaining a sample with the materials in question for any type and size of shoes (Karavana, 2012).

For this reason, appropriate techniques of production with suitable materials must be selected after determining the uses of shoes well. Selecting and using materials not suitable for manufacturing footwear both restrict all vital activities and cause foot discomfort and health problems.

It should be kept in mind that the boots and footwear to be manufactured for military purposes shall be used under different and severe geographical and climatic conditions and shall be directly related to the ability to move of military personnel. Turkey has a very wide surface area and incorporates a great variety of geographical features. In this context, different soil characteristics have occurred in different regions (Table 1).

Table 1. Regional distribution of Turkey's soils according to pH values (Eyüpoğlu, 1999)

Regions	Soil Sample Numbers	Strong Acidic (%)	Middle Acidic (%)	Weak Acidic (%)	Neutral (%)	Weak Alkali (%)	Strong Alkali (%)
Thracian and Marmara	26563	-	3.6	15.9	55.8	24.7	-
Black Sea	36291	2.7	9.2	16.1	31.4	40.3	0.3
Middle Anatolia	76688	-	0.2	1.7	16.8	79.8	1.5
Southeast Anatolia	25523	-	0.5	3.5	44.1	51.8	0.1
East Anatolia	12023	-	0.1	6.6	34.5	58.5	0.3
Aegean	22695	0.2	2.3	11.2	45.6	40.5	0.2
Lakes	27575	-	0.1	1.3	20.0	78.4	0.2
Mediterranean	16095	-	0.1	1.3	14.6	83.6	0.4
TOTAL	243453	1044	5206	16135	72721	146867	1480
Average of Turkey		0.4	2.2	6.6	29.9	60.3	0.6

Consequently, using high-quality and suitable materials in manufacturing military boots and footwear is of vital importance in increasing the performance expected from military personnel (Sarı and Bitlisli, 2000). As is the case with other fields, technology develops in the defense industry and it necessitates military boots to provide the desired fastness, durability and comfort under various chemical conditions. In military operations, where several tasks are carried out for a long period, fulfillment of the expected physical requirements by military boots is highly effective in the accomplishment of such tasks.

The objective of this research is to examine the resistance to acidic and alkaline mud solutions of the military boots used under a wide range of environmental conditions and thus to introduce the physical effects of acidic and alkaline soils on the physical life of military boots.

MATERIAL AND METHOD

Material

Military Boots

In this research, nine pairs of defect- and fault-free military boots with rubber sole manufactured by cemented construction method were used as material.

Acidic and Alkaline Mud Solutions

10 l acidic and 10 l alkaline artificial mud solutions were prepared in laboratory with the purpose of observing the physical changes that occur in the military boots used in the fields having acidic and alkaline soils.

Method

Preparation of Acidic and Alkaline Mud Solutions

In the preparation of mud solutions, firstly saturation slurry was obtained by adding 70 ml distilled water into 100 g neutral soil. Then, the pH of saturation slurry was adjusted to 4.5 with 1M HCl for acidic mud solution and to 8.5 with 0.1M NaOH for alkaline mud solution.

Mechanical Walking Test

Three pairs of boots were randomly selected for control group, acidic and alkaline mud solutions. Then, each boot was enumerated. After that, acidic and alkaline mud solutions were filled in the tanks of SATRA-TM505 model dynamic footwear water resistance tester. Finally, the military boots put on by the mechanical legs of the engine were submerged into the mud solutions and exposed to 200000 steps mechanically.

Physical Tests

In order to evaluate the physico-mechanical changes of upper and sole of military boots, determination of hardness of vulcanized or thermoplastic rubber (TS ISO 48, 1998), determination of abrasion resistance of footwear outsoles (TS EN 12770, 2004), determination of adhesion strength between upper and sole (TS EN ISO 20344, 2007), determination of tensile strength and percentage extension of leather (TS 4119 EN ISO 3376, 2006), determination of tear load-double edge tear of leather (TS 4118-2 EN ISO 3377-2, 2005), determination of stitch tear resistance of leather (TS EN ISO 23910, 2008), determination of water vapour permeability of leather (TS EN ISO 14268, 2004) and determination of air permeability of leather tests were examined.

Statistical Analysis

The results that were obtained were evaluated in SPSS 15.0 statistics programme. For the stated purpose, a descriptive statistical test, ANOVA and Duncan test were carried out.

RESULT AND DISCUSSION

One of the most important criteria in determining the physico-mechanical characteristics of processed leathers is tensile strength, which is applied to almost all types of leathers (Olivannan et. al., 1977). Upon the examination of Table 2, the average tensile strength of military boots' upper leathers of control, alkali and acidic trials was found to be 23.762 N/mm^2, 16.645 N/mm^2 and 16.048 N/mm^2, respectively. It was determined that the differences between the tensile strength values of trials were found statistically significant ($p<0.05$). After the mechanical walking test with acidic and alkaline mud solutions, decreases in the tensile strength values were determined. It is understood that these values is lower than the acceptable quality standards of upper leathers (UNIDO, 1996).

It is useful to take elongation value into consideration as well as tensile strength because a low elongation value results in easy tear while a high elongation value causes leather goods to become deformed very quickly or even lose usability. An increase in the elongation values of the upper leathers exposed to acidic and alkaline mud solutions was determined (Table 2).

The measure of processed leather's performance and strength during use is determined by means of tear load. Table 2 shows that there is a big decrease in the double edge tear load value of upper leather of acidic trial. In terms of double edge tear load, the difference between control and alkaline mud solution trials were found insignificant ($p>0.05$). Besides, differences of tear load values between acidic mud solution trial and other two trials were found statistically significant ($p<0.05$).

As seen in Table 2, differences between the trials were found slightly significant in terms of stitch tear resistance ($p<0.05$). These values are higher than the limit values recommended for upper leather (UNIDO, 1996).

Water vapour and air permeability values can change depending on the structural properties of leather, porosity, thickness and tanning types (Kanlı et al., 2010). It can be seen from Table 2 that the lowest water vapour permeability and air permeability tests results were obtained from control group. It is not surprising to have the lowest water vapour permeability and air permeability values for control group. The decrease in water vapour permeability and air permeability depends on the porosity of the upper leather (Milasine et. al., 2003). Statistical analysis shows that water vapour permeability and air permeability values of upper leather obtained from alkaline and acidic mud solutions trials are higher than the control group. Differences between the trials were found statistically insignificant in terms of air permeability ($p>0.05$). Besides, differences of water vapour permeability values between control group and other two trials were found statistically significant ($p<0.05$).

Table 2. Some physical tests values of military boots' upper

Trials		T. S. (N/mm^2)	P. E. (%)	T. L. (N)	S. T. R. (N/mm^2)	W. V. P. (mg/cm^2.h)	A. P. (cm^3/cm^2.s)
Control	X±S.E.	23.76±3.53^a	46.69±2.14^b	122.50±4.65^a	176.18±15.10^a	1.56±0.13^b	0.77±0.14^a
Alkaline	X±S.E.	16.65±1.49^b	57.60±3.48^a	119.73±3.21^a	157.89±6.96^{a,b}	3.43±0.45^a	1.77±0.64^a
Acidic	X±S.E.	16.05±1.68^b	53.23±2.84^{a,b}	84.57±8.31^b	136.08±10.03^b	2.87±0.52^a	1.97±0.70^a

X, S.E., T.S., P.E., T.L., S.T.R., W.V.P. and A.P. mean average, standard error, tensile strength, percentage extension, tear load, stitch tear resistance, water vapour permeability and air permeability, respectively.

$^{a, b, c}$ values in the same column with different superscript letters are significantly different ($p<0.05$).

If the tests conducted on upper leathers are evaluated in general, it is possible to say in the light of previous studies that, as some of the tanning agents between the fibers of the upper leathers that belong to the military boots exposed to alkaline mud solution are removed under the influence of alkaline or as tanning deteriorates in patches, free movement of leather fibers increases but a considerable decrease is not seen in their resistance and thus percentage elongation value increases and water vapour and air permeability values increase compared to control group (Başaran et. al., 2011). On the other hand, in the upper leathers that belong to the military boots exposed to alkaline mud solution, acidic hydrolyses occurs in leather fibers under the influence of acid. It is thought that, due to the separations in collagen's molecular chains, leather structure weakens and thus tensile strength, tear load and stitch tear resistance values are found to be lower compared to the leathers in other two experimental groups.

Table 3. Some physical tests values of military boots' sole

Trials		Upper/Sole Adhesion Strength (N/mm)	Abrasion Resistance (mm^3)	Hardness (Shore A)
Control	X±S.E.	6.13 ± 0.05^a	134.33 ± 3.28^c	70.50 ± 0.29^a
Alkaline	X±S.E.	3.10 ± 0.01^b	158.67 ± 3.33^b	70.50 ± 0.29^a
Acidic	X±S.E.	2.57 ± 0.17^c	205.67 ± 9.94^a	70.50 ± 0.29^a

$^{a, b, c}$ values in the same column with different superscript letters are significantly different ($p<0.05$).

As shown in Table 3, upper/sole adhesion strength values' differences between the trials were found statistically significant ($p<0.05$). It was detected that there was a decrease in upper/sole adhesion strength values. The lowest upper/sole adhesion strength value is 2.57 N/mm in the acidic mud solution trial. Similarly, differences of the abrasion resistance values between the trials were also found statistically significant ($p<0.05$). After the acidic and alkaline mud solutions trials, increases in the abrasion resistance values were determined. Also, the highest abrasion resistance value belongs to the acidic mud solution trial as 205.67 mm3. Interestingly, hardness values of military boots' soles of each trial didn't change while abrasion resistance values of soles were decreasing. And, the difference between the hardness values of each trial was found insignificant ($p>0.05$).

It was found that an upper/sole adhesion strength value of military boots' soles in the alkaline mud solution trial was higher than that in the acidic mud solution trials. On the other hand, an abrasion resistance value of these soles in the alkaline mud solution was found to be lower than that in the acidic mud solution trial (Table 3). It is understood that military boots' soles were affected by acidic mud solution much more than alkaline mud solution.

CONCLUSION

It was found that acidic and alkaline mud solutions caused degradations in the chemical structure of both sole and upper materials of the military boots subject to research and reduced the physical properties of the materials in question, resulting in shorter physical life for boots.

Military boots are manufactured according to the standards set by relevant institutions and required to maintain their properties through their physical life. For this reason, it is necessary to take into consideration the external environmental conditions under which military boots are used.

For meeting the requirements expected from military boots during usage, it is also highly important to separately analyze the properties of the materials to be used in production. In addition, production by considering that changes may occur in the pre-assembly properties of the materials due to the interactions between materials as a result of assembly shall increase productivity in terms of both micro and macro economics.

REFERENCES

Başaran, B., Bitlisli, B.O., Ocak, B., Önem, E. (2011), "Effect of different atmospheric conditions on some physical properties of leather", *Journal of Textile and Apperal*, 21(2), 194-197.

Eyüpoğlu, F. (1999), "Türkiye Topraklarının Verimlilik Durumu", *KHGM Toprak ve Gübre Araştırma Enstitüsü Yayını*, Teknik Yayın No: T-67, Genel Yayın No: 220, Ankara.

Kanlı, N., Zengin, C.A. and Bitlisli, B.O. (2010), "The Effects of Different Finishing Types on Water Vapour and Air Permeability Properties of Shoe Upper Leathers", *ICAMS 2010 Proceedings Book*, 63-66.

Karavana, H.A. (2012), “Manufacturing Technology of Leather Products-II”, unpublished lecturer notes, Ege University Engineering Faculty Leather Engineering Department, Bornova, İzmir.

Milasiene, D., Jankauskaite, V. and Arcisauskaite, R. (2003), “Prediction of Stress Relaxation in Laminated Leather Layers”, *Material Science (Medžiagotyra)*, 9(1), 73-79.

Olivannan, M.S., Muthulingam, P., Sadulla, S., Kumar, A., Rao, J.B., Salvarangan, R. (1977), “Process for the manufacture of suede garment leathers from chrome crust goat skins”, *Leather Science*, 24(8), 272-276.

Sarı, Ö. and Bitlisli, B.O. (2000), “Problems stemming from upper leathers in military shoes and boots and suggested solutions”, *Infantry 2000 Symposium CD*, Tuzla Infantry Cadet School Command, Istanbul, Turkey.

TS 4118-2 EN ISO 3377-2 (2005), “Leather - Physical and mechanical tests; Determination of tear load - Part 2: Double edge tear”, *Turkish Standard Institution*, 7.

TS 4119 EN ISO 3376 (2006), “Leather – Physical and mechanical tests - Determination of tensile strength and percentage extention”, *Turkish Standard Institution*, 9.

TS EN 12770 (2004), “Footwear-Test methods for outsoles – Abrasion resistance”, *Turkish Standard Institution*, 10.

TS EN ISO 14268 (2004), “Leather - Physical and mechanical tests - Determination of water vapour permeability”, *Turkish Standard Institution*, 16.

TS EN ISO 20344 (2007), “Personal protective equipment - Test methods for footwear”, *Turkish Standard Institution*, 66.

TS EN ISO 23910 (2008), “Leather - Physical and mechanical tests - Measurement of stitch tear resistance”, *Turkish Standard Institution*, 13.

TS ISO 48 (1998), “Rubber, vulcanized or thermoplastic-Determination of hardness (Hardness between 10 IRHD and 100 IRHD)”, *Turkish Standard Institution*, 20.

UNIDO (1996), *Acceptable quality standards in the leather and footwear industry*. UNIDO Publication Sales No. UNIDO.95.4.E, Vienna.

CLASSIFICATION OF FOOT TYPES, BASED ON PLANTAR FOOTPRINTS

AURA MIHAI, MARIANA PASTINA

"Gheorghe Asachi" Technical University of Iasi-Romania, mpastina@tex.tuiasi.ro

The present studies have been conducted in order to develop a rational classification technique of foot typologies, based on parameters derived from plantar footprint. Absence of an absolute dimension on the foot typology has driven to a considerable variation in choosing the measurement types in order to determine foot type. The plantar footprint examination is a rapid, non-invasive, simple method that can quantify the foot configuration. According to the obtained results, the subjects will be divided into four categories, subjects with: Normal Foot, High Arched Foot, Flat Foot, Hallux-Valgus Foot. The necessity for this classification is found both in the subsequent analysis of foot anthropometrical parameters and in modelling and designing prophylactic footwear.

Keywords: foot, footprints, pressure plate.

INTRODUCTION

Plantar foot pressure, the ground reaction forces and kinematic measurements are widely used for gait analysis in order to characterize normal or abnormal function of the human foot. Compared to traditional systems, the combination of these data gives a more complete, detailed and accurate foot loads during their activities (Giacomozzi C. and al. 2000). The foot is the source of direct contact with the supporting surface, and therefore plays an important role in all moments of static or moving. During walking, the foot contributes in absorbing the shocks; it adjusts to irregular surfaces and contributes to generating the push-off impulse (Saltzman C.L. and Nawoczenski D.A., 1995). Foot type it is a general term widely used to describes a number of architectural features of the foot in order to obtain clues of its dynamic functioning. Foot dynamics is perceived as being linked to a variety of musculoskeletal symptoms, including personal injury from running and plantar pain, especially on the heel. Biomechanical studies have progressed, by comparing the presence, absence or the size of typological parameters, between groups, with or without foot pathology under investigation. Despite widespread use of these parameters, it was recognized that an objective and quantitative analysis of foot typology it still remains elusive. This is in contrast with the suggestion that, in order to identify the relationship between typology and foot pathology is first necessary to use a classification system that allows accurate recognition of each statement (Mathieson I. and al. 1999).

Plantar footprints were often studied in the past for various reasons. Many scientists around the world have focused attention on analysis of hominid fossils traces, orthopaedic studies and other medical studies, anatomical studies and anthropological, genetic and dermatological studies, biomechanical studies, ergonomics and forensic studies (Kewal K., 2008). Classification of different types of foot using the Footprint Angles and Chippaux-Smirak Index varies by the parameters analyzed, indicating the dependence to foot plantar print and the wide variety of foot morphology. It has been proposed a basic classification technique which allows for rational classification of foot types. Comparisons between initial classification and classification using individual parameters showed significant discrepancies between the parameters studied (Nikolaidou M.E. and Boudolos K.D., 2006).

Clinical measurements of foot structure have been developed to quantify certain aspects of foot geometry for diagnosing various diseases. Such type of measurement is the width of median-longitudinal arch. This can be achieved using the following parameters: Chippaux-Smirak index - the ratio between minimum width of midpoint and the widest width of toes, Arch Angle - the angle between the line connecting the metatarsal posterior-extreme point and the heel posterior-extreme point (Papuga M. O. and Burke J. R., 2010).

METHOD

To obtain the plantar footprint was used Rsscan pressure plate and the associated system, Footscan 7 Gait, 2nd Generation, 0,5 Gait Scientific System, produced by RSscan International (www.rsscaninternational.com).

In order to determine the foot types, the plantar footprints were taken from 60 women, aged 20-30 years and weighing 45-70 kg. All participants fulfilled the following criteria: without gait problems, without foot injury, without systemic medical conditions that may influence the gait. Foot pressures were taken on barefoot. For statistical measurements, subjects were asked to stand with both feet on the pressure plate, in an equilibrium position. For dynamic measurements, subjects were asked to walk normally on the plate, marking a measurement for the right foot and one for the left foot. The procedure was repeated three times for each subject analyzed. Unlike traditional methods of taking plantar footprints, a dynamic footprint is obtained, using this system, the software automatically links images in all phases of walking. Images were exported to scale 1:1 and 9 dimensions were measured to calculate the main parameters of the footprint, as shown in the legend below.

Legend:

UV – foot length

AB – heel width

AC – distance between the intersection of AB with UV

DE – on footprint – distance between the intersection of BF with AH

DE' –3D foot shape – correspondence of **DE** – on footprint

FG – fingers with

FH - distance between the intersection of FG with UV

α – arch angle (FPS)

β – angle of I finger deviation, hallux-valgus angle (HVA)

CSI –Chippaux-Simark index

where CSI= $\frac{DE}{FG} * 100$ (%) (1)

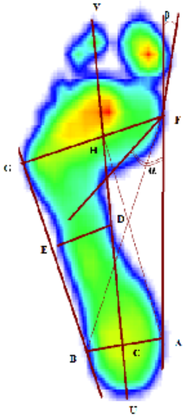

Figure 1. Plantar footprint

RESULTS AND DISCUSSIONS

CIS, FPS, HVA indexes were calculated, based on the measured parameters for each subject separately and applying the above calculus relationships.

Using the obtained results, the subjects were classified, considering each index type.

Table 1. Chippaux-Simark index

Foot type	Index values	Left	Right
High arched (H)	[0,20)	9	8
Normal (N)	[20,30)	24	20
Intermediary (I)	[30,40)	21	22
Low arch (L)	[40,45)	4	7
Flat (F)	>45	2	3

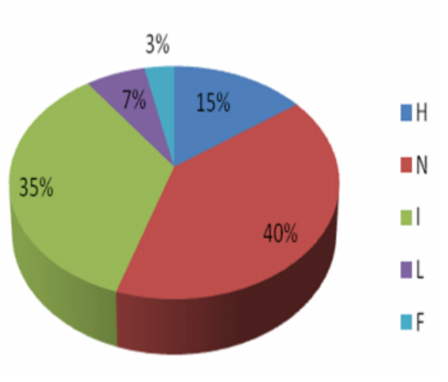

Figure 2. Left foot

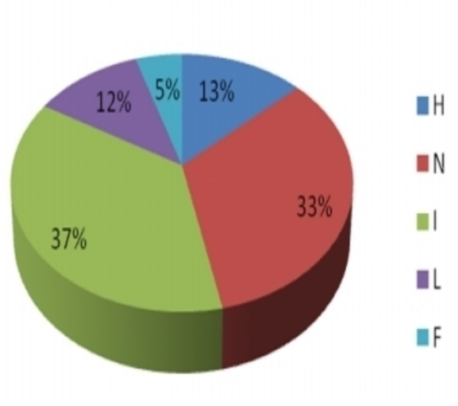

Figure 3. Right foot

As we can see, there are differences between subjects' right foot and left foot, but these differences are maintained within normal limits.

Following the analysis using Chippaux -Simark index for the left foot, has resulted that 15% of subjects have high arched foot, 7% with a tendency to flattening, 3% with flat feet and the remaining 75% normal and intermediate foot. For the right foot, Chippaux -Simark index showed that 13% of subjects have high arched foot, 12% with a flattening tendency, 5% flat foot and the remaining 70% normal and intermediate foot.

Table 2. FPS - arch angle (α)

Foot type	Index values	Left	Right
High arched (H)	>50	17	22
Normal (N)	[40,50)	34	30
Intermediary (I)	[35,40)	4	3
Low arch (L)	[30,35)	1	1
Flat (F)	[0,30)	4	4

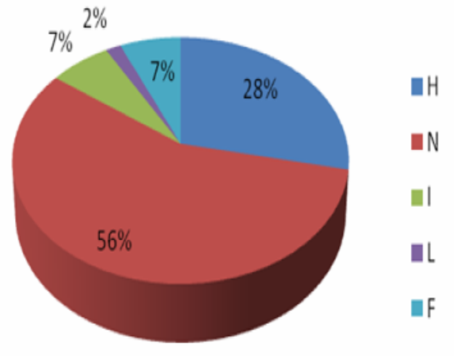

Figure 4. Left foot

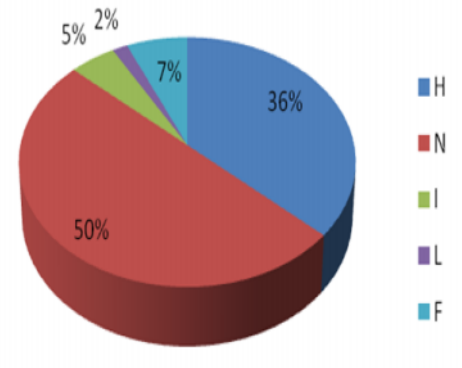

Figure 5. Right foot

Following the analysis using the arch angle, α, for the left foot, the results are presented in the following way: 28% of subjects have high arched foot, 2% a flattening tendency, 7% flat foot and the rest of 63% have normal or intermediate foot. For the right foot, the results showed that 36% of subjects have high arched foot, 2% a flattening tendency, 7% flat foot and the remaining of 55% have normal or intermediate foot.

Table 3. HVA - Hallux-Valgus angle β

Foot type	Index values	Left	Right
Hallux-Valgus (HV)	>15	4	2
Outward movement (De)	[10, 15)	6	5
Normal (N)	[0, 10)	32	28
Inward movement (Di)	<0	18	25

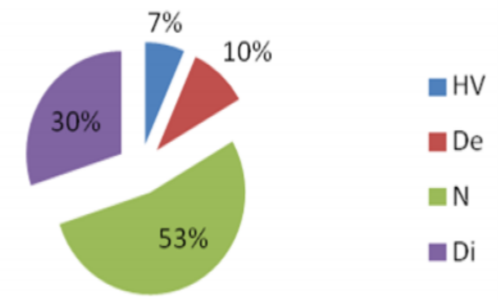

Figure 6. Left foot

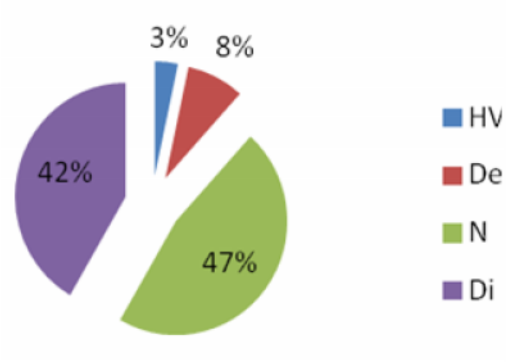

Figure 7. Right foot

The hallux-valgus angle is used to detect the presence on the foot of hallux-valgus condition. For the left foot, 7% have a hallux-valgus foot, 10% have a risk of developing this condition, 53% of subjects have a normal foot, and 30% of cases have an inward deviation of the first finger. For the right foot, 3% have hallux-valgus condition, 8% are at risk of development this anomaly, 47% with normal foot, and 42% have an inward deviation of the first finger.

Table 4. Foot types - Centralized results

Index	Subjects	Foot	H (%)	N (%)	I (%)	L (%)	F (%)	HV (%)	De (%)	N (%)	Di (%)
Chippaux-Simark-CSI	Women	Left	15	40	35	7	3	-	-	-	-
		Right	13	33	37	12	5	-	-	-	-
FPS(α)	Women	Left	28	56	7	2	7	-	-	-	-
		Right	36	50	5	2	7	-	-	-	-
HVA (β)	Women	Left	-	-	-	-	-	7	10	53	30
		Right	-	-	-	-	-	3	8	47	42

CONCLUSIONS

According to the obtained results, the subjects will be divided into four categories, subjects with: Normal Foot, High arched Foot, Flat Foot, Hallux-Valgus Foot.

These studies have been conducted in order to develop a rational classification technique of foot typologies based on parameters derived from plantar footprint. The plantar footprint examination is a rapid, non-invasive, simple method that can quantify the foot configuration.

The necessity for this classification is found both in the subsequent analysis of foot anthropometrical parameters and in modelling and designing prophylactic footwear.

Acknowledgements

This paper was realised with the support of EURODOC “Doctoral Scholarships for research performance at European level” project, financed by the European Social Found and Romanian Government.

REFERENCES

Giacomozzi, C., Macellari, V., Leardini, A., Benedetti, M.G. (2000), “Integrated pressure-force-kinematics measuring system for the characterisation of plantar foot loading during locomotion”, *Medical & Biological Engineering & Computing*, 38, 156-163.

Kewal, K. (2008), “Establishing correlation of footprints with body weight—Forensic aspects”, *Forensic Science International*, 179, 63–69, available online at www.sciencedirect.com.

Mathieson, I., Upton, D., Birchenough, A. (1999), “Comparation of footprint parameters calculated from static and dynamic footprints”, *The foot*, 9, 145-149.

Nikolaidou, M.E., Boudolos, K.D. (2006), “A footprint-based approach for the rational classification of foot types in young schoolchildren”, *The Foot*, 16, 82–90, available online at www.sciencedirect.com.

Papuga, M.O., Burke, J.R. (2010), “The reliability of the associate platinum digital foot scanner in measuring previously developed footprint characteristics: a technical note”, *Journal of Manipulative and Physiological Therapeutics*, 34(2), 114-118, available online at www.sciencedirect.com.

Saltzman, C.L., Nawoczenski, D.A. (1995), “Complexities of foot architecture as a base of support”. *J Orthop Sports Phys Ther*, 21, 354–60.

***, RSscan, www.rsscaninternational.com

INVESTIGATIONS ON DETERMINATION OF ANTIOXIDANT PROPERTIES OF CERTAIN PLANT PRODUCTS AND THEIR EFFECTS ON THE PREVENTION OF CR(VI) AND FORMALDEHYDE FORMATION IN LEATHER

HASAN OZGUNAY[1], ALTAN AFSAR[1], SELIME COLAK[1], GOKHAN ZENGIN[1],
ONUR YILMAZ[1], URANA DANDAR[1], DEMETRA SIMION[2], CARMEN CORNELIA GAIDĂU[2]

[1] *Ege University, Faculty of Engineering, Leather Engineering Department, Izmir, Turkey*

[2] *INCDTP - Division: Leather and Footwear Research Institute, 93 Ion Minulescu st., sector 3, postal code: 031215, Bucharest, Romania*

The effectiveness of antioxidant materials on the prevention of free radical formation is well known. The tannins as phenolic materials are also known to have antioxidant properties, however, the antioxidant effectiveness shows variation regarding to the type and structure of tannins. In leather manufacturing direct use of Cr(VI) and formaldehyde is forbidden, however, there is always a risk of conversion of Cr(III) to Cr(VI) and formation of free formaldehyde subsequent to the manufacturing. Free radicals usually play an important role of formation of these toxic substances in leather. In the present study, Valonea and Henna was selected as tannin and their antioxidant capacities were determined by FRAP and TEAC/ABTS methods. Furthermore, these vegetable tannins were used in leather processes and their effect on prevention of Cr(VI) and free formaldehyde formation was examined.

Keywords: valonea, henna, Cr(VI).

INTRODUCTION

With regard to chrome tannage, the most important technical issues concerning ecology and consumer health are: avoiding chromium (VI) and avoiding formaldehyde release (Germann, 2008). Normally chrome tanning merely involves Cr(III), however, there have been many reports, Cr(VI) has been abnormally detected in some leather samples, this has been widely debated (Cory, 1997; Rydin, 2002; Katz & Salem, 1994).

The exact origin of Cr(VI) in leather is not well understood. However, pigments based on lead chromate (Girard & Hubert, 1996; Cory, 1997), the incompletely reduced chromium tanning agents and metal complex dyes containing Cr(VI) are known to be the primary sources of hexavalent chromium, which can be easily avoided in processing. But the most difficult aspect of the problem is the possibility of oxidative conversion of leather bound Cr(III) to Cr(VI) during manufacture (Font et al., 1998; Hauber & Germann, 1999). Fatliquors based on oils with a high degree of unsaturation and other post-tanning and finishing auxiliaries bearing uncured oxidative catalysts used in the processing of leather could, theoretically, aid in the conversion of free Cr(III) to Cr(VI) (Nickolauss, 1995; IUC-8, 1998).

Regarding the problems associated with formaldehyde (Wolf, 2002; Lampard, 2001; Meyndt & Germann, 2004), formaldehyde is used as a condensation agent in the production of processing chemicals such as syntans, resin tanning agents and dyeing auxiliaries. These condensation products show varying stability to hydrolytic reactions and this can lead to the release of formaldehyde. In addition there are possible synergistic effects through interactions with the leather matrix, and the possible formation of aldehydes on ageing of unsaturated organic substances (e.g. fatliquors) (Germann & Meyndt, 2005).

In time, the chemicals used in production and other environmental factors like heat, light and etc. may cause aging and some changes and deformations in leather products e.g.: oxidation of Cr(III) to Cr(VI), decrease in shrinkage temperature, fading or yellowing, loss of physical resistance, odor problems due to oxidations of fatliquors or formaldehyde release. These deformations generally occur due to the oxidant groups, which are called free radicals, arise depending on the factors mentioned above.

Hindering formation of free radicals prevents occurrence of the many cases mentioned above. Antioxidants are used for hindering free radical formation. As is known in the food and medicine sectors, the tannins have a great antioxidant activity (Bors & Michel, 1999). Vegetable extracts which poses multiple phenolic hydroxyls have been shown by experiment to be strong inhibitors of oxidation to Cr(III) into Cr(VI) (Congzeng et al., 2010). Retanning using vegetable tannins like quebracho and sumac extracts have been demonstrated to be efficient against chromium VI formation in the leathers exposed to light (Zalacain et al., 2000).

In the present study henna (Lawsonia Inermis) which have been extensively used for centuries in the Middle East, the Far East and Northern Africa as dye for nails, hands, hair and textile (Afzal et al., 1980) and Valonea which is one of many well-known vegetable tannins used in tanning and retanning processes for leather making were used in leather production as retanning and/or natural coloring materials and their effects on chromium IV formation was investigated. In the research we have also determined antioxidant powers of henna and valonea in order to establish a connection with their antioxidant powers and chromium VI formation preventing effects.

EXPERIMENTAL

Material

Commercial valonea tannin (in extracted form) and henna powder (in grinded form) were used in the research.

Method

Determination of Antioxidant Powers of Valonea and Henna

Antioxidant properties of vegetable materials were measured by FRAP (Iron (III) Reducing Antioxidant Power) and TEAC/ABTS (Trolox Equivalent Antioxidant Capacity) methods (Ozgen, M. et al., 2006) (Ozgen et al., 2006).

Use of Valonea/Henna in Leather Production

A wet-blue hide which was shaved to 1.25 mm thickness was used for the trials. The croupon area of the leather was divided into pieces in size of 15x21 cm as experiment samples. The leather samples processed according to recipe in Table 1. Two pieces were processed without any vegetable material as blank samples according to the same recipe.
Considering the commercial henna was not an extract, before deciding the amounts of materials that will be used in trials henna powder was extracted at 50°C for 4 hours and the extractable solid amount was determined gravimetrically (25%). As ¼ amount of the henna will pass in to the float 4%, 10% and 20% (over the wet-blue weight) decided to be used in trials while 1%, %2.5 and 5% of valonea were used.

Determination of the Colors of Leather Samples

Minolta CM-508d spherical spectrophotometer (Minolta Co. Ltd. Japan) with 8 mm diameter of measurement area was used for measuring the colors of the leather samples. Spectral reflectance values were measured between 400-700 nm range with 20 nm intervals, and 16 readings were obtained for each sample. The measurements were done under the conditions of CIE 10° standard observer angle and CIE standard D65 light source. The reflectance readings were converted to CIE L*a*b* values by using related formulas, and color differences were calculated by CIELAB 1976 color difference formula.

Artificial Aging of Leather Samples and Cr(VI) and Formaldehyde Tests

Cr (VI) and formaldehyde contents of the leather samples were determined according to IUC 18 and IUC 19 (2002) standard test methods. In this part of the research we aimed to investigate possible effects of valonea and henna on Cr(VI) formation under drastic conditions. For this purpose after determining the initial Cr(VI) and formaldehyde contents of the leather samples they exposed to UV light (360 nm) and kept at 80°C for 7 days.

Table 1. The recipe of process

Process	%	Product	°C	Min	
Washing	200	Water	35		
	0.2	HCOOH		30	
Neutralization	150	Water	35		
	2.5	Neutralizing syntan		15	
	0.5	$NaHCO_3$		45	pH:5-5.5
Washing	200	Water	35	20	
Retanning	150	Water	40		
	x	Vegetable material (Valonea / Henna)		15	
	2	Condensed naphthalene sulphone acid		15	
	3	Phenol sulphone condensation product		15	
	3	Melamine-Urea formaldehyde resine		15	
Fatliquoring			45		Float heated
	5	Sulphited mix of natural fatliquors			
	2	Synthetic fatliquor			
	2	Synthetic fatliquor		45	
	1	HCOOH		30	
	0.5	HCOOH		30	pH: 3.8
Washing	200	Water	35	20	

RESULTS AND DISCUSSION

For the analysis, 0.1 g of henna was extracted in 25ml of methanol for 24 hours. 0.1 g of valonea was dissolved in 25 ml of water: acetone mixture (1:1) before the analysis. Both solutions were diluted appropriately and their antioxidant powers were calculated according to trolox equivalents.

Antioxidant Properties of Valonea and Henna

Considering the results obtained by both methods; it was clearly seen that antioxidant power of valonea was considerably higher than henna. At this point it is necessary to mention and take in to consideration that the valonea sample used in the analysis was in extracted form while the henna sample was not extraction product.

Table 2. Antioxidant powers of henna and valonea according to FRAP

Vegetable Material	Antioxidant powers (mmol/L)
Henna	2.3
Valonea	48.1

Table 3. Antioxidant Analysis Results (TEAC/ABTS)

Vegetable Material	Antioxidant powers (mmol/L)
Henna	2.4
Valonea	28.0

Colors of the Leather Samples Treated with Valonea/Henna

Considering the CIE L, a, b values obtained by color measurements; it was detected that b* values of the leather samples have a tendency to increase which means an increase in yellow tones in accordance with the increasing amount of vegetable material used.

Table 4. Colors of the leather samples treated with valonea/henna

	Samples	L	a
■	Blank 1	79.73	-2.94
■	Blank 2	81.84	-3.53
■	1% Valonea	72.72	-1.67
■	2.5% Valonea	72.57	-1.28
■	5% Valonea	72.94	-0.57
■	4% Henna	75.34	-1.61
■	10% Henna	70.21	-0.10
■	20% Henna	69.26	1.46

Cr (VI) and Formaldehyde Contents of Leather Samples

Before aging, Cr(VI) was not detected neither in blank nor in valonea or henna treated leather samples. After artificial aging treatment 23.6 and 35.5 ppm Cr(VI) was detected in blank samples which were not treated with any vegetable material. That means an important amount of Cr(III) oxidized to Cr(VI) due to the applied drastic conditions (Table 5).

Considering valonea treated leather samples; it was seen that increasing amount of valonea use, prevented Cr(VI) formation quite effectively. In case of henna use, the amount of Cr(VI) formation was also decreased, but it was not as effective as valonea.

Valonea's and henna's Cr(VI) formation prevention effects were found in accordance with their antioxidant powers.

Before aging, varying values between 13.55-22.6 ppm regarding formaldehyde content were detected in leather samples. The results were not surprising as the synthetic tannins were specially selected to be having formaldehyde problem. Generally considering formaldehyde contents of the leather samples treated with vegetable materials, it can be seen that they have lower formaldehyde content than the blank leather samples. In spite of that it was concluded it was not possible to talk about formaldehyde preventing effect of vegetable materials used in trials.

Table 5. Cr(VI) and formaldehyde contents of leather samples before and after aging

Sample	Before aging Cr (VI) (ppm)	After aging Cr (VI) (ppm)	Before aging Formaldehyde (ppm)	After aging Formaldehyde (ppm)
Blank 1	0	23.6	22.6	19.4
Blank 2	0	35.5	18.45	18.7
1% Valonea	0	6.6	13.85	9.55
2.5% Valonea	0	2.7	19.9	7.9
5% Valonea	0	0.65	13.55	5.05
4% Henna	0	13.35	15.6	9.5
10% Henna	0	12.0	14.35	10.1
20% Henna	0	7.9	16.35	11.65

Formaldehyde contents of the leather samples were detected over again after aging treatment. From the evaluation of the results, it was clearly seen that the amounts of formaldehyde in the leather samples treated with vegetable materials, especially with valonea, were decreased considerably. Their formaldehyde contents were almost 50% lower than the blank samples. At this point the results derived us to think that an amount of formaldehyde was draw away during artificial aging treatment, in blank samples an amount reoccurred due to the aging but the valonea and henna possibly prevented some of the reactions that will result with formaldehyde release.

CONCLUSIONS

Both analysis methods (FRAP and TEAC/ABTS) applied in order to investigate antioxidant powers of henna and valonea revealed that the antioxidant capacity of valonea was much higher than henna.

After processing the leather samples, Cr(VI) was detected neither in blank nor in valonea or henna treated leather samples. However, after accelerated aging considerable amounts of Cr(VI) formation was observed in all leather samples. From the evaluation of the Cr(VI) contents of the leather samples, it was seen that valonea and henna treated leather samples were having lower Cr(VI) comparing to reference samples in accordance with their antioxidant capacities. That means antioxidant powers of vegetable materials determine their Cr(VI) formation prevention ability in chromium leather products.

Similar to the Cr(VI) results, the free formaldehyde contents of the leathers processed with valonea and henna tannin were lower than the reference leathers. Moreover, the valonea treated leathers showed lower free formaldehyde levels than the leathers treated with henna. Their formaldehyde contents were almost 50% lower than the blank samples. At this point the results derived us to think that an amount of formaldehyde was draw away during artificial aging treatment and valonea and henna possibly prevented some of the reactions that will result with formaldehyde release.

REFERENCES

Afzal, M., Al-Oriquat, Al-Hussan, J.M. and Mohammed, N. (1980), Flavone glycosides from Lawsonia inermis, *Heterocycle*, 14, 1973-1976.

Bors, W. and Michel, C. (1999), "Antioxidant capacity of flavanols and gallate esters: pulse radiolysis studies", *Free Radical & Medicine*, 27, 1413-1426.

Germann, H.P. (2008), "The Ecological Tannage-Challenges and Progress", SLTC Procter Memorial Lecture, *Journal of the Society of Leather Technologists and Chemists*, 92, 229.

CIE (Commission Interantionalle DeL'Eclairage) (1976), Official Recommendations on Uniform Colour Spaces Colour Differance Equations Metric Colour Terms, 10.

Congzeng, Y., Rui, W., Xingyuan, M. and Mingyang, Y. (2010), "Antioxidant Effects of phenolic compounds on unsaturated lipids preventing the oxidation of Chrome(III)", *Journal of the Society of Leather Technologists and Chemists*, 94(1), 33.

Cory, N.J. (1997), "A Practical Discussion Session to Deal with Opportunities for Improvement of Customer/End User Satisfaction", *Journal of the American Leather Chemists Association*, 92(5), 119-125.

Font, R., Cuadros, M., Lalueza, J., Orus, C., Reyes, M.R., Costa-Lopez, J., Marsal, A. (1998), "Presence of Cr (VI) in Sheep Skins: Influence of Tannery Process", *Journal of the Society of Leather Technologists and Chemists*, 82(49), 91-95.

Germann, H.P., Meyndt, R. (2005), "Formaldehyde-Free Leather: A Realistic Objective?" In: Proceedings XXVIII IULTCS Congress, Florence, Italy.

Girard, L. and Hubert, J. (1996), "Speciation Of Chromium (VI) and Total Chromium Determination in Welding Dust Samples by Flow-İnjection Analysis Coupled to Atomic Absorption Spectrometry", *Talanta*, 43(11), 1965-1974.

Hauber, C. and Germann, H.P. (1999), "Investigations on a Possible Formation and Avoidance of Chromate in Leather", *World Leather*, 12(6), 73.

IUC-8 (1998), Determination of chromic oxide content, *Journal of the Society of Leather Technologists and Chemists*, 82, 200.

IUC 18 (IUC: The Official Methods of the International Leather Chemists' Societies for Chemical Leather Analysis) (2002), Determination of Chromium VI Content.

IUC 19 (IUC: The Official Methods of the International Leather Chemists' Societies for Chemical Leather Analysis) (2002), Determination of Formaldehyde Content in Leather.

Katz, S.A. and Salem, H. (1994), *The Biological and Environmental Chemistry of Chromium*, VCH Publishers, New York.

Lampard, G. (2001), "Formaldehyde - The Final Straw?" *Leather International*, Nov., 203, 65.

Meyndt, R. and Germann, H-P. (2004), *Leder und Häutemarkt*, 5, 8.

Nickolauss, G. (1995), "Does leather contain chromium (VI)?", XXII International Union of Leather Technologists and Chemists Societies congress, Friedrichshafen, 47.

Ozgen, M., Rees, R.N., Tulio, A.Z., Miller, A.R. & Scheerens, J.C. (2006), "Modified 2,2'-Azino-bis 3-ethylbezothiazoline – 6-sulphonic acid (ABTS) Method to Measure Antioxidant Capacity of Selected Small Fruits and Comparison to Ferric Reducing Antioxidant Power (FRAP) and 2,2'-Diphenil-1-Picrilhydrazyl (DPPH) Methods", *Journal of Agriculture and Food Chemistry*, 54, 1151- 1157.

Rydin, S. (2002), "Chrome (VI) in Consumer Products", *Leather International*, 204(4727), 44-45.

Wolf, G. (2002), Formaldehyde in Leather: Causes and Avoidance, *World Leather*, February/March, 46-52.

Zalacain A, Alonso G. L.; Prodanov M., et al., (2000), "Determination of the tanning capacity of a rhus coriaria L. extract and its antioxidant activity", *Journal of the Society of Leather Technologists and Chemists*, 84, 212-215.

FINITE ELEMENT ANALYSIS FOR INSOLE-SOLE PROTOTYPES

MARIANA PASTINA[1], AURA MIHAI[1], NIKOLAOS BILALIS[2]

[1] *"Gheorghe Asachi" Technical University of Iasi, Romania, amihai@tex.tuiasi.ro*

[2] *Technical University of Crete, Greece*

3D finite element models for an insole with various thicknesses as well for an individual sole were created for this study. Based on these models, analyzes were made in order to obtain the distribution of strain and effort on their surfaces, in different conditions of use. To achieve the above, data have been purchased, concerning the shape of insole and sole (foot 3D scanned, shoe last modelling, shoe bottom parts modelling) and the properties of specific materials used to obtain them. The goal was to determine the effectiveness for the bottom part of footwear, for certain materials. There have been registered a significant diminution of efforts, on sole and insole, when the insole thickness increased, for two combinations of materials, EVA low density and PU flexible, EVA medium density and PVC soft, making it to be recommended for customized shoes.

Keywords: foot, prototype, insole and sole materials.

INTRODUCTION

Computer simulation of the foot and footwear is crucial not only to create realistic animations, but also acts as an instrument of economic evaluation in designing functional footwear. The most popular approach for simulating the foot and footwear is mainly based on FEM (Finite Element Method). Most studies have focused on the bottom of the shoe, the top of the shoe is rarely studied (Tang Y.M. and Hui K.-C., 2011). Finite element analysis contributes to experimental approach for predicting the loads distribution on the foot or for different objects, which provides information such as internal forces and deformations (Cheunga J.T.M. and al., 2005). Computer simulations can provide detailed and standardized analysis of design variables in order to guide strategies of prescribing customized footwear (Erdemira A. and al. 2005). Finite element modelling compensates for the limits of geometry and of experimental conditions, being allowed so, the evaluation of behaviour for the analyzed products (Erdemira A. and al. 2006). Insole design is usually intuitive and not always based on scientific principles. In addition to material and geometry, its thickness can have a considerable influence on adjusting plantar pressures, the thicker the insole, the more efficiently is (Goskea S. and al. 2006). Finite element analysis is time consuming and must be done by persons well trained in this field (Yarnitzkya G. and al. 2006). When studying the effectiveness of shoe design on foot mechanics, scientists adopt the finite element analysis of loads. Based on these analyzes, it was found that the stiffness of the sole and insole influences the effort of the foot inside the shoe (Spearsa I.R. and al. 2007). Effective analyses can be conducted to explore the impact on the foot, and the shoes, by changing sole's or insole's thickness, stiffness or material (Yu J. and al. 2008). Finite element analysis facilitates efficient evaluation of various structural and material parameters, for the footwear without it being fabricated. The models that exist in the literature show the potential of understanding the biomechanics of foot and footwear. However, the complicated geometry for most of the models, makes difficult to do a precisely simulation of them (Cheung J. T.M. and Zhang M., 2008).

METHOD

The purpose of this study is to create 3D finite element models for insoles and soles and based on these models, analyzes were made in order to obtain the distribution of strain and effort on their surfaces, in different conditions of use. To achieve the above, data have been purchased, concerning the shape of insole and sole (foot 3D scanned, shoe last modelling, shoe bottom parts modelling) and the properties of specific materials used to obtain them. The goal is to determine the effectiveness for the bottom part of footwear, for certain materials. 3D shapes of insole and sole have been built using the DELCAM software, which are part of the CAD family of programs (Computer Aided Design), Crisipin ShoeDesign and PowerShape. These models must then be exported and recognized by the interface of a software program type FEA (Finite Element Analysis), which will interpret the objects constituting the model and determine the conditions on the outline. In addition to preparing these models and transforming it for the analysis method, FEM, information has been added, for the measurement units, the physical and mechanical properties. This analysis has been done with ANSYS software, version 13.0. It was assumed that the materials have elastic-plastic behaviour, isotropic and homogeneous. Following the experiments in the recent years and the numerous tests, has been demonstrated that EVA foam (ethylene-vinyl acetate) can be used to make soles, insoles and midsoles. Shock absorption properties depend on its density. EVA deformation used to make footwear have a linear variation, and the studies conducted by Tsuyoshi Nishiwaki and Junichiro Tateishi in 2011 show that density decreases with the increase of deformation effort. According to this research, an average density led to a depreciation of shocks, being recommended for shoe insoles (Nishiwaki T. andTateishi J., 2011). Aoife Healy and al. in 2011, have established that the pressures in the heel area are reduced by bottom components based on PU (polyurethane) medium density, medium density EVA and EVA low density. They also established that the same things happen in the metatarsals area (Healy A. and al. 2011). Another item recommended by the studies found in literature is soft PVC (polyvinyl chloride) medium (Brueckner K. and al. 2011).

The novelty of the present research is the procedure of combining materials to obtain a complex of insole and sole with different thickness. Based on data from the literature there have been considered the following groups of materials and their properties:

Table 1. Materials properties

	EVA low density	EVA medium density	PVC soft	PU flexible
Density (g/cm^3)	0.923	0.941	1.245	1.250
Young Modulus (MPa)	11	60	20 - 50	60
Poisson Coefficient	0.49	0.49	0.40	0.40
Tensile Yield Strength (MPa)	2.5	7.31	20	-
Tensile Ultimate Strength (MPa)	1.9	12.5	15.8	20 – 30

Being a static analysis, the entire weight is distributed evenly on both feet. The loading force is:

$$G = m * g, \tag{1}$$

Where:

G - force of gravity;

m - body weight (for this study, subject's weight is 50 kg);
g - gravitational acceleration, 9.81 m/s^2.

RESULTS

It was designed and imported a sole of 10 mm thickness and the heel of 20 mm, and an insole with different thicknesses, 1, 3, 5 and 7 mm.

Von Misses stress results showed an increase or decreases of efforts depending on the material and insole thickness, as presented in figures 2÷7. The values obtained correspond to situations in practice, when it is observed that after a period of wearing a footwear product, in these regions, is identified a degree of depreciation of the material. An example of Von Misses equivalent stress is illustrated in Figures 1. a) and b).

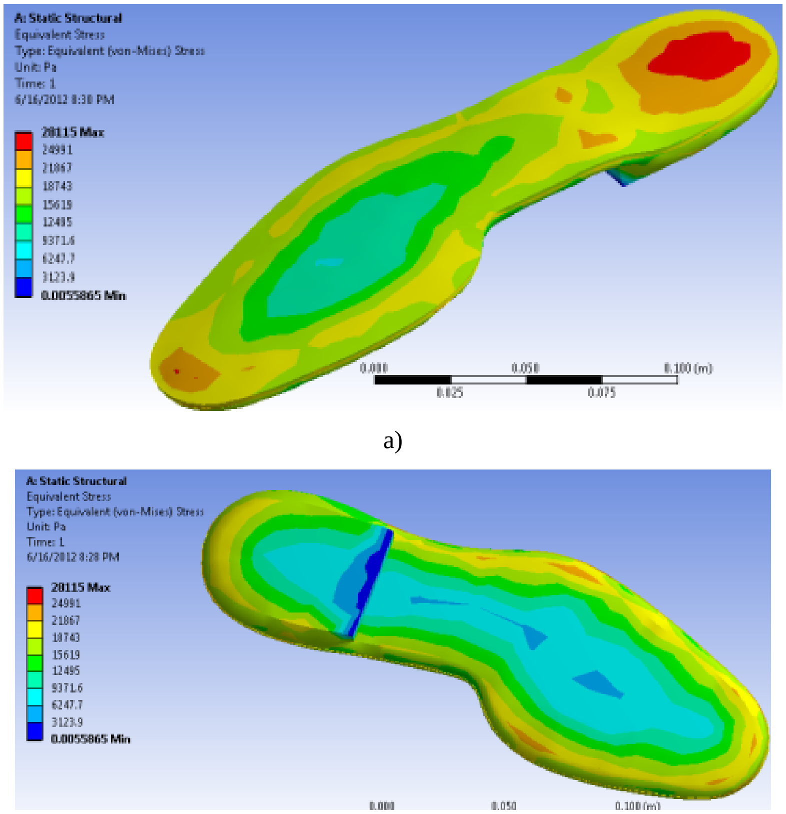

a)

b)

Figure 1. EVA low density +PU flexible – insole of 3 mm thickness

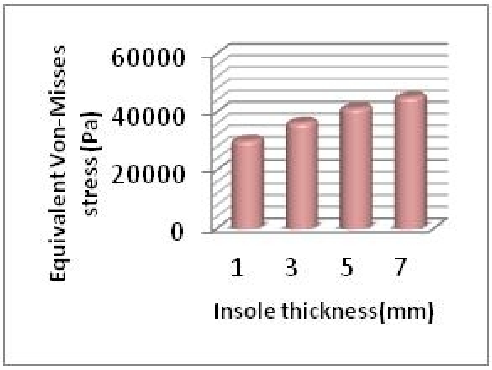

Figure 2. Equivalent Von-Misses stress (Pa) - EVA low density + EVA medium density

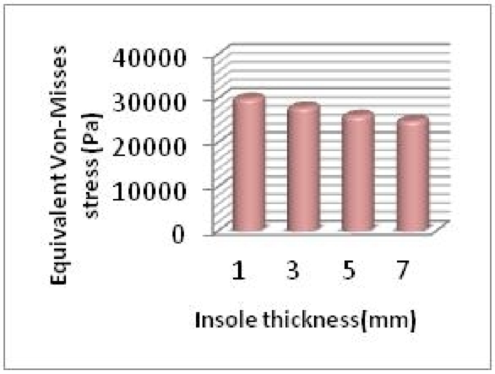

Figure 3. Equivalent Von-Misses stress (Pa) - EVA low density + PU flexible

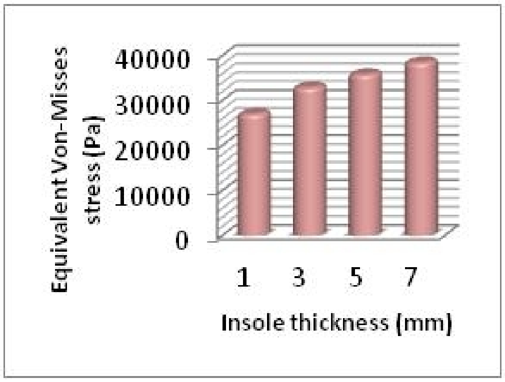

Figure 4. Equivalent Von-Misses stress (Pa) - EVA low density + PVC soft

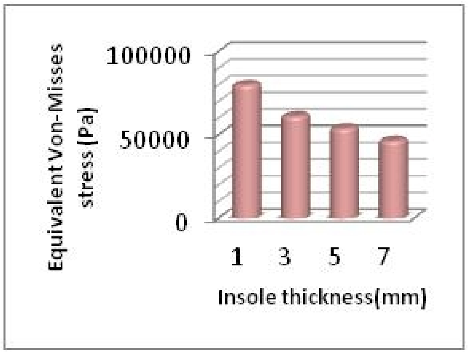

Figure 5. Equivalent Von-Misses stress (Pa) - EVA medium density + PU flexible

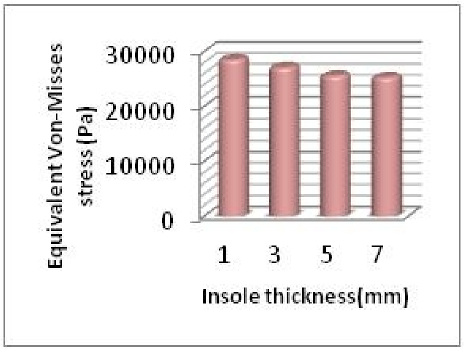

Figure 6. Equivalent Von-Misses stress (Pa) - EVA medium density + PVC soft

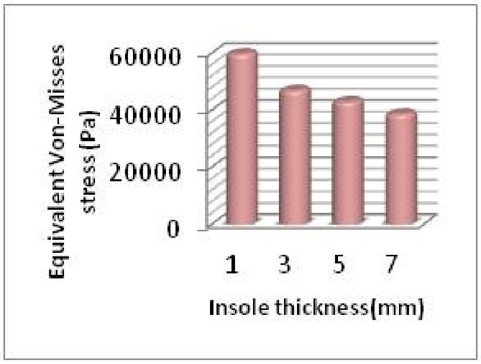

Figure 7. Equivalent Von-Misses stress (Pa) - PVC soft + PU flexible

CONCLUSIONS

A significant reduction of efforts on the sole, while the insole thickness increases, which then are transmitted to the foot, are registered by two combinations of materials, EVA low density + PU flexible and EVA medium density + PVC soft. Considering these results, the materials combination which provides a reduction of efforts, are recommended in producing bottom components of footwear. In case of EVA low density + EVA medium density there is an increase of stress with the increase of insole's thickness, and in case of PVC soft + PU flexible there are observed a decrease of efforts while the insole increases its thickness, but even so, these values remain larger than the above cases.

Based on finite element analysis, it can be concluded that changes on insole and design and the use of different materials for insoles and soles can significantly redistribute the efforts / deformations on the foot.

Acknowledgements

This paper was realised with the support of EURODOC "Doctoral Scholarships for research performance at European level" project, financed by the European Social Found and Romanian Government.

REFERENCES

Brueckner, K., Heidnefelder, J., Odenwald, S., Milani, T.L. (2011), "Mechanical and biomechanical characterization of running shoes with different midsole materials before and after aging", *Footwear Science*, 3(S1), 18-19.

Cheung, J.T.-M., Zhang, M., Leunga, A. K.-L., Fan, Y.-B. (2005), "Three-dimensional finite element analysis of the foot during standing—a material sensitivity study", *Journal of Biomechanics*, 38, 1045–1054.

Cheung, J.T.-M., Zhang, M. (2008), "Parametric design of pressure-relieving foot orthosis using statistics-based finite element method", *Medical Engineering & Physics*, 30, 269–277.

Erdemira, A., Saucermanb, J.J., Lemmonc, D., Loppnowd, B., Tursoe, B., Ulbrechtf, J.S., Cavanagh, P.R. (2005), "Local plantar pressure relief in therapeutic footwear: Design guidelines from finite element models", *Journal of Biomechanics*, 38, 1798–1806.

Erdemira, A., Viveirosb, M.L., Ulbrechtc, J.S., Cavanagh, P.R. (2006), "An inverse finite-element model of heel-pad indentation", *Journal of Biomechanics*, 39, 1279–1286.

Goskea, S., Erdemirb, A., Petreb, M., Budhabhattib, S., Cavanagh, P.R. (2006), "Reduction of plantar heel pressures: Insole design using finite element analysis", *Journal of Biomechanics*, 39, 2363–2370.

Healy, A., Dunning, D., Chockalingam, N. (2011), "Effect of insole material on plantar pressure", *Footwear Science*, 3(S1), 69-70.

Nishiwaki, T., Tateishi, J. (2011), "Basic research on midsole material designing", *Footwear Science*, 3(S1), 122-123.

Spearsa, I.R., Miller-Youngb, J.E., Sharmac, J., Kerd, R.F., Smith, F.W. (2007), "The potential influence of the heel counter on internal stress during static standing: A combined finite element and positional MRI investigation", *Journal of Biomechanics*, 40, 2774–2780.

Tang, Y.M., Hui, K.-C. (2011), "Human foot modeling towards footwear design", *Computer-Aided Design*, 43, 1841–1848.

Yarnitzkya, G., Yizharb, Z., Gefen, A. (2006), "Real-time subject-specific monitoring of internal deformations and stresses in the soft tissues of the foot: A new approach in gait analysis", *Journal of Biomechanics*, 39, 2673–2689.

Yu, J., Cheung, J.T.-M., Fan, Y., Zhang, Y., Leung, A.K.-L., Zhang, M. (2008), "Development of a finite element model of female foot for high-heeled shoe design", *Clinical Biomechanics*, 23, S31–S38.

ASPECTS REGARDING THE DEVELOPMENT OF THE MEDICAL FOOTWEAR INDUSTRY IN ROMANIA

DANIEL PETCU, DANA DESELNICU, SERGIU ADRIAN GUTA, GHEORGHE BERIJAN

INCDTP - Division Leather and Footwear Research Institute Bucharest, 93 Ion Minulescu St.,
email: icpi@icpi.ro

Medical footwear is a product of a complex interdisciplinary field, whose efficacy is proven in numerous scientific articles. Evidence-based prescription and design of this type of shoes can make significant contributions to health. The objective of this study is the analysis of the development stage and potential of this area in Romania. Relevant companies were interviewed through an online questionnaire consisting of 17 questions, addressing the following fields: products, technologies used in design and production, information, personnel, prescription of medical devices. The questionnaire was addressed to footwear manufacturing companies, and the inclusion criterion was the existence of a contractual relationship with the National Health Insurance Agency. A total of 10 companies answered. The number of technicians in a company involved in design and execution is 2-17 people; most companies think a more detailed prescription is necessary; a small number of companies are willing to invest in research, since the money available does not meet co-financing criteria imposed by regulations. Given that Romania ranks 7th most populated country in the EU, the medical footwear industry has great development potential. In order to achieve this objective, a contribution of all institutions involved in prescribing and designing this type of footwear is required.

Keywords: medical footwear, industry, development.

INTRODUCTION

Orthopedic footwear can help improve quality of life by reducing pain intensity manifested in the musculoskeletal system of the lower limbs and reducing pressure at the interface of contact between foot and support surface (Jannink et al., 2006). The action that shoes and medical devices placed inside the shoes can exert on the human body can generate both adverse effects on health (Barkema et al., 2011; Russell, 2010) and positive effects in the conservative treatment of mechanical disorders of the lower limbs such as ankle equinus, Achilles tendinitis, lower limbs discrepancies, forefoot ulcers (Rosenbloom, 2011; Hutchins et al., 2009).

In accordance with the law, “medical device” designates “any instrument, device, mechanism, material or other article used alone or in combination, including software necessary for its proper application, that the manufacturer intended for human beings and which does not fulfill its main action in/on the human body by pharmacological, immunological or metabolic means, but may be assisted in its function by such means, for the purpose of:

- diagnosis, prevention, monitoring, treatment or pain relief;
- diagnosis, monitoring, treatment or compensation for an injury or a handicap;
- investigation, replacing or changing the anatomy or a physiological process” (Decision no. 54/2009).

Both orthopedic shoes, foot orthoses and partial foot prostheses are included in the category of medical devices, according to the list of medical devices for the recovery of organic or functional deficiencies in ambulatory care, items D, G3 and H (Order no. 1723/950/2011 of the Ministry of Health). The special character given by medical device status stems from the fact that they “are provided for a specified or indefinite period, based on the prescription issued by the physician who has signed a contract with the health insurance agency, directly or through legal representatives" (Order no. 1723/950/2011 of the Ministry of Health). Another key feature of these products is that they are customized devices, designed and produced on demand. "Customized device" refers to "any device specifically made in accordance with written prescriptions of a duly qualified medical practitioner that sets specific design characteristics for the device and is intended to be used only by an individual patient. The above-mentioned prescription may also be issued by any other person authorized by virtue of their professional qualifications" (Decision no. 54/2009; Council Directive 93/42/EEC, 1993). The institutional framework and development direction of the educational system in the footwear field regarded as medical device were dealt with in previous papers (Petcu et al., 2008, 2009). A fundamental element of this complex medical footwear prescription-design-manufacturing system is the activity of production units, intended to be analyzed in this work.

OBJECTIVES

The National Research and Development Institute for Textile and Leather, Division: Leather and Footwear Research Institute has proposed to conduct a realistic dissemination of the current situation in the medical footwear production sector. The objective is to contribute to formulating new directions and joint research projects necessary for the development and modernization of this important area of activity.

METHOD

Within INCDTP – Division ICPI an online questionnaire was developed, entitled "Questionnaire on the activities related to prescribing, designing and manufacturing of the therapeutic, orthopedic footwear and in-shoe medical devices", which could be accessed online at the address: http://icpi.ro/chestionar/chestionar.php. The questionnaire was available online between 1 April and 30 July 2011. In the questionnaire structure, questions were grouped in relation to the following categories of subjects of interest:

1. Products,
2. Technologies used in design and production,
3. Information,
4. Personnel,
5. Prescription of medical devices,
6. Other aspects related to activity in this area.

Based on lists of medical device suppliers in contractual relationships with Health Insurance Agencies of Counties, a list of companies manufacturing orthopedic shoes or lower limb braces was prepared by consulting the websites of these institutions. A number of 28 manufacturers in contractual relationships with Health Insurance Agencies were identified. A cover letter signed by ICPI division management, explaining the objectives of the questionnaire, which also included the link for online access to it, was mailed to the contact addresses provided by each manufacturer from the list and to the Romanian Association of Footwear, Leather Goods and Other Leather Article Producers. After a first phase of centralization of responses received, the companies that did not respond were contacted by phone or by email in order to present the questionnaire and to make a request for its filling in.

RESULTS

Given the nature of this industry, evidenced by the definitions mentioned in the introduction of this paper, the contractual relationship between respondent and health insurance agency was established as a criterion for inclusion. Of the total number of 28 companies identified as complying with the criterion for inclusion, a total of 9 (32.1%) could not be contacted. Three of the 9 (32.1%) companies who responded did not fill in the questionnaire, answering by mail, and thus their answers cannot be equated with a questionnaire response. A total of 6 companies (21.4%) filled in the questionnaire online (Figure 1). For this analysis, the questionnaire answer of a company that is not in contractual relationship with the health insurance agency was not taken into account.

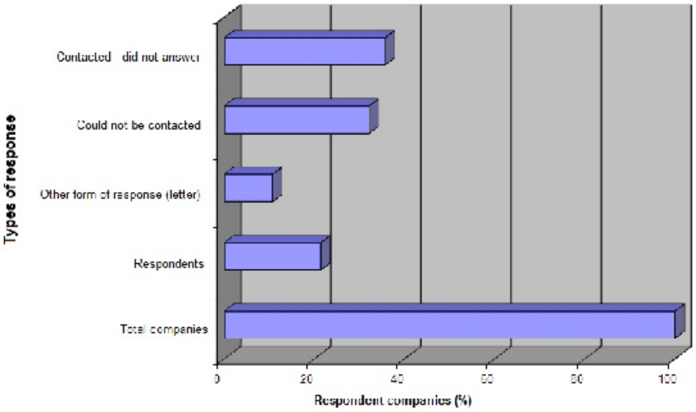

Figure 1. Structure of answers to online questionnaire

To facilitate interpretation of results, companies that have filled in the online questionnaire will be hereinafter generically called respondents.

The share of respondents' activities is: 41.7% - footwear production, 48.8% - orthotics/prosthetics, 0% - medical rehabilitation, 9.5% - other activities (e.g. commercial activities). All respondents stated that they manufacture shoes, while 66.7% also conduct orthosis/prosthesis development activities. Respondent companies operate in this market since 2001, with a total average of 7 employees (minimum 2, maximum 17) involved in the design and execution of these types of medical devices.

In the “Products” category, the share of companies stating that they produce one of the products of interest to this study, is shown in Figure 2. Thus, all respondents said that they produce partial foot prostheses, orthoses for foot statics correction, arch supports and orthopedic shoes, while additionally, 83.3% make functional foot orthoses, 50% produce shoes for certain diseases (diabetes, arthritis etc.), 50% make accommodative foot orthoses, 33.3% produce post-operative shoes and 16.7%, other devices for the foot up to the malleoli.

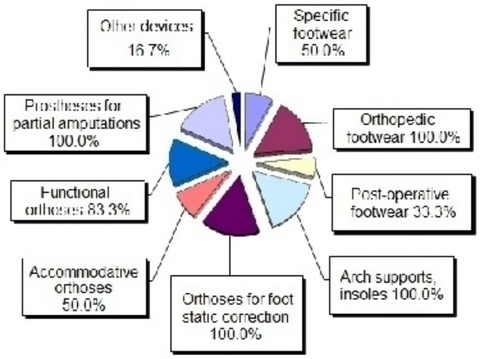

Figure 2. Categories of medical foot devices, made by respondent companies

It is noted that specialized products for foot pathologies of interest for this study and defined as medical devices by Romanian law are the following: shoes for deformities, shortenings, amputations of metatarsus; orthoses for foot statics correction; foot orthoses; partial foot prostheses. In contrast to this situation, the U.S. national social insurance program, Medicare, is much more complex, including, for example, a group of special shoes and braces for people with diabetes (Centers for Medicare & Medicaid Services). A clear definition of the types of medical devices for the treatment of foot pathologies is also required, because the same term has different meanings for different manufacturers. For example, searching the internet for “foot orthoses” yields results on products with totally different therapeutically actions.

In terms of technologies used in designing and manufacturing of medical devices, an inclination towards traditional methods based on manual techniques can be indirectly emphasized. Computerized techniques are mentioned in 33.3% of respondents, and they mainly aim footprint scanning for arch support manufacturing (2D podoscopy). Only one company says it uses 3D foot scanning. The use of CAD-CAM technology in design and execution of these products is an indicator of the gap between the specialized industry in our country and that in developed countries, where, for example, 3D foot scanning is an indisputable fact.

Regarding information sources used, 50% of respondents said that they participate in scientific meetings on topics related to footwear, orthotic/prosthetic products or medical issues concerning medical footwear and devices. Also, 50% of respondents participate in fairs and exhibitions. None of the respondents said they attend training courses on issues related to medical footwear in the country or abroad. None of the respondents are subscribed to a specialized journal, while 83.3% use the Internet for information. Also, 83.3% of respondents feel a specialized publication for the area of footwear with medical applications and medical devices inserted in footwear would be useful. A solution to this can be editing a special supplement of the Leather and Footwear Journal published by ICPI, entirely dedicated to this field, where interested companies can have the opportunity to publish articles, opinions or present their own activity.

The training of personnel involved in the design of these devices is very diversified. Thus: 33.3% of employees graduated from high school, 33.3% graduated from post-secondary school (ortho-prosthetist technician), 66.7% graduated from university (technical college, medical bioengineering, kinesiology), 16.7% attended postgraduate courses (Masters' in foot biomechanics).

Regarding the technical indications contained in the prescription of these devices, all respondents said that the patient's disease is specified, 66.7% said that the prescription is simply an indication of the type of device, 33.7% said that prescription does not contain all necessary information, requiring also the experience of the company. Only 16.7% said that the prescription contains all information necessary for shoe production, while 33.3% believe that prescription contains all information needed for insoles, arch supports and orthoses. In all cases the prescription sheet is drafted by the physician, while only 16.7% of respondents can provide their own prescription sheet. A 66.7 percentage believe a more detailed prescription is needed which would:

- correlate the diagnosis with the type of shoes,
- contain the exact type of device and special constructive elements,
- contain complete anatomical morphological data (such as specifying the exact amount of lower leg discrepancies or full analysis of dysfunctionalities in both feet, not only the most affected one, etc.).

All companies surveyed identify the partnership with the insurance system as the main problem they are facing (Figure 3).

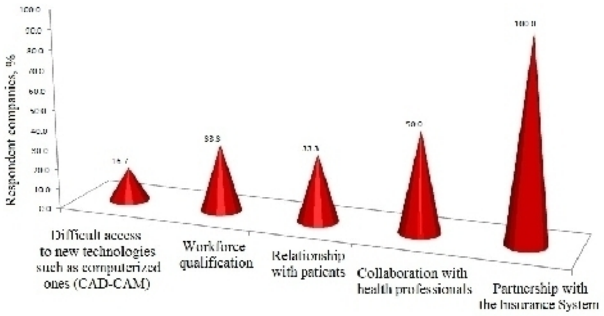

Figure 3. The main sources of difficulty which the respondent companies face

A percentage of 50 consider collaboration with health professionals to be problematic, especially due to medical prescription, while workforce qualification skills and relationship with patients is considered problematic by 33.3% of respondents. Last in the list of main problems was the difficult access to new technologies such as computerized technologies (CAD-CAM), indicated by only 16.7% of respondents.

Investment in research is around the values of 300-800 euro per year or 10% of amounts discounted on time by insurance agencies. None of the respondents indicated interest in development of research/development activities in any of the following areas: medical device prescription, product design, materials, manufacturing technologies, relationships with patients, training systems. Also, the amounts indicated by respondents as being available for investment in research are insufficient to meet co-financing requirements imposed by participation in research projects.

None of the respondents mentioned other important aspects of their activity that were not included in the questionnaire.

CONCLUSIONS

This study revealed that the medical footwear industry is still in its incipient phase in our country. Romania ranks 7th most populated country in the EU, which sets the premises for a development potential.

Several conclusions can be drawn:

- In terms of respondents, the main source of difficulty is the partnership with health insurance agencies. Comparing the structure of products settled through the insurance system in various countries, we find that in Romania, the list of medical devices of interest for this study contains fewer categories;

- A clarification of the definitions of each type of medical device is needed to improve both the act of prescription and communication between professionals involved in prescribing and designing these devices;

- Companies operating in this area are small companies with limited potential for investment in CAD-CAM technology or research activities. This is likely to affect the elaboration of a coherent and sustainable development strategy of this specialized field;

- The existence of a professional association to support training and economic activities of its members, using the existing model in advanced countries, can be a powerful stimulus of development in this area.

This study has several limitations. Thus, the small number of respondents is insufficient to consider the conclusions of this study generally valid. The novelty of interviewing through an online questionnaire can be interpreted as an impediment in getting responses, given that a number of companies do not have experience with this type of interview.

REFERENCES

Barkema, D.D. et al. (2011), "Heel Height Affects Lower Extremity Frontal Plane Joint Moments during Walking, *Gait Posture*, doi:10.1016/j.gaitpost.2011.11.013.

Centers for Medicare & Medicaid Services, "Medicare Coverage of Diabetes Supplies & Services", available online at: http://www.medicare.gov/publications/pubs/pdf/11022.pdf.

Hutchins, S. et al. (2009), "The Biomechanics and Clinical Efficacy of Footwear Adapted with Rocker Profiles — Evidence in the Literature", *The Foot*, 19, 165–170.

Jannink, M. et al. (2006), "Effectiveness of Custom-made Orthopaedic Shoes in the Reduction of Foot Pain and Pressure in Patients with Degenerative Disorders of the Foot", *Foot Ankle Int.*, 27(11), 974-9.

Petcu, D. et al. (2008), "Institutional Framework Required to Obtaining Footwear and Foot Orthoses for Preventive and Therapeutic Purposes", Proceedings of 2nd International Conference, ICAMS 2008, Bucharest, 582-586.

Petcu, D. et al. (2009), "Directions of Development of Systems Training in the Footwear Field", Presentation and Training Session in the VTC-Shoe Project, Iasi, 5-7.

Rosenbloom, K.B. (2011), "Pathology-Designed Custom Molded Foot Orthoses", *Clin Podiatr Med Surg*, 28, 171–187, doi:10.1016/j.cpm.2010.11.001.

Russell, B.S. (2010), "The Effect of High Heeled Shoes on Lumbar Lordosis a Narrative Review and Discussion of the Disconnect", *Journal of Chiropractic Medicine*, 9, 166–173.

*** (1993), Council Directive 93/42/EEC of 14 June 1993 concerning medical devices, available online at: http://eur-lex.europa.eu/.

*** (2009), Decision no. 54/2009 of 29/01/2009, published in The Official Journal of Romania, Part I no. 94 of 17/02/2009 regarding conditions of marketing medical devices, available online at: http://www.ms.ro/?pag=148.

*** (2011), Order of the Ministry of Health and of the president of the National Health Insurance Agency no. 1723/950/2011 for approval of Methodological Regulations of applying the Framework Contract in 2012, available online at: http://www.cnas.ro/norme-contract-cadru/norme.

THE INFLUENCE OF THE HYDRODYNAMIC DRAFT TUBES ON THE LIQUIDS MIXING QUALITY

IULIANA-MARLENA PRODEA, V. VALERIU JINESCU, NICOLETA TEODORESCU

University Politehnica of Bucharest, Romania, email:improdea@yahoo.com, vvjinescu@yahoo.com, nicoleta_teodorescu@yahoo.com

It was experimentally analyzed the influence of the hydrodynamic draft tubes (working in a functional unit with the mixer) on the liquids mixing quality, in the case of the rotating mixing devices. It was aimed to find (discover) the functional optimum by the optimization of the mixing system structure.

Keywords: rotating mixing devices; draft tubes; liquids mixing quality.

INTRODUCTION

The mixing operations are widely applied in different industries, implying different substances, with specific flowing behaviour, that's why many researches were done regarding the mixing phenomena (Jinescu, V.V., 1989, Paul, L.E, et al, 2004, Zalc, J.M., et. al. 2002, Jinescu V.V., et. al., 2002, Alvarez - Hernandez, M.M et. al., 2002, Sterpu, A.E., et. al, 2010).

In this paper there are presented a part of the experimental results of an extensive research made in order to optimise the rotative mixing devices and draft tubes, aiming to obtain a functional optimum (Prodea, I.M., 2010). This problem is studied from an original prospective that of determining of the optimum draft tubes geometry. The funded solutions were simple, not expensive, efficacious and easy to apply

It is analyzed the interaction between the mixer and the draft tube, seeking the improvement of the mixing quality and the energetic consumption.

EXPERIMENTAL INSTALLATION

The experimental installation is presented in Figure 1.

There were used, in turn, two glass cylindrical vessels (R1 and R2 - Table 1), provided with 3 vertical baffles and a central draft tube. The rotating mixing device has variable rotative speed (8 – 290 rot/min) and can be controlled by a computer, with a dedicated soft.

On the mixing device shaft were mounted, in turn, a standardised and a non-standardized (original) propeller – Table 2. The generated flow pattern, in both cases, was axial descendent

The draft tubes were made using cylindrical and taper elements resulting the configurations $T_{t,1} \div T_{t,9}$, presented in Fig.2.

A UV lamp was used to examine the induced flow pattern. The working fluid was a biphasic system made of oil (discontinuous phase)/water (continuum phase). The measurements were done at the ambient temperature ($\approx 20\,°C$).

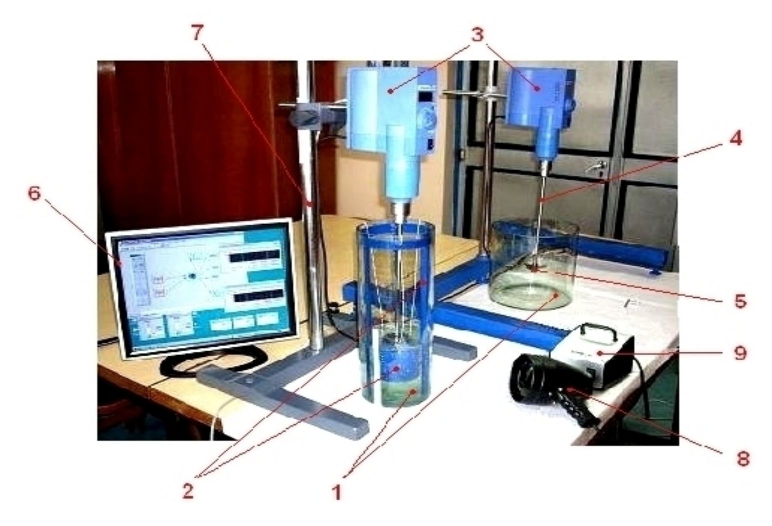

Figure 1. Experimental installation (Prodea, I.M., 2010): 1 – cylindrical vessel; 2 – interior static devices (baffles and draft tube); 3 – mixer device driver; 4 – shaft; 5 – mixer; 6 – computer; 7 – support; 8 –UV lamp; 9 – lamp source.

Table 1. Vessels characteristics (Prodea, I.M., 2010)

Vessel	Inner diameter [mm]	Vessel height [mm]	Liquid volume V_l [mm³]	Oil layer thickness [mm]
R1	$\boldsymbol{D}_{\boldsymbol{R}1} = 135$	$\boldsymbol{h}_{\boldsymbol{R}1} = 400$	$1932{,}374 \cdot 10^3$	$\boldsymbol{h}_{\boldsymbol{ulei},\boldsymbol{R}1} = 5$
R2	$\boldsymbol{D}_{\boldsymbol{R}2} = 180$	$\boldsymbol{h}_{\boldsymbol{R}2} = 260$	$4580{,}442 \cdot 10^3$	$\boldsymbol{h}_{\boldsymbol{ulei},\boldsymbol{R}2} \cong 6{,}7$

EXPERIMENTAL MEASUREMENTS

It is analysed the interaction (hydrodynamic draft tube-mixer) in the case of a dispersion oil/water, for each possible couple (mixer-vessel) according the configurations presented in Figure 3 (Prodea, I.M., 2010). There were used, in turn, the draft tubes presented in Figure 2. Each draft tube was placed at certain *h* height from the vessel bottom (Figure 4).

There were 4 positions of the mixer placed in the draft tube: *(a)* beneath the draft tube*;(b)* at the inferior limit of the draft tube*; (c)* in the middle of the draft tube*; (d)* at the upper limit of the draft tube.

The experimental measurements were done at the same rotative speed, for both mixers, $\boldsymbol{n}_1 = \boldsymbol{n}_2 = 290$ *rot/min*, respectively, so that one assures the generation of a turbulent flow during mixing operation.

Table 2. Mixers used in experimental measurements (Prodea, I.M., 2010)

Mixer	 Mixer 1	 Mixer 2
Mixer span (diameter) d_a $[mm]$	$d_{a,1} = 50\,mm$	$d_{a,2} = 50\,mm$
Characteristic ratio $\frac{d_a}{D}$	$\frac{d_{a,1}}{D_{R1}} \cong 0{,}37$; $\frac{d_{a,1}}{D_{R2}} \cong 0{,}28$;	$\frac{d_{a,2}}{D_{R1}} \cong 0{,}37$; $\frac{d_{a,2}}{D_{R2}} \cong 0{,}28$

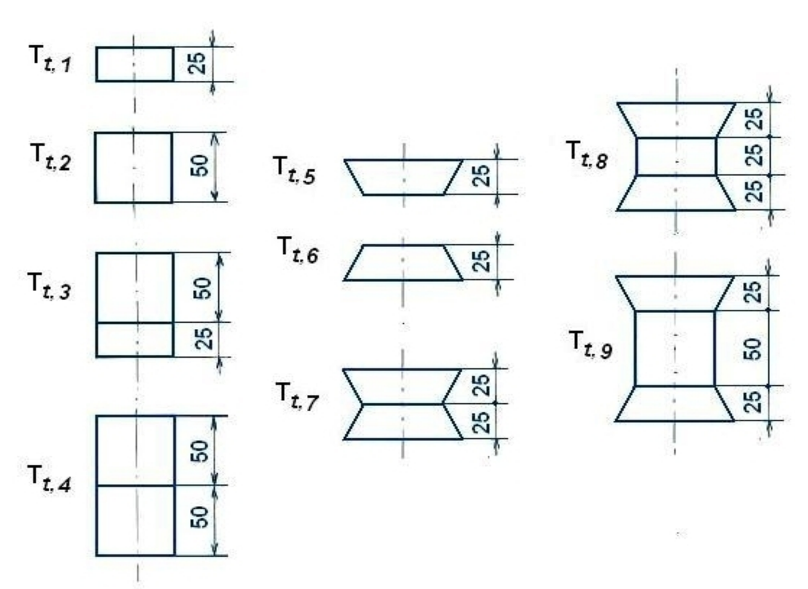

Figure 2. Draft tubes (Prodea, I.M., 2010)

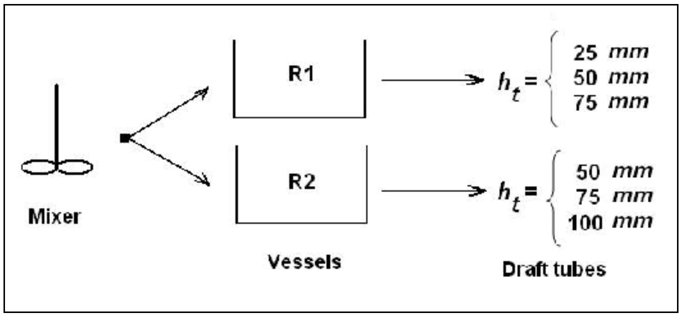

Figure 3. Experimental configurations (mixer, vessel, draft tube)

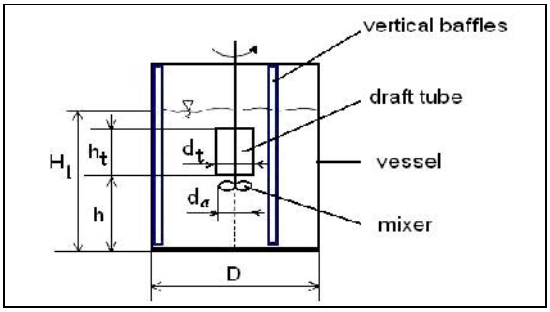

Figure 4. Mixing system configuration

EXPERIMENTAL RESULTS. INTERPRETATION

For each studied configuration (vessel - mixed – hydrodynamic draft tube) was measured the torque momentum and was evaluated the mixing quality using an original method (Prodea, I.M., 2010), i. e. a scale with coefficients between 0 and 5, defined function of a series of parameters essentially for a homogenous emulsion.

A good mixing was obtained only using simultaneously vertical baffles, and draft tubes.

The experiments aimed the determination of the optimum draft tube geometry and the optimum positioning of the draft tube related both to vessel bottom and to mixer.

To compare the obtained performances in the case of each tested mixing system, in order to establish the optimum, it was used both the mixing quality coefficient and the specific mixing power, N_{sp}, calculated with:

$$N_{sp} = \cdot \frac{\pi \cdot n}{30} \cdot \frac{M_t}{V_l}, \tag{1}$$

Where n is rotative speed of the mixing device shaft; M_t - measured torque; V_l - liquid volume (table 1).

In the Figures 5.a, 5.b, 5.c, - 6.a, 6.b, 6.c are emphasized, based on experimental results, the influence of the mixer geometry and its position related to the vessel/draft tube on the mixing efficiency; also it was take into account the influence of the geometry's draft tube on the mixing quality.

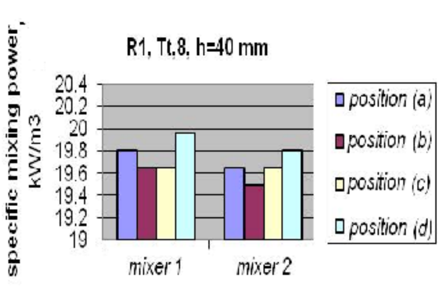

Figure 5. a) Mixer geometry and positioning influence on the specific mixing power

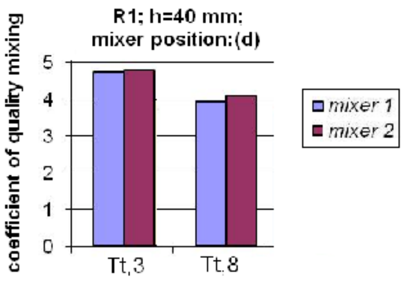

Figure 6. a) Draft tube and mixer geometry on the mixing quality

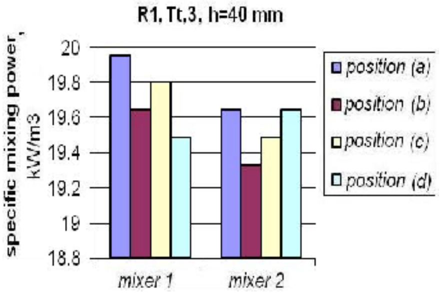

Figure 5. b) Mixer geometry and positioning influence on the specific mixing power

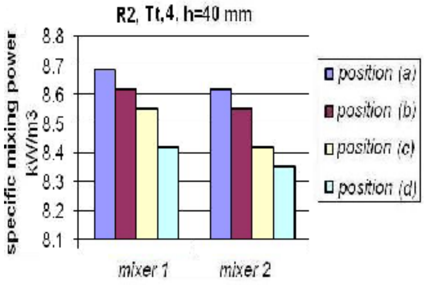

Figure 6. b) Draft tube and mixer geometry on the mixing quality

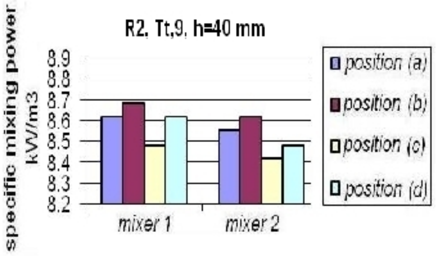

Figure 5. c) Mixer geometry and positioning influence on the specific mixing power

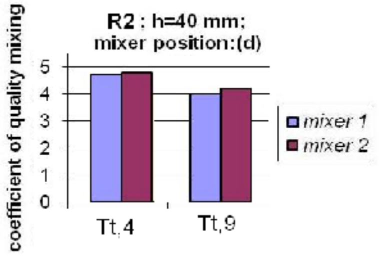

Figure 6. c) Draft tube and mixer geometry on the mixing quality

One observes that, no matter how the mixer is used, for the mixing configurations made with the vessel R1, the best results for the mixing quality were obtained in case of the draft tubes $T_{t,3}$ and $T_{t,8}$, while using the vessel R2, the best results were obtained with the draft tubes $T_{t,4}$ and $T_{t,9}$. Comparing the experimental results, the optimum configurations were $T_{t,8}$ (for vessel R1) and $T_{t,9}$ (for vessel R2) together with the mixer 2, placed in position *(d)* related the draft tube.

CONCLUSIONS

The interaction mixer-draft tube was analyzed from the prospective of the influence of the draft tube on the flow pattern generated by the mixer and, implicitly, on the mixing quality and efficiency parameters. There were stated, in this way the optimum configurations of the mixing systems for the analysed cases.

Regarding the draft tube, one can draw the following conclusions:

a) the optimum draft tube height, $\boldsymbol{h_{t,optim}}$, depends on the liquid height $\boldsymbol{H_l}$ ($\frac{\boldsymbol{h_{t,optim}}}{\boldsymbol{H_l}} \cong \frac{1}{2}$); b) the optimum positioning of the mixer is *(d)*, corresponding to the upper limit of the draft tube.

An original approach was used in order to find the optimum mixing system, which involves original mixing quality coefficients (Prodea, I.M., 2010), leads to simple solutions, low cost needed, reaching, apart of the functional optimum, also, an economic one.

REFERENCES

Alvarez - Hernandez, M.M., Shinbrot, T., Zalc, J.M., Muzzio, F.J. (2002), “Practical Chaotic Mixing”, *Chemical Engineering Science*, 57, 3749–3753.

Jinescu, V.V. (1989), *Technological Equipment for Process Industries* (in Romanian), vol. IV, Technical Press, Bucharest.

Jinescu, V.V. Prodea, I.M., Ion, N.A. (2002), “The necessary power and energy consumed in mixing processes in high-capacity recipients” (in Romanian), *Revista de Chimie*, 53(12), 802-808.

Paul, L.E, Atiemo – Obeng, A.V., Kresta, M.S. (2004), *Handbook of Industrial Mixing: Science and Practice*, John Wiley & Sons, Inc., New Jersey.

Prodea, I.M. (2010), *Contributions to optimisation of mixing devices in process industries* (in Romanian), PhD Thesis, University Politehnica of Bucharest.

Sterpu, A.E., Teodorescu N., Prodea, I.M., Popescu, E., Niţă, I. (2010), “Mathematical Models for Power Consumption at the Mixing of some Lubricating Greases”, *Environmental Engineering and Management Journal* (Iaşi), 9(8), 1063–1068.

Zalc, J.M., Szalai, E.S., Alvarez, M.M., Muzzio, F.J. (2002), “Using CFD to understand chaotic Mixing in laminar stirred Tanks”, *AIChE Journal*, 48(10), 2124-2134.

.

THE INTERACTION BETWEEN THE THERMO – HYDRODYNAMIC DRAFT TUBE AND THE MIXER IN THE CASE OF THE ROTATING MIXING DEVICES

IULIANA-MARLENA PRODEA, V. VALERIU JINESCU, NICOLETA TEODORESCU

University Politehnica of Bucharest, Romania, improdea@yahoo.com, vvjinescu@yahoo.com, nicoleta_teodorescu@yahoo.com

It is experimentally analyzed the influence of the heating coil acting as a thermo – hydrodynamic draft tube, placed inside the mixing vessel, on the heat transfer, in the case of the rotating mixing devices. It is aimed to obtain the functional optimum.

Keywords: rotating mixing devices; heating coil; draft tube.

INTRODUCTION

Mixing operation of the liquids, with the rotating mixing devices, have multiple applications in the process equipment industries (for example the chemical reactions acceleration; the homogenization of the multiphase blends; the stabilisation of the suspensions, emulsions and dispersions by mixing operation; the improvement of the heat transfer; some biochemical and physic-chemical process intensification) (Jinescu, V.V., 1989, Nagata, S., 1975, McDonough, R.J., 1991).

The design and the construction of the mixing equipment are based on the study of the specific hydrodynamic phenomena, as it is presented in the literature (Alvarez, M.M., et. al. 2002, Szalai, E.S., et. al, 2004, Jinescu, V.V., et. al, 2003).

Here are presented the experimental research results made (Prodea, I.M., 2010) aiming the improvement of the heat transfer in the case of a vessel provided with a inner heating coil, using for this rotating mixer devices. The heating coil fulfil, simultaneously, a double role, both heat exchanger and cylindrical hydrodynamic draft tube, which works in functional unity with the mixer. So the heating coil is named thermo-hydrodynamic draft tube.

It is studied the interaction between the utilized mixer and the heating coil, aiming a functional optimum from the point of view of the obtained heat transfer. That's why it is considered, for the selected mixer type, its position relatively to the heating coil and the position of the unit mixer- heating coil relatively to the vessel. The economic aspects are also taken into account.

EXPERIMENTAL INSTALLATION

The experimental installation is presented in figure 1, water is the inner fluid. The measurement were done at $60°C$.

The glass vessel (1 in the figure 1) has the inner diameter $D = 190\,mm$ and the height $h = 290mm$, being thermal insulated in exterior. The level of the liquid H_l is maintained constant during the experiments (equal with the inner diameter).

For the experimental measurement were used, two mixers (Figure 2): a propeller with the diameter $d_{a,1} = 50\,mm$ (which determines an axial flow pattern) and a 6 blades Rushton turbine with $d_{a,2} = 65\,mm$ (which determines a radial flow pattern).

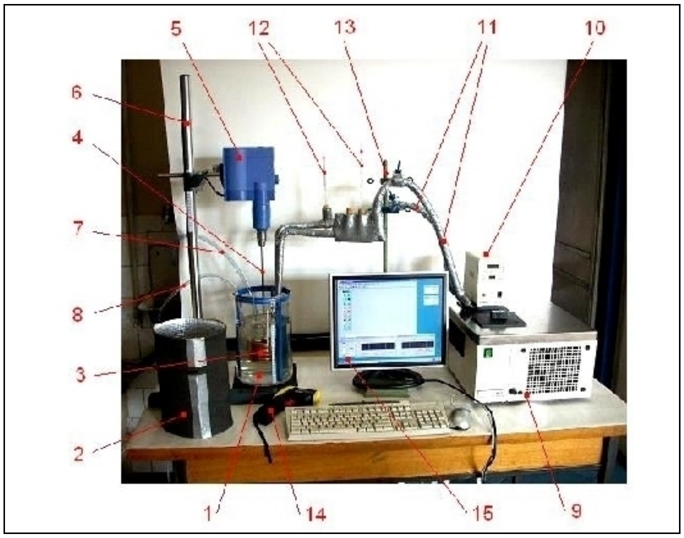

Figure 1. Experimental installation (Prodea, I.M., 2010): 1 – glass cylindrical vessel with vertical baffles; 2 – exterior heat insulation (removable) provided with a monitoring gap; 3- heating coil (with a draft tube function); 4 – mixing device shaft; 5 – driving device (IKA LABORTECHNIK, Eurostar model); 6 – support; 7 – water supply hose (entrance); 8 – water evacuation hose (exit); 9 – heating recirculation bath (THERMOHAAKE DC 30, K15) (Teodorescu, N., 2003); 10 – temperature controller; 11 – rubber hoses thermal insulated (for the heating fluid); 12 – thermometers (one for the entrance of the heating fluid and one for the exit);13 – support; 14 – infrared thermometer (NAMICON); 15 – computer.

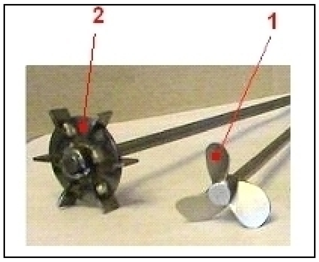

Figure 2. The mixers used in the experimental work (Prodea, I.M., 2010): 1 - propeller; 2 - 6 blades Rushton turbine

The heating coil was shaped to function as a cylindrical draft tube with the inner diameter $\boldsymbol{d_t} = 60\boldsymbol{mm}$ and the height $\boldsymbol{h_t} = 105\boldsymbol{mm}$. For this experimental set-up (with the cylindrical hydrodynamic draft tube) was observed the best mixing quality (Prodea, I.M., 2010, Jinescu, V.V. et. al., 2010).

EXPERIMENTAL MEASUREMENTS

The experiments were done (Prodea, I.M., 2010) for different configurations vessel – thermo-hydrodynamic draft tube (heating coil) – mixer (table 1), and different rotation speeds: $\boldsymbol{n}_1 = 290$ *rot/min* for the mixer 1; $\boldsymbol{n}_2 = 223{,}07$ *rot/min* for the mixer 2, so that the peripheral speed of the two mixers is the same.

Table 1. The configurations vessel – draft tube (heating coil) – mixer

Configuration	Position of the heating coil related to the bottom vessel (Fig.3)	Mixer	Position of the mixer related to the heating coil (Fig.4)
A	$\boldsymbol{h} = 60\,\boldsymbol{mm}$	1	(d)
B	$\boldsymbol{h} = 60\,\boldsymbol{mm}$	2	(e)
C	$\boldsymbol{h} = 60\,\boldsymbol{mm}$	2	(a)
D	$\boldsymbol{h} = 60\,\boldsymbol{mm}$	---	---
E	$\boldsymbol{h} = 35\,\boldsymbol{mm}$	1	(d)
F	$\boldsymbol{h} = 35\,\boldsymbol{mm}$	2	(e)
G	$\boldsymbol{h} = 35\,\boldsymbol{mm}$	---	---

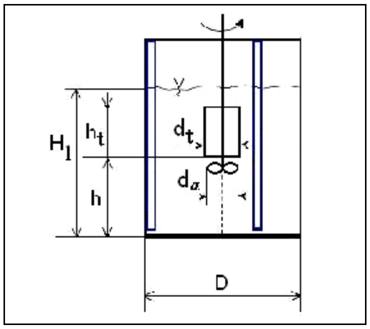

Figure 3. Mixing system configuration (Prodea, I.M., 2010)

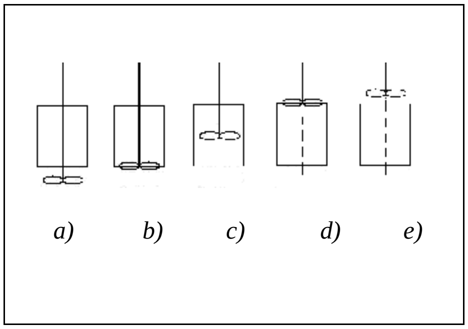

Figure 4. The possible positions of the mixer in the draft tube (Prodea, I.M., 2010)

It was aimed in each case the evaluation of the influence of the flow pattern generated by the mixer on the heat transfer from the heating coil to the liquid.

The experimental measurements were done at fixed temperature of the heating fluid ($T = 60°C$) and constant flow rate, in the case of assuring constant temperature for the water inside the vessel. It was obtained equilibrium between feeding water flow rate and the exit water flow rate, so the water quantity in the vessel remained also constant during measurements.

For each vessel - thermo-hydrodynamic draft tube- mixer was measured a temperature difference, $\boldsymbol{\Delta T} = \boldsymbol{T_i} - \boldsymbol{T_e}$, where $\boldsymbol{T_i}$ is the heating fluid temperature at the entrance in the heating coil and $\boldsymbol{T_e}$ at the exit, respectively.

EXPERIMENTAL RESULTS. INTERPRETATION

In Table 2 there are indicated the mean values of the registered temperatures differences between the temperature of the heating fluid at the entrance and that of the exit from the heating coil, for each of the configuration mentioned above.

Table 2. Experimental results (Prodea, I.M., 2010)

Configuration	$(\Delta T)_m$, [°C]
A	11,48
B	12,47
C	10,97
D	7,01
E	9,63
F	11,66
G	7,83

The thermal power $\dot{Q}$ (provided from the quantity of the thermal fluid ceded heat and taken over by the vessel's water), in the case of each configuration, can be determined using the following relation:

$$\dot{Q} = \dot{m}_{ag} \, c_{ag} \, (\Delta T)_m \tag{1}$$

where $\dot{m}_{ag}$ - heating fluid mass flow rate, c_{ag} - specific heat; the values $(\Delta T)_m$ are indicated in table 2.

For whatever two configurations j and k ($j \neq k$, j and k being whatever of the configuration $A \div G$), the ratio of the thermal powers can be calculated based on correlation (1):

$$\frac{\dot{Q}_j}{\dot{Q}_k} = \frac{(\Delta T)_{m,j}}{(\Delta T)_{m,k}} \tag{2}$$

$$\text{If } (\Delta T)_{m,j} > (\Delta T)_{m,k} \;\Rightarrow\; \frac{(\Delta T)_{m,j}}{(\Delta T)_{m,k}} > 1 \;\Rightarrow\; \dot{Q}_j > \dot{Q}_k \tag{3}$$

$$\text{If } (\Delta T)_{m,j} \le (\Delta T)_{m,k} \;\Rightarrow\; \frac{(\Delta T)_{m,j}}{(\Delta T)_{m,k}} \le 1 \;\Rightarrow\; \dot{Q}_j \le \dot{Q}_k \tag{4}$$

Based on relations (2), (3) and (4), analysing the table 2, the conclusions on the experimental results are:

- For the ***B*** configuration is obtained the best heat transfer from the heating coil to the mixed fluid, so the mixer 2 (the Rushton turbine), which provide a radial flow, is superior, from this point of view, to the mixer 1 (propeller), for similar exploitation conditions (it is take into account the fact that the position of the mixer 1/draft tube assembly related to the vessel is the optimum one (Prodea, I.M., 2010, Jinescu, V.V. et. al., 2010) – which correspond to the maximum pumping capacity, for the given experimental conditions);
- Whatever the heating coil position in the vessel, in the case of the placement, in turns, in similar positions with respect to the heating coil, of a propeller and a Rushton turbine, respectively, the best choice from the heat exchange point of view is that which produce radial flow;

- Comparing the configurations ***D*** and ***G***, in which is used only the thermal draft tube (heating coil), without the mixer, it was observed that the heat exchange is better in the case in which the heating coil is placed deeper in the working fluid;

- No matter what configuration with mixer, it was observed an intensification of the heat exchange with respect the configurations without mixer;

- Analyzing the obtained results in the case of ***A*** and ***E*** configurations**,** it is emphasized the fact that the heat transfer is better in the case ***A***, in which the fluid flow determined by the mixer/draft tube assembly is more intense.

In figures 5 and 6 are presented the comparisons between the heat transfer, by means of the temperature difference of the heating fluid at the entrance and exit, respectively, for the two mixers and thermal/thermo-hydrodynamic draft tubes (made from the heating coil). The measurements were done with and without mixer.

One can see that the $\Delta T = T_i - T_e$ varies very little in time, but is quite different in the case in which a mixer is used, versus the case without mixer. In the case of using mixers, no matter what, 1 or 2, the higher heating coil is placed the better heat transfer is obtained.

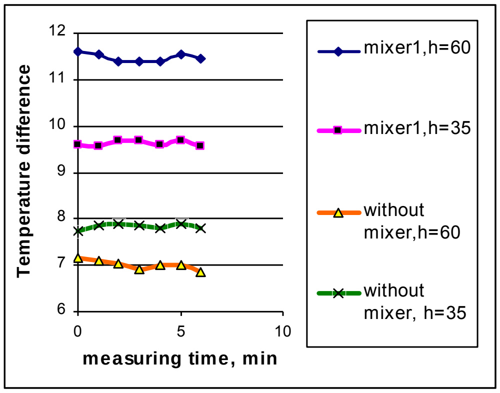

Figure 5. The influence of the configuration mixer 1/position in the vessel on the heat transfer, measured by $\Delta \boldsymbol{T} = \boldsymbol{T_i} - \boldsymbol{T_e}$ (^{o}C); rotation speed n = 290 rot/min.

In the case of the heating coil without mixer, the optimum position is contrary – the deeper heating coil position in the vessel the better heat transfer was obtained. These two tendencies happened because the mixer determines the thermo-hydrodynamic function of the heating coil. In the case of no mixer used, the heating coil has only heat exchanger role (even if making the temperatures uniform in the vessel determines a low intensity flow).

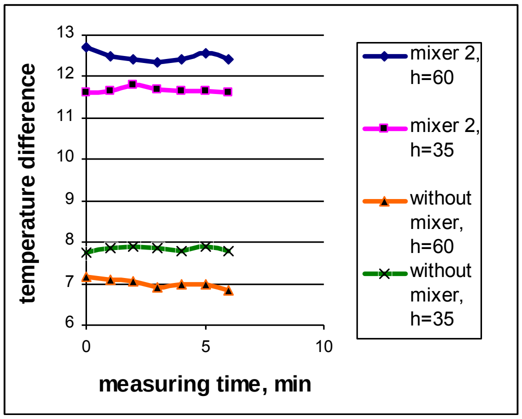

Figure 6. The influence of the configuration mixer 2/position in the vessel on the heat transfer, measured by $\Delta T = T_i - T_e$ (^{o}C); rotation speed n=223 rot/min.

CONCLUSIONS

For the applications aiming the intensification of the heat transfer, from the experiments performed, one can finally conclude that is advisable to choose a mixer which produces a radial flow pattern, placed in the upper side, above the heating coil, over a mixer which produces an axial one. The process efficiency, in this case, will be better and total costs will be lower. The other transitory conclusions were presented above.

REFERENCES

Alvarez, M.M., Zalc, J.M., Shinbrot, T., Arratia, P.E., Muzzio, F.J. (2002), Mechanism of Mixing and creation of structure in laminar stirred tanks", *AIChE Journal*, 48(10), 2135–2148.

Jinescu, V.V. (1989), *Technological Equipment for Process Industries* (in Romanian), vol. IV, Technical Press, Bucharest.

Jinescu, V.V. Prodea, I.M., Teodorescu, N., (2010), "Research on mixing in liquid medium by using rotating mixing devices in draft tube configurations" (in Romanian), The XVI National Symposium of Construction Equipment SINUC 2010, Bucharest, Section I, 74–80.

Jinescu, V.V., Ion, N.A., Prodea, I.M. (2003), „Some considerations on optimisation of mixing installations" (in Romanian), *Revista de Chimie*, 54(5), 431-435.

McDonough, R.J. (1991), *Mixing for the process industries*, Van Nostrand, Reinhold, New York.

Nagata, S. (1975), *Mixing. Principles and applications*, John Wiley and Sons, New York.

Prodea, I.M. (2010), *Contributions to optimisation of mixing devices in process industries* (in Romanian), PhD Thesis, University Politehnica of Bucharest.

Szalai, E.S., Arratia, P., Johnson, K., Muzzio, F.J. (2004), "Mixing analysis in a tank stirred with Ekato Intermig (R) impellers", *Chemical Engineering Science*, 59(18), 3793–3805.

Teodorescu, N. (2003), *Applied rheology. Laboratory Guidelines* (in Romanian), MatrixRom Press, Bucharest.

CROSSLINKING AND GRAFTING ETHYLENE-PROPYLENE–TERPOLYMER RUBBER WITH ACCELERATED ELECTRONS IN THE PRESENCE OF POLYFUNCTIONAL MONOMERS

MARIA DANIELA STELESCU[1], ELENA MANAILA[2], GABRIELA CRACIUN[2], NICULINA ZUGA[3]

[1]*National Research and Development Institute for Textile and Leather – Leather and Footwear Research Institute, 93 Ion Minulescu St., Bucharest, Romania, dmstelescu@yahoo.com*

[2]*National Institute for Laser, Plasma and Radiation Physics, Electron Accelerators Laboratory, 409 Atomistilor St., 077125, Magurele, Romania*

[3]*Constantin Cantacuzino National College, 3 George Cair St., Targoviste, Romania*

In this work, we have studied the effects of polyfunctional monomers on the physical properties of ethylene-propylene–terpolymer rubber crosslinked with electron beam or peroxides. The polyfunctional monomers used were triallylcyanurate, triallylisocyanurate, trimethylolpropane trimethacrylate, zinc diacrylate and ethylene glycol dimethacrylate. Using polyfunctional monomers has led to decreasing optimum cure time t_{90} and increasing physical properties of peroxide or electron beam cured systems by increasing the efficiency of productive radical reactions. The most efficient polyfunctional monomer for ethylene-propylene–terpolymer rubber has been trimethylolpropane trimethacrylate. The results show that electron beam irradiation gave the best results. In addition, crosslinking by electron beam also shows a series of advantages, such as: (1) the resulted products are pure, as no peroxide is added; (2) lack of wastes; (3) reduced crosslinking time and power expenditure; (4) the resulted products are sterile, and (5) improved characteristics of crosslinked products.

Keywords: ethylene-propylene–terpolymer rubber, polyfunctional monomer, electron beam, physical-mechanical properties.

INTRODUCTION

Modification of thermoplastic and rubbery materials by electron beam (EB) radiation is a potential method for development of new polymers and composites. Irradiation of polymeric materials results in grafting and subsequently formation of a three dimensional network through the union of generated macro radicals. Radiation-initiated reactions can be categorically classified as three types: crosslinking, scission and grafting. Crosslinking is the intermolecular bond formation of polymer chains. The degree of crosslinking is proportional to the radiation dose. It does not require unsaturated or other more reactive groupings. In contrast, scission is the opposite process of crosslinking in which the rupturing of C–C bonds occurs. Grafting is a method where monomers are introduced laterally onto the polymer chain. Grafting proceeds in three different ways: pre-irradiation; peroxidation and mutual irradiation technique. For example, in the mutual irradiation technique, both the polymer and the polyfunctional monomers are irradiated simultaneously to form the free radicals and thus addition takes place. Some of the examples of radiation polyfunctional monomers are trimethylolpropane triacrylate (TMPTA), trimethylolmethane tetraacrylate (TMMT), tripropyleneglycol diacrylate (TPGDA), maleimides, thiols, and halogenated compounds. These polyfunctional monomers are prone to form more radicals on irradiation quicker than high molecular weight polymers and thus a lower amount of radiation dose is required to achieve the required properties. On the other hand, aromatic amines and quinones are used as anti-radicals (Bhowmick et al., 2006).

In this work, we have studied the effects of polyfunctional monomers on physical properties of ethylene-propylene–terpolymer rubber crosslinked with electron beam or peroxides. The polyfunctional monomers used were triallylcyanurate, triallylisocyanurate, trimethylolpropane trimethacrylate, zinc diacrylate and ethylene glycol dimethacrylate. The effects of irradiation dose in presence and absence of polyfunctional monomers on the crosslinking and structure of ethylene propylene rubber were investigated.

EXPERIMENTAL

The following raw materials were used: (1) EPDM rubber (Keltan 8360) (Mooney viscosity is 78.80 ML_1 at 25ºC, 54.68% ethylene content, ENB 5.41 W_t %, (2) Polyfunctional monomers: triallyl cyanurate (TAC) Luvomaxx TAC DL 70 (26% percentage of ash, density 1.34 g/cm^3, 30% active synthetic silica), triallyl isocyanurate (TAIC) Luvomaxx TAIC DL 70C (pH 2.6, density 1.34 g/cm^3), trimethylolpropane-trimethacrylate (TMPT) Luvomaxx TMPT DL 75 (22% percentage of ash, pH 9.2, density 1.36 g/cm^3, 75 ± 3% active ingredient), ethylene glycol dimethacrylate (EDMA) Luvomaxx EDMA DL 75 (23% percentage of ash, 75 ± 3% active ingredient, density 1.25 g/cm^3), zinc diacrylate (ZDA) ZDA GR 75 (density 1.23 g/cm^3). (3) Dibenzoyl peroxide Perkadox 14-40B (1.60 g/cm^3 density, 3.8% active oxygen content, 40% peroxide content) as vulcanizing agent for vulcanization of control samples.

Blends have been made by means of blending technique, on a laboratory roll with electric heating at 120±5°C, total blend time of 5', friction of 1:1.1. The blend constituents were added in the following sequence and amounts: 100 phr EPDM and 3 phr polyfunctional monomers (TAC, TAIC, TMPT, EDMA and ZDA respectively).

Plates required for physical-mechanical tests have been made by compression molded, using an electrically heated hydraulic press, at a temperature of 160ºC, pressure of 150 MPa and time of 3 min. to obtain sheets of 11.5 x 11.5 x 0.2 cm^3.

Control samples were prepared similarly, with the following specifications: 8 phr of dibenzoyl peroxide as vulcanizing agent was added and the blend vulcanization was achieved in a hydraulic press at 160^{o}C; the vulcanization time was measured by means of Monsanto Rheometer (see Table 1).

The resulted plates were subjected to EB vulcanization with ILU-6M accelerator of 1.8 MeV and 10.8 kW output power. The ILU-6M is a resonator-type accelerator, operating at 115±5 MHz. This accelerator generates electron beam pulses of 0.375 ms duration, up to 0.32 A current peak intensity and up to 6 mA mean current intensity. The cross-sectional size of the scanned EB at the ILU-6M vacuum window exit is 1100 mm x 65 mm. The EB effects are related to the absorbed dose (D), expressed in Gray or J kg^{-1}. The single pass dose with conveyor under the ILU-6M scanner is adjustable from 12.5 kGy to 50 kGy. For EB treatment the rubber sheets were cut in rectangular shape of 0.15 x 0.15 m^2. The layers of three sandwiched sheets were irradiated by repeatedly passing on a conveyor under the ILU-6M scanner in atmospheric conditions and at room temperature of 25°C. Distance between ILU-6M vacuum window exit and conveyor surface was 33x10^{-2} m. The conveyor speed was 2.36x10^{-2} m s^{-1}. Single pass dose measured with ceric-cerous sulphate dosimetry system was 25 kGy. For the samples passing several times under the scan, the accumulated dose was from 50 kGy to 200 kGy.

According to the Technical Report Series No. 277 (IAEA Vienna, 1987), the absorbed dose is the major parameter in the accelerated electron radiation. The vulcanizing and grafting process performances are provided by the strict control of this parameter.

The relation defining the absorbed dose is:

$D = d\varepsilon/dm$ (1)

where:

$d\varepsilon$ is the mean energy given up by the ionizing radiation to the mass amounts dm of the substance interacting with this ionizing radiation.

dm is emphasized to be very low but not so low that the mean energy $d\varepsilon$ given up by the radiation would undergo a significant fluctuation.

Absorbed dose is measured in J/kg. The SI unit measure for the absorbed dose is the gray (Gy):

1 Gy = 1 Joule/kg. (2)

The rad unit is also used, with the following relation between the Gy and rad:

1 Gy = 100 rad (3)

A relevant example: a material irradiated by 2 Mrad (20 kGy) means that AE (accelerated electron beam) have deposited 2.10^8 ergs or about 10^{19} eV per gram substance.

Tensile strength and tearing strength tests were carried out with a Schoppler strength tester with testing speed 460 mm/min, using dumb-bell shaped specimens according to ISO 37/1997, respectively angular test pieces (type II) in according to ISO 34-1/2000. Hardness was measured by using a hardener tester according to ISO 7619/2001. Elasticity was evaluated with a Schob test machine. The cure characteristics of the compounds were measured at 160°C using an oscillating disk rheometer (Monsanto), according to the SR ISO 3417/1997. Delta torque or extent of crosslinking is the maximum torque (MH) minus the minimum torque (ML). Scorch time (t_{s2}) is taken as the time to reach 2% of the delta torque above minimum. Optimum cure time (t_{90}) is the time to reach 90% of the delta torque above minimum. The cure rate index (CRI) is a measure of the rate of vulcanization based on the difference between optimum vulcanization time (t_{90}) and incipient scorch time (t_{s2}). It was calculated according to the following formula:

$CRI = 100/(t_{90} - t_{s2})$ (4)

RESULTS AND DISCUSSIONS

The physical-mechanical and rheological properties of the EPDM rubber samples with polyfunctional monomers crosslinking with peroxide are presented in Table 1. Table 1 indicates that the use of polyfunctional monomers has led to the decrease of the minimum torque and to the decrease of the optimum curing time. The best curing time and the highest curing rate index were obtained when using ZDA, and the best value of polymer fraction incorporated in the network, which indicates cross-linking density, was obtained for the blend containing TMPT. Physical-mechanical properties of obtained blends depend on the type of polyfunctional monomer used. Using polyfunctional monomers has led to an increase in hardness and the highest values (68°ShA) were obtained using TMPT, EDMA, ZDA. Elasticity decreased as a result of introducing polyfunctional monomers in the blend, and the lowest values were obtained for TMPT (57%). Tensile strength, tear strength and elongation at break have shown an improvement upon the introduction of polyfunctional monomers, and the best results were obtained using ZDA. Residual elongation shows an insignificant increase as a result of using polyfunctional monomers, having low values, and indicating an efficient cross-link of the blend.

Table 1. Rheological and physical-mechanical characteristics of samples crosslinked with peroxide

Characteristics /The type of PFMs	Free	TAC	TAIC	TMPT	EDMA	ZDA
Rheological characteristics						
ML(dN/m)	9	3.8	5.7	4.2	4.5	0.5
MH (dN/m)	44	52.8	51.2	51	49	33.5
ΔM, (dNm)	35	49	45.5	46.8	44.5	33
T s2 (minutes)	1’15’’	1’	42’’	24’’	54’’	42’’
T90 (minutes)	18’	16’45 "	16’15 "	16’00 "	14’30 "	14’00 "
CRI	0.843	0.858	0.856	0.860	0.857	0.843
Physical-mechanical characteristics						
Hardness, °ShA	61	66	66	68	68	68
Elasticity, %	70	60	59	57	59	60
Tensile strength, N/mm^2	1	1.3	1.1	1.1	1.2	1.4
Elongation at break, %	60	60	60	80	67	80
Residual elongation, %	5	5	3	2	3	4
Tear strength, N/mm	2.8	4.2	4.2	4.8	4.9	7.4

Physical-mechanical characteristics of the blends with different types of polyfunctional monomers (PFM) vulcanized by EB are presented in Figures 1-6. Hardness (Figure 1) increases as the irradiation dose increases, however, the obtained values are lower than those of blends cross-linked with benzoyl peroxide. The TMPT-containing blend showed a rapid increase of hardness up to a value of irradiation dose of 10 Mrad, then the hardness value remained constant; in the other blends, hardness increased with the increase of irradiation dose. Elasticity (Figure 2) has very high values (58-75%).

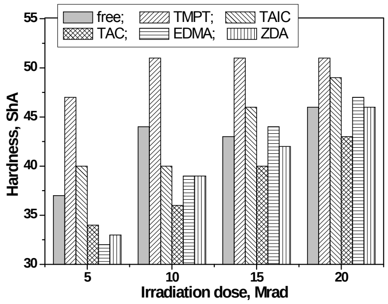

Figure 1. Hardness versus electron beam (EB) irradiation dose and polyfunctional monomers type

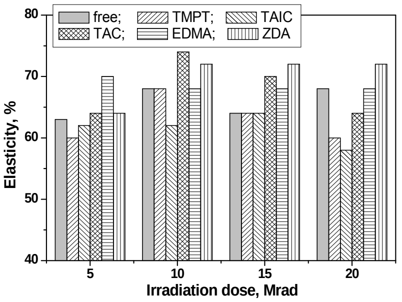

Figure 2. Elasticity versus electron beam (EB) irradiation dose and polyfunctional monomers type

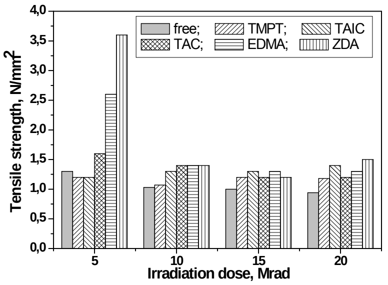

Figure 3. Tensile strength versus electron beam (EB) irradiation dose and polyfunctional monomers type

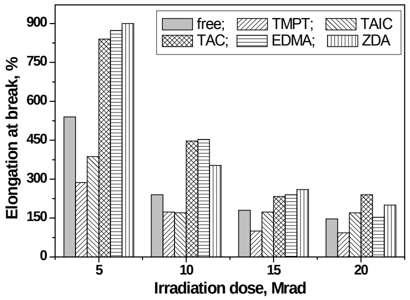

Figure 4. Elongation at break versus electron beam (EB) irradiation dose and polyfunctional monomers type

Tensile strength (Figure 3), elongation at break (Figure 4), residual elongation (Figure 5) and tear strength (Figure 6) show a peak at 5 Mrad, then decrease. Elongation at break and residual elongation show similar values to those of blends cross-linked with benzoyl peroxide for irradiation dose values of 15 and 20 Mrad respectively. Tensile strength and tear strength have low values because the elastomer is not charged, however, values obtained at doses of 5, 10, 15 Mrad are superior to those of blends cross-linked using benzoyl peroxide.

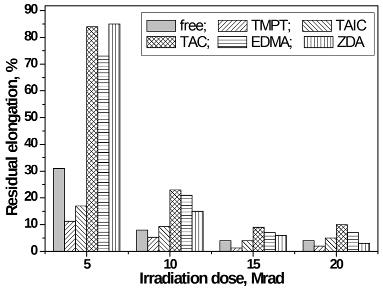

Figure 5. Residual elongation versus electron beam (EB) irradiation dose and polyfunctional monomers type

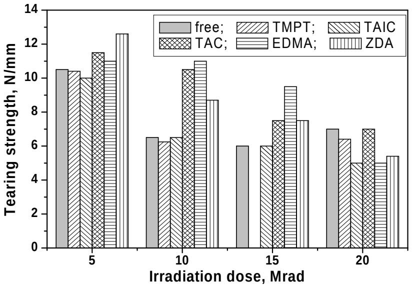

Figure 6. Tearing strength versus electron beam (EB) irradiation dose and polyfunctional monomers type

CONCLUSIONS

Using polyfunctional monomers has led to decreasing optimum cure time t_{90} and increasing physical properties of peroxide or electron beam cured systems by increasing the efficiency of productive radical reactions. The most efficient polyfunctional monomer for ethylene-propylene–terpolymer rubber has been trimethylolpropane trimethacrylate. The results show that electron beam irradiation gave the best results. In addition, croslinking by electron beam also shows a series of advantages, such as: (1) the resulted products are pure, as no peroxide is added; (2) lack of wastes; (3) reduced crosslinking time and power expenditure; (4) the resulted products are sterile, and (5) improved characteristics of crosslinked products (Stelescu et al., 2011; Manaila et al., 2007).

REFERENCES

Bhowmick, A.K. and Vijayabaskar, V. (2006), "Electron beam curing of elastomer", *Rubber Chem. Technol*., 79, 522.

International Atomic Energy Agency Vienna (1987), "Absorbed Dose Determination in Photon and Electron Beams", *Technical Reports Series*, No. 277, 4

Manaila, E., Zuga, M.D., Martin, D. et al. (2007), "Ethylene-propylene terpolymer rubber processing by electron beam irradiation", 6th International Conference of the Balkan-Physical-Union, August 22-26, 2006, Istanbul, Turkey, Vol. 899, 785-785.

Stelescu, M.D., Manaila, E. and Zuga, N. (2011)**,** "The use of polyfunctional monomers in the radical cure of chlorinated polyethylene", *Polymer Journal*, 43, 792-800.

EFFECT OF GALLIC ACID CONTENT ON TANNIN - TITANIUM (III) COMBINATION TANNING

BO TENG[1,2], XIAOYUN JIAN[1], WUYONG CHEN[1,2]

[1] *National Engineering Laboratory for Clean Technology of Leather Manufacture, Sichuan University, Chengdu 610065, P. R. China, teng.boo@hotmail.com*

[2] *The Key Laboratory of the Education Ministry of Leather Science and Engineering, Sichuan University, Chengdu 610065, P. R. China, correspondence author: wuyong.chen@163.com*

The combination tanning using titanium (III) and hydrolysable tannin extracts was reported as a better tannage to improve the properties of leather than condensed ones. One of the most obvious differences between these tannin extracts was the gallic acid content. To clarify the effect of this reactive structure on tannin-Ti (III) combination tanning, Acacia Mangium tannin extract (no gallic acid), Oil Orange tannin extract (25% gallic acid) and Strawberry Tree tannin extract (40% gallic acid) were selected for tannin-Ti (III) complex and tanning experiments. The quantity of precipitation, pH of complexation system and shrinkage temperature was used as main evaluation factors of this investigation. Under different temperature and pH conditions with different dosages of tannin extracts and Ti (III) agent, their complex ability and tanning ability were studied respectively. The result shows that: The gallic acid in tannin extracts could improve its complex ability with Ti (III) under different temperature and pH conditions. The tannin extracts with more gallic acid, showed higher effective complexation index and better reactivity to complex with Ti(III). So, higher thermal stability was obtained with less tanning agent. Under tanning condition, the more the gallic acid content in tannin extracts, the higher the thermal stability of leather presented. This research could provide a reference for the Ti (III) - vegetable extracts combination tanning.

Keywords: gallic acid; tannin extract; combination tanning

INTRODUCTION

In order to reduce the consume of chrome tanning agent, as well as to reduce the pollution in tanning industry, various of agents and tanning methods were tried for leather making, and replacing traditional leather process. But only the metal salt-vegetable tannin combination methods were reported as a practical one to manufacture leathers with ‘chrome like’ properties (Covington, 1998). Mimosa tannin extract, Quebracho tannin extract, Larch tannin extract, Myrobalan tannin extract and titanium (III) sulfate were used as the combination tanning agent by A. D. Covington, and leathers with high thermal stability were also obtained after treated by this method (Covington et al., 1998). What is interesting is that, compared with condensed tannins, leathers with higher shrinkage temperatures were all produced by hydrolysable tannins in this combination tanning system. As we know, content of gallic acid group was considered as the most obviously structural difference between hydrolysable and condensed tannins. In addition, these gallic acid groups were also regarded as the important factor for the formation and stabilization of tannin-metal complexes. But study on the effect of gallic acid content on tannin-Ti (III) combination tanning ability has not reported yet. So Strawberry Tree tannin extracts (40% gallic acid), Oil Orange tannin extracts (25% gallic acid) and Acacia Mangium tannin extracts (no gallic acid) (Figure 1) (Chen et al., 2011) were selected for combination tanning experiment and complex experiment with Ti (III) respectively, to study the effects of these structural differences on their complex and combination tanning ability and provide a valuable reference for the Ti (III) - vegetable extracts combination tanning methods.

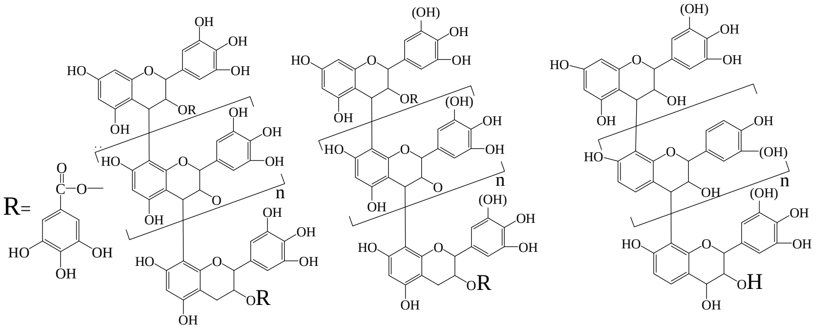

Strawberry Tree tannin **Oil Orange tannin** **Acacia Mangium tannin**

Figure 1. The structural characteristics of tannins (Chen et al., 2011)

EXPERIMENTAL

Materials

Acacia Mangium tannin extract (68.12% tannins); Oil Orange tannin extract (66.25% tannins); Strawberry tree tannin extract (65.33% tannins) contains equivalent sediment and obtained from Baise tannin extracts factory, all the chemicals used in complex experiment were analytical grade, other chemicals used in tanning experiment were commercial grade. Cowhide were sourced from Chengdu as raw materials, after treated by conventional liming, deliming and bating process, pH was then adjusted to 5.0, the hide was used for tanning experiment. Tannin extracts solution with concentration of 0.02 g/ml, was adjusted to pH 4.0 with sulfuric acid. Sulfate titanium (III) was also diluted into a concentration of 0.01g/ml, and the pH was adjusted to 1.0 with sulfuric acid, the Ti (III) and tannin extracts solutions for complex experiments were prepared.

Complex at Different Temperature

Mixtures containing 10ml Ti (III) and 5ml tannin extract were diluted to 30ml with deionized water, and then kept in different temperature conditions as 20, 30, 40, 50 and 60°C for 2 hr respectively. After centrifuged for 0.5 h with 2 kr/min rotating speed, the precipitations were dried at 120°C.

Complex at Different Tannin Extracts-Ti (III) Mass Ratios

Mixtures containing 10ml Ti (III), and tannin extract solutions with volume of 0, 2, 4 ,6, 8, 10, 12, 14, 16, 18, 20, 22, 24, 26 ml (mass ratio ranged from 0 to 5.2 with step as 0.4) were added respectively, and diluted to 30 ml with deionized water. After heated at 40°C for 2 hr, the pH of mixtures was measured and centrifuged for 0.5 hr with 2 kr/min rotating speed, and then the precipitation was dried at 120°C.

Tanning with Different Dosage of Tannin Extracts

Matched pieces of bated hide were taken from the back and flank areas. The chemicals used in the following procedure were based on the weight of the bated hide.

Tannin extracts at concentrations of 10, 12, 14, 16, 17, 18, 19 and 20% with 50%float were added into drums, while rotated at 30°C for 48hr under rotated speed of 15r/min. After which complete penetration of tannin extract were ascertained, the leather was washed for 5min, then followed by 2.5% Ti (III) treatment for 4 h. The leather was neutralized to pH 4.0, and temperature was raised to 50°C for another hour. Then the shrinkage temperature of leather was measured using a shrinkage tester.

Other pieces of bated hide were taken and treated by 20% tannin extracts with 50% float, while rotated for 48h with rotation speed of 15r/min at 30°C. Samples were washed for 5 min, then 0.5, 1.0, 1.5, 1.7, 1.9, 2.1, 2.3 and 2.5% Ti(III) with 50% float was added and treated for 4hr. Samples were neutralized to pH 4.0, followed by rotation for another hour at 50°C. Then the shrinkage temperature of tanned leather was tested.

Complex under Different pH

Samples were composed of 10ml Ti (III) and 5ml tannin extract solution, and then neutralized to a serious pH by NaOH with concentration of 1 mol/L. After diluted to 30ml with deionized water, the samples were placed at a 40°C condition for 2 hr, and then centrifuged for 0.5hr with 2kr/min rotating speed. Afterwards, the precipitation was dried at 120°C and weighted.

Neutralized to Different pH

Bated hides were taken, 20% tannin extract with 50% float were added. After treated for 48 hr at a rotation speed of 15 r/min, leathers were washed for 10 min and 2.5% Ti (III) was added besides rotated for another 4 h. While pH was adjusted to a serious value with $NaHCO_3$, temperature was raised to 50°C for 1hr, and shrinkage temperature was tested.

Tanning under Optimum Conditions

Table 1. Optimum condition of tannin-Ti (III) combination tanning

	Sample 1	Sample 2	Sample 3
Tanning	Acacia Mangium (16%)	Oil Orange (17%)	Strawberry tree (19%)
	30°C, run for 48 hr		
Retanning	Ti(III) 1.7%	Ti(III) 1.9%	Ti(III) 2.3%
	Adjusted to pH 4.5, run for 1 hr at 50°C		

Marched pieces of bated hide were tanned under optimum condition (Table 1). Shrinkage temperature, Tensile strength and tear strength of the tanned leather were tested as QB/T2713-2005, QB/T2710-2005 and QB/T2711-2005 standard procedures. Each value reported is an average of four (2 along the backbone, 2 across the backbone) experiments.

RESULTS AND DISCUSSIONS

Effect of Temperature on Complexation

Figure 2 shows the precipitation of tannin-Ti (III) reactions as a function of temperature (20 to 60°C). The amount of precipitation increased with temperature rising obviously. Furthermore, under any temperature conditions, the greatest amount of precipitation were produced by complex reactions between Strawberry tree tannin extracts (contains 40% gallic acid) and Ti (III), as Acacia Mangium tannin extract (no gallic acid) showed the least value. These results indicated that, like the phenomenon of other tannin-metal complex reactions (Di, 2002), tannin-Ti (III) complex reactions were influenced by both heating process and tannin extract species.

Basic structural unit of these tannin extracts was flavan-3-ol, reacted with metal ions through adjacent phenolic hydroxyl groups on B ring (Shi et al., 2002), as well as formed stable chelates (Figure 3). Gallic acid group reacted with metal ions through hydroxyls on pyrogallol structure; in addition, the reaction ability was also enhanced by electron attract effect of gallic acid structure. Compared with flavan-3-ol units, gallic acid was easier to react with Ti (III). Therefore, with temperature from 20 to 60°C, gallic acid in tannins improved its complex ability with Ti (III). So, more precipitation was generated.

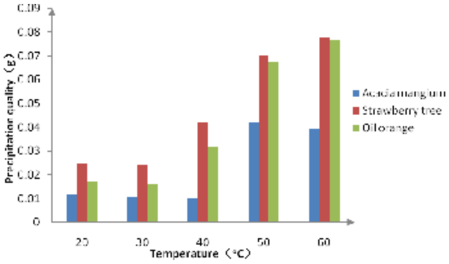

Figure 2. Relation between precipitations and temperature

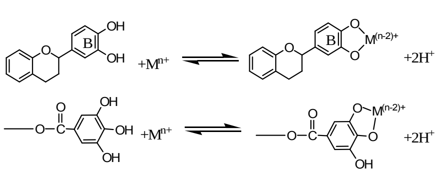

Figure 3. Reactions between tannin and metal ion

Effect of Tannin Extract and Ti(III) Amount on Combination Tannage

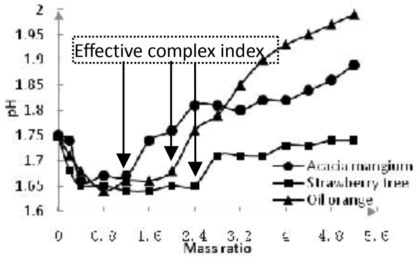

Figure 4. Relation between tannin/titanium(III) mass ratio and pH

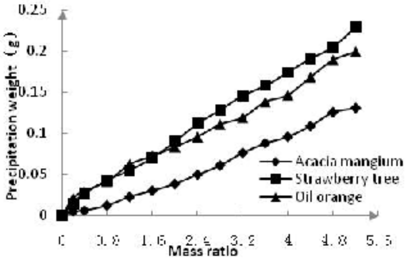

Figure 5. Relation between tannin/titanium(III) mass ratio and precipitation weight

Figure 4. indicates that as a few amount of tannin extracts was added, hydrolysis of phenolic hydroxyl was in progress and H^+ was released, while system pH dropped and maintained at a stable state. As tannin/Ti (III) ratio increased, the complex reaction and dissociation reaction processed completely, buffered properties of tannin extract began to play a leading role in this system, and resulted in the increasing of pH value. The pH value right before its increasing trend was identified as a very important point. The mass ratio at this point was regarded as the equivalent weight of complex reaction i.e.

effective complexation index of the reaction (Di, 2001). The more gallic acid contained in tannin extracts, the higher effective complexation index it was shown.

The positive correlation was observed between precipitation quantities and tannin extract dosages (Figure 5). Furthermore, tannins with the highest effective complexation index (Strawberry tree tannin), produced maximum amount of precipitations. On the contrary, tannins with smallest effective complexation index, showed the minimum value. These results also indicated that with any dosage of tannins, the degree of Ti (III) tannin complex reaction correlated positively with gallic acid content of tannins.

Table 2. Effect of tannin extract dosage on shrinkage temperature (°C)

Tannin dosage	10%	12%	14%	16%	17%	18%	19%	20%
Acacia mangium	90.8	88.2	89.9	92.5	92.3	93.1	96.4	96.0
Strawberry tree	89.7	92.2	97.3	106.1	105.4	105.3	106.2	105.6
Oil orange	84.1	93.9	98.2	102.4	104.7	103.4	104.0	103.0

Table 3. Effect of Ti(III) dosage on shrinkage temperature (°C)

Ti (III) dosage	0.50%	1.00%	1.50%	1.7%	1.9%	2.10%	2.30%	2.50%
Acacia mangium	81.2	88.5	88.6	88.2	92.8	90.0	95.4	95.1
Strawberry tree	86.7	89.1	95.9	105.9	105.2	103.3	104.1	105.4
Oil orange	84.5	86.0	94.5	100.7	104.1	104.4	103.0	104.5

Effect of tannin extracts and Ti(III) dosages on leather shrinkage temperature was shown on Table 2 and Table 3. For the Strawberry tree tannin extract with the most amount of gallic acid content (40%), the shrinkage temperature obtained the highest value by using lest dosage of tannin extract (16%) and Ti(III) (1.7%); For the Oil Orange tannin extract with less amount of gallic acid content (25%), shrinkage temperature achieved the highest value by using more tannin extract (17%) and Ti (III) (1.9%). For the Acacia Mangium tannin with no gallic acid content, shrinkage temperature obtained the highest value by using the most dosage of tannin extract (19%) and Ti(III)(2.3%). Thus, the more gallic acid content on tannin extracts, the higher dosage of tanning agents were used to obtain their highest shrinkage temperature.

Effect of pH on Thermal Stability of Leather

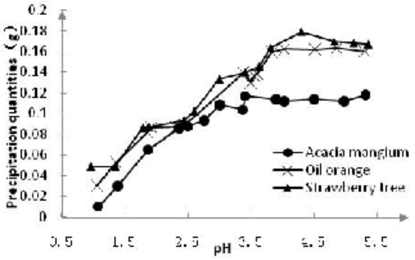

Figure 6. Precipitation quantities under different pH

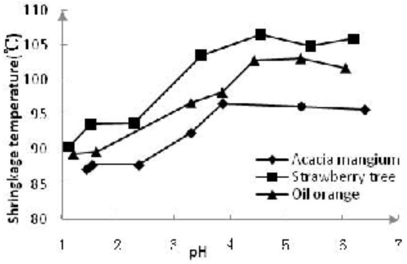

Figure 7. Relation between pH and shrinkage temperatures

Figure 6 and Figure 7 indicated the process of complex reactions were facilitated by the increase of pH, as well as the thermal stability. In addition, under same pH conditions, the Ti (III) reacted with tannin extracts with more gallic acid (Strawberry tree), generated more precipitations and higher shrinkage temperatures were obtained. On the contrary, for the reaction between tannins without gallic acid (Acacia Mangium) and Ti (III), least quantities of precipitations were got, and the leather showed the lowest shrinkage temperatures. Therefore, under the tannin-Ti(III) combination tanning condition, thermal stability of leather was enhanced due to the facilitated of gallic acid on complex reactions. Moreover, similar trends were found at different pH conditions.

Evaluation of Leather Made under Optimum Conditions

Table 4. Properties of leather produced by tannin-Ti (III) combination tanning methods under optimum conditions

Properties	Acacia Mangium	Strawberry tree	Oil orange
Shrinkage temperature (°C)	96.2	106.0	104.1
Tensile strength (MPa)	16.2	18.7	20.3
Tear strength ($N\cdot mm^{-1}$)	42.4	36.7	38.2

Table 4 indicated higher shrinkage temperature was obtained with Strawberry tree which contains more gallic acid; lower shrinkage temperature was presented by Acacia Mangium which contains no gallic acid under the optimum conditions. But there is no such association between physical properties and the content of gallic acid.

CONCLUSIONS

Tannin extracts with different content of gallic acid were used for complex and tanning experiment with Ti(III). The result shows that: the effective complexation index as well as the tannin-Ti (III) complex ability, was improved by gallic acid in tannins under different temperature and pH conditions; with increase of gallic acid contained in tannin extracts, leather produced by tannin-Ti (III) combination tannage showed higher thermal stability and required less tanning agents; under optimized tanning condition, leather treated by tannins with more gallic acid, exhibited higher shrinkage temperature in this combination tanning system.

Acknowledgements

The authors wish to thank the Ministry of Science and Technology of China for financial support of the cooperation project (item No.2009DFA42850, No.40-3).

REFERENCES

Chen, W., Li, G. (2011), *Tanning Chemistry*, China Light Industry Press, Beijing.

Covington, A.D. (1998), “The 1998 John Arthur Wilson memorial lecture: new tannages for the new millennium”, *JALCA*, 93, 168-183.

Covington, A.D., Lampard, G.S. and Pennington, M. (1998), “An investigation of titanium (III) as a tanning agent”, *JSLTC*, 82(2), 78-80.

Di, Y. (1999), “*Studies on the complexing regularity of the chemical degradated vegetable tannins and its application*”, Si Chuan University.

Shi, B. and Di, Y. (2000), *Plant Polypheno*, Science Press, Beijing.

EVALUATION OF THE SHEEPSKIN MATTRESS IN TERMS OF PRESSURE RELIEVING CAPABILITY

JIN ZHOU[1, 2], QIUYUE TANG[1], YOURAN ZHANG[1], WEICAI YU[1], CARMEN GAIDAU[3], WUYONG CHEN[1]

[1] *National Engineering Laboratory for Clean Technology of Leather Manufacture, Sichuan University Chengdu 610065, P. R. China, wuyong.chen@163.com*

[2] *Faculty of Technology, Tomas Bata University, Zlin 760 01, Czech Republic, rufuszhou.scu@gmail.com*

[3] *INCDTP - Division: Leather and Footwear Research Institute, Bucharest 031215, Romania*

The aim of this study was to quantitatively evaluate the effectiveness of sheepskin mattress in pressure relieving. The pressure distribution of rigid mattress (CM), air mattress (AM) and standard medical mattress (SMM) in supine posture of 18 students before and after the intervention of the own-made sheepskin mattress (FM) were measured by mFLEX system and variables of peak pressure (PP) and average pressure (mmHg) (AP) and contact area (cm2) (CA) at total, back, sacrum and heel area were used for comparisons. Paired-T test with a significant level of 0.05 shows that the usage of FM significantly increased total CA by mean of 30% for three basis mattresses, then reductions about 8% for PP and 10% to 40% for AP were also observed. At back area, both PP and AP decreased by average of 30% for CM and AM; whereas only 10% reducing of PP was reported at sacrum for CM and SMM but at which the magnitude of pressure was still high. With exception of heel area, the outcomes were proved to be reliable where CoV and ICC ranged 5.1%-23.2% and 0.70-0.97. It can be concluded that the sheep skin mattress was effective in relieving the magnitude of contact pressure and it could be used in the routine patient's care to prevent the ulceration.

Keywords: pressure measurement; sheepskin mattress; ulceration prevention.

INTRODUCTION

According to a clinical report from US, the incidence of ulceration among the long-tem hospitalized patients ranged 10 to 18% (Clark, 2002; Janet Cuddigan, 2001) and this ulceration was majorly induced by a long duration of the low pressure, despite that the high peak pressure was more risky, such as diabetic patients who usually suffered from the ulceration because of the high peak plantar pressure (De Simon et al., 2002; Klaesner et al., 2002; Nijs et al., 2009). The prerequisite of the low pressure ulcer was the long time loading and the occurrence of ischemia lesion (Cherry, 1997; Defloor, 2000)which was due to the ischemia situation caused by the pressure larger than 10kPa (Basler, 1927). Thereby the critical purpose of nursing was to lower the applied pressure as well as to shift the position of loading periodically. The protrusion of bones such as the scapula at back, sacrum of buttock and foot calcaneus which constructed a plane to support the body weight usually had a relatively high contact pressure. Particular at the sacrum area, as the majority of the body mass is concentrated, the highest incidence of ulceration was found (Daideri et al., 2006; Jakobsen and Christensen, 1987; Rithalia and Gonsalkorale, 2000).

The occurrence of ulcer not least prolonged the duration in hospital, but it also largely increased the amount of expenses in medical treatment. A survey from UK reported that the total cost has been estimated as 1.4 to 2.1 billion pounds annually (Bennett et al., 1998). Thereby the strategies of prevention appear crucial. Fortunately, current literatures concluded a series of constant low pressure (CLP) systems aimed at lowering the incidence of ulceration. These systems were classified into two groups

(McInnes et al., 2011): one was Low-tech CLP which reduced the magnitude of pressure by the way of increasing contact area, including foam mattress and sheep skin mattress; another was High-tech CLP, such as alternative pressure air mattress (APAM), of which the contact area could be adjusted by the inflation or deflation of air units, meanwhile purpose inflation or deflation periodically shifted the centre of pressure and avoided the long duration of load on the same place.

Sheep skin mattress (SSM) with long and high density furs provides a larger area to support, simultaneously the air flow which is important for trauma healing under the contact surface is also available; further, SSM with merits of reasonable price and reusability indicated that it could be widely applied in clinics. Unfortunately only positive clinical effects in ulcer prevention have been reported by Jolley et al. (Jolley et al., 2004) and McGowan et al. (McGowan, 2000), no quantitative evaluation has yet been studied.

Therefore, this study aimed at quantitatively evaluating the effectiveness of sheep skin mattress in pressure relieving. Since significant outcomes of sheep skin has been reported, two hypotheses were assumed: firstly, the sheep skin mattress would alleviate the pressure distribution, reduce its magnitude and provide a much larger area for contact; secondly a good reliability would be observed under the back and sacrum area where more pressure loaded.

METHODS

Subjects

Eighteen healthy (11 males and 7 females) students aged 20 to 27 were recruited from Sichuan University. The body weight and height were first measured and then BMI was calculated. Those students with BMI over 24.5 and with a history of back pain were excluded. The aims and methods were explained and participants have given their formal approvals prior to the measure. All procedure of this study was supervised by ethic committees of Sichuan University and followed the principles of Declaration of Helsinki.

Mattress

Four types of mattress were provided. They were: sheep skin mattress (FM) (60 x 90 x 5cm, own-fabricated, Chengdu, China) which was tanned under the guidelines of Australian Medical Sheepskin-Australian Standards As4480.1; standard medical mattress (SMM) (180 x 90 x 6cm, HuaZhiJie Li, co., Chengdu, China) which was composed by three centimeter foam mat and three centimeter coir mat; normal air mattress (AM) (180 x 90 x 6cm, HuaZhiJie Li, co., Chengdu, China) where the distance between two air strips was 10cm; rigid mattress (180 x 90 x 3cm, HuaZhiJie Li, co., Chengdu, China) used as control mattress (CM) was made of coir mat. So six types were available for measure: FM+SMM, FM+CM, FM+AM, SMM, CM and AM.

Pressure Measurement

MFLEX pressure measuring system (mFLEX: 32 x 32, Rsscan international, Belgium) was utilized. The area of pressure sensors is 1920 mm x 762 mm, the number of sensor is 1024, the range of measure is 0-100mmHg (0-13 kPa) and the frequency is 5Hz. Calibration was made before measure. Four areas were selected for analysis (Allen et al., 1993) (Figure 1): total, back, sacrum and heel area, under which peak pressure (PP) (mmHg), average pressure (AP) (mmHg) and contact area (CA) (cm2) was computed by software of mFLEX (V4.0, Rsscan international, Belgium). To avoid the measurement error caused by different analysts, only on experienced researcher was assigned to complete all the analysis.

Participants were asked to wear the leisure clothes and three to five minutes warm up was also provided before measure. When the subjects lay in the bed in supine posture (Figure 2), the mFLEX system was switched on, and ten seconds data was recorded when the pressure distribution became stable. The same procedure was repeated in other two successive days.

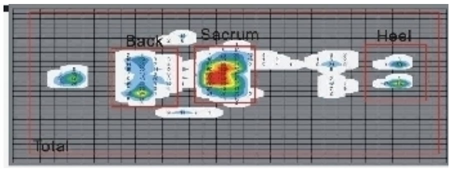

Figure 1. Four masks model for contact pressure for analysis

Figure 2. Supine position used in pressure measurement

Data processing and statistical analysis

The data was first averaged and the normal distribution was then tested by Q-Q plot. Paired-t test and reliability assessment were proposed for statistical analysis. Coefficiency of variance (CoV) and intraclass correlation coefficiency (ICC) (Hopkins, 2000) was suggested for reliability assessment, where CoV= typical error / mean value of three trials. The higher the CoV is, the lower the repeatability (Ramanathan et al., 2010). Further, when ICC<0.5, the reliability is poor; while 0.5<ICC<0.75 or ICC>0.75 indicates a medium or good to excellent reliability (Leslie Gross Portney, 1993). Software of SPSS (V16.0, SPSS Inc, USA) was used for statistical analysis with significant level of 0.05.

RESULTS

The mean age of students is 24.2 ± 1.7 y, mean height is 167.9 ± 8.2 cm, mean body weight is 58.8 ± 7.7 kg and mean BMI is 20.8 ± 1.4. All obtained data in supine posture confirmed the normal distribution.

In total area, compared with CM, FM+CM significantly decreased the PP by 7 % (p=0.02) and AP by 33% (p=0.000). The use of FM also significantly ameliorated the amplitude of pressure of SMM by 8.8% for PP (p=0.01) and 11% for AP (p=0.01). Meanwhile, 40% AP of AM was significantly lowered by FM. The total CA of CM, SMM and AM were significantly increased by 40%, 19% and 31% respectively when FM was intervened (p=0.000 for all).

At the back (Figure 3), PP and AP of FM+CM were reduced by 44% and 33% respectively and the CA arose by 32% (p=0.000 for all), in contrast with alone usage of CM; while similar results were found for FM+AM where the reduction of magnitude of pressure was 23% (p=0.01) for PP and 37% (p=0.001) for AP, as well as 22% augment of CA was reported (p=0.003). No significant differences were found between SMM and FM+SMM (p>0.05).

Under sacrum area (Figure 3), since CA of CM and SMM increased significantly by 38% and 25% with the help of FM, the PP of course was significantly reduced by 10% for both mattress (p=0.02 for all), as well as decreased by 26% and by 17% for AP of CM (p=0.000) and SMM (p=0.01). Neither the amplitude of pressure of AM at sacrum area, nor of CA was significantly ameliorated by the overlay of FM (p>0.05).

For the heel area, the overlay of FM significantly reduced the pressure value (p=0.000 for PP and AP) and simultaneously increased the contact area (p=0.003) at heel of CM. However, only the AP of SMM (p=0.01) and AM (p=0.03) was improved by FM.

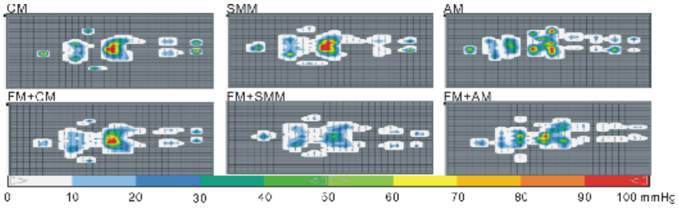

Figure 3. The pressure re-distribution after the usage of sheep skin mattress

The reliability of CA was shown to be excellent, where CoV and ICC ranged 5.1% to 10.7% and 0.92 to 0.97 was found at total, back and sacrum area. Meanwhile, a moderate to good reliability of AP and PP was observed at these three areas and CoV and ICC ranged 8.0% to 23.2% and 0.70 to 0.93. However, all the three pressure variables at heel displayed a poor reliability by showing a higher CoV (28.7% - 62%) and lower ICC (0.22 - 0.76) value.

DISCUSSION

In this study the pressure distribution of three types of mattress with and without overlay of sheep skin was recorded by mFLEX pressure measuring system and the effectiveness of sheep skin mattress in pressure relieving was quantitatively assessed. The results showed that the sheep skin overlay significantly reduced the magnitude of contact pressure and simultaneously increased the contact area; moreover all the results were proved to be reliable, with exception of heel region.

The clinical evaluation for sheep skin mattress in ulcer prevention was first reported by Mcgowan et al. (McGowan S, 2000). They recruited 297 post-operated patients who were prescribed with the sheep skin mattress during their nursing period and the results demonstrated that the mattress significantly reduced the incidence of ulceration (RR=0.30, 95% confident interval: 0.17 to 0.52). Besides, Jolley (Jolley et al., 2004) described a positive result from 539 in-hospitalized patients by using the sheep skin mattress in G2 ulcer prevention. The incidence of ulcer of traditional nursing approach was 9% (20/223), while it decreased to 5.5% (12/218) (RR=0.58， 95% confident interval: 0.35 to 0.96) after the intervention of the sheep skin mattress. Thereby the sheep skin mattress could be considered as an optimal protocol in ulcer prevention for the long-term hospitalized patients.

Our results showed that before the usage of sheep skin, SMM recorded pressure distribution as high as CM, with exception of back area, so this finding implied that the current hospital mattress did not satisfy the basic needs of pressure relief. After the FM was applied, both the magnitude of pressure and the contact area were ameliorated. Accidently, in our result, despite the AM was usually considered as a low-tech CLP , it was found to be less effective in reducing pressure value by showing the pressure as large as control mattress, especially at Back (PP=84.8mmHg, AP=30.3mmHg) and sacrum area (PP=99.7mmHg, AP=40.3mmHg). Thereby, the AM should be used with caution.

The low CoV and high ICC value of all three pressure variables obtained from three independent trials implied that the reliabilities at all four regions excluding the heel were shown to be good to excellent. Our results were supported by the current explanation (Gurney et al., 2008; Zammit et al., 2010) where the larger area and higher load was, the better reliability should be.

Although the hypotheses have been proved, several limitations should be considered whilst interpreting the results. Firstly, the hospital mattress used in our study was designed under the standard of China and was not the same as the one reported in literatures. So comparisons between the results should be with caution. Secondly, the result of this study was obtained from healthy subjects and the result should not be generalized to other population. Since anthropological variations would result the significant differences in contact pressure, for instance the elder population received a lower peak pressure at sacrum area. Thirdly, some PP exceeded the maximum rang (100 mmHg) of measure system during measurement, however the part of pressure higher than 100 mmHg was meaningless, where capillary circulation was already cut off when the pressure passed 10 kPa (76 mmHg)(Basler, 1927). Future works still need to explore whether the capillary circulation or thermal stability being improved or not by the sheep skin mattress.

CONCLUSION

The pressure distribution of three basic mattresses was ameliorated by the intervention of sheep skin mattress, where total CA were significantly enlarged and both PP and AP were reduced. The optimal improvement was seen at back area of CM and AM and at sacrum area of CM and SMM, in which the large amount of pressure was eliminated. Moreover, the outcomes of all regions excluding heel area were manifested to be reliable. Overall, sheep skin mattress as an effective CLP system can be widely used in the clinics to prevent ulceration.

Acknowledgements

This study was supported by the project of “new leathers and furs with microbiological resistance for medical use” (2009DFA42850) and by the items from Agency of Science and Technology of Sichuan Province for financial support (item No. 2009HH0004).

REFERENCES

Allen, V., Ryan, D.W., Murray, A. (1993),“Repeatability of subject/bed interface pressure measurements”, *J. Biomed. Eng.*, 15, 329-392.

Basler, A. (1927), “Bestimmung stutzpunkte des aut die einzehen sohlen bezirkewirkenden teilgwiches des menschlichen korpers”, *Abderhaldens Hamduch*, 559-557.

Bennett, R.G., Baran, P.J., DeVone, L.V., Bacetti, H., Kristo, B., Tayback, M., Greenough, W.B. (1998), "Low airloss hydrotherapy versus standard care for incontinent hospitalized patients", *Journal of the American Geriatrics Society*, 46, 569-576.

Cherry, G.W., and Ryan, T.J. (1997), "The Decubitus Ulcer in Clinical Practice", in: C., L., Parish, J.A.W., & J. T. Crissey (Eds.), *Pathophysiology*, Springer, Berlin, 33-43.

Clark, M., Bours, G., Defloor, T. (2002), "Summary report on the prevalence of pressure ulcers", *EPUAP Review*, 4, 49-57.

Cuddigan, J., Ayello, E.A. (2001), "Pressure Ulcers in America: Prevalence, Incidence, and Implications for the Future. An Executive Summary of the National Pressure Ulcer Advisory Panel Monograph", *Advances in Skin & Wound Care: The Journal for Prevention and Healing*, 14, 208-215.

Daideri, G., Berthier, F., Brocker, P., Darmon, M.J., Mignolet, F., Quaranta, J.F., Staccini, P. (2006), "Prevalence of pressure sores in a university hospital in 2003", *Rev. Epidemiol. Sante Publique*, 54, 517-527.

De Simon, S., La Penna, A., Napoletano, M., Uccioli, L. (2002), "Hallux valgus in diabetic patients: relation with peripheral neuropathy", *Diabetologia*, 45, A337-A337.

Defloor, T. (2000), "The effect of position and mattress on interface pressure", *Applied Nursing Research*, 13, 2-11.

Gross Portney, L. (1993), *Foundations of Clinical Research: Applications to Practice*, Appleton and Lange, Connecticut.

Gurney, J.K., Kersting, U.G., Rosenbaum, D. (2008), "Between-day reliability of repeated plantar pressure distribution measurements in a normal population", *Gait Posture*, 27, 706-709.

Hopkins, W.G. (2000), "Measures of reliability in sports medicine and science", *Sports Med.*, 30, 1-15.

Jakobsen, J., Christensen, K.S. (1987), "Transcutaneous oxygen tension measurement over the sacrum on various anti-decubitus mattresses", *Danish Medical Bulletin*, 34, 330-331.

Jolley, D.J., Wright, R., McGowan, S., Hickey, M.B., Campbell, D.A., Sinclair, R.D., Montgomery, K.C. (2004), "Preventing pressure ulcers with the Australian Medical Sheepskin: an open-label randomised controlled trial", *Med. J. Aust.*, 180, 324-327.

Klaesner, J.W., Hastings, M.K., Zou, D.Q., Lewis, C., Mueller, M.J. (2002), "Plantar tissue stiffness in patients with diabetes mellitus and peripheral neuropathy", *Archives of Physical Medicine and Rehabilitation*, 83, 1796-1801.

McGowan, S., Montgomery, K., Jolley, D, Wright, R. (2000), "The role of sheepskins in preventing pressure ulcers in elderly orthopaedic patients", *Primary Intention*, 8, 1-8.

McInnes, E., Jammali-Blasi, A., Bell-Syer, S.E.M., Dumville, J.C., Cullum, N. (2011), "Support surfaces for pressure ulcer prevention", *Cochrane Database of Systematic Reviews*, 4.

Nijs, N., Toppets, A., Defloor, T., Bernaerts, K., Milisen, K., Van Den Berghe, G. (2009), "Incidence and risk factors for pressure ulcers in the intensive care unit", *J. Clin. Nurs.*, 18, 1258-1266.

Ramanathan, A.K., Kiran, P., Arnold, G.P., Wang, W., Abboud, R.J. (2010), "Repeatability of the Pedar-X in-shoe pressure measuring system", *Foot and Ankle Surgery*, 16, 70-73.

Rithalia, S.V., Gonsalkorale, M. (2000), "Quantification of pressure relief using interface pressure and tissue perfusion in alternating pressure air mattresses", *Arch Phys Med Rehabil*, 81, 1364-1369.

Zammit, G.V., Menz, H.B., Munteanu, S.E. (2010), "Reliability of the TekScan MatScan (R) system for the measurement of plantar forces and pressures during barefoot level walking in healthy adults", *Journal of Foot and Ankle Research*, 3.

INVESTIGATION OF THE OPTIMAL ARCH DESIGN OF THE LAST FOR HEEL-HEIGHTED SHOE WITH LOW, MID AND HIGH HEEL HEIGHT

JIN ZHOU[1, 2], WEIWEN ZHANG[1], PETR HLAVÁČEK[2], BO XU[1], WUYONG CHEN[1]

[1] *National Engineering Laboratory for Clean Technology of Leather Manufacture, Sichuan University Chengdu 610065, P. R. China, Corresponding author: wuyong.chen@163.com*

[2] *Faculty of Technology, Tomas Bata University, Zlin 760 01, Czech Republic, rufuszhou.scu@gmail.com*

This study aimed at evaluating the effect of arch shape of the last on the insole pressure distribution of lady shoes with 20mm, 50mm and 80mm heel height. The right foot of ten girls in barefoot standing on the shoe heel was scanned in 3D format in order to obtain the data of foot arch. Three types of last were designed: control last (CL), higher last (HL) and lower last (LL). The arch shape of CL was designed based on the foot, while the arch of HL and LL was modified by 2.5mm higher or lower than that of control last in the position of cuboids. Insole pressure variables of peak pressure (PP), contact area (CA) and pressure-time integral (PTI) at hind, mid and fore foot were analyzed by paired-T test with the significant level of 0.05. The result shows that no significant differences were observed in mid foot between comparisons of HL and CL and CL and LL in each heel height. However, HL demonstrated a significantly lower PP and PTI than CL at forefoot in the 20mm and at hind foot in the 80mm heel height respectively; while LL only demonstrated a significantly larger PP than CL under hind foot in 50mm heel height. It can be concluded as that the last with an appropriate arch support was helpful for attenuating the magnitude of pressure in forefoot and hind foot.

Keywords: high heel shoes, insole pressure, arch shape of last.

INTRODUCTION

High-heeled shoes are considered as one of the “bad” design for women, because it changes their normal gait by shifting the centre of body mass forward and significantly increases the vertical forces at forefoot (Ebbeling et al., 1994; Lee et al., 2001) by which lower limb pains or even the foot deformities might be triggered (Ebbeling et al., 1994; Lee et al., 2001; Stephens, 1992). Although, the influences of the high-heeled shoe on the kinematic and kinetic characteristics during walking have been seriously discussed (Cho and Choi, 2005; Kouchi and Tsutsumi, 2000; Speksnijder et al., 2005; Stefanyshyn et al., 2000), harmful effects on the health reported by researchers did not hamper its prevalence through the whole footwear history. Therefore only the work could be done is to design the shoes as comfort as possible to diminish the negative effects.

The last decides the wearing of shoe, though, the shape of arch determines the comfort of high heeled last, since the arch of the foot not merely acts as the force transmitter, but also as force absorption whilst walking. But when the heel of foot elevated, the length of medial and lateral longitudinal arch was shortened (Kouchi and Tsutsumi, 2000) and the shortened fascia made the foot too rigid to roll over, by which a higher plantar pressure could be observed. In order to attenuate the forefoot pressure caused by the high-heeled shoe, interventions and therapy strategies were conceived, such as metatarsal pad, total contact insert, arch supported insoles (Cole et al., 2005; Hong et al., 2005; Yung-Hui and Wei-Hsien, 2005; Cong et al., 2008). Despite these approaches improved the tension of foot arch and alleviated the concentration of peak pressure on the forefoot, unfortunately these approaches were not designed based on the last and the introduction of these inserts might cause the new uncomforting problems in shoe wearing. In addition, the influence of arch shape of the last on insole pressure distribution was still not clear.

Therefore, this study aimed at evaluating the effects of arch shape of the last on the insole pressure distribution of lady shoes with 20mm, 50mm and 80mm heel height. As Hawes et al (1994) suggested that the closeness of matching of the last to that of the human foot will decide comfort of fit in shoe wearing, it was hypothesized that the better last was designed according to the arch of foot.

METHODS

Subjects

Ten female students from Sichuan University were recruited. Their mean age is 24(0.2) y, mean height is 1.60 (0.04) m, mean body weight is 49.8(4.4) Kg, mean foot length is 230(2.4) mm and mean width is 87.7 (2.4) mm. Subjects with deformities such as flat foot or hallux valgus were excluded by visual inspection. Aims and methods were explained and subjects have given their approvals. Besides, the study was supervised by the ethical committee of the University and the procedures followed the Helsinki declarations.

Foot Measurement and Last Design

Only right foot in barefoot standing on the shoe heels with height of 20mm, 50mm and 80mm was measured by a three dimensional laser scanning system (INFOOT USB: Standard type, I-Ware Laboratory Co., Ltd, Japan). The main positions of right foot such as the top of hallux, prominence of first and fifth metatarsophalangeal joints, position of cuboids and the end of heel were marked manually and they were read by the software of system (INFOOT measurement interface V2.9, I-Ware Laboratory Co., Ltd, Japan).

The sagittal profile along with foot longitudinal axis (the foot longitudinal axis is the line passing through the end of heel to the centre of second toe, based on this axis, the foot is divided into medial and lateral part) was extracted from the marked foot model in 3D software (Powershape, Delcam Co., Ltd, UK) (Figure 1a). The arch curve was defined as the part of profile between the first metatarsophalangeal joint to the position of the heel contact (red line in Figure 1a); and then it was equally cut by 10 perpendicular lines and produced 10 joints (Kouchi and Tsutsumi, 2000) in which coordinates of each joint were recorded (Figure 1b). Process of average was made for each coordinate and an average foot arch section was constructed.

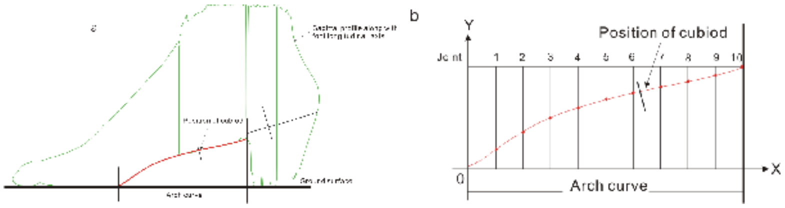

Figure 1. The arch shape analysis

The three types of last were provided (Figure 2): control last (CL) (red line) was the one that applied the average foot arch as the arch curve of last; while the higher last (HL) (dash-dot black line) was the one that the arch section was modified by 2.5mm higher than the control last in the position of cuboids; similarly, the lower last (LL) (dash blue line) was the one 2.5mm lower. The 2.5mm reduction in height of cuboids implied the 3.5 mm decreasing in the instep girth which is the half size degree of sizing system. This difference in the last industry is usually considered to be enough to result the perception of unfit. Except midfoot, the other part of last was kept unchanged for the same heel height and all of the last used in this study were hand-made by the same last engineer.

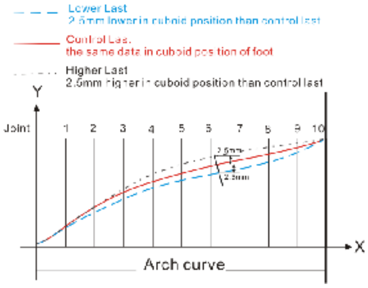

Figure 2. Three types of arch shape of last

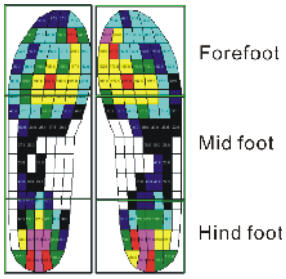

Figure 3. Three masks model for insole pressure analysis

In-shoe Plantar Pressure Measurement

The Novel insole system (Pedar-X, Novel GmbHgmbh, Germany) was applied in the data collection. The sole region of foot was divided by Novel multimask (Novel Multimask software, Novel GmbHgmbh, Germany) into 3 main parts: heel, midfoot, forefoot (Figure 3) under which pressure variables of peak pressure (PP) (kPa), contact area (cm^2) (CA) and the pressure-time integral (kPa*s) (PTI) were calculated. Three successful measure of right foot was required for each subject.

Statistical Analysis

Paired-t test was applied for the difference comparisons between the control and lower last and control and higher last respectively. All the analysis was performed by the SPSS software with significant level a=0.05 (v.16.0; SPSS Inc, Chicago, USA).

RESULTS

Contact Area

As the arch heightened, more midfoot contact was found (Table 1). But only significant differences were found in midfoot between the CL and LL in 80mm heel height (p=0.00), where CA of CL was larger than that of LL. Besides, a significant larger CA was also observed in forefoot (p=0.04) between the two types of last. No significant differences were shown between CL and HL in all three heel height groups.

Table 1. Result of in-shoe plantar pressure measurement and the comparisons between the three types of last (Mean (SD)

		20mm heel height		50mm heel height		80mm heel height	
	region-Last	mean	P value		P value	variable	P value
CA (cm^2)	FF-HL	40.3(1.0)	0.27a	40.3(1.9)	0.76a	39.2(1.6)	0.70a
	FF-CL	39.7(1.6)	0.58b	40.2(2.1)*	0.02b	39.5(2.9)*	0.04b
	FF-LL	40.0(1.4)		40.9(1.6)		38.4(3.6)	
	MF-HL	33.1(3.9)	0.57a	27.7(4.5)	0.97a	20.6(4.4)	0.18a
	MF-CL	32.9(3.9)	0.73b	27.7(4.9)	0.07b	21.3(4.0)*	0.00b
	MF-LL	32.6(5.3)		26.5(4.5)		18.1(4.9)	
	HF-HL	26.90(0.4)	0.40a	26.2(0.8)	0.26a	25.9(1.4)	0.94a
	HF-CL	26.8(0.7)*	0.01b	26.4(0.8)	0.60b	25.9(1.1)	0.66b
	HF-LL	26.1(1.0)		26.2(1.1)		25.7(1.7)	
PP (kPa)		242.4(59.6)*	0.03a	239.0(45.1)	0.32a	274.3(102.2)	0.92a
		260.9(68.0)	0.46b	251.9(69.6)	0.38b	275.1(94.9)	0.41b
		253.3(90.5)		264.1(76.8)		297.9(70.7)	
		164.0(32.6)	0.57a	162.1(47.1)	0.67a	177.5(101.5)	0.51a
		166.5(33.7)	0.23b	157.0(54.7)	0.82b	184.8(89.1)	0.81b
		177.1(26.3)		154.5(56.3)		190.1(88.5)	
		182.4(30.8)	0.28a	127.6(23.4)	0.99a	103.7(15.1)*	0.01a
		174.9(24.1)	0.08b	127.5(16.9)*	0.00b	116.3(19.9)	0.09b
		163.3(23.9)		145.7(24.9)		123.1(23.5)	
PTI (s*kPa)		70.1(16.5)*	0.01a	91.2(12.9)	0.30a	126.5(48.8)	0.07a
		80.1(22.7)	0.77b	85.8(21.1)	0.29b	109.9(28.3)	0.12b
		81.1(28.6)		90.2(23.6)		123.1(24.2)	
		61.9(11.6)	0.55a	72.5(16.2)	0.25a	83.6(47.2)	0.66a
		63.9(12.9)	0.21b	69.6(18.5)	0.39b	80.6(30.9)	0.97b
		67.6(12.3)		66.9(18.1)		81.0(38.5)	
		65.2(14.3)	0.18a	57.3(10.5)	0.20a	51.2(8.1)*	0.02a
		59.7(12.8)	0.81b	59.8(10.3)	0.21b	58.4(10.2)	0.13b
		58.7(15.6)		62.8(13.0)		62.3(14.4)	

* Significant level < 0.05. FF: forefoot, MF: mid foot; HF: hind foot; HL: higher last, CL: control last; LL: lower last. “a” implies the comparison between HL and CL; “b” implies the comparison between CL and LL.

In terms of 20mm heel height, more CA was demonstrated significantly under hind foot, in contrast with that of LL (p=0.01).

Peak Pressure

No significantly PP reduction in midfoot was recorded as more mid foot contacted with the insole. But in the 20mm heel height, the PP of HL was significantly smaller than that of CL at forefoot (p=0.03) as well as at hind foot in 80mm heel height (p=0.01). PP of CL was significantly decreased by 12%, when compared with LL in the 50mm heel height (p=0.00).

Pressure Time Integral

A trend of decreasing of PTI under midfoot was found as the arch height elevated in each heel height, but they were not statistically significant. Whereas, in the region of forefoot in 20mm heel height (p=0.01) and at hind foot in 80mm heel height (p=0.02), the PTI of HL was significantly smaller than that of CL.

DISCUSSION

This study compared the insole pressure distribution of three types of last in 20, 50 and 80mm heel height, where one last was designed based on the data of foot and the other two ones were modified to be higher or lower than foot arch in arch shape. The results showed that for each heel height, the higher last obtained the preferable insole pressure distribution than other two types.

To improve the comfort perception of high-heeled shoes, Hawes et al. (1994) suggested that the last should be constructed as close as possible to the foot. Following this principle, methods were devised to minimize the spaces between the shoe and foot, such as different kinds of insert. Hong et al. (2005) recommended a type of total contact insert and their outcomes showed that this inserts was more effective on reducing the insole pressure of high heel shoes than being used in low heel or flat shoes. Additionally, insoles with heel cup and arch support were also reported to be helpful for the pressure redistribution at the heel and medial foot (Yung-Hui and Wei-Hsien, 2005). But the approaches above did not follow the shape of last, so that when the inserts were used, in-shoe spaces would be decrease and undesirable comfort perception would receive. Therefore the design of arch shape in the viewpoint of last would positively resolve this problem.

In our study, although the arch of last was elevated, no significant differences were shown between CL and HL and CL and LL in each heel height. However, HL in the 20mm and 80mm heel height demonstrated a significantly lower PP and PTI under forefoot and hind foot. Moreover, when comparing with LL, CL demonstrated a significant higher CA of CL at mid foot in the 80mm heel height and a significant lower PP of hind foot were found in the 50mm heel height. This reduction of PP in the same place was also found in the HL. The outcome above indicated that an appropriate arch support was beneficial in lowering the magnitude of pressure distribution at forefoot and hind foot and this found was supported by the Cong et al (2008) who concluded that as the depth of shank increased and midfoot obtained more loading, PTI of forefoot decreased. Therefore, the assumed hypothesis was disapproved since only a moderate performance of CL was observed.

Limitations of this study should be considered when interpreting the results. Firstly, only 2.5mm of change was made for the higher and lower last. Although this difference indicated a half size change in instep girth, as the results shown in our study, this change was not enough to trigger more explicit differences between the comparisons.

Secondly, the results should not be generalized to other female populations, since the measurement was based on the foot of young female students whose foot length was within 230 ± 5 mm. Confounding variables such as pathologies have significantly influence on the pressure distribution. The future studies need to continue to explore the influence of the arch shape of the last on the insole pressure distribution, where the arch height should be modified much more, such as 5 mm or even 7.5 mm which indicates the one or one and half size changes in the instep girth.

CONCLUSION

The main findings could be concluded as below: HL attenuated the amplitude of the pressure under forefoot in 20mm and hind foot in 80mm heel height respectively and an appropriate arch support was helpful for attenuating the amplitude of pressure in forefoot and hind foot in each heel height, so the HL was the optimal arch design of the last for the high heel heighted shoe.

Acknowledgements

This study was supported by the project of “New leathers and furs with microbiological resistance for medical use” (2009DFA42850) and by the items from Agency of Science and Technology of Sichuan Province for financial support (item No. 2009HH0004).

REFERENCES

Cho, W.H., Choi, H.K. (2005), “The mechanism of postural balance control of high-heeled women”, in: Kim, Y.J., Bae, H.D. (Eds.), *Advances in Fracture and Strength*, Pts 1- 4, 2303-2307.

Cole, C., Seto, C., Gazewood, J. (2005), “Plantar fasciitis: Evidence-based review of diagnosis and therapy”, *Am. Fam. Physician*, 72, 2237-2242.

Cong, Y., Luximon, Y., Zhang, M. (2008), “Effect of Shank Curve of High-heeled Shoe on the Plantar Pressure Distribution”, in: Peng, Y., Weng, X. (Eds.), *Apcmbe 2008: 7th Asian-Pacific Conference on Medical and Biological Engineering*, 500-502.

Ebbeling, C.J., Hamill, J., Crussemeyer, J.A. (1994), “Lower-extremity mechanics and energy-cost of walking in high heeled shoes”, *Journal of Orthopaedic & Sports Physical Therapy*, 19, 190-196.

Hawes, M.R., Sovak, D., Miyashita, M., Kang, S.J., Yoshihuku, Y., Tanaka, S. (1994), “Ethnic differences in forefoot shape and the determination of shoe comfort”, *Ergonomics*, 37, 187-196.

Hong, W.H., Lee, Y.H., Chen, H.C., Pei, Y.C., Wu, C.Y. (2005), “Influence of heel height and shoe insert on comfort perception and biomechanical performance of young female adults during walking”, *Foot Ankle Int*., 26, 1042-1048.

Kouchi, M., Tsutsumi, E. (2000), “3D foot shape and shoe heel height”, *Anthropological Science*, 108, 331-343.

Lee, C.M., Jeong, E.H., Freivalds, A. (2001), “Biomechanical effects of wearing high-heeled shoes”, *International Journal of Industrial Ergonomics*, 28, 321-326.

Speksnijder, C., Vdmunckhof, R., Moonen, S., Walenkamp, G. (2005), “The higher the heel the higher the forefoot-pressure in ten healthy women”, *The Foot*, 15, 17-21.

Stefanyshyn, D.J., Nigg, B.M., Fisher, V., O'Flynn, B., Liu, W. (2000), “The influence of high heeled shoes on kinematics, kinetics, and muscle EMG of normal female gait”, *Journal of Applied Biomechanics*, 16, 309-319.

Stephens, M.M. (1992), “Heel pain- shoes, exertion, and haglunds deformity”, *Physician Sportsmed.*, 20, 87-88.

Yung-Hui, L., Wei-Hsien, H. (2005), “Effects of shoe inserts and heel height on foot pressure, impact force, and perceived comfort during walking”, *Appl Ergon*, 36, 355-362.

IV.
ENVIRONMENT

ADVANCED WATER TREATMENT WITH FLOCCULANT MATERIALS OBTAINED BY RADIATION TECHNOLOGIES

GABRIELA CRĂCIUN, ELENA MĂNAILĂ

National Institute for Laser, Plasma and Radiation Physics, Electron Accelerators Laboratory, #409 Atomistilor St., 077125 Magurele, Romania, e-mail: gabriela.craciun@inflpr.ro

Paper presents the correlation between physical and chemical characteristics of some polymeric materials obtained by electron beam irradiation and their efficiency in potable water treatment. The interest was focused upon some potable water quality indicators established by Romanian Rule Regarding Potable Water Quality: turbidity (T), organic matter (OM) and total organic carbon (TOC). In order to provide measurable improvements in water quality we have studied the effects of different treatments based on flocculants and various combined treatments based on electrolytes and flocculants. The electrolytes used was $Al_2(SO_4)_3$. Using these polymeric materials in potable water treatment brings several advanteges such as: (a) reduce with 25% up to 50% the quantity of classic electrolytes needed; (b) concentrations of 10 to 100 times smaller of classic materials are used; (c) they do not produce metallic residuals in the resulted sludge, which does not affect the metabolism of plants and animals; (d) reduce with almost 60% the volume of the resulted sludge in comparison with the volume resulted from classic material treatment; (e) reduce with approximately 5-10 times the contact, stationary and decantation time which determines a shorter process of water purifying.

Keywords: water treatment, flocculants, radiation technologies.

INTRODUCTION

Water for public supply can be obtained from underground sources by wells sunk into aquifers, or from surface sources such as purpose-built reservoirs or lakes and rivers. The safety of the water is of utmost concern because several million people die each year after consuming contaminated water. All the above-mentioned sources can be subject to pollution. In the case of underground water, polluted surface water can enter the saturation zone of an aquifer and so lead to its contamination. Pollution can come from waste tip leachate containing heavy metals and organic compounds, farm run-off containing nitrates and pesticides, and industrial wastes which may have been deliberately dumped down old coal mine shafts (http://openlearn.open.ac.uk/). River water can be affected by farm drainage, sewage works and industrial effluents, and also the run-off water from roads. The prime function of water treatment is to produce a safe product, so several stages are involved: (1) the removal of suspended matter and rendering of the water clean, colorless and free from disagreeable taste and odor; (2) the disinfection of the water so that the numbers of bacteria are reduced to an appropriate level; (3) the removal of chemicals harmful to health and the reduction to low levels of chemicals that might otherwise interfere with normal domestic and industrial requirements; (4) the reduction of the corrosive properties of the water and protection of the pipe supply system; (5) the minimisation of the amount of material passing into the supply system which might encourage biological growth (http://openlearn.open.ac.uk/).

Coagulation is always considered along with flocculation and is used to remove particles which cannot be removed by sedimentation or filtration alone. These particles are usually less than 1 μm in size and are termed colloids. They have poor settling characteristics and are responsible for the colour and turbidity of water. They include clays, metal oxides, proteins, micro-organisms and organic substances such as those that give the brown coloration. The important property which they all have is that they carry a negative charge and this, along with the interaction between the colloidal particles and the water, prevents them from aggregating and settling in still water. The particles can be aggregated by adding either multivalent ions or colloids having an opposite (positive) charge. These are added as chemical coagulants. Chemicals commonly used as coagulants in water treatment are aluminium and ferric salts which are present as the ions Al^{3+} and Fe^{3+}. These positively charged multivalent ions neutralises the naturally occurring negatively charged particles, thus allowing the particles to aggregate (Porteous 2000; http://openlearn.open.ac.uk/).

The acrylamide polymers are very efficacious for water treatment but acrylamide is a toxic monomer and therefore their use are governed by international standards that provide the residual acrylamide monomer content in them be less than 0.05%. The acrylamide copolymers radiation technology was first developed on a semi-industrial scale with electron beam (EB) at the NILPRP, Accelerators Laboratory–Bucharest (Martin et al., 2004; Martin et al., 2002). The major advantages of radiation induced polymerization processes are: very easy to manipulate the molecular weight, from low to very high, by simply changing the feed composition as well as the composition of the product by incorporating different monomers; precise control of charge density as the monomer feed composition is controlled at the initial stages only; precise control of molecular weight distribution; no flammable and toxic solvents used; no production of waste matter or evolution of noxious gases; no production of hazardous effluents; very low monomer contents; very clean process. The use of polyelectrolytes with improved properties, such as by radiation technologies, will help the transposition of the EU Drinking Water Directive (98/83/EC) (Martin et al., 2006).

EXPERIMENTAL

The EB induced polymerization uses the Coulomb interaction of the accelerated electrons with atoms or molecules of the irradiated medium. By these interaction ions, thermalized electrons, excited states and radicals are formed and thereby the polymerization process is driven. Ionizing radiation polymerization is similar to conventional free radical addition polymerization. The initiation step in both reactions requires the admittance of some external energy. In ionizing polymerization, the energy is supplied by the ionizing radiation. The main function of the ionizing radiation in the polymerization process is limited to the primary events, the initiation step which leads to the production of free radicals and to a few specific secondary effects. The subsequent steps of propagation, termination and chain transfer proceeds as in a chemically catalyzed process. In radiation-initiated polymerization, any substance added to a monomer is radiolyzed, since the absorption of ionizing radiation is a purely electronic process, and this leads to an additional production of free radicals. Thus, due to water presence in the EB irradiated system, our experiments show that the role of the radicals originated from irradiated water is predominant over those of the radical, which come directly from the monomer irradiation.

Preparation of our P_n polyelectrolyte types is based on co-polymerization of aqueous solutions containing appropriate mixtures of acrylamide (AMD) and acrylic acid (AA) monomers and certain agents, such as complexing agents for impurities inhibition, chain transfer agents for cross-linked structure inhibition and initiators for monomer conversion optimization. The typical chemical composition (Martin et al., 2006) of the aqueous solutions to be irradiated for acrylamide-acrylic acid copolymer preparation is: (1) total monomer concentration (TMC): 40%; (2) monomers ratio (AMD/AA): 4/1-9/1;

(3) complexing agent concentration: 0.1% (5% solution of ethylene diamine tetra acetic acid); (4) chain transfer agent (CTA) concentration: 0.075%-0.2% (10% solution of sodium formate); (5) initiator (I) concentration: 0%-0.8% (2% solution of sodium persulfate); (6) NaCl concentration: 8-12%.

For the preparation of acrylamide-acrylic acid copolymers our interest was focused on the basic optimization of the characteristics involved in waste water treatment, such as, conversion coefficient (CC), residual monomer concentration (M_r), intrinsic viscosity (η_{intr}) or average M_w and linearity coefficient given by Huggins' constant (k_H). For the EB irradiated solutions in which water concentration decreases to less than 40%, the polymerization rate decreases and the conversion coefficient (CC) decreases, although the radiation absorbed dose level is increased. Thus, irradiated water radicals facilitate the polymerization process and decrease the required absorbed dose level in the lower range, of 0.9-1.1 kGy for AMD-AA copolymers. Also, due to the bigger AMD radiation reactivity (r_{AMD} =1.6) in comparison with AA reactivity (r_{AA}=0.6) and because the ratio of the residual monomer contents of AMD and AA is in inverse proportion to their reactivities ratio, the residual monomer concentration of AMD (a toxic monomer) is about 2.8 times smaller than the residual monomer concentration of AA, in the composition of acrylamide-acrylic acid copolymers.

For potable waters the interest was focused upon the following quality indicators established by Romanian Rule Regarding Potable Water Quality: turbidity (T), organic matter (OM) and total organic carbon (TOC). The factors affecting the selection of the appropriate polyelectrolyte are: the nature of the suspended particles (organic/inorganic content, net surface charge density, solids content of substrate, pH content of substrate, temperature of the system), the end result to be achieved (rapid separation of the solid matter from the fluid, clarity of the separated fluid) and dynamic and shear effects (mixing/conditioning of polymer and suspended particles, nature of shear forces associated with the dewatering equipment used). In many cases, polyelectrolytes are used as coagulation aids together with electrolytes ($Al_2(SO_4)_3$, $FeSO_4$ and $Ca(OH)_2$) (Martin et al., 2006).

RESULTS AND DISCUSSION

In order to provide measurable improvements in water quality we have studied the effects of different classical treatments with electrolytes (classic treatment type - CT) and the effects of various combined treatments with electrolytes + polyelectrolytes (combined treatment type - CT+P). Various CT or/and P concentrations were tested. Also, many polyelectrolytes of P type with various characteristics were used. Polyelectrolytes with a wide range of intrinsic viscosity values (molecular weights) were tested. To set these concentrations were performed laboratory tests on raw water coming from a surface river that is the source of drinking water for a large city in Romania, using laboratory facility type JAR-TEST. For both raw water and treated water were followed the same quality indicators: turbidity (T), measured in nephelometric turbidity units - NTU, organic matter (OM), measured in milligrams of $KMnO_4$ per liter - mg $KMnO_4$/l and total organic carbon (TOC), measured in milligrams of C per liter - mg C/l. These quality indicators are the most difficult to comply with the limits set by standards for drinking water quality. Raw water characteristics were: T = 28.6 NTU, OM = 24.33 mg $KMnO_4$/l, TOC = 35 mg C/l and pH = 8.06. First tests were conducted using solutions of $Al_2(SO_4)_3$ with different concentrations.

In Figure 1 are presented the coagulation – flocculation experiments results obtained from the classical treatment (CT) with $Al_2(SO_4)_3$ solutions with concentrations between 10 and 35 mg/l. It can be observed that the best results were obtained for concentrations of 25 and 30 mg/l. We kept for use in the combined coagulation – flocculation experiments based on electrolytes and polyelectrolytes (CT+P) the concentration of 25 mg/l.

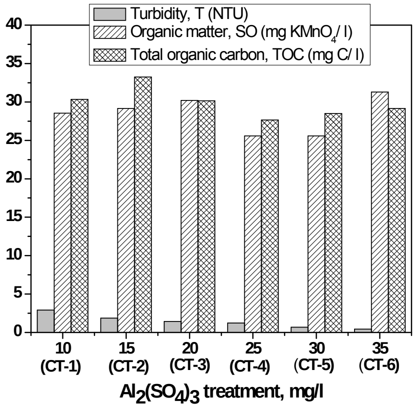

Figure 1. Coagulation – flocculation experiments results using $Al_2(SO_4)_3$ solutions with concentrations between 10 and 35 mg/l

In Table 1 are presented the physical and chemical characteristics of the polyelectrolytes obtained by EB irradiation, selected to be used for the combined coagulation – flocculation experiments based on electrolytes and polyelectrolytes. We chose polyelectrolytes with $C_c > 90\%$ and consequently $M_r < 0.05$ %, $k_H < 0.5$ and a wide range of η_{intr}. A high conversion coefficient always assures a low value of residual monomer concentration so the presence of the toxic acrylamide in the final product is very low. Also, AMD-AA copolymers exhibit good water solubility only for $k_H < 0.5$.

From our experience the value of η_{intr} always exhibits a maximum value associated with a minimum value for k_H. So, when k_H is higher than 0.5 a cross-linked structure in the final product has occurred, polyelectrolyte becomes water-insoluble and η_{intr} exhibit lower values.

Table 1. Physical and chemical characteristics of the polyelectrolytes obtained by EB irradiation and used in the combined coagulation-flocculation experiments

	Physical and chemical characteristics of polyelectrolytes			
Polyelectrolytes	CC (%)	η_{intr} (dl/g)	K_H	M_r (%)
Polyelectrolyte 1 (P1)	93.46	7.89	0.31	0.012
Polyelectrolyte 2 (P2)	97	8.18	0.17	0.06
Polyelectrolyte 3 (P3)	100	10.18	0.18	0
Polyelectrolyte 4 (P4)	97.67	10.59	0.24	0.006
Polyelectrolyte 5 (P5)	99.1	14.57	0.2	0.0014
Polyelectrolyte 6 (P6)	91	15.76	0.17	0.017

Polyelectrolytes are usually used for potable water treatment in very small amounts (0.2 mg/l in our case) and their application reduces the amount of electrolyte necessary in the range of 20-40% and the acquirement of very low values for the quality indicators. In Figures 2-4 we have represented the treated water quality indicators T, OM and TOC as a function of the applied treatment (CT+P).

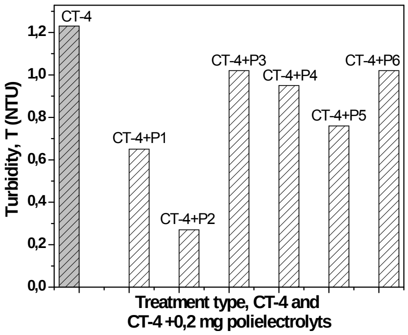

Figure 2. The effect of different treatment types on T

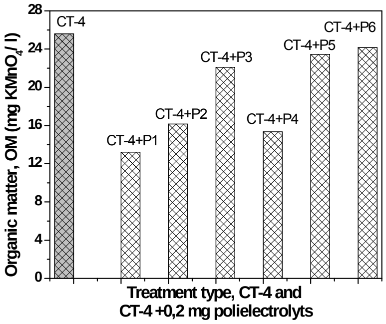

Figure 3. The effect of different treatment types on OM

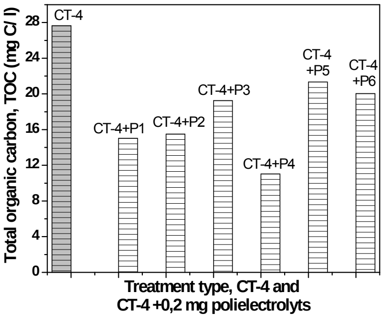

Figure 4. The effect of different treatment types on TOC

As is shown in Figure 2, after combined treatments application the quality indicator T does not show a decrease with η_{intr} as we expected. Polyelectrolytes having a high intrinsic viscosity proved to be less efficient than those having low intrinsic viscosity. P1 (η_{intr} = 7.89 dl/g) and P2 (η_{intr} = 8.18 dl/g) were the best in T reduction (47% and 78% respectively, versus CT) while P5 (η_{intr} = 14.57 dl/g) and P6 (η_{intr} = 15.76 dl/g) gave poor results in T reduction (17% and 15% respectively, versus CT).

From Figures 3 and 4 we see that in terms of both OM and TOC quality indicators, they exhibit the same tendency as T. Polyelectrolytes P1 and P2 reduce OM with 48% and 37% respectively versus CT, while P5 and P6 reduce OM only with 0.08% and 0.05% respectively versus CT also. In the case of the quality indicator TOC, P1 and P2 decreased it with 45% and 44% respectively versus CT, while P5 and P6 reduce TOC only with 23% and 27% respectively versus CT.

P4 which has a good intrinsic viscosity (η_{intr} = 10.59 dl/g), although it achieved a reduction of T with only 22% compared with CT, but reduced OM with 40% and TOC with 60%. This last result is better than any of the above (CT+P1, CT+P2, CT+P5 or CT+P6).

CONCLUSIONS

In this paper are presented the results obtained with a classic treatment (CT) and combined treatments (CT+P) applied on raw water coming from a surface river. The polyelectrolytes used in the combined treatments (P) were chosen with $C_c > 90\%$ and consequently $M_r < 0.05$ %, $k_H < 0.5$ and a wide range of η_{intr}. The best reduction efficiency on water quality indicator T, after combined treatments applying was obtained in the case of P1 and P2 use. The best reduction efficiency on water quality indicators OM and TOC, after combined treatments applying were obtained in the case of P4 use. Polyelectrolytes used in the combined treatments CT+P1, CT+P2 and CT+P4 have lower intrinsic viscosities than those of polyelectrolytes used in combined treatments CT+P5 and CT+P6. So, a high intrinsic viscosity is not always sufficient to ensure all quality indicators reduction. Each quality indicator is associated with a certain type of polyelectrolyte which exhibits the maximum ability to its reduction. Never the polyelectrolyte with the highest η_{intr} gives simultaneous reduction of all quality indicators. Also, for a given polyelectrolyte there is a different amount for each quality indicator, which gives the best result.

REFERENCES

Martin, D., Ighigeanu, D., Mateescu, E., Craciun, G., Calinescu, I., Iovu, H., Marin, G. (2004), “Combined microwave and accelerated electron beam irradiaton facilities for applied physics and chemistry”, *IEEE Transactions on Industry Applications*, 40(1), 41-52.

Martin, D., Mateescu, E., Craciun, G., Ighigeanu, D., Ighigeanu, A. (2002), “Polymeric flocculants processing by accelerated electron beams and microwave heating”, *Radiation Physics and Chemistry*, 64(5-6), 423-428.

Martin, D., Craciun, G., Manaila, E., Ighigeanu, D., Togoe, I., Oproiu, C., Margaritescu, I., Iacob, N. (2006), “Waste Treatment by Microwave and Electron Beam Irradiation”, 2nd Environmental Physics Conference, 18-22 February 2006, Alexandria, Egypt, Book of Abstracts, 28-30.

Porteous, A. (2000), *Dictionary of Environmental Science and Technology*, 3rd edition, John Wiley & Sons (T210 Set Book).

***, http://openlearn.open.ac.uk/

REMOVAL OF AMMONIUM IONS FROM WATER BY RAW AND ALKALI ACTIVATED BENTONITE

RAMAZAN ALI DIANATI TILAKI

Department of Environmental Health, Faculty of Health, Mazandaran University of Medical Sciences, Sari-Iran, dianati.tilaki@gmail.com

Ammonium ions in water poses adverse effects on aquatic life and in elevated level presents risk for human health. Zeolites as low cost and ecofriendly sorbent, has very good capacity to remove ammonium ions. The purpose of the present study was to examine the efficiency and comparison of raw and alkali modified bentonite as low cost sorbent for removal of ammonia nitrogen (NH_4-N) from water. Natural calcium bentonites originating in Iran were treated with 6.0M NaOH aqueous solution at the temperature of 150°C under atmospheric pressure for 6 hours. The alkali modified bentonite were washed several times with distilled water, dried in an oven at a temperature of 110°C and then used as sorbent. Batch experiments were conducted to delineate effect of initial ammonium concentration (5,10 and 50ppm) and bentonite dose (1.0,5.0 and 10.0 gL^{-1}) on removal and sorption capacity of raw and alkali activated bentonite. Results showed that time required to reach equilibrium in removal of ammonium by the examined bentonites was 30.0 Min. Removal efficiency of raw and modified bentonites for ammonium removal with 45.0 Min. contact time was 25 to 50 percent. By increasing contact time to 4 and 18h ammonium removal efficiency for both raw and modified bentonite didn't changed definitely. Increasing bentonite dose from 1.0 to 10.0 gL^{-1} slightly increased sorption efficiency. Increasing ammonium concentration from 5.0 to 50.0 mgL^{-1} didn't clear effect of removal efficiency. Bentonite can be used for ammonium removal from water environment

Keywords: ammonia, water, Bentonite.

INTRODUCTION

Ammonia in surface water supplies often is a result of runoff in agricultural areas where fertilizer applied to the ground. Another way that high levels of ammonia in water appear is from aquifers in animal feed lots. Ammonia is oxidized to nitrate by bacterial action. In drinking water the maximum ammonia concentration Of $1.5mgL^{-1}$ is recommended by the World Health Organization (WHO) to avoid changes of taste and odor of water. Natural levels of ammonia in ground waters are usually below $0.2mgL^{-1}$. Higher natural contents (up to $3mgL^{-1}$ are found in strata rich in humic substances in forests. The presence of ammonia at higher levels is an important indicator of fecal pollution (Mažeikien et al., 2010). The removal of NH_4^+-N can be accomplished by physical, chemical, biological or a combination of these methods. Available technologies include adsorption, chemical precipitation, membrane filtration, reverse osmosis, ion exchange, air stripping, breakpoint chlorination and biological nitrification and denitrification. Each of these methods has its own specific limitation (Hussain et al., 2006). There are many researches that show the zeolite can be used to remove ammonia from water. Among the zeolites, Clinoptilolite was used most frequently as ammonia sorbent (Abd El-Hady et al., 2001, Miladinovic et al., 2004, Liu et al., 2008, Rahmani et al., 2006, Asilian et al., 2007). Bentonite is a clay mineral which is largely composed of Montmorillonite, which is mainly a hydrous aluminum silicate. Bentonites typically exhibit a cation exchange capacity (CEC) of 70 -100meq/gram (Kashani Motlagh et al., 2008; Karimi et al., 2009).The chemical and mineralogical structures of the bentonites, which are activated by heating in strong acids, undergo considerable transformations. The surface acidity and the porous structure of bentonites can be changed to the desired extent by acid activation (Onal et al., 2011). Many studies performed on the alkaline reaction of bentonite have been directed, obviously, to the montmorillonite alteration. Previous studies on the reactivity of montmorillonite in alkaline solutions indicated the collapse of expandable smectite layers, in particular the formation of illite or illite/smectite mixed-layers (Cuevas et al., 2006).

The aim of the present study was to investigate the effect and adsorption behavior of raw and alkali activated calcium bentonite to remove ammonium ion from aqueous solution.

MATERIALS AND METHODS

Natural Calcium Bentonite mined in Iran was used as starting material. Bentonite was washed several times with distilled water to remove impurities, dried in an oven at 110°C for 24h and then used as raw bentonite. The modification of raw bentonite was performed under alkaline condition. The mixture consisting 50 g of a raw bentonite and 500 mL of 6.0 M NaOH solution was placed in a reflux vessel and heated in an oven at 100°C under atmospheric pressure for 6.0h. Then the mixture was placed in a cone to settle out. The settled product was washed several times with distilled water until the pH of supernatant became natural (around 7), dried in an oven at 105°C for 24h and then used as modified bentonite.

The batch study was conducted to establish the removal pattern of ammonium ions using raw and alkali activated bentonite. The investigations on the adsorption capacity of bentonite for ammonium ions were conducted in two phases: (1) the preliminary investigations and (2) the main investigations. The preliminary investigations aimed at the evaluation of the impact of selected amounts of bentonite on the removal degree of N-NH_4^+ in the following concentrations 5.0, 10.0 and 50.0 mg L^{-1} N-NH_4^+.The samples with the addition of 0.1 g of bentonite were shaken for 10 minutes. The removal degree of ammonium ions was evaluated. With the reference to the obtained results from the preliminary investigations, further experiments were conducted with 0.1, 0.5 and 1.0 g of raw and modified bentonite separately in order to achieve higher degree of ammonium ions removal. Also, the contact time of the sorbents and the solution was extended to 4.0 and 18.0h to determine the effect of contact time on the amount of removed N-NH_4^+ ions.

Three solutions with the following concentrations: 5.0, 10.0, and 50.0 mg L^{-1} N-NH_4^+ were prepared from the standard solution of ammonium chloride at concentration of 1 g L^{-1}. Samples of 0.1, 0.5 and 1.0g of raw and alkali activated bentonite were weighed separately and 100 ml of N-NH_4^+ solutions were added. The prepared samples were shaken for 10,20,30,45 and 60 minutes and after that the samples were centrifuged at 4000 rpm for 15 min. Each solution was prepared in triplicates.

Equilibrium isotherm were determined by contacting a fixed mass of sorbent (0.1, 0.5 and 1.0 g separately) with 100 mL of NH_4^+-N concentrations (5.0, 10.0 and 50.0 mgL^{-1}) were tested. The isotherm constants and least squares correlation coefficients (R^2) of both models were compared to determine the best-fit isotherm model for this study. All experiments were conducted at room temperature (23 ± 2°C). Ammonia nitrogen concentration was measured by EPA Method (350.2) using a HACH DR/2800 Spectrophotometer set at 425 nm wavelength.

RESULTS AND DISCUSSION

The equilibrium time determined (time after that bentonite did not remove further ammonium from solution) for both raw and alkali activated bentonite was 30.0 Min. In the Figure 1 removal efficiency of raw bentonite and alkali modified bentonite was compared. As it can be seen from Figure 1 with ammonium concentration of 5.0 ppm, by increasing sorbent dose efficiency has been increased. Also the figure shows that modification of bentonite by alkaline solution has increased ammonium sorption efficiency.

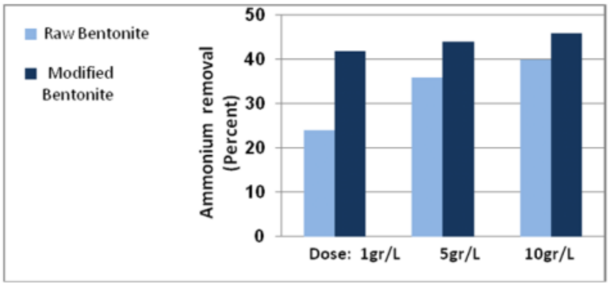

Figure 1. Comparison between percent of ammonium removal by different dose of raw and modified bentonite with initial concentration of ammonium (Ci=5ppm) and contact time (t=45Min.)

Yujiro Watanabe et al. (2005) reported that the structure of natural zeolite such as mordenite and clinoptilolite after treatment with 3.0M NaOH solution at 150°C was changed to Phillipsite and by this type of modification the amount of ammonium removal from solution by modified zeolite was two-fold greater (1.92 mmol g^{-1}) than that taken up by the starting material. Figure 2 shows that ammonium removal efficiency of sorbents for 10 ppm initial concentration of NH_4^+-N, are slightly lower in comparison with Figure 1. The results also shows that modified bentonite has greater ammonium sorption efficiency.

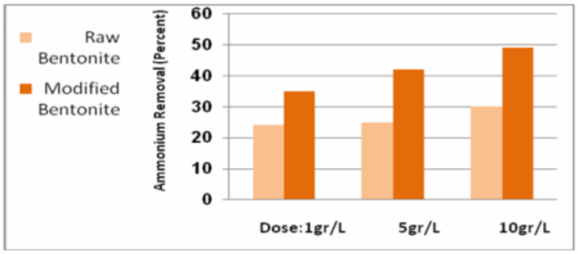

Figure 2. Comparison between percent of ammonium removal by different dose of raw and modified bentonite with initial concentration of ammonium (Ci=10ppm) and contact time (t=45Min.)

In another study, J. Cuevas et al. (2006), reported that Spanish reference benonite (FEBEX) was modified with alkaline solution (mixture of NaOH, KOH and $Ca(OH)_2$) with pH in the range of 12-13. The solid/alkaline solution ratio was 1/3 or 80 g of bentonite and 240 ml of solution and time of contact was from 7 days up to 365 days at 35, 60 and 90°C. The aim of their work was to clarify the effect of the alkaline plume induced by concrete on bentonite. By their of modification, they observed that the pH of solution was decreased after two month of contact and concluded that “One of the most important observations made during the interaction between alkaline solutions and bentonite was that montmorillonite can be considered as an important buffer agent of the pH in the bentonite. The pH decrease is mainly due to the dissolution of montmorillonite and the deprotonation of aqueous silica (i.e. $H_4SiO_4 \rightarrow H_2SiO_4^{2-} + 2H^+$), and also to the incorporation of OH^- in the structure of newly-formed minerals or the retention of OH^- in the external surface of smectite may play a significant role”. Also they reported that the change in structure of bentonite was dependent to temperature and contact time and it can be resulted that the cation exchange capacity of alkaline modified bentonite was greater than raw bentonite (J. Cuevas, et al. 2006).

In the another research it is reported that three modified bentonites, hydroxy-aluminum pillared bentonite (Al-Bent), hydroxy-iron pillared bentonite (Fe-Bent), and cetyl trimethylammonium exchanged organo-bentonite (CTMAB-Bent) were prepared, characterized, and its adsorption properties for ammonia nitrogen were evaluated in batch experiments. The results showed that the ability of ammonia nitrogen adsorption of modified bentonites was far more than that of raw bentonite. The adsorption capacity followed the order: Al-Bent > Fe-Bent > CTMAB-Bent > raw bentonite (Liangguo Yan et al, 2009). In the Figure 3 efficiency of different dose of raw and modified bentonite for removal of 50ppm ammonium was compared. As it can be seen from this figure, with increasing the initial concentration of ammonium, the removal efficiency of sorbent didn't changed compared to Figure 1. Moreover with different dose of sorbent, the removal efficiency was in the range of 35 to 40 percent. As it can be seen from all figure, ammonia removal efficiency of alkaline modified bentonite was higher than raw bentonite. alkali activated bentonite has more cation exchange capacity than raw bentonite.

The effect of increase in contact time on removal efficiency of bentonites has been shown in Figure 4. As it can be seen from this figure, by increasing the contact time to 4 and 18 h, the ammonium removal efficiency of raw bentonite did not change very definitely compared to previous results.

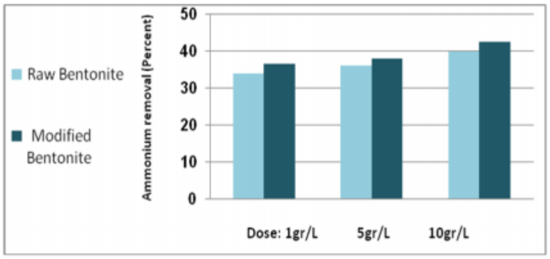

Figure 3. Comparison between percent of ammonium removal by different dose of raw and modified bentonite with initial concentration of ammonium (Ci=50ppm) and contact time (t=45Min.)

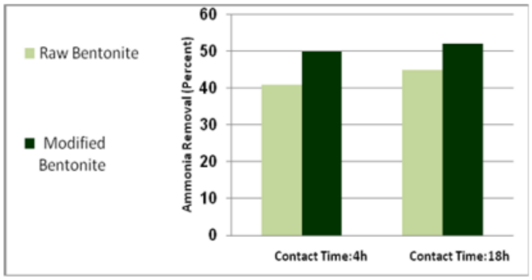

Figure 4. Comparison between contact time for ammonium removal by raw and modified bentonite with dose 10gr/L and initial concentration of ammonia(Ci=50ppm)

It is reported that zeolites and bentonite due to their adsorption properties and high affinity to ammonium ions, are capable of removing ammonium and undesirable odors from the environment and because of that can appear beneficial in the treatment of animal excrements (Venglovsky et al., 1999). In another research it is reported that addition of bentonite counteracted the inhibitory effect of ammonia during thermophilic anaerobic digestion of cattle manure. The effect was observed only when the ammonia concentration was increased gradually. In batch experiments bentonite had a similar stimulatory effect leading to a decreased Lag phase and increased methane production rate. This results indicating that bentonite can remove ammonia from solution which is toxic for methanogenesis bacteria (Angelidaki et al., 1993). In order to decide which type of isotherm fits better the sorption experimental data, we plotted the quantities log (x/m) vs. log Ce for the Freundlich isotherm and 1/q vs. 1/Ce for the Langmuir isotherm. The R^2 values (goodness of fit criterion) computed by linear regression for the two types of isotherms are presented in Table 1 for both sorbents. The data of Table 1 indicate that the Langmuir and Freundlich isotherms are best suited for sorption of NH_4^+- N by both raw and modified Ca-Bentonite.

Table 1. Goodness of fit of the Freundlich and Langmuir isotherms to the sorption experimental data

Sorbent	R^2 Values					
	Freundlich isotherm			Langmuir isotherm		
Raw Ca-Bent.	M=0.1g	M=0.5g	M=1g	M=0.1g	M=0.5g	M=1g
	0.98	0.94	0.95	0.99	0.88	0.91
Mod.Ca-Bent.	0.98	1.0	0.99	0.96	0.99	0.99

T.C. Jorgensen and L.R. Weatherley (2003), reported that ammonia removal from wastewater by zeolite clinoptilolite via ion exchange are best fitted with Langmuir adsorption model. They reported that the Langmuir model provided a close fit for the ion-exchange equilibrium. The Langmiur model assumes only one solute molecule per site and also assumes a fixed number of sites. Whilst the Langmuir model was developed for adsorption process, it can be seen that the experimental data in this ion exchange process are in accordance very well with adsorption model (Jorgensen and Weatherley, 2003).

CONCLUSION

From the results of this study it can be concluded that, raw calcium bentonite can remove around 25 to 45 percent (depending on sorbent dose and sorbate concentration) of ammonium ions present in aqueous solution. Treatment of raw bentonite in the NaOH 6.0 M solution at 100°C for 6h will cause increase around 25 to 50 percent (depending on ammonium concentration) in ammonium sorption efficiency. Raw or treated bentonite can be used for ammonia removal in many places such as animal farms, sludge digestion plants and biogas reactors.

Acknowledgement

This work was supported by grants from vice-chancellor for research of Mazandaran University of Medical Sciences, Sari-Iran.

REFERENCES

Abd El-Hady, H.M., Grünwald, A., Vlčková, K., Zeithammerová, J. (2001), “Clinoptilolite in Drinking Water Treatment for Ammonia Removal”, *Acta Polytechnica*, 41(1).

Angelidaki, I. and Ahring, B.K. (1993), “Effect of the clay mineral bentonite on ammonia inhibition of anaerobic thermophilic reactors degrading animal waste”, *Biodegradation*, 3, 409-414.

Asilian, H., Mortazavi, S.B., Kazemian, H., Phaghiehzadeh, S., Shahtaheri, S., Salem, M. (2004), “Removal of Ammonia from Air, using Three Iranian Natural Zeolites”, *Iranian J Publ Health*, 33(1) 45-51.

Cuevas, J. et al. (2006), “The alkaline reaction of FEBEX bentonite: a contribution to the study of the performance of bentonite/concrete engineered barrier systems”, *Journal of Iberian Geology*, 32(2), 151-174.

Hussain, S. et al. (2006), “Physico-chemical method for ammonia removal from synthetic wastewater using limestone and GAC in batch and column studies”, *Bioresource Technology*, 98, 874–880.

Jorgensen, T.C. and Weatherley, L.R. (2003), “Ammonia removal from wastewater by ion exchange in the presence of organic contaminants“, *Water Research*, 37, 1723-1728.

Kashani Motlagh, M.M., Amiri Rigi, Z., Yuzbashi, A.A. (2008), “To Evaluate an Acid Activated Bentonite from Khorasan (Iran) for Use as Bleaching Clay”, *IUST International Journal of Engineering Science*, 19(5-2), 83-87.

Karimi. L., Salem. A. (2011), “The role of bentonite particle size distribution on kinetic of cation exchange capacity”, *Journal of Industrial and Engineering Chemistry*, 17, 90–95.

Liu, C. et al. (2008), “Study on Ammonia-Nitrogen and Humic Acid Removal Using Aluminum Oxide Molecular Sieve and Modified Clinoptilolite”, *Clean*, 36(5–6), 512 – 516.

Miladinovic, N., Weatherley, L.R., Lopez-Ruiz, J.L. (2004), “Ammonia Removal form Saline Wastewater by Ion Exchange”, *Water, Air, and Soil Pollution: Focus*, 4, 169–177.

Mažeikien, A. et al. (2010), “Laboratory Study of Ammonium Removal by using Zeolite (Clinoptilolite) to treat drinking water”, *Journal of Environmental Engineering and Landscape Management*, 18(1), 54–61.

Onal, M., Sarikaya, Y., Alemdaroglu, T. (2002), “The Effect of Acid Activation on Some Physicochemical Properties of a Bentonite”, *Turk J Chem*, 26, 409-416, TUBITAK.

Rahmani, A.R. and Mahvi, A.H. (2006), “Use of Ion Exchange for Removal of Ammonium: A Biological Regeneration of Zeolite”, *Global NEST Journal*, 8(2), 146-150.

Venglovsky, J. et al. (1999), “Adsorption properties of natural zeolite and bentonite in pig slurry”, *Vet.Med. Czech*, 44(11), 339-344.

Watanabe, Y. et al. (2005), “Hydrothermal modification of natural zeolites to improve uptake of ammonium ions”, *J Chem Technol Biotechnol*, 80, 376–380.

Yan, L., Xin, X., Xu, Y., Yu, H., Du, B. (2009), “Removal of ammonia nitrogen from water by modified bentonite”, 3rd International conference on Bioinformatics and Biomedical Engineering, ICBBE 2009.

DEVELOPMENT OF ELECTROCHEMICAL METHOD FOR DETERMINATION OF HEAVY METALS IN LEATHER AND LEATHER INDUSTRY WASTEWATERS

VOLODYMYR KHOMENKO, ILONA SENYK, VIKTORIIA PLAVAN, VIACHESLAV BARSUKOV

Kiev National University of Technology and Design, 2, Nemirovich-Danchenko str., Kiev 01011 Ukraine, email: v-barsukov@i.ua

In this work an electrochemical method for determining the content of heavy metals in leather and leather industry wastewaters has been developed. The method is based on usage and improvement of stripping voltammetry, which allows simultaneous determination of several elements in a solution as well as different degrees of oxidation for each element. Such heavy metals in industry wastewaters as Pb, Cd and Cu can be determined by a very express way with a determination limit of 0.01- 0.05 ppm. The content of any metal can be calculated easily from the current – potential curve, which is similar to a spectral dependence. In this work a special method has been developed for chromium determination, which is of greater importance for leather industry. This method is a little bit more complicated, but it enables not only a general content of chromium to be estimated, but also a partial content of Cr (III) and Cr (VI) in leather and leather industry wastewaters. The employment of the proposed electrochemical method has different advantages in comparison with the existing chemical techniques and allows one to save time, chemicals and to improve the quality of determination for heavy metals. The limit of detection the above-mentioned metals was 0.01-0.05 ppm using 0.4M KCl solution as a background electrolyte.

Keywords: wastewaters, Cd, Pb, Cu, Cr (III) and Cr (VI) determination.

INTRODUCTION

In developing modern technologies a burning issue is the environmental one, connected with monitoring contamination of the environment with heavy metals such as Cd, Pb, Cu, Cr (III) and especially Cr (VI). These metals are highly toxic, capable of accumulating in both living things and the environment. The permissible content of heavy metals in natural water must not exceed 0,001 %. Conventionally, atomic adsorption, inductively coupled plasma mass spectrometry and other expensive analytical methods are used for their reliable determination. Therefore, development of alternative methods, which would be relatively cheap and sensitive, is an urgent problem.

Such electrochemical method as stripping voltammetry is characterized by a relatively low cost of the equipment along with quite high sensitivity. A comparative analysis of advantages and disadvantages of different techniques was reported in (Bersier, P. M., et al, 1994). The analysis enables a conclusion to be drawn that in many cases the stripping voltammetry method is a competitive alternative one by its sensitivity to a number of elements. A major advantage of this method is an opportunity to determine several elements simultaneously as well as different degrees of oxidation for each element. That is why the improvement and employment of this method is a relevant question of today for different industries, including leather industry.

Disadvantages, which decrease the effectiveness of the existing stripping voltammetry method, are a limited scope of metals that can be determined, the necessity to remove oxygen from the solution under study and to find out an optimum composition of the solution. To this must be added a low potential sweep rate (< 2 mV/s), long concentration time (over 10 min) and relatively narrow potential ranges used in the analysis. Our task in this work was to improve the method and to work out a procedure for detecting trace concentrations of ions of heavy metals such as Cd, Cu, Pb and Cr in aqueous solutions.

The stripping voltammetry method is considered to be a relatively new analytical technique, which is being more and more frequently used in analytical chemistry and electrochemistry (Kiptoo, J., et al, 2010, Brainina, K. et al 1993). The stripping voltammetry determination of metal content in aqueous solutions of electrolytes involves a few steps, the main ones being accumulating the analyte at the working electrode and dissolving the concentrate. The method is based on the ability of elements to undergo electrochemical deposition from the solution at the indicator electrode at controlled boundary-diffusion current with subsequently dissolving in the process of anode polarization at a certain potential characteristic of every element. The analysis was carried out with an electrochemical module containing a rotating disc electrode with a working surface of 0.07 cm^2. A three-electrode electrochemical cell was used in this work. The case of the cell from glassy carbon was used as an auxiliary electrode. In all the studies an Ag/AgCl reference electrode and a glassy carbon disc indicator electrode were employed. The indicator electrode's rotation rate was 1000 rpm. Electrochemical measurements were performed using a VMP3 potentiostat (from Princeton Applied Research, Great Britain). Reliability of the results of electrochemical measurements was verified by atomic-absorption spectrometer SOLAAR S4 (from ThermoElectron Co., the USA).

RESULTS AND DISCUSSION

Determination of Cd, Pb and Cu

One of the principal considerations in improving the stripping voltammetry method was to achieve a high speed of conducting the analysis, which can be done by minimizing the concentration time as well as by using a high-rate (20 mV/s) potential sweep. Besides the method proposed requires minimum currents (up to 10 µA). This current value allows the employment of relatively cheap electronic devices for the equipment.

In this work a procedure schematically shown in Figure 1 has been proposed for stripping voltammetry measurements. The glassy graphite working electrode was preliminarily modified by forming a mercury micro-surface in the solution under investigation at a potential of 0 V. The electrodeposition of the elements at the indicator electrode proceeds at a given potential (E_k) for a given time of electrolysis (t_k). Electrochemical dissolution of the elements from the electrode surface occurs via linear potential change at a given sweep rate (S). After the electrochemical dissolution of microscopic depositions of the metals the electrodes were electrochemically cleaned at a given potential (E_c) for a given time of electrolysis ($t_{cleaning}$).

The experiment revealed the following conditions as optimum ones: the background electrolyte is 0.4 M KCl solution, $E_k = –1.20$ V, $E_c = 0.45$ V, S= 20 mV/s, $t_k = 60-180$ s, $t_{cleaning}$ is 60 s. The above conditions allowed clearly separated peaks of anode dissolution for cadmium, lead, copper and mercury. The chosen t_k and S values allowed continuous operation of the glassy graphite electrode modified with mercury without additional calibration.

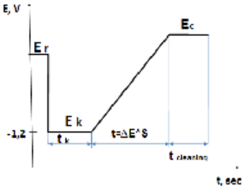

Figure 1. Change in the electrode potential of the indicator electrode in stripping voltammetry determination of the content of heavy metals in aqueous solutions

In this work a limiting concentration has been accurately determined for the ions of cadmium, copper and lead in the background electrolyte solution. The sensitivity of the method was found to improve considerably on using a rotating disc electrode. Figure 2 shows stripping voltammograms of anode dissolution at the stationary electrode (curve 1) and rotating indicator electrode (curve 2). According to experimental data the sensitivity of the method increases by several orders of magnitude upon using a rotating disc electrode.

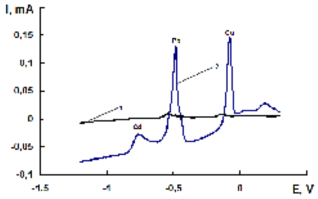

Figure 2. Stripping voltammogram for anode dissolution of metals in 0.4M KCl solution containing 0.1 ppm. The stripping voltammogram was taken for two cases: with a stationary indicator electrode (curve 1) and with rotating one (curve 2, 1000 rpm)

It should be noted that the time of deposition is the most essential factor affecting the accuracy of determination of heavy metals in aqueous solutions. The optimum concentration time (t_k) has been established to be 180 s, which allows a rapid stripping voltammetry measurement without decreasing the accuracy.

The accuracy of the analytical capability of stripping voltammetry was further increased by using a glassy carbon electrode modified with mercury. The microscopic mercury film was deposited directly in the solution analyzed by adding 0.1 ppm mercury nitrate so that the surface of working electrode was being modified in-situ.

Figure 3 presents stripping voltammograms for determination of cadmium at modified and non-modified electrodes. The anode dissolution current for cadmium at the modified electrode has shown a 25% increase compared to that at the non-modified one. It should be noted that the width of peaks of stripping voltammetry curves for modified electrodes is much smaller, which also contributes to the improvement of the method. Compared to glassy carbon electrodes, the positive effect of the electrode being modified is due to the fact that when modified the electrode enables concentration of ions of many metals which are reduced at quite low potentials and gives more reproducible results. In determining the ions of heavy metals the electrolytic accumulation involves forming metal amalgams, for example:

$$Pb^{2+} + 2e + Hg = Pb(Hg), \quad (1)$$

whereas upon the reverse sweep there is registered the anode oxidation current of the product by the scheme: Pb(Hg) - 2e = Pb^{2+} + Hg.

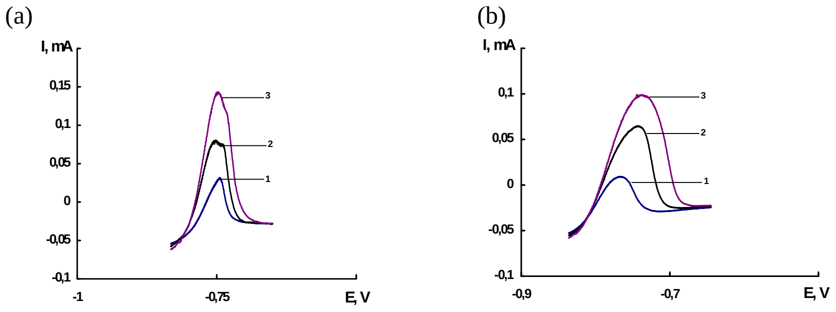

Figure 3. Stripping voltammogram for anode dissolution of cadmium (0.1 ppm) in 0.4M KCl solution for two cases: with a modified electrode (a) and with a non-modified glassy carbon electrode (b)

Mercury film electrodes compare favorably to stationary mercury drop electrodes, because on using them practically all the metal is accumulated in the thin Hg film and in anode dissolution it completely goes into solution, whereas in the case of drop electrodes a considerable amount of the reduced metal diffuses into the Hg drop and does not take part in the anode process.

According to the proposed procedure, limits of detection were determined for cadmium, copper and lead. Figure 4 shows a root-mean-square deviation of anode dissolution current for cadmium (a), copper (b) and lead (c) in the 0.05-2 ppm concentration range, which amounted practically 1.

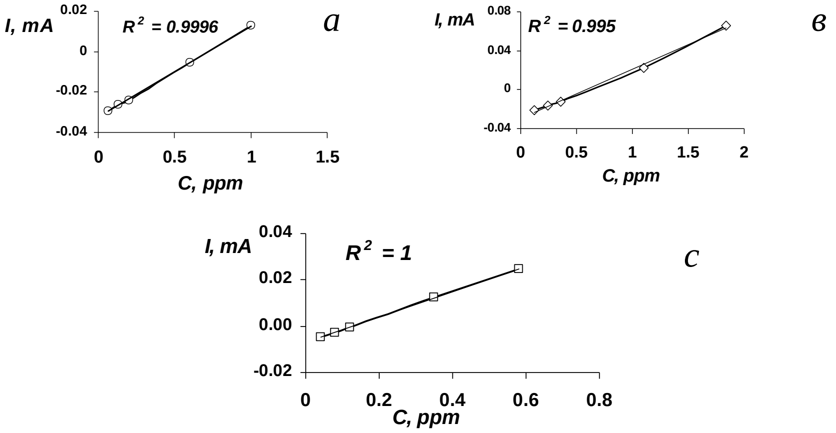

Figure 4. The height of anode dissolution current peaks for cadmium (a),copper (b) and lead (c) vs the concentration of metal ions in 0.4M KCl solution

Thus, the concentration limit of detection of the above-mentioned metals of the order of 0.05 ppm can be determined by the procedure proposed for the stripping voltammetry method, the error being no more than 10%.

Chromium Determination

The anodic stripping voltammetry cannot be directly employed to determine chromium in solutions due to the fact that the metal is highly inert and it is difficult to deposit it cathodically at the indicator electrode. That is why in this work an indirect method was proposed for determination of Cr ions.

Previous studies showed that the stripping voltammetry method is a reliable one to determine trace concentrations of the ions of heavy metals. So, the analytical signal obtained for the above ions can be used to determine the concentration of chromium ions. Cr (VI) ions are capable of forming scarcely soluble chromates with some heavy metals. Thus, adding chromium ions to the background solution containing a certain amount of a heavy metal will decrease their concentration. The method was based on the reactions of Cr (VI) with lead ions

$$2\,Pb(NO_3)_2 + K_2Cr_2O_7 + H_2O = 2\,PbNO_3\downarrow + 2\,KNO_3 + 2\,HNO_3 \qquad (2)$$

Analytical measurements were taken in the background electrolyte of 0.4M KCl solution containing a certain amount of lead ions (1-50 ppm). Prior to the measurements, the indicator electrode was prepared. The preparation involved the following steps:

- the electrode was washed with bidistilled water;
- the electrode was dried with filter paper;
- a thin layer of the working surface was cut away with an emery cloth.

In taking the measurements regeneration of the surface of the indicator electrode was carried out by cathode polarization at 0.5 V.

As much as 25 $см^3$ of the background solution was put into the electrolyzer and 0.1-0.5 ml $K_2Cr_2O_7$ solution with a concentration of 0.001 or 0.01M was subsequently added. The working electrode and the reference electrode were then immersed.

Analysis was carried out under the following conditions:

- preconcentration for 180 s with stirring at a potential of 1.0 V;
- recording cathode voltammograms at a linear sweep rate of 50 mV/s in the 1.00-0.50 V potential range.

The recording was done 2-3 times. The content of chromium (VI) in no-load test was determined for every new lot of the chemical used.

According to the proposed technique, the potential of maximum anode current was observed at -0.4 V (Figure 5).

Figure 6 shows that the anode dissolution current for lead decreases proportionally with increasing chromium concentration in the background electrolyte.

Thus, the proposed method can be successfully used to determine the amount of Cr (VI) in solutions. It is worth mentioning that the method enables quantitative determination just for Cr (VI), which is deposited as lead chromate.

To determine the total content of chromium, the chromium (III) should be oxidized before performing a second striping voltammetry analysis by similar procedure. The content of chromium (III) is calculates as the difference between the second and first results of the striping voltammetry analysis.

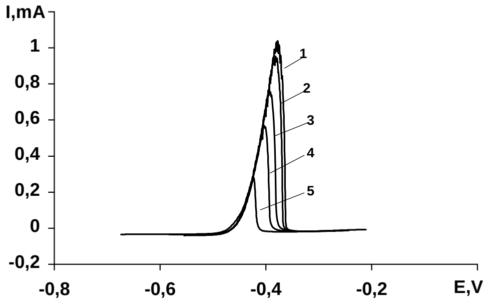

Figure 5. Stripping voltammogram for lead in KNO3 solution with a chromium concentration of: 1-0.02 ppm; 2- 0.041 ppm; 3-0.061 ppm; 4-0.082 ppm; 5-0.1 ppm

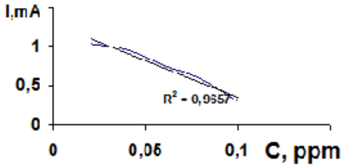

Figure 6. The anode dissolution current for vs chromium concentration in the background electrolyte (0.4M KNO_3)

Reliability of the measurements was verified with the atomic-absorption spectrometer SOLAAR S4. The detection resolution for Cr (III) and Cr (VI) was established to be 0.01- 0.05 ppm, the relative error not exceeding 4%.

REFERENCES

Bersier, P.M., Howell, J. and Bruntlett, C. (1994), “Advanced electroanalytical techniques versus atomic absorption spectrometry, inductively coupled plasma atomic emission spectrometry and inductively coupled plasma mass spectrometry in environmental analysis”, *Analyst*, 119, 219-232.

Brainina, K. and Neyman, E. (1993), “Electroanalytical Stripping Methods”, *Chemical Analysis: A Series of Monographs on Analytical Chemistry and Its Applications*, 1st edition, Wiley-Interscience, Hoboken, 198.

Kiptoo, J., Ngila, J.C. and Silavwe, N.D. (2010), “Speciation studies of selected heavy metals in different water systems: Application of stripping voltammetry and solid-phase extraction employing chelating agents with atomic spectrometric detection”, VDM Verlag Dr. Müller, Saarbrücken, 180.

ESTABLISHMENT OF AVERAGE MOLECULAR STRUCTURE MODEL FOR COLLAGEN EXTRACTED FROM LEATHER SOLID WASTE WITH CHROMIUM

YUNJUN LAN[1], ZHIWEN DING[2], XIAOYAN PANG[2]

[1] *College of Chemistry and Materials Engineering, Wenzhou University, Zhejiang, 325027, email:lanbo3611@163.com2*

[2] *China Leather and Footwear Industry Research Institute Beijing China, 100015, email: pang_xiaoyan@126.com3; ding-zhiwen@263.net1*

Collagen protein was extracted from cowhide leather solid waste with chromium by hydrolysis of alkaline and cycle method. Then different molecular weight ranges of collagen protein were got by ultrafiltration. Collagen protein was characterized by High Performance Liquid Chromatography(HPLC) and Multi-angle Laser Scattering meter and the average molecular weight was got, based on that the average molecular structure model was established. The study will provide the theory basis for the modification research of collagen.

Keywords: collagen; ultrafiltration; average molecular structure model.

INTRODUCTION

Animal skin is the most abundant resources of collagen protein type I. Because the collagen protein molecules has natural unique skeleton, animals' skins were used to make leather. But only about 25% of the raw materials are made skin in leather industry, the rest as solid waste are threw away during leather making process, such as splitting, shaving, buffing and trimming. In the production of leather, the leather solid waste with chromium contains the collagen protein of 90% (calculated by dry basis). Leather solid waste with chromium was produced about 200,000 tons every year in leather industry in China. Recently, the worldwide scholars are committed to the study on reusing of leather solid waste. It is a kind of way that the collagen protein was extracted by the process of alkaline, acid and enzymatic method and then was modified to reuse for the leather solid waste with chromium. As we all know, collagen protein extracted by above simple extraction method contains heavy metals chromium. If the leather solid waste was recycled to the leather fields, it will not to enter the food chain and endanger the health of human body. The classification of collagen protein and the establishment of the average molecular model are the basis for the modification research for reusing the leather solid waste with chromium. Small molecular weight of the collagen protein production was modified to produce leather retanning filling agent, high molecular weight collagen protein production was modified to produce leather finishing agent, which provides an effective way for reusing of leather solid waste with chromium.

EXPERIMENT

Main Chemicals

Cowhide leather solid waste with chromium was provided by Dongming leather Ltd. Co.; MgO, $Ca(OH)_2$ and NaOH are CP; acetonitrile and sodium acetate are Fisher

Scientific; hydrochloric acid is AR. All the chemicals provided by Beijing chemical reagent Co.

Main Equipment

Cup type ultrafiltration system, SCM-310, produced by Shanghai Institute of Applied Physics, Chinese Academy of Sciences; HPLC, Agilent 1100 produced by America Agilent Co.; DAWN EOS Multi angle Light scatterer, produced by America Wyatt Co.

Ultrafitration and Classification for Collagen Protein

Collagen protein molecules with different molecular weight have the different appearance size. Under certain pressure, when the collagen protein of different molecular weight across the hole film with certain pore size, collagen protein molecules with small molecular weight can pass the hole membrane, and collagen protein with big molecular weight will be intercepted. Collagen protein will be speared to different molecular weight from the mixture by a series of pore membrane with different diameter size. And then relatively concentrated molecular weight of collagen protein was got.

Cowhide chromium-contained leather solid waste was used to extracted collagen protein by the method of alkaline and circulation. And the Collagen protein was classified by different size of ultrafiltration membrane.

Alkaline hydrolysis process: add 800% (weight percent) water to cowhide wet blue shaving scraps and use alkaline 5% (weight percent) of MgO, $Ca(OH)_2$ and NaOH respectively, the hydrolysis temperature is 90°.

Circulation hydrolysis process: Leather solid waste with chromium was hydrolyzed and chromium sludge was got after filtered. Filtrate 1 and chromium cake was got after the chromium sludge was hydrolyzed again. Filtrate 2 was got after washing the chromium cake. Then combine the filtrate 1 and filtrate 2 and collagen protein hydrolysate with low concentration was got which was reused to hydrolyze the leather solid waste with chromium high concentration of collagen protein solution was got. The specific process routes see Figure 1.

The ultrafiltration membrane of intercepted molecular weight for 50,000, 30,000, 10,000, 5,000 and 2,000 were used in turn. The collagen protein with different molecular weight range including more than 50,000, 30,000~50,000, 10,000~30,000, 5,000~10,000, 2,000~5,000 and less than 2000 were got.

Collagen Protein Characterization and Establishment of Average Structure Model

High performance liquid chromatography (HPLC) and multi-angle laser scattering were used to determine the molecular weight distribution and the content of amino acid composition of collagen. The amino acid composition of per gram collagen protein mixture was confirmed so as to confirm the average amino acid composition, average molecular formula and average molecular weight. Then the average collagen protein molecular structure model was established based on above research.

The determination of molecular weight distribution: the conditions of performance liquid chromatographic is that chromatographic column: TSK2000; detected wavelength: 230nm; mobile phase: 0.1mol/L PBS containing 0.1mol/L NaCl; flow rate: 0.5 ml/min; loading quantity of sample: 20μl.

The determination of the amino acid composition: protein hydrolysis: 6mol/L HCL, 110°C, hydrolyzed time 16h, DNFB derivative; chromatography SBC18 pillars, detected wavelength 360nm, mobile phase: A 0.05mol/L acetic acid sodium, B 50% acetonitrile, gradient elution; loading quantity of sample: 5μl.

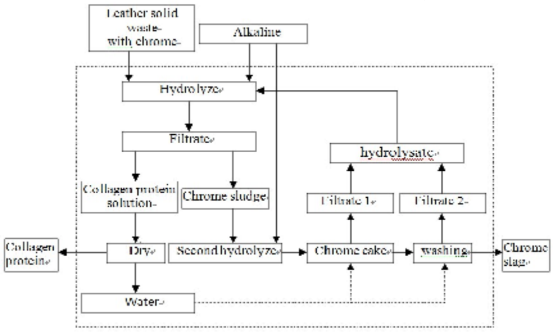

Figure 1. Technique route of small molecular weight collagen protein extracted by circulation method from leather solid waste with chrome

RESULTS AND DISCUSSION

Ultrafitration for Collagen

Collagen solution was graded by above method and the collagen content of different level was determined. The results are shown in Figure 2.

Figure 2 shows the proportion of collagen protein with molecular more than 50,000 is 55.1% hydrolyzed by MgO, 34.5% hydrolyzed by $Ca(OH)_2$ and 6.9% hydrolyzed by NaOH. It is because the basicity of NaOH and $Ca(OH)_2$ is stronger than MgO, so the proportion of collagen protein with small molecules weight hydrolyzed by NaOH and $Ca(OH)_2$ is higher than MgO. The proportion collagen protein with molecules weight less than 10,000 is 48.8% hydrolyzed by NaOH, 23.8% hydrolyzed by $Ca(OH)_2$ and 15.5% hydrolyzed by MgO. Above results shows that molecular weight of collagen protein concentrated relatively was got by ultrafiltration classification.

Collagen protein extracted by alkaline and circulation method was graded by the same way and the results as shown in Figure 3 below.

The results can be seen in Figure 3, for the extraction of collagen protein from leather solid waste with chromium, large molecular weight is got mainly by alkaline method. The proportion of molecular weight more than 30,000 is 79.6% and the molecular weight less than 10,000 is only 9.5%. But small molecular weight is got mainly by circulation method. The proportion of molecular weight less than 5,000 is 62.9% and the molecular weight more than 30,000 is only 15.3%.

From the results of above study, we can see the collagen protein extracted from leather solid waste with chromium can be separated to different range of molecular weight by ultrafiltration method. Molecular weight of over 30,000 can be collected to prepare the protein finishing agent and the molecular weight in below 10,000 can be collected to prepare the retanning and filling agent based on this technology.

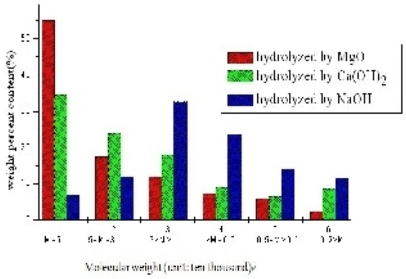

Figure 2. Classification results of collagen hydrolyzed by different alkaline

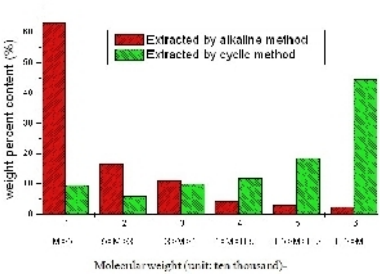

Figure 3. Classification results of collagen extracted by alkaline and cyclic method

Establishment of Collagen Average Molecular Structure Model

Analysis of Amino Acid of Collagen

Table 3 shows the results of amino content of amino acid per 1000 amino acid. The quantity of Glycin is the biggest. There is not tryptophan in the collagen protein.

Average Molecular Weight

Figure 4 is the spectrogram of Reverse Phase HPLC of amino acid composition. Figure 5 is the distribution of collagen molecular weight. The percent of collagen with different molecular weight can be seen from Figure 5 and Table 1. Table 2 shows the number average molecular weight of collagen is 7,018.9.

Establishment of Collagen Average Molecular Structure Mode

Because the collagen protein extracted from leather solid waste is a mixture of different molecular weight, how to show the collagen protein formula has been a problem for a long time. Now a way of average formula for collagen protein is developed and the average molecular structure model was established which is important for the study on the modification of collagen.

From Table 3 we can see the number of amino acid of average each collagen protein molecules is 77, the average collagen protein formula is $C295H456N90O108S$ and the molecular weight is 7,016 g/mol.

Table 4 shows that the number activity group of average 1mol collagen: carboxyl group 10mol, amine group 14mol (including: primary amine 6mol, aliphatic secondary amine 3.5mol, secondary amine on imidazole ring 0.3mol, C=NH 3.5mol), hydroxyl group 13mol (aliphatic hydroxyl group 12mol, phenolic hydroxyl group 0.15mol).

Table 1. Different percent of different molecular weight composition

Molecular weight(unit: ten thousand)	Percent (%)
1.9	2.6
1.1	8.7
0.82	34.9
0.59	27.1
0.46	15.7
0.35	11

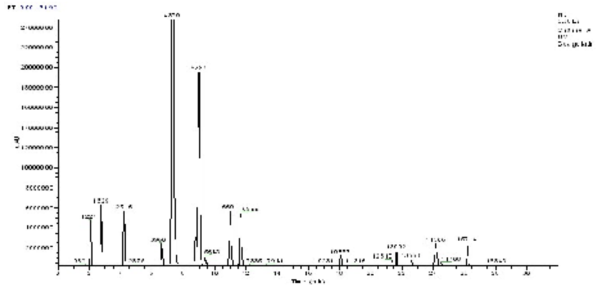

Figure 4. Reverse Phase HPLC of amino acid composition

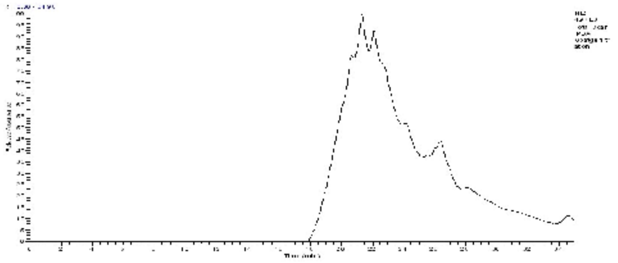

Figure 5. Distribution of collagen molecular weight

Table 2. Analysis of number average molecular weight of collagen protein

Molecular weight (unit: ten thousand)	Percent (%)	Value(unit: ten thousand)
1.9	2.6	0.0494
1.1	8.7	0.0957
0.82	34.9	0.28618
0.59	27.1	0.15989
0.46	15.7	0.072222
0.35	11	0.0385
Number average molecular weight		0.70189

Table 3. Analysis of the establish of average molecular structure model for collagen

Amino acid	Abb	Mw	Amino acid/1000	Total Mw	Proportion %	Molecular formular	Quantity of amino acid
Asparagin	Asp	115	51	5865	6.43	$C_4H_5NO_3$	3.9
Glutamic acid	Glu	129	70	9030	9.90	$C_5H_7NO_3$	5.4
Hydroxyproline	HyP	113	102	11526	12.63	$C_5H_7NO_2$	7.9
Serine	Ser	87	37	3219	3.53	$C_3H_5NO_2$	2.8
Glycin	Gly	57	318	18126	19.87	C_2H_3NO	24.5
Threonine	Thr	101	17	1717	1.88	$C_4H_7NO_2$	1.3
Arginine	Arg	156	46	7176	7.86	$C_6H_{12}N_4O$	3.5
Proline	Pro	97	129	12513	13.72	C_5H_7NO	9.9
Alanine	Ala	71	115	8165	8.95	C_3H_5NO	8.9
Valine	Val	99	21	2079	2.28	C_5H_9NO	1.6
Methionine	Met	131	8	1048	1.15	C_5H_9NOS	0.6
Isoleucine	Ile	113	12	1356	1.49	$C_6H_{11}NO$	0.9
Leucine	Leu	113	23	2599	2.85	$C_6H_{11}NO$	1.8

Amino acid	Abb	Mw	Amino acid/1000	Total Mw	Proportion %	Molecular formular	Quantity of amino acid
Tryptophan	Trp	186	/	/	/	/	/
Phenylalanine	Phe	147	12	1764	1.93	C_9H_9NO	0.9
Histidine	His	137	4	548	0.60	$C_6H_7N_3O$	0.3
Cysteine	Cys	103	2	206	0.22	C_3H_5NOS	0.15
Lysine	Lys	128	31	3968	4.35	$C_6H_{12}N_2O$	2.4
Tyrosine	Tyr	163	2	326	0.36	$C_9H_9NO_2$	0.15
Total			1000	91231	100	$C_{295.2}H_{455.6}N_{90.4}O_{107.6}S_{0.75}$	76.9

Table 4. Num. of activity groups in the average molecular structure model of collagen protein

	Activity group	mol/mol collagen protein
Amine group	Primary amine group	5.9
	Aliphatic secondary amine group	3.5
	Secondary amine on imidazole ring	0.3
	C=NH	3.5
Hydroxyl group	Aliphatic primary hydroxyl group	2.8
	Aliphatic secondary hydroxyl group	1.3
	Secondary hydroxyl group in five membered ring	7.9
	phenolic hydroxyl group	0.15
	carboxyl group	10

CONCLUSION

Collagen was got by hydrolysis of alkaline and cycle method from cowhide leather solid waste with chrome. Then different molecular weight ranges of collagen were got by ultrafiltration. Collagen was characterized by High Performance Liquid Chromatography and Multi-angle Laser Scattering meter and the average molecular weight was got, based on that the average molecular structure model was established. The study has resolved the problem of collagen raw material with composition complex and difficult to characterize which will provide the theory basis for the modification research of collagen.

Acknowledgements

The authors wish to thank National High Technology Research and Development Program of China (863 Program) (Project No.2011AA06A108; National Natural Science Foundation of Republic of China (Project No.21146003) and Open Fund Project of Wenzhou University (Project No.100061200121 and 100061200117) for the financial support.

REFERENCES

Ding, Z., Yu, S., Zhang, W. et al. 2007, “Preparation and Application of amino resin modified collagen protein retanning and filling agent”, *China Leather*, 36(9), 54-57.

Liu, K., Ding, Z., Tang, K. (2007), “Study on the collagen modified polyurethane finishing agent for leather”, *China Leather*, 36(19), 37-40.

Xu, Y., Sun, J., Pang, X., Ding, Z. (2010), “Mechanism of Polyurethane Modified Collagen and its Application (III)—retanning and filling agent of polyurethane modified collagen protein”, *China Leather*, 39(5), 12-14.

Zhao, S. (1998), “Study on the collagen extracted by enzyme from fresh pigskin”, *Science and Technology of Food Industry*, (5), 16-17.

ALTERNATIVES FOR RECOVERY OF PROTEINS EMBEDDED IN CHROME LEATHER WASTES

MIHAELA-DOINA NICULESCU[1], PETER JURKOVIČ[2], JÁN MATYAŠOVSKÝ[2],
CARMEN GAIDAU[1], JÁN SEDLIAČIK[3]

[1] *INCDTP - Division: Leather and Footwear Research Institute of Bucharest, 93 Ion Minulescu St, 3, Bucharest, Romania, icpi@icpi.ro*

[2] *VIPO s.a., Partizanske, Gen. Svobodu 1069/4, 958 01 Partizánske, Slovakia, vipo@vipo.sk*

[3] *Technical University, Faculty of Wood Sciences and Technology, Masaryka 24, 960 53, Zvolen, Slovakia, janos@vsld.tuzvo.sk*

The present research highlights the possibility of extracting the protein component from chrome leather waste in the leather industry through various techniques and using it in various agricultural and industrial applications. To obtain extracts of collagen intended for agriculture, hydrolysis of chrome leather waste was experimented at atmospheric pressure, under enzymatic-alkaline conditions, while collagen extracts for adhesives were obtained through a new process of de-chroming chrome leather waste, in three extraction baths, followed by hydrolysis with inorganic and organic acids, and lyotropic agents. For characterization of collagen extracts chemical analysis techniques (gravimetric, volumetric) and instrumental techniques (potentiometry, AAS, FT/IR ATR, HPLC) were used. New types of collagen extracts, with relatively low average molecular weight (Mmed. <10 kDa) were obtained, enriched in essential amino acids (threonine, valine, phenylalanine, leucine, isoleucine), conditioned for applications as additives in foliar fertilizers, with the role of stimulation and nutrition of plants under stress conditions, as well as concentrated collagen extracts with modeled rheological properties in order to be combined with adhesives in the wood industry (urea-formaldehyde), which led to reductions in formaldehyde emissions from wood materials joined using glue, by about 40%.

Keywords: wastes, protein, recovery.

INTRODUCTION

Chrome leather wastes resulting from natural leather processing can be grouped into two different categories: a) chromium-containing finished leather wastes; b) chromium-tanned leather, wet blue, but only the leather wastes in category b) are likely to induce negative effects on the environment and on human health (Kolomaznik, K., et al, 2008, Font, J. et. al., 1999), under currently practiced uncontrolled storage conditions. For these reasons, research presented in this paper focused on extracting proteins from unfinished chrome leather.

Numerous studies of protein extraction from leather have reported hydrolysis as the most effective process for solubilization of collagenous proteins. By combining the effect of chemical agents with the effect of temperature and period of execution of processes, different stages of collagen hydrolysis are obtained, characterized by average molecular weight of hydrolysates. Using enzymatic hydrolysis for disaggregation of chromium containing leather waste is an option that stands out through the advantages offered by the use of proteolytic enzymes and by the moderate reaction conditions: temperature not too high, up to 70°C, pH between 7 and 10, atmospheric pressure and a lower salt content in collagen hydrolysates (Janocova, D., et al, 2002).

In recent years research (Hrncirik, J. et al, 2005, Taloi, D. et al, 2008) indicates that hydrolysis must be addressed in a complex way, in several stages, with different mechanisms of development, initiated by different chemical agents, which complement each other. Hydrolysis offers the the advantage of obtaining hydrolysates containing amino acids, which recommends them as protein additives for agricultural fertilizers. Other new methods of dechroming leather waste without Cr^{3+} oxidation to Cr^{6+} (Matyašovský, J. et al, 2011) enable the formation of collagen gels, with industrial applications, for example, in the production of adhesives for wood. The most frequently used polycondensation adhesives in the wood industry are the urea-formaldehyde (UF) and phenol-formaldehyde (PF) adhesives. The release of harmful formaldehyde is an open problem, but the free liquid formaldehyde that UP and FP adhesives contain can be related to reactive amino groups that the proteins contain; therefore collagen from leather waste could be a viable solution in modifying classical adhesives.In addition, collagen has adhesive properties. The secondary structure of proteins dispersed in solution may be responsible for increasing the contact area and strength of adhesion to other surfaces such as wood materials, with which it interacts during the hardening process, achieving a strong binding (Sun, S., et al, 2000).

This paper discusses aspects related to the advanced extraction of the protein component from chrome leather wastes resulting from the natural leather processing industry and the possibilities of valorising it in agriculture and the wood industry.

EXPERIMENTAL

Experimental Techniques

In order to obtain collagen hydrolysate for agricultural, experiments were done with hydrolyses of chrome leather waste, at atmospheric pressure, under alkaline conditions (using lime) at temperatures between 70 and 98°C, with durations up to 6 hours, coupled with enzymatic hydrolysis at temperatures up to 70°C, with Oropon ON2 and Alcalase 2.5 L, for 2-4 hours. The collagen hydrolysate for adhesive preparations was obtained by dechroming chrome leather waste, in three extraction baths, followed by hydrolysis with inorganic and organic acids, as well as lyotropic agents (Matyašovský, J. et al, 2011). Collagen hydrolysate thus obtained, with a dry matter content of 45%, was used in proportions of 3%, 5% and 8% as additions to UF resins - Kronores CB 1100 from Kronochem Co.

Methods of Analysis

Chemical analysis techniques (gravimetry and volummetry) and instrumental techniques (potentiometry, AAS, FT/IR ATR, HPLC) were used for characterization of collagen hydrolysates. Free formaldehyde in plywood samples was determined according to standard method EN 120 (perforator method), and formaldehyde emission from plywood was determined using standard method EN 717-1 (chamber method).

RESULTS AND DISCUSSIONS

Characterization of Collagen Hydrolysates

Dermal substance content from collagen hydrolysate is an important parameter in the hydrolysis process, and Figure 1 highlights the fact that the highest value, 90.98% in dry matter, was recorded as a result of alkaline hydrolysis at the temperature of 80°C, for 6 hours.

Average molecular weight of hydrolysates, Figure 2, is found in a relation well defined by the ratio of total nitrogen and amino nitrogen, which shows the degree of conversion of total nitrogen into amino nitrogen and which decreases as the degree of hydrolysis increases.

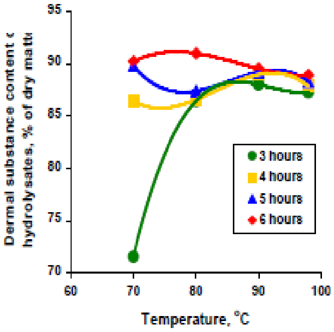

Figure 1. The influence of temperature on the dermal substance of hydrolysates

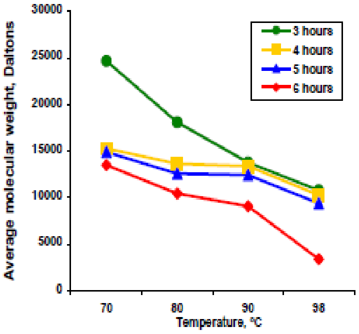

Figure 2. Variation of average molecular weight of collagen hydrolysates in relation to temperature

For process optimization, the solution of relaunching the hydrolytic process under milder conditions, but providing an enrichment in amino nitrogen of the hydrolysate, with an effect of reducing the molecular weight of collagen hydrolysate below the 10000 Da value, is the most favourable solution. Enzymatic hydrolysis brings significant improvements in terms of reducing molecular weights and thus in terms of amino acid content of collagen hydrolysates obtained by alkaline hydrolysis. In Figure 3 it can be noted how the enzymatic hydrolysis helps polypeptide chains to split, leading to increased amino nitrogen content and thus reducing the average molecular weight.

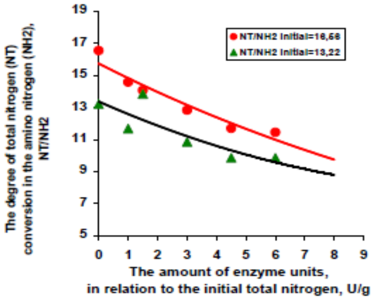

Figure 3. The influence of enzyme amount on the hydrolysis degree

Although collagen hydrolysates were obtained from chrome leather wastes, it was found that they can be considered free of chromium, because atomic adsorption spectrometry revealed that they have a chromium content of 15 to 45 ppb (10^{-9}), situated within the upper limit of 50 mg/l for drinkable water.

Amino acid content of alkaline hydrolysates, compared to that of alkaline-enzymatic hydrolysates, determined by HPLC chromatography, is presented in Table 1.

Table 1. Amino acid content of collagen hydrolysates

No.	Amino acids	Content, mg/100ml, of hydrolyzed collagen, derived from hydrolysis: A - alkaline, AE - alkaline enzyme			
		A1	AE1	A2	AE2
1	Ac. aspartic	2.72	10.10	32.91	19.88
2	Ac. glutamic	6.35	11.17	24.53	16.54
3	Serine	4.33	5.64	193.29	99.95
4	Histidine	2.95	20.17	38.41	29.66
5	Glycine	6.74	1.37	26.49	17.53
6	Threonine	-	15.12	-	-
7	Alanine	13.63	7.39	-	-
8	Tyrosine	-	-	-	75.31
9	Valine	-	7.45	-	53.56
10	Phenylalanine	-	-	-	32.96
11	Isoleucine	-	1.24	-	49.14
12	Leucine	-	4.49	-	139.45
13	Proline	36.07	0.21	25.36	35.75
	Total	72.79	84.35	340.99	569.73

Applications in Agriculture

It should be noted that enzymatic hydrolysis has an important contribution to enriching hydrolysates with amino acids, including essential amino acids (threonine, valine, phenylalanine, leucine, isoleucine). The presence of essential amino acid in collagen hydrolysates is important for applications in agriculture, as they are precursors of many bioactive substances which stimulate the metabolism of plants, their growth and development. In the metabolic process, amino acids are used by plants in the synthesis of their protein. Free amino acids penetrate plant cells, where they increase photosynthetic activity and chlorophyll synthesis, and their role is manifested especially under stress conditions (Gaidau, C. et al, 2009). Control of amino acid content in collagen hydrolysates by further hydrolysis enables the formulation of a wide range of foliar fertilizers with distinct roles in any period of vegetation, as well as the development of new classes of fertilizers for different types of crops.

Applications in the Wood Industry

Adhesive compositions for the wood industry are a viable alternative to applications of collagen recovered from chrome leather wastes. For these applications, specific parameters that control both technical performances in the binding process and ecological implications were studied.

It was found that the addition of concentrated collagen hydrolysate, obtained from chrome leather waste, in the composition of urea-formaldehyde resin does not significantly affect the polymerisation time of adhesive blends, ranging between 74-77 seconds, compared to the standard sample for which it is 78 seconds.

Dynamic viscosity, however, recorded significant changes in relation to the amount of collagen hydrolysate in the composition and the time elapsed from the mixture preparation, aspect illustrated in Figure 4. Apparently, the experiments show that the addition of 8% collagen hydrolysate is the most favourable solution, because in the range of 170-320 minutes, dynamic viscosity is at the same level as the standard adhesive.

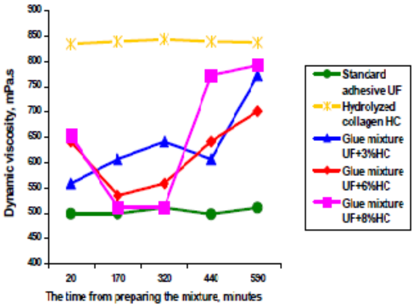

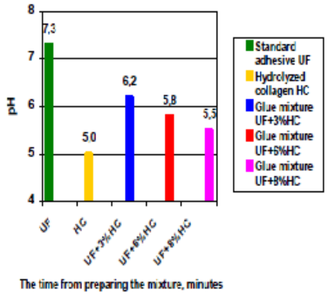

Figure 4. Dynamic viscosity of collagenous adhesive blends

Figure 5. pH change of adhesive blends

However, in practical terms, for acceptable deviations for this parameter, compared to standard UF adhesive, in as wide a range of time, the addition of collagen hydrolysate should not exceed a value of 6%. The impact degree of the pH value, illustrated in Figure 5, supports this aspect. pH is an important parameter in practical terms, as a too acidic or too alkaline pH may degrade the structure of elements the adhesive preparation comes into contact with.

In terms of environmental implications, the most important parameters in the binding process are free formaldehyde content and formaldehyde emission. Free formaldehyde content of plywood, determined through the perforator method, is situated in the range of 2.0-2.2 mg/100g dry material, for samples bound with UF-collagen hydrolysate mixture for the control sample, bound with standard UF adhesive it is 5.2 mg/100g dry material; therefore approximately 2.5 times lower.

The influence of collagen hydrolysate addition in urea-formaldehyde adhesive on the formaldehyde emission is shown in Figure 6 and can be quantified by a reduction of emission by approximately 40%.

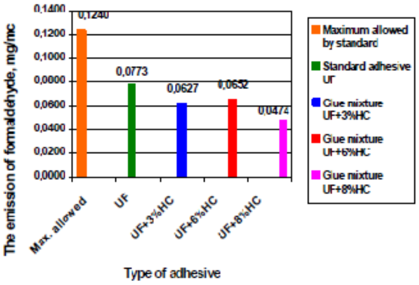

Figure 6. Formaldehyde emission from plywood

The results of FTIR-ATR spectroscopy analysis are comparable with reports from the literature (Essawy, H.A., et al, 2009, Belbachir, K. et al, 2009), and confirm the chemical reactions between UF resin and collagen hydrolysate.

CONCLUSIONS

Chrome leather wastes are an economic source of proteins with applications in agriculture and industry.

Collagen hydrolysates obtained by alkaline hydrolysis and enriched in amino acids by complementary enzymatic hydrolysis can be used as additives in the composition of foliar fertilizers.

Control of amino acid content in collagen hydrolysates by further hydrolysis enables the formulation of a wide range of foliar fertilizers, specific to certain crops or periods of vegetation.

Dechroming chrome leather shavings, using an innovative process, without oxidation of Cr^{3+} into $Cr^{6+,}$ allows obtaining concentrated hydrolysates, suitable for preparations with adhesive properties.

Using mixtures of urea-formaldehyde adhesives with collagen hydrolysate leads to reduction of formaldehyde emissions from bound wood materials by approximately 40%.

Acknowledgements

This paper was written in the framework of bilateral cooperation project Romania-Slovakia „Innovative materials from leather industry by-products", financing contract no. 466/28.02.2011, concluded with UEFISCDI, and contract no. APVV-SK-RO-0022-10 (Slovakia).

REFERENCES

Belbachir, K., Noreen, R., Gouspillou, G. (2009), "Collagen Types Analysis and Differentiation by FT-IR Spectroscopy", *Anal. Bioanal. Chem.*, 395(3), 829-837.

Essawy, H.A., Moustafa, A.A.B., Elsayed, N.H.. (2009), "Improving the Performance of Urea-formaldehyde Wood Adhesive System Using Dendritic Poly(amidoamine)s and Their Corresponding Half Generations", *J. Appl. Polym. Sci.*, 114, 1348-1355.

Font, J. et. al. (1999), "Influence of Various Factors on Chromium (VI) Formation by Photo Aging", *J. Soc. Leather Techol. Chem.*, 83, 300.

Gaidau, C., Ghiga, M., Stepan, E., Taloi, D., Filipescu, L. (2009), "Additives and Advanced Biomaterials Obtained from Leather Industry By-products", *Rev. Chim.*, Bucharest, 60(5), 501-507.

Hrncirik, J., Dvorackova, M., Hruska, F., Kupec, J., Kolomazik, K. (2005), "Kinetics of Alkaline Hydrolysis of the Insoluble Protein Fraction Following Enzymatic Hydrolysis of Chrome-Tanned Shavings", *J. Am. Leather Chem. Assoc.*, 100(1), 1–7.

Janocova, D., Kolomaznik, K., Vasek, V. (2002), „Optimization of Chrome Shavings Treatment by Enzymatic Digestion", International Carpathian Control Conference ICCC Malenivice, Czech Republic.

Kolomaznik, K., Adamek, M., Andel, I., Uhlirova, M. (2008), "Leather Waste - Potential Threat to Human Health, and a New Technology of its Treatment", *J. Hazard. Mater.*, 160(2-3), 514-520.

Matyašovský, J., Sedliačik, J., Jurkovič, P., Kopný, J., Duchovič, P. (2011), "De-Chroming of Chromium Shavings without Oxidation to Hazardous Cr6+", *J. Am. Leather Chem. Assoc.*, 106(1), 8-17.

Sun, S., Zhong, Z. (2000), "Adhesives from Modified Soy Proteins", in *Proceedings of the Wood Adhesives 2000 Nevada*, Forest Prod. Soc., 5–6.

Taloi, D., Gaidau, C., Niculescu, M. (2008), "Leather Waste Hydrolysis Assisted by Active Mathematical Modeling", in Proceedings of the 2nd International Conference on Advanced Materials and Systems, Bucharest, 23-24 Oct. 2008, 319-324.

RECENT DEVELOPMENTS IN CLEANER PRODUCTION AND ENVIRONMENT PROTECTION IN WORLD LEATHER SECTOR

SENGODA GOUNDER RAJAMANI

International Union of Environment (IUE) Commission of IULTCS, Chennai- 600 028, India, email: dr.s.rajamani@gmail.com

International Union of Environment (IUE) Commission of IULTCS has got 40 technical members from all major Leather producing countries, UNIDO and European Union (EU). The recent environmental regulations and systems developed in world leather sector with specific reference to Europe, India, China and Latin America are dealt in this technical paper. The safe disposal of sludge which is estimated about 5 million tons/year from the world leather sector is one of the major unresolved issues in many countries. The leather production activities, especially raw to semi finishing processes are being shifted from United States, West European countries and Japan to Asian and South American countries. Environmental regulations and standards are similar in developing and developed countries. Certain parameters are more stringent in developing countries when compared to the developed countries. Major investments are being made for the environmental systems and resettlement of tanneries from the urban areas to the industrial parks. New regulations such as restriction on use of chemicals, control on salinity and water recovery under zero discharge concepts, management of chromium containing sludge etc. envisage continued Research & Development activity.

Keywords: Environment, IUE Commission, World Leather

INTRODUCTION

The International Union of Environment IUE Commission is a vibrant wing of IULTCS with about 40 technical members from 32 countries and invitees from United Nations Industrial Organization (UNIDO), European Union (EU) and other relevant international organizations. The IUE Commission regularly meets every year in one of the member countries and update the development. The meeting for the year 2011 was held during September 2011 in Valencia, Spain. The next meeting is scheduled during October 2012 in Montevideo, Uruguay. The lists of IUE members are given in Table 1.

Table 1. Members of IUE Commission

S.No.	Country	Representatives
1.	Argentina	Ms. Patricia CASEY / Mr. Carlos CANTERA
2.	Australia	Ms. Catherine MONEY
3.	Austria	Dr. Hans ANDRES
4.	Brazil	Ms. Katia Fernanda STREIT, Prof. Dr. Mariliz Gutterres
5.	China	Mr. Chen ZHANGUANG / Madam ZHANG SHUHUA / Mr Su CHAOYING
6.	Colombia	Mr. Juan Manuel SALAZAR
7.	Croatia	Mr. Jakov BULJAN
8.	Czech republic	Prof. Dr. Karel KOLOMAZNIK
9.	Denmark	Mr. Johannes O. Borge
10.	European Union	Mr. Gustavo Gonzalez Quijano, Bruxelles, Belgium
11.	France	Mr. Thierry PONCET, Secretary IUE
12.	Germany	Dr. Heinz Peter GERMANN
13.	Greece	Mr. Pantelis PANTELARAS
14.	India	Dr. S. Rajamani, Chairman, IUE Commission

S.No.	Country	Representatives
15.	Italy	Dr. Gianluigi Calvanese
16.	International Tanners Council, UK	Mr. Paul Pearson
17.	Japan	Dr. Keiji Yoshimura
18.	Mexico	Mr. Ricardo Weiss
19.	New Zealand	Ms. Ngaire Foster
20.	Poland	Dr. Maciej URBANIAK
21.	Portugal	Mr. Filipe Crispim
22.	Romania	Dr. Luminita Albu / Dr.Loannis Loannidis
23.	Slovenia	Dr. Anton GANTAR
24.	Spain	Dr. Rita Puig / Dr.Lluis Labastida Azemer
25.	Switzerland	Dr. Campbell Page / Dr Jens FENNEN
26.	The Netherland	Mr. Arnold Mulder
27.	Taiwan	Mr. George Huang / Mr.Thomas Yu
28.	Tunisia	Dr. Abdessatar TOUMI
29.	Turkey	Dr. Volkan CANDAR / Dr Murat TOZAN
30.	UNIDO, Vienna	Mr. Ivan Kral
31.	United Kingdom	Dr. Wolfram SCHOLZ / Ms.Christine Ohren-Bird
32.	United States	Mr. E Hurlow / Mr.Mainul Haque
33.	Uruguay	Mr. Ricardo Hourdebaigt

WASTE DISCHARGES AND ENVIRONMENTAL MANAGEMENT

The capacity of world leather process is 15 million tons of hides and skins per year. Wastewater discharge from tanneries is more than 600 million m^3/ year. The estimated solid waste generation from tannery process is about 6 million tons/year. The disposal of large quantity of sludge which is about 5 million tons/year from effluent treatment plants is one of the major unresolved issues in many countries.

The IUE commission has developed essential guidelines and practices adopted in cleaner production, treatment of effluent, solid waste management and environmental regulations. The updated IUE documents with number and title are given in Table 2.

ENVIRONMENTAL UPDATES

Almost all the leather processing countries including Asian and African countries have introduced pollution control standards similar to the standards adopted in United States, European Union and other developed countries. In view of the serious environmental issues, cleaner production and implementation of Common Effluent Treatment Plants (CETPs) in tannery clusters, relocation and resettlement of tanneries from urban towns to designated industrial areas had been done in countries such as Spain, Turkey, India, China etc with major investments. Many countries such as Bangladesh, Egypt etc. have planned to relocate the cluster of tanneries from the cities to new industrial zones with CETPs.

Table 2. IUE Commission Documents

S.No.	Doc.No.	Title
1.	IUE 1	Recommendations on cleaner technologies for leather production
2.	IUE2	Recommendations for tannery solid by-product management
3.	IUE 3	Document on total dissolved solids in tannery effluent

S.No.	Doc.No.	Title
4.	IUE 4	Assessment for chromium containing waste
5.	IUE 5	Typical performance for tannery wastewater treatment
6.	IUE 6	Typical pollution values related to tannery processes
7.	IUE 7	Chargeable effluent parameters in various countries
8.	IUE 8	Recommendations for odour control in tannery
9.	IUE 9	Recommendations for sewer adapted for tannery effluents
10.	IUE 10	Guidelines for restricted products in leather
11.	IUE 11	Recommendations for occupational safety and health aspects

The sustainability of the small-scale units has become a serious issue in leather sector due to enforcement of environmental regulation in many countries 400 small-scale tannery units have been closed in China during 2007 to 2009. Currently environment is the major area of research carried out by the leather research institutes and universities. More than 50% of the research publications in the world leather sector deal with cleaner production & waste management.

With a view to control salinity and environmental protection in countries such as Brazil the hides and skins from the slaughter house needs to be processed immediately without preservation using common salt. During the International recession period there was no demand for the wet blue/finished leather, and the disposal of unsalted hides and skins had become a major environmental issue in Brazil. Currently the organized slaughter houses in Brazil and other countries are building their own tanneries to process fresh hides and skins without applying salt for preservation. Management of high chlorides and salinity in the tannery effluent has become a serious environmental threat in many countries including Spain, India & China etc. They have started adopting membrane system for water recovery and costly treatment of the saline rejects from the membrane system.

The recent developments in cleaner production and waste management in selected leather producing countries are given in Table 3.

SUSTAINABILITY IN MEETING ENVIRONMENTAL CHALLENGES

The leather production activities especially raw to semi-finished leather are being shifted from the developed nations such as United States, West European countries, to North African, Asian and Latin American countries. The major leather producing countries such as China, Italy, India etc. are facing problems due to enforcement of stringent regulations. The sustainability of the small-scale units is becoming a serious issue to meet the environmental requirements. Major investment is being made for environmental protection and resettlement of tanneries from the urban areas to the industrial parks with common effluent treatment plants. New regulations such as ban on use of certain chemicals, salinity and water recovery under zero discharge concept, disposal/ management of chromium containing sludge etc. envisage continued research & development activity. Innovative tanning processes which will greatly reduce are prevent the water usage are needed together with reduction of chromium and other chemicals use.

Table 3. Research & Development in Environmental Protection

S.No.	Country	Research & Development
1.	ARGENTINA	R & D on Cleaner Production, Establishing standard procedures in analysis and publication, Environmental Regulations through Commission of Ecology Control. Restriction / Refusal for the disposal of chrome containing sludge to the common landfill "Green Peace" Movement targets for effluent treatment and management are some of the recent challenges in Argentina.
2.	BRAZIL	Photo-Electro Oxidation and Electro dialysis for water recovery and reuse. R&D activities in the Federal University of Rio Grande do Sul and SENAI Leather Center. Controlled incineration of chromium tanned wastes and development of constructed wetlands for effluent treatment in some tanneries at pilot scale are some of the recent field applications. Meeting toxicity standards, restriction in the disposal of chrome containing sludge even in common secure land fill site is one of the recent challenges.
3.	CHINA	Currently there are about 800 tanneries. Till now, about 12 CETPs are in operation, Some more are under planning. Planned to reduce volume by 10% and pollution load at source. The tanneries are permitted to expand the capacity without increase in the water usage. One of the major tanneries has implemented the MBR and RO system for water recovery and reuse. As such there is no specific restriction on the Total Dissolved Solids (TDS) or salinity norms for the disposal of treated effluent. However meeting the BOD, COD norms for the saline streams from RO is one of the issues to be addressed. As a sustainability measure new license are given to tanneries with process of capacity of more than 3000 tons /year.
4.	COLOMBIA	In view of the serious environmental issues, cleaner production, implementation and maintenance of Effluent Treatment Plants have become necessary in all the tanneries in Colombia. During the recent years, there had been many changes in the regulations related to environmental impacts for the general industry in Colombia. Those changes are related to waste water discharges and now the latest addition is odour control.
5.	FRANCE	Tallow extracted from fleshing converted into alternative energy source, Reed bed system is installed for effluent treatment.
6.	INDIA	Designed to establish a biggest CETP in Asia with a budget of about 60 million USD in Kanpur city with a capacity of 48,000 m3/day (48 MLD) for 450 tanneries. Zero Liquid Discharge concept by adopting membrane system for recovery of water from tannery effluent has been implemented in the South Indian tanneries at a cost of about 100 million USD. Disposal of the saline stream from membrane units in land locked areas is one of the unresolved technical issues. Decentralized secure landfill system linked with CETPs for leather sector had been implemented in many tannery clusters. (First of its kind in the world). R&D activities on bio processing are under progress.

S.No.	Country	Research & Development
7.	NEW ZEALAND	Enzymes and unhairing process is becoming more popular. Elimination of salting of skins by introducing chilling process in selected areas, Sulphide oxidation, pH & settleable solids control and discharge of effluent into public sewer system.
8.	POLAND	Processing of organic materials and converting into fuel called as bio-coal, Co-fermentation of chromium-free tannery wastes with municipal sewage sludge and conversion into fertilizer.
9.	ROMANIA	Cleaner Production programmes are being carried out with the co-operation of INCDTP / ICPI, Institutions COTANCE etc. in Romania.
10.	SPAIN	The tannery clusters with CETP are located in Igualada near Barcelona and Lorca near Murca a coastal town in the southern part of Spain. The individual tanneries with ETPs and leather product units are located around Valencia and in Vic (Barcelona). The CETP in Igualada with a capacity of 9 MLD has been established with a capital cost of 13 million Euro. Under utilization of the CETP, high operation costs and disposal of hazardous category sludge are some of the issues to be addressed. Membrane Bio Reactor with Reverse Osmosis (RO) for water recovery has been established in a CETP near Lorca. The water recovery system from a tannery CETP is first of its kind in the world and was commissioned during 2004-2005. The system has faced with some technical and economical issues in saline water evaporation system in the landlocked area. R & D activities on cleaner production and waste minimization are being carried out by the institutions in Spain: INESCOP, AIICA and EEI (Universitat Politecnica de Catalunya)
11.	TAIWAN	Currently there are about 50 tanneries in operation in Taiwan. The tanneries are having individual treatment plants with capacities ranging from 300m3–2000m3/day. They adopt conventional physio-chemical and biological treatment systems.
12.	TUNISIA	Integrated cleaner production programme has been carried out for 12 vegetable tanneries in Tunisia, Research & Development on solid sludge is under progress in co-operation with CTC.
13.	TURKEY	Two major CETPs have been established and are in operation near Istanbul (Tuzla) and Izmir. The tanneries had been resettled in industrial zones. R &D activity are being continued on cleaner production. Sludge disposal is a major problem similar to other countries.
14.	UNITED KINGDOM	Bio-diesel from tallow, Bio-ethanol from protenised wastes; short-term preservation of raw hides; technical assistance on cleaner production; adoption of membrane system etc. to other countries.
15.	URUGUAY	There are about 23 working tanneries in Uruguay. Two of them are bigger ones and about six of them are medium scale units. The big and some of the medium tanneries have effluent treatment plants and they have also specific secure landfill places to dispose the solid wastes. Many cleaner production projects are being carried out with the involvement of several organizations. Currently, the main environmental problem to be addressed in Uruguay is the disposal of solid waste generated by the tanneries located on the Southern part of the country.

Acknowledgement

The contributions of the IUE members listed in Table 1 from all the 33 countries, UNIDO and European Union are acknowledged. Special efforts and inputs from Mr. Ivan Kral, UNIDO, Mr. Thierry PONCET, Ms Catherine MONEY, Prof. Dr. Karel KOLOMAZNIK, Ms. Patricia CASEY, Prof. Dr. Mariliz Gutterres, Ms. Katia Fernanda Streit, Mr. Chen ZHANGUANG, Madam ZHANG SHUHUA, Mr. Su CHAOYING, Mr. Johannes O. Borge, Dr. Heinz Peter GERMANN, Dr. Campbell page, Mr Jakov BULJAN, Dr. Wolfram SCHOLZ, Mr. Elton Hurlow, Prof. Tony COVINGTON and Dr. Shi Bi technical committee members of IULTCS are greatly acknowledged.

The support and contributions of COTANCE, European Union (EU), National Research & Development Institute for Textile and Leather (INCDTP), Division Leather & Footwear Research Institute (ICPI), Leather Research Institute by name “Asociación Española de las Industrias del Curtido y Anexas (AIICA)” located in Igualada, particularly by Dr.Agusti Marshal, Dr. Ms. Luisa F. Cabeza and Mr. Daniel Sanchez Esteve from Spanish Leather Chemists Association are greatly acknowledged.

Central Leather Research Institute (CLRI), China Leather Industry Association (CLIA), Taiwanese Leather Industry Association (TLIA), Indian Leather Technology Association (ILTA), Latin American Congress Federation of Leather Industry Chemists and Technicians (FLAQTIC 2012) are acknowledged.

REFERENCES

IUE Commission documents (2008), Recent developments in cleaner production and environment protection in World Leather Sector.

Milá, LL., Doménec, X. et al. (2002), “Use of LCA in the procedure for the establishment of environmental criteria in the Catalan ecolabel of leather”.

Minutes of the 2011 IUE Commission Meeting held during September 2011 in Valencia, Spain.

Rajamani, S. and Casey, P. (2010), “Environmental update in Leather Producing Countries – Argentina”, *Leather News India*.

Rajamani, S. et al. (2010), “Environmental Update in Leather Producing Countries – China”, *Leather News India*.

REMOVAL OF IONS FROM DILUTE SOLUTIONS BY EMULSION LIQUID MEMBRANES TECHNIQUE

DEMETRA SIMION[1], GEORGETA POPESCU[2], CRISTINA MĂRUŢĂ[2], CARMEN GAIDĂU[1], HASAN OZGUNAY[3]

[1] *INCDTP - Division: Leather and Footwear Research Institute, 93 Ion Minulescu st., sector 3, postal code: 031215, Bucharest, Romania, demetra.simion@yahoo.com*

[2] *Research Center for Macromolecular Materials and Membranes, Spl. Independentei 206, sector 6, 79611 Bucharest, P.O. Box 15-143, Romania*

[3] *Ege University, Faculty of Engineering, Leather Engineering Department, 35100 Bornova, Izmir, Turkey*

The separation of uranyl ions from dilute solutions can be realized by a facilitated transport using a carrier, dissolved in an membrane. This process was realized by emulsion liquid membranes technique and is a solution to a problem of environmental pollution. By this method, aqueous solutions containing uranyl ions in the range 2–10 mg/L were extracted and concentration reduced to under 0,4 mg/L, so that these solutions can be delivered to surface waters. The inverted emulsions used in extractions were obtained by stirring equal volumes of organic phase and aqueous stripping solution containing NaHCO3 and Span 80. Liquid membranes containing mobile complexing agents have been widely studied in the form of inverted emulsions known as emulsion liquid membranes (ELM). The present work is original because presents the possibility of using ELM method to separate the uranyl ions UO22+ from dilute solutions and waste waters. By dispersing the inverted emulsion Water/Oil in the phase source, a liquid membrane is realized between the two phases, source and receiving solution. In conclusion it was demonstrated the possibility of applying the ELM technique using ammonium quaternary salts as carrier to remove the uranyl ions from waste waters with high extractions yields (85-90%).

Keywords: uranyl ions, organic membrane, emulsion liquid membranes technique.

INTRODUCTION

Liquid membranes containing mobile complexing agents have been widely studied in the form of inverted emulsions known as emulsion liquid membranes (ELM). The method has been proposed for the first time by Li (1971). The present work presents the possibility of using ELM method to separate the uranyl ions UO_2^{2+} from dilute solutions and waste waters. The extraction mechanism implies the use of an ammonium salt, Aliquat 336 (trioctyl methyl ammonium chloride) as carrier, dissolved in the liquid membrane formed of kerosene. The inverted emulsion is obtained by stirring the organic phase (kerosene) containing the carrier with the receiving phase, a solution of $NaHCO_3$, 1M in the presence of emulsifier (Span 80).

By dispersing the inverted emulsion W/O in the phase source, a liquid membrane is realized between the two phases, source and receiving solution.

Extraction of uranyl ions UO_2^{2+} take place if H_2SO_4 is added to the source phase when the uranyl sulfate anion is formed (1):

$$UO_2^{2+} + 2\,SO_4^{2-} \leftrightarrow UO_2\,(SO_4)_2^{2-} \qquad (1)$$

The uranyl – sulfate anion reacts at the interface with the carrier Aliquat 336 to form a complex soluble in organic phase. This complex is transported to membrane / receiving phase where a reaction with HCO_3^- take place to form an insoluble in organic phase uranyl -carbonate complex $UO_2\,(HCO_3)_2^{2-}$ (Fontas et al., 1997; Noble & Stern, 1995; Kobuke, 1980, STAS 1990). In this way, the concentration of uranyl – ions in receiving phase are taking place against the concentration gradient. In the some time, HCO_3^- is transported in countercurrent from receiving phase to source phase.

MATERIALS AND METHODS

The solution of uranyl ions were obtained by dissolving uranium octoxid (U_3O_8) in concentrated nitric acid and dilution with distilled water to concentration between 4–10 mg/L.

The organic membrane were composed of kerosene (Merck) having dissolved the carrier, Aliquat 336 (Fluka) and the emulsifier (Span 80). Equals volumes of organic phase and receiving solutions ($NaHCO_3$ 1 M) were stirred using a Cole & Parmer high speed stirrer to obtain the inverted emulsions. The extraction of uranyl ions from dilute solutions were realized by dispersing the inverted emulsion in the source phase (at 1 :15 ratio) for times between 5-30 min.

The yield of extractions were expressed as the ratio of uranyl ions extracted to initial quantity in system.

RESULTS AND DISCUSSIONS

The main factor that determines the yield of extraction of uranyl ions is the pH of the source phase as illustrated in Figure 1.

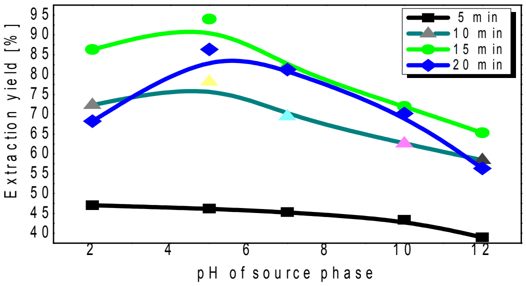

Figure 1. The influence of phase source's pH on the extraction yield

The curve yield versus pH are going through a maximum at around pH=5. The higher yield value are obtained at longer extraction times reaching a plateau. The extending extraction time over a certain value is detrimental probably to the destruction of inverted emulsions during stirring and reintroduction of receiving solution to source phase. The extraction yield are also affected by the emulsion / source phase ratio (Figure 2).

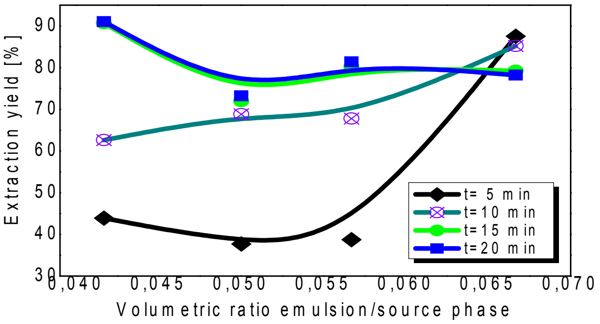

Figure 2. The influence of volumetric ratio emulsion/ source phase on the extraction yield

The extraction yield is also affected by the ratio of organic phase to receiving aqueous phase in inverted emulsion as illustrated in Figure 3.

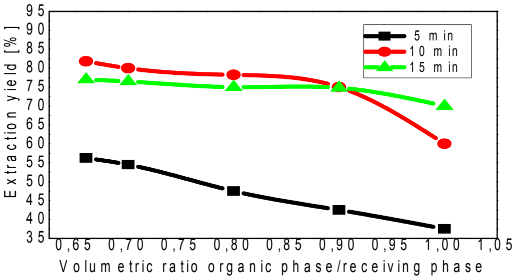

Figure 3. The influence organic phase ratio/receiving phase on the extraction yield

The increase of organic phase to aqueous phase leads to a decrease in yields, the maximum yield being obtained for 1 : 1 ratio.

Besides the yield of extraction versus carrier and emulsifier nature as well as the characteristics of emulsion formulation, the speed of transport from source phase to receiving solution care be characterized by the flux of uranyl ion defined by:

$$\gamma_{net} = \frac{C_{RP}}{MSt} = \left[mol/cm^2.s\right] \qquad (2)$$

where: C_{RP} is the concentration of uranyl ions in the receiving phase after time t, s – area of separation between two phases and M – molecular weight of transported species.

The net flux vs. time is presented in Figure 4.

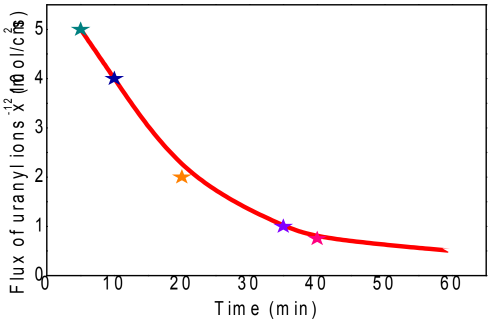

Figure 4. The influence of the time on the uranyl ions' flux

The net flux is decreasing in time as result of diminished concentration in phase source but the value are much higher, 100 times the fluxes obtained in the SLM technique for the same system. These data demonstrates the high efficiency of the ELM method due to higher contact area realized by dispersion of inverted emulsion.

CONCLUSION

It was demonstrated the possibility of applying the ELM technique using ammonium quaternary salts as carrier to remove the uranyl ions from dilute solution (waste waters) with high extractions yields (85-90%) the remaining uranyl ions concentration in the source phase are located under the value admitted for surface water delivery.

REFERENCES

Fontas, C., Antico, E., Salvado, V., Valiente, M., Hidalgo, M. (1997), *Anal. Chim. Acta*, 346, 199-206.
Kobuke, Y., Tabushi, I., Ando, K. (1980), *J. Am. Chem. Soc.*, 102, 5948-49.
Lin, N.N. (1971), *Ind. Eng.*, 10, 215.
Noble, R.D., Stern, S.A. (1995), *Membrane Separation Technology: Principles and Applications*, Elsevier, Amsterdam.
STAS 12849/1-90.

STUDY ON THE RECYCLING OF SOME POLYMERIC MATERIALS: EXPERIMENTAL ANALYSIS

NICOLETA TEODORESCU[1], VIOLETA DOINA PANDELESCU (STROE)[2]
[1] *Politehnica University of Bucharest, Mechanic and Mechatronics Engineering Faculty, Industrial Process Equipment Department*
[2] *S.C. Rolmira S.R.L.*

The paper presents the experimental studies which were done on LDPE and on a new biodegradable polymeric material (which is known that can replace HDPE or/and LDPE), in order to know if it can be recycled and what is the difference between the rheological behaviours of these two materials. From this study can conclude if it is possible to use only recycled polymeric materials to make new products and to establish the limits of the recycling.

Keywords: recycling, biodegradable, rheological behaviours.

INTRODUCTION

The measurement of viscoelastic properties of plastics are most commonly done on molten polymers (Ştefănescu et al., 2009). For these experiments there were chosen two polymeric materials, one is a low density polyethylene grade B21/2.0 from Rompetrol Petrochemical (2008), and the other one is a biodegradable polymeric material Mater-Bi, grade NF803 (produced by Novamont, an Italian research company dedicated to environmental alternatives to polyethylene-based plastics). Both materials are processed by blowing-extrusion on annular die for making thin packaging films, bags and shopping bags.

The paper will show the influence of the recycling process on the rheological behaviour of the two polymeric materials mentioned above.

THE EXPERIMENTAL RESULTS

First it was measured, for each material at the first and at the tenth pass the MFI (melt index flow) in g/10 min, which presented obvious differences, as one can see in the Figures 1 and 2.

On the capillary rheometer were done measures on the two materials resulting the rheograms ($\tau - \dot{\gamma}$). There were performed the two corrections Bagley and Rabinowitsch (Teodorescu, 2003).

Finally there were obtained the rheograms for all the temperatures, but here are presented only a part of them, Figures 3–6.

The rheograms for each capillary were approximated by exponential curves with a good error (R^2 - average square error), which shows that the model is very similar to the experimental results.

LDPE shows changes in molecular weight after recycling. Molecular weight decrease showing a mild slope rheograms (Figure 1 and Figure 2).

The NF803 material becomes sticky and very fluid at 180°C on capillary 1 (L/d=3,521) which is the shortest. At the same temperature on capillary 3 (L/d=12,494), the extrudate shows less elasticity (it can be broken with fingers).

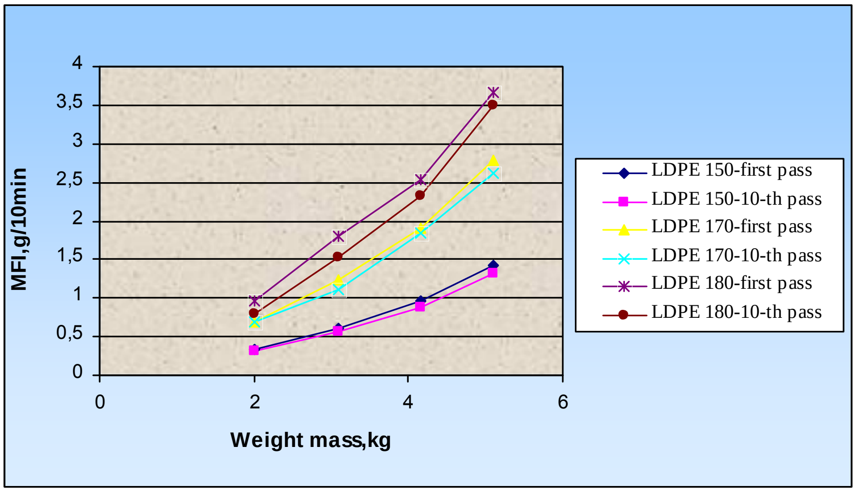

Figure 1. Melt flow index, capillary 2(L/d=6,566), LDPE - first and tenth pass

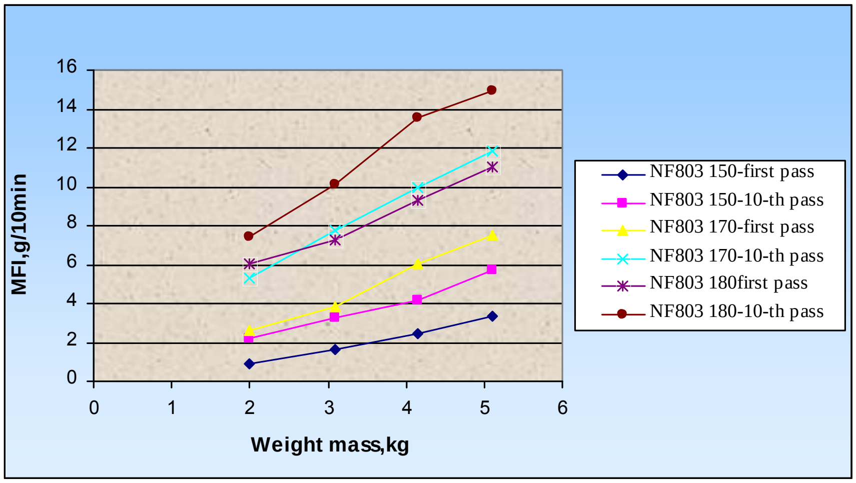

Figure 2. Melt flow index, capillary 2 (L/d=6,566) NF803 - first and tenth pass

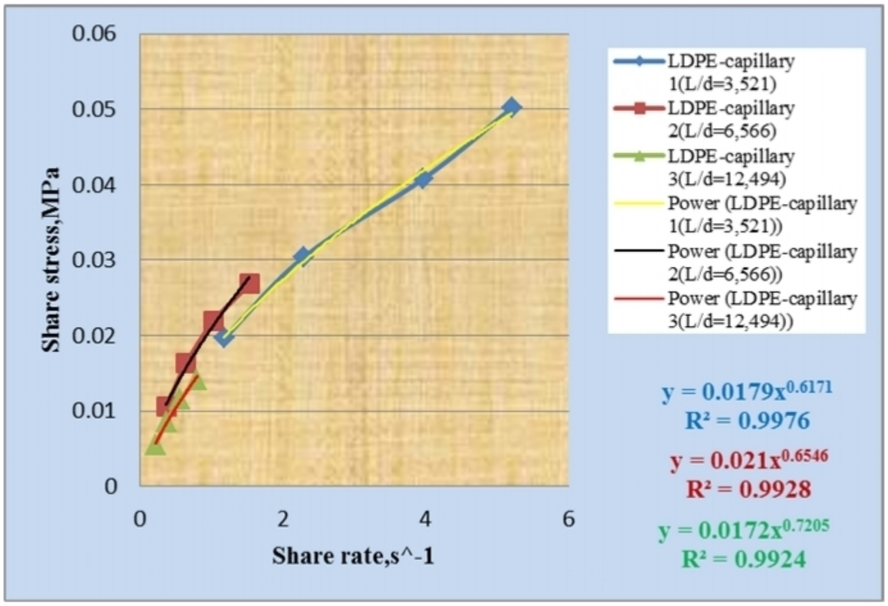

Figure 3. LDPE virgin (the first pass) rheograms, T=150°C

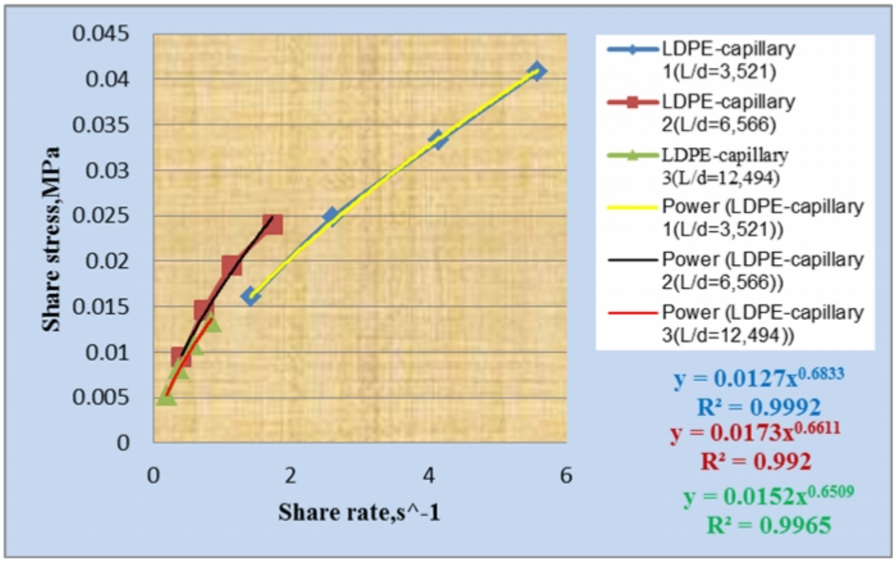

Figure 4. LDPE recycled (the tenth pass) rheograms, T=150°C

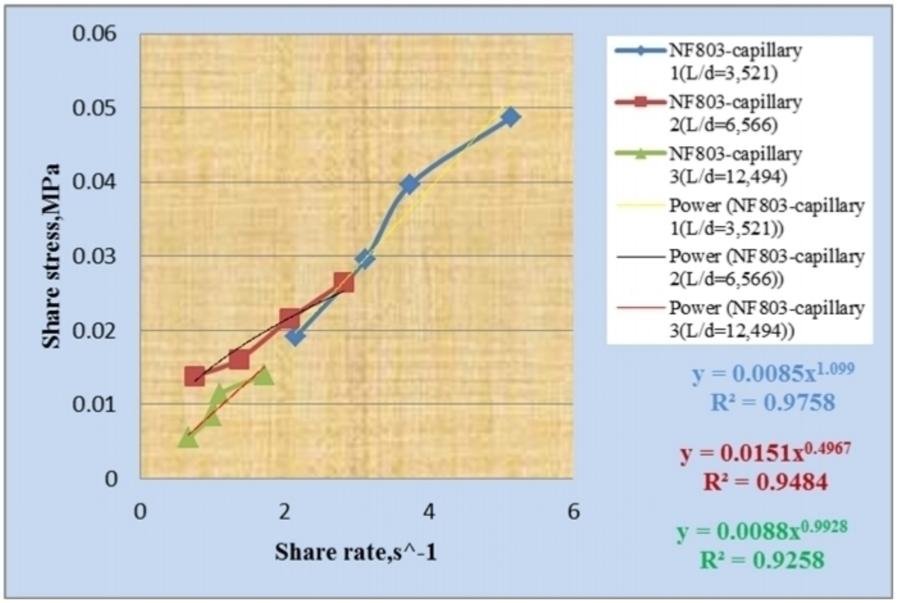

Figure 5. NF803 virgin (the first pass) rheograms, T=150°C

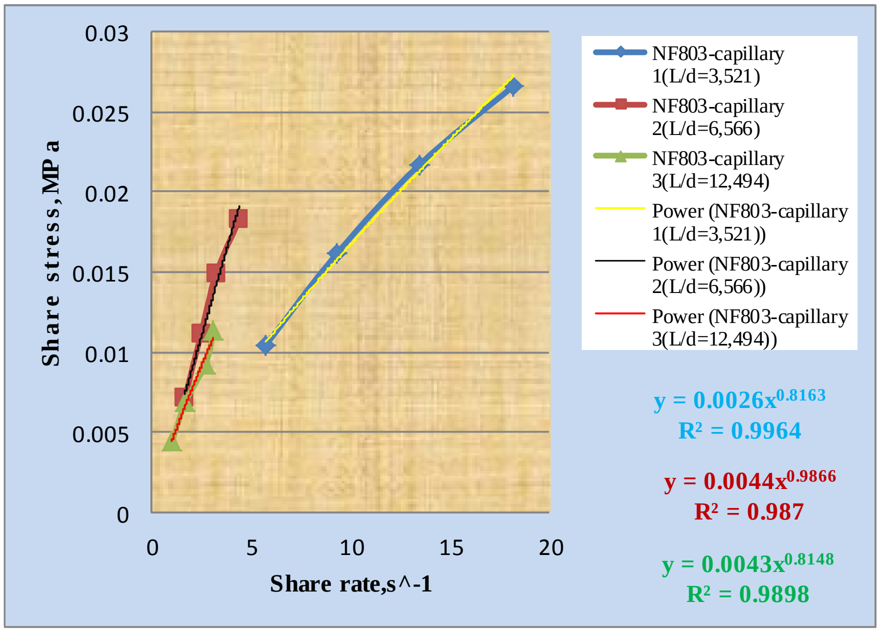

Figure 6. NF803 recycled (the tenth pass) rheograms, T=150°C

After recycling, the rheological parameters m and ν show a non-linear decrease with the temperature for LDPE, more significant form than for ν, as it results from the equations presented in Tables 1 and 2.

Table 1. The temperature influence on the m values – capillary 1 (L/d=3,521)

No.	Polymeric materials		Mathematic models	R^2
1.	LDPE	First pass	$m = 10^{-5} \cdot T^2 - 0{,}0039 \cdot T + 0{,}3719$	1
		Tenth pass	$m = -4 \cdot 10^{-6} \cdot T^2 + 0{,}0012 \cdot T - 0{,}0743$	1
2.	NF803	First pass	$m = 6 \cdot 10^{-6} \cdot T^2 - 0{,}0024 \cdot T + 0{,}2209$	1
		Tenth pass	$m = 3 \cdot 10^{-5} \cdot T^2 - 0{,}01 \cdot T + 0{,}8016$	1

For NF803, the tendency of decreasing for *m* is the same until the temperature approaches the value of 170°C, when a strong increase can be observed (Table 3).

Table 2. The temperature influence on the ν values – capillary 1 (L/d=3,521)

No.	Polymeric materials		Mathematic models	R^2
1.	LDPE	First pass	$v = -0{,}0003 \cdot T^2 - 0{,}1186 \cdot T - 9{,}5199$	1
		Tenth pass	$v = -2 \cdot 10^{-2} \cdot T^2 - 0{,}0006 \cdot T + 0{,}8318$	1
2.	NF803	First pass	$v = -0{,}0002 \cdot T^2 + 0{,}0792 \cdot T - 6{,}0825$	1
		Tenth pass	$v = -0{,}0004 \cdot T^2 + 0{,}1282 \cdot T - 9{,}7327$	1

CONCLUSIONS

- The use and the recycling of the polymeric products cause brutal modifications of the internal structure and of the physical and chemical properties. This determines a significant change in the flow properties at reprocessing.
- The operation of the capillary rheometer may simulate many polymer conversion processes.
- Rheological behaviour of virgin and recycled polymeric materials (LDPE and the biodegradable one) was studied in this paper and there were made rheograms which gives information regarding rheological parameters.
- The rheograms for each capillary were approximated by exponential curves with good accuracy (R^2 – the average square error approaches 1), which shows that the model is in concordance with the experimental results.
- Because of the changes in the molecular weight of the LDPE because of the recycling it was observed a mild slope rheograms (Figure 1 and Figure 2).
- At the first pass, on the capillary 1(L/d=3,521), NF803 has a dilatant fluid behaviour (Figure 3) but at the tenth pass this behaviour changes in a pseudoplastic one (Figure 4) because of the thermo-mechanical degradation of the starch component.
- The NF803 material becomes sticky and very fluid at 180°C on capillary 1 (L/d=3,521) which is the shortest. At the same temperature, on capillary 3 (L/d=12,494), the extrudate shows less elasticity (it can be broken with fingers).
- After recycling, the rheological parameters m and ν show a non-linear decrease with the temperature for LDPE, more significant for m than for ν,

(Tables 1 and 2).

- For NF803, the tendency of decreasing for *m* is the same until the temperature approaches the value of 170°C, when a strong increase can be observed (Table 1).

From the experiments one can conclude that, even the biodegradable polymer can be recycled during its life time, which is a very important thing for the products obtained with the major flaws, avoiding premature disposal. This turns into saving money and less environmental pollution.

For the traditional polymers (in this case LDPE), theoretical, the recycling is unlimited, but it is very important in the processing of the recycled polymers to know how the rheological properties change with the number of the recycling. One can observe that even similar polymers (with almost same properties at the first processing) behave quite different as the number of recycling is bigger. So the experiments (like the ones' presented in this paper) are very valuable for the applications.

REFERENCES

Novamont SpA, Scheda Tecnica Mater-Bi NF803.

S.C. Rompetrol Petrochemicals S.R.L. (2008), SS – 59: B21/2.0-Low Density Polyethylene Standard Specification.

Ştefănescu, M.F., Teodorescu, N., Jugănaru, M.R. (2009), "Ecological use of the solid polymeric wastes-Case study: Plastics properties modifications in the recycling process", The second Int. Conference on Polymers Processing in Engineering, Galaţi, Romania, Oct. 2009.

Teodorescu, N. (2003), *Applied Rheology. Laboratory Guidelines* (in Romanian), Matrixrom.

STUDY ON THE RECYCLING OF SOME POLYMERIC MATERIALS: MATERIALS CHARACTERISTICS; EXPERIMENTAL PROCEDURES

NICOLETA TEODORESCU[1], VIOLETA DOINA PANDELESCU (STROE)[2]

[1] *Politehnica University of Bucharest, Mechanic and Mechatronics Engineering Faculty, Industrial Process Equipment Department*

[2] *S.C. Rolmira S.R.L*

The paper presents the general recycling problems of the polymeric materials biodegradable or non-biodegradable. For this reason there were chosen two materials, one is LDPE and the other one is a new biodegradable polymeric material (which is known that can replace HDPE or/and LDPE).This part presents the physical and mechanical properties of the two materials and the experimental procedures.

Keywords: recycling, biodegradable, plastics.

INTRODUCTION

Plastics are more difficult to recycle than metal, paper or glass. The plastics recycling process normally involves cleaning it, shredding it into flakes, than melting the flakes into pellets. The pellets are melted into a final product. Some products work best with only a small percentage of recycled content and other products can be made successfully with 100 percent recycled content.

The difficulties of plastics recycling consist of their molecular architecture (molecular weight and molecular weight distribution, degree of branching) and rheological behavior. Plastics are complex rheological materials in that they exhibit both viscous and elastic (usually called viscoelastic) properties under varying conditions of stress, strain and temperature (Ştefănescu et al., 2009).

Thermoplastics (at least most of them) are recyclable and reused until their degradation determine poor mechanical properties. The recycling possibilities are: - recycling to obtain new products (when the wastes must be separated in fractions of polymers with similar characteristics); - biological or thermal treatment (if the waste is mixed) in order to obtain biogas (together with other organic waste materials and/or composts) and energy recovery respectively.

Mechanical recycling supposes melting and recasting in order to re-use the plastics in new products. The unavoidable quality losses are not too severe and the energy required is low, so the processing costs are reasonable. The collecting of small size parts can be limitative in terms of money. So it is unrealistic to believe that all plastic debris are mechanical recyclable. It is common accepted that ~20% of the used plastics are to be mechanical recycled .

Feedstock recycling supposes the breaking down of the plastics into chemical and petrochemical feedstock (in liquid or gaseous form), which can be used in the processing of other chemical products. It is generally agreed as a more efficient procedure than mechanical recycling. About 90% of the used plastics could be recycled in this way but the prices can be limitative.

Energy recovery consist in incineration and is the best choice for a number of plastic wastes varieties (including plastics with high proportion of foreign materials even those containing residues) (Teodorescu et al., 2009).

To make an option for the recycling technology one studies the life circle of plastics, which begins with primary resources, continues with extraction and processing, obtained product, use of the product, continues with recycling and disposal which can damage the environment with emissions and waste. (Teodorescu et al., 2009).

The recycling process needs recovery logistics from the consumers (including transportations which require on their turn the use of fossil fuels and generate air emissions). So recycling is admitted only if it requires fewer resources than can be gained by this process.

There is an increasing demand to develop eco-friendly products (that means material produced from renewable resources and highly biodegradation of the product) (Teodorescu et al., 2009), such as bio-plastics.

For producing a bio-plastic product only 65% of the energy consumed by producing a petroleum-based product is needed, which means that by producing only bio-plastic products we will save 35% of the energy we now waste on making traditional plastics. If we take into consideration that annual plastic products used only weights than 50 million tones we will understand why bio-plastic products are so badly needed (Thanate Tan, 2009).

The use and the recycling of the polymeric products (both bio and fossil based) cause brutal modifications of the internal structure, of the physical, chemical, electrical properties which determine a significant change in flow properties at reprocessing. The type and the magnitude of the properties changing depend also on the type of chosen recycling technology. (Teodorescu et al., 2009). So it is very important to know precisely how the processing properties as well as in reuse properties are changing, needing each time a thorough experimental research, which is in our intention to pursue.

In this paper we will present the main physical and mechanical properties of two polymeric materials, one is LDPE and the other one is a biodegradable polymeric material made of renewable raw materials of agricultural origin and from non genetically modified starch.

THE EXPERIMENTS

For the experiments a capillary rheometer (Figure 1), a scales and a PC were used.

The capillary rheometer characteristics are: inner cylinder diameter D = $9{,}5^{+0{,}015}$ mm, heated cylinder length 171.5 ± 0.063 mm, capillary dies dimensions L/d [mm/mm] 8/2.272 (capillary 1), 17,4/2,605 (capillary 2), 30/2.401 (capillary 3), temperature regulator scale 0…400°C, weight masses 2; 2,1; 4,15 and 5,1 kg. The virgin materials were tested at 150°C, 170°C, and 180°C, than nine times recycled, without testing and at the tenth pass the materials were measured at the same temperatures and weight masses. For all recycling experiments the materials were cut approximately at the dimensions of the virgin initial pellets.

To obtain the rheograms (τ-$\dot{\gamma}$), for both materials, from the experimental measurements performed ($\overline{m}$– the average masses of the samples [kg]; t – test time (cutting interval) [s] and G_i – weight masses [kg]) were used the relations (1)-(4) (Teodorescu et al., 2003).

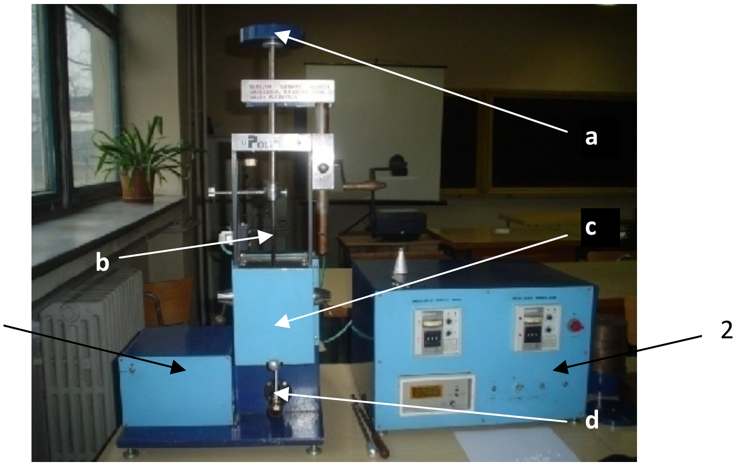

Figure 1. Capillary rheometer (Ştefănescu et al., 2009): 1 - mechanical device; 2 - automation block; a - weight; b - piston; c - heater; d - cutter

$$\tau = \frac{\Delta p}{4 \cdot \frac{L}{d}} \tag{1}$$

$$\dot{\gamma}_{a,p} = \frac{32}{\pi \cdot d^3} \cdot Q_v \tag{2}$$

$$\Delta p = 4 \cdot \frac{G_i}{\pi \cdot 9.5^2} \tag{3}$$

$$Q_v = \frac{\overline{m}}{t \cdot \rho} \tag{4}$$

where the symbols are: τ – share stress [Pa], $\dot{\gamma}$ – share rate [s^{-1}], Δp – pressure drop [Pa], L/d – capillary dies dimension, L – capillary length, d – die diameter, Q_v – flow rate, [m^3/s].

For the experiments were used:

A) a low density polyethylene grade B21/2.0 (produced by Rompetrol Romania) which has the properties presented in Table 1.

Table 1. LDPE properties (S.C. Rompetrol Petrochemicals S.R.L., 2008)

Properties	UM	Limits	Test method
Appearance:	-	Uniform color granules without extraneous matter	Visually
Contamination (oxidizes and other defects)	% m/m	Max. 0,01	Visually /Gravimetrically
Physical			
Melt flow index(3) (190°C, 2,16kg)	g/10 min	1,8 - 2,20	ASTM D1238
Density (23^{0}C)(1,3)	g/cm^3	0,919 - 0,925	ASTM D792
Thermal			
Vicat softening temp. (1,2) (A-50°C/h-10N)	°C	Min.90	ISO 306/A
Mechanical/optical properties for film(4)			
Tensile strength at brake(2) (23°C, v = 500 mm / min)			
- machine direction		Min. 13	ISO 527/3
- cross section		Min. 11	
Elongation at brake(2) (23°C, v = 500mm / min)			
- machine direction	%	Min. 200	ISO 527/3
- cross direction		Min. 300	
Haze(3)	%	Max. 10	ASTM D1003
Gloss,45^{0}(3)	UL	Max. 50	ASTM D2457
Slip agent content	Ppm	Min. 350	Own method

1) The medium value of the physical/mechanical and thermical properties is measured on the standard samples made by compression proces (ASTM D4703/C) conditioned at room temperature (ISO 291) or unconditioned (performed in one our maximum from specimen output-nominal density).
2) Periodical tests
3) Batch test
4) Film thickness-0,04mm,Blow up rate-1:2

Aplications: extrusion, clarity films for packages, with a good transparency.

B) a biodegradable polymer Mater-Bi, grade NF803 (produced by Novamont, an Italian research company dedicated to environmental alternatives to polyethylene-based plastics) with the properties presented in table 2.

Table 2. Biodegradable material, Mater-Bi NF803, properties (Novamont SpA)

Properties	UM	Limits	Method	Notes
Melting temperature	°C	110	DSC	granules
Melt flow index (150°C, 5kg)	g/10min	3,5	ASTM D1238	
Density (23°C)	g/cm^3	1,27	Picnometer	granules
Tensile strength at brake	MPa	25	ASTM D882	Film thickness-0,03mm
Elongation at brake	%	300	ASTM D882	Film thickness-0,03mm

Properties	UM	Limits	Method	Notes
Young module	MPa	230	ASTM D882	Film thickness 0,03 mm
Share strength	N/mm	45	ASTM D1938	i MD
	N/mm	45	ASTM D1938	p MD
	N/mm	76	ASTM D1938	i MD
	N/mm	76	ASTM D1938	p MD
Haze	%	89	ASTM D1003	
Water vapour permeability	Gx30μm/m^{2}x24h	700	ASTM E398	Film of 30μm, 38^0/90%RH

Mater-Bi is the first completely biodegradable and compostable bio-polymer ever invented. The processes are protected by more than 50 patents. It comes from renewable resources of agricultural origin and from non-genetically modified starch, it reduces greenhouse gas emissions, and the consumption of energy and non renewable resources, and it completes a virtuous circle: the raw materials of agricultural origin return to the earth through processes of biodegradation and composting, without releasing polluants. (Novamont SpA).

This polymeric material respects the fundamental requirements of EN 13432 standard for complete biodegradation under composting conditions which are:

- conversion to CO_2, water and biomass via microbial assimilation of the test material;
- 90% conversion of the test polymer to CO_2;
- same rate of biodegradation as natural materials – leaves, paper, grass and food scraps;
- time of biodegradation – 180 days.

CONCLUSIONS

The NF 803 material has been used in our country since 2009 and was developed as an alternative to polyethylene-based plastics used in packaging industry.

Our intention for the next paper is to know if, in the period mentioned above (180 days), the biodegradable material can be recycled and how the recycling process influence the rheological behavior of the two polymeric materials. So it is also tested, to see how rheological properties changes, the LDPE, to have a comparison possibility, to evaluate the recycling properties for both polymers.

REFERENCES

Novamont SpA, Scheda Tecnica Mater-Bi NF803.

S.C. Rompetrol Petrochemicals S.R.L., (2008), SS – 59: B21/2.0-Low Density Polyethylene Standard Specification.

Ştefănescu, M.F., Teodorescu, N., Jugănaru, M.R. (2009), "Ecological use of the solid olymeric wastes-Case study: Plastics properties modifications in the recycling process", The second Int. Conference on Polymers Processing in Engineering, Galaţi, Romania, Oct. 2009.

Tan, T. (2009), "Bioplastic – An Altenative To Petroleum-based Plastic", available at articlesbase.com.

Teodorescu, N., Ştefănescu, M.F., (2009), "Ecological use of the solid polymeric wastes-Quality and economic limitations", The second Int. Conference on Polymers Processing in Engineering, Galaţi, Romania, Oct. 2009.

Teodorescu, N. (2003), *Applied Rheology. Laboratory Guidelines* (in Romanian), Matrixrom.

RESEARCH ON THE PHYSICAL PROCESSES INVOLVED IN AIR REGIME IN SOIL

PETRE VOICU[1], GABRIEL ZAINESCU[2], DANIELA RADUCU[1], DANA DESELNICU[2], MIRCEA SEVASTEL[3]

[1] *Research Institute for Soil Science and Agrochemistry 61 Marasti Blvd., 71331, Bucharest, Romania*

[2] *INCDTP – Division: Leather and Footwear Research Institute, 93 Ion Minulescu str., 031215, Bucharest, Romania, email: icpi@icpi.ro*

[3] *University of Agronomical Sciences and Veterinary Medicine 61 Marasti Blvd., 71331 Bucharest, Romania*

Technological components of cultivation systems of the soil, especially tillage and all interventions from surface caused by harvesting, harvest transport, maintenance cultivation, have a great impact on soil condition in general, but especially on the physical state of soil, and also have a great impact regarding aeration conditions from the surface and from soil profile. Intensity effects on soil depend on the one hand of the natural conditions in which the soil formed and weather conditions from crop growing season and on the other hand depend on anthropogenic factor generated by the technological system. Because changes in soil aeration are extremely dynamic, determinations regarding characterization of air movement and air content should be made in dynamic during the entire period of air stress. The data obtained are useful in establishing optimal conditions for application tillage systems. Also, knowing aeration conditions specific for different cultivation allows to set necessary need for drainage and to use appropriate agricultural works. Therefore, especially in irrigated areas were more strongly manifested physical processes of soil degradation at surface. Experiments were performed in the south areas from Romania on preluvosoil from Tancabesti/Periş using an apparatus for determining permeability named Eijkelkamp model.

Key words: soil, air, permeability

INTRODUCTION

Technological components of crops, especially tillage and all interventions from the surface caused by harvesting, transport, maintenance have a great impact on soil condition in general, but especially on the physical condition and the conditions of aeration from soil surface and soil profile (Trandafirescu, 1987).

Intensity effects depend on the one hand of the natural conditions where soil is and weather conditions during the growing crop and on the other hand by anthropogenic factor generated by the technological system. Because changes in soil aeration are extremely dynamic determination regarding characterizing air movement and the air content should be made dynamic throughout all the period of air stress. The data obtained are useful in establishing optimal conditions for application of tillage systems. Today it is widely agreed that taking soil in culture, in addition to positive effects, which led directly to increased productivity, had also negative consequences that decrease soil fertility (Canarache, 1990).

The negative effect caused by a layer compaction of soil on air-fluid properties, involves a study to obtain as much information about the process of compaction, its extension and its consequences on plant growth and measurement of air permeability soil should give in this sense, information about the process of compaction, along with other data regarding settlement and hydric regime from soil. In the layer it is evident a stratification, both in terms of the status settlement, alternating layers of soil more compact with the loos, and in terms of accumulation of nutrient, which limits water absorption and root development. Accumulation and movement of macro and micronutrients in soil and their transfer in plant mass (especially phosphorus) is a less studied and cited in the literature (Håkansson, 1992). Anthropogenic soil compaction effects on loading of the soil with polluting elements, conduct of chemical processes such as nitrification and denitrification, oxidation and reduction are also rarely addressed (Soane, 1975, Horn et al., 1993). Applications of measures regarding air movement in soil in compaction studies allow understanding, both short-term effects such as aeration processes taking place in the seedbed and to the long term, such as restructuring the soil after introduction of practical systems with minimal work, zero-tillage, or during the soil self-recovery after the exercise of traffic or poor conditions of work performed.

Synthesis of all research regarding anthropogenic compaction emphasized that the more compact settlement may also have some positive effects on production under low soil moisture, as long as the aeration porosity is not the limiting factor, i.e. no values below 10% v/v (Davies, 1999). Also, knowledge of different cultures aeration conditions and deciding on whether the application allows drainage and appropriate agricultural work. After 1970, agricultural technology systems tillage became more intense, and the soil was becoming increasingly required, especially as a result of generalizing conventional works and to make an excessive number of works for seedbed preparation. Therefore, especially in irrigated areas were more strongly manifested physical processes of soil degradation from surface (Voicu, 2008). One of these experiences was organized in the south of the country on the reddish brown soil fromTancabesti/Peris, determinations are made with permeameter Eijelkamp.

MATERIALS AND METHODS

Air permeability measurements were performed in ICPA with permeameter Eijelkcamp on cylinders harvested from all four types of compaction intensity (0, 2, 5 and 10 crossings), the same cylinder which were subjects to different levels of water retention (pF_1, $pF_{1,6}$, pF_2). It was trying to present the correlation between water content and air from samples, knowing that the two phases are complementary in the soil. Moments of induced of soil compaction were chosen to highlight the possible changes that would occur in the soil, especially in the upper layer, in the autumn (determined mainly by the specific work of harvesting and transport, and the preparation soil for sowing) and spring.

Stages of sampling were performed to separate the effects of anthropogenic from natural factors. Thus, we were able to study the possible effects of natural factors (precipitation and temperature) that acts mainly in winter, with mechanical role in natural processes (wetting and drying, heating and cooling, inflation and contraction) of recovery physical condition of soil.

RESULTS AND DISCUSSION

Effects of the Main Experienced Factors on Soil Permeability to Air

The obtained results refer at two stages from agricultural year: immediately after compaction induced (spring and fall) and after completion of mechanical maintenance works. Results are given for the first 40 cm of soil profile, on four layers from 10 to 10 cm, correlated with depth of the main types of tillage.

Induced moments of compaction in soil were chosen to highlight the possible changes that would occur in soil, especially in the upper layer, in the autumn (determined mainly by the specific work of harvesting and transport, but also determined by the soil preparation for sowing crops) and spring.

The two stages for sampling were performed to separate the effects of the natural factors from anthropogenic factors. Thus, we were able to study the possible effects of natural factors (precipitation and temperature) that acts mainly in winter, with have a great role in mechanical natural processes (wetting and drying, heating and cooling, inflation and contraction) of recovery physical condition of the soil.

Data obtained for samples collected after the autumn compaction is presented in Figure 1 only for extreme variants (C0 and C10).

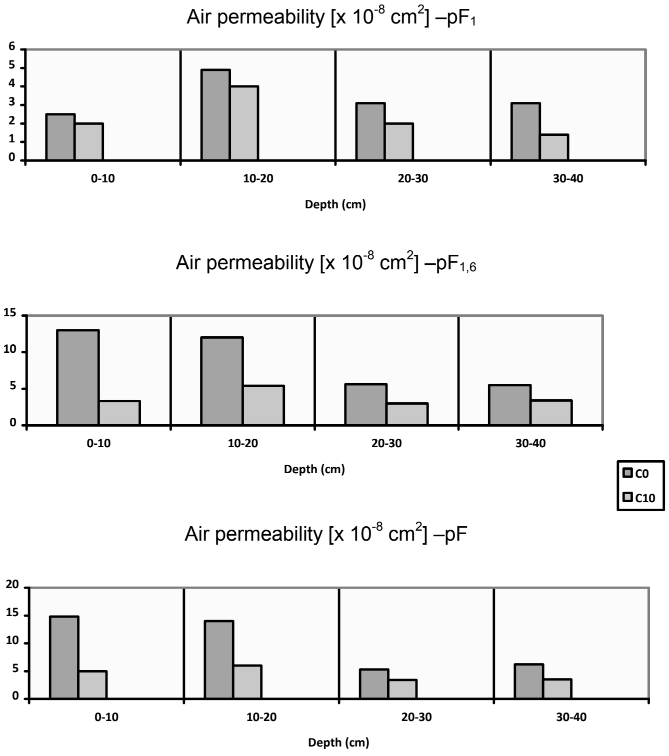
Air permeability [x 10^{-8} cm^2] –pF$_1$

Air permeability [x 10^{-8} cm^2] –pF$_{1,6}$

Air permeability [x 10^{-8} cm^2] –pF

Figure 1. Effect of anthropogenetic compactation on air permeability at different stage of water retention (Tancabesti, Peris)

In version “maximum compacted”, it was found that air permeability is extremely low throughout the soil profile, especially in surface horizons. These results were expected, given that samples were collected immediately after compaction, so the soil had not sufficient time to achieve stability through natural processes, processes like freeze-thaw or wetting-drying, or by anthropogenic processes determined by technological factors. If we look deeper in the profile, air permeability increased slightly in the second depth, reaching a minimum at depth of 40 cm, being in the same range of variation (low air permeability).

Analyzing the obtained data, we can say that in the loose version (control) permeability for air behavior is the one expected: in the upper layer is lower, permeability for air increases significantly with depth (increasing more evident at higher values of the suction, $pF_{1,6}$, pF_2). By comparison, appears unexpected differences in maximum compacted version, in upper layer at all three levels of water retention, air permeability is very high, they are decreasing with increasing the soil profile. High values of permeability for air for this version may be due because of numerous cracks from the soil, which created preferential paths of water and air circulation. The cumulative effect of compaction and maintenance of soil is observed at 10-20 and 20-30 cm depths; where at higher suction growth is not as obvious as the witness version, although air permeability increases. The results led to conclusion that work in the spring and summer (from seedbed preparation, maintenance cultivation) has the greatest importance in the appearance and development of more compact layers in the soil profile, at least in the first 40 cm.

In general, aeration conditions in the upper soil profile are much improved, being in agreement with other physical properties: apparent density, water content at various stages of retention, aeration limit and aeration deficiency index (Table 1).

Table 1. Main physical attributes in plot maximum compacted (C10) reddish brown soil from Tancabest/Peris

Depth (cm)	Characteristic					
	DA ($g\ cm^{-3}$)	Water content (% v/v) at different suctions			LA (% v/v)	Ida (%)
		$pF_{1,0}$	$pF_{1,6}$	pF_2		
0-10	1,17	48	41	38	40	-379
10-20	1,46	41	38	36	24	-150
20-30	1,42	45	40	38	26	-205
30-40	1,52	43	40	38	22	-89

To assess air content should be taken into account the aeration limit - LA (indicating maximum humidity that the soil is likely to have without aeration to be poor) and aeration deficiency index - Ida, both indicators showing full aeration conditions satisfactory.

Using assessment indicators for the air content in soil, from year 2009 (in year three of experiments) it was calculated total porosity and aeration porosity at three different moments: after compaction in autumn, after compaction in spring and after mechanical maintenance work.

Soil permeability for water is one of the important physical characteristics that it offers a suggestive image regarding changes of air regime in soil because air and water are two additional phases in the soil. Air permeability of soil with low values must be accompanied by a hydraulic conductivity with great values.

From the first stage of making observations, immediately after exercise surface traffic immediately, and until to the next stage, after maintenance work, saturated hydraulic conductivity values decrease sometimes over 3-4 times, especially in witness version, in most cases reaching the middle values.

High values of this feature, for a soil so tamp, could be explained by improving macro and mezzo-fauna activity, especially with earthworms, activity which determined the continuity improving and growth of macro-pores volume, because increased amount of plant debris that remained on the soil surface after harvesting manual work and have then been incorporated into the soil by plowing in the autumn. It is known that during the application of irrigation or rainfall water percolating into the soil, forcing the elimination of an equivalent volume of air. Also, water is very little responsible for increasing the oxygen content in the soil (at a temperature of 20°C a quantity of oxygen brought by a volume of water in soil is about 30 times lower than that of an equal volume air).

The main effect of soil compaction is to reduce the porous volume and redistribution of different size groups of the pores. These changes had direct effects on many physical properties, processes with a higher intensity or less intensity including the aeration capacity, gas exchange, water retention, permeability, resistance at penetration, root penetration and indirectly many chemical and biological processes (especially de-nitrification processes, nodule formations, micro and mezzo-fauna from soil, especially modified because of decreasing soil aeration).

Porosity, total porosity, macro-porosity (pores larger than 50 µm) regarding pores larger than 30 µm and distribution by size for pore presents important changes because of the compaction (Figure 2). The maximum compacted version, total porosity reaches minimum values, falling below 50% (the middle value domain), while the aeration porosity is situated with domain of low values, between 7 and 12% v/v. The only depth where aeration porosity is good is the surface layer (PA 20%). Distribution after size of different categories of pores suffers important changes under the influence of compaction, especially in the uppers and lowers tilling layer, as well as water content at different levels of water retention. As expected, when we advance on the profile, macro-pores volume transmission (those with diameter > 50 µm, which have active role in the processes of aeration of the soil) greatly decreases, reaching values even below the minimum of 10% v/v which represents deficient aeration conditions for plant development.

Results come to confirm existent data in materials regarding the effect of aerations of the soil to different chemical and biological process in soil (Table 2).

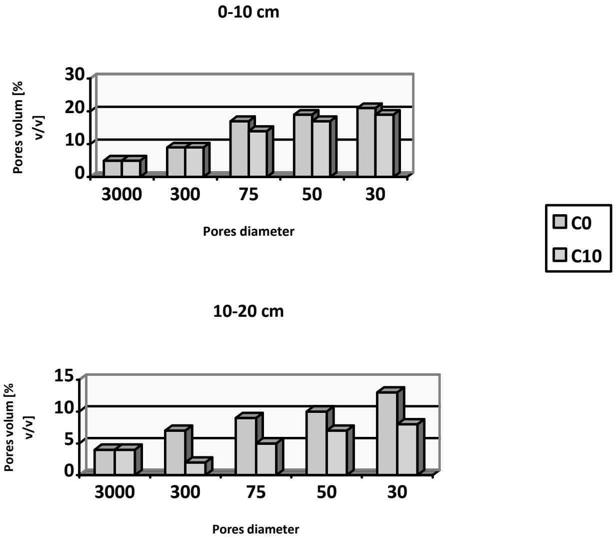

Figure 2. Effect of compaction intensity on distribution by pores size (depth 0-10 and 10-20 cm)

Table 2. Microbiological activity under the influence of compaction[*]

Indexes of characterization of biological activity	Uncompacted	Compacted 10 passes
No. of bacteria (million g^{-1} soil)	163	30
No. of microscopic fungi (thousand g^{-1} dry soil)	2231	79
Dehydrogenase activity (mg formazan 10^{-2} g^{-1} dry soil)	3,5	1,2

[*]After Dumitru et al. (2002)

CONCLUSIONS

Air from soil is with water and nutrients, one of the most important factors affecting soil fertility. The purpose of this paper was to study the soil aeration, which is a complex subject, including air movement and content, using a wide range of indicators which are determined and/or calculated and/or estimated by various methods for understanding many factors which determines the state of aeration and its influence on soil processes and plant response.

From obtained data you can be seen, as expected, that in witness version, after compaction and after maintenance, aeration porosity does not present restrictive values, it is in small to medium value (between 10 and 20% v/v), and total porosity is about 50% v/v. These data show favorable conditions for normal development of various processes in the soil. We should note that from all the mechanisms regarding air movement in the soil, it was study the convection one, although it participation in air movement has not very high proportions. Unlike the diffusion mechanism for assessing indicators (coefficients of diffusion of gases) are strongly dependent on the nature of each component of soil air, air permeability (pointer of movement by convection) is independent of the gas circulating in the soil. Despite these advantages of air permeability, this indicator has not been determined so far in Romania, this research is a first.

REFERENCES

Canarache, A. (1990), Physics of agricultural soils (in Romanian), Ceres, Bucharest, 221-249.

Dumitru, E., Enache, R., Gus, P., Dumitru, M. (1999), Residual effects of some agricultural practices on the physical state of the soil (in Romanian), Risoprint, Cluj-Napoca, 205.

Hakanson, I. (1992), “Subsoil compaction by high axle load traffic”, *Soil Tillage Res*, 29, 105-306.

Horn, R. (1993), “Mechanical properties of structured unsaturated soil”, *Soil Technology*, 6, 47-75.

Soane, B.D. (1975), “Studies on some soil physical properties in relation to cultivation and traffic”, *Bull. Min. Agric. Fish and Food Tech*, 29, 160-182, London.

Trandafirescu, T., Chivulete, S., Canarache, A., “Influence of repeated compacting and decompacting of brown reddish soil from Moara Domneasca on the physical characteristics and yield of corn and soy” (in Romanian), Public SNRSS, 23A.

Voicu, P. (2008), *Research on using polymers in agriculture* (in Romanian), Bren, Bucharest, 205.

Zainescu, G.,Voicu, P., Albu, E., Sandru L. (2008), Romanian patent request no. A 00655: Innovative Process of Obtaining Biocompost Hide Based on Wastes.

DETERMINATION OF HEAVY METAL TOXICITY OF FINISHED LEATHER BY METPLATE TEST

IHSAN YAŞA[1], GÜLŞAH ÇAKMAK[1], HUSEYIN ATA KARAVANA[2]

[1] *Industrial and Basic Microbiology Department, Faculty of Science, Ege University, Bornova, Izmir 35100, Turkey, email: ihsan.yasa@ege.edu.tr*

[2] *Leather Engineering Department, Engineering Faculty, Ege University, Bornova, Izmir 35100, Turkey*

In this study the heavy metal toxicity of finished leather has been analyzed using enzyme activity inhibition bioassay, the MetPLATE and heavy metal contents of the samples were compared by % inhibition levels. The toxicities of soluble forms of heavy metals in leather were revealed by analyzing leather samples in the artificial alkali sweat solution and the toxicity characteristic leachate procedure solution (TCLP). Total heavy metal concentrations of finished leather have been determined by means of Inductively Coupled Plasma Optical Emission Spectrometry (ICP-OES). According to the test results obtained, the heavy metal toxicities of finished leather, especially in terms of chromium, have been found at above the critical limits. % inhibition levels of the finished leather samples were found to be in the range of 13.20-99.35%, which mainly came from chromium, cobalt and copper.

Keywords: heavy metal toxicity, leather, MetPLATE.

INTRODUCTION

Toxic effects of heavy metals on human health are very well known: damages of organs, disorders in the respiratory tract and lung diseases, dysfunction of heart, blood and blood producing organs, disorders in nervous system, skin diseases, abnormalities in fertility and pregnancy. Accumulation of heavy metals in body tissues and binding to enzymes may disrupt the functioning of cells, which may also lead to development of tumors or cancers (Apostoli, 2002).

The problems arise when metals are extracted from the products such as textile or leather. Metals may represent a health hazard to consumers by causing allergenic skin reactions, also metals present in leather material may contribute to problems during processing. In addition, when leather wastes are released to the environment, the heavy metals within the leathers may harm the ecosystem and threaten human health by transferring indirectly into the food chain.

Chemical and instrumental analyses have been carried out to determine the environmental effects of various inorganic substances within the leather. These analyses provide the necessary information to some extent, but cannot determine the effects of heavy metals on biological systems. One of the methods revealing toxicity on living cell is Met PLATE test, which is used in solid waste samples, waste effluents, soils etc. (Aslan et al., 2006).

In this study the heavy metal toxicity of finished leather has been analyzed using enzyme activity inhibition bioassay, the MetPLATE and heavy metal contents of the samples were compared by % inhibition levels. The toxicities of soluble forms of heavy metals in leather were revealed by analyzing leather samples in the artificial alkali sweat solution and the toxicity characteristic leachate procedure solution (TCLP). Total heavy metal concentrations of finished leather have been determined by means of Inductively Coupled Plasma Optical Emission Spectrometry (ICP-OES).

EXPERIMENTAL

The toxicities of totally 20 pieces different finished leathers (10 pieces shoe upper and 10 pieces of shoe lining leathers) have been investigated. The test samples were cut into small pieces and these pieces were ground with a Restch SKI mill in order to make analyses according to SLC 2. The mill was thoroughly cleaned before processing each sample (SLTC, 2008).

The leather samples were analysed in two diffrent ways by preparing in artificial alkali sweat solution and toxicity characteristic leachate prosedure (TCLP) to determine the toxicities of soluble forms of heavy metals which are found in leather samples. All analyses for each sample were carried out in triplicate and all reagents in this study except for chlorophenol-red-b-D-galactopyranoside (Sigma) were obtained from Merck.

Toxicity of leathers was determined using a slightly modified MetPLATE enzymatic test. A toxicity test was then run according to Rossel et al. (1997). The six tubes used for the bioassay process were divided into two groups of three tubes each. The first group of tubes was called sample S and the control was called C. The second group of tubes were called blank B. The initial step of the assay was 0,9 ml of leachate transferred to each of the test tubes S and B. 0.9 mL of MiliQ of distilled water was added to tube C. In the second step of the assay, 0.1 mL of Escherichia coli EW1b bacteria was added to all tubes. The tubes were vortexed for 10 s and then incubated at 35°C while shaking for 1 h. Following a 1-h contact period, 0.5 mL of 125 ppm chlorophenol-red-b-D-galactopyranoside was added as an enzyme substrate in a 0.15 M K-PO4 buffer (pH 7.0) to tubes S and C, to B tube 0.5 ml of distilled water was added and all the tubes were incubated at 35°C until a reddish color developed. Next, suspensions S, C, B were centrifuged at 10,000 rpm for 5 min. One milliliter of each filtrate was pipetted on to quartz cell and absorbance at 575 nm was read using a Varian Cary 300 Bio UV–Visible spectrophotometer.

Percent inhibition was estimated as follows:

Inhibition, % = $\left[\frac{C-S}{S}\right] \times 100$ (1)

Total heavy metal concentrations of soluble forms of heavy metals in the leachate samples have been determined by means of inductively coupled plasma optical emission spectrometry (ICP-OES, Perkin Elmer Optima 2100 DV). Tests were carried out to detect the metals most used in the tanning industry, and some of those for which limits have been set by the EU (Basaran et al., 2006).

All the test results obtained from MetPLATE and ICP-OES analysis were assessed as inhibition % and according to the OEKO-TEX® Standard 100, respectively.

RESULTS AND DISCUSSION

As presented in Table 1, the total metal concentrations of 7 metals in shoe lining leather groups were determined in varying concentrations in the range of 0.00–0.07 for ppm Cu, 0.00–0.00 ppm for Cd, 0.00–0.01 ppm for Ni, 0.00–15.86 ppm for Zn, 0.00–0.03 ppm for Co, 0.00–0.29 ppm for Pb and 3.47–41.72 ppm for Cr.

The total metal concentrations of 7 metals in shoe upper leather groups were determined in varying concentrations in the range of 0.00–12.58 for ppm Cu, 0.00–0.00 ppm for Cd, 0.00–0.02 ppm for Ni, 0.00–0.00 ppm for Zn, 0.00–0.03 ppm for Co, 0.00–0.02 ppm for Pb and 2.82–33.88 ppm for Cr as presented in Table 2.

The concentrations of some heavy metals in our study were parallel to those determined by Basaran et al. (2006) in his report (0.34–0.55 ppm for Cd, 10,160–19,201 ppm for Cr, 35.37–79.46 ppm for Cu, 4.19–14.42 for Pb, 2.26–3.27 for Ni and 4.19–27.35 for Zn).

Table 1. Heavy metal contents in shoe lining leathers by ICP-OES (ppm)

Heavy metals		Cu	Cd	Ni	Zn	Co	Pb	Cr	Total	Inhibition, %
TCLP solution	A1	0,00	0,00	0,00	0,00	0,03	0,00	64,35	64,38	56,91
	A2	0,00	0,00	0,01	0,00	0,02	0,00	33,36	33,38	6,70
	A3	0,001	0,00	0,00	0,00	0,01	0,00	10,94	10,95	32,78
	A4	0,00	0,00	0,01	0,00	0,01	0,00	5,07	5,09	28,88
	A5	0,002	0,00	0,00	0,00	0,02	0,00	30,60	30,62	12,16
	A6	0,00	0,00	0,00	0,00	0,01	0,00	23,16	23,17	8,61
	A7	0,00	0,00	0,00	0,00	0,02	0,00	40,53	40,55	16,13
	A8	0,00	0,00	0,00	0,00	0,04	0,00	40,15	40,19	29,81
	A9	0,00	0,00	0,00	0,00	0,02	0,00	16,38	16,40	48,65
	A10	0,00	0,00	0,00	0,00	0,02	0,00	41,72	41,74	22,68
Sweat solution	A1	0,07	0,00	0,01	0,00	0,02	0,00	14,10	14,19	48,82
	A2	0,06	0,00	0,01	0,00	0,01	0,01	4,88	4,97	34,80
	A3	0,06	0,00	0,01	0,00	0,01	0,04	6,70	6,82	N.D.
	A4	0,04	0,00	0,02	0,00	0,01	0,27	4,67	5,00	N.D.
	A5	0,01	0,00	0,00	1,46	0,01	0,00	6,65	8,13	26,16
	A6	0,00	0,00	0,00	15,86	0,01	0,00	2,95	18,82	23,79
	A7	0,05	0,00	0,01	0,00	0,01	0,14	4,00	4,20	42,84
	A8	0,06	0,00	0,01	0,00	0,03	0,29	5,30	5,68	31,79
	A9	0,01	0,00	0,00	0,00	0,01	0,03	3,47	3,52	17,57
	A10	0,06	0,00	0,00	0,00	0,01	0,05	4,08	4,20	43,53

*N.D. – not determined

Chromium was found to have the highest concentrations compared to the other metals for leathers treated with TCLP solution, exhibiting almost 98% of the total metal contents analyzed. These high chromium concentrations are due to main tanning modern process, which is carried out predominantly with basic chrome sulfates (Thorstensen, 1983). However, Cd, Cu, Pb, Ni and Zn, which are definitely not used during the treatment of hides, have also been identified in the constitution of the leathers. These metals originate from leather dyes, pigments, pesticides, or contaminated equipment used in the tanneries during the treatment of the hides. However, the concentrations of these elements are negligible compare with those of Cr. The variations in heavy metal concentrations within and between groups relate to the intensity of the tanning and coloring processes. Furthermore, heavy metal levels are also affected by the dye and pigment mixtures used according to the desired color of the leathers (Sharphause, 1989).

Table 3 shows the heavy metal toxicity of shoe lining leathers under study, according to the MetPLATE assay. The percent inhibition of b-galactosidase enzyme varied from 6.70% to 56.91% and 17.57% to 48.82 for leathers treated by TCLP and artificial alkali sweat solutions, respectively. Based upon the percent inhibition, all leather samples appear to display meduim-level heavy metal toxicity.

Table 2. Heavy metal contents in shoe upper leathers by ICP-OES (ppm)

Heavy metals		Cu	Cd	Ni	Zn	Co	Pb	Cr	Total	Inhibition, %
TCLP solution	Y1	0,00	0,00	0,00	0,00	0,01	0,00	5,23	5,25	23,41
	Y2	0,00	0,00	0,00	0,00	0,01	0,00	16,60	16,62	68,29
	Y3	0,00	0,00	0,00	0,00	0,02	0,00	15,59	15,61	59,13
	Y4	0,00	0,00	0,00	0,00	0,01	0,00	4,32	4,33	26,70
	Y5	0,00	0,00	0,00	0,00	0,01	0,00	17,30	17,31	55,34
	Y6	1,21	0,00	0,01	0,00	0,02	0,00	11,88	13,12	86,52
	Y7	0,03	0,00	0,00	0,00	0,01	0,00	10,54	10,58	47,19
	Y8	0,00	0,00	0,00	0,00	0,01	0,00	8,04	8,05	49,02
	Y9	0,00	0,00	0,00	0,00	0,01	0,00	10,21	10,22	51,17
	Y10	0,00	0,00	0,00	0,00	0,02	0,00	33,88	33,90	48,83
Sweat solution	Y1	0,00	0,00	0,02	0,00	0,01	0,02	2,94	2,99	13,20
	Y2	0,05	0,00	0,01	0,00	0,01	0,00	6,65	6,72	16,64
	Y3	0,01	0,00	0,00	0,00	0,02	0,00	5,38	5,41	33,72
	Y4	0,00	0,00	0,01	0,00	0,01	0,00	2,82	2,84	26,04
	Y5	0,02	0,00	0,01	0,00	0,01	0,00	5,19	5,23	27,00
	Y6	12,58	0,00	0,02	0,00	0,03	0,00	3,44	16,06	45,35
	Y7	0,57	0,00	0,01	0,00	0,01	0,00	5,76	6,35	17,25
	Y8	0,06	0,00	0,00	0,00	0,02	0,01	5,45	5,54	26,90
	Y9	0,02	0,00	0,01	0,00	0,02	0,00	7,61	7,66	24,38
	Y10	0,03	0,00	0,00	0,00	0,01	0,02	7,74	7,81	18,00

*N.D. – not determined

Table 3. Total heavy metal content and toxicity in shoe lining leathers

Sample	TCLP solution leachate		Sweat solution leachate	
	Total heavy metal content, ppm	Inhibition, %	Total heavy metal content, ppm	Inhibition, %
A1	64,38	56,91	14,19	48,82
A2	33,38	6,70	4,97	34,80
A3	10,95	32,78	6,82	N.D.
A4	5,09	28,88	5,00	N.D.
A5	30,62	12,16	8,13	26,16
A6	23,17	8,61	18,82	23,79
A7	44,55	16,13	4,20	42,84
A8	40,19	29,81	5,68	31,79
A9	16,40	48,65	3,52	17,57
A10	41,74	22,68	4,20	43,53

*N.D. – not determined

Table 4 presents the heavy metal toxicity of shoe upper leathers under study, according to the MetPLATE assay. The percent inhibition of b-galactosidase enzyme varied from 23.41% to 86.52% and 13.20% to 45.35 for leathers treated by TCLP and artificial alkali sweat solutions, respectively. Based upon the percent inhibition, all leather samples appear to display meduim-level heavy metal toxicity.

Table 4. Total heavy metal content and toxicity in shoe upper leathers

Sample	TCLP solution leachate		Sweat solution leachate	
	Total heavy metal content, ppm	Inhibition, %	Total heavy metal content, ppm	Inhibition, %
Y1	5,25	23,41	2,99	13,20
Y2	16,62	68,29	6,72	16,64
Y3	15,61	59,13	5,41	33,72
Y4	4,33	26,70	2,84	26,04
Y5	17,31	55,34	5,23	27,00
Y6	13,12	86,52	16,06	45,35
Y7	10,58	47,19	6,35	17,25
Y8	8,05	49,02	5,54	26,90
Y9	10,22	51,17	7,66	24,38
Y10	33,90	48,83	7,81	18,00

*N.D. – not determined

Considering the fact that every year million tons of leather goods are discarded and the leather industries generate finished leather solid waste, and that their disposal contributes tons of toxic metals to the environment. This points to the need for recycling instead of disposing to landfill. Also, leather process recipes should be revised to reduce the heavy metal content of leather in order to produce ecological leather products.

CONCLUSION

In this study the heavy metal toxicity of finished leather has been analyzed using enzyme activity inhibition bioassay, the MetPLATE and heavy metal contents of the samples were compared by % inhibition levels. The toxicities of soluble forms of heavy metals in leather were revealed by analyzing leather samples in the artificial alkali sweat solution and the toxicity characteristic leachate procedure solution (TCLP). According to the test results obtained, the heavy metal toxicities of finished leather, especially in terms of chromium, have been found at above the critical limits. % inhibition levels of the finished leather samples were found to be in the range of 6.70% -86.52%, which mainly came from chromium, cobalt and copper.

REFERENCES

Apostoli, P. (2002), *J. Chromatogr., B*, 778, 63.

Aslan, A., Gulumser, G., Ocak, B. (2006), "Increasing the efficiency of chromium tanning by using collagen hydrolysates from shavings", *J Soc Leather Technol Chem*, 90, 201–204.

Basaran, B., Iscan, M., Bitlisli, B.O., Aslan, A. (2006), "A study on heavy metal contents in different types of finished leathers", *J Soc Leather Technol Chem*, 90, 229–234.

Rossel, D., Tarradellas, J., Bitton, G., Morel, J.L. (1997), "Use of enzymes in soil ecotoxicology: a case for dehydrogenase and hydrolytic enzymes", in: Tarradellas, J., Bitton, G., Rossel, D. (eds.), *Soil ecotoxicology*, CRC, USA, 179.

Sharphause, J.H. (1989), *Leather technician's handbook*, Leather Producers Association, Northampton.

SLTC (2008), "Official methods of analysis, society of leather technologists and chemists", SLTC, Northampton.

Thorstensen, T.C. (1983), *Practical leather technology*, Krieger, USA.

V.
CULTURAL HERITAGE

APPLICATION OF NON -DESTRUCTIVE ANALYSIS FOR INVESTIGATION OF PAINTED WOOD ARTIFACTS OF AZERBAIJAN

DINARA ABBASOVA[1], CIPRIAN CHELARU[2]

[1] *Institute of Radiation Problems of AzNAS, Baku, Azerbaijan, dinara_abasova@hotmail.com*

[2] *INCDTP - Division: Leather and Footwear Research Institute,Bucharest, Romania*

In the XVIII century Azerbaijan, decorations for window had a very complex design, nicely colored. Optical microscopy is useful to determine the metals content. By means of Micro XRF analysis we were able to determine that there were As base colors. The knowledge that we have about the ornaments from the XVII century is that in that period As base colors were used.

Keywords: decoration, Micro XRF, metal content

INTRODUCTION

Long history of Azerbaijan combined together the most colorful traditions and customs that have existed there for many centuries, independently of each other.

That is why the culture of each region of Azerbaijan has its own special features. Such Azerbaijan cities as Baku, Ganja, Shamakhi, Barda, Tabriz, Shaki, Gabala, Nakchivan and others have their own unique cultural character. Some of them are famous due to music, some due to philosophers and poets, some became worldwide known because of handicrafts such as carpets. But almost every town has something in common with others: its architecture. You cannot find any old Azerbaijan city which does not have at least a few ancient architectural monuments.

METHODS

Optical Microscopy Analysis – Non-Destructive Visual Evaluation of the Artifact

Figure 1 displays the stereomicroscope that was used to see the damage spared on the sample surface and also the color of pigment, information that is very useful in identification of used pigment.

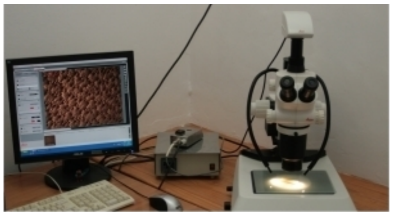

Figure 1. Stereomicroscope used for analysis

Micro XRF Analysis – Non-Destructive Surface Mapping the Sample Surface of Sample

Figure 2 displays the Micro XRF device that was used to determine metal content on analyzed sample.

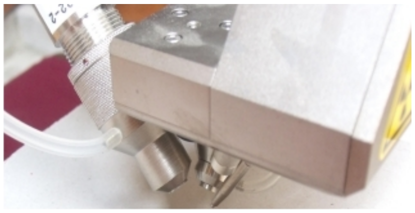

Figure 2. Micro XRF device

The analyzed piece was one window wood painted ornament, from XVII century - Figure 3.

Figure 3. Window frame made from painted wood – before restoration

From the window ornament was removed one small part – Figure 4, in order to determine the degradation state and also to identify the metal content from pigment used for painting, in order to know how to restore the wood frame.

a b

Figure 4. Sample of window frame, analyzed on stereomicroscope (a), analyzed by MicroXRF (b)

OPTICAL MICROSCOPY ANALYSIS

Using this non-destructive method of analysis it is possible to see in detail the defects that occur on the surface of sample, to see the area where they are present and also to measure them.

In the Figure 5 it is easy to see the two main cracks, five secondary cracks and multiple small cracks. These cracks have different length and orientation.

Figure 5. Crack size and orientation

Figure 6 displays a main crack and several small cracks, with different length and orientation. It is also possible to see one wood defect.

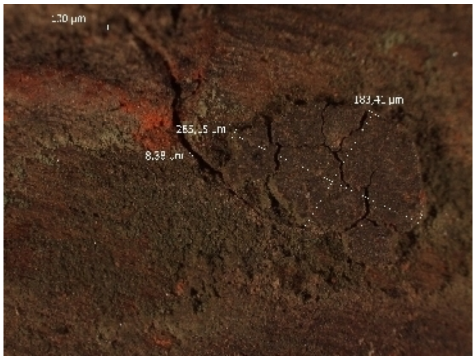

Figure 6. Wood defect and cracks

Figure 7 displays a large crack and also a big degradation of wood in the area. The presence of red color in this area indicates that, for this area, a large amount of pigment was used, most probably, iron based pigment.

Figure 7. Wood degradation and pigment content

The Figure 8 displays a inner part of decoration, some overlay parts. This indicates that in order to make such a deep detail, the manufacturer must work very hard.

Figure 8. Layers of wood in the sample

MICRO XRF Analyses

The Micro XRF analysis was made on small area – 90 mm^2 – Figure 4 (b).

Measurement conditions:

- High voltage/kV: 50
- Current/µ A: 600
- Time/s: 5
- Energy range/keV: 50
- Anode: Mo
- Optic: Lens 0.060
- Atmosphere: Air

The analysis identified different types of metals, figure 9-13:

- easy metals:
    - Ca – 2.800

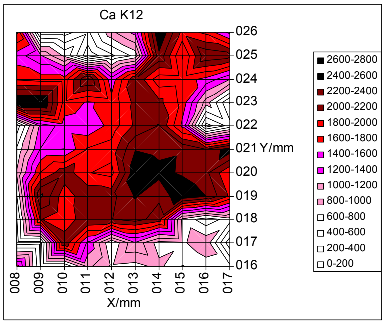

Figure 9. Metal concentration (Ca) on samples surface

- heavy metals:
    - Fe –11.100
    - Cu – 120.000

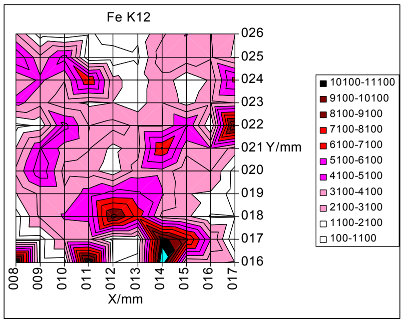

Figure 10. Metal concentration (Fe) on samples surface

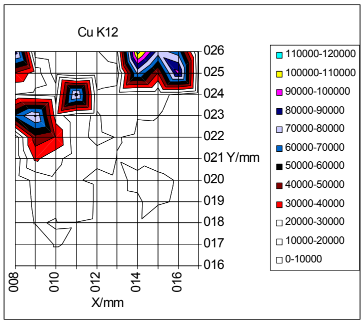

Figure 11. Metal concentration (Cu) on samples surface

- toxic metals:
    - Pb – 90.000
    - As – 75.000

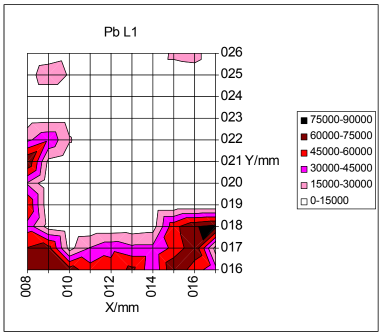

Figure 12. Metal concentration (Pb) on samples surface

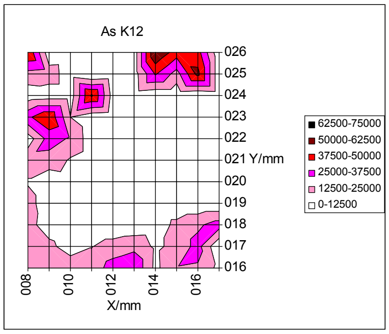

Figure 13. Metal concentration (As) on samples surface

After the experts evaluated all the aspects of the window frame, the restoration was done so that it would not affect the chemical composition or the aspect of the artifact. The information collected was useful to understand the pigment content used for painting the wood used as window decoration. Figure 14 displays the final aspect of the artifacts.

Figure 14. Window frame made from painted wood – after restoration

CONCLUSIONS

Optical microscopy reveals major and minor cracks on the samples surface and it shows the area where advanced degradation is present. Using optical microscopy it was possible to see layers of wood, layers made by the manufacturer. Optical microscopy also indicates the presence of one red pigment in large amount.

Micro XRF analysis displays a more complete image about the pigments used on this window frame.

Ca – it is present all over the surface – the most probable color where it is present was white.

Fe – it is present all over the surface – the most probable color where it is present was red. but the amount used was three times higher than the white pigment.

Cu – it is present only in small area but the amount is very high – ten times higher than Fe – the most probable color where it is present was blue.

Pb – it is present only in small area but the amount is very high – similar to Cu – the most probable color where it is present was yellow.

As - it is present only in small area but the amount is very high – similar to Pb – the most probable color where it is present was green.

The presence in the same place of Cu and As also indicates that the painter used blue (Cu based pigment) and yellow (As based pigment) to obtain the green color.

In the XVII century, the painted decoration was very common and because of this reason, even on a small sample a lot of metals were found, that are the main component of pigments.

Acknowledgement

The authors thank the National History Museum of Azerbaijan for allowing investigation in their collection, to Dr. Yakup KALAYCI from Elemental Analysis Laboratory of Saraykoy Nuclear Research and Training Center of Turkish Atomic Energy Authority, who made Micro-XRF analysis.

Research work has been done in frame of the IAEA Regional project RER/0/034 “Using Nuclear Techniques for the Characterization and Preservation of Cultural Heritage Artefacts in the European Region” in Turkey and Romania in 2011.

REFERENCES

www.azhistorymuseum.az

STUDY ON ANCIENT RHINO BONE FOUND IN AZERBAIJAN

DINARA ABBASOVA[1], CIPRIAN CHELARU[2]

[1] *Institute of Radiation Problems of AzNAS, Baku, Azerbaijan, dinara_abasova@hotmail.com*

[2] *INCDTP - Division: Leather and Footwear Research Institute, 93 Ion Minulescu, Bucharest, Romania*

From the moment of Earth formation – 4.6 billion years ago, the process that prepares “the birth of life” begins to emerge. No longer than 700 million years after the Earth was born we can say that life exists on the blue planet. Fully formed animals appear after 3.2 billion years of evolution – simple animal - Precambrian Period. No more than 560 million years must pass, divided in three Eras in order to arrive in the Pleistocene Era. Ice core from the Antarctic indicates that at the end of Pleistocene era there was a glaciation. In the Pleistocene the majority of animals such as woolly rhino, woolly mammoth, cave bear, cave lion had already adapted to cold. The presence of woolly rhino (Coelodonta antiquitatis) in the current place of Azerbaijan, indicates the existence of this type of animal in the south part of Eurasian continent during the Late Pleistocene and places them in the Eurasian belt distribution. AMS (Accelerator Mass Spectrometry) analysis “says” that the rhino lived around 44.000 years ago, in the middle of the last Ice Age (110.000-10.000 years ago). Micro XRF analysis reveals a large amount of S, Fe, Ti, As, Sr. The large concentration of SO_2 is due to oil which was found in that area, that indicates a big vegetation in that period.

Keywords: woolly rhino, glaciation, Late Pleistocene.

INTRODUCTION

Time. A term that brings many questions around us. The moment for planet formation is much disputed but we have approximate age - 4.6 billion years. Life. It seems that life does not to wait too long to “colonize” the newly formed planet, so after only 700 million years the first cells are appearing (prokaryotes). After this “spark” it took 3.2 billion years of evolution for the emergence of the first animals – simple animals. Figure 1 shows how Earth looked when the first animals started to appear.

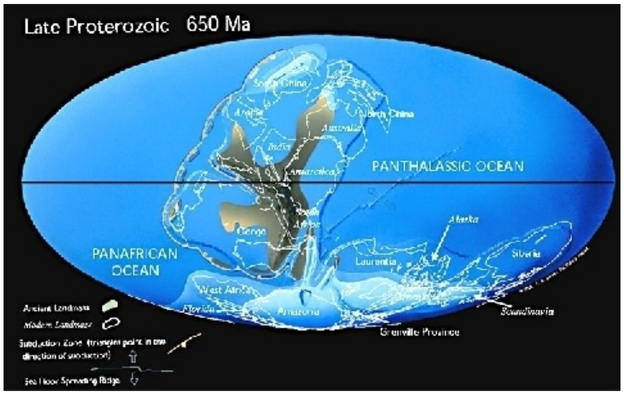

Figure 1. 650 million years ago, first animals start to appear

It is possible to see that the position of continents was different from what it is today. Because our planet is a dynamic one, the position of continents has continued to change, the process continues today; Figure 2 illustrates very well the evolution of continental surface.

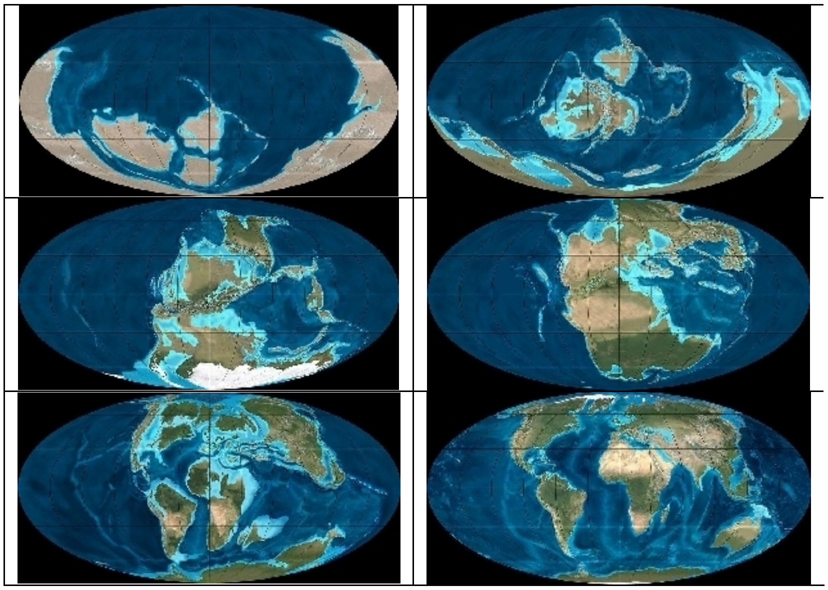

Figure 2. Continental surface evolution

It is well known that clime has changed over time. Latest studies indicate that every 12,000 years a glaciation occurs, which lasts an average of 100,000 years. The atmosphere CO_2 concentration is directly linked with temperature variation. It was established by the researchers that a concentration smaller than 230 p.p.m.v. (parts per million by volume) starts the cooling effect of the atmosphere. The information provided by the ice core taken from the Antarctic reveals that 110,000 – 10.000 years ago, at the end of Late Pleistocene, the level of CO_2 dropped under 230 p.p.m.v and in that period the 8th Ice Age took place. Figure 3 displays the variation of CO_2 concentration in Earth's atmosphere.

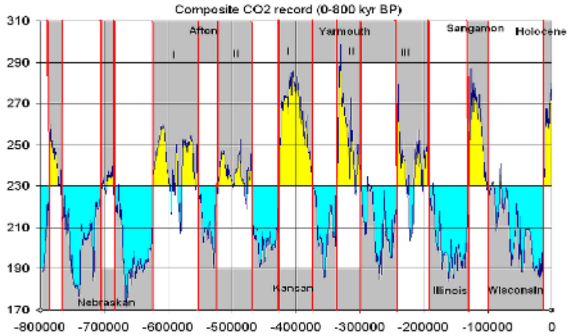

Figure 3. CO_2 concentration in Earth's atmosphere recorded in ice core from the Antarctic

EXPERIMENTAL

Animal type determination - comparing the skull with the skulls of known animals. Bone sample was taken from the National Museum of History of Azerbaijan National Academy of Sciences.

C^{14} radio date - approximate period of animal life – made with AMS (Accelerator Mass Spectrometry) - Radiocarbon and Trituim Laboratory of Rudjer Boskovic Institute, Croatia.

Optical microcopy analysis - aspect of bone at microscope level – made with Leica stereomicroscope - INCDTP- ICPI, Bucharest, Romania.

RESULTS

After long studies about the skull found in Azerbaijan - Figure 4 - and after it was compared with different rhino skulls – Figure 5, it was established that it is a rhino.

Figure 4. Skull found in Azerbaijan

Woolly Rhinoceros

Sumatran Rhinoceros

Modern Rhinoceros

Figure 5. Different rhino skulls

Optical microscopy of skull bone – Figure 6 – displays a good health of bone, without visible signs of struggle or disease.

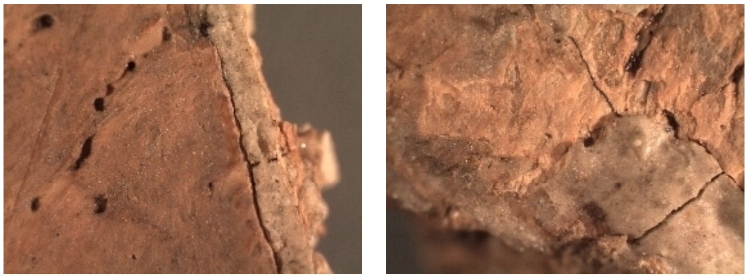

Figure 6. Optical microscopy of skull bone

After this assumption it was necessary also to determinate the period when this animal lived. The most used method for dating is C^{14} radio date. C^{14} radio date was possible to do using AMS (Accelerator Mass Spectrometry) technique – principle described in Figure 7.

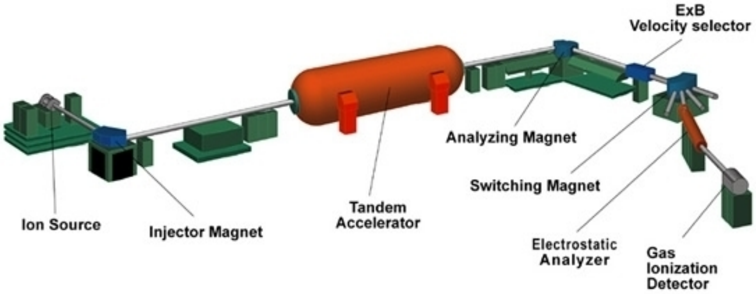

Figure 7. Accelerator Mass Spectrometry principle

AMS technique measures long-lived radio nuclides that occur naturally in our environment. AMS uses a particle accelerator in conjunction with ion sources, large magnets and detectors to separate out interferences and count single atoms in the presence of $1x10^{15}$ (a thousand million million) stable atoms.

The radio nuclides are used for a wide variety of dating and tracing applications in the geological and planetary sciences, archaeology, and biomedicine.

AMS analysis “says” that the animal has 43.960 years.

By AMS analysis an oil/petroleum trace was identified on the bone, information that tells us that the rhino lived in a place with many trees which in time transformed into oil/petroleum or after some time the petroleum reached the surface and contained the bone.

In terms of “Earth evolution stages” this value is placed in the Pleistocene Era - 2.588 - 0.0117 million years ago, more precisely in the Late Pleistocene (0.126-0.0117 million years ago).

In the Late Pleistocene (110.000 and 10.000 years ago) the 8th Ice Age took place and so, the 43.960 years indicate that this animal lived in the middle of the last Ice Age. Figure 8 illustrates the possible appearance of the woolly rhino.

Figure 8. Woolly rhino

Azerbaijan is in the area where it was predicted that the woolly rhino lived – Figure 9. This area starts from France, engulfing all the Europe and extending to all Russia and the most part of China, remains are found even in the Tibetan Plateau.

Figure 9. Woolly Rhino distribution on Eurasian land in the Late Pleistocene

In the same period also lived many cold adapted animals, like woolly mammoth (Figure 10), cave bear (Figure 11). Contemporary with this animals, another animal was present that began to climb the evolution ladder at the start of Pleistocene Era - 2.5 million years earlier – Modern Human.

Figure 10. Woolly mammoth

Figure 11. Cave bear

CONCLUSIONS

Due to comparative studies on skull found in Azerbaijan, it was established that it is a rhino skull.

The health of the rhino was good, due to the aspect of bone (skull) that did not present any deformation because of struggle or disease.

C^{14} radio carbon dating showed that the skull is 43,960 years old.

This age places the existence of this animal in the Late Pleistocene (0.126 million years ago - 0.0117 million years ago) which is a part of the Pleistocene Era (2.588 million years ago - 0.0117 million years ago).

At the beginning of Pleistocene Era, the race for surviving and colonizing the Earth had started for another animal – Modern Human.

Information obtained from the ice core extracted from the Antarctic indicates that the 8th Ice Age occurred between 100.000 and 10.000. This indicates that animals of that time were completely adapted to the Ice Age conditions.

Geographical position of Azerbaijan confirms the extended area of woolly rhinoceros, which contains all of Europe and North-West of Asia.

Acknowledgement

This work has been done in frame of the project IAEA RER 8/0/15 “Using Nuclear Techniques for the Characterization and Preservation of Cultural Heritage Artifacts in the European Region”.

REFERENCES

http://www.scotese.com/earth.htm
http://www.dailymail.co.uk/sciencetech/article-1108642/The-beasts-raise-dead-Return-mammoth-matter-time.html
http://www.rhinoresourcecenter.com/images/Woolly-rhino-03_i1298079508.php
http://phys.org/news/2011-09-important-woolly-rhino-fossil.html

HOW PARCHMENT RESPONDS TO TEMPERATURE AND RELATIVE HUMIDITY: A COMBINED MICRO DSC, MHT, SEM AND FTIR STUDY

ELENA BADEA[1], CRISTINA CARŞOTE[2], WILFRIED VETTER[3], IRINA PETROVICIU[2], LUCREŢIA MIU[4], MANFRED SCHREINER[3], GIUSEPPE DELLA GATTA[5]

[1] *Faculty of Sciences, University of Craiova, Romania, on leave at the University of Turin, Italy*

[2] *National Museum of Romanian History, Centre of Research and Scientific Investigation, Bucharest, Romania, email: elena.badea@unito.it*

[3] *Institute of Science and Technology in Arts, Academy of Fine Arts, Vienna, Austria*

[4] *INCDTP - Division: Leather and Footwear Research Institute, Bucharest, Romania*

[5] *Department of Chemistry, University of Turin, Italy*

Micro differential scanning calorimetry (micro DSC), micro hot table (MHT) method, scanning electron microscopy (SEM) and Fourier-transform infrared (FTIR) spectroscopy measurements were used to investigate the synergistic effects of temperature (*T*) and relative humidity (RH) on deterioration of parchment from microscopic to molecular level. Samples were obtained by exposing new parchments to various *T* and RH environments, for increasing time periods, in climate chambers. Ageing treatments were carried out in the compass of the EC Project “Improved Damage Assessment of Parchments” and Romanian–Austrian Bilateral Project “The Influence of Environmental Factors on the Conservation of Collagen-based Museum Objects”.

Keywords: parchment, collagen denaturation, environmental sensitivity

BACKGROUND

The almost entire intellectual heritage of the Western World, from classical times to the Renaissance, has been delivered to us on parchment in form of scrolls, manuscripts, codices, notary documents, dynastic fonds, papers of the secretaries of State, archives of ecclesiastical institutions and ancient noble families. Large collections of parchment documents exist in public and private libraries, archives and religious institutions. However, in the context of climate change and global energy crisis restrictions their protection still represents a conservation problem not yet solved. The current standards based on the “gold” statement “one-size-fits-all collections”, namely $T = (20 \pm 2)$°C and RH = (50 ± 2)% appear no longer appropriate for storing and displaying all parchment collections (2011 ASHRAE Handbook - Heating). The extent to which these standards can determine the conservation practice should be viewed in terms of their implications on collection longevity, available resources and climate changes. Focused research enabling to establish new improved guidelines for balancing cost and long term preservation are greatly requested for collections care.

This paper reports the results of a study on parchments aimed at furthering our knowledge on how they respond to *T* and RH, quantifying the damage and unambiguously evaluating the stability of historical objects. Micro differential scanning calorimetry (micro DSC), micro hot table (MHT) method, scanning electron microscopy (SEM) and Fourier transform infrared (FTIR) spectroscopy can be used to profile parchment heritage collections, identify environmentally sensitive objects and suggest if less restricted environmental standards are practicable.

MATERIALS AND EXPERIMENTAL METHODS

Samples

Samples were obtained by exposing new parchments to accelerated ageing at various T (40°C to 80°C) in controlled RH atmosphere (40% to 80%) for 1, 2, 4, 8, 16 and 32 days using climate chambers. Parchments were also exposed to 40% and 80% RH in alternating days at both 40°C and 80°C.

Techniques

Micro Differential Scanning Calorimetry (micro DSC) measurements were carried out in excess water conditions with a high-sensitivity SETARAM micro differential scanning calorimeter (micro DSC III) (Badea et al., 2012a).

Micro Hot Table (MHT) method visualizes the shrinkage motion of collagen fibres dispersed in water under constant heating rate using a hot table equipped with a central processor for temperature and a stereomicroscope with a digital camera for the motion recording (Larsen et al., 2007).

Scanning Electron Microscopy (SEM) observations were made with a Leica 420 Stereoscan apparatus equipped with a tungsten filament at 5 to 30 kV accelerating voltage. Samples were short-pulse coated with graphite and analysed on their flesh side at increasing magnifications.

Fourier-Transform Infrared (FTIR) spectroscopy measurements were performed with an Alpha Bruker Optics spectrometer equipped with Opus 6.5. software. Spectra were collected in the range 4000 cm^{-1} to 450 cm^{-1} with a resolution of 4 cm^{-1}. Both grain and flesh sides were analysed.

RESULTS AND DISCUSSIONS

Deterioration of parchment is a complex process whose path generally develops from an intact fibre structure of high thermal and mechanical stability through different stages with decreasing stability until a terminal stage characterised by a destroyed fibre that may transform into gelatine by contact with water or storage in moist conditions.

Thermal Stability

Micro DSC and MHT method measure collagen thermal denaturation and shrinkage activity, respectively, as manifestation of thermal denaturation (i.e. triple-helix conversion to random coil) at fibre, fibrillar and molecular levels.

Micro DSC in Excess Water

When collagen thermal denaturation occurs, DSC provides a direct measurement of the associated enthalpy change $\Delta_d H$ (peak area) together with the peak maximum temperature T_d, peak half-width $\Delta T_{1/2}$ and peak maximum height $C_p^{ex}(\text{max})$ (Figure 1). During accelerated ageing by humid heating the progressive loss of the interactions that stabilize collagen structure is expressed by DSC peak lowering, broadening and shifting towards lower temperatures (Larsen et al., 2007). We found that T_d linearly decreases in function of ageing temperature regardless of the RH value. Principal Component Analysis (PCA) confirms that ageing temperature has a much more intensive effect on DSC parameters than RH (Badea et al., 2012a). This is also illustrated by the grouping of samples in clusters depending on ageing temperature independently of RH value (Figure 2).

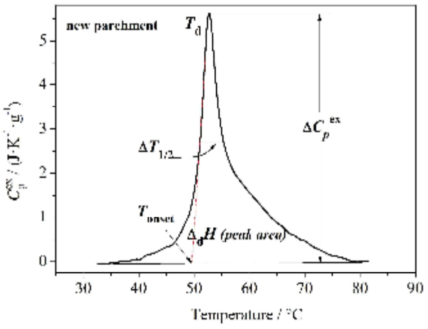

Figure 1. Typical thermal denaturation DSC curves for new parchment

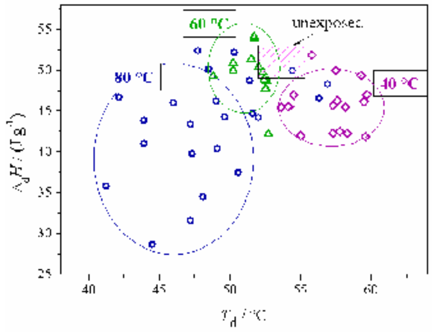

Figure 2. Sample clustering in function of ageing temperature in the $\Delta_d H$ vs T_d plot

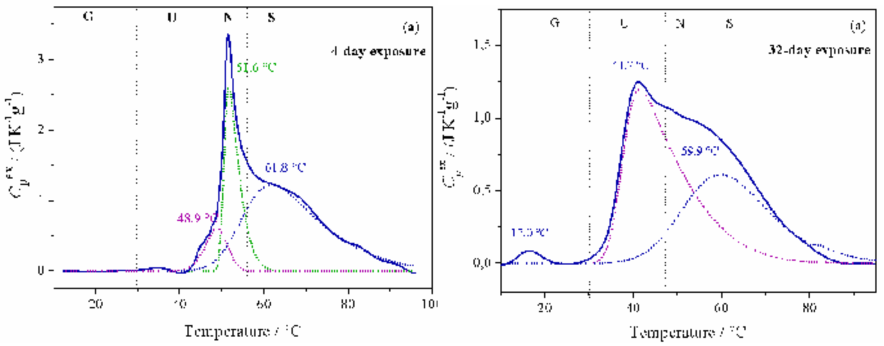

Figure 3. Collagen populations with distinct thermal stability in parchments exposed to 80°C and daily alternating 40% and 80% RH for 4-day and 32-day periods

Dynamic alterations of DSC peak shape during ageing due to the variation of collagen populations with distinct thermal stability is revealed by mathematical deconvolution of the DSC peak as illustrated in Figure 3. Classification of collagen populations in four groups in function of their thermal stability, i.e. native (N) $48°C \leq T \leq 56°C$, stabilised (S) $T > 56°C$, unstable (U) $30°C < T < 48°C$ and gelatin-like (G) $T \leq 30°C$, and their percent quantification has been obtained (Badea et al., 2012a; Larsen et al., 2007). In Figure 3 a progressive conversion of N into U collagen, more susceptible to convert to gelatin whether RH fluctuates, is revealed for parchments exposed to 80°C. A parallel decrease of S collagen occurs even though its thermal stability remains practically unmodified. S collagen is stabilised by a high concentration of crosslinks and can thus better and longer withstand deterioration. After a 32-day ageing period all N collagen was partly transformed into U collagen and partly fully denaturated (more than 50% by comparison to a new parchment). Denaturation induced by exposure to 60°C reached a maximum of 20% at 80% RH and is mainly ascribable to a partial destabilisation of collagen with lowest thermal stability, whereas at 40% RH a slight thermal stabilization occurs after short exposure times and confers parchment better capability to stand against deterioration. Parchments exposed to 40°C for 32 days displayed an increased stability regardless of the RH level most likely due to more compact packing of collagen fibrils as a result of new inter-fibrillar water bridges and crosslinks (Badea et al., 2012a).

MHT Method

Shrinkage activity is described as a sequence of temperature intervals: no activity–A1–B1–C–B2–A2–complete shrinkage (Larsen et al., 2007). T_f and T_l are the temperatures at which the first/last fibre motion is observed, T_s is the shrinkage temperature (i.e. the starting temperature of C interval) and $\Delta T = T_l - T_f$ is the total length of the shrinkage interval. T_s showed to be close to the extrapolated onset temperature of DSC peak, T_{onset}, for parchments exposed to accelerated ageing (Badea et al., 2011; Budrugeac and Miu, 2008). This difference may however increase for historical samples due to their much higher heterogeneity of damage (Figure 4) (Badea et al., 2012b).

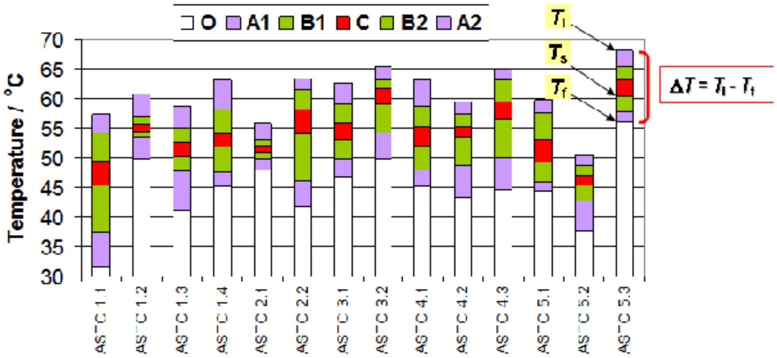

Figure 4. Shrinkage activity of some historical scrolls (The Castellanie Collection, 14th-15th cent, The State Archives of Turin). Large variations among the subsamples from the same scroll (e.g. ASTO 1 and ASTO 5) are observed.

Summarizing the results of our MHT study on accelerated aged parchments we can assert the following:

- For T_f > 45°C and T_s < 50°C parchment is stable. Below these values shrinkage could be observed even at room temperature and partial or total dissolving of collagen fibres occur at T_f < 35°C and T_s < 40°C.
- For highly damaged samples neither B2 nor A2 intervals can be observed and in some cases the C interval may also be absent (Badea et al., 2012b).
- Simultaneous presence of very high ΔT (i.e. more than 30°C) and very low T_s (less than 40°C) denotes the presence of both gelatin and crosslinked collagen.

Fibres Morphology

SEM observations confirm that accelerated ageing at 80°C and 40% RH, causes substantial loss of structural water in triple helices resulting in shrunk fibres. At 80°C and 80% RH collagen mainly tends to convert to gelatine as indicated by the formation of a glassy surface after 32-day exposure (Figure 5a). RH alternation promotes both shrinkage and gelatinisation (Figure 5b) and accelerates the progression of damage.

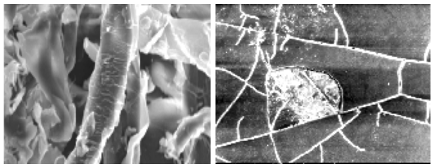

Figure 5a. SEM images of shrunk fibres (2000x) to 80°C and 40% RH and extended glassy surface (500x) to 80°C and 80% RH after 32 days

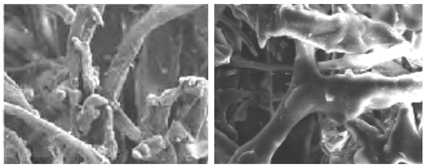

Figure 5b. SEM images (4000x) of shrunk and swollen, melt-like fibres after 8 and 32-day exposure to 80°C and daily RH alternations (40% - 80%)

Molecular Alterations

The parameters characterising molecular alterations were calculated from the ATR spectra (Badea et al., 2008; Giurginca et al., 2009) for samples exposed to 80°C and 80% RH. Slight gelatinisation was revealed by an increase in the separation of the amide I (A_I) and amide II (A_{II}) bands after 32-day exposure. The triple helix denaturation was indicated by the A_{III}/A_{1450} ratio decrease during ageing. However, no significant deterioration by hydrolysis was observed as suggested by the A_I/A_{II} ratio which remained rather constant during ageing. No signal was detected at 1740 cm^{-1} (the carbonyl vibrations) which corresponds to degradation by oxidation.

IMPLICATIONS OF THIS STUDY FOR CONSERVATION PROFESSIONALS

Micro DSC, MHT, SEM and FTIR measurements revealed the loss of stability at all structural levels of collagen in parchments subjected to humid heating. Only micro DSC provides a bulk characterisation of samples, whereas SEM, MHT and FTIR characterise their surface layers. Several conclusions of importance for conservation practice can be drawn:

- Ageing temperature induced significant variation of DSC parameters, whereas RH was less influential. However, exposure to 40% and 80% RH in alternating days enhanced the deterioration effect of temperature.
- High T and RH values play a synergistic role in triggering denaturation and gelatinisation processes.
- Parchment showed to withstand moderate RH levels ($40\% \leq RH \leq 60\%$) for $40° \leq T \leq 60°C$ for 32 days without significant structural alterations.
- At $T = 80°C$ significant alterations were found regardless of the RH level. Collagen partially converts to gelatine in parchments exposed to 80°C and 80% RH.
- Gelatinisation, previously reported for parchments exposed to dry heating at 100°C and chemical pollutants (NO_x and SO_2) (Della Gatta et al., 2005; Budrugeac et al., 2010), is an irreversible damage and gelatine a highly disordered and fragile material that cannot withstand the same level of mechanical stress as collagen and may be dissolved by water or damp environment.

Generally damage evolves from the surface to the inner structure of parchment, from macroscopic to molecular levels. However, it is not uncommon for a seemingly well-preserved parchment appearing macroscopically intact to have significant damage at the molecular level or *vice versa*. This is due to the fact that parchment may deteriorate by different mechanisms at different levels of its structure. Simple visual observation is therefore unable to provide information on the impairment of hierarchical organisation of collagen, the main component of parchment, and hence on the stability of a parchment. On the other hand, it should be noticed that changes in materials' characteristics do not necessarily reflect the evolution in the damage of parchment's structure. To determine if damage is superficial or have partially or totally penetrated the whole structure of a parchment.

As far as historical parchments are concerned, one might infer that those with the most part of their collagen in unstable (U) intervals are significantly more susceptible to rapid ageing and deterioration. These fractions, having lost their native supercoiled organisation, may collapse even at room temperature if exposed to RH > 60% or large RH fluctuation. On the other hand, the parchments characterised by the persistence of more than 50% of collagen in native (N) and stabilised (S) intervals are less susceptible to T and RH fluctuations. Their reinforcement by a massive crosslink formation enables more relaxed environmental standards during storage and display (Badea et al., 2012b; Badea et al., 2012c).

REFERENCES

American Society of Heating, Refrigerating and Air-Conditioning Engineers, Inc. (2011), *ASHRAE Handbook - Heating, Ventilating, and Air-Conditioning Applications*, (I-P Edition), Chapter 23 Museums, galleries, Archives and Libraries.

Badea, E., Della Gatta, G., Usacheva, T. (2012a), "Effects of temperature and relative humidity on fibrillar collagen within parchment: a micro Differential Scanning Calorimetry (micro DSC) study", *Polymer Degradation and Stability*, 97, 346-353.

Badea, E., Sommer Poulsen, D., Mühlen Axelsson, K., Della Gatta, G., Larsen, R. (2012b), "Standardised methods for damage ranking in parchment: from microscopic evaluation to collagen denaturation assessment", e-Preservation Science, submitted.

Badea, E., Della Gatta, G., Miu, L., Carşote, C., Petroviciu, I., Larsen, R., Odlyha, M., Braghieri, A., Benedetto, S. (2012c), "Damage assessment of historical parchments: a protocol for preventive conservation", *Restitutio, Conservation- restoration bulletin*, Muzeul Satului "Dimitrie Gusti", No. 4 (in print), Bucharest.

Badea, E., Della Gatta, G., Budrugeac, P. (2011), "Characterisation and evaluation of the environmental impact on historical parchments by DSC", *J. Therm. Anal. Calorim.*, 104, 495-506.

Badea, E., Miu, L., Budrugeac, P., Giurginca, M., Mašić, A., Badea, N., Della Gatta, G. (2008), "Study of deterioration of historical parchments by various thermal analysis techniques, complemented by SEM, FTIR, UV-VIS-NIR and unilateral NMR investigations", *J. Therm. Anal. Calorim.*, 91, 17-27.

Budrugeac, P., Miu, L. (2008), "Effect of accelerated thermal ageing on the thermal behaviour of the recently made parchments", *J. Therm. Anal. Calorim.*, 94, 342-355.

Budrugeac, P., Badea, E., Della Gatta, G., Miu, L., Comănescu, A. (2010), "DSC study of deterioration caused by environmental chemical pollutants to parchment, a collagen based material", *Thermochim. Acta*, 500, 51-62.

Della Gatta, G., Badea, E., Ceccarelli, R., Usacheva, T., Mašić, A. (2005), "Assessment of damage in old parchment by DSC and SEM", *J. Therm. Anal. Cal.*, 82, 637-649.

Giurginca, M., Lacatusu, I., Miu, L., Petroviciu, I. (2009), "Parchments behavior under extreme heat and fire conditions", *Mater. Res. Innov.*, 13, 337-339.

Larsen, R., Poulsen, D.V., Minddal, K., Dahlstrøm, N., Fazlic, N. (2007), "Damage of parchment fibres on the microscopic level detected by the micro hot table (MHT) method", in: R. Larsen (Ed.), Improved Damage Assessment of Parchment (IDAP) Collection and Sharing of Knowledge (Research Report No 18), EU-Directorate-General for Research, Luxembourg, 69–72.

PREPARATION OF A NOVEL WRITING PARCHMENT WITH ALUM

YING GONG[1,2], WUYONG CHEN[2], FAN CHENG[2], JIPING CHEN[1], SHUANG YANG[2], LUCRETIA MIU[3]

[1] *College of Chemistry and Chemical Engineering, Yunnan Normal University, 650500, Kunming, China, email: gongying_2004@163.com*

[2] *National Engineering Laboratory for Clean Technology of Leather Manufacture, Sichuan University, 610065, Chengdu, China, correspondence author: wuyong.chen@163.com*

[3] *The National Research and Development Institute for Textile and Leather, Division Leather and Footwear Research Institute, 031215, Bucharest, Romania. Email: lucretia.miu@certex.ro*

A novel writing parchment was prepared by tanning with an aluminum salt. The moisture content of this parchment was approximate to 10%, and its acidity was maintained at a pH value of 6.5. As for the surface of the parchment, the color of the grain face was similar to the fresh side, with the luminance value around 90 and the brightness value about 80%. Furthermore, the contact angle for deionized water on both sides increased slowly at a rate of 0.2 ^{o}/s with prolonged contact time, and it climbed up to a value next to 100^{o} after 60s contact. These data indicated that the new parchment was a hydrophobic material suitable for writing with water-based inks. The pores of goatskins were retained as demonstrated with the SEM images of parchments. Both the AFM and XRD studies further confirmed that the micro-structure of the collagen fibers was not destroyed distinctly during the preparation process with tanning. What is more, the shrinkage temperature of the parchment would be higher than 90ºC, and its stitch tearing strength exceeded 22N/mm because of the enhanced cross-linking between the aluminum ion and the collagen fibers. In a word, this research suggested a feasible option to manufacture writing parchments of high stability.

Key words: parchment, aluminum tanning, writing ability

INTRODUCTION

Parchment is a laminar material made from goatskins or calfskins, which were endowed with fine stability, strength and longevity and popularly used for writing. For example, parchment documents are valuable stuffs recording the historical and cultural information for the European civilization dated to the second millennium BC.

In the old times goatskins were manufactured to the traditional parchments by unhairing, liming and washing, and then simply drying at room temperature under tension. Most commonly goatskins were tightened on a wooden frame known as a stretching frame (Reed 1972). However, this type of parchment without tanning was apt to decompose with the variations of environmental conditions, especially the relative humidity and temperature (Bowden, Brimblecombe 2002).

As reported, scientists are interested in characterizing the properties and origins of parchments and replicating the damaged parchment documents. As we all know, a professional team was sponsored by senior researcher Lucretia Miu, professor Budrugeac Petru and researcher Cristina Carsote in Romania, who had developed several techniques to analyze these parchments. For example, (a) both Microscope Heating Table and Thermal Analysis techniques (i.e. Differential Scanning Calorimeter, et al.) were exploited to determine the shrinkage temperature (Ts) of parchments, which was then used to elucidate the causes to the degradation of historical parchments, such as the gelatinization, hydrolysis and oxidation happened to the collagen. (b) Some instruments, like Fourier Transform Infrared Spectroscope containing Attenuated Total Reflectance and Atomic Force Microscope, were adopted to display the degradation degree. (c) X-ray Diffractometer and X-ray Fluorescence Spectroscope were used to reveal the compositions of parchments, which could be utilized to replicate historical parchments (Budrugeac et al. 2010, 2011; Carsote et al. 2008; Miu 2011).

In 2009, professor Chen Wuyong (China) jointed in this research team and finished some work on the reproduction of parchments. Firstly, they adopted the traditional process to prepare parchments and the liming time was optimized to maximize the removal efficiency of fats and the loose of the elastic fibers. Then, both the bating and pickling processes were exploited to remove the pigments in the skins so as to obtain parchments of white color (Yang et al. 2012). However, this type of parchment was a little acid, which may result in the degradation of collagen in the following storing stage and the diffusion of inks like a feather when written on.

Mineral tanning is a tannage using the coordination reaction between metal ions (i.e., Cr^{3+}, Al^{3+}) and the carboxyl groups in collagen, which could give animal skins excellent strength and stability. In this study, aluminum tanning was exploited to prepare parchments with goatskins. As revealed, this tanned parchment had luminous surface of a little hydrophobicity, high shrinkage temperature and stitch tear strength, suggesting that the parchment prepared with alum was a collagen-based material of high thermal stability and fine writing ability. In brief, this study provided an option to the replication and substitution for the deteriorated parchments in museum.

EXPERIMENTAL

Preparation of Parchments

Fresh goatskins, purchased from a local slaughterhouse, were treated with the following processes in turn: soaked at a pH value of 7; unhaired by padding a 90g/L Na_2S solution on the flesh side and then pulling out the loose hair; limed with lime (CaO mass content higher than 60%) for 8d (pH>12); relimed with lime for another 8d (pH>12); shaved to a thickness of 0.8mm; delimed with formic acid to a pH value of 6; bated with trypsase (activity as 12000U/g) (pH=8); tanned with alums ($KAl(SO_4)_2.12H_2O$ mass content as 90%) and then neutralized to a pH value of 7 with sodium formate. Next the titanium white (size range 50nm-100nm) was coated on the flesh side with the dosage as $5g/m^2$ during the following drying process under tension. In the end, the fresh side was buffed with a 320 mesh sand paper to get a fine face. The final product, namely parchment, was a laminar material with a thickness of 0.3mm.

The parchment is neutral with a pH value of 6.5±0.2 as analyzed with QB/T 2724-2005 method. Its water content was determined as 10%±0.5% using QB/T 3812.12-1999 method, which was a little higher than the moisture content for writing papers required in the GB/T 12654-2008 standard. This may be due to the high hydrophilicity of collagen in the parchment.

Determination of Color

The colors of the parchment were quantified according to the Commission International de l'Eclairage (CIE) system of color measurement with 100 standard observer data (McLaren 1983). Color values (*L, a, b* and *C*) and the diffuse reflectance at 457nm (R457, %) were recorded using a Premier 8200 color photometer (USA) with the standard white board (*L*=100) as the control.

Determination of Shrinkage Temperature

The sample pan was obtained by hermetically sealing of a parchment piece of around 3 mg together with 35μL deionized water and stoking this for 24 h. Each sample pan together with a reference empty pan was heated from 30ºC to 120 ºC with a heating rate of 10 ºC/min using a PC 200 DSC tester (Germany). The heat flow curves were recorded to get the shrinkage temperature.

Determination of the Stitch Tear Strength

The resistance to stitch for parchment was tested according to GB/T 17928-1999 method. Three rectangular specimens (100mm×20mm) were sampled perpendicular and parallel to the back bone of parchment individually. The data were averaged to represent the stitch tear strength of tanned parchment.

Contact Angle Analyses

Deionized water drop with a volume of 10μm was deposited on the surface of parchment sample (40mm×40mm) using an OCA 20 video contact angle tester (Germany) and the angle of contact was measured after 5s and 60s in turn. Then, the rate of change in wettability was calculated as following:

$$R = (A - a)/55 \qquad (1)$$

Where R, rate of change in wettability, ^{o}/s; A and a, average angle of contact for five drops after 5s and 60s respectively, ^{o}.

Scanning Electron Microscope Study

A JSM-5900LV scanning electron microscope (Japan) was used for the analysis. The micrographs for the grain sides of parchments were obtained by operating the SEM at low vacuum (10^{-4}Pa) with an accelerating voltage of 20kV.

Atomic Force Microscope Study

A SPM-9600 atomic force microscope (Japan) was exploited to observe the microstructure of the collagen fibers in parchments. The AFM images were obtained in an ambient condition at room temperature (20ºC with 65% relative humidity. The other testing conditions were as following: NSG 11 probe with observing size as 1μm.

X-ray Diffraction Analyses

An X'Pert Pro X-ray diffractometer (Netherlands) was used to obtain the X-ray diagrams of the grain surfaces of parchments. The testing conditions were as following: generator voltage as 40kV, tube current as 35mA, 2θ as 5^{o} to 50^{o}.

RESULTS AND DISCUSSIONS

Properties for the Surface of Parchments

The color values for parchments were analyzed with the standard white board (*L*=100) as the control, and the results were listed in Table 1. The color was similar for the grain and flesh side of parchments, and the luminance (*L*) was approximate to a value of 90, only 10% below the standard white board. What is more, the brightness (R_{457}) of parchment was round 80%, only a little higher than the value of 75% for the writing paper required in GB/T 12654-2008 standard. All these results indicated that the color for the tanned parchment was fit for writing application.

Table 1. Color values for parchments

Color values	*L*	*a*	*b*	*C*	R_{457} (%)
Grain side	89.48±0.46	-0.62±0.06	5.46±0.13	5.46±0.10	79.03±0.02
Flesh side	90.19±0.34	-0.59±0.04	4.84±0.10	4.89±0.12	79.81±0.02

As shown in Table 2, the initial contact angle of the tanned parchment at 5s contact was just a little lower than 90^{o}, while it increased by a value of 10^{o} after 60s contact. As described in ASTM D 724-1999 method, the excellent penetration of inks would happen when the angle of contact for a writing paper had a tendency of increase between measurement after 5s and 60s, and the contact angle located in the range of 90^{o} to 100^{o}. In this study, the contact angle for water on the surface of tanned parchment was approximate to 100^{o}, and it rose slowly at a rate of 0.2 ^{o}/s with the prolonged contact time. These data demonstrated that the liquid drop (i.e. water, water-based inks) could penetrate well in the tanned parchment. Furthermore, it had been found that there was no feather phenomenon on parchment when writing with the standard ink defined in ASTM D 724-1999 standard. In a word, this kind of tanned parchment would be suitable for writing.

Table 2 The angle of contact for deionized water on the parchments

Samples	Angle of contact（°）		Rate of change in wettability *R*(^{o}/s)
	5s	60s	
Grain side	84.0±0.3	95.9±0.4	-0.2
Flesh side	86.7±0.4	97.5±0.5	-0.2

The scanning electron micrographs for the grain side of parchments were shown in Figure 1. The images with different magnifications revealed the pores on the grain side. There was slight variation in the pore structure indicating that the particular surface characteristics of animal skins would be retained for parchments.

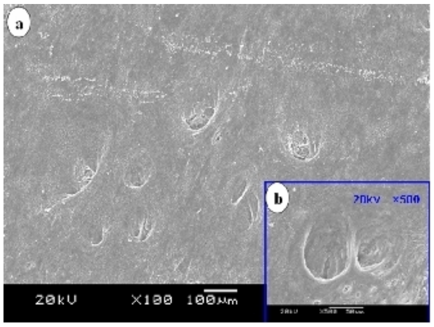

Figure 1. SEM images for the grain side

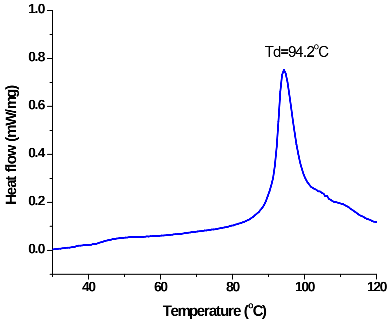

Figure 2. DSC curve for the parchment

Physical Properties of Parchments

Hydrothermal structural stability of collagen-based materials is characterized by shrinkage when it is heated in water. Moreover, the temperature at which fully hydrated material shrinks under definite conditions is called the shrinkage temperature (*Ts*). As displayed in Figure 2, the shrinkage temperature was 94.2ºC for the tanned parchment, much higher than that for the historical parchment in the museum (lower than 70 ºC). It is evident that the hydrothermal stability of parchment was elevated by tanning, which would result in the enhancement of the resistance to the degradation reactions, such as the gelatinization, hydrolysis and oxidation of collagen (Budrugeac et al. 2010).

The stitch tearing strength of the parchment was determined as 23.4±0.6 N/mm and 22.7±0.4 N/mm for the samples perpendicular and parallel to the back bone line respectively. Parchment, as a writing material, is commonly binded together for conservation. These data demonstrated that this type of parchment had enough strength for bookbinding.

Microstructure for Collagen in Parchments

The microstructure for the collagen fibers was shown in Figure 3. The collagen fibers were characteristic axial *D*-periodic cross-striated fibrils, which proved that the microstructure of collagen was not damaged with tanning.

Figure 4 showed the X-ray diagram for the tanned parchment. There were two peaks in the X-ray curve, the diffraction angle (2θ) of which were located at about 7^o and 20^o. As reported, the two peaks in the X-ray diagram of the collagen fiber in the hide represented the side-chain distance peak (Peak ***a***) and the backbone reflection peak (Peak ***c***) (Heidemann & Keller 1970; Gong et al. 2011, 2012). In this study, the existence of the two peaks further confirmed that the microstructure of collagen fibers was not deteriorated with tanning, which was also demonstrated with the *D*-period structure in AFM image (Figure 3). Furthermore, the other peaks around 10^o and 20^o , i.e. peak ***b, d, e*** and ***f,*** indicated the presence of aluminum sulfate like $Al_2(SO_4)_3.17H_2O$ and $Al_3(SO_4)_2(OH)_5.17H_2O$.

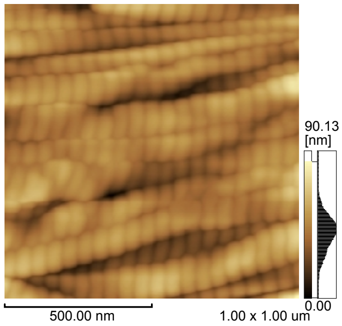

Figure 3. AFM image for the parchment

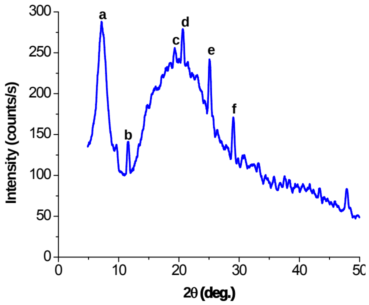

Figure 4. XRD curve for the grain side

DISCUSSIONS

As for a writing material, parchment should own not only the excellent writing quality, but also suitable strength and stability. The surface of the tanned parchment is white with luminance as 90 and brightness (R_{457}) as 80%, moreover, it is a little hydrophobicity with the angle of contact for water approximate to 100^o. These data prove that this new parchment is fit for writing application in accordance with the GB/T 12654-2008 standard "Writing Paper". The shrinkage temperature and the stitch tear strength of parchment are higher than 90 ºC and 22N/mm individually, both of which are superior to the properties for the historical parchments (Budrugeac et al. 2010, 2011; Carsote et al. 2008; Miu 2011) and the pickled parchments (Yang et al. 2012). It is evident that the thermal stability and mechanical properties are effectively enhanced with aluminum tanning. As a result, the resistance to degradation for the parchment would be probably strengthened. Furthermore, it could be speculated that this tanned parchment is suited to bookbind and will be of long longevity. In conclusion, the presented tanned parchment is an available choice for writing material.

CONCLUSIONS

A novel parchment was designed with aluminum tanning on the basis of traditional procedure. This type of parchment had fine writing ability, high hydrothermal stability and mechanical properties. Moreover, there was not any distinct damage in the pore structure and the microstructure of collagen in parchment. These results confirmed the success of the new writing parchment with aluminum tanning.

Acknowledgments

The authors wish to thank the Ministry of Science and Technology of China for financial support of the cooperation project (No.2009DFA42850, No.40-3).

REFERENCES

ASTM D 724 (1999), Standard Test Method for Surface Wettability of Paper (Angle-of-Contact Method), USA Standard.

Bowden, D., Brimblecombe, P. (2002), *Microanalysis of Parchment*, Rene Larsen (Ed.), Archetype Publications Ltd., London.

Budrugeac, P., Badea, E., Della Gatta, G. et al. (2010), "A DSC study of deterioration caused by environmental chemical pollutants to parchment, a collagen-based material", *Thermochimica Acta*, 500, 51–62.

Budrugeac, P., Cucos, A., Miu, L. (2011), "The use of thermal analysis methods for authentication and conservation state determination of historical and/or cultural objects manufactured from leather", *Journal of Thermal Analysis and Calorimetry*, 104, 439-450.

Carsote, C., Petroviciu, I., Matei, C. et al. (2008), "Degradation Level Evaluation and 2 Parchments Restoration from the National Military Museum 'Ferdinand I' Collection", *Revista Romana de Conservare si Restaurare a Cartii*, (1), 10-15.

GB/T 12654 (2008), Writing paper, China standard.

GB/T 17928 (1999), Leather-Determination of the stitch tear strength, China Standard.

GB/T 7974 (2002), Paper, board and pulp - Measurement of brightness - Diff / Geometry, China standard.

Gong, Y., Cheng, K., Zhang, T. et al. (2011), "Automated clean leather dyeing assisted by wringing, ultrasound and microwave", *JALCA*, 106(4), 127-132.

Gong, Y., Zhang, T., Chen, W. (2012), "Behavior of fatliquored leathers in a microwave field", *JALCA*, 107(2), 60-67.

Heidemann, E., Keller, H. (1970), "X-ray studies of tanned collagen", *JALCA*, 65(12), 512.

McLaren, K. (1983), *The Color Science of Dyes and Pigments*, Adam Hilger, Bristol.

Miu, L. (2011), "Particular problems in leather and parchment conservation and restoration-Using Nuclear Techniques for the Characterization and Preservation of Cultural Heritage Artefacts in the European Region", IRASM – IFIN-HH Radiation Processing Centre, Magurele - Ilfov, ROMANIA.

Reed, R. (1972), *Ancient Skins, Parchments and Leathers*, Seminar Press Ltd., Berkeley Square, London.

Yang, S., Gong Y., Chen W. et al. (2012), "Parchment replicating with leather technology", *Leather Science and Engineering*, 22(2), 10-16.

THE SHROUD OF TURIN: SPECTRAL AND COLORIMETRIC ANALYSIS FOR INNOVATIVE LIGHTING

PAOLA IACOMUSSI, GIUSEPPE ROSSI

Istituto Nazionale di Ricerca Metrologica INRIM, Strada delle Cacce 91, Torino, 10135 Italy

p.iacomussi@inrim.it, g.rossi@inrim.it

This paper describe the INRIM methodology to define a light spectrum able to guarantee a defined perception of a work of art avoiding degradation. The method is based on the measurement of spectral reflection factors of a number of points of the artifact surface. Several significant points on the Turin Shroud, measured in the past, have been used to define the lighting condition during the last Shroud exhibition of 2010.

Keywords: color measurement, lighting, color perception.

INTRODUCTION

Colour is an important characteristic a works of arts surface and during the display plays a relevant role. Colorimetric investigations contribute, on one side to the knowledge of the works of arts and on the other to verify conservation conditions. Any drift of the colours greater than the natural aging, means an incorrect conservation, and as early is discovered as early it is possible to adopt the convenient measures to reduce deterioration. The measurement of colour is also the basis for designing and realizing lighting systems for expositions with optimization of colour rendering and conservation.

Lighting a works of art represents a difficult exercise of balancing two different and opposite aspects: perception and conservation. INRIM developed a method, initially called IEN method ables to overcome the known difficulties of the Color Rendering Index method when polychromatic surfaces are exposed to low light levels based on spectral investigations on the works to lights.

LIGHTING OF WORKS OF ART

The choice of an illuminating source must be performed following the basic principles of:

- minimal degradation of materials;
- better colour rendering index;
- good visibility of details (maximum contrast);
- agreement with the international recommendation for conservation (limitation of illuminance levels, thermal load, UV radiation)

Usually the illuminating studies of works of art are based on the CIE Colour Rendering Index (CRI) (CIE 1995) and Kruithoff diagram.

CRI is a suitable method to identify the colour rendering properties of light sources, on the basis of resultant colour shifts of 14 standardised colour samples: it is only a general method and light sources with equal value of the CRI can render differently the same work of art because the 14 standard samples cannot be representative of the colours and reflection spectra involved in the specimen. Furthermore, CRI fails when the light source is a LED light, because colour perception in LED lighting doesn’t follow the same rules of the traditional sources and CIE has not already provide a suitable method specific for LED.

Kruithoff diagram links the illuminance, i.e. the quantity of light incident on a surface, to the acceptability of the perceived colour of this surfaces when it is lightied by sources with different Correlated Colour Temperature (CCT). In this application CCT can be considered as the expression of the colour of the light: lights with large amount of blue are perceived as cold lights and have high CCT values. Kruithoff diagram is, again, a general method that identify the combination of illuminance and CCT able to produce pleasant perceived colours. But there is not large consensus about these results and, because the strong hidden correlations with light source emission spectrum, specimen spectral characteristics and visual adaptation, the diagram suggestions could fail at low illuminance levels, that are mandatory for works of art conservation (CIE 2004).

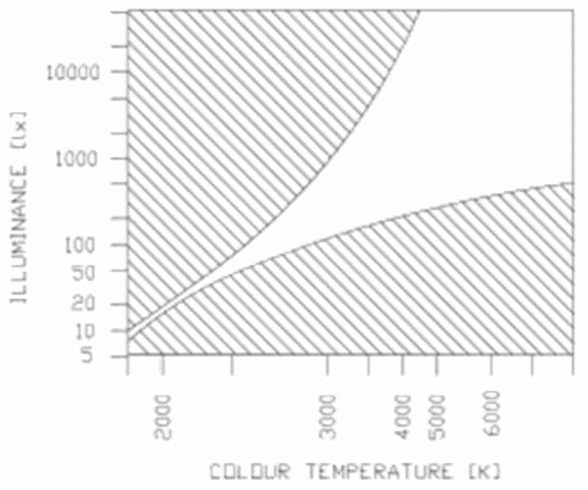

Figure 1. Kruithoff diagram (unpleasant combinations are in the dashed area)

The INRIM Method

The INRIM methodology (P.Iacomussi et al. 2001) defines the luminous source properties, with the aim of achieving the best colour rendering (working on the emission spectra) and of avoiding colour and objects degradation (working on the illuminance level). The colour rendering properties of different types of lamps, or of a combination of them, is evaluated taking account of the spectral reflection factor of several points of the work of art and, especially for painting, of the type of illumination available to the artist.

The methods is fully described in references and consists of several steps:

- measurement of the spectral reflectance of the objects (spectral characterization of the work of art).

  This can be done with devices able to spectrally evaluate the radiation. INRIM developed two dedicated devices and methods:

  1. a system based on an imaging spectrograph and a tunable filters with two CCD detectors (MIR),

   2. a Principal Component Analysis method for spectral reconstruction from data obtained with multi RGB devices (calibrated scanners or CCD cameras),
- definition of the correct source (or mix of sources) with the procedure derived from the CIE colour rendering index method but with the measured spectral reflectancies of the lighted object;
- calculation with a modified radiosity algorithm of the photometric and spectral reflected radiation considering the influence of the spectral reflections in the environment (including BRDF behaviour) around the object (e.g. walls);
- visualisation on a calibrated monitor for subjective verifications of the colour perception of object when it is lighted by the reference source and by the selected sources.

Applications

In early 2000 the INRIM method was applied to several important works of arts, Giotto's frescoes at Cappella Degli Scrovegni (L. Fellin et al 2001) and Leonardo's Cenacolo in order to define which commercial and traditional light source is able to assure the same colour perception of a priori reference source. In 2010 the enhanced INRIM method was applied to study the Turin Shroud Exhibition using a light source with spectral components digitally controlled.

TURIN HOLY SHROUD EXHIBITION

The Holy Shroud exhibition - in its more literal meaning of the act to show, display - requires a lighting able to facilitate the visual task of pilgrims to decipher the details of the image in a sufficiently obscured behaviour to not to disturb the concentration and the mystical approach to the cloth and to satisfy ambient parameters for the perfect preservation of specimen and avoid any possible image damage.

Perceive visually the Shroud is not an easy task. The "sign" of the figure that emerges from the background with the many details of the passion is somewhat masked by other factors such as burns or stains on the fabric. Also in terms of colour, as shown by the measurement (carried out by IEN-INRIM in 1978, 1998 and 2010) of spectral reflectance of the image differs minimally from that of the background fabric.

Colorimetry of the Turin Shroud

The Holy Shroud appears almost monochromatic, and the chromaticity coordinates are placed in a very small region of the CIE 1931 Chromaticity diagram. This region is enlarged in Figure 2, where the zones (stain, background, burning, body, blood, etc.) appear not very much separated, and their identification through the colour seems to be difficult. Basically the perceived image of the body is the result not of a difference in colour (like the "red" blood), but in brightness, appearing much darker than the background as is clearly show in Figure 3, were the spectral reflection factor of few sample points is plotted.

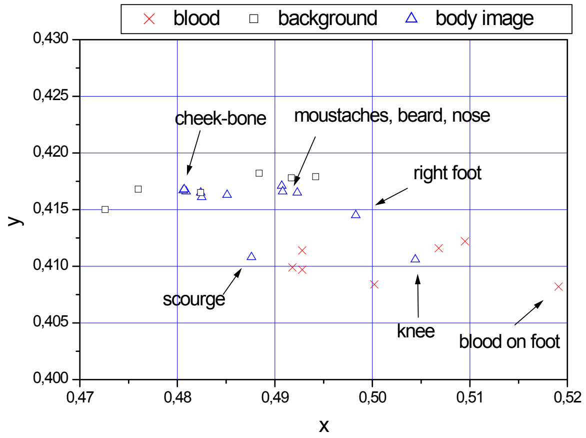

Figure 2. Chromaticity coordinates of measured points in the chromaticity diagram, enlarged area

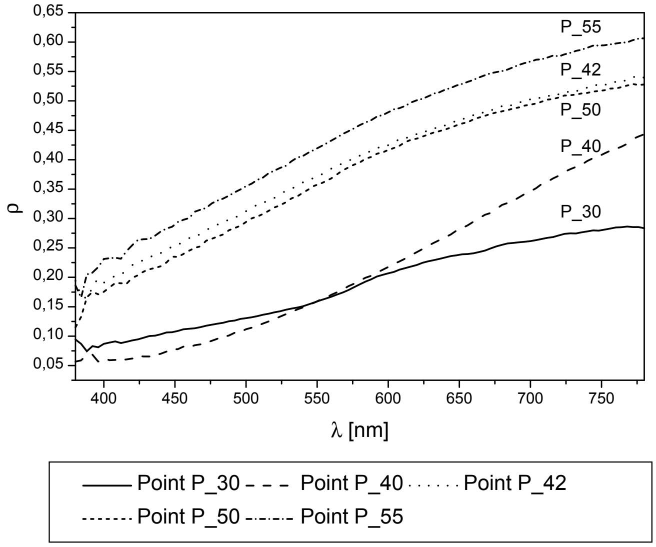

Figure 3. Spectral reflection factors of different zones of the Holy Shroud: P30 blood (right forearm); P40 burning; P42 water stain; P50 right eye; P55 background

Lighting the Holy Shroud Exhibition

The emission spectrum of the sources was calculated with the triple aim of:

- perceive the colors of the Shroud as if it were illuminated by diffuse daylight, mimicking the ancient Shroud exhibition where the Shroud was exposed outdoors;
- increase the contrast between image and background, thereby making more visible the signs of the Man of the Shroud;
- minimize the incident light, keeping it below the regulatory limits, to optimize the conservation conditions.

In this special lighting set up the main problems to overcame are:

- Geometrical constraints (specular reflections from the protective glass pane, shadows, illuminance uniformity) due to the very angulated light positions vs Shroud position;
- Spectral constraints due to the presence of a thick and green security glass and the Shroud it self and the necessity to compensate the colour shift due to the double path of the light (from source to Shroud surface and from Shroud surface to observer);
- Perception constraints due to conservation, religious behaviour, image characteristics (difference in brightness rather in colour);

Literature and standards (CIE 2004 UNI 1999), generally report a permitted illuminance level for sensible materials of 50 lx with an annual dose of 50 klx h/year for extremely sensible materials and 150 klx h/year for sensible material, but some authors prefer lower values of illuminance. In the Shroud exhibition we reached a lower values than 50lx. Considering the spectral constraint due to the spectral transmittance factor of the security glass (Figure 4), the emission spectrum of the source was modified to compensate the green surplus and to enable the perception of colours as if the Shroud was lighted by Daylight.

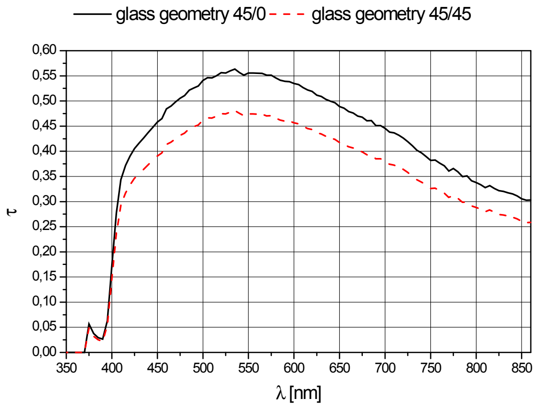

Figure 4. Security glass spectral transmittance factor (0/45 and 45/45)

Acknowledgements

The authors gratefully acknowledge the support of the Turin Shroud Commission for the assignment of the Turin Shroud Lighting, and Mr. G. Scialpi for his help in the measurements.

REFERENCES

CIE Commission Internationale de l'Eclairage (1995), Method of measuring and specifying colour rendering properties of light sources, CIE 13.3.
CIE Commission Internationale de l'Eclairage (2004), Control of damage to museum object by optical radiation CIE 157.
Iacomussi, P., Rossi, G., Soardo, P., Fellin, L. (2001), "A new method for studing lighting design for works of arts', Proceedings of Lux Europa 2001 The 9th European Lighting Conference, Reykjavik (IS).
UNI (1999), Standard 10829:1999 Condizioni Ambientali di Conservazione.

SCIENTIFIC ASPECTS OF DEGRADATION AND CONSERVATION OF HERITAGE ARTIFACTS

OVIDIU IORDACHE[1], IOANA STĂNCULESCU[2], VIKTORIIA PLAVAN[3], LUCREȚIA MIU[1]

[1] *National R&D Insitute for Textile and Leather, Bucharest, Romania, lucretia.miu@certex.ro*

[2] *Horia Hulubei National Institute for Physics and Nuclear Engineering, Măgurele & University of Bucharest, Faculty of Chemistry, Bucharest, Romania*

[3] *Kiev National University of Technology and Design, Kiev, Ukraine*

This study will give a better insight on how irradiation can be used to treat and preserve delicate historical objects by clearing them of contaminants such as insects, fungi and bacteria. Historic and culturally important objects are at risk of microbial deterioration. Microbial deterioration of heritage materials occurs primarily through the formation and growth of biofilms—microorganisms attached to a surface and embedded within a microbial produced polymer matrix. Gamma irradiation is used to kill contaminants and bacteria that may infest old artifacts, without altering or damaging the original composition of the artifact. This radiation technique offers the most delicate and reliable method of disinfecting old or fragile cultural heritage materials; it helps to conserve them and paves the way for restoration. This research is meant to give support to a new research which should investigate the effect of various doses of irradiation on both heritage artifacts and microbial strains that usually affect these artifacts.

Keywords: artifacts, deterioration, gamma irradiation

INTRODUCTION

Scientific contribution to the conservation of cultural heritage has grown to a great extent in the last decade. Physical, chemical and biological factors interact with constitutive materials inducing changes both in their compositional and structural characteristics. A certain aspect of matter transformation is due to the metabolic activity connected with the growth of living organisms (Tiano, 2002). Many cultural heritage objects that are not stored in the right conditions may become infected with biological contaminants that can destroy them and that may also present hazards to the experts working closely with them. Microbial processes act in conjunction with physical and chemical deterioration and in most instances are inseparable from it. The material composition of the object as well as the external environment can, in part, determine the community of microorganisms that is present and the mechanism of deterioration. However, microorganisms can also alter the physical and chemical properties at a material surface, thereby affecting other deterioration mechanisms (Mitchell, 2010). The main types of damages derived from metabolic activity of organisms are related with physical, chemical and aesthetical mechanisms, while the intensity of these damages are strictly correlated with: type and dimension of the organism involved; kind of material and state of its conservation; environmental conditions, micro-climatic exposure; level and types of air pollutants (Tiano, 2002).

Conservative interventions using direct and indirect methodologies have been applied in order to stop or slow-down the biodeterioration process.

The preservation of cultural heritage artifacts using irradiation is a little known but highly effective application of nuclear technology. Irradiation can be used to treat and preserve delicate historical objects by clearing them of contaminants such as insects, fungi and bacteria.

Currently the most common method used for hygiene of these materials is ethylene oxide treatment, which is toxic to human and harmful for the natural environment. The promising alternative for this technique can be ionizing radiation. Gamma irradiation has already been applied to control of pest organisms in large volumes of books and archives as well as in wooden sculptures (Chmielewska et al., 2011).

In comparison to standard chemical procedures, irradiation has the advantage of being able to treat a whole specimen through its packaging. The object is not physically touched, and no chemicals are used, so there are no toxic residues, and hence no risks for curators, visitors or the environment. In addition, complex and delicate items can be treated quickly, reliably and at a low cost. Characterized by deep penetration and low dose rates, gamma radiation effectively kills microorganisms throughout the product and its packaging with little temperature effect. After the irradiation treatment, both bioburden (microbial load of the items) and degradation effects (chain scission, etc.) depend on the absorbed dose. High radiation doses will highly decrease the bioburden (exponential decay) and low doses will produce less degradation on the irradiated materials. Physical-chemical analysis can be used to assess the restoration results: SEM, AFM, FT-IR, TA, DLS, ED-XRF and ICP-AES (Ion et al., 2011).

Textile Based Artifacts Bioburden and Decay Mechanisms

Fibers with a high amount of lignin are more resistant to microbiological attack than purified fibers, while textiles contain sizing (starch and dextrin) are more susceptible.

The following structural features of fibers and textiles also affect biodegradation: degree of polymerization, length of cellulose chain, fiber crystallinity and orientation. Furthermore, mechanical, and photochemical degradation increase susceptibility to biodeterioration. Loosely woven fabrics are less resistant than tightly woven fabrics because they hold more dirt and biological pollutants between fibers, creating favorable conditions for biological attacks (Menier, 1988).

The most frequent biodeteriogens of cellulosic textiles are micro-fungi (*Ascomycetes* and *Deuteromycetes*) and bacteria of cellulolytic and non-cellulolytic species, many of which have been mentioned for the wood and paper biodeterioration. The most active agents of textile deterioration are fungi. Among *Deuteromycetes*, there may be found several species of *Alternaria*, *Aspergillus*, *Fusarium*, *Memnoniella*, *Myrothecium*, *Neurospora*, *Penicillium*, *Scopulariopsis*, *Stachybotrys*, *Stemphylium*, etc. Quite frequent and particularly harmful because of its high cellulolytic activity is the genus *Chaetomium* of *Ascomycete* (Kowalik, 1980; Vigo, 1980). *Zygomycetes* such as *Mucor* and *Rhizopussometimes* often occur on textiles.

Leather Based Artifacts Bioburden and Decay Mechanisms

Leather is composed mostly of the protein collagen, which displays a discrete structural hierarchy, from the molecular to microscopic levels (it is a complex material based on collagen and tannin, with special properties). Collagen degradation at any or all levels of the structural hierarchy over time may influence the physical characteristics of historically important documents (the organic nature, the influence of the physical-chemical factors: environmental pollution, the acid-basic treatments, temperature, humidity; biological and microbiological factors: bacteria, fungi, contribute to the occurrence of structural alterations).

Parchment is composed of collagen, some amount of keratin and elastin, and a minimal amount of albumin and globulin. Collagen is one of the proteins most resistant to microorganisms attack, it can only be hydrolyzed by specific enzymes, collagenases, produced by some anaerobic bacteria of the genus *Clostridium* (Feiden, 1982; Kowalik, 1980).

The parchment's susceptibility to biodeterioration depends by the raw material, its method of production and its conditions of preservation. Under aerobic conditions, only bacteria can attack partially decomposed collagen, among which are strains of *Bacillus* (*e.g., B. mesenthericus*), *Pseudomonas*, *Bacteroides*, and *Sarcina*. Ancient parchment materials can also be attacked by certain species of fungi of the genera *Cladosporium*, *Fusarium*, *Ophiostoma*, *Scopulariopsis*, *Aspergillus*, *Penicillium*, *Trichodernia*, etc., (Hueck, 1972). As a result of biodeterioration, parchment loses its original properties and becomes hard and brittle, often with deformation of the structure. The microbial attack also causes variegated spots, white films and fading of the texts.

Bacteria under conditions of high humidity attack untanned skins. Tanned leathers are not readily subject to bacterial attack, but are degraded by fungi (Tiano, 2002).

Fungi that attack tanned leather often belong to lipolytic species and utilize the fats present in leather as a source of carbon. In this case the proteins are not directly affected, but can be damaged by organic acids released as metabolic end products and the artifact becomes stained and stiff (Varonina et al., 1981; Von Endt et al., 1986).

Proteinaceous materials like parchment and leather are also susceptible to attack by insects: *Dermestidae* and *Tineidae* are the main families that can selectively attack either collagenous or keratinous materials (Varonina et al., 1981; Von Endt et al., 1986). Occasionally, cellulose and proteinaceous feeders cause damage to parchment and leather materials. The insect damage appears as superficial erosion, deep erosion, holes or loss of material (Tiano, 2002).

Effect of Gamma Radiations on Living Cells

Gamma irradiation is electromagnetic radiation of short wavelength emitted by radioactive isotopes as the unstable nucleus breaks up and decays to reach a stable form. DNA is the principal cellular target governing loss of viability after exposure to gamma irradiation. DNA damage occurs predominantly by the indirect action of gamma rays, which interact with other atoms or molecules, particularly water, to produce reactive free radicals. Cell death (defined for proliferating cells as loss of reproductive capability) is predominantly induced by double-strand breaks in DNA, separated by not more than a few base pairs, which can generally not be repaired by the cell (Hall & Giaccia, 2006).

Although several studies have investigated the effect of gamma irradiation on the viability of micro-organisms, little information is available regarding its effect on microbial DNA. In particular, whether gamma irradiation eliminates amplifiable DNA, detectable using quantitative broad-range PCR, is unknown. DNA may fail to amplify due to DNA degradation, such as alteration in primer binding sites or reduction of the DNA into fragments smaller than the target. If gamma irradiation effectively eliminates amplifiable DNA, it could be used widely in laboratory and clinical practice for prevention of DNA contamination of PCR reaction reagents, laboratory equipment, surgical instruments and containers for specimen collection and transportation (Trampuz, 2006).

Gamma rays, electromagnetic waves with high penetrating power, pass through materials without leaving any residue. Fungi have been successfully inactivated from different materials, such as paper, wood and soil with radiation doses ranging from 6 to

15 kGy. The insect infestation control can be performed by submitting wooden objects to lower radiation doses, *e.g.* 0.2 – 0.5 kGy whereas the fungi and microorganisms infestation can be prevented by doses of 3 – 8 kGy and 15 – 20 kGy, respectively (Magaudda, 2004). However, the disinfestation of cultural heritage using gamma radiation is a extremely efficient process, but this does not protect the material to a re-infestation (U.S. Department of Agriculture, 1974).

Gamma radiation as sterilizing treatment causes direct damage to cell DNA through ionization inducing mutation and killing the cell. It also has an indirect effect as a result of radiolysis of cellular water and formation of active oxygen species, free radicals and peroxides causing single and double strand DNA breakages (Silva et al., 2006).

Effects of Gamma Radiations on Cultural Heritage Artifacts

Gamma radiation has proven to be a clean and safe alternative for the treatment of biodeteriorated objects. Its high penetration capability and the possibility to be applied to a broader range of materials (as opposed to temperature treatments), make this option an attractive alternative in art preservation, conservation and decontamination (Adamo et al., 2001; Gonzalez et al., 2002).

The longer irradiation time and the higher irradiation doses, enhance the possibility for oxygen in air interacts with radicals originated from material irradiation processes. Pigment alterations caused by gamma irradiation have been reported in other works (Rizzo et al., 2002). A dose of 30 kGy is considered to be harmless and therefore proposed as the maximum irradiation dose to be applied in the decontamination treatment of tested parchments (Nunes, 2012).

The complexity of cultural heritage artifacts matrix makes it a good substrate for growth of biodeteriorating organisms. Different treatment methods have been applied during the last years aiming towards its decontamination. However, there is very little information about the effects of gamma radiation on the physical properties of parchment (*i.e.* changes in color and texture, elasticity, etc.).

Texture is a multi-parameter attribute that was first studied between the 19th and 20th centuries (Bourne, 1978; Szczesniak, 2002). Texture recently became an important parameter to analyze the structural changes in materials by decontamination processes (Pang et al., 2007; Araujo, 2007).

Color, as well as texture, is a physical parameter that has been employed in decontamination studies in order to understand the effects of different lethal agents on the physical properties of materials (Zaied et al., 2007; Landfeld et al., 2010), and also to prevent changes in the aesthetics of treated documents.

The structural damage of collagen has been widely reported as the decrease of R-CONHR’, the degradation of amides (broken –C-N bonds in the amide structure of collagen and formation of $ROCNH_2$ and O=CR bonds) (Bowes & Moss, 1962; Grant et al., 1973) and increase of C-O and C=O bonds, thermal denaturation (Liu et al., 1989), and general oxidative degradation (Bowes & Moss, 1962).

Bioburden of 14th Century Leathers from the 16th Han Grave of the Bakhchisaray (Crimea), from Ukraine

The goal was the isolation and identification of fungi species, obtained from archaeological leathers, Exposure in Czapek-Dox environment was used, to establish biological load.

Paecilomyces variotii was the predominant species found on the samples. Samples were kept under observation for 10 days. Mold growths began to show after 6-7 days of incubation. They were maintained in the thermostat at a temperature of 30°C and air humidity of 90%.For biological analyses, there have been used samples in low amount and after the treatment they were kept under observation for a few days.

After several days, maintained in the thermostat at controlled temperature and humidity, different types of bacterial and fungal colonies began to appear. The next fungi species are specific for leather: *Paecilomyces varioti*, *Aspergillus flavus*, *Penicillium sp.*, *Aspergillus niger*, *Trichoderma viride*. There have been identified species commonly found in soil such as *Rhizopus sp.*, but also species that attack textile fiber and cellulose such as *Myrothecium verrucaria* (Gavriliuc et al., 2010).

DISCUSSION

Gamma rays can be used for decontamination and disinfestation purposes without damaging the art work artifacts even if the treated material is once more exposed to radiation source, *i.e.* due to a re-infestation by biodeteriorating agents (Severiano et al., 2009).

In the example shown, regarding the biological load of archeological leathers, the necessity of gamma radiation treatment was highlighted for this type of artifacts, for safe restoration and preservation purpose.

The main objectives of the project will be studying of the microbiological contamination of the cultural heritage items (textiles and leather), cultural heritage deposits and workplaces in order to establish a maximal contamination limit which will lead to a minimum required dose for the treatment. Also, future works will be concentrated on study regarding the radiation induced degradation on cultural heritage items and this will lead to a maximum allowed radiation dose for the treatment. The tests will be performed on both recent (reference) and naturally and/or artificially aged materials. For subtracting the cumulative effects, tests will be performed both to the whole material as it appears in the cultural artifacts and to constituents, raw materials and additives.

Acknowledgement

This work was financed by the ANCS, PN-II-PT-PCCA-2011-3-1742 project, “Improvement of occupational environment quality in cultural heritage deposits. Validation of gamma radiations treatment of textile and leather cultural goods (TEXLECONS)” contr. no. 213/2012.

REFERENCES

Adamo, M., Brizzi, M., Magaudda, G., Martinelli, G., Plossi-Zappala, M., Rocchetti, F., Savagnone, F. (2001), “Gamma radiation treatment of paper in different environmental conditions: Chemical, physical and microbiological analysis”, *Restaurator*, 22, 107–131.

Araújo, M.M., Thomaz, F.S., Fanaro, G.B., Duarte, R.C., Aquino, S., Corrêa, B., Villavicencio, A.L.C.H., (2007), “Irradiation as a decontamination processing for rice paper sheet”, *Proceedings of the International Nuclear Atlantic Conference (INAC)*, Associação Brasileira de Energia Nuclear—ABEN.

Bourne, M.C. (1978), “Texture profile analysis”, *Food Technol.*, 32, 62–66.

Bowes, J.H., Moss, J.A. (1962), “The effect of gamma radiation on collagen”, *Radiat Res*, 16, 211–223.

Chmielewska, D., Gryczka, U., Migdal, W., Ignatowicz, S. (2011), “Application of radiation methods to preservation of cultural heritage”, *Journal of Entomological and Acarological Research*, 43(2), 237-244.

Feilden, B.M. (1982), “Insects and other pests as causes of decay”, *Conservation of Historic Buildings*, London, Butterworth Scientific, 131-151.

Gavriliuc, N.A., Ibrahimova, A.M., Plavan, V., Miu, L., Budrugeac, P., Giurginca, M., Gaidau, C. et al. (2010), “Tomb of Khan Hadji Gherai (research on archeological materials 2003-2008)”, Zaporojie Kiev, Ukraine, 104-135, ISBN 978-966-2994-34-6.

Gonzalez, M.E., Calvo, A.M., Kairiyama, E. (2002), “Gamma radiation for preservation of biologically damaged paper”, *Radiat. Phys. Chem.*, 63, 263–265.

Grant, R.A., Cox, R.W., Kent, C.M. (1973), “The effects of gamma irradiation on the structure and reactivity of native and cross-linked collagen fibers”, *J Anal Chem*, 115, 29–43.

Hall, E.J, Giaccia, A. (2006), *Radiobiology for the Radiologist*, Lippincott Wilkins & Williams, Philadelphia, USA.

Hueck, H.J. (1972), “Textiles pests and their control”, *Textiles Conservation*, London, J. E. Leene, 76-97.

Ion, R.M., Doncea, S.M., Ion, M.L. (2011), “Nanomaterials for Chemical and Biological Restoration of Old Books”, *New Approaches on Book and Paper Conservation-Restoration Conference*, Austria, Horn, 9-11 May.

Kowalik, R. (1980), “Microbio deterioration of library materials. Part 1”, *Restaurator*, 4, 99-114.

Landfeld, A., Erban, V., Kovářı́ková, E., Houška, M., Kýhos, K., Průchová, J., Novotná, P. (2010), “Decontamination of cut carrot by persteril® agent based on the action of peroxyacetic acid”, *Czech. J. Food Sci.*, 28, 564–571.

Liu, B., Harrell, R., Davis, R.H., Dresden, M.H., Spira, M. (1989), “The effect of gamma irradiation on injectable human amnion collagen”, *J Biomed Mater Res*, 23, 833– 844.

Magaudda, G. (2004), “The recovery of bio teriorated books and archive documents trough gamma radiation: some considerations on the results achieved”, *Journal of Cultural Heritage*, 5, 113-118.

Menier, J. (1988), “Sur quelques insectes deprédateur desarchives”, Patrimoine culturel et alterations biologiques. *Actes des journees d’etudes de la S.F.I.I.C.*, Poitiers, 17-18 November 1988, 45-52.

Mitchell, R., McNamara, C.J. (2010), *Cultural Heritage Microbiology - Fundamental Studies in Conservation Science*, ASM Press, 1 edition.

Nunes, I., Mesquita, N., Cabo Verde, S., João Trigo, M., Ferreira, A., Carolino, M.M., Portugal, A., Botelho, M.L. (2012), “Gamma radiation effects on physical properties of parchment documents: Assessment of Dmax”, *Radiation Physics and Chemistry*, Elsevier.

Pang, N.S., Jung, I.Y., Bae, K.S., Baek, S.H., Lee, W.C., Kum, K.Y. (2007), “Effects of short-term chemical disinfection of gutta-percha cones: identification of affected microbes and alterations in surface texture and physical properties”, *J. Endod.*, 33, 594–598.

Rizzo, M.M., Machado, L.D.B., Borrely, S.I., Sampa, M.H.O., Rela, P.R., Farah, J.P.S., Schumacher, R.I. (2002), “Effects of gamma rays on a restored painting from the XVIIth century”, *Radiat. Phys. Chem.*, 63, 259–262.

Severiano, L.C., Lahr, F.A.R., Bardi, M.A.G. and Machado, L.D.B. (2009), “Influence of gamma radiation on mechanical and thermal properties of Cedrella fissilis and Ocotea porosaused in works of art”, *2009 International Nuclear Atlantic Conference - INAC 2009*, Rio de Janeiro, RJ, Brazil, September 27 to October 2, 2009, ASSOCIAÇÃO BRASILEIRA DE ENERGIA NUCLEAR - ABEN ISBN: 978-85-99141-03-81.

Silva M., Moraes, A.M.L., Nishikawa, M.M., Gatti, M.J.A., Alencar, M.A.V., Brandão, L.E., Nóbrega, A. (2006), “Inactivation of fungi from deteriorated paper materials by radiation”, *International Biodeterioration & Biodegradation*, 57, 163-167.

Szczesniak, A.S. (2002), “Texture is a sensory property”, *Food Qual. Prefer.*, 13, 215–225.

Tiano, P., (2002) - “Biodegradation of Cultural Heritage: Decay Mechanisms and Control Methods”, CNR - Centro di studio sulle “Cause Deperimento e Metodi Conservazione Opere d’Arte”, 50121 Firenze, Italy.

Trampuz, A., Piper, K.E., Steckelberg, J.M. and Patel. R. (2006), “Effect of gamma irradiation on viability and DNA of Staphylococcus epidermidis and Escherichia coli”, *J. of Medical Microbiology*, 55, 1271–75.

U.S. Department of Agriculture, Forest Service, Forest Products Laboratory (1974), *Wood Handbooks*, U.S Department of Agriculture, Washington D.C. & USA.

Varonina, L.L., Nazarova, O.N., Petushkova, U.P. and Rebrikova, N.L. (1981), “Damage of parchment and leather caused by microbes”, ICOM Committee for Conservation, 6th Triennial Meeting. Ottawa, 21-25 September 1981, Preprints, Paris, ICOM, 1913.1-19/3.11.

Vigo, T.L. (1980), “Protection of textiles from biodeterioration”, *Conservazione e Restauro dei Tessili*, Convegno Internazionale, Como, 18-26.

Von Endt, D.W. and Jessup, W.C. (1986), “The deterioration of protein materials in museums”, *Biodeterioration 6, Proceedings of the Sixth International Biodeterioration Symposium*, eds. S. Barry and D.R. Houghton, Great Britain, Cab International, 332-337.

Zaied, S.F., Youssef, B.M., Desouky, O., El Dien, M.S. (2007), “Decontamination of gum arabic with γ-rays or electron beams and effects of these treatments on the material”, *Appl. Radiat. Isot.*, 65, 26–31.

STUDY OF DETERIORATION OF ARCHEOLOGICAL COLLAGEN BASED ARTEFACTS

VIKTORIIA PLAVAN[1], LUCRETIA MIU[2], MARINA DARAGAN[3], NADIA GAVRILYUK[3], VIACHESLAV BARSUKOV[1], ALIA IBRAGIMOVA[4]

[1] Kiev National University of Technologies and Design, 2, Nemirovich-Danchenko str. Kiev, 01011, Ukraine, e-mail: plavan@live.ru, chemi@voliacable.com,

[2] INCDTP - Division: Leather and Footwear Research Institute (Bucharest, Romania)

[3] Institute of Archaeology from National Ukrainian Academy of Sciences (Kiev, Ukraine)

[4] The Bakhchisarai State Historical and Cultural Preserve (Crimea, Ukraine)

Specimens of the Scythian archaeological leather and tendon from the fourth century BC and archaeological leather from XVI century were investigated. To analyses of amino acid composition of the archeological leather an ion-exchange liquid-column chromatography was employed. At the microscopic level, damage in fibred structure is detected and measured by optical microscopy and scanning electron microscopy and leather hydrothermal stability by the Micro Hot Table technique. Animal types of leather was identifying by optical microscopy. Such macro and microscopic damages of leather as loss of tear strength, fraying, cracking and gelatinization of fibers, correlated with changes into the underlying structure of collagen. Ageing of leather affect the amount of polar amino acids in the collagen, primarily lysine, arginine, and asparagine and glutamine amino acids. The relationship between the amounts of basic and acidic amino acids B for the new leather is 0.52, whereas for the archaeological leather and tendon it is 0.49-0,12 and 0,24, correspondingly, which reflects the degree of oxidation decomposition of collagen. The shrinkage temperatures of archaeological leather and tendon were about 45-50^{o}C. X-ray fluorescence determines the chemical elements like: Fe, Cu, Ca, S, Zn, Mn, etc. on the surface of the archaeological leather and tendon.

Key words: ageing of leather, archaeological leather, amino acid composition

INTRODUCTION

It is known that there is a relationship between the visual damage of leather, which manifests itself in its physical properties on microscopic and macroscopic levels, and the changes revealed by structural, thermochemical, thermophysical and chemical analyses, in which the assessment is carried out in the leather fragments. Such visual macro- and microscopic damage as loss of strength, fraying, brittleness and fibre gelation in leather can correlate with the changes in collagen structure. In some cases, the changes can be connected with chemical transformations caused by the oxidation and hydrolysis processes which occur in protein chains and acid residues on a molecular level. When dried, archeological leather is characterized by considerable shrinkage, becomes brittle and fragile, which can be hardly reverse.

The goal of this work was study of deterioration of archeological collagen based artefacts in order to develop science-based technologies for leather recovering, which would allow leather items to be stored and exhibited.

MATERIALS AND METHODS

The following specimens were studied:

1) leather from Khazi Gerai khan's Turbe tomb № 16 from XVI century. The cover of coffin from tomb № 16 was covered with heavy lavishly-decorated greenish cloth with floral design. Under the cloth a leather covering was revealed. It consisted of four

separate pieces of leather from different raw-hide types (calfskin, sheepskin) nailed on the cover;

2) specimens of archeological leather of the remains of a shoe from Scythian burial place №2, burial mound №5 dating back to the IVth century B.C. (Figure 1). The remains were found in 1971 in Balhakovo, Mykolaiv region. Visual assessment of the remains showed that the leather was badly damaged as it was hard, brittle and fragile. However, it was fairly dense.

3) specimens of collagen-containing material, probably tendon (Figure 2), which was used by Scythians to make bows (Scythian burial place № 4, burial mound № 8 dating to the third quarter of the IVth century B.C.). Visual assessment of the material showed that it was brittle, fragile and having a dense film on its surface, even though it had been polyacrylate- pretreated by archeologists.

The assessment of damage focuses on collagen, which is the major component of leather showing the damage on every structural level. On the macroscopic level the changes caused by the damage are characterized by colour, hardness and thickness and can be measured by ordinary physical techniques. On the microscopic level the damage to the fibre structure can be detected and measured with an optical microscope or a scanning electron microscope and by determining hydrothermal stability of the leather with the help of Micro Hot Table. Such methods as liquid column chromatography and X-ray fluorescent analysis are used for determining physical-chemical properties of collagen and measuring the structural damage of its fibrils and microfibrils on the mesoscopic and nanoscopic levels as well as for assessing chemical and structural damage of leather on the molecular level. To conduct qualitative and quantitative analyses of amino acid composition of the archeological leather and collagen-containing material, ion-exchange liquid-column chromatography with the 339 M automatic analyzer (Microtechna, the Czech Republic) was employed.

RESULTS AND DISCUSSION

The destruction of vegetable-tanned leather results from two processes: acid hydrolysis and oxidative degradation of collagen and tannins (Larsen, R., et al, 1994). In oxidative degradation of collagen there is observed transformation of positively charged amino acid residues into negatively charged ones, whereas in undamaged collagen the positively charged and negatively charged amino acid residues are balanced. A change in this balance, including that caused by oxidative degradation of leather, leads to leather destruction. The relationship between the amounts of basic and acidic amino acids $B = \frac{\Sigma(Arg\ Lys)}{\Sigma(Asp, Glu)}$ reflects the degree of oxidation decomposition of collagen.

In this study the content of basic amino acids in the new and archeological leather was determined with results being presented in Figure 1. The results show that ageing affects the amount of polar amino acids, primarily of lysine and arginine, as well as aspartic and glutamic acids in leather. The content of proline also increases.

Basically, oxidative degradation of collagen results in a decreased amount of basic amino acids and proline, whereas the content of acidic amino acids increases. Apart from other reasons this is due to an increase in the amount of collagen degradation products.

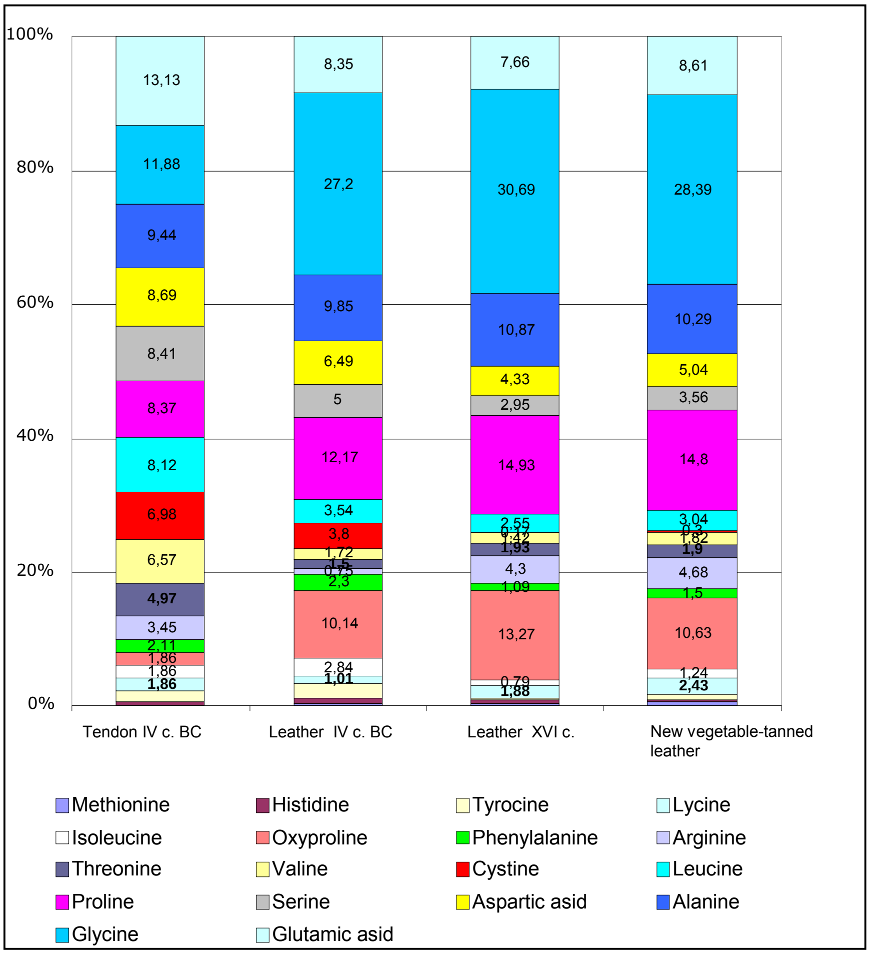

Figure 1. Amino acid composition of the archeological leather and collagen-containing material

Hydrolytic degradation of collagen leads to an increased amount of basic amino acids due to breaking the peptide bonds. The total amount of arginine and lysine is 7.11% for the new leather, 6.18% for the XVI c. leather and 1.76% for the leather dating back to the IV c. BC, that is the decrease amounts to 0.93 and 5.35 correspondingly. If there occurred only the oxidative degradation in collagen, the content of acidic amino acids would increase by the same value. As a matter of fact, there is observed a decrease in the content of acidic amino acids of 1.66% for the XVI c. leather and 1.19% for the leather dating back to the IV c. BC. If the ageing resulted only from the hydrolytic degradation of collagen, the amount of acidic amino acids would increase due to the breaking of the peptide bonds. Thus, the values prove that the ageing is caused by a complex action of both the processes. For the new leather the ratio B is 0.52, whereas for the old leather B=0,51 and B=0,12 for the XVI c. leather and for the leather dating back to the IV c. BC, correspondingly.

A tendon is a tough band of connective tissue that attaches muscles to bones. Tendons are composed of bundles of type I collagen fibres closely packed together, with some amounts of type III and V collagen. The bundles of collagen are held up together with proteoglycans. Type III and IV collagens are distinguished by a higher content of cystine, due to which they are capable of forming additional disulphide bonds stabilizing the complexes of collagens with proteoglycans.

This is corroborated by the data on the amino acid composition of a tendon portion. The content of cystine amounts to nearly 7% compared to 0.2% for the new leather. Due to this the tendons have a high strength and a low capability of stretching.

The total amount of basic amino acids (arginine and lysine) in the tendon specimen is 5.31%. The total amount of acidic amino acids (glutamic and aspartic acids) is 21.82%, which is much higher than that for other specimens probable due to an increased amount of collagen degradation products. For the IV c. BC tendon B = 0,24, which is indicative of a smaller degree of collagen degradation on ageing compared to the leather dating back to the same historical period. This must be accounted for by the high content of cystine in the structure of type III collagen, which is a component of the tendon, in contrast to type I collagen, which is a major component of the leather.

The temperature range over which the shrinkage of collagen fibres takes place is visually determined by the MHT method (Larsen et al., 2002). Results of determination of the shrinkage temperature range for the specimens under study are presented in Table 1.

Native fibres of the skin collagen of mammals shrink at temperatures of about 65-68°C. There is certain differentiation in the temperature for different species of mammals and different topographical areas of the skin. After vegetable tanning the shrinkage temperature ranges from 66 to 90°C, after formaldehyde tanning it is 75-90°C, and after chrome tanning it is 80-120°C.

Table 1. Shrinkage temperature of collagen fibres determined by the MHT method

Samples	Shrinkage temperature, °C						
	Initial temperature	A_1	B_1	C	B_2	A_2	Final temperature
Leather XVI c.	29.3	46.8	49.8	**51.7**	52.8	53.7	55.6
Leather IV c. BC	24.6	28.7	34.4	**45.3**	50.3	58.4	66.4
Tendon IV c. BC	27.8	36.9	44.9	**46.9**	57	61.9	67

The shrinkage temperature of the new leather determined by the conventional method was found to be 80°C. The results presented show that ageing causes a 10-25°C decrease in the shrinkage temperature of the archeological leather compared to the specimens of the new vegetable-tanned leather.

The content of arginine and lysine in the specimens correlates with the shrinkage temperature values (Figure 2). As it was said above, the ratio of the amounts of basic and acidic amino acids reflects the degree of oxidative degradation of collagen. That is the higher the content of basic amino acids, the lower the degree of the oxidative degradation.

It is known from results of previous studies (Plavan, V.P., et al, 2010) and historical literature that vegetable tanning was used in leather manufacture in the XVI century, whereas nomadic and semi-nomadic peoples manufactured leather using smoke and feces, for example urine of cattle or horses. Now it is known that it is mainly amine groups of lysine and arginine that are involved in the interaction with organic materials like tannins. Thus, vegetable tanning increases the leather resistance to oxidative degradation.

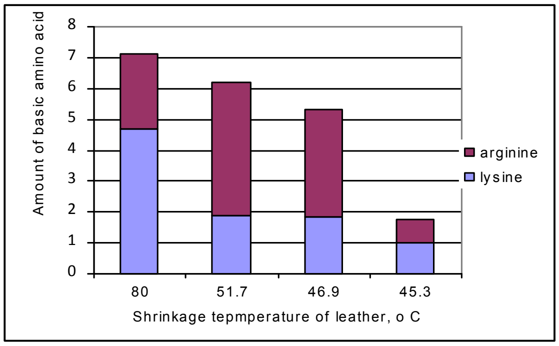

Figure 2. Dependence of the leather shrinkage temperature from content of basic amino acids

The distribution of chemical elements over the leather surface was determined by the XRF analysis. It was established that the leather contains such chemical elements as calcium, copper, iron, silicon, zinc, phosphorus, sulphur and others. The XVI c. leather specimens contain a lot of copper and iron in their surface. This is explained by the employment of metal items (cramps, angle pieces, etc) in upholstering tombs with leather. Copper easily corrodes in the air and leaves behind a green-blue deposit on the leather, which was noticed in the visual assessment.

The IV c. BC leather and tendon specimens have a great deal of iron and copper on their surface. There were also revealed calcium, manganese, nickel, zinc, titanium and other elements on the surface.

Visual assessment of the XVI c. leather shows that it has such visible damage as brittleness, hardness, warping, cracked grain and frayed edge. There is noticeable damage caused by moisture, mineral deposits and mould, traces of a blue metallic deposit (which must be due to copper oxidation). However, there is observed a fairly distinct of the grain, which allows one to determine the type of raw hide the leather was made of, most probably sheepskin, by using microscopy. The IV c. BC leather specimens are brittle and breaking. The structure of its derma is densified with signs of gelatinization. The grain is indistinct. Therefore, determination of the type of raw hide is quite complicated, though results of optical microscopy indicate that the leather must have been made from goatskin. It appeared impossible to evaluate the structure of derma of the IV c. BC leather by scanning electron microscopy because of its high density and its being stained with earth. The specimen of the IV c. BC tendon was covered with acrylate by archeologists in order to strengthen and store it. That is why it was also impossible to evaluate the structure of the material by scanning electron microscopy.

CONCLUSIONS

1. Ageing of leather affect the amount of polar amino acids in the collagen, primarily lysine, arginine, and asparagine and glutamine amino acids. The relationship between the amounts of basic and acidic amino acids B for the new leather is 0.52, whereas for the archaeological leather and tendon it is 0.49-0,12. For the IV c. BC tendon B = 0,24, which is indicative of a smaller degree of collagen degradation on ageing compared to the leather dating back to the same historical period. This must be accounted for by the high content of cystine in the structure of type III collagen, which is a component of the tendon, in contrast to type I collagen, which is a major component of the leather.
2. The shrinkage temperatures of archaeological leather and tendon were about 45-50°C. Ageing causes a 10-25°C decrease in the shrinkage temperature of the archeological leather compared to the specimens of the new vegetable-tanned leather. The content of arginine and lysine in the specimens correlates with the shrinkage temperature.
3. X-ray fluorescence determines the chemical elements like: Fe, Cu, Ca, S, Zn, Mn, etc. on the surface of the archaeological leather and tendon.
4. The derma structure of leather specimens from IV c. BC is densified with signs of gelatinization. The grain is indistinct. Results of optical microscopy indicate that the leather must have been made from goatskin.

REFERENCES

Larsen, R., Vest, M. and Bogvad Kejser, U. (1994), STEP leather projects: evaluation of the correlation between natural and artificial ageing of vegetable tanned leather and determination of parameters for standardization of an artificial ageing method. Research report № 1, Bjarnholt Repro, Copenhagen.

Larsen, R., Poulsen, D.V. and Vest, M. (2002), “The hydrothermal stability (shrinkage activity) of parchment measured by the micro hot table method (MHT)”, in Larsen, R. (ed.), *Microanalysis of Parchment*, Archetype Publications Ltd., London, 55-62.

Plavan, V.P., Miu, L. (2010), “Evaluation of the archaeological leather from Durbe Burial site of Khan‘s Hadji-Geray ”, in Gavrilyuk, N.A., Ibragimova, A.M. (eds.), *Durbe Burial site of Khan`s Hadji-Geray*, Dikoe pole, Zaporozhye, Kiev (in Russian and Ukrainean).

ELEMENTS OF SYMBOLIC ANTHROPOLOGY IN DEVELOPING THE CULTURAL IDENTITY OF THE FASHION PRODUCT

MARLENA POP

INCDTP - Division: Leather and Footwear Research Institute, 93 Ion Minulescu, Bucharest, Romania, email: pop_marlen@yahoo.ca

The art of costumes, made of textile or animal origin fibres, is one of the oldest cultural technologies of humanity, integrated in both the public and the domestic spaces of life. The artistic and cultural imaginary, predominantly feminine, has found an ideal place of expression, because the tradition of social and cultural praxis has a millenary individuality and continuity. In the creative interior of this equally artistic and technological area, the cultural identity of the product is defined by the cultural archetype or pattern which transcends the primary message and reveals, through the symbolic qualities of decorative elements and of ancient artistic techniques, a whole specific universe. Following the scientific line of CG Jung in defining the archetype, but also the philosophy of Mircea Eliade, who said that "symbol, myth, archetypal image are related to the substance of spiritual life, that we can hide, mutilate and degrade them, but never remove them", the paper proposes to decode that Romanian archetypal syntax, defined by elements of symbolic anthropology, which make up the traditional costume. Analyzing cultural archetypes and patterns which define Romanian spirituality, expressed through symbolic elements and motifs of garb with ritual role, the paper will highlight elements of symbolic anthropology expressed through avant-garde concepts of modern product design. Thus, the paper will argument the thesis that cultural identity sells any product, provided that the authentic intrinsic cultural value is respected, defined and promoted, because the European cultural economy is not only a desideratum and a top strategy, it is also a dynamic multicultural reality directed towards sustainability of heritage values.

Keywords: symbolic anthropology, archetypes, Romanian cultural patterns, cultural identity, fashion product.

INTRODUCTION

In terms of visual arts, including fiber arts and fashion, cultural identity is represented by artistic imagination, expressed through theme, language and message, basically, through its symbolic codes. However, artistic imagination is revealed not only through explicit visual semiotics and rhetoric but also through the ineffable emotional transgression, which is much more difficult to decode by psychologists, philosophers and aestheticians. Cultural identity in the visual arts is defined by the archetype that transcends artistic work, beyond the artist's personal myths, beyond semiotic myths of cultural fashion; basically by transgressing the direct message of the artistic work and the intentionality of the artist, the archetype reveals only the original reference point of our historical and spiritual being. Following the scientific line of C.G. Jung in defining the archetype, but also the philosophy of Mircea Eliade, who said that "symbol, myth, archetypal image are related to the substance of spiritual life, that we can hide, mutilate and degrade them, but never remove them" (Eliade, 1978) we are trying to decode that particular Romanian mythical archetypal syntax, which is expressed in our contemporary art as well. The transition from culture theory to artistic practice is made by deciphering the imaginary, the functions of archetypes and by understanding myths.

THE STRUCTURE OF ROMANIAN MYTHOLOGY

Fundamental myths: Myth of spirituality - Miorita ("The Little Ewe"), Myth of ethnogenesis - Baba Dochia ("The Old Dokia"), Myth of the creator - Mesterul Manole

(Master Manole), Erotic myth - Zburatorul (Incubus); cosmogonic and astral myths: Creation of Heaven, Tree of Heaven, Vamesii vazduhului, The Holy Sun, Cosmic Egg, Sun Wheel, Calusarii (Calucenii), Zburatorul (Incubus), Fat-Frumos (Prince Charming) and his counterpart Ileana Cosanzeana, the Sun and the Moon, The Fire of Life, Joimaritele (Old maids), Sanzienele (Fairies), Stele logostele (Stars) etc.

Myths of heroes: Zamolxis, The Good Twin God, Mistricean, Decebalus, Trajan, Bessarabians, Stefan the Great, Michael the Brave, Avram Iancu, Master Manole, The Novac brothers, Pintea the Brave, Gruia, Iorgovan and folk characters Pacala, Pepelea.

Myth is the expression of an encoded message whose decoding key we must find. Myths always include basic symbols, narratively exploiting the power of the symbol to make transparent the cryptic dimensions of reality (Ghinoiu, 2008).

There are two fundamental dimensions of the symbol: gnoseologic and ontologic. Both appear in Eliade's analysis without being explicitly denominated as such. His effort focuses on the disclosure of internal coherence of symbolic systems. Just by being universal (objective) structures of the human spirit, archetypes become cultural “symbols”. “Due to their inherence in any important human enterprise, they gain aesthetic value” (Jung, 2003).

ARCHETYPAL SYMBOLS IN ROMANIAN ANCIENT TEXTILE CRAFTS

Symbolic ornaments reflect customs, myths, personifications, beliefs, figurative representations of institutions, aspects of folk knowledge and practices. Archetypal symbols found as dominant motifs in ancient textile crafts are divided in the following groups: mythological, ethnographic-folkloric, religious, emblematic-heraldic mythical symbols: “solar signs”, “suns with little fir trees”, “sun”,” sun wheels”, “sun and reel" ethnographic symbols: “fir tree leaf”, tree of life” whose significance is “eternal youth and life without death”, “four-leaf clover” which stands for luck; religious symbols: “cross”. Romanian archetypal symbols: solar signs, tree of life, fir tree, red apple, four-leaf clover, cross, prosphora, bison head, vulture, white doves (Vulcanescu, 1987).

MOTIFS - ROMANIAN CULTURAL PATTERNS IN THE FOLK COSTUMES ORNAMENTATION

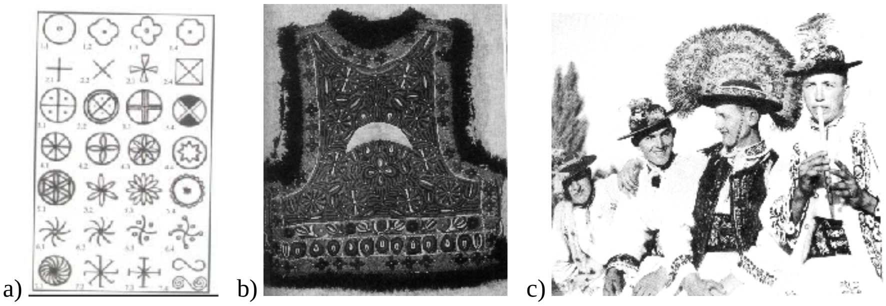

Figure 1. a) Solar archetypes-motifs on carpets and garments, b) Solar cult motifs on fabrics and clothing ornaments, c) Bistrita-Nasaud, men's celebration clothes

“Imagery and imagology of Romanian folk creations are an invitation to a journey in which motifs encountered on different objects, are abstractly or concretely presented, zoomorphical or anthropomorphical, geometrical or stylized, phytomorphic or cosmomorphic, social, symbolic and last but not least skeuomorphic. One of the most common motifs is the "zig-zag" - abstract, geomorphic, also known as "calita-ocolita", "carnel" or "waves". Another type of "self-mirror", of mirror of macrosocial consciousness, is built by interpreting cosmomorphic ornamentation found in our ethnocultural space." (Stanciulescu et al., 2008). The solar cult of our ancestors is found in solar archetypes expressed by the following motifs: solar wheels, representations of the heavenly bodies, the succession of seasons (Figure 1, images a, b, c). In addition to the sunlight cult, there are the cult of moonlight, star and rainbow.

ROMANIAN FOLK COSTUME-PRIESTLY DIGNITY

Analyzing archetypes and cultural patterns which define Romanian spirituality, the philosophical and artistic argument developed by analysis of Romanian myths and textile motifs, will also allow analysis of contemporary clothing patterns, as well as understanding and interpreting the traditional symbolism expressed through the Romanian avant-garde concepts of textile design.

Celebration, ritual or wedding clothes were "bridges" to eternal life based on the belief that clothes - especially shirts - are "the house of man, of his body" (Stoica et al., 1985). A Romanian peasant blouse seems to us a manuscript with strange hieroglyphs, a waist belt, through its motifs, an important ritual whose clothing purpose is derived, a head ornament, through the hierarchy of life of its wearers, seems nothing but an object of feminine coquetry. Stylistic rigour is too severe to not precede aesthetics, decorativeness, usefulness (Figure 2). It forces us to consider things from a different angle, from another perspective. Folk art chromatically reintroduces us into a world of white, basic colour in Romanian art, especially in the folk costume. "A people in white. The choice of colour in ancient cultures always has a ritual significance." (Anghel, 2003). Color responds to a concept, it is assigned some value in the order of cosmic representation; its assimilation or rejection separates communities in terms of ethnicity, just as distribution or right of jewelry hierarchically separate or place individuals within the family or clan. "Regardless of the motifs that separate ethnographic areas and which are, it seems, rudiments of tribal disintegration, in our country, white is unifying, a sign of ethnic particularities with underlying spirituality" asserts Paul Anghel.

Figure 2. Ancestral folk costume

THE TRANSFER OF SYMBOLIC ANTHROPOLOGY ELEMENTS IN FASHION

Elements of ancestral symbolic anthropology, characteristic of the Romanian folk costume, can be correctly transposed and reinterpreted if scientific methods of conceptual transfer are used at the level of visual language, or reinterpreted using high-level conceptual design methods. The cultural transfer of signs, motifs and their symbolic, mythical and ritual meanings is understood by means of the praxis of visual semiotics. Visual semiotics has the purpose of establishing or explaining the connections between a sign (signifier - the meaning, the signification of the clothing item) and the represented object (signified - the object and shape of clothing), in the context of a wide range of application areas. Transfer of cultural patterns and symbols through the fashion product takes place at different levels of stylization and visual reinterpretation. In Figure 3, images 1-4, the experimental concepts of designer Andra Clitan prove the existence of four levels of stylization of Maramures motifs, from integration of a Maramures carpet motif in the tailoring of a modern clothing item, using a manual Maramures weaving style as raw material for a fashion piece (skirt with rose pattern), stylization of motif and its integration into the author's style (white blouse with Maramures lace motif) to the suggestion of the motif and, therefore, of the symbols it carries in a piece where the symbolic dominant is given by the structure of felt used in the winter “clop” (traditional Maramures hat).

Figure 3. Andra Clitan – “Mara Mi”, “My Maramures” 2010, www.andraclitzan.ro

Interpretation of Romanian cultural patterns by a foreign designer, in the case of our example, by the French designer Philippe Guliet, beyond the innovative show of the collection in the Romanian cultural environment at the end of 2011, is not an easy endeavour (Figure 4).

Figure 4. Philippe Guilet – "Preconceptions", Project 100% RO, 2011, www.100-100.ro

The designer has read the message of textile arts and folk costumes only at aesthetic level, and that of techniques used for embroidery, lace, weaving or sheepskin coats only as manual work. Perhaps the French designer did not mean to send the symbolic and mythical message of Romanian spirituality, which does not forsake any of its components. When the reference of plastic semiosis is a folk costume, the ornamentation must not be separated from the tailoring style because the cultural identity of the product is lost, and the stated purpose of such a collection, which is always "the valorisation of cultural heritage", no longer exists, being destroyed precisely by the cultural mixture. The affirmation is truly highlighted by making a bullfighter bolero jacket with bead embroidery and Bistrita motifs, English renaissance collars made of Maramures fabrics or Spanish or French tailoring with some Romanian decorations. In these pieces, dominated by a multicultural message, Romanian cultural patterns become intransmissible and unidentifiable, losing themselves in the general expressiveness of the product, since the Spanish bolero is still a Spanish bolero, and its rich Bistrita ornamentation does nothing but aesthetically enrich this piece and does not say anything about its symbolism and origin. Through his collection "Preconceptions" the French designer has managed to prove only the existence of an active creative endeavour in Romanian crafts, ancient in its symbolic, mythical and ritual structure, at any time ready to integrate as superior element in Romanian cultural products.

CONCLUSIONS

Economic and cultural globalization, through its mechanisms of levelling life, consumption and product recreation, has led, over the past 25 years, to the destruction of national identity in products and to an overestimation of international brands. The development of concepts such as sustainability in fashion, fast-fashion, slow-fashion and ethic-fashion has recently brought back into question the need for national cultural identity, verbally and visually expressed through the product. Going back to the origins manifests in fashion concepts of the last two seasons through the interpretation of fashion themes related to the national heritage in very high cultural and artistic registers in terms of visual language. Conceptual design, through innovation and avant-garde ideas, has the role of creating national cultural identity in fashion, by re-evaluating cultural, spiritual and hand-made heritage, while the fashion industry must request these design products and services. Positive national cultural identity, as added value in fashion, sells any product very well, because the European cultural economy is not only a desideratum and a top strategy, it is also a present and future multicultural reality.

REFERENCES

Anghel, P. (2003), *Ancestry and Perennity* (in Romanian), Litera, Bucharest.
Eliade, M. (1978), *Aspects of Myth* (in Romanian), Univers Press, Bucharest.
Ghinoiu, I. (2008), *Romanian Pantheon* (in Romanian), Romanian Academy Press, Bucharest.
Jung, C.G. (2003), *Complete Works 1, Archetypes and the Collective Unconscious* (in Romanian), Trei, Bucharest.
Stanciulescu, T.D., Grigoriu, A., Pop, M. (2008), *Biophotonic Clothing* (in Romanian), Performantica, Iasi.
Stoica, G., Petrescu, P., Bocse, M. (1985), *Dictionary of Folk Art* (in Romanian), Scientific and Encyclopedic Press, Bucharest.
Vulcănescu, R. (1987), *Romanian Mythology* (in Romanian), RSR Academy Press, Bucharest.

RESEARCH AND INVESTIGATION OF ECCLESIAL HERITAGE BOOK-LEATHER COVER

NICOLETA VORNICU, CRISTINA BIBIRE

Metropolitan Center of Research T.A.B.O.R, Metropolitanate of Moldavia and Bukovina
Iasi, Romania,email: cmctaboriasi@yahoo.com

This paper presents physic-chemical and biological investigation of the leather used in the manufacture covers to three books Antologhion, 1840, Minei 1845, Ceaslov 1874 from old book repository Library Dumitru Staniloaie. Techniques investigation used are: XRF, FTIR, electron microscopy and microscopoie optics. The results provided information on the type of skin tanning type, nature and degree of biological attack and helped to establish the conservation status of these books, the active preservation and enhancement of existing in the exhibition.

Keywords: leather, book, cultural heritage

INTRODUCTION

Conservation of heritage, the two sides of the: preservation and restoration, is a research complex, involving interdisciplinary. Elucidation of the mechanism of degradation of various organic and mineral materials in the structure of national heritage objects, explaining phenomena that occur over time between the systems involved in the processes of destruction and elimination or reduction of their activity is a fundamental issue of conservation and restoration.

The objects are subject progressive degradation processes due to the collaboration between several factors. Besides the natural process of aging, imminent any organic materials, suffered materials that make up objects of art have been some alterations complex physical, chemical and biological. Degradation of leather may be the result of sewing techniques, improper use or action of environmental conditions.

OBJECTIVES

This paper presents physic-chemical and biological investigation of the leather used in making the covers of three books: Antologhion, 1840, Minei 1845 and Ceaslov 1874 from the old book store “Dumintru Staniloae” Library.

Figure 1. (a). Antologhion, brown leather (b). Mine, brown leather imprinted with gold leaf; (c). Ceaslov, brown leather

METHODS

Investigative techniques used are: XRF, FTIR, electron microscopy and optical microscopy.

Optical Microscopy

By examining with a microscope Olympus SZX 160 was made from the skin surface evaluation of the covers of the three books emphasizing mood garnet and shell follicle, which is the main parameter characterization to identify your skin type.

Scanning Electron Microscopy

Scanning electron microscopy called (Scanning Electron Microscopy, SEM) is a technique for investigating high-resolution surfaces, whose application in the study of heritage objects are many and varied (Vornicu, Sturge). Analysis of skin samples taken from three items analyzed was performed using a scanning electron microscope (SEM / ESEM - EDAX) - Quanta 200 and followed highlighting skin morphology.

Analysis by X-ray Fluorescence Spectrometry Technique

X-ray fluorescence spectral allows non-destructive elemental analysis of samples of old leather. Experimental determinations were made with an X-ray fluorescence spectrometer portable type Innov X Systems Alpha Series. It is equipped with an X-ray tube with a W anticathode, working at maximum parameters of 35kV and 40μA, fluorescence radiation is detected and analyzed with a Si detector (PIN) with thermoelectric cooling and operation is controlled by a minicomputer. For plotting spectra and semi-quantitative analysis software was used for light Soil matrix mode is selected during arousal from 60 sec.

FTIR Analysis

FTIR analysis was carried out using a Vertex 70 Bruker, 30 – 25 000 cm^{-1} FTIR spectrometer, KBr beamsplitter & RT-DLaTGS detector (mid-infrared), T222/3 multilayer beamsplitter & RT-DTGS-FIR detector.

Skin samples of skin powder and tablets were mixing potassium bromide (KBr). The resulted product was pressed in pellets with KBr.

RESULTS

The results provided information on skin type, type of tanning, nature and extent of biological attack.

The preliminary optical microscopically investigation shows that the examined leather has the characteristics of the modified cow skin, due to the various degradations; the used method was the comparison of the stereo microscopically images with those of an whiteness sample. Scanning electron microscopy (SEM) is a method that is often used to investigate the skin, collagen, etc.

Biological degradation (Figure 2a) the books have musty areas which demand biological investigations although the active conservation of these books will be made by means of prevention and not by biological care.

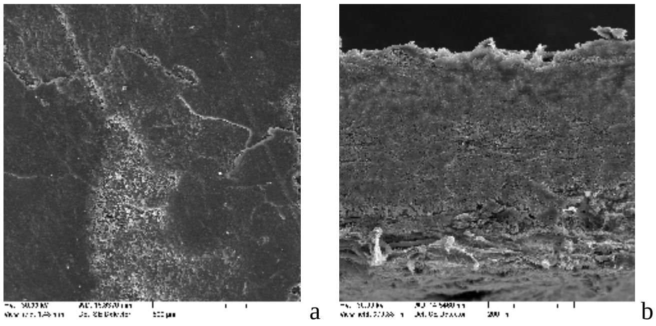

Figure 2. SEM image Antologhion: a. grain surface of dyed leather; b. SEM analysis of cross-section of dyed leather

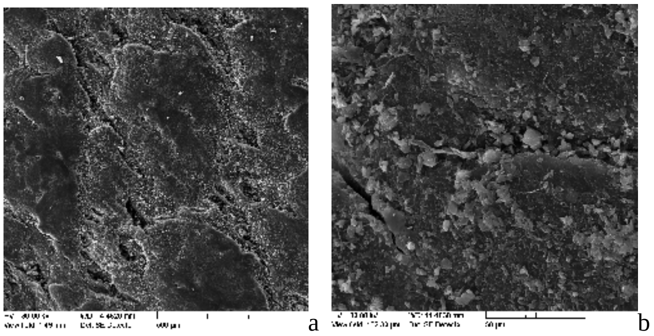

Figure 3. SEM image Minei: a. grain surface of dyed leather; b. SEM analysis of cross-section of dyed leather

Electron microscopy particles are easily recognized vegetable tannin (Figure 3b) leather in between collagen fibers sleeping network.

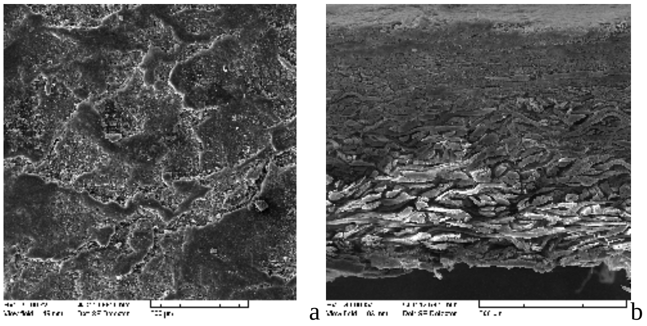

Figure 4. SEM image Ceaslov: a. grain surface of dyed leather; b. SEM analysis of cross-section of dyed leather

Electron microscopy performed at varying degrees of magnification confirms that the analyzed samples are cattle leather.

Cow reticular layer of skin is made of connective fiber bundles thick, strongly developed, intertwined, very irregular, with a natural boundary formed by braiding fibers to fine hypodermis. Calf skin, normally be considered as having histological structure of beef hides all small size. Samples analyzed with age and wear high degree of dehydration shows advanced morphology of the collapse.

However, if the 3 samples us can say that the skin was taken from an adult animal, as shown in the papillary layer (gren). Both the macro observation and SEM images observed in this biological attack. Sampling was done by fingerprinting and cultivation was carried out on two types of media: Czapek-Dox agar for fungi and for bacteria. Identified the presence of active species and Aspergillus niger to Antologhion Ceaslov.

In order to identify the mineral composition of skin to cover the three objects used X-ray fluorescence is nondestructive This investigation and provide information about skin type but also how tanning. The results of registration for each type of sample spectra are shown in Figures 5, 6, 7 indicating the presence of elements Ca, K, S, Cu, Pb, Zn and Fe. which is due to skin composition (Ca, K) or remaining traces of processing stages.

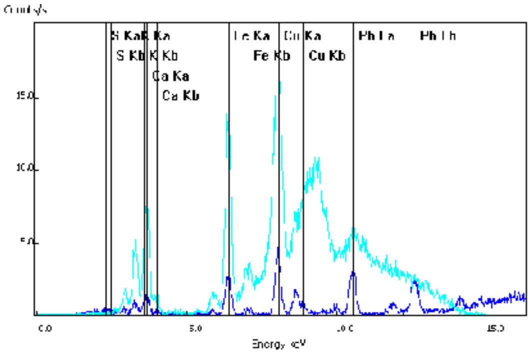

Figure 5. XRF spectrum for Antologhion

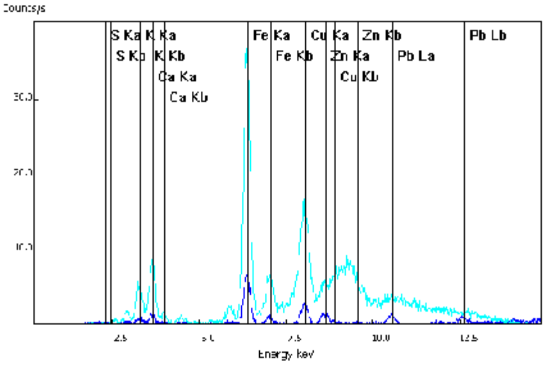

Figure 6. XRF spectrum for Minei

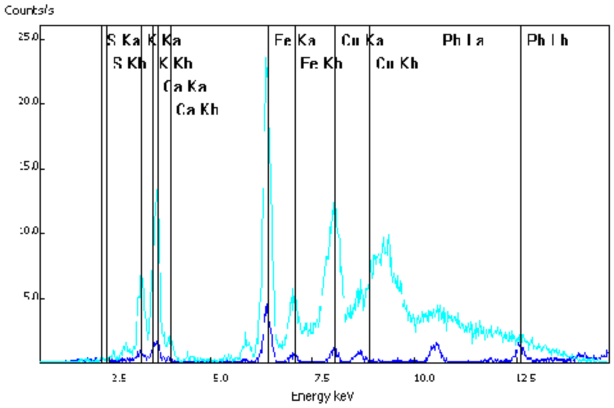

Figure 7. XRF spectrum for Ceaslov

Leather minerals varies depending on the breed, age and sex of the animal, from 0.25 to 0.65% on dry skin. Most of these substances is formed NaCl. The skin also contains phosphates, carbonates, sulfates, chlorides of K, Mg, Ca, Na, less Fe, Al, S (Larsen, 1994).

FTIR analysis was only performed in order to identify your skin type. Skin samples were scratched with a sterile scalpel blade obtaining a skin powder was mixed and compressed with potassium bromide (KBr). Was used as a standard sample powder from pig and goat skin. It was found that all spectra were almost the same as the skin is almost identical composition. Differentiation could be watching so called “regions of interest”, which are the following long wave and 500-400 cm^{-1}, 1200-1000 cm^{-1} and 700-600 cm^{-1}. (Elwathig). Following overlapping peaks for the three samples was noted that these spectra shows a bit visible in the region 472-470 cm^{-1} indicating the highest molecular absorption for carbonyl functional group (-C = O) and amide. This shows us that the covers are leather cow.

CONCLUSIONS

The data obtained have helped to establish the conservation status of these books, the preservation and valuing active within the existing exhibition.

To identify characteristics of skin covers the three books we used optical microscopy electron microscopy showed that in all three cases it is the skin of cattle. Electron microscopy provided information on this biological attack Ceaslov and Antologhion, identification was achieved by specific laboratory techniques, signaling is the present species Aspergillus niger to Antologhion and Ceaslov. SEM image of particles present in vegetable tannin indicate vegetable tanning of the skin. It is obvious that type SEM analysis provides quantitative information and qualitative nature. Non-destructive XRF analysis by identifying elements expressed in ppm of skin covers the three provided information on the composition but also the type of tanning. If SEM analysis determined that cover skin for FTIR spectroscopic analysis objects determine the types of functional groups present in skin products confirming data previously obtained.

REFERENCES

Elwathig, M., Mirghani, S., Mohd Salleh, H., Che, Y. and Jaswir, I. (2012), "Rapid Authentication of Leather and Leather Products", *Advances in Natural and Applied Sciences*, 6(5), 651-659.

Kite, M., Thomson, R. (2005), *Conservation of leather and related materials*, 4-10.

Larsen, R. (1994), STREP Leather Project Evaluation of the Correlation between Natural and artificial Ageing of Vegetable Tanned Leathers, Final Report, Copenhagen.

Sturge, T. (2000), *The conservation of leather artifacts: case studies from the Leather Conservation Centre*, Leather Conservation Centre, Northampton, 26–27.

Vornicu, N. and Bibire, C. (2001), *Biodeterioration of Artworks* (in Romanian), Trinitas, Iasi.

Wess, T.J., Drakopoulos, M., Snigirev, A., Wouters, J., Paris, O., Fratzl, P., Collins, M., Hiller, J.C. and Nielsen, K. (2001), "The use of small-angle X-ray diffraction studies for the analysis of structural features in archaeological samples", *Archaeometry*, 43, 117–129.

VI.
INNOVATION

CONSTRUCTIVE MEASURES TO INCREASE SEISMIC SAFETY IN URBAN AREAS

OANA MIHAELA BANU[1], IOANA OLTEANU[1], ANDREI ALISTAR[2], MIHAI BUDESCU[1]

[1] *“Gheorghe Asachi” Technical University of Iasi, Faculty of Civil Engineering and Building Services, Department of Structural Mechanics, 43rd, D. Mangeron Blvd., Iasi, Romania, oanam_ionita@yahoo.com, zita_01040@yahoo.com, mbudescu@tuiasi.ro*

[2] *“Popp si asociatii” - 136 Calea Grivitei, B building, sector 1, Bucharest, Romania, andrei.alistar@p-a.ro*

Several structural systems are considered in Romania. One of the most common is the reinforced concrete frame system. For this type of structures the weak beam-strong column design concept is used. Structural damages from previous earthquake show that the strength increase of the secondary elements has a negative influence on the overall behaviour of the structure. In order to improve the behaviour of the structure in case of an earthquake several studies were conducted. The present paper presents results for some constructive measures that direct the development of the plastic hinge away from the column and into the beam, as the design concept states. The proposed measures are for the slab connection to the beams and for the infill masonry. Capacity curves for the studied situations were obtained using a nonlinear static analysis. The studies have been carried out on one storey reinforced concrete frame structure and on a plane three storey reinforced concrete frame structure respectively. The results emphasize that the proposed measures lead to a more suitable behaviour for frame structures in seismic areas.

Keywords: failure mechanism, constructive measures, plastic hinge.

INTRODUCTION

Considering safety and serviceability requirements several structural models can be used for a building. Frame structures, dual systems, wall systems are some of the existing structural systems, using different materials. The most common one in the world, because is easy to erect and to modify the interior spaces and also is cost effective, is the reinforced concrete frame structure (Murty et al., 2006).

For these types of structure norms have special requirements that need to be satisfied, as is for example the weak beam – strong column concept. This principle is mandatory in order to have an adequate failure mechanism – first the secondary elements and then the principal ones. Even though this concept is been considered in the design stage, experience from past earthquakes reveals that is not enough. The influence of non-structural elements – slabs, parapets, partition walls have a significant contribution in the overall behaviour of the structure, leading to unfavourable failure mechanism (for example to the failure of columns first) (FEMA 454, 2006).

The paper aim is to present two constructive measures that can enhance the failure mechanism in case of earthquake. Both measures were tested for reinforced concrete frame structures and are intended for the infill walls and for the slab. A nonlinear static analysis has been performed for these measures in order to show that the plastic hinges were directed from the columns, as they were in the initial model, into the beams, as they appear in the final version.

The nonlinear analysis is inherently more accurate than the linear analysis because it takes into account the plastic behaviour of the structure. The inconvenience of this analysis method is that the user must be able to predict the locations where the plastic hinge will develop in the structure. This may not be possible for more complicated structures.

CASE STUDY

Additional Stiffness Due to Infill Walls

The infill of the frame structures with different materials as autoclaved concrete blocks (ACB) is widely spread. The problem this solution rise is due to their different behaviour. The frame structure is relatively flexible and somehow ductile, while unreinforced masonry is very stiff and fragile and may «explode» under the effect of only small deformations. At the beginning of an earthquake the masonry carries most of the earthquake actions but as the shaking intensifies the masonry fails due to shear or sliding. The appearance of diagonal cracks is characteristic of a seismic failure (Bachmann, 2003).

Two failure mechanisms can be identified: when the columns are stronger than the masonry, or vice-versa, Figure 1.a and 1.b. In the first case the masonry is completely destroyed and falls out, while in the second one the columns can be damaged, which may leads to collapse (Bachmann, 2003).

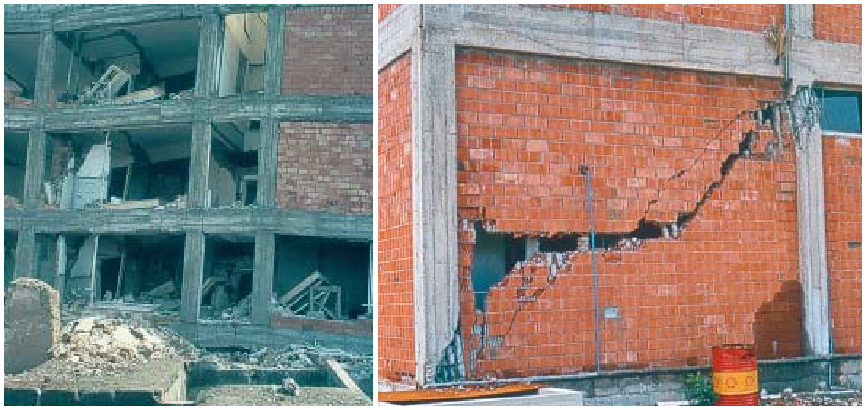

Figure 1.a. Stronger columns lead to the falling out of the masonry (Erzincan, Turkey 1992); 1.b. Strong masonry sheared the columns (Adana-Ceyhan, Turkey 1998)

For the first analysis a 3 storey, 2D reinforced concrete frame structure of C20/25 concrete was considered. For the columns cross section the following dimensions were considered 50cm by 50cm and for the beams were 30cm by 50cm. The infill wall mechanical characteristics were as follows: modulus of elasticity, E, equal to 1210MPa; density equal to 2700 kg/m3 and compression strength, f_c, equal to 14MPa. The infill wall, with 15 cm thickness, has a door opening, 90cm wide by 210cm tall, for each level. The second model for this case considers a seismic joint of 5cm modelled as rubber with the following mechanical properties: modulus of elasticity, E, equal to 2MPa, Poisson's ratio, υ=0.49 and density 912 kg/m^3.

Figure 2 presents a comparison between the capacity curves for the two considered cases obtained through a static nonlinear analysis performed in SAP2000. It can be noticed an increase in the structure's flexibility and a significant increase in the maximum displacement, even though the bearing capacity decreases. Another important change that occurs in the overall behaviour of the structure is represented by the plastic hinge location. In the first situation the plastic hinge appear at the base of the ground floor column leading to the collapse of the structure very fast, Figure 3.a. In the second case, when the seismic joint is considered the plastic hinge appears first in the beam, and then in the columns. In this case the design concept of weak beam – strong column is fulfilled, Figure 3.b.

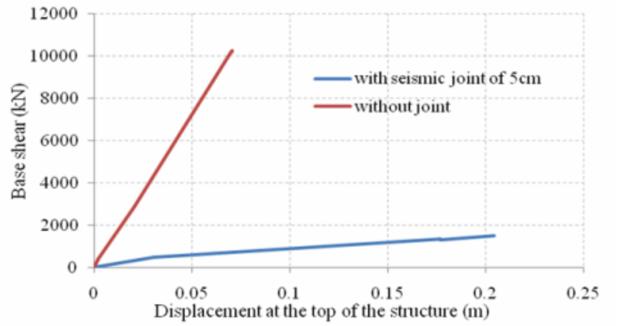

Figure 2. Capacity curves comparison

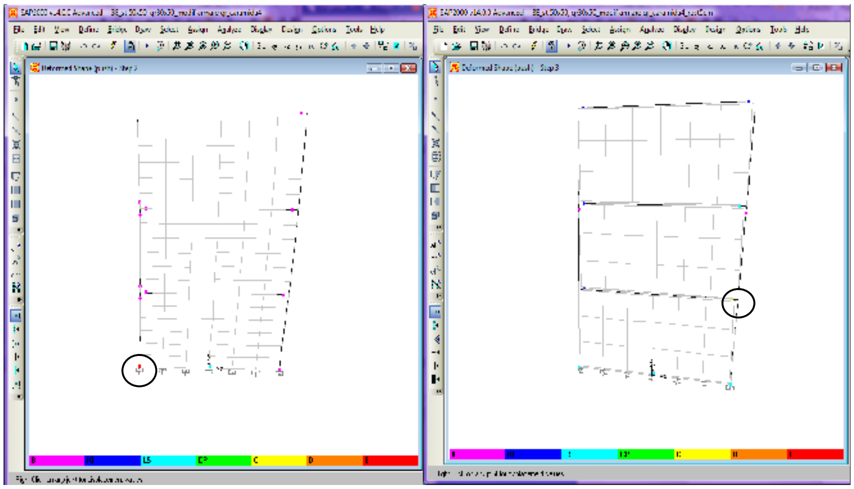

Figure 3.a. Plastic hinge development for the infill without joint; 3.b. Plastic hinge development for the infill with 5cm seismic joint

Slab Decoupling from the Beams

It was observed that considering the slab in the analysis of a frame structure lead to a significant increase in the stiffness of the structure. Another problem was observed in the plastic hinge development. The additional stiffness due to the slab direct the plastic hinge from the beams into the column. In order to solve this problem we propose the introduction of a bitumen joint between the slab and the beam in the area where the plastic hinge could appear. Several types of joints were analyzed in ATENA 3D software, but the paper presents only the most efficient joint.

The considered structural model is represented of a single storey reinforced concrete structure with an opening of 6m and 3m high, and with 50cm by 50cm column cross section and 30cm by 50cm beam cross section. The slab thickness is of 15cm.

Performing a nonlinear static analysis of the considered models, the concrete cracks development evolution has been studied (Figure 4.a and Figure 5.a). Also the internal stresses state evolution in the reinforcing system has been analysed (Figure 4.b and Figure 5.b). Figure 4 represents the results for the initial frame, while Figure 5 consists of the results for the frame with the considered bitumen joint.

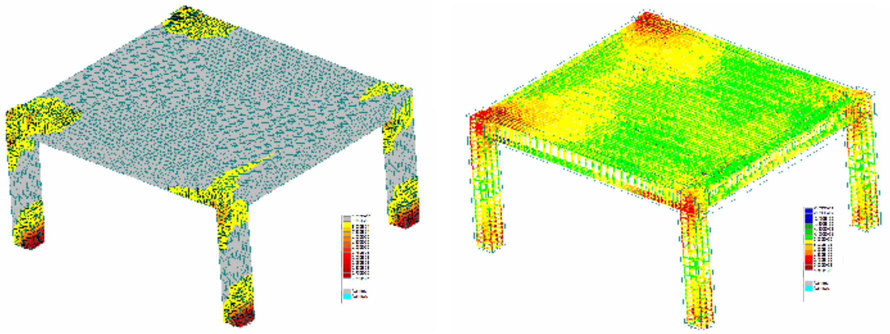

Figure 4. Reinforced concrete frame without joint: (a) concrete cracks development; (b) stress development in the reinforcement for a 1000kN loading

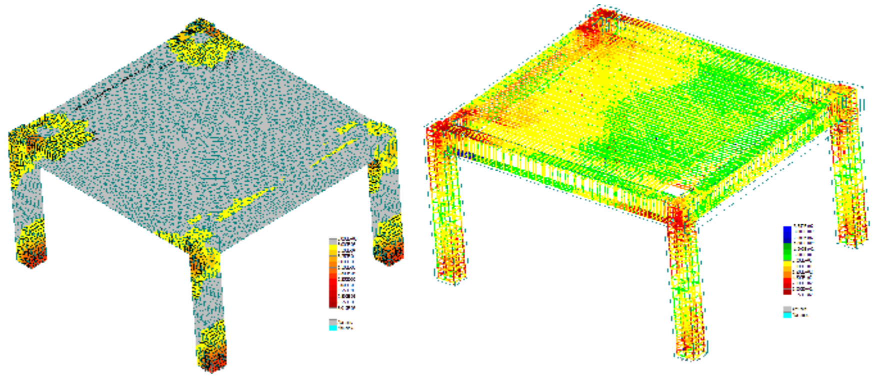

Figure 5. Reinforced concrete frame with bitumen joint: (a) concrete cracks development; (b) stress development in the reinforcement for a 1000kN loading

Figure 4.a. and 5.a. emphasize the way the plastic hinge is redirected away from the columns and into the beams in order to form an adequate failure mechanism.

CONCLUSIONS

The structural engineers are in a unique position to make proper decisions during the design stage of the constructions that can reduce their future vulnerability to natural disasters. To implement successful measures for this purpose, the engineer must be able to assess the risk from natural disasters, as earthquakes and to predict future risk patterns.

The two proposed constructive measures can enhance a failure mechanism in case of earthquake in order to ensure the weak beam – strong column concept. As it is well known, this principle is mandatory in order to have an adequate structural behaviour – first the failure of the secondary elements and then of the principal ones.

For this reason all beam-to-column connections have to be moment-resistant and stronger than the beams. This way the plastic hinges will be developed in the body of the beam and not in the column or in the joint.

In the case of the infill walls measure, it was observed that the use of a seismic joint had as a consequence the plastic hinge development first into the beam.

Also in the case of the second proposed measure, the slab decoupling form the beams by using a bitumen joint had lead to the same favourable consequence.

REFERENCES

Bachmann, H. (2003), *Seismic Conceptual Design of Buildings – Basic principles for engineers, architects, building owners, and authorities*, Swiss Federal Office for Water and Geology, Switzerland.

FEMA 454 (2006), *Designing for Earthquakes - A Manual for Architects*.

Murty, C.V.R., Brzev, S., Faison, H., Irfanoglu, A., Comartin, C.D. (2006), *The seismic performance of reinforced concrete frame buildings with masonry infill walls*, National Information Center of Earthquake Engineering, Kanpur, India.

P100-1/2006, *Seismic Design Code – Part I – Guidelines for Building Design* (in Romanian).

VULNERABILITY ASSESSMENT - AN EFFICIENT APPROACH TO IMPROVE STRUCTURAL SAFETY OF LOCALLY DAMAGED REINFORCED CONCRETE FRAME STRUCTURES

OANA MIHAELA BANU[1], IOANA OLTEANU[1], ANDREI ALISTAR[2], MIHAI BUDESCU[1]

[1] *"Gheorghe Asachi" Technical University of Iasi, Faculty of Civil Engineering and Building Services, Department of Structural Mechanics, 43rd, D. Mangeron Blvd., Iasi, Romania, oanam_ionita@yahoo.com, zita_01040@yahoo.com, mbudescu@tuiasi.ro*

[2] *"Popp si asociatii" - 136 Calea Grivitei, B building, sector 1, Bucharest, Romania, andrei.alistar@p-a.ro*

The latest improvements in structural analysis, as well as the continuous interest concerning the innovative building materials and the knowledge of their properties, have determined the civil engineers to build efficient modern structures, with an increased degree of robustness. Within the main aims of the structural design is to provide safety to structures. For this reason, a special attention has to be paid to the potential sources of abnormal loads that should be examined when designing for progressive damage performance. Significant research activities have been carried out to gain a better understanding upon the possibilities of studying and improving the integrity of structures. Nowadays, all these may be achieved through accurate analyses on the overall structural behaviour by using non-linear finite element computer programs. The objective of this paper is to present a vulnerability assessment procedure. A numerical analysis of a plane four storey reinforced concrete frame structure has been carried out. The recorded and processed results for the progressively damaged structure are presented. The structural stability and the vulnerability of the discussed structure have been assessed by considering the local damage effect upon a perimeter and a central column.

Keywords: structural integrity, vulnerability, robustness.

INTRODUCTION

Within the main aims of the structural design it was always the safety providing to structures and the risk reducing for the inhabitants' life. In the traditional design these objectives are achieved by designing structural components against some specified limit states. But, as the latest cases of structural failure and progressive collapse showed, this approach is not sufficient, since it does not exclude the risks implied by local damages to a structure due to accidental events. The effect of such events on structural integrity becomes very important for the non-robust structures. For this kind of structures some local damage can generate a chain reaction of failures causing further on the collapse of the whole structure or of a major part of it. This phenomenon is called progressive collapse (Val and Val, 2006).

A perception upon the lack of robustness can be obtained through vulnerability analysis. According to the dictionary definition of vulnerability as "susceptibility to damage", a structure is considered to be vulnerable if small damages can cause disproportionate consequences to this. Consequently, a vulnerability analysis is concerned with the structure configuration in order to identify the vulnerable failure scenarios. Considering these failure scenarios, structural configuration can be modified until the vulnerability is reduced thus making the structure more roust (Agarwal et al., 2006).

One of the structural properties that can prevent the collapse of an entire structure when only parts of it are damaged or entirely destroyed is the structural robustness. As it can be easily understood, a robust structure is also a collapse resistant one. Special attention must be given to the behaviour of the structural elements and of their connections to improve their strength, redundancy, toughness, ductility and energy absorption, as well as their provision of alternative load paths under extreme events (England et al., 2008). Continuous, high redundant structures with ductility will absorb local damage very well. It is obvious that other structural systems, such as large panel or bearing wall systems, pre-cast concrete slabs or steel joist floors supported on masonry walls, and any building system that do not posses sufficient ductility are more vulnerable because of the difficulties in providing continuity and ductility in such systems (Mendis, P. and Ngo, T., 2003).

CASE STUDY

In this stage of the research activity there have been studied different plane and spatial reinforced concrete frame structures. The plane frame structure considered within this study has four storeys above the ground level, each of 3.00m high. The load bearing system of the structure consists of reinforced concrete columns and beams. The static equivalent load applied on the beams of the structure was a uniformly distributed live load of 18kN/m. The structural members properties are indicated in the following table:

Table 1. Structural members properties

Structural member	Width [cm]	Height [cm]	Concrete class
Columns	55.00	55.00	C20/25
Beams	30.00	60.00	C20/25

Plane Frame Analysis Performed Using ROBOT Software

First, the plane frame structure has been modelled and the structural static analysis has been carried out using the Autodesk Robot Structural Analysis 2010 system. The configuration of this plane frame structure is shown in Figure 1.

For the purpose of the analysis, the local damage of the central column from the first floor of the structure due to an extreme loading has been simulated. After that, the damage state of the structures has been assessed. In order to analyse a progressively damaging phenomenon, the central column from the first floor was not instantaneously removed from the structures. Instead of this, the flexural stiffness of the column was reduced step by step from 100% to 10%.

At each step of flexural stiffness reduction, the evolution of the bending moments of the beams along the axis no.1 and of the axial force in the central column from the intersection of the axis no.1 with “B” axis on each floor were recorded.

The influence of the local damage from the first floor of the structure upon the load bearing elements from the upper floors was also evaluated. Using the normalized values of the internal force members, a series of charts has been drawn (Figure 2 and Figure 3). Since the number of these charts is very large not all of them could have been included in this paper.

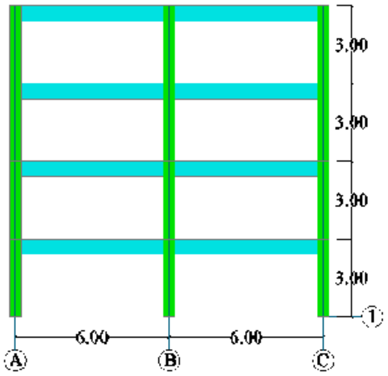

Figure 1. The studied plane frame structure

In the selected charts M_A and M_B represent the values of the bending moment evaluated at the end sections of the beams and N_{max} represent the maximum value of the axial force at the bottom of the central columns from "B" axis. The numerical indexes refer to the considered storey and the index "c" refers to the value of the effort at the current step of the analysis.

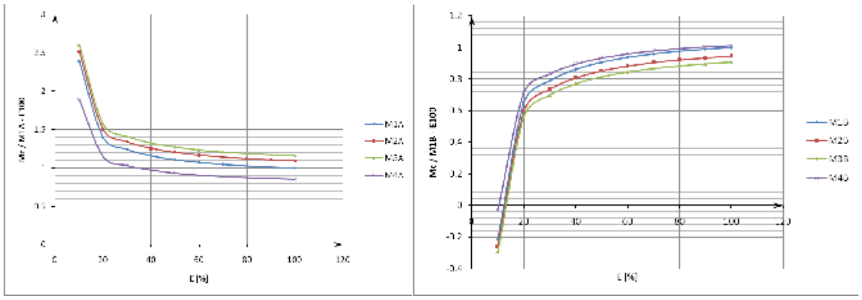

Figure 2. Bending moments MA and MB evolution on each storey of the plane frame structure

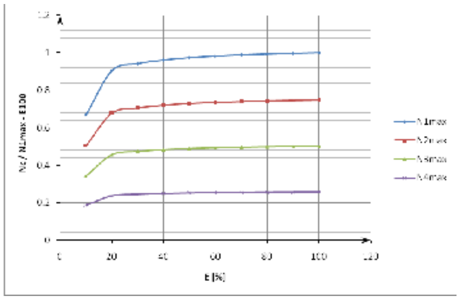

Figure 3. Axial force Nmax evolution on each storey of the plane frame structure

As it can be seen from the previous diagrams, the structural elements from the upper floors are affected in the same proportion, the internal forces curves (i.e. bending moment for beams and axial force for columns) developed for each storey having almost the same shape. An inflection point in the evolution of the internal forces occurs when the flexural stiffness of the central column is reduced at 30%.

When the flexural stiffness of the central column is reduced to 10%, the absolute values of bending moment on the beams, MA, increase suddenly and the bending moment, MB, becomes positive.

Plane Frame Analysis Performed Using ATENA 3D Software

The same structure and the same loading scenario have been assumed for a non-linear static analysis by using ATENA 3D software. An accurate meshing with tetrahedral type finite elements of the structural members has been performed and the overall behaviour of the structure has been analysed.

For the purpose of this paper, it was considered to be more relevant to present from the recorded results, those related to the final step of the analysis. In this stage, the flexural stiffness of the central column is already reduced to 10% from its initial value. The concrete cracks development evolution into the beams has been studied. As it was expected and as it can be observed from Figure 4, the concrete cracks developed at the lower face of the beam ends adjacent to the central columns are more widely spread than those developed at the upper face, at the opposite ends of the beams. But the last ones are more pronounced since the bending moments at these ends of the beams are higher.

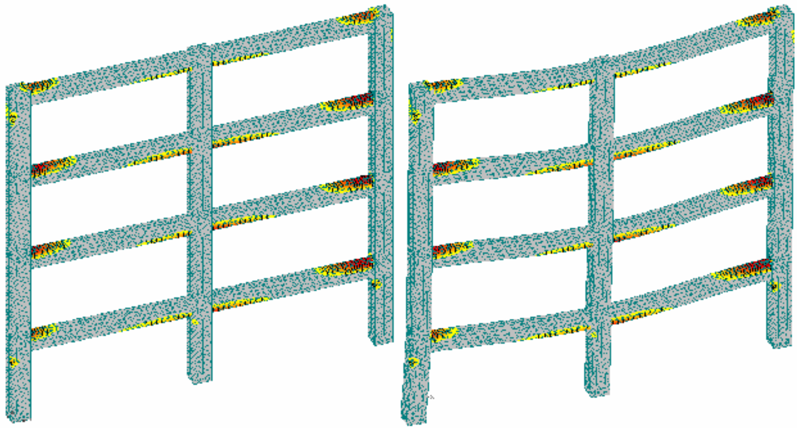

Figure 4. Concrete cracks development into the beams adjacent to the damaged column
a. undeformed shape; b. deflected shape

Another scenario was proposed for study considering a two times higher load acting on the beams. In this stage the concrete cracks development evolution into the columns is more pronounced and the results reveal the fact that the structure is in danger to collapse. As it can be observed from Figure 5, the concrete cracks developed into the central column indicate the fact that the concrete doesn’t work properly anymore. The cracks width is even higher than 0.6mm and due to this fact the ones from the beam are almost imperceptible on the figure.

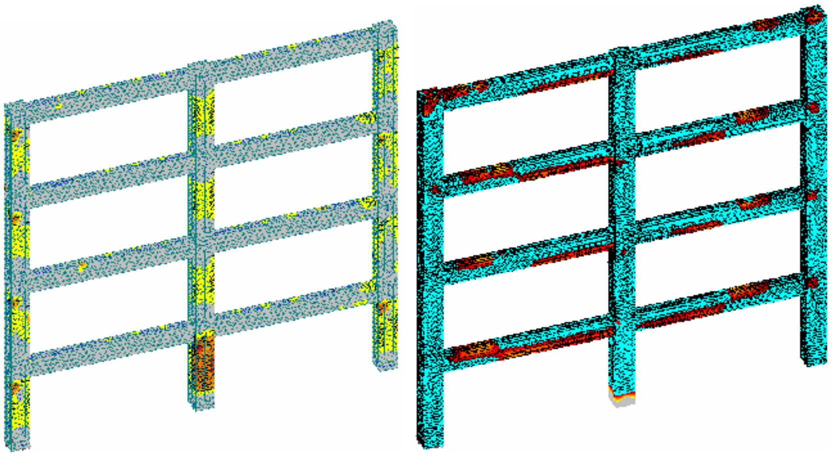

Figure 5. Concrete cracks development in the second case scenario

The internal stress state of the reinforcing system in this case scenario is shown in Figure 6. Since the bearing capacity of the concrete was exceeded, the longitudinal reinforcement reaches the yielding limit at the upper side of the central column. It can be easily observed in the detail from Figure 7.

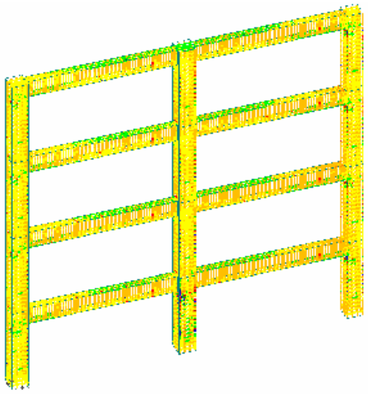

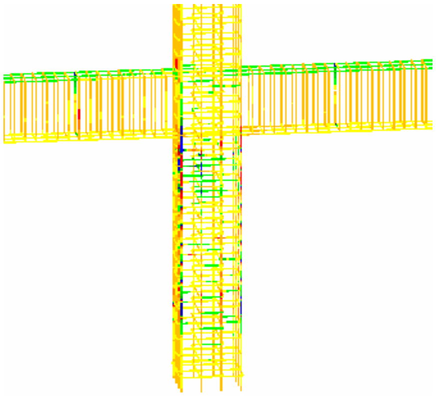

Figure 6. Internal stress state in the reinforcing system in the second case scenario

Figure 7. Detail of the internal stress state in the longitudinal reinforcement of the central column

CONCLUSIONS

Based on the performed analyses of the behavior of load-bearing elements it has been found out that for a flexural stiffness damage ratio higher than 60% in columns, the development of internal force members may lead to a local damage or to the collapse of the entire framing system.

Usually, the occurrence of internal force members (i.e. bending moment for beams and axial force for columns) which do not exceed 30% in columns and 20% in beams can be redistributed to the adjacent elements.

For some specific types of buildings to which exists the risk of producing local damages it is necessary to assume some scenarios regarding the progressive collapse. These scenarios have to take into consideration the local measures needed for the reducing of structural vulnerability and thus for the preventing of global collapse.

The influence of local damage is diminished on the vertical direction with each new level added to the structure, the supplementary levels having a positive effect upon its behavior.

REFERENCES

Agarwal, J., England, J., Blockley, D. (2006), "Vulnerability analysis of structures", *Journal of the International Association for Bridge and Structural Engineering IABSE, Structural Engineering International (SEI)*, 16(2), 124-128.

England, J., Agarwal, J., Blockley, D. (2008), "The vulnerability of structures under extreme events", *Journal Computers and Structures*, 86(10), 1042-1051.

Mendis, P. and Ngo, T. (2003), "Vulnerability Assessment of Concrete Tall Buildings subjected to Extreme Loading Conditions", in *The Proceedings of the CIB-CTBUH International Conference on Tall Buildings*, 8-10 May, Malaysia.

Val, D.V. and Val, E.G. (2006), "Robustness of Frame Structures", *Journal of the International Association for Bridge and Structural Engineering IABSE, Structural Engineering International (SEI)*, 16(2), 108-112.

TITANIUM-TANNED LEATHER

JOAQUIN FERRER[1], MARIA ESTHER RIQUELME[1], VICENTE SEGARRA[1], MARIA VICENTA GALIANA[2], SILVINO NAVARRO[2]

[1] *Centre for Technology and Innovation (INESCOP), Polígono Industrial Campo Alto – 3600 Elda (Spain), medioambiente@inescop.es*

[2] *Industrias del Curtido, S.A. (INCUSA), Avda. Alicante, s/n – 46460 Silla (Spain)*

Nowadays, the stabilisation with chrome salts is the most widely used technique for leather production, accounting for more than 90% of leather tanned worldwide. However, the leather industry is currently subject to constant environmental pressure, which has led to a continuous search for and implementation of improvements in production processes, as well as the thinking of new market strategies, such as the development of more environmentally friendly tanning processes. Titanium has some advantages with regard to conventional chrome tanning, i.e. it is a non-toxic, inert and non-allergenic element. Besides, titanium tanning avoids chrome contamination in tannery effluents and in wastewater treatment sludge, which improves the overall environmental impact of the process. The project 'Eco-friendly leather tanned with titanium (TiLEATHER)' was conceived with the aim of launching this technology into the European market. This project is co-funded by the European Commission and is coordinated by the Centre for Technology and Innovation (INESCOP). This paper presents the main results obtained in the framework of the TiLEATHER project after the physical-chemical characterisation of different leather samples and footwear styles produced with said leather.

Key words: leather, titanium, tanning.

INTRODUCTION

Titanium was first considered as a possible tanning agent in 1930, as its properties allow it to react with collagen carboxyl groups present in leather. Titanium used as a tanning agent has been proven to produce leather with a level of quality suitable for commercial use. What is more, it is a non-toxic metal and gives additional advantages in that it is biocompatible, inert and avoids possible allergic reactions derived from contact with the skin.

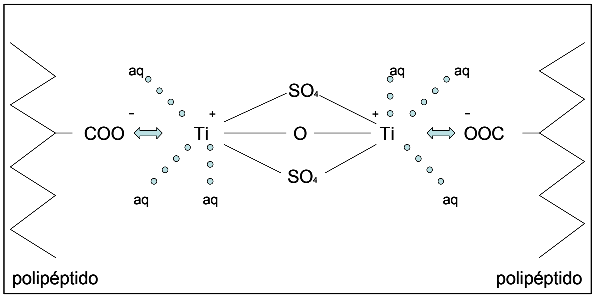

Figure 1. Titanium and skin collagen bond

Nowadays, more than 90% of leather produced worldwide is tanned using chromium salts. This tanning technique can imply certain environmental risks derived from the possible chromium oxidation. However, the leather industry is currently subject to constant environmental pressure, which has led to a continuous search for and implementation of improvements in production processes, as well as the thinking of new market strategies, such as the development of more environmentally friendly tanning processes.

For this reason, in recent years the Centre for Technology and Innovation (INESCOP) has been researching into new tanning agents that provide alternatives to chrome-tanned leather, as is the case of titanium-tanned leather, in particular in the framework of the project titled “Eco-friendly Leather Tanned with Titanium (TiLEATHER)”, co-funded by the European Commission through the “CIP ECO-INNOVATION” Programme.

The new titanium tanning technique is a sustainable alternative that allows chrome to be completely eliminated from tanning processes.

In order to launch this technology into the European market, the tannery Industrias del Curtido, S.A. (INCUSA) is producing titanium-tanned leather under the registered trade name SANOTAN®.

This paper presents the main results obtained in the framework of the TiLEATHER Project after the physical-chemical characterisation of different leather samples and footwear styles produced with said leather.

EXPERIMENTAL

After having set up a new production line for titanium tanning, the first cattle hides tanned with titanium on an industrial scale were obtained, and then their properties were physically and chemically characterised. What is more, a further step was taken with the production of several shoe styles made of titanium-tanned leather by the footwear manufacturing companies participating in the project, with a view to checking the suitability of said leather for footwear production.

Physical and Chemical Characterisation of Titanium-Tanned Leather

For the physical and chemical characterisation, titanium-tanned leather was subjected to different quality tests according to International standards. Tables 1 and 2 summarise the results obtained:

In view of the obtained results, titanium-tanned leather meets the requirements for footwear manufacturing.

It is to be noted that an optimum shrinkage temperature value was obtained, which is a critical parameter for footwear manufacture using this leather. As can be observed, the shrinkage temperature exceeded 75°C, which is not usually achieved using tanning agents other than chrome.

Physical and Chemical Characterisation of Footwear Produced with Titanium-Tanned Leather

Secondly, in order to test the suitability of titanium-tanned leather for footwear production, different footwear styles with different material assembly methods were manufactured. Figures 1, 2 and 3 show some of the shoe styles manufactured by the different project partners.

Table 1. Results of physical tests on titanium tanned leather

Tests	Standard Test Method	Average values	Recommended values
Thickness (mm)	UNE-EN ISO 2589:2003	2.2	>1.1
Shrinkage temperature (ºC)	UNE-EN ISO 3377-2:2003		>70
Initial		79	
At 10% shrinkage		83	
Flex resistance (No. cycles)	UNE-EN 13512:2002		
Dry		>200,000	-
Wet		>12,000	-
Tear strength (N)	UNE-EN ISO 3377-2:2003	398.5	>50
Tensile strength (N/cm2)	UNE-EN ISO 3376:2003	20.4	>15
Elongation at break (%)	UNE-EN ISO 3376:2003	66.25	-
Water vapour permeability (mg/cm2.h)	UNE-EN ISO 20347:2005	5.5	-

Table 2. Results of chemical tests on titanium-tanned leather

Tests	Standard Test Method	Average values	Recommended values
Moisture content (%)	UNE-EN ISO 4684:2006	10.9	-
Substances soluble in dichloromethane (% extracted matter)	UNE-EN ISO 4048:2008	10.0	-
pH	UNE-EN ISO 4045:2008	3.58	-
Chlorophenols (ppm)	UNE-EN ISO 17070:2007	< 0.1	<0.1(1)
Formaldehyde (ppm)	UNE-EN ISO 17226-1:2008	34.7	<150(1)
Extractable metals (ppm)	UNE-EN ISO 17072-2		As, Cd and Pb <100(1)
Cr		10.9	
Ti		9100	
Pb		< 0.5	
Cd		< 0.2	
As		< 2	

(1) Values according to the ecological criteria of the European Eco-label for footwear (Decision 2009/563/EC)

Tests were conducted on the different footwear styles in order to check their compliance with the minimum requirements of the European Eco-label for footwear (Decision 2009/563/EC) or, in the case of professional footwear, with the requirements set out in the European Standard for professional footwear (UNE-EN ISO 20344). The tests carried out are listed in the Table 3.

Table 3. Summary of tests on the different shoe styles made of titanium-tanned leather

Parameter analysed	Samples 1, 2 and 3		Samples 4, 5 and 6		Samples 7, 8 and 9	
	Average values	Requirements *	Average values	Requirements **	Average values	Requirements ***
Cr (VI) (ppm)	<3	<3	< 3	<3	< 3	<3
Formaldehyde (ppm)	9.4	<150	37	<150	5	<150
PCP and TCF (ppm)	< 0.1	<0.1	< 0.1	<0.1	< 0.1	<0.1
Cr (ppm)	< 20	-	< 20	-	< 20	-
Pb (ppm)	< 20	<100	< 20	<100	< 20	<100
Cd (ppm)	< 20	<100	< 20	<100	< 20	<100
As (ppm)	< 20	<100	< 20	<100	< 20	<100
Flex resistance (No. cycles)						
Dry	> 100	100	> 100	-	> 100	80
Wet	> 20	20			> 20	20
Tear strength (N)	206	≥ 60	220	120	199	≥ 60
Colour fastness to rubbing						
Discharge						
Dry (10 cycles)	5	-	-	-	4	-
Wet (10 cycles)	3				1	
Degradation						
Dry (10 cycles)	4	-	-	-	4	-
Wet (10 cycles)	4				4	
Water vapour permeability (mg/cm^{2}h)	-	-	4.8	> 0.8	-	-
Water vapour coefficient (mg/cm^2)	-	-	47.6	> 15	-	-
Water resistance						
Penetration 1 hour (g)	-	-	3.9	< 0.2	-	-
Absorption 1 hour (%)			81	< 30		

*Requirement of the European Eco-label for the inside of school footwear.

** Requirement according to the Standard UNE-EN ISO 20344 for professional footwear.

*** Requirement of the European Eco-label for the inside of casual footwear.

Figure 1. Professional footwear

Figure 2. Children's footwear

Figure 3. Men's and women's footwear

After conducting the tests, the different styles tested meet the limits required for each type of footwear.

CONCLUSIONS

The main conclusions drawn after the physical and chemical characterisation of titanium-tanned leather and footwear made of the same are the following:

- Titanium-tanned leather poses and alternative already available on the European and the international market.
- Titanium-tanned leather completely avoids the use of chrome in the tanning process.
- Titanium-tanned leather meets the technical specifications for footwear manufacturing according to the requirements of the European Eco-label for footwear.

REFERENCES

Covington, A.D. (1997), *Modern tanning chemistry*, Chemical Society Reviews, 111-126.
Galiana, M.V., Navarro, S., Segarra, V., Ferrer, J. and Riquelme, E. (2011), "New type of titanium tannage", XXXI IULTCS Congress September 2011, Valencia, Spain.

AESTHETIC SHAPES OF FOOTWEAR ACCESSORIES PERCEIVED AS SOURCES OF VIRTUAL SHOW

TRAIAN FOIASI

INCDTP - Division Leather and Footwear Research Institute, Bucharest, email: icpi@icpi.ro

Accessories are created in order to express the wearer's personality, to emphasize certain features, while toning down others; by means of accessories, shapes recombine endlessly, thus giving way to new possibilities to be highlighted as sources of show. Accessories, much like other footwear components, are able to provide industrial customers with clear and practical solutions regarding fashion forecasting 18 to 24 months in advance. These will be the starting point for their implementation in the footwear industry. Aesthetics, as shape and perception of accessories, which by means of their structure, material and last, but not least, their design and cutting-edge technology, give strength and visual impact according to the latest fashion trends. Contrary to studies on the chemicals used in leather processing and treatment in relation to foot hygiene, accessories respond through their degree of destructibility and the aesthetics, which is ephemeral anyway. Metals which may cause inconveniences to some, may be beneficial for others, just the same as semiprecious or precious stones are not compatible to each individual. Fashion, in its high complexity, highlights the social environment where the individual moves. This study presents several themes in fashion accessories for footwear and leather goods.

Keywords: design, accessories, footwear.

INTRODUCTION

Creativity, aesthetic and artistic knowledge, as well as psychology and marketing define the world of high-class fashion design. The preciousness of materials, metallic and non-metallic accessories, dynamical shapes full of grace and inventiveness, anticipation as aesthetic phenomenon are defining elements in designers' creations. Fantasy impels creators to play with shapes and colours, yet it must not be forgotten that fashion is meant for potential buyers, wearers of designers' suggestions, in real life circumstances. What best outlines the creation is the originality of suggestions and the functionality of solutions.

Accessories, or more simply put, ornaments which make up the foreshadowed object carry more and more poignantly the mark of designers, and the pressure is enormous. The reason is obvious: creations become real jewellery objects, and the imagination of those who design them seems to have no boundaries. The ornament is able to highlight and emphasize the aesthetic shape and the final quality of the product, as long as it is not conceived as an added touch of artificial beauty. It gains major aesthetic value as long as it is not superfluous, flashy or discordant, but rather corresponds to an aesthetic necessity, stimulating good taste (Achitei & Breazu, 1993).

ARTISTIC CONCEPT, ANTICIPATION AS DEFINING AESTHETIC PHENOMENON IN ACCESSORY DESIGN

The themes proposed in this study develop a wide range of artistic and technical approaches which will highlight some fashion trends regarding accessories for footwear and leather goods.

Freedom of Expression, Playfulness, Joy

Figure 1. Art session

Developing interweaving networks of textile materials and fibre optic with knots embellished with strass, semiprecious stones with irregular structure convey freedom of expression and innovation (Figure 1).

Accessories Specific to Leather Goods, Large Shapes, Gravity

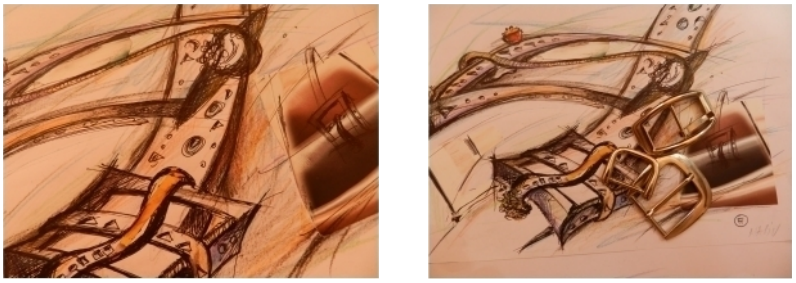

Figure 2. Massive

Through their composition and shape, the metals used give a sense of massiveness, but their degree of destructibility make them ephemeral (Figure 2).

Anticipatory Artistic and Technological Concept

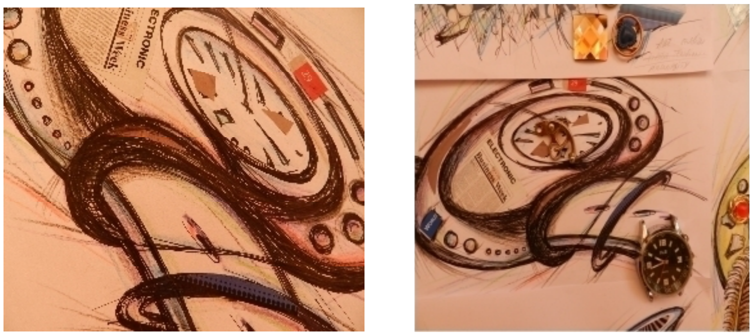

Figure 3. Message design

Cutting-edge communication systems, information, message, decoding are components of avant-garde accessories. Titanium, carbon, nickel, static finishes contribute to the preciousness of artistic concepts (Figure 3).

Relaxation, Richness, Show-biz

Figure 4. By night

Precious metal jewellery become customized accessories specific to a category of people who "associate" or "identify" themselves with uniqueness (Figure 4).

Rigour, Elegance, Freshness

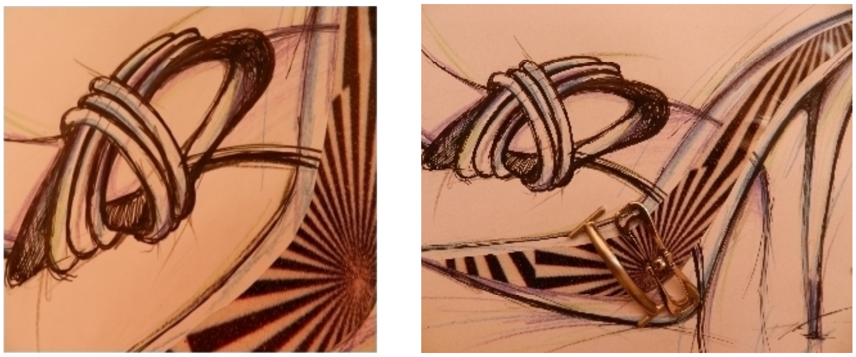

Figure 5. Geometric attraction

The sophisticated play of graphic representations combined with layering technologies characterize a line of elegance, rigour and freshness (Figure 5).

CONCLUSIONS

Interpretation of trends is focused on structures. These are defined as the shape and materials which trigger for and against arguments. The contrast of round and warm shapes against angular and rigid ones remains our restless play of identification with what we want. All these suggestions lead to an individualization of the product which will finally become a geometric attraction, a charming night, massive through its size, an art session, a message of the designer.

REFERENCES

Achitei, Gh. and Breazu, M. (1993), Aesthetics (in Romanian), Academy Press, Bucharest.

Foiasi, T. (2012), "Cultural Models in Haute-Couture Fashion. Part II – Sizes, Materials and Colours in Haute-Couture Fashion", Revista de pielarie incaltaminte (Leather and Footwear Journal), 12(1), 53-62.

*** (2012), Ars Sutoria, 380, Milano.

THE MOHAIR – PRECIOUS SOURCE OF RAW MATERIAL IN ROMANIA

CARMEN GHITULEASA[1], LILIOARA SURDU[1], ANA MARIA MOCIOIU[1], AUREL CONSTANTIN[2]

[1] *National R&D Institute for Textiles and Leather Bucharest (INCDTP), Lucretiu Patrascanu, 16, 031283 Bucharest, Romania, e-mail: certex@ns.certex.ro, webpage: http://www.certex.ro*

[2] *FERM PROD SRL Scarlatesti, Braila, Romania, e-mail: fermprod@gmail.com*

Returning to Nature is a growing tendency in the textile industry. Chemical fibers had known spectacular, even fascinating developments over time, trying to imitate nature in all its specific aspects. Despite this expansion of the production and processing of chemical fibers with extremely diversified and sophisticated characteristics, the specific properties of natural fibers and especially those of animal hairs could not be equalized. The use of these precious raw materials, the so-called noble fibers or “luxury hair fibers” overcame the barriers of "luxury" products, becoming a characteristic of the textile product market in the last years. In Romania, Angora goats were brought under the form of donations, in order to reinvigorate Romanian livestock farms. INCDTP initiated in collaboration with the FERM PROD ltd company from Braila county (area favorable in terms of environmental conditions and climate) an acclimatization project in Romania of a nucleus of Angora goats. The paper presents aspects regarding: the acclimatization process of animals, their breeding and multiplication; the comparative study of the main characteristics of Romanian Angora mohair type of fibers: physical-mechanical, chemical, electron microscopy, thermo gravimetrical properties; aspects regarding the processing of mohair/wool fibers blends and/or wool type chemical fibers, for obtaining woven fabrics with superior aesthetical and comfort characteristics.

Keywords: Romanian mohair, acclimatization, characteristics, fibers

INTRODUCTION

The tendencies of fashion towards clothes having special comfort characteristics have determined, in the last period, the manufacturers to focus their attention towards a greater usage of natural animal fibres. Usually known under the generic title of noble animal fibres, they present specific characteristics: soft, fluffy, handle, bulky, superior thermal isolation, breathable characteristic, air and humidity permeability, that give to the products containing such fibres an increased degree of comfort in wearing; possibility of adjusting to different environmental temperatures, maintaining he thermal equilibrium of the body.

The market researches indicate that the society’s evolution has determined, and still does, a certain change of the consumers’ perspective. Their requests and exigencies go beyond the level of quality textile products, reaching a superior one: natural fiber products, with a high added value, that bring “services” to the consumer, such as: comfort, easy care, functionality, “anti” properties: anti-soiling, anti-felting, anti-moths, odour control.

Globally, the major concerns of the consumer goods textiles’ manufacturers meet these requests and refer to: the use to the full extent of natural textile fibers; the increase of the added value of the products; achieving quality products that combine the engineering factors with the aesthetic and economic ones; achieving quality products that combine the engineering factors with the aesthetic and economic ones.

The paper presents aspects regarding the acclimatization process of the goats, a study of the complex structural properties of Romanian Angora mohair, as compared to those corresponding to wool fibres, through: electronic microscopy, thermo gravimetrical analysis, birefringence analysis.

There are also examined the physical-mechanical and chemical properties of raw and washed mohair fibers and their evolution during the acclimatization of goats, starting with 2003.

Further, there are presented aspects regarding the manufacturing of the Romanian mohair fibres for obtaining yarns and woven fabrics containing mohair, wool fibres and/or wool type chemical fibres, with superior aesthetic and comfort characteristics and high added value.

ASPECTS REGARDING THE ACCLIMATIZATION PROCESS OF THE ANGORA GOATS

Starting the acclimatization process, some conclusions are presented:

- animals have adapted easily to the new living conditions; after five years of breeding the Angora goats at FERM-PROD, one can say that the acclimatization process is completed: quantity of mohair: 4-6 kg fiber per animal; most animals are now the 4th-5th-6th generation; goats that produce two kids are in percentage of 50-60%;
- nevertheless, because of the inbreeding process, there were noticed the following aspects: the percentage of healthy kids at calving, the body weight and the quantity of fiber per animal and animal size were reduced.

In this situation, the specialists from FERM-PROD made tests for cross-breeding: 20 females were crossbred with males of normal breed. The following aspects were noticed: some kids kept the mother genetic character and there can be noticed the fleece aspect, specific to Angora; other kids have mainly their father character and the Angora specific aspect lost.

At present, there are carried out actions for purchasing 5 Angora males from Turkey, in order to restore the specific characteristics of the breed.

CONTRIBUTIONS TO THE STUDY OF THE PHYSICAL-MECHANICAL CHARACTERISTICS OF THE ROMANIAN MOHAIR FIBRES

Regarding to the main physical-mechanical characteristics for Romanian mohair fibers (2003 and 2010), as compared with Romanian wool fibers, the following aspects there are highlighted:

- ➢ Mean diameter is found around 30 μm, for the fibers coming from adult goats, value comparable with the one corresponding to the semi-fine wools, sort 29P (21); no modifications are noticed as far as samples in the 2010 production are concerned, as compared to the 2003 production;
- ➢ Mean length of the mohair fibers in the 2010 production shows a higher value (140 mm), in comparison with fibers in the 2003 production (100.2 mm);
- ➢ Staple fibers content has high values in case of mohair against wool, as this is generally a characteristic specific to goats (Angora, Cashmere) and camellids (camels, alpaca), being formed out of the fibers layer next to the animals skin (ca. 14% of total fleece);
- ➢ A reduction of the breaking resistance is determined for the 2010 production fibers, as compared to the 2003 production fibers, phenomenon that can be interpreted as an effect of the acclimatization process and of animals consanguinization;
- ➢ Friction coefficient values prove a sensible increase in case of 2010 production fibers, against the 2003 ones, process that can be explained by possible changes of the scales, which, due to acclimatization, thickened and became more prominent;
- ➢ Number of wrinkles for the mohair fibers is 0.7 wrinkles/cm, with 86% lower against the one corresponding to wool fibers (5.3 wrinkles/cm); these aspects are due to differences existing between the two types of fibers at the level of cuticle cells and are

worth being considered when designing the fibrous blends and, further, when managing the technological processing stages;

- Luster is influenced by the cuticle cells characteristics, which determine an increase of the even reflecting component to the decrease of the diffuse reflecting one, thus leading to a more intense luster gained, as compared to wool;
- Whiteness degree determined by the Elrepho method amounts to 37.90 for the mohair, which highlights a white color with a soft yellowish tint favoring the fibers luster.

It can also be observed that the variation coefficient of all characteristics is high; this is a specific characteristic of animal hairs. Also, it can see that the number of crimps is low, as compare with wool fibers; the friction coefficients, fiber/fiber and fiber/metal have also low values. This aspect determines the lowest adherence of the mohair fibers.

CONTRIBUTIONS TO THE STUDY OF THE STRUCTURAL PROPERTIES OF THE ROMANIAN MOHAIR FIBRES

The mohair (keratin fibre) is characterized from the morphological point of view by the existence of three distinctive cellular layers: cortical layer, cuticle layer and medulla. Medulla is specific for coarse fibres, with diameter over 35-38 μm. For emphasizing the longitudinal aspect of the fibres, there are effected electronic microscopy analyses, in the laboratories of our institute: fibres – production 2003 and fibres – production 2010.

Figures 1 and 2 highlight the fibres longitudinal surface for mohair and wool fibres.

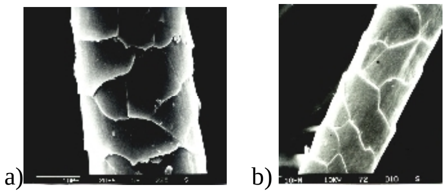

Figure 1. The aspect of the longitudinal surface for the wool fibres (a) and the 2003 mohair fibres (b) (Ghituleasa, 2004b)

The existence of some fine denticulate cuticle cells, with sharp peaks and with smaller thickness (scale height) in comparison with wool fibre scales can be observed.

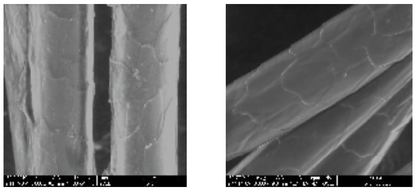

Figure 2. The aspect of the longitudinal surface for 2010 raw mohair fibres a) raw fibers, b) washed fibers (Ghituleasa, 2004b)

The impurities, sebum and fat adherent of the fibres can be observed on the raw fibers. It can be observed that the longitudinal surface aspect of the mohair fibres is more uniform as compared with wool fibres. There are not significant differences between analyzed fibres (2010 as compared with 2003).

The specific surface scale appearance is one of the factors that determine the high natural luster degree and the improved tinctorial properties of mohair fibers.

The keratin fibres, in general, are characterized by the existence of two types of cortical cells, ortho and para, present in different ratios within the morphological structure of the cortex. The orto-para quantitative ratio and also the distribution of these cells in the fibres cortex are characteristics that modify substantially their properties.

The analyses of electronic microscopy undertaken in the specialized laboratories in the institute have emphasized for the mohair fibres a cortical structure formed of orthocells and para heterotype cells (cells of transition from ortho to para). The undertaken research has emphasized a close connection between the cortical structure and crimping of the fibres. The mohair fibres have a reduced number of crimps (0,7/cm) and a monotype distribution (ortho-cortical cell and of transition ortho →para). Figure 3 presents the aspect of the cross-section for the mohair fibres. For the emphasizing of the cortical structure a coloration specific to the paracortical cells (silver nitrate 2.5%) has been effected in the investigation laboratories in the institute.

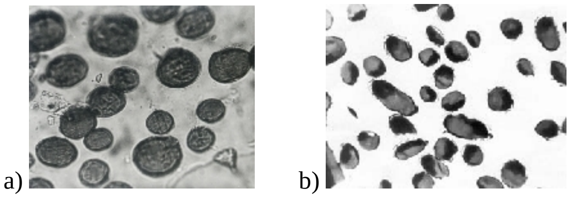

Figure 3. Aspect of the cross-section for mohair fibers (a) and wool fibers (b) (Ghituleasa, 2004b)

In the section it can be observed that there are not clear differences of colour inside the cortex as it is in the case of fine wools, that proves the character of ortho- paracortical transition of the cells. The lack of the para cells, strongly reticulated, generates a labile character and an increased reactivity of fibres towards the chemical agents.

The thick mohair fibers with a diameter exceeding 38-40μm are characterized by the presence of the medullar channel, situated at the center of the cross-section.

The presence of the medullar channel roots back in the insufficient keratinization of the fiber and represents, at the same time, a result of the lower inclusion of sulphur-containing amino-acids (cystine).

THERMOGRAVIMETRICAL ANALYSES

a) DTG results of the mohair and wool fibres samples (2003), were recorded by MOM 1500 D Budapest. The initial temperature was T_o=26°C.

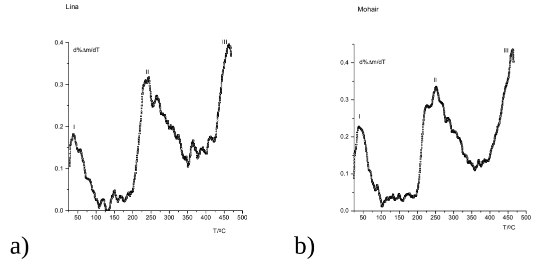

Figure 4. DTG curves for wool (a) and mohair fibers (b) (Ghituleasa, 2010)

Table 1. The variation of percentage mass loss, depending on temperature, for 2003 mohair fibres and wool fibres (Ghituleasa, 2010)

Temperature, °C	Mass loss, % Δm		Ratio % Δm
	Mohair	Wool	mohair/wool %
125	10,7	8,7	123
192,5	13,2	10,5	125,7
363,5	48,8	42	116,1
466	72,2	66,5	109

The analyses of the Figure 4 and of the data presented in the Table 1 allow the emphasizing of the following aspects:

- The rising of the temperature up to 125° determines a process of eliminating water by evaporation, corresponding to a mass loss of 10,7% for mohair fibres by about 23% higher than the adequate value of the wool fibres, which is 8,7%. During this interval, the average temperature of heat absorption adequate to the maximum speed of eliminating humidity (first peak endothermic) has values between 50-80°C. The higher value of mohair fibres mass loss due to humidity elimination can be in relation with the higher water content of these fibres and with the structural differences specific to the process of orthokeratinisation, emphasized by analyses of electronic microscopy and X-rays diffraction.
- After the humidity elimination, the thermic degradation of the fibres occurs in two stages: decomposition and thermo-oxidation.
- The more the temperature rises, the more the procentual mass decreases, both for mohair and for wool; the fibres decomposition occurs. It is emphasized that when temperature is about 200-228°C, when the value of mass loss is 13,2-15%, a supercontraction of fibres associated with a shortening of the molecular chain occurs.

The second endothermic peak appears at the temperature of 260-275°C and occurs at the level of heterotype para-cortical cells, with a higher cystine content.

- Starting with this temperature, the fibres samples decompose quickly. During the decomposition process, the mohair loses 9-25% mass more than wool does, with close values of temperature. Thus, at temperature of 360°C the mass loss has the value of 48,8% for mohair and 42% for wool.
- The second stage of the fibre degradation starts with a temperature of 400°C, when the fibres thermo-oxidation occurs and the value of mass loss of 72,2% for mohair and of 66,5% for wool. At 500°C the thermal decomposition is complete.

b) Equipment used for 2010 mohair fibres was STA 6000 -PerkinElmer. Mass samples was about 4.1 mg. Temperature range was between 25-700 °C.

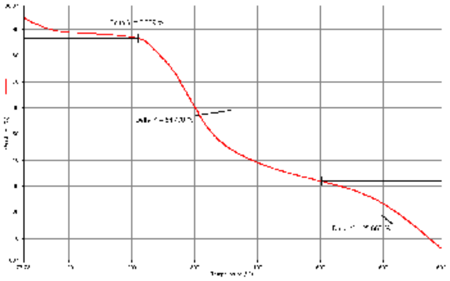

Figure 5. The variation of mass loss, depending on temperature, for 2010 mohair fibres (Ghituleasa, 2010)

Table 2. The variation of percentage mass loss, depending on temperature, for 2010 mohair fibres (Ghituleasa, 2010)

Temperature, °C	Mass loss, % Δm
27 – 225	8,089
225 – 500	54,47
500 – 692	25,67
> 700	11,78

It can be observed that the biggest mass loss (thermo degradation of the fibres) occurs for 225-500°C. The analyses of the Figure 5 and of the data presented in the Table 2 emphasize that there are not differences between the temperature behavior of the 2003 and 2010 mohair fibres. The wool and mohair fibers different behavior under the temperature action is caused by the ortho-keratinization process specific to mohair that generates a more labile or instable structure, which is bulkier and richer in the water content.

CONCLUSIONS

On the global level, the use of "rare" animal fibers, also known under the name of "noble, precious, special fibers" has increased considerably in the recent years.

Taking into account the global trends in the field, the acclimatization of a nucleus of Angora goats in Romania, the setting up of a new autochthonous base of valuable raw material and the evaluation of the possibilities of efficient processing of these fibers, represent an alternative for the Romanian zootechnical sector and a challenge for the scientific research and textile industry of our country.

The issues presented demonstrate the importance given to mohair fiber production and processing in Romania and motivate the continuation and extension of the researches on highlighting opportunities for the efficient turning to account of this valuable raw material.

Research will continue for developing the range of products containing mohair fibers. Mohair can become a valuable source of raw material for the textile industry in Romania.

Acknowledgement

Authors would like to thank professor dr. Mihai Ciocoiu from Technical University of Iasi, Romania, for his support in developing this research.

REFERENCES

Ghituleasa, C. (2004a), "Textile articles with improved characteristics destined for consumer goods" Research project INCDTP, Bucharest, Romania.

Ghituleasa, C. (2004b), "Theoretical and experimental contribution regarding the physical-mechanical, physical-chemical and for textile manufacturing of the Romanian mohair fibres", PhD Thesis, Technical University Gh. Asachi, Iasi.

Ghituleasa, C., Visileanu, E., Ciocoiu, M. (2003), "Romanian Angora Mohair Fibers – Characteristics, Application Fields", *Journal of Natural Fibers*, Poland.

Ghituleasa, C., Visileanu, E. (2004), *Animal Natural Fibres*, CERTEX Publishing House, ISBN 973-85532-3-7, 19-45, Bucharest, Romania.

Ghituleasa, C. (2010), "Study regarding animals hairs at the national and global level", Research project INCDTP, Bucharest, Romania.

APPLICABILITY OF VULNERABILITY INDEX ON GIS SURVEYING SYSTEM

IOANA OLTEANU, ANA-MARIA TOMA

"Gheorghe Asachi" Technical University of Iasi, Faculty of Civil Engineering and Building Services, Department of Structural Mechanics, 43rd, D. Mangeron Blvd., Iasi, Romania, zita_01040@yahoo.com, anamtoma@ce.tuiasi.ro

The continuing changes in the seismic codes make mandatory a vulnerability inventory for buildings designed according to previous norms. The variety of the existing structural models, the materials and the utilized technologies lead to the need of individual studies. The objective of these studies is to determine a damage index for each building and to define them on the city map. In this way risk areas are determined and suitable scenarios for quick post-disaster relief measures can be taken in order to minimize the damages. This is a valuable tool that can enable decisions makers to direct the help to the most needed locations. The paper considers a recent developed methodology that is based on the capacity curve evaluated through a nonlinear static analysis. The considered vulnerability method uses damages stages defined in RISK- UE project specifications in order to assess the vulnerability index. The vulnerability index expresses the exposure of a structure in terms of damage probability and iunie 2012spectral displacement. In this paper the damage indexes for 12 reinforced concrete frame structures are evaluated. These indexes are then considered on a GIS map in order to determine the actual state of the structures of a city.

Keywords: vulnerability index, capacity curve, GIS system.

THEORETICAL BACKGROUND

The pushover analysis is a nonlinear static incremental procedure able to describe, in a simplified way, the structural behavior to seismic actions. The pushover analysis is defined in the Federal Emergency Management Agency document 273 as a nonlinear static approximation of the response of the structure when subjected to earthquake load (FEMA 273, 1997). The static approximation consists of applying a lateral horizontal load pattern upon a structural model considering the material nonlinearity and monotonically increasing the loads until the collapse of the structure is reached.

The capacity curve, determined through pushover analysis, allows identifying the weak structural members and the failure mechanisms. The curve is in fact the relation between the base shear and the displacement at the roof of the structure (ATC-40. 1996), (Zou and Chan, 2005).

The building performance is evaluated by intersecting of the capacity curve of the structure with the demand curve corresponding to the seismic action, called performance point, which approximates the expected seismic performance of the structure under a known earthquake (ATC-40. 1996), (Mohamed Nour, 2007).

In order to apply the capacity spectrum method the following steps are required: (1) perform the pushover analysis of the building; (2) plot the capacity curve of the building; (3) represent it in a ADRS format, that is, as a capacity spectrum; (4) calculate and plot the bilinear representation of the capacity spectrum; (5) plot the demand spectrum of the considered earthquake; and finally (6) intersect capacity and demand spectra to obtain the performance point, and thus the expected spectral displacement, Figure 1. The performance point is calculated by using the equal displacement approximation described in ATC-40 (Fajfar, 2000), (Mohamed Nour, 2007).

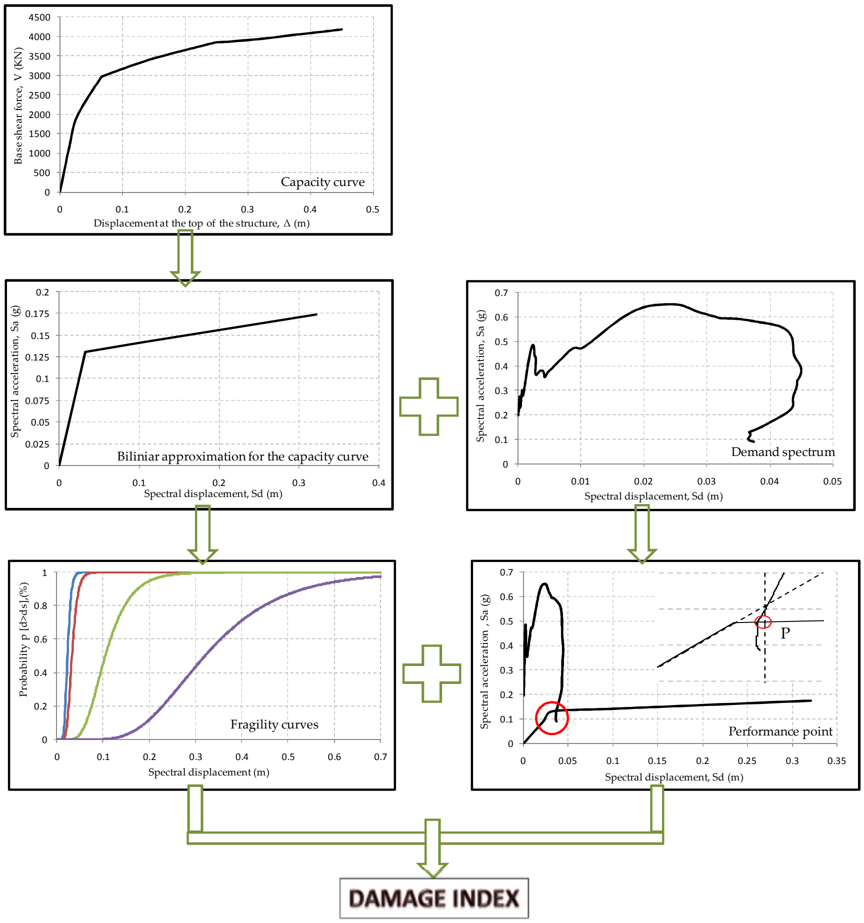

Figure 1. Considered steps for damage index evaluation

Fragility curves define the probability that the expected global damage *d* of a structure exceeds a given damage state *dsi*, as a function of a parameter quantifying the severity of the seismic action. Thus, for each damage state, the corresponding fragility curve is completely defined by plotting *P[d≥dsi]* in the ordinate and the spectral displacement *Sd* in the abscissa (Barbat et al. 2009).

A simplified procedure to obtain fragility curves starting from the bilinear representation of the capacity curves is described in the Risk-UE handbook. The considered approach proposes four damage states: *slight* – the damage is considered negligible, *moderate* – slight structural damage and moderate nonstructural damage, *severe* – moderate structural damage and heavy nonstructural damage and *collapse* when structure is in imminent danger of collapse (Milutinovic and Trendafiloski, 2003).

The probability for each damage state is computed as a subtraction. The probability of occurrence of the slight damage state is p1=pfc1-pfc2, for the moderate damage state it is p2=pfc2-pfc3, for the severe damage state it is p3=pfc3-pfc4 and for collapse damage state it is p4=pfc4, Figure 2 (Barbat et al., 2006).

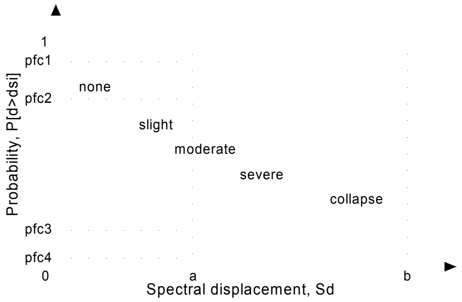

Figure 2. Fragility curves general representation

Considering the fragility curves and the performance point, the damage index can be evaluated for a specific value, *a*, of the spectral displacement using the following relation (Olteanu et al., 2011):

$$\mathrm{DI}(Sd = a) = \frac{1\cdot p1+2\cdot p2-3\cdot p3+4\cdot p4}{4} \qquad (1)$$

CASE STUDY

For this case study 12 reinforced concrete frame structures were considered with different characteristics. Structures with one level, 3 levels, 6 levels and 9 levels were considered each with 2, 4 and 6 openings respectively. The structures were realized of C20/25 concrete with reinforcement of PC52 and OB37. The minimum reinforcement percentages from the current codes were considered (STAS 10107, 1990).

A pushover analysis was performed for each structure in SAP2000 in order to obtain the capacity curve. Then, these results were used to compute the bilinear approximation and the damage states for each structure. The accelelogram for Vrancea earthquake from March 1977 was considered for the demand curve. The capacity curve was intersected with the demand curve considering the methodology from the equal displacement approximation presented in ATC-40. in order to obtain the performance point.

The results for all the 12 models are presented in a synthetic way in Table 1. The table contains the yield displacement, dy, the ultimate displacement, du, the fundamental period, T, spectral displacement, Sd(P) and spectral acceleration, Sa(P) corresponding to the performance point. M is the ductility coefficient evaluated as a ratio between the ultimate displacement and the yield displacement.

It is noticed from these results that the number of spans do not influence significantly the results, in contrast with the number of levels.

The physical damage of a structure, which quantifies the average loss of a particular structure starting from a seismic hazard scenario and the structural vulnerability, can be accomplished using damage probability matrices, which express the conditional probability P [D = j | i] to obtain a damage level j, due to an earthquake of severity i

(Whitman et al. 1974). Table 2 represents the damage index matrix and contains also a mean value for the damage index, Dsm.

Table 1. Results synthesis for the considered models

Structure	dy (m)	du (m)	T(s)	μ	Sd(P)	Sa(P)
g.f_2spans	0.0065	0.0506	0.1961	7.75	0.0028	0.4140
g.f_4spans	0.0083	0.0497	0.2009	5.99	0.0028	0.4140
g.f_6spans	0.0083	0.0519	0.3315	6.27	0.0028	0.4140
3f._2spans	0.0221	0.1308	0.4977	5.91	0.0351	0.4011
3f._4spans	0.0205	0.1310	0.4946	6.40	0.0342	0.3829
3f._6spans	0.0238	0.1214	0.4936	5.09	0.0338	0.4196
6f._2spans	0.0332	0.2100	0.8740	6.32	0.0436	0.1810
6f._4spans	0.0319	0.1973	0.8526	6.18	0.0437	0.1842
6f._6spans	0.0312	0.1906	0.8453	6.10	0.0437	0.1846
9f._2spans	0.0352	0.3408	1.1150	9.70	0.0370	0.1282
9f._4spans	0.0323	0.3209	1.0712	9.95	0.0383	0.1317
9f._6spans	0.0328	0.3165	1.0564	9.64	0.0392	0.1342

Table 2. Damage index matrix

Structure	Probability for each damage state					
	None	Slight	Moderate	Severe	Collapse	Dsm
g.f_2spans	0.9348	0.0445	0.0207	0.0000	0.0000	0.0215
g.f_4spans	0.9912	0.0047	0.0041	0.0000	0.0000	0.0032
g.f_6spans	0.9911	0.0048	0.0041	0.0000	0.0000	0.0033
3f._2spans	0.0017	0.1466	0.6471	0.2041	0.0005	0.5138
3f._4spans	0.0009	0.1195	0.6803	0.1988	0.0004	0.5195
3f._6spans	0.0071	0.2340	0.5776	0.1807	0.0006	0.4834
6f._2spans	0.0136	0.2783	0.6343	0.0738	0.0000	0.4421
6f._4spans	0.0092	0.2506	0.6449	0.0953	0.0001	0.4566
6f._6spans	0.0075	0.2354	0.6485	0.1086	0.0001	0.4646
9f._2spans	0.0712	0.3620	0.5640	0.0029	0.0000	0.3746
9f._4spans	0.0306	0.2646	0.6990	0.0058	0.0000	0.4200
9f._6spans	0.0285	0.2566	0.7077	0.0072	0.0000	0.4234

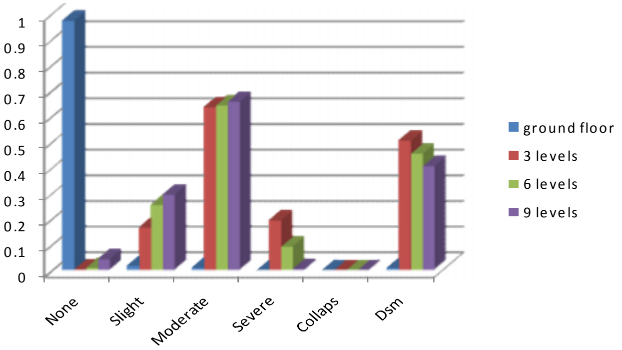

Figure 3. Synthesis of the mean damage index

A graphical representation of the mean damage index in represented in Figure 3. It can be concluded that the ground floor structure is extremely rigid, being situated almost 100% in the non damaged state. At the other limit are the 3 levels structures, with a mean damage index of 0.5, which means that it will suffer the most damage in case of an earthquake similar to Vrancea 1977. Also the damage state with the highest percentage is the moderate one, for all the structures with more than 3 levels.

Another important remark is that none of the considered structure will reach collapse, meaning that they are well designed.

GIS MAPS, VISUALIZATION OF DAMAGE STATES

Buildings have partially or totally collapsed during recent earthquakes in Turkey 1999, Italy 2009, Haiti 2010, Chile 2010 and Japan 2011. As demonstrated by the on-site investigations, it is possible that many of the observed collapses have been the result of lack of understanding the regional seismic hazard, the behavior of structural materials under dynamic loads, and the post-elastic behavior of structural systems (Villaverde, 2007). Knowing where such events have occurred and the geographic limits of their impacts is clearly important. When combined with information on human populations, infrastructure and other spatially distributed phenomena that may be relevant to response and recovery, it becomes clear that the technologies that acquire, interpret and disseminate such information (GIS, remote sensing, GPS, etc.) are essential in all aspects of disaster from preparedness, prevention and protection through detection to response and recovery.

Geographic information and technology provide the basis for estimating and mapping risk, for planning evacuation routes and shelters, for determining areas where human populations are most likely to have been impacted following a disaster and for assigning resources during recovery, among many other vital and important tasks (Goodchild, 2008; Toma and Atanasiu, 2011). An example of the applicability of GIS technology in visualizing the spatial distribution of the structural damage in a urban sample are is shown in Figure 4. The user can select to view only the buildings with a certain level of damage. Moreover, the program can display all the buildings for which a degradation coefficient or the vulnerability index is computed and display them with different colors depending on the values of the coefficient (Toma et al., 2011).

Figure 4. Buildings shown according to their degree of degradation (NetSET-GIS)

CONCLUSIONS

The interaction between GIS maps and seismic risk assessment is a modern tool and many cities are already mapped according to a damage index. This tool helps authorities to know the actual situation and to prepare emergency scenarios.

The current study shows that the vulnerability of the structure is inverse proportional with the number of stories. The ground floor structure can be considered an exception because of their extremely rigid behavior. The study also shows that in case of an earthquake similar with the recording from 1977 the majority of the buildings will suffer a moderate damage and retrofit measure will be needed.

The most vulnerable structures are the 3 stories, which have a probability of damage for the performance point over 50%.

The study was conducted only on reinforced concrete frames and further research should be done on other structural systems in order to have a complete database.

REFERENCES

ATC-40 (1996), Seismic Evaluation and Retrofit of Concrete Buildings. Applied Technology Council. Report: SSC 96-01, Volume 1, Seismic Safety Commission, Redwood City, California.

Barbat, A.H., Carreño, M.L., Pujades, L.G., Lantada, N., Cardona, O.D., Marulanda, M.C. (2009), "Seismic vulnerability and risk evaluation methods for urban areas. A review with application to a pilot area", *Structure and Infrastructure Engineering*, 6(1), 17-38.

Barbat, A.H., Pujades, L.G., Lantada, N. (2006), "Performance of Buildings under Earthquakes in Barcelona, Spain", *Computer-Aided Civil and Infrastructure Engineering*, 573-593.

Fajfar, P. (2000), "A Nonlinear Analysis Method for Performance Based Seismic Design", *Earthquake Engineering and Structural Dynamics*, 16(3), 573-592.

FEMA-273 (1997), NEHRP Guidelines for the Seismic Rehabilitation of Buildings, FEMA-273. Building Seismic Safety Council. Federal Emergency Management Agency, Washington, D.C., USA.

Goodchild, M.F. (2008), "GIS and Disasters: Planning for Catastrophe", *Computers, Environment and Urban Systems*, 30(2), 70-80.

Milutinovic, Z.V., Trendafiloski, G.S. (2003), RISK-UE, An advanced approach to earthquake risk scenarios with applications to different European towns, Contract: EVK4-CT-2000-00014, WP4: Vulnerability of current buildings.

Mohamed Nour El-Din Abd-Alla. (2007), "Application of Recent Techniques of Pushover for Evaluating Seismic Performance of Multistory Buildings", Master thesis, Faculty of Engineering at Cairo University.

Olteanu, I., Alistar, A., Budescu, M. (2011), "Nonlinear analysis of reinforced concrete frames in ATENA 3D", *Bulletin of Polytechnic Institute of Iasi*, Construction. Architecture Section, Tome LVII, Fasc. 2, 93–103.

Toma, A.M. and Atanasiu, G.M. (2011), "Seismic Risk Evaluation Based on Digital Mapping of a Romanian Urban Area", *Proceedings of the 8th International Conference on Urban Earthquake Engineering (8CUEE)*, Tokyo, Japan, paper ID: 12-124.

Toma, A.M., Atanasiu, G.M. and Toma, I.O. (2011), "GIS-based seismic risk evaluation of tall residential buildings of Romanian urban areas – case study for the city of Iasi", *Proceedings of the International Conference on Engineering UBI2011 "Innovation and Development" – ICEUBI2011*, Colvilha, Portugal, paper ID: CT19-5.

Villaverde, R. (2007), "Methods to Assess the Seismic Collapse Capacity of Building Structures: State of the Art", *ASCE Journal of Structural Engineering*, 133(1), 57-66.

Whitman, R.V., Reed, J.W., Hong, S.T. (1974), "Earthquake damage probability matrices", *Proceedings of 5th European conference on Earthquake Engineering*, Rome, Italy.

Zou, X.K., Chan, C.M. (2005), "Optimal seismic performance–based design of reinforced concrete buildings using non-linear pushover analysis", *Engineering Structures*, 27, 1289-1302.

VULNERABILITY ASSESSMENT OF REINFORCED CONCRETE FRAME STRUCTURES DESIGNED ACCORDING TO ROMANIAN CODES

IOANA OLTEANU, ANA-MARIA TOMA

"Gheorghe Asachi" Technical University of Iasi, Faculty of Civil Engineering and Building Services, Department of Structural Mechanics, 43rd, D. Mangeron Blvd., Iasi, Romania, zita_01040@yahoo.com, anamtoma@ce.tuiasi.ro

The damaged produced worldwide by earthquakes and their secondary effects during the past decade show that the vulnerability assessment of the entire building stock should be evaluated. Various methodologies for the evaluation of the seismic vulnerability have been proposed as a result of research work carried out worldwide. The easiest way to describe the vulnerability of a structure is to represent a lognormal function of the relation between the probability of damage and the spectral displacement. The present paper focuses on the assessment of the seismic vulnerability of reinforced concrete structures. The procedure is based on the capacity curve obtained through a nonlinear static analysis and on four damage states described according to RISK-UE project specification. The vulnerability index is computed based on the values obtained from the fragility curves. The main parameters considered in the present paper for the vulnerability assessment were the number of stories, number of spans and the slab thickness. The considered structures were designed according to the prescriptions of the Romanian seismic code for Iasi location.

Keywords: vulnerability curve, reinforced concrete frame, slab thickness.

INTRODUCTION

Disasters from recent natural hazard, Figure 1, reveal the urgent need to a real evaluation of the building stock all around the world. Research projects, such as HAZUS, Risk-UE and CAPRA, developed different procedures to assess buildings vulnerability state. For example, HAZUS is based on experts' opinion (HAZUS 1999).

Figure 1. Reinforced concrete frames damaged in L'Aquilla earthquake 6th of April 2009 and Chile earthquake 27th of February 2010

Risk-UE project proposes a deterministic procedure for seismic risk evaluation in urban areas, which uses the capacity spectrum curve and the demand curve (Mouroux şi Lebrun 2006), (Freeman 1978). The method permits evaluating the expected seismic performance of structures by comparing, in spectral coordinates, their seismic capacity with the seismic demand described by Acceleration-Displacement Response Spectra and adequately reduced in order to take into account the inelastic behavior (Fajfar 2002).

CAPRA, meaning Comprehensive Approach on Probabilistic Risk Assessment, evaluates the losses from natural disasters by means of the probabilistic matrix. This program is the first one that proposes to consider multi-hazard analysis for vulnerability assessment of a location (ERN-AL 2010).

ROMANIAN SEISMIC CODES

Romanian seismic codes suffered significant modifications during the last 70 years. The first seismic code is from December 1941, and came as the result of major damages caused by the earthquake from 10th of November 1940. The code was based on Italian regulation and used to consider the seismic force as 5% of total gravitational forces, uniformly distributed on the structure slab (Ştefan and Covatariu 2005).

In 1963 a reviewed version, called P13-63 was adopted. The code considered the observations made on disastrous earthquakes for seismic areas and observations done in international conferences. At that time recordings of the seismic activity in Vrancea region did not exist.

An improved version, P13-70, contained modifications of foreign codes and research results from our country and worldwide. These modifications led to a significant reduction of the conventional seismic force, for all structure types. It was noticed that neither code correctly considered the plastic behavior of structures during strong earthquakes.

The effects for 4th March 1977 earthquake, together with on site observations and the ground acceleration recording at the INCERC seismic station, determined two new codes P100-78 and P100-81. A major modification was represented by the introduction of the normalized design elastic spectrum specific for sub crustal earthquakes from Vrancea. The consideration of the maximum ground acceleration and reduction of the seismic force in accordance with the structure ductility was considered. The torsion effect is considered for the first time in P100-81 code.

P100-92 represents modern codes which contain zoning maps. The importance class is introduced in this norm and the type of the structure is considered in the reduction coefficient consideration.

P100-2004 represents the first code elaborated in Eurocode format, having as major aim the harmonization of the national design code with the European one. The current norm is P100-2006, which represents the transition code from P100-2004 to Eurocode 8. The two codes are already very similar.

Figure 2 represents a graphical comparison of the values for the seismic force in different codes presented above. The graphical comparison is for a reinforced concrete frame P+7E, with medium ductility. The behavior factor according to the code is 4.725. The period of vibration is 0.6 s. The seismic forces for two seismic areas were evaluated – Focsani and Iasi. The considered foundation soil is of medium stiffness.

The results are presented in Figure 2. It can be stated that P100-63, the first seismic norm was the most restrictive one. The other values are less, but with an increase tendency until the current code. Also it is clear that Focsani city, which is closer from the epicenter area, has more restrictive values for the seismic force.

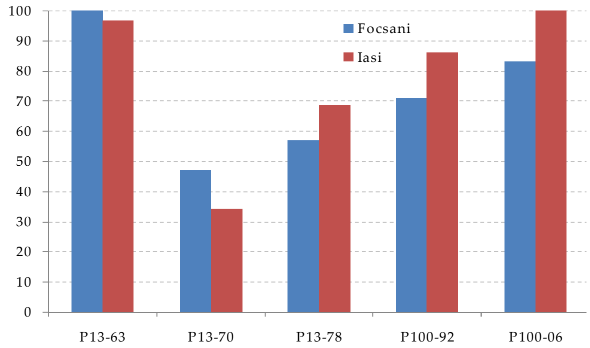

Figure 2. Comparison for the seismic force evaluated with different codes

SEISMIC VULNERABILITY ASSESSMENT METHODOLOGY

The following dimensions characterize the vulnerability concept: physical, economic, social, educational, political, institutional, cultural, environmental and ideological. For all of these Wilches-Chaux proposed the notion of global vulnerability. The paper concentrates on the physical dimension of the concept. This is correlated with the exposure degree and the fragility of the exposed elements (Cardona 2004).

Structures with different characteristics are compared based on a seismic vulnerability assessment methodology which was considered in the Risk-UE project (Milutinovic and Trendafiloski 2003).

Vulnerability is defined as the physical, economical, politic or social predisposition to suffer damages in case of a natural or entropic hazard. The hazard refers to a latent danger or an external risk factor for an exposed element, which can be expressed as the probability to produce an event with a specific intensity, for a specific location, in a moment during the service life time of the building (Olteanu, 2011).

The behavior of reinforced concrete structures is dependent of the ratio between the columns height and the beams length, as well as of the strength of the column and beam cross section. Grünthal has defined five damage levels considering the effect earthquake can have on structures, EMS – 98 (Earthquake Measure Scale). Similar to this, in Risk-UE project are identified 5 damage states, with some differences from the EMS-98 intensity scale (Grünthal 1998). The main difference occurs at the top damage states.

The physical expected damage, which quantifies the mean damages for a specific structure can be determined using probability damage matrix, vulnerability functions and fragility curves.

Capacity curves are the results of a pushover analysis, method used for the seismic performance evaluation of existing structures, but also for the design process. The method consist in loading the structure with a specific load pattern which is increased monolithically until the structure reaches a target displacement, measured at the top of the structure. According to FEMA 273 the loading pattern approximates the possible distribution of stresses in the structure in case of an earthquake.

Using the capacity curves and the damage states described in Risk-UE specifications, fragility curves can be obtained. These curves present the probability of damage for each damage state at every displacement value of the structure. It was considered that their interpretation is difficult and researchers proposed the vulnerability curves instead (Barbat et al., 2008).

Vulnerability curves quantify damage as a function of parameters that characterize the seismic action, the spectral displacement for example, as it is considered in this paper. From theoretical point of view, the vulnerability curves represent the mathematical probability of structural damage, for each value of the spectral displacement.

VULNERABILITY ASSESSMENT

Several buildings were considered in order to be able to compare structures with different geometric and plan configuration. All the structures have in common the structural system and the material – reinforced concrete structure. The buildings were design according to current Romanian codes – STAS 10107-90, P100-2006, for Iasi location, considered as condominium buildings.

Table 1 contains main characteristics for the used structures and the fundamental periods. A 3 m story height was considered and 3m for the span was used. For the 3 storey structures the following cross section were used: for the columns 50 cm by 50 cm and for the beams 30 cm by 50 cm. Meanwhile for the 9 storey model the following cross section were obtained: beams of 30 cm by 50 cm and columns of 70 cm by 70 cm for the first 5 storeys and 50 cm by 50 cm for the rest of the floors.

Table 1. Models description and fundamental period

Model	Levels	Spans	Slab thickness	Period
RC1	3	3x3	10 cm	0.231 s
RC2	3	3x3	20 cm	0.262 s
RC3	3	3x6	10 cm	0.239 s
RC4	3	3x6	20 cm	0.273 s
RC5	9	3x3	10 cm	0.591 s
RC6	9	3x3	20 cm	0.637 s
RC7	9	3x6	10 cm	0.608 s
RC8	9	3x6	20 cm	0.651 s

A static nonlinear analysis was performed for the buildings using SAP 2000 computer software. Capacity curves are obtained as results; Figure 3 a. and b., which are used further in the vulnerability assessment procedure.

Using these capacity curves and the damage states defined according to Risk-UE specification, fragility curves were evaluated and then vulnerability curves were compared. In Figure 4, vulnerability curves for more structures considering the same number of storeys and different number of spans and slab thickness are compared. For the 3 storey structures the difference are insignificant, meanwhile for the 9 storey structures the differences can be seen with the naked eye. For this situation it can be state that the most unfavorable situation is when an asymmetric structure with a thick slab is considered.

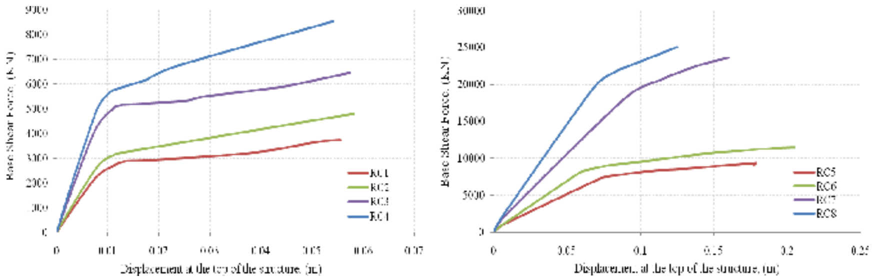

Figure 3. Capacity curves for: a. 3 stories structures; b. 9 stories structures

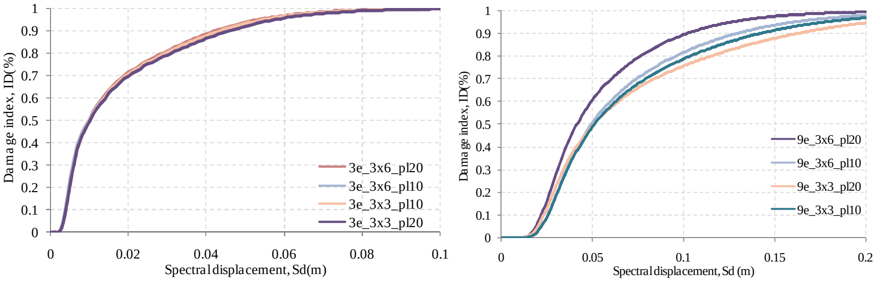

Figure 4. Vulnerability curves

In Figure 5 are compared also vulnerability curves. In the left figure, two parameters are considered as variables – the number of storeys and the slab thickness. It can be noticed that the 3 storey structures are more vulnerable and that the 9 storey ones are more flexible structures with a higher capacity to dissipate seismic energy. If the slab thickness is considered as variable parameter it can be concluded that the over strength produced by a heavier slab is bigger and in consequence the overall behavior of the entire structure is less flexible.

In Figure 5 right, where the main parameters are the number of stories and the number of spans, it can be stated that the number of spans have less influence of the damage index, than the slab thickness has. Also, again it was noticed a significant difference of the results between structures with 3 and 9 storeys.

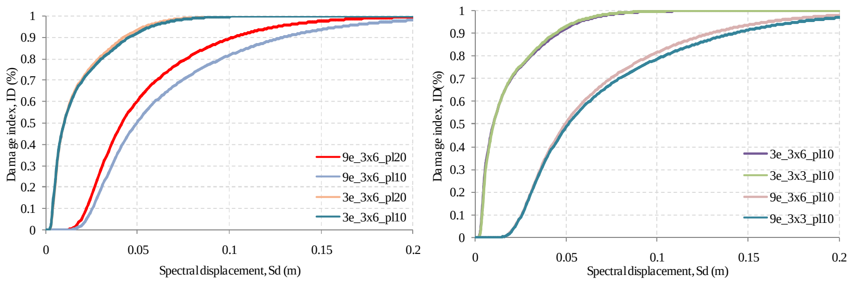

Figure 5. Vulnerability curves

CONCLUSIONS

The continuum changes of seismic codes make mandatory to update the design process. The evolution of Romanian seismic code in past year reveals the interest of the authorities on constructing safer structures.

The study show that the less number of stories a structure has, more vulnerable is. Also is noticed that the number of spans does not influence the overall behavior of the structure, in contrast with the slab thickness.

The additional stiffness a slab introduces for a structure is well known and the study reveals that the introduced stiffness is directly proportional with the slab thickness.

The study reveals the need of particular measures for each structure type in order to increase their capacity to dissipate seismic energy and to have a good overall behavior in case of earthquake.

REFERENCES

Barbat, A.H., Pujades, L.G., Lantada, N. (2008), “Seismic damage evaluation in urban areas using the capacity spectrum method: Application to Barcelona”, *Soil Dynamics and Earthquake Engineering*, 851–865.

Cardona, O.D. (2004), “The need for rethinking the concepts of vulnerability and risk from a holistic perspective: a necessary review and criticism for effective risk management”, in: G. Bankoff, G. Frerks, and D. Hilhorst, eds., *Mapping vulnerability: disasters, development and people*, London, UK: Earthscan Publishers, 37–51.

ERN-AL (2010), CAPRA - Comprehensive Approach for Probabilistic Risk Assessment. www.ecapra.org. Evaluación de Riesgos Naturales – América Latina.

FEMA-273 (1997), NEHRP Guidelines for the Seismic Rehabilitation of Buildings, FEMA-273, Building Seismic Safety Council, Federal Emergency Management Agency, Washington, D.C., USA.

Freeman, S.A. (1978), “Prediction of response of concrete buildings to severe earthquake motion”, *Proceedings of Douglas McHenry International Symposium on concrete and concrete structures*, publication SP-55, American Concrete Institute, Detroit, Michigan, USA.

Grünthal, G. (1998), *European macroseismic scale 1998* (volume 15), Luxemburg: Centre Européen de Géodynamique et Séismologie, Cahiers du Centre Européen de Géodynamique et de Séismologie.

HAZUS 99-SR2 (1999), Estimated annualized earthquake losses for the United States. Federal Emergency Management Agency (FEMA), Washington, USA.

Milutinovic, Z.V., Trendafiloski, G.S. (2003), RISK-UE, An advanced approach to earthquake risk scenarios with applications to different European towns, Contract: EVK4-CT-2000-00014, WP4: Vulnerability of current buildings.

Mouroux, P., Lebrun, B. (2006), “RISK-UE project: an advanced approach to earthquake risk scenarios with application to different European towns”, in C.S. Oliveira, A. Roca and X. Goula (eds.), *Assessing and Managing Earthquake Risk*, 479 - 508, Springer.

Olteanu, I. (2011), *Vulnerability assessment for reinforced concrete frame structures in seismic areas* (in Romanian), POLITEHNIUM.

P100-1/2006 – Antiseismic Design Code – Part I –Rules for building design (in Romanian).

P100-78. Design Code for civil constructions, sociocultural, agricultural and industrial buildings (in Romanian).

P100-81. Design Code for civil constructions, sociocultural, agricultural and industrial buildings (in Romanian).

P100-92. Antiseismic Design Code for civil constructions, sociocultural, agricultural and industrial buildings (in Romanian).

P13-63. Design Code for civil constructions, sociocultural, agricultural and industrial buildings (in Romanian).

STAS 10107 (1990), Design code for structural elements design of reinforced concrete and prestressed concrete, Romanian Standardization Institute (in Romanian).

Ştefan, D., Covatariu, G. (2005), “The seismic force development related to Romanian designing codes”, *Revista Intersecţii*, 5(3), 57-66.

PLAN CONFIGURATION INFLUENCE ON VULNERABILITY OF REINFORCED CONCRETE FRAME STRUCTURES IN SEISMIC AREAS

IONUŢ OVIDIU TOMA, IOANA OLTEANU, ANA MARIA TOMA, MIHAI BUDESCU

"Gheorghe Asachi" Technical University of Iasi, Faculty of Civil Engineering and Building Services, No. 43rd, Prof. D. Mangeron Blvd., Iaşi, Romania, 700050, emails: iotoma@ce.tuiasi.ro, ioanaolteanu@ce.tuiasi.ro, anamtoma@ce.tuiasi.ro, mbudescu@tuiasi.ro

The evaluation of the expected physical damage, which quantifies the average loss of a particular structure starting from a seismic hazard scenario and the structural vulnerability, can be accomplished by using damage probability matrices, vulnerability functions, or fragility curves. The latter express the probability that an expected global damage d of a structure equals or exceeds a given damage state ds, as a function of a parameter quantifying the severity of the seismic action. The most recent trends in the evaluation of vulnerability for risk analysis operate with simplified mechanical models essentially based on the Capacity Spectrum Method. Vulnerability assessments of reinforced concrete frame structure were conducted especially on regular structures. However, modern architecture tends to introduce more and more asymmetric structures. In this paper a comparison between the behaviour of symmetric and asymmetric structures, from the lateral stiffness point of view, in case of an earthquake is made in terms of vulnerability.

Keywords: capacity curve, spatial RC frame structures, plan configuration, vulnerability assessment.

INTRODUCTION

Due to the increased public awareness to the effects of natural disasters, with particular focus on earthquakes, great emphasis is being placed on the role of disaster mitigation and vulnerability assessment in planning for sustainable development (Kappos et al., 2008; Erdik et al., 2011). Communities can use risk and vulnerability assessment results to reduce the impacts from hazards through the development or revision of emergency response, disaster recovery and hazard mitigation strategies (Faccioli, 2006). Evaluating the seismic vulnerability in a region is of critical importance in the field of structural engineering (Ansal et al., 2010).

Seismic vulnerability aims to quantitatively assess the extent of damage in a building for a given earthquake (Lee and Ko, 2007). Currently there are two main formulations for achieving this, namely the damage probability matrix and the vulnerability curves. The latter describes the probability of a structure to exceed a certain damage limit state in terms of a selected ground motion (Borzi et al., 2008).

Researchers all over the world proposed various analytical methods of assessment for the seismic vulnerability based on the non-linear time history analysis (Singhal and Kiremidjian, 1996; Massi, 2004). The method involves running many analyses of prototype structures for which structural characteristics were randomly varied subjected to a set of representative earthquakes. However, running nonlinear time history analyses for large sets of structures subjected to various seismic scenarios can become time consuming and computationally unfeasible. This led to the development of alternative methods.

The Capacity Spectrum Method of ATC-40 (ATC, 1996) is one alternative to the non-linear time history analysis. Due to its simplicity, the structural engineering profession quickly adopted the new nonlinear static procedure, also known as pushover analysis (ATC-40, 1996; FEMA-356, 2000). It is now generally recognized that when pushover analysis is carefully applied it is able to provide useful information that otherwise cannot be obtained by either linear static or dynamic analysis (Inel and Ozmen, 2006). Pushover analysis is carried out for either user-defined nonlinear hinge properties or default-hinge properties. Reports in the literature show that plastic hinge length and characteristics no influence on the base shear capacity but significantly influence the displacement capacity of the frames (Inel and Ozmen, 2006; Shakery et al., 2010).

In this paper a comparison between the behavior of symmetric and asymmetric structures, from the lateral stiffness point of view, in case of an earthquake is made in terms of vulnerability. The analysis procedure is based on the Capacity Spectrum Method.

NUMERICAL SIMULATIONS

The structures considered in this paper are 3D models of reinforced concrete frame structures with 3 and 6 storeys having a plan configuration of 3 bays by 3 spans, Figure 1, and 3 bays by 6 spans, Figure 2. The span was 6 meters and the storey height was 3 meters. The columns, the beams and the slabs were made of concrete class C20/25. The thickness of the slab was kept constant to 10 cm for all analysis cases.

The vulnerability of the considered structures was assessed by means of nonlinear static analysis, also known as pushover analysis as defined by FEMA-356. The pushover analysis considers a lateral horizontal load pattern applied to a structural model considering the material nonlinearity. The load is and monotonically increased until the collapse of the structure is reached.

The numerical simulations were conducted by means of SAP2000 computer program. The plastic hinges were defined according to Table 6-7 from FEMA 356 code for the beams and according to Table 6-8 from the same code for the columns (Inel and Ozmen, 2006).

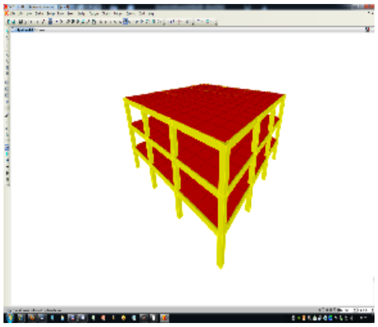

Figure 1. The 3 storey model

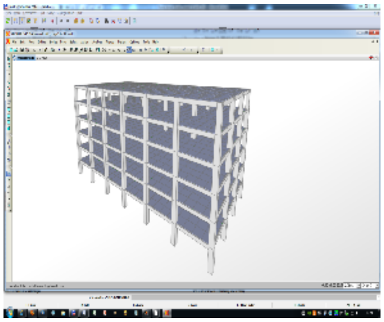

Figure 2. The 6 storey 3 bays by 6 spans model

The plastic hinges in case of beams depend solely on the effect of bending moments whereas in case of columns the combined effects of the axial force and biaxial bending are considered (Cedolin et al., 2008).

The obtained capacity curves from the pushover analysis were used to assess the damage state of each considered structure. The accelerogram for Vrancea earthquake from March 1977 was considered for the demand curve (URBAN-INCERC, 2012). The capacity curve was intersected with the demand curve considering the methodology from the equal displacement approximation presented in ATC-40 in order to obtain the performance point.

The second step of the procedure consisted in determining the vulnerability functions, also known as fragility curves, associated to each analysis case. They express the probability that an expected global damage *d* of a structure equals or exceeds a given damage state *ds*, as a function of a parameter quantifying the severity of the seismic action.

RESULTS AND DISCUSSIONS

The present paper presents some preliminary results on the influence of the plan configuration on the vulnerability of three-dimensional reinforced concrete frame structures located in seismic areas. For this purpose, nonlinear static analysis was conducted on four reinforced concrete frames designed according to Romanian codes. The considered analysis cases are shown in Table 1. The obtained results are discussed in terms of the influence of lateral stiffness, as a direct result of the plan configuration, on the vulnerability of the considered frame structures.

Table 1. Analysis cases and geometrical details

Analysis Case	No. of bays	No. of spans	No. of storeys	Slab thickness [cm]	Bay length [m]	Span length [m]	Storey height [m]
3s_3x3	3	3	3	10	6	6	3
3s_3x6		6					
6s_3x3		3	6				
6s_3x6		6					

Figure 3 presents the fragility curves for the 3s_3x3 analysis cases. The direction of the monotonically increasing load applied on the structure was considered along the bays, that is along the shorter side of the model.

As It can be seen from Figure 3, the plan configuration does not seem to influence the behaviour of the structure because the fragility curves for each corresponding damage state overlap with the sole exception of the *Collapse* state. In this latter case, the distribution of the lateral stiffness of the structure only slightly influence the outcome of the results leading to smaller values for the probability of *Collapse* given a value of the spectral displacement.

The fragility curves for the 6 storey structure, considering two plan configurations, are shown in figure 4. Contrary to the previously obtained results, the distribution of the lateral stiffness along the two horizontal orthogonal directions plays a significant role in the outcome of the results. The analysis case having 6 spans is stiffer, hence resulting in more restrictive safety conditions for a given value of the spectral displacement than in the case when the number of spans is equal to the number of bays. This observation is valid for *slight, moderate* and *severe* damage probability scenarios.

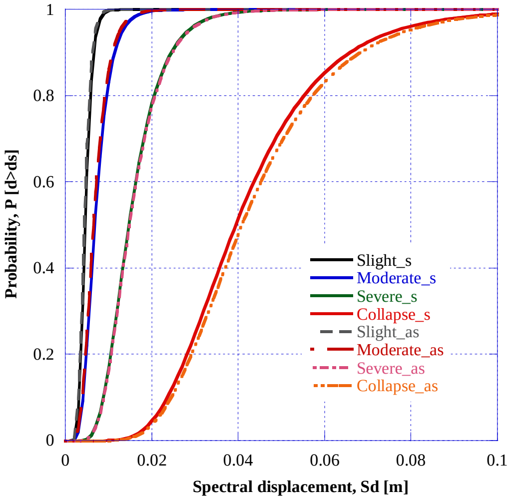

Figure 3. Fragility curves for the considered numerical models with 3 storey

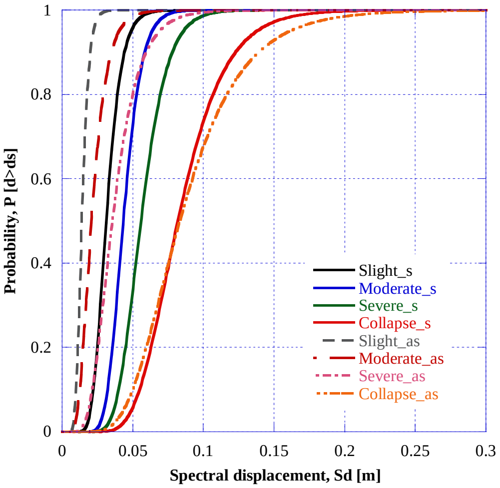

Figure 4. Fragility curves for the considered numerical models with 6 storey

The influence upon the shape of the fragility curve associated with the *Collapse* state is only minor, very similar to the previous observations.

From the analysis of the results shown in Figure 3 and Figure 4 it can be concluded that the taller structure allows for larger spectral displacements for every considered damage state. This is in agreement with the generally accepted structural design concept stating that taller structures are more flexible than low rise buildings allowing more earthquake energy to be dissipated through lateral displacement.

The observations are in agreement with the obtained results for the fundamental periods of vibrations for the 3 storey and 6 storey structures. The computed values were

0.2314 seconds for the 3s_3x3 analysis case and 0.3809 seconds for the 6s_3x6 case, respectively.

CONCLUSIONS

The present paper presents some preliminary results on the influence of the plan configuration on the vulnerability of three-dimensional reinforced concrete frame structures located in seismic areas. For this purpose, nonlinear static analysis was conducted on four reinforced concrete frames designed according to Romanian codes.

Based on the obtained results it can be concluded that the number of spans do not influence significantly the results, in contrast with the number of storeys. This is especially valid for the fragility curve associated with the *Collapse* state. For the *Slight*, *Moderate* and *Severe* damage probability scenarios the increased lateral stiffness results in more restrictive safety conditions for a given value of the spectral displacement.

On the other hand, it can be concluded that the taller a structure is, the larger the values of the spectral displacement are for every considered damaged state.

REFERENCES

Ansal, A., Kurtulus, A. and Tonuk, G. (2010), "Seismic microzonation and earthquake damage scenarios for urban areas", *Soil Dynamics and Earthquake Engineering*, 30(11), 1319-1328.

Applied Technology Council (1996), *Seismic evaluation and retrofit of concrete buildings*, vol. 1 and vol. 2, ATC-40, California, U.S.A.

Borzi, B., Pinho, R. and Crowley, H. (2008), "Simplified pushover-based vulnerability analysis for large-scale assessment of RC buildings", *Engineering Structures*, 30, 804-820.

Cedolin, L., Cusatis, G., Eccheli, S. and Roveda, M. (2008), "Capacity of rectangular cross-sections under biaxially eccentric loads", *ACI Structural Journal*, 105(2), 215-224.

Erdik, M., Şeşetian, K., Demircioglu, M.B., Hancilar, U. and Zulfikar, C. (2011), "Rapid earthquake loss assessment after damaging earthquakes", *Soil Dynamics and Earthquake Engineering*, 31(2), 247-266.

Faccioli, E. (2006), "Seismic Hazard Assessment for Derivation of Earthquake Scenarios in Risk-UE", *Bulletin of Earthquake Engineering*, 4, 341-364.

Federal Emergency Management Agency (2000), *Prestandard and commentary for seismic rehabilitation of buildings*, FEMA-356, Washington DC, U.S.A.

Inel, M. and Ozmen, H.B. (2006), "Effects of plastic hinge properties in nonlinear analysis of reinforced concrete buildings", *Engineering Structures*, 28, 1494-1502.

Kappos, A.J., Panagopoulos, G. and Penelis, G.G. (2008), "Development of a seismic damage and loss scenario for contemporary and historical buildings in Thessaloniki, Greece", *Soil Dynamics and Earthquake Engineering*, 28(10-11), 836-850.

Lee, H.-S. and Ko, D.-W. (2007), "Seismic response characteristics of high-rise RC wall buildings having different irregularities in lower stories", *Engineering Structures*, 29, 3149-3167.

Masi, A. (2004), "Seismic vulnerability assessment of gravity load designed RC frames", *Bulletin of Earthquake Engineering*, 1(3), 371-395.

National Research and Development Institute for Construction, Urbanism and Sustainable Territorial Development "Urban-Incerc", 2004, last accessed, May 2012, http://www.incerc2004.ro/accelerograme.htm

Shakery, K., Shayanfar, M. A. and Kabeyasawa, T. (2010), "A story shear-based adaptive pushover procedure for estimating seismic demands of buildings", *Engineering Structures*, 32, 174-183.

Singhal, A. and Kiremidjian, A.S. (1996), "Method for probabilistic evaluation of seismic structural damage", *ASCE Journal of Structural Engineering*, 122(12).

VII.

QUALITY MANAGEMENT AND COMPETITIVENESS

STATISTICAL ANALYSIS OF THE ABSORPTION OF STRUCTURAL FUNDS IN ROMANIA

MARGARETA FLORESCU[1], MERAL KAGITCI[1], GHEORGHE COARA[2]

[1] *The Bucharest Academy of Economic Studies, Bucharest, Romania, icefaceus@yahoo.com*

[2] *INCDTP - Division: Leather and Footwear Research Institute, 93 Ion Minulescu, Bucharest, Romania, icpi@icpi.ro*

Excellence and scientific basis of European dimensions, especially long-term research, are of major importance for dynamic knowledge-based economy. Absorptive capacity represents the degree to which a country is effectively and efficiently capable to spend the financial resources from the Structural Funds. It can analyze the absorptive capacity in terms of institutional-state system administered as European funds, through the beneficiaries through which addresses these funds, which has two distinct characteristics, namely absorption capacity of the supply side (of funds) and the absorption capacity of the demand side.

Keywords: structural funds, evolution, implementation, statistical analysis, econometric estimations

INTRODUCTION

Excellence and scientific basis of European dimensions, especially long-term research, are of major importance for dynamic knowledge-based economy. Create excellence poles around public research institutions tend to exert a powerful mobilizing effect of R & D investments in companies in the sector properly, including those which in other circumstances, would not invest in research and development. So the question is put R & D effectiveness in achieving public scientifically strong, competitive, which can benefit the companies in Europe.

The total transfers allocated to Romania under Cohesion Policy for 2007-2013 depend on the ongoing negotiations in Brussels on the new financial perspective. For the period 2010-2013, financial transfers to Romania will depend on the outcome of the EU. As a working hypothesis, if the financial package sums 2007-2009 (5.439 billion euros) in the guidance package proposed for 2010-2013 (12 560 million) to reach a total amount of transfers allocated of 17.999 billion euros.

The absorption capacity represents the degree to which a country is effectively and efficiently capable to spend the financial resources from the Structural Funds. If we consider that to do this is necessary, on the one hand the absorption capacity of the institutional system created by the State to manage the funds in case and, on the other hand, the absorption capacity of the beneficiaries to which are addressed these funds, we might consider it's that there are two distinct features, namely the absorption capacity of the supply side (of funds) and the absorption capacity of the from the inquiry side.The status of the absorption of structural funds and cohesion on the seven operational programs are registered with a degree of absorption of 14.13% in 2011. The figures absorption of these funds in 2011 is: absorption rate - 14.13%; pre-financing paid to beneficiaries - 6,792,009,361 lei; reimbursements paid to the beneficiaries - 5,394,958,047 lei; grant agreement number - 6923; number of projects approved - 8869.

ECONOMETRIC APPROACHES OF THE EUROPEAN UNION STRUCTURAL FUNDS ABSORPTION IN ROMANIA

Structural Funds are: an expression of solidarity between EU countries, a fundamental objective, is achieved by raising living standards and competitiveness between countries. They are oriented towards financial assistance to member countries with development and eliminate economic and social disparities between Member States. The literature is dealing with absorption problem from three perspectives. Thus absorption capacity, measured by how a state is able to use funds in an efficient, has three major implications namely macroeconomic absorption capacity, absorption capacity of financial and administrative capacity of absorption. The first, namely macroeconomic capacity is measured in terms of GDP, the upper limit of 4% of GDP. Financial capacity refers mainly to the ability of central and local authorities to co-finance projects and programs promoted by the EU as well as planning and budgeting to ensure multi-year contributions.

Mathematical Models to Quantify the Economic Impact of Structural and Cohesion Funds on the Economies

Given the crucial role that structural and cohesion funds have in the regional development promoted by the EU, has become indispensable to quantify their impact on the economies of "destination". An example is HERMIN model, used in many EU countries, which is based on quantitative estimation of the impact on the economies those funds. The model was used mainly for structural funds both for the ex-ante and ex-post model is one more sector and allows on the one hand assessment of the economic system as a whole and on the other propagation effects impact on the sector funds to which they were targeted. HERMIN model captures both macroeconomic relationships and links that are generated by the first and very important impact at regional level. The mechanisms underlying the Hermin model is the Keynesian conventional model still has the neo-classical features, which are in fact associated with the sub omponent of aggregate demand. (John Bradley, Edgar Morgenröthe, Gerhard Untiedt, "Macro evaluation of the structural funds regional using the modeling framework HERMIN").The type HERMIN is focused on key economic characteristics of the economies of the EU periphery, characteristics that relate mainly to:

-opening the country's economic and international trade exposure and internal and external shocks;

-relative measures and characteristics of goods sectors "tradable" and "non-tradable" and research and production technology and changes structural;

-mechanisms for determining wages and prices;

-degree of flexibility of labor market functioning under the influences of labor migration in international and inter-regional context;

-the role of public sector and government debt and the interactions between public and private sectors in terms of policy implementation.

The HERMIN Model Adapted at the Romanian Economy: HEROM Model

The impact assessment of EU financial instruments in order to achieve the economic and structural cohesion design of Romania has led to a design of a model HERMIN adapted to the Romanian economy, namely HEROM model. In order to achieve economic convergence, the model has certain advantages HEROM are perfectly tailored to our economy. Such a structure model based on transition economies, the type of economy to which our country's domestic macroeconomic framework aims. It is also based on the sectors of an economy, something that leads to better highlight the sectorial changes and the interactions between sectors. This model has been used by some Romanian specialists, to assess both quantitative and qualitative impact of structural funds on the Romanian economy, considering as a starting point two basic scenarios, namely: economic growth without structural and structural funds. Evaluation results revealed that the case scenario for the existence of structural funds growth is 2 percentage points higher than in scenario based on their absence, indicating the course of events and restrictions that could affect these projections. Considering the analysis period as 2007-2020, GDP in 2020 would reach 25% or higher scenario includes funds are of course notable growth during the injection of funds, 2007-2013.

The model was then extended to analyze the impact of structural funds on exports and imports made by our country during the analyzed period, based on the two scenarios considered.Having regarded to that, the trade balance is determined ultimately by external economic relations, the exports were noticed significant differences in terms of Hermin Model are the two scenarios (Figure 2), which can only be a good thing for the growth experienced by our country.

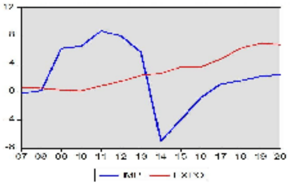

Figure 2. The evolution of the impact of structural funds calculated as the difference between the values of the two scenarios; Data source: www.eurostat.eu, author’s calculations

Also, an aspect worth mentioning is the impact on the two sectors, that of tradable goods (T) and the non-marketable assets (N), here resulting in a notable contribution in the T benefits whose output was estimated to increase approximately 38% in 14 years to 25% of the N output associated budget deficit will be considerably higher during the injection of funds, followed by a moderate decrease until the end of the analysis (Table 1).

Table 1. The scenario with funds and the scenario without funds. The percentage difference values for the two scenarios (Source: Report INSSE2009 http://www.fonduri-ue.ro/)

Years	PIB (expense method)	PIB (method based on the costs factors)	Budget deficit
2007	5.36	5.88	10.58
2008	5.30	5.70	15.01
2009	7.15	7.61	19.85
2010	9.02	9.58	15.50
2011	9.78	10.29	18.73
2012	10.45	10.99	22.59
2013	17.70	18.98	24.73
2014	16.66	17.65	-9.74
2015	15.21	16.01	55.21
2016	16.62	17.75	-13.84
2017	16.86	18.10	-7.21
2018	17.14	18.48	-4.32
2019	19.31	21.03	-5.00
2020	24.02	25.39	-7.12

Of course there are limitations and drawbacks here, such as those who started hypothesis of the existence of two scenarios, "funds" and "no money" and the absorption rate of 100% in the first scenario. Studies show that professionals in countries that have experienced various funds injected absorption rates over time and thus consideration of scenarios with different absorption rates for 2007-2013 would have been a more appropriate and effective. The impact analysis of social assistance provided by the EU on imports and exports in case of different absorption rates in the two scenarios mentioned above are summarized in Tables 2 and 3 and the following diagrams in Figure 3.

Table 2. Negative Scenario (Source: http://www.ipe.ro/rjef)

	Absorption Rate (%)	Imports (%)	Exports (%)
2008	30	1.86	0.15
2009	40	2.47	0.12
2010	45	2.92	0.07
2011	60	5.20	0.52
2012	70	5.55	1.22
2013	80	4.53	1.87

Table 3. Positive Scenario (Source: http://www.ipe.ro/rjef)

	Absorption Rate (%)	Imports (%)	Exports (%)
2008	35	2.17	0.18
2009	48	2.96	0.14
2010	59	3.83	0.09
2011	79	6.84	0.69
2012	89	7.06	1.56
2013	95	5.38	2.22

But further integration of the economies not only helps in its growth, but has beneficial effects on other EU member states. Also, economic growth in emerging economies over the last 5 years has contributed about 0.2-0.4% in economic growth in EU countries with traditions. The econometric estimation of the impact of EU integration has on economic growth data were used for the period 1996-2007 on a sample of 106 developed countries and developing and following regression equation:

Creşterea PIB_real/locuitor = 11,14 - 1.43PIB_real/locuitor_initial - 7.03rata_de_viaţă +
(2.95)** (4.51)*** (-3.89)***
+ 0.12Investiţii/PIB + 0.02acces_învăţământ_superior -
(3.89)*** (1.78)*
- 0.014rată_inflaţie + 0.62indice_libertate_economică_1995 +
(-2.32)** (3.01)**
+ 0.85modificare:indice_libertate_economică_1995-2005 +
(3.98)***
+ 0.98variabilă_dummy_NMS + 0.67variabilă_dummy_Africa
(1.82)* (1.69)*

where *, **, *** represent statistical significance levels of 10, 5 and 1%, t statistic is shown in parentheses.

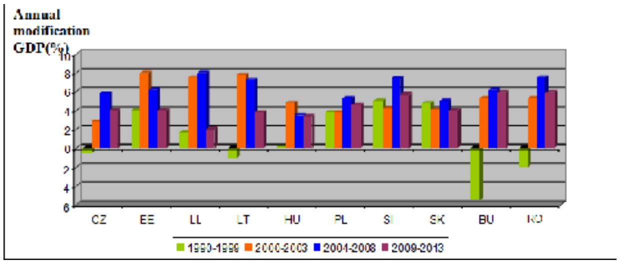

Figure 3. Growth before and after the access of EU countries; Source: IMF World Economic Outlook, September 2011

Basically we can conclude that economic and financial integration has brought with it accentuated economic growth and rhythms, some new states already having GDP / capita higher than in countries with tradition in the EU. From the perspective of the complexity analysis, the model HEROM describes much better the dynamics of the Romanian economy to similar patterns of growth. Pre-accession funds (PHARE, SAPARD, ISPA) has been granted to Romania through a program started before 2000 and were continued until 2009. The degree of absorption of EU pre-accession funds is 67.88%, much higher than the absorption of structural funds. The only problem you might encounter in Romania in the pre-accession funds could be represented by the need to return the amounts entered on the basis of completed projects on time. Because the model requires a large data set, we still considered a simplified version of the model to capture the funds from the EU influence on macroeconomic and specific industries on GDP and FBC. The data used in the model have the stages for the period 2000-2010.

For the econometric model building we chose the exogenous variable (to represent the value of EU funds as proxy variable) PHARE pre-accession funds and made the difference from the previous period to capture the dynamics of variable. Among the pre-accession funds to Romania these have meant 45% of the total pre-granted in 2007 and 2008, in addition, areas of intervention covering several levels of the Romanian economy. As endogenous variable we chose GDP variation (DPIBV) and FBC (DFONDURI_STRUCTURALE) have resulted as two regressions which highlights the extent to which structural funds variation causes variations in GDP / FBC. Amount of funds received in 2007 totals and a share of projects completed in 2006. Previous contracts regressions; we conducted tests that capture the Granger causality between the variables:

Sample:2000-2009
Lags:2

Null Hypothesis	Observations	F-Statistic	Probability
DFONDURI_PHARE does not Granger Cause	7	3.11272	0.24315
DFBC does not Granger Cause DFONDURI_PHARE		1.93899	0.34025

According to the test, with a probability of 34% is wrong if the null hypothesis is rejected. Supports the null hypothesis that there is a causal relationship between the variation of PHARE funds and variation FBC funds. In conclusion, we reject the null hypothesis with a confidence level of 64%, meaning we can say that with a probability of 54% variation PHARE funds directly influence changes in GDP:

Sample:2000-2009
Lags:2

Null Hypothesis	Observations	F-Statistic	Probability
DFONDURI_PHARE does not Granger Cause	7	3.13879	0.22529
DFBC does not Granger Cause DFONDURI_PHARE		0.89864	0.54388

In the case of the relationship between changes in GDP and changes in PHARE funds, alternative hypothesis is accepted with probability 77%, i.e. 77% chance that there are direct causal relationship between two variables appear. From the economic point of view it can be argued that structural funds outside GDP / FBC are influenced by a number of other factors.

According to the statistical output (regression) is more strongly influenced DPIBV DFBC variation than the structural funds, but the difference shown by the coefficient of determination (R^2) for the two models is within 1% (Table 4).

Table 4. DPIBV DFBC variation

Tests	DFBC-DFONDURI_PHARE	DPIBV-DFONDURI_PHARE
T-student	3,140551	3,185251
R²	0,584891	0,591737
F-statistic	9,863057	10,14582
Durbin-Watson	2.502	2.018

Explicitly, the two regressions can be written as:

$$DFBC = 1.31\ (E-05) - 0.5 \cdot DFONDURI\_PHARE + 1771.6$$

$$DPIBV = 13.31\ (E-05) - 0.5 \cdot DFONDURI\_PHARE + 9594.907$$

Analysis of estimation results show a number of weaknesses of the model, including: reduced number of observations; proxy variable describes selected with a probability of 45% pre-development funds; there is the possibility of differences between European funds and changing the time of granting GDP; absorption remains low compared with other Member States; crime problem with European funds and their return necessities, Romania is the first place from this point of view, seeing is required to return some money.

In conclusion, the influence of European funds on the level of GDP and FBC is rather weak, although the economic situation of Romania (liquidity shortages) more competitive with projects to attract external funds.

CONCLUSIONS

From what has been presented we have the following results:

- Like the pre-accession funds (SAPARD, PHARE, ISPA), structural funds are a form of grant, which are operational in Romania since 2007. These funds are allocated to various projects through development programs containing specific measure by directions of development and be eligible for this funding.
- Romania benefits from structural funding of about 28-30 billion euros from EU in 2007-2013.
- According to the 2007-2013 financial perspective agreed at the European Council in December 2005, Member States whose average GDP per capita in 2001-2003 was below 40% of the EU-25 will receive transfers from the Structural and Cohesion Funds of up to 3, 8% of national GDP.
- There are several directions that will be used in structural and cohesion funds in 2007-2013 so that funding would generate economic and social development: infrastructure, economic competitiveness, human capital development, public administration, development planning.
- Structural and cohesion funds will strengthen the Romanian business environment.

REFERENCES

Guston, D. (2001), “The Expanding Role of Peer Review processes in the United States“, *Public Research, Inovation and Technology Policies in U.S.*, 4-31.

Jasanoff, S. (1990), *The Fifth Branch: Science Advisers as Policy Makers*, Harvard University Press.

Lütkepohl, H. and Kratzig, M. (2004), *Applied Time Series Econometrics (Themes in Modern Econometrics)*, Cambridge University Press.

Weller, A.C. (2001), *Editorial peer review: its strength and weaknesses*, ASIST monograph series, Medford.

***, http:// www.ec.europa.eu/research/enquiries

*** (2002), Treaty on European Union, OJ C 325/24.12.2002, available at http://eur-lex.europa.eu/ro/treaties/index.htm, accessed on September 8, 2009.

*** (2006), Decision no. 1982/2006/CE du Parlement Européen et du Conseil du 18 décembre 2006 relative au septičme programme-cadre de la Communauté européenne pour des actions de recherche, de développement technologique et de démonstration (2007-2013).

BUILDING INFORMATION MODELING FROM THE PERSPECTIVE OF A CONTRACTOR

TOMAS FUNTIK

Slovak University of Technology in Bratislava, Faculty of Civil Engineering, Department of Building Technology, Radlinskeho 11, Bratislava, tomas.funtik@stuba.sk

In today's world of constant progress and development of technology over time, market conditions are changing significantly. We are observing constant pressure to improve quality and reduce prices not only in construction. These challenges can be achieved with innovative approaches, improved systems, and last but not least, the use of latest technology and software. Within the planning and preparation of construction works the progress is represented by information model (BIM - Building Information Model or Modeling) whereby we are able to meet the challenges and expectations of investors. This approach completely changed view of the existing methods used and practices of construction firms in the segment. Conception contributes to more effective and systematic work, excluding the amount of error, respectively reduces discrepancies prior to execution phase. The current authors and experts in this area suggest the need to use BIM as an effective tool of managed information throughout the life cycle of a building. As shown in various case studies, use of BIM can achieve savings of up to 10% off the cost. The paper focuses on the study of this approach and to learn the basic principles for subsequent application to structural and technological practices.

Keywords: building information model, pre-construction planning, project management.

INTRODUCTION

Construction of buildings and structures requires more precise planning for its successful execution. With the ever increasing demands for quality, safety, environmental protection, and also the increasing cost of inputs such as labor, building materials and mechanisms, the need for more thorough preparation for the effective, smooth and safe construction is growing.

These conditions are constantly forcing engineers in the field of AEC no only to improve existing technologies and methods in construction, but also put higher attention and focus to planning. Virtual model of a building or a building information model is a solution that allows managing simple or complex projects, but in principle it is a tool for more efficient construction.

CONSTRUCTION PLANNING

Preparation of construction may vary from the perspective of an investor, contractor, architect, as each pursues other interests. For purposes of this paper I will focus mainly on the preparation in terms of the contractor.

Planning of a construction is critical and very challenging activity in the field of management and construction projects. Before the construction we consider different options and we can influence the course or even the overall result of the project. Planning involves the selection of technology, definition of tasks, estimating of resources required and duration of each task as well as any interaction between them. A good plan is essential for well established budget and schedule.

Term planning can encompass a wide range of activities. For the purpose of this work we would understand it as developing of a technological, qualitative, time and cost parameters of the project which is subject to conditions and restrictions the project is executed in.

The planning processes are linked to the intention of the project, and thus to the purpose, strategy and objectives we want to achieve. We express the intention of the project by defining individual activities that determine the project structure (WBS - Work Breakdown Structure) and specifications of work (SOW - statement of work) and also organized structure of the project (OBS - Organization Breakdown Structure).

It is necessary to define the project on the timeline. Planning of schedule includes:

- defining activities,
- determine the logical links,
- estimate the duration of activities (deterministic, stochastic),
- create a schedule (determining slacks and critical path).

The planning process also determines resource needs during the project. In particular, there is the need for labor, materials and finances. This process is integral part of scheduling. Within developing the plan we can focus on cost control or monitoring construction progress.

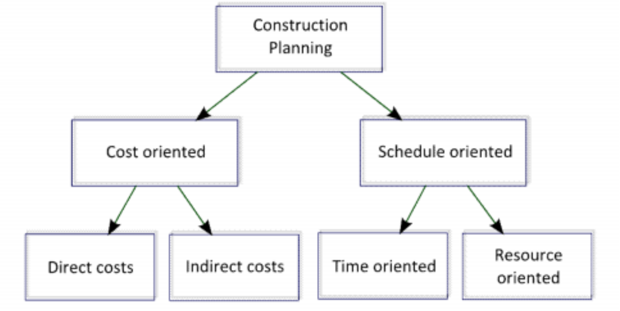

Figure 1. Planning of a Construction (Hendrickson, 2008)

Some projects are primarily broken down by category of costs. Such plans are called price or cost-oriented. The cost categories are allocated to direct and indirect costs.

In other cases we consider the criticality of the duration of each task, and those are subject to emphasize for planning. This ensures either to retain in correct order with adequate links (time-based plan) or effectiveness of planning according to available resources over time (resource-based plan).

Quality planning has a major impact on the overall cost of the work. We can make decisions at various stages of the life cycle that can mean not only savings, but also overcharge of the project. Extent of influence shows the Figure 2. It therefore follows that the more advanced stage, the less opportunity to influence the cost. In these phases is however focused the most of the cost.

Therefore it is necessary to begin with precise planning in the early stages of project life cycle and there must be not only investors, developers and architects involved but also other participants such contractors, facility managers and so on. The need for communication and exchange, collection, adding and updating of information not only support suitability but the necessity of using information models.

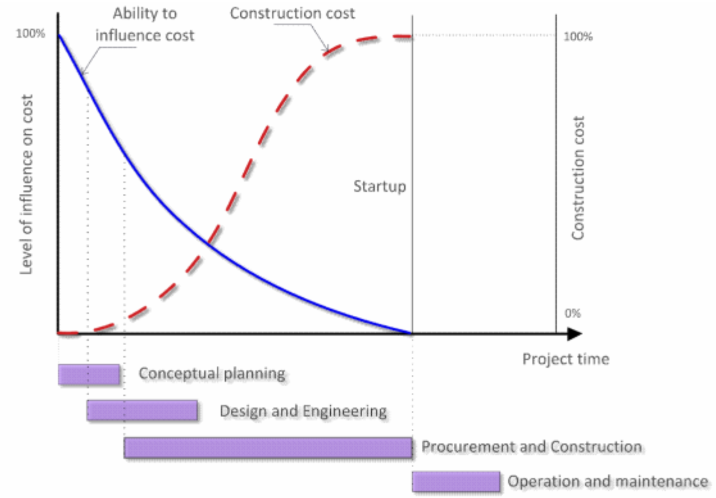

Figure 2. Effect of planning in various stages of the project cost (Hendrickson, 2008)

BUILDING INFORMATION MODELING

At present, very often occurs term “BIM” in the construction industry. While abroad it has already found his indispensable place and no bigger project can be done without it, we are still waiting for its application in our region.

BIM at its basic precondition counts with cooperation among different stakeholders at different stages in its life cycle. It is necessary to enable them with proper cooperation links to enter, exclusion, modification or update the information in the BIM which reflect the roles of each stakeholder.

As widely known, BIM must use parametric modeling. In general, parametric tools are best for creating highly sophisticated and complex products in an industry that is heavily regulated by standards. The opposite method is explicit form of modeling.

Advantages of Using BIM

“Managing building information using a building information model can lead to substantial cost savings, from design and construction through to maintenance.” (Smith M., 2011).

It is proved that the model saves time mostly by better coordination of information and early detection of potential irregularities or clashes. This reduces the number of necessary site control and coordination is easier. Significant advantage of BIM comparing to current methods using numbers of layouts is to coordinate information, thereby avoiding unnecessary delays and errors.

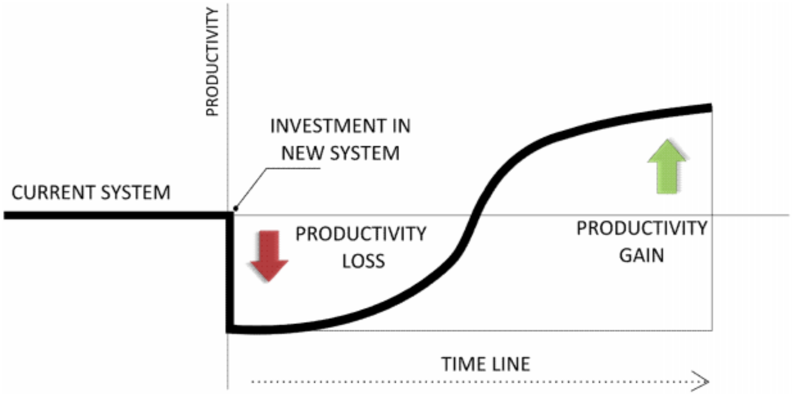

Figure 3. BIM productivity curve (Chadwick, 2011)

During the process of implementation of BIM due to introduction of innovations we may observe temporary reduction of the productivity. This decrease is caused by the transition to new technologies, which require considerable investment. Reduced productivity also affects the ability of interested workers to adapt to new conditions and user interface.

Over time, when the learning phase is completed, we can expect rapid increase of productivity, which reached a level that could never be achieved without BIM.

In the BIM system all of construction process participants build up a team together from the very first stages of design and they exchange the necessary information. It is essential that all changes are automatically coordinated throughout the project life cycle. The result is therefore a high quality project.

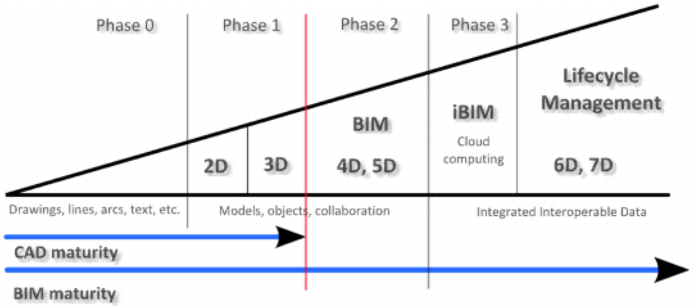

Figure 4. BIM and CAD maturity (Chadwick, 2011)

When comparing the capacity of programs or systems, we find that BIM system is much more complex and mature. While CAD systems end up with their options for 3D imaging, BIM allows xD planning.

Software Solutions for Contractors

There are many systems widely used on the market suitable for contractors planning of a construction. I will mention three of them for purpose of this paper along with short description. They vary in some functions but the key features are similar.

Vico Office Suite

This software solution consist of 3D, 4D and 5D modules allowing create visualization, clash detection, quantity takeoff, scheduling, production control and finally the estimating. Scheduling system is location-based, not CPM (critical path method). Within the program you are using databases, not a collection of files so you can easily create a new field to track your interest.

Office allows import of Revit, ArchiCAD and Tekla models and other also allowing exchange through IFC (Industry Foundation Classes).

Synchro

With this software you can easily prepare visualization of construction progress including project scheduling and advanced risk management. Other tool is synchronization with design changes and supply chain management with cost allocation. You can consider many alternatives for various schedule scenario or different resource allocations which helps you evaluate possible time and cost savings.

Synchro integrates well through the import of over 30 CAD file types including the DWF, DWG, SKP, DGN, file types. In all cases the 3D import and synchronization of updated 3D files is keyed off the Object Name and it's CAD system assigned GUID.

Synchro alone will meet or exceed your project BIM for Delivery requirements for CPM scheduling, EVA from the cost loaded schedule, and ability to read the 3D model data.

Autodesk Navisworks Manage

Autodesk declare it is a comprehensive review solution for analysis, simulation, and coordination of project information. Multidisciplinary design data can be combined into a single integrated project model for interference management and clash detection. It is build to automatically detect clashes and interferences and it will allow you to open current clash in original software application.

Navisworks allows interoperability with ArchiCAD, Primavera, MS Project and many other.

Benefits of BIM for Contractors

Contractors are according to official reports least involved in the BIM. But the success of a project is depending also on them or using other words if any of stakeholders fail to participate on BIM the very important idea becomes unfulfilled. According to the SmartMarket Report published by McGraw-Hill Construction in 2011 the big difference is mainly in the adoption of BIM by contractors, which is slightly better in North America with 50% share over 24% in Western Europe.

Advantages are obvious and contractors definitely may benefit by using the potential of BIM. Among other it allows them to enable the use of sophisticated networking tools that connect different software. Their outcomes are integrated within the model.

By better visualization of a project they have an opportunity to use it for marketing presentation of construction progress. Having the complete model of a future building allows analyzing simulated situations and identifying conflicts that may occur during the construction. By reducing the errors fewer corrections are to be done.

Using a virtual model we may integrate many environmental aspects and optimize resources before the construction phase of a project. This all lead to improved coordination of construction progress and hence significant savings of financial resources.

CONCLUSION

Based on the analysis of the current condition of the problem it is possible to evaluate the potential benefits of BIM. In order to integration and smooth information transmission in the life cycle of a building BIM adoption is essential also by contractors. Without functional interconnection and information exchange from participants in the process of construction in the early project stages, we can use all their efforts just as expensive visualization. If the contractor does not have suitable software capabilities and trained staff who are willing to go with the times and be innovative, they should not apply for more complex projects, as they would not be able to handle it under current market conditions. They can not compete with BIM adopters in terms of quality and resource management as they lead to significant savings (either time or cost). However, it is interesting to observe that despite the undeniable benefits that BIM systems offer so far they are not widely used in this region.

REFERENCES

Chadwick, M.W. (2011), “Cost of not using BIM”, Polytechnic Institute of NYU, http://www.marcharch.com/files/Cost_of_Not_Using_BIM.pdf

Eastman, Ch. (2009), *BIM Handbook*, John Wiley & Sons, Inc., ISBN 978-0-470-18528-5.

Hendrickson, Ch., (2008), *Project Management for Construction*, Edition 2.2, ISBN 0-13-731266-0.

McGraw-Hill Construction (2011), SmartMarket Report.

Smith, D.K., Tardif, M. (2009), *Building Information Modeling, A Strategic Implementation Guide*, John Wiley & Sons, Inc. New Jersey, ISBN 978-0-470-25003-7.

Smith, M. (2011), “BIM in construction”, http://www.thenbs.com/topics/BIM/articles/bimInConstruction.asp.

Stockings, W.H. (2002), *The Process Of Construction Planning*, University of Eindhoven, ISBN 90-6814-131-7.

Vlček, K. (1998), *Stavebnotechnologická príprava stavieb*, Jaga Group, Bratislava, ISBN 80-88905-00-1.

***, http://bim.construction.com/research/FreeReport/BIM_Europe/

***, www.synchroltd.com

***, www.vicosoftware.com

***, www.autodesk.com

ARTISTIC TECHNOLOGIES FOR DEVELOPMENT OF CULTURAL LEATHER PRODUCT

MARLENA POP

INCDTP - Division: Leather and Footwear Research Institute, 93 Ion Minulescu, Bucharest, Romania, email: pop_marlen@yahoo.ca

The foray into structures of artistic image in environmental decorative arts aims, on the one hand, at the comparative analysis of artistic discourse in three different registers of expression: the decorative and the plastic register, and on the other hand, it aims to identify the icono-plastic sign as carrier of the archetypal message, in two distinctive types of logos: poetic and narrative. The third register of expression is the material one, defined by artistic technologies. Aesthetic interpretation stays in the area of deciphering the artistic message, mostly symbolic, while semiotic analysis aims to decipher the inner mechanisms of the image, and the artistic imagination, defining icono-plastic signs. Undertaking the materialization of the work, throughout the whole trajectory of achieving the decorative cultural product, is called artistic technology. It is a creative technology at the conceptual level, but framed within technical steps to achieving the environmental decorative product, which are very clearly defined as technological operations. Coming out of the major area of aesthetics and subjected to semiotic analysis, the artistic image transgresses, in theory, from a harmonic matrix of analysis, specific to aesthetics, into an expressive matrix, specific to discourse analysis, visual rhetoric. The whole approach, as well as the result of semiotic analysis of a decorative art project idea, will lead, step by step, to outlining an artistic technology, which becomes itself part of the cultural product symbolics, a technological style thus emerging. Artistic technology analyzed in terms of semiotics, which is the subject of the case study for the “Red apple” project is leather embroidery, industrially manufactured. The purpose of the whole scientific endeavor is to shape the guidelines of a framework artistic technology to further develop a number of artistic products with cultural identity, for modern domestic environmental spaces: private homes with determined environmental design or public spaces: institutions, libraries, airports etc.

Keywords: artistic technology, cultural leather product, semiotic analysis, environmental design.

INTRODUCTION

Out of a relative aesthetic taxonomy, textile arts are by definition decorative arts, using a variety of artistic techniques and technologies. Artistic technology is that set of technical steps that lead to achieving a decorative environmental cultural product, made of various materials, specific to textile arts. By means of the case study presented in the paper, the project “Red Apple” is proposed as semiotic analysis of the plastic discourse which will lead to a new approach to artistic leather technologies. Traditional techniques of hand embroidery on leather, specific to fur craft, were adapted to mechanical sewing technologies that achieve many decorative or plastic effects on the compositional surface of an artistic material such as leather. Artistic technologies require integration of plastic materials, in this case leather, in the cultural concept of the decorative product, because the technology itself has plastic value in the compositional framework developed. Thus, the technical elements such as stitch type, its density, assembling components, substrate, framing, carry the semiotics of the same artistic concept, which transmits a single message.

THEORETICAL-EXPLANATORY AND METHODOLOGICAL GUIDELINES

A macrosemiotic analysis involves discovering the work through its specific analysis, offering the receiver the possibility to make his own interpretation, by means of three levels of understanding. These levels of understanding can be assimilated differently, depending on the repertoire of the receiver, but parameters required for an accurate and complete reception must already exist in the decorative work.

1. The pre-iconographic level of analysis refers to elements through which the public perceives the work at a first reading: classification of compositional objects, surface aspects of texture, shape and color, the relationship between the viewer and the work;
2. The iconographic level deals with understanding iconic signs and relationships between them, and therefore the message of the work, which is given by all the elements of the artistic language: texture, shape and color, which produce a direction of communication.

Texture

- Material (linen, cotton, silk, hemp, sisal, wool, microfiber, technical textiles, waste, etc.);
- Dyes and pigments (classes of pigments: mineral, natural, organic, metallic);
- Personal technique or artistic technology (manual techniques or industrial technologies for weaving, printing, embroidery, knitting, sewing etc.).

Shape

Expression of shape in textile arts is done both two-dimensionally and three-dimensionally, using various techniques, ranging from haute-lisse to textile sculpture or installation or, on the contrary, textile miniature. The signifiers of shape are the same as for painting, sculpture or graphics.

The “position” parameter is analyzed according to the background and the center of the compositional image, i.e. the center of interest, corresponding to the semantic axis.

The “size” parameter is defined according to the scale of the viewer and the background size. At the one-dimensional level, the basic /large/-/small/ opposition becomes /long/-/short/ and at three-dimensional level, there is the /voluminous/-/non-voluminous/ pair. Size is also based on perspective. The signified of size is called “dominance”.

The “orientation” parameter is defined as a virtual movement in the background on a path whose model can be established. This movement can be /centripetal/ or /centrifugal/. But whether it is centripetal or centrifugal, it may seem to be oriented /vertically/ (i.e. /ascending/ or /descending/) or /horizontally/, /right/ or /left/. The signified of orientation is balance, which can be defined depending on two variables: “potentiality of movement” and “stability”.

Colour

At the level of expression, colour can be defined by three variables: the dominant color, brightness and saturation. Chromatics may acquire meaning also by reference to an iconic sign: thus, red can be interpreted by its similarity with blood, blue by its similarity with the sky etc., depending on the cultural symbolism the author and the viewer belong to.

The plastic sign is a synthesis of all three forms of expression: texture, shape, colour, and its meaning, rather vague and imprecise, emerges only in context of the image; each element becomes significant depending on the one next to it and their particular relationships lead to what is known, at value level, as originality, personal style, manner.

3. The iconological level - the viewer aesthetically recreates the artwork and restores the creative path, projecting onto the artwork the whole range of ideas that have supposedly led to its creation.

The viewer has a great freedom in reading in the case of the plastic sign, but equally, also requires a plastic culture, i.e. a more elaborate repertoire for it. There is a hierarchy of reading systems that, far from being mutually exclusive, can be used together: the visual artwork can be read like a text, integrating it into a cultural architext, but it can also be read by knowing the specific code used in its making. Even if the iconological method looks especially towards the aesthetic value of artworks, while semiotics examines how visual language is signified, they are not mutually exclusive, but complementary.

CASE STUDY, RESULTS AND DISCUSSIONS

Figure 1. Concept of a decorative leather cultural product

The demonstrational case study, presented below, outlines the stages of a concept of a decorative leather cultural product, for environmental space (Figure 1).

Recent ethnographic research, also presented in Roman Ethnographic Atlas, coordinated by Ion Ghinoiu, impose the idea that the "tree of life" in Romanian ancestral culture is neither the fir tree, taken 200 years ago from German culture and used in various holiday rituals, nor the oak, present as a heraldic symbol in some medieval coats of arms, but the red apple tree. Not the royal yellow apple tree, neither the green apple, but the wild red apple present in Romanian culture for thousands of years. Its very millennial presence in this area before the invasions of Celts and Pelasgians, in whose cultures it represents Axis Mundi, translated in our language as the "sky axle", as well as the symbolism developed on the iconic structure of Neolithic testimonies found in ceramics, in the Gumelnita culture, have led the authors of the Atlas to argue that the iconic sign of the tree of life is the "red apple tree". This iconic sign appearing as "tree of life" in most Moldovan Orthodox frescoes and Oltenia rugs has a positive connotation of direction in life and not a negative one, as spread by Christianity.

In the case study, regarding "Red Apple Tree" project development, archetypal symbol of the apple can be identified both as carrier of artwork message, of the artist's intentionality and by the very material structure and project technology.

The Structure of the "Red Apple Tree" Project

The artist's intentionality - transfer of a cultural message, regarding one of the Romanian archetypal symbols, the tree of life, defined by the "red apple tree" - is expressed by:

- Typology of the artwork: two-dimensional embroidery on leather, made with industrial equipment, although the technique specific to Romanian fur and leather crafts is manual;
- Texture: structures of various types of leathers in terms of animal origin, assortment, technological processing and colour finishing, on flax textile substrate and wooden support;
- Shape: relatively rectangular, of 120x105 cm, two-dimensional;
- Composition enclosed with decorative framing and a center of interest in the common perception of the viewer. The figurative archetypal symbol is included in this hub of dynamic axes of the composition as a figurative symbol - the red apple tree. The frame is divided into several descriptive registers that include icono-symbolic Romanian signs. Only in the horizontal register there is an archetypal symbol of time, the Greek infinite motif, today a motif of globalized culture.
- Th colour palette has earthy tones, with accents of red and blue.
- The central, dominant icono-symbolic sign of the red apple tree is shown decoratively; the whole work is easy to read, following the narrative path of the composition. It is surrounded by many archetypal icono-plastic signs for the Romanian culture: the snake, the cross, the spiral, the ladder, the egg, the zig-zag.

The semantic triad texture - shape - color communicates the circumscription of the artwork into a cultural identity only by means of the icono-symbolic signs expressed by motifs and by the narrative logos. This type of artwork requires a more specialized repertoire of the viewer.

The semiotic hypothesis, which is confirmed through the case study, implies that the level of expression is not opposed to, but correlated with the content of the artistic image. Creating plastic meaning does not take place only between isolated elements, such as the iconic sign bearing a symbol and the plastic one which is an expression of the semiotic code, but also between two types of levels, compositional, spatial or temporal. The efficiency of similar effects derives from dimensional density or homogeneity of parts. This principle of reading an artistic work is a semi-symbolic one. The iconic sign is, by definition, a carrier of message of the artwork, and it is demonstrated that the archetypal symbol is embedded in it, transposed through the artistic technology used.

CONCLUSIONS

The semiotic analysis of the artistic project demonstrated that:

- the visual language of an artistic work includes a cultural archetype in its semiotic structure, whether it is conveyed by the artist's intention of the plastic message;
- plastic expression is not opposed to, but correlated with the content of the artistic image;
- creating plastic meaning does not take place only between isolated, icono-plastic elements, but also between two types of levels, compositional, spatial or temporal;
- the archetypal imagery of the artist is found in his work both through the topic, subject, message and through the rhetorical peculiarities of the plastic discourse;
- the plastic rhetoric, as a decorative style used in artwork development, as a cultural product, is also transferred to the artistic technology used, in this case, industrial leather embroidery;
- the artistic technology used in cultural product development is an intrinsic part of it, for which a technological style can be developed.

REFERENCES

Barthes, R. (1964), “Rhetorique de l’image”, in Communications, n. 4.

Boldureanu, I.I. (2006), *Traditional Oral Culture: Themes, Concepts, Categories* (in Romanian), Marineasa, Timişoara.

Durand, G. (1977), *Anthropological Structures of the Imaginary* (in Romanian), Univers, Bucharest.

Evseev, I. (1994), *Dictionary of Cultural Symbols and Archetypes* (in Romanian), Amarcord, Timisoara.

Francastel, P. (1992), *Figurative Reality* (in Romanian), Meridiane, Bucharest.

Ghinoiu, I. (2008), *Romanian Pantheon* (in Romanian), Romanian Academy Press, Bucharest.

Gombrich, E.H. (1986), *Art and Illusion* (in Romanian), Meridiane, Bucharest.

Pop, M. (2012), “Cultural Archetypes and Patterns in Contemporary Romanian Textile Arts”, in International Conference on Arts & Society, III, *The International Journal of Arts Theory and History*, Birmingham Institute of Art and Design, Birmingham, UK.

Vranceanu, A. (2002), *Literary Models in Visual Narration* (in Romanian), Cavaliotti, Bucharest.

MANAGEMENT METHODOLOGY FOR RESEARCH AND DEVELOPMENT PROJECTS

MARIUS SIMION

National Research & Development Institute for Industrial Ecology, 71-73 Drumul Podu Dambovitei, district 6, Bucharest, email: ecoind@incdecoind.ro

In 1989 the Central Computer and Telecommunications Agency (CCTA), an United Kingdom government agency, developed a structured method for effective project management called PRINCE (PRojects IN Controlled Environments). PRINCE was originally based on PROMPT (a PM method created by Simpact Systems Ltd. in 1975) and in 1989 effectively substituted PROMPT within Government projects. CCTA continued to develop this method, and in 1996 PRINCE2 was launched. PRINCE2 is extensively used by the United Kingdom government and now is a de facto standard widely recognised for all projects not for information projects only. Any research and development project could be guided by the PRINCE2 principles. The paper offers a way to adapt and adjust PRINCE2 to a pre-established project methodology of an authority which finances projects such as Executive Unit for Financing Higher Education, Research, Development and Innovation (UEFISCDI). PRINCE2 was tailored to suit the UEFISCDI methodology and was designed an adapted process model diagram. The goal of paper is not to substitute PRINCE2 processes and templates with those of a default methodology but only according them. Applying PRINCE2 methodology for any research project is a guarantee that the project could be kept under control in terms of time, cost and quality.

Keywords: project management methodology, PRINCE2, process model diagram.

INTRODUCTION

The word project comes from the Latin verb “proicere” which means “something to put forwards”. The word project thus actually originally meant “something that comes before anything else happens”. A definition for project is: unique effort that includes risk, with a clearly defined start date and finish date, made towards achieving the targets established, respecting certain parameters related to cost, time and quality.

In agreement with PRINCE2 a project is a temporary organization that is created for the purpose of delivering one or more business products according to an agreed Business Case (The Stationery Office, 2009).

The Project Management (PM) is a fairly common activity, which many of us do it. Most times we cannot realize that. Instinctively. Project management has been practiced since early civilization. Great Pyramids, the Great Wall of China, monumental cathedrals are just a few examples of projects. But also daily and usually things such as travels and vacations. From the begining the civil projects complexity rised a number of problems. Until 1900 the management of civil engineering projects was done by architects and engineers. Frederick Taylor (1856-1915), for the first time considered the design activity in the work processes. His contribution represents foundations of modern tools of PM such as WBS (Work Breakdown Structure) and resource allocation. As a discipline, Project Management was developed from several fields of application including civil construction, engineering and military operations planning, with contributions of Henry Gantt (1861-1919) in planning and control techniques, and Henri Fayol (1841-1925) with his theory on the five functions of management. Both were students of Taylor. Their work forms the basis of knowledge of project and program management. Before 1950, most of the projects were managed using only Gantt charts and informal techniques and tools. The 1950s marked the beginning of the modern PM era. Many techniques have been assembled into a single coherent system of PM. During this period two mathematical models were developed the project planning: CPM (Critical Path Method) and PERT (Program Evaluation and Review Technique).

According with PRINCE2 the Project management is planning, delegating, monitoring and controling of all aspects of the project, and the motivation of those involved, to achieve the project objectives within the expected performance targets for time, cost, quality, scope, benefits and risks (The Stationery Office, 2009).

Project Management is the PDCA (Plan-Do-Check-Act) of all aspects of the project.

Planning *(**P**lan)*
↓
Delegating *(**D**o)*
↓
Monitoring *(**C**heck)*
↓
Controlling *(**A**ct)*

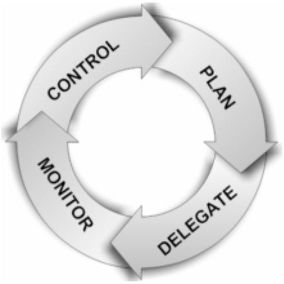

Figure 1. Project Management according to PRINCE2

PROJECT MANAGEMENT METHODOLOGY

The Need for a Methodology

Project management is just common sense (Bentley, 2002). Of course it is. So why many of us do it wrong? A good planning and control not mean automatically a happy ending for the project. Anticipation of an unpredictable event and a risk response plan does not guarantee achieving the project objectives.

An answer might be that most of us doesn’t learn from our mistakes. We not use our gained experience to improve the model, do not assemble the techniques and methods of PM in a functional mechanism as a whole. Or we do not have a holistic view of the project.

PRINCE (PRojects IN Controlled Environments) is a structured project management method for effective project management. This method is based on experience from thousands of projects and from contributions of many project managers, teams and project sponsors, academics, trainers and consultants. This method was established by the Central Computer and Telecommunications Agency (CCTA) which was an United Kingdom government agency and initially used for information system projects. PRINCE was originally based on PROMPT (a project management method created by Simpact Systems Ltd. in 1975) and in 1989 effectively substituted PROMPT within Government projects. The Office of Government Commerce (the former CCTA) continued to develop the method, and in 1996 PRINCE2 was launched. PRINCE2 is extensively used by the United Kingdom government, and now is a de facto standard widely recognised for all projects not just for information system projects.

The main feature of the PRINCE2 methodology is that It is scalable and flexible so it can be tailored to the project environment. A key approach of the method is that it clearly distinguishes the process management and techniques involved in the process itself.

There are many proven techniques for planning and controling used to support PRINCE2. Examples are Critical Path Method (CPM) in the planning process and Earned Value Management (EVM) in the progress control.

However PRINCE2 develops own techniques such as Product-based Planning (PBP) or Quality Review Techniques (QRT).

PRINCE2 Principles

The purpose of PRINCE2 is to provide a project management method that can be applied regardless of project scale, type, organization, geography or culture. This is possible because PRINCE2 is principles-based. The seven PRINCE2 principles are:

1. Continued business justification
2. Learn from experience
3. Defined roles and responsibilities
4. Manage by stages
5. Manage by exception
6. Focus on products
7. Tailor to suit the project environment.

PRINCE2 Structure

There are three parts to the structure of the method itself (Figure 2):

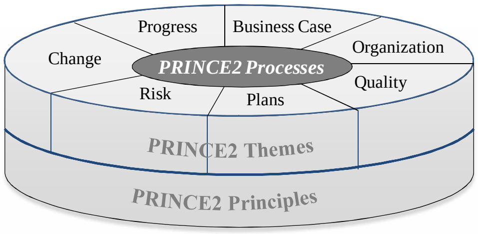

Figure 2. The structure of PRINCE2

- Techniques (Product-based planning and Quality review techniques)
- Themes (Business Case, Organization, Quality, Plans, Risk, Change, Progress)
- Processes. PRINCE2 is a process-based approach for project management. There are seven processes in PRINCE2 (Figure 3):
    1. Starting Up a Project (SU)
    2. Directing a Project (DP)
    3. Initiating a Project (IP)
    4. Controlling a Stage (CS)
    5. Managing Product Delivery (MP)
    6. Managing a Stage Boundary (SB)
    7. Closing a Project (CP)

Each management process is a structured set of activities designed to accomplish a specific objective. It takes one or more defined inputs and turns them into defined outputs.

National Authority for Scientific Research (UEFISCDI) is the specialized authority of central public administration subordinated to the Ministry of Education, Research, Youth and Sport, which performed its duties in research field. This authority is a public institution, funded by the state. Financing is achieved by launching competitions of research projects.

RESULTS AND DISCUSSION

The aim of the paper consists in adapting and adjusting PRINCE2 to a pre-established project methodology of an authority which finances projects such as Executive Unit for Financing Higher Education, Research, Development and Innovation (UEFISCDI).

PRINCE2 was tailored to suit that methodology and designed the adapted process model diagram (Figure 3).

The purpose is not substitution of PRINCE2 processes and products with those of a default methodology but only according them (Simion, 2011).

Pre-project

Project Mandate is equated with the call for open competition for research projects. UEFISCDI transmits the Information package, Guide for applicants and Annexes. These documents represents the methodology of UEFISCDI for a program competition.

In Starting Up a Project process the project manager (PM) writes a Project Brief (an outline Business Case, a plan, product descriptions, quality, estimates resources, costs, time, risks and tolerances) and fills in Form B (technical paper).

Initiation of the Project

In Initiation stage the Project Board (Direction level) decides if the outline Business Case of the project is desirable, viable and achievable, and therefore worthwhile investing in. The Direction makes retouches and aproves the Project Initiation Documentation (PID).

In this stage this documentation for application is written:

- Accompanying documents (Partners collaboration agreement, Project plan and other documents),
- Forms and UEFISCDI templates (Forms A1, A2, B and C).

Initiation Notification is similar to Proposal Submission of documentation to UEFISCDI on written support and online. The Authority evaluates the project proposal and gives the acceptance or not for financing or rejects it. The acceptance ends with a contract signing that means the project is authorized.

Stage Execution

From the point of Authorize Project forward the project enters into the PRINCE2 mechanism of stage controling, product delivery and managing the stage boundary as we see in Figure 3.

There is a cyclical sequence of processes finishing with outputs, products which correspond with initially established acceptance criteria. Many times during this stage project manager sends Highlight Reports or an Exception Report to the Board and requests for advice. These could be followed by request for an exception plan, request for UEFISCDI consultation or an ad-hoc direction given by the Board. It's possible that any overrun of cost, time which cannot be solved in limits of tolerances of project to be proposed for viewing by UEFISCDI for a contract addendum. Tolerance is the permissible deviation from a plan without bringing the deviation to the attention of the next higher authority.

The control of project is achieved through control elements anchored in different moments of time. The purpose of control is to ensure that the proiect remains viable against its Business Case and produces the required products which meet the defined quality criteria. Controls ensure that, for each level of the proiect management team, the next level up of management can monitor progress, compare achievement with plan, review plans and options against future situations, detect problems and identify risks, initiate corective action and authorise further work.

A stage is ending with an Internal approval meeting recorded in an Internal Approval Minutes and delivering documentation to UEFISCDI.

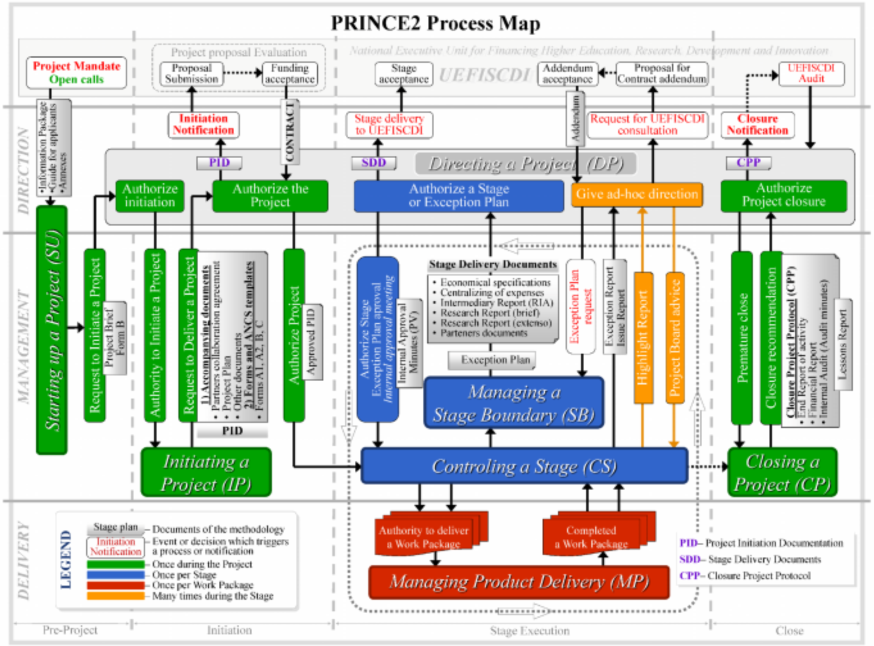

Figure 3. Process Model Diagram

Closing the Project

The purpose of the Closing a Project process is to provide a fixed point at which acceptance for the product is confirmed and to recognize that objectives set out in the original PID have been achieved.

As a result of project closing the Board authorizes the closure through a Protocol consisting of an End Report of activity, Financial Report and Internal Audit.

CONCLUSIONS

Applying PRINCE2 methodology for any research and development project is a guarantee that the project could be kept under control in terms of time, cost and quality.

PRINCE2 Advantages

- It is scalable and flexible so it can be tailored and adjusted to the project environment.
- It is now generally accepted as PM Standard in European area.
- Product-based orientation will clarify what the project will offer, why, when, by whom and for whom.
- Divide the project into stages easy managed and controlled.
- It has well-defined organizational structure for project management team.
- It is focused on economical justification (Business Case) and implementation of the control should be made relatively to the original purpose and economical parameters established.
- It is a tool for diagnosing, facilitating, ensuring and assessing work done in the project, solving problems and for auditing.
- Promotes learning and continuous improvement in organizations.
- Can be integrated into the organization's Management Quality System.

PRINCE2 Disadvantages

- Writing and maintaining PRINCE2 documents, registries and reports implies a relatively large work volume.
- Managemnent Component of Configuration in earlier versions than 2009, although these versions can be applied in many project fields, they show a clear tendency for use in IT projects. The PRINCE2 2009 version has placed this component in the background, solving this issue.

REFERENCES

Bentley, C. (2002), *PRINCE2, a practical handbook*, Butterworth-Heinemann, Oxford, Great Britain.

Nicolescu, O., Verboncu, I. (2008), *Management Methodologies* (in Romanian), University Press, Bucharest, Romania.

Simion, M. (2011), “Product-oriented management methodology for research and development projects”, Master's thesis, ASE, Faculty of Cybernetics, Statistics and Economic Informatics, Computerized project management Master.

The Stationery Office on behalf of the Office of Government Commerce (2009), *Managing Successful Projects with PRINCE2*, London, Great Britain.

THE QUALITY – A FACTOR FOR COMPETITIVENESS OF ORGANIZATIONS

NICOLETA SPOREA, MARIANA-FLORENTINA ŞTEFĂNESCU, ION DURBACĂ

University POLITEHNICA of Bucharest, nsporea@yahoo.com, marianastefanescu2007@yahoo.com, ion.durbaca@yahoo.com

The quality of products and services is an important element of a strategy of each organization. The intention of the authors is to indicate the possibilities for improving competitiveness, primarily through implementation of Six Sigma concept.

Keywords: competitiveness, quality, Six Sigma

INTRODUCTION

The quality has become a strategic tool of the global organization management, and an important element of competitiveness. It also represents an essential factor for the civil society and environment.

Quality can be interpreted and explained in different ways. However, the fact is that the starting point for the definition of this term is collection of data about customers' demands, since they are crucial arbiters of quality assessment. If we have in mind the results of numerous studies, according to which quality means perfection, consistency, elimination of defects, and/or reduction of losses due to the elimination of defects, delivery speed, compatibility with standards, reliability, etc., it can be said that quality should be viewed in a broader sense, or not only as the quality of products and processes, but also as a quality business (Soin, 1992; Kaplan & Norton, 2001; Brue, 2002).

Competitiveness of a organization depends on its ability to innovate and develop. Some organization get some advantages over the larger competitors in the world because of the pressures and challenges that are subject. They won because of the existence of strong rivals at home, some aggressive vendors and local customers hard to keep.

The relationship quality - competitiveness is determined for any business because we notice that the needs of clients have been varied. Today is no longer enough to satisfy the consumers' needs, but must get the maximum results by exploiting their inclinations for the novelty of product. The quality increase must turn, therefore, in the growth of competitiveness.

If the quality management is observed in its evolutionary way, one can identify four approaches to quality management:

- approach based on the product – the quality will be provided if the characteristics or attributes of products have been identified; according to those characteristics and attributes, presence of quality is ascertain; this approach assumes quality control;
- approach based on manufacturing – the quality will be provided if the product has all characteristics predicted by the engineers specifications; this approach corresponds to total quality control;
- approach based on the product users - the quality will be provided if it fully meets the demands of customers or if it is "suitable for use"; this approach assumes total quality management;

- approach based on values - the quality will be provided if the product meets customers' needs, and also has an acceptable price, or if the variability of the process in which the product is produced is controlled at an acceptable level of costs; this approach corresponds to Six Sigma quality management.

FACTORS AND INDEXES OF COMPETITIVENESS

Competitiveness of an organization is shown in its capacities and market expansion which is carried out e.g. through increased production of up-to-date high quality products.

Competitiveness is a feature of an organization connected with the environment in which the company operates.

M. Stankiewicz defines competitiveness as the ability of an organization to efficiently pursue its market aims; this ability can be implemented owing to the knowledge how to create a favorable image of an organization and how to use technological and organizational innovations.

Competitiveness implies elements of productivity, efficiency and profitability. But it is not an end in itself or a target. It is a powerful means to achieve rising living standards and increasing social welfare, - a tool for achieving targets.

A few dimensions of competitiveness can be identified, and they are (Chase, et al., 2004):

- Quality ("make it good"),
- Delivery speed ("make it fast"),
- Delivery reliability ("deliver when promised"),
- Volume flexibility ("change its volume"),
- Innovativeness ("change it").

These factors of competitiveness can be classified into three dimensions: costs (in terms of product price), quality and reliability (in terms of product functionality and continuous fulfillment of customers' requirements), time and flexibility (in the sense that the product is always available to customers and that is always delivered on time, or that new products and processes are introduced in time). According to Skinner (Rao et al., 1996), the dimensions of competitiveness are in the trade-off relationship, because it is not possible to simultaneously achieve high quality, low costs and on-time delivery of products.

The Global Competitiveness Report is published yearly by the World Economic Forum. World Economic Forum measures competitiveness of national economies through Business Competitiveness Index (BCI), Growth Competitiveness Index (GCI), and Global Competitiveness Index. Business Competitiveness Index has been introduced by Michael Porter, in 2000. This index is based on microeconomics variables. Growth Competitiveness Index was introduced by Sachs and McArthur, in 2001. It is based on a stronger academic fountain in economic growth theory. The index that was last mentioned is the latest compared to the previous two. Therefore it is logic to expect that it includes both macroeconomic and microeconomic factors of competitiveness.

Since 2005, the World Economic Forum has based its competitiveness analysis on the Global Competitiveness Index, which measures the set of institutions, policies, and factors that set the sustainable current and medium-term levels of economic prosperity. This index is calculated as a weighted average of many different components, each measuring a different aspect of competitiveness and ranking on the scale from 1 to 7.

These components are grouped into 12 pillars of economic competitiveness: institutions, infrastructure, macroeconomic environment, health and primary education, higher education and training, goods market efficiency, labour market efficiency, financial market development, technological readiness, market size, business sophistication and innovation (Schwab, 2010). Scores for these components in Romania are given in the Figure 1.

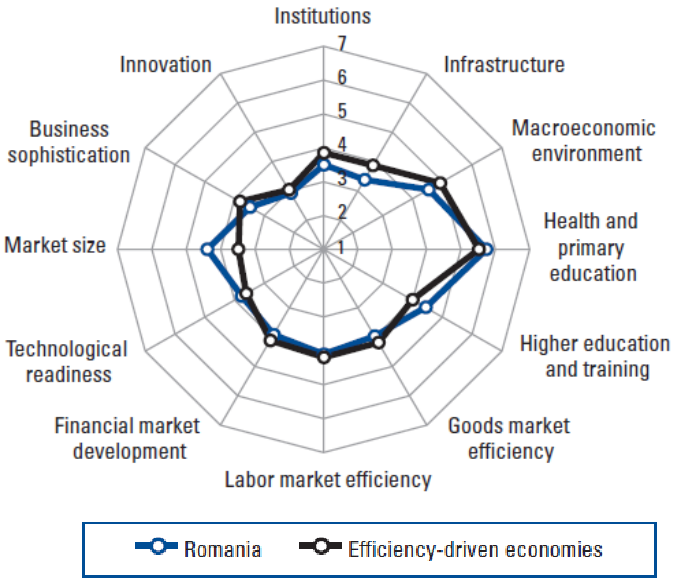

Figure 1. Scores of 12 pillars for Romania

The 12 pillars mentioned in Figure 1 are not independent variables. The variables are related to each other and tend to reinforce each other. For example the variable innovation contained by the 12th pillar would not be possible without good educated and trained labor force so 5th pillar (Porter Michael E., Schwab Klaus 2008). Results of Global Competitiveness Index for Romania are given in Table 1.

Global Competitiveness Index score is 4.1, which is quite low compared to the country which is leader (Switzerland with GCI score of 5.7), but still not so bad.

The Report on Business from 2010 (World Bank survey) and Global Competitiveness Report for 2011-2012, unfortunately show the same fact – deterioration of Romanian economy competitiveness. Romanian's competitiveness has decreased from 67 (in 2010) to 77 (in 2011). These facts must be a warning for creators of Romanian economic policy and the basis for improvement of conditions for doing business in Romania.

Table 1. Rank and GCI value

ROMANIA	2011-2012		2010-2011		Change	
	Rank	Score	Rank	Score	Rank	Score
Global Competitiveness Index	77	4.1	67	4.2	-10	-2.3%
Institution	99	3.5	81	3.7	-18	-5.4%
Infrastructure	95	3.4	92	3.4	-3	0%
Macroeconomic environment	87	4.5	78	4.5	-9	0%
Health and primary education	66	5.7	63	5.8	-3	-1.7%
Higher education and training	55	4.4	54	4.5	-1	-2.2%
Goods market efficiency	96	4.0	76	4.1	-20	-2.4%
Labor market efficiency	92	4.1	76	4.3	-16	-4.6%
Financial market development	84	3.9	81	4.0	-3	-2.5%
Technological readiness	60	3.8	58	3.8	-2	0%
Market size	44	4.4	43	4.4	-1	0%
Business sophistication	102	3.5	93	3.5	-9	0%
Innovation	95	2.9	87	2.9	-8	0%

THE SIX SIGMA CONCEPT

Six Sigma is a revolutionary business process geared toward dramatically reducing organizational inefficiencies that translates into bottom-line profitability. It started in the 1980s at Motorola (Smith, L. 2001); then, organizations such as General Electric, Allied Signal, and Seagate worked with the initiative during the 1990s and made it the most successful business initiative of the era.

Six Sigma is not a statistical tool that is used for decades, but the business concept for improvement of the business quality. The Six Sigma concept involves a continuous process improvement, incremental improvement or “kaizen” (Japanese term for continuous improvement), where the improvement process is directed towards correcting of the existing processes, focusing on key factors that determine the results of the process.

The concept of Six Sigma is to eliminate defects. Six sigma is the goal, but it’s less important than the objective of pursuing continuing process improvement. Sometimes the Six Sigma implementation team needs to set more realistic goals, depending on customer requirements and expectations and the complexity of the product or service. Smart managers know that the six sigma quality level is an idea; what’s real is the focus on identifying defects and eliminating their root causes.

Key to the Six Sigma methodology of the 1990s is a five-step process—Define, Measure, Analyze, Improve, and Control (DMAIC). By systematically applying these steps (with the appropriate tools), practitioners of this approach have been able to save substantial costs. The first phase of this process is the define phase and it includes defining customers' requirements, key process for their fulfillment and performance standards. After defining, the next phase is measure, in which managers have to establish a system of measures and to evaluate the performance of key processes and activities. Information obtained by measurement become subject of analysis, the phase during which managers have to identify potential areas for improvement. Implementation of the improvement must be evaluated and controlled, so therefore the control represents the last phase of the DMAIC process.

The path from the initiative for the establishment of the Six Sigma concept, till the appearance of effects of the implementation is not easy, but is recommended if the organization wants to provide or increase competitive advantage (Figure 2).

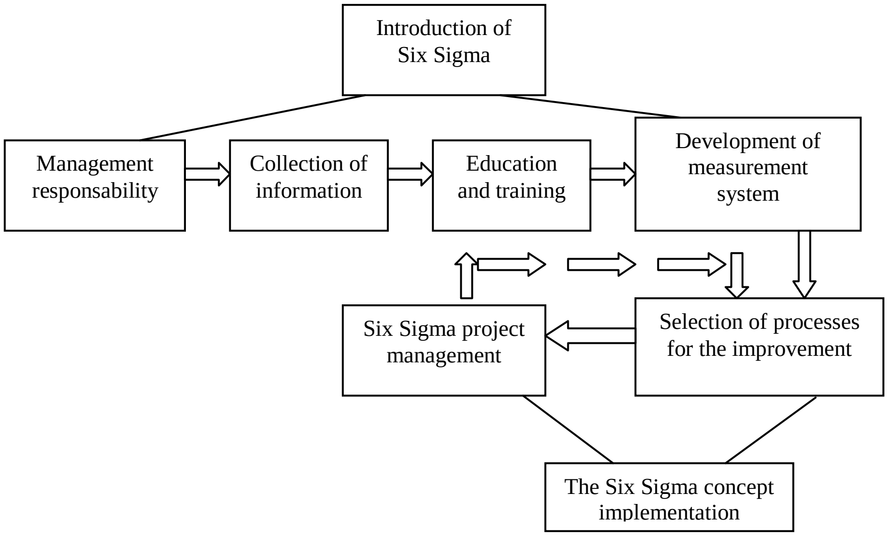

Figure 2. The Six Sigma concept: from the initiative to implementation

To implement this concept successfully, the continuous collection of information, stablishing a system of measurement, as well as education and training of employees is necessary. Such "behaviour" of the organization is an important condition for achieving competitive advantage in the new economy.

The Six Sigma concept is based on Deming's idea of "striving for continuous improvement" and Taguchi's view according to which "any deviation from the target value causes an increase in costs". The pursuit of the Six Sigma concept is to reduce variation, because decrease of variation causes increase of productivity, measured either as the amount of output per unit of input, or as the amount of output per unit of time, and therefore it is recommended for organization with purpose of competitiveness improvement.

CONCLUSIONS

Based on the results of the research conducted in 2010 and 2011 years, in Romanian organization, when the quality and the quality improvement are factors of competitiveness, it can be said that there is negative tendency, but not enough dramatically.

The usage of tools and instruments that contribute to discovering the opportunities for quality improvement is not sufficient. The introduction of modern concepts and methods for quality management is characteristic for higher management levels.

The Six Sigma concept should help managers in resolving the paradox that assumes providing the shortterm financial results through improvement projects, and, at the same time, development capacity for the future, through investment in human capital and key processes.

REFERENCES

Brue, G. (2002), *Six Sigma for Managers*, McGraw-Hill, New York.

Chase, R., Jacobs, R., Aquilano, N. (2004), *Operations Management for Competitive Adventage*, McGraw Hill, Irwin.

Kaplan, R.S., Norton, D.P. (2001), *The Strategy Focused Organization: How Balanced Scorecard Enterprises Thrive in the New Business Environment*, Harvard Business School Press, Boston.

Porter, M.E., Schwab, K. (2008) ,"The Global Competitiveness Report 2008-2009", World Economic Forum SRO-Kundig, Geneva.

Rao, A., Carr, P., Dambolena, I., Kopp, J. (1996), *Total Quality Management: A Cross Functional Perspective*, John Wiley & Sons, New York.

Schwab, K. (2010), "The Global Competitiveness Report 2010–2011", World Economic Forum, SRO-Kundig, Geneva.

Smith, L. (2001), "Six Sigma and the Evolution of Quality in Product Development". *Six Sigma Forum Magazine*, 28-35.

Soin, S.S. (1992), *Total Quality Essentials: Using Quality Tools and Systems to Improve and Manage Your Business*, McGraw-Hill, New York.

Stankiewicz, M.J. (2002), The competitiveness of the company: building the competitiveness of enterprises in conditions of globalization, TNOiK Home Organizer, Torun.

AVOIDING EMERGING RISKS BY USING THE ENGINEERING DESIGN

MARIANA-FLORENTINA ŞTEFĂNESCU, ION DURBACĂ, NICOLETA SPOREA
University POLITEHNICA of Bucharest, marianastefanescu2007@yahoo.com, ion.durbaca@yahoo.com, nsporea@yahoo.com

In process industries there are specific risks, such as current and emerging. The first category includes environmental and technical risks, and the second category includes biological hazards, chemical and psycho-social risks. The 6th Environmental Action Programme has appealed for a Thematic Strategy for Urban Environment with the objective to "contribute to a better quality of life through an integrated approach to urban areas" and help " a higher level of quality of life and social welfare of citizens by providing an environment that generates no pollution level effects on human health and the environment and encouraging sustainable urban development". In this respect, the paper presents a calculation example of stack height dispersion of an energy-energy power plant of 500 MW for avoiding emergent risk of polluted air from the building site of the plant.

Keywords: emergent risk, polluted air, engineering design.

INTRODUCTION

As our society evolves under the influence of the new technologies and under the changing economical and social conditions, as well as employment, working practices and processes of the organizations in process industries are constantly changing. These new situations involve emerging risks and new challenges which, in turn, require specific policy, administrative and technical approach ensuring a high level of safety and health at work.

To reduce risks to their health emerging for workers, in the industrial units which have large combustion plants, and for unemployed persons in the immediate vicinity caused by the increasing air pollution, it is necessary to take effective measures aimed at technical contribute to improving the environmental quality and thus human health and safety factors.

Further is an example of calculation of the height of the cart polluting emissions dispersion into the atmosphere, as recommended by EU environmental legislation on air quality, which, through the integrated environmental documents, establishes the conditions for removal from the flue gas emissions. In this respect, the competent authority responsible for environmental protection establishes the stack height so that environment and health are protected.

CALCULATION OF THE DISPERSION OF THE CART HEIGHT

This paper presents a calculation example for height of the chimney dispersion in a lignite thermal power installation of 500 MW, a trader in the process industries, establishing the assessment area, such as to lead to maintain air quality, according to European environmental reference documents (guidelines and recommendations, BAT etc.).

Data Base

Data base is presented in the Table 1.

Table 1. Values for data base

Data base	Values
Thermal power (PT)	500 MW
Calorific value (PC_i)	18 MJ / kg brown coal
Specific volume of waste gas for coal	5 Nm³ / kg brown coal
Reference oxygen	6%
Diameter of the chimney outlet (d_i)	3 m
Waste gas temperature (t_g)	70°C
Thermal power plant cart height available	100 m

Emission Limit Values

Emission limit values are presented in the table below.

Table 2. Emission limit values

Emissions	Mean daily values [mg / Nm ³]	95% of all hourly average values [mg / Nm ³]
Dust	30	60
SO_2	200	400
O_x	200	400

Calculating the Height of the Chimney Dispersion

Calculating the height of the chimney dispersion is achieved in the following steps:

Step 1: waste gas flow calculation, R [Nm ³ / h] issued (after removing the water content of water vapor in the normal state):

- Maximum fuel consumption:

500 mW / 18 MWS / kg = 27.8 kg / s = 100 t / h waste gas flow emitted (at 0% oxygen): 5 m³ / kg x 100,000 kg / h = 500,000 Nm ³ / h; (1)

- Tail gas flow rate (6% oxygen):

500,000 m³ / h x 21 / (21-6) = 700,000 Nm ³ / h (2)

Step 2: calculation of emission mass flow, Q [kg / h] for:

- Dust:

Q = 700,000 Nm ³ / hx 60 mg / Nm ³ = 42 kg / h (3)

- SO_2:

Q = 700,000 Nm ³ / hx 400 mg / Nm ³ = 280 kg / h (4)

- NO_2:

Q = 700,000 Nm ³ / hx 400 mg / Nm ³ (x) x 0.64 *) = 180 kg / h (5)

Note:

- Transformation factor of NO_x in NO_2 is 0.64.
- For combustion of solid coal (lignite), the percentage of NO_2 in the NO_x emissions (in the waste gas) is about 10%. The rest (90%) is emitted as NO, (approx. 60% of NO resulted will be oxidized, turning into NO_2).

It is calculated as follows:

- mass concentrations of NO_2 in the exhaust gas immediately after firing, the limit value CNOx = 400 mg / Nm ³ (calculated as NO_2), is determined as follows:

$CNO_{2,\ combustion}$ = 400 mg/Nm^3 x 0.1 = 40 mg / Nm ³; (6)

- mass concentrations of NO_2 by oxidation of NO to NO_2 waste gas route:

CNO_2 (by NO oxidation) = (400 mg / Nm ³ - 40 mg / Nm ³) * 0.6 = 216 mg / Nm ³ (7)

- Determining the transformation factor f from NOx to NO_2:

$CNO_{2, total}$ = 40 mg / Nm ³ + 216 mg / Nm ³ = 256 mg / Nm ³; (8)

f = 256 mg/Nm^3 / 400 mg / Nm ³ = 0.64. (9)

Step 3: Calculation of the ratio Q / S

There is a key factor in determining specific pollutant dispersion stack height and this is noted S. According to German Engineers Union Directive (2002) Annex 7, S factor values are shown in Table 3.

Table 3. S factor values for different kind of emissions

dust	SOx	NO_2	HCl	HF	CO
0.08	0.14	0.1	0.1	0.0018	7.5

In these conditions the following values result:

- for Q / S - powder:

42 kg / h / 0.08 = 525 kg / h (10)

- for Q / S - SO_2:

280 kg / h / 0.14 = 2000 kg / h (11)

- for Q / S - NO_2:

180 kg / h / 0.1 = 1800 kg / h (12)

Relevant is the largest coefficient Q / S, and in this case it results for SO_2: Q / S = 2000 kg / h.

Step 4: Determination of the height of the chimney dispersion from diagram*).

Data needed are presented in the Table 4:

Table 4. Values for data needed

Data needed	Values
Diameter of the basket of dispersion (the outlet), d	3 m
Waste gas temperature, t	70°C
Flow waste gas, dry, R	700,000 Nm^3 / h

Using the diagram presented in Figure 1 the dispersion stack height (H ') results about 55 m.

*) Diagram translates gases dispersion in graphic format in Figure 1.

If there is vegetation compact or compact construction which occupies more than 5% of the evaluated area, then the dispersion stack height (H ') must be increased by an additional amount (J).

Step 5: Considering building / vegetation

Where, compact construction, existing or under a plan approved construction, compact or vegetation have more than 5% of the land assessed, then dispersion stack height (H ') be increased by an additional amount (J). The J [m] will cause the diagram in Figure 2, where we noted: H [m] - built chimney dispersion height (H = H '+ J); J [m] - the average height of existing or approved compact construction or compact vegetation from existing plane.

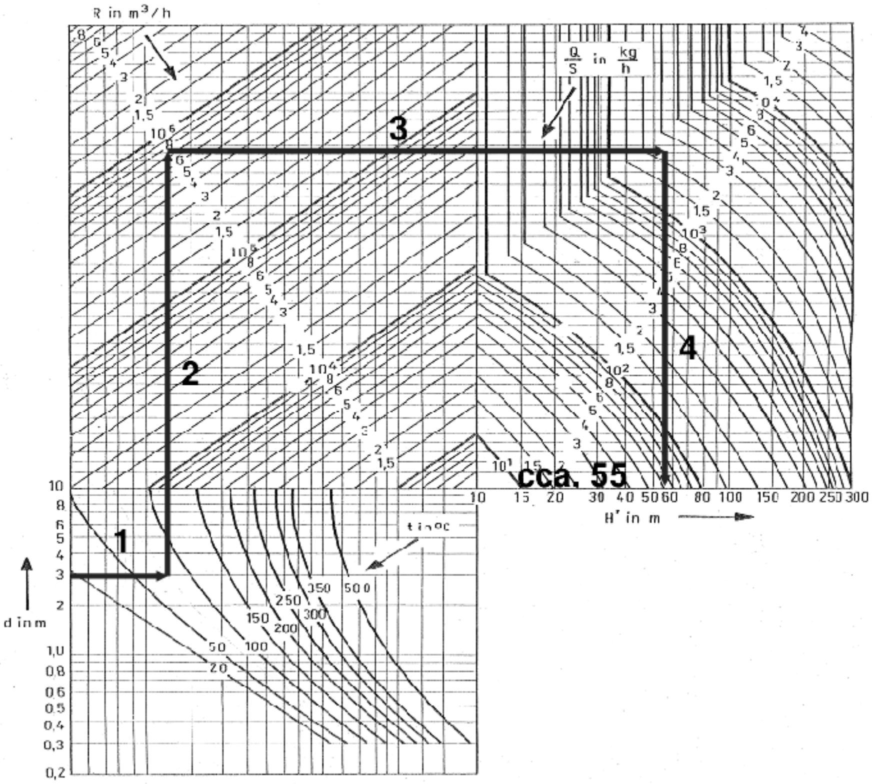

Figure 1. Diagram for determining the stack height dispersion

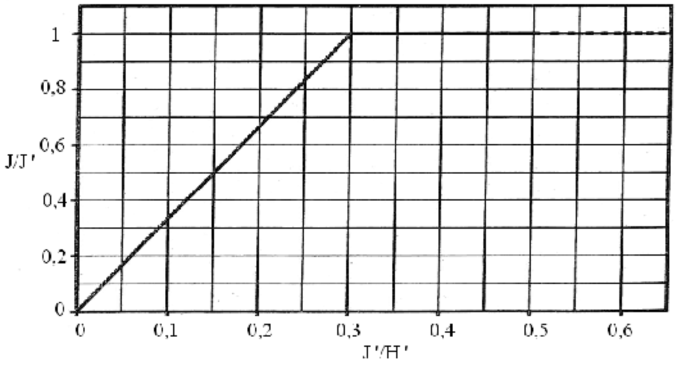

Figure 2. Diagram for determining the value of J

Step 6: Considering the relief form

For determination the height of the chimney dispersion will be taken into account a non linear relief form, if the facility is located in a valley or dispersion of emissions is disturbed by the bumps relief. Where appropriate, then the stack height of dispersion will be increased by a correction factor. All sites located in valleys or low altitude places, it must be checked if ensure the free flow of air and with it and waste gas. For all of these it must be taken into account the emergence of a whirlwind called Lee inside Valley, created by the flow direction across the valley, which acts on the gas evacuated cart. The area is bounded by a line with a slope of 15° which starts from the top margins of the valley to the horizontal (Figure 3). It must be checked if the cart height breaks the line, or the exhaust flow is achieved. If the free flow condition is not met by the cart height by issuers, it is expected immissions accumulation. Thus, the dispersion height cart will be raised so that its outlet to be located above the cavity zone.

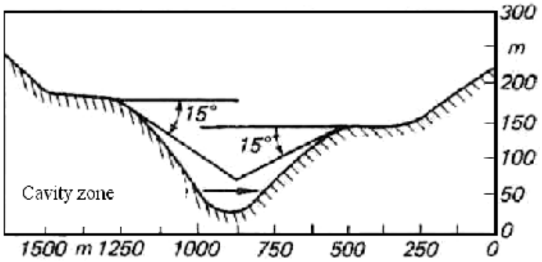

Figure 3. Example for line location of 15 degrees and limiting the cavity area

Detailed specifications for the determination of the correction factor are listed in bibliographic sources (Lazaroiu, 2006; Council Directive 2001/80/CE; German Engineers Union Directive, 2002; NEUE TA LUFT, 2002).

Area Evaluated for Analysis Immissions of the Thermal Power Plant Site

As “New German Technical Guide for Air Quality Control - TA Luft Neue” the field for the immissions evaluation (see Figure 4), caused by thermo-electric power plant, is the area that is completely inside the circle around the dispersion cart, which is 50 times the actual height of the chimney and in which the additional pollution is more than 3.0% of the concentration long-term of the immissions.

In this case, it will consider the actual height (100 m) of the emissions dispersion cart from the existing thermal power plant.

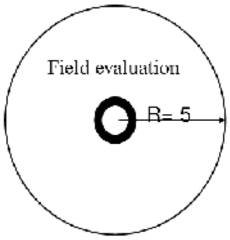

Figure 4. Scope of Assessment: 50 x 100 m = 5 km

Checking Immissions Situation

Using the dispersion calculation, someone may check if out of assessment area, there are additional immissions pollution powders, respectively NO_2 <1.2 mg / Nm ³ and SO_2 <1.5 mg / Nm ³.

In the European reference documents are recommended the following limits of annual immissions:

- Powders (PM10): 40 mg / Nm ³
- SO_2: 50 mg / Nm ³
- NO_2: 40 mg / Nm ³.

CONCLUSIONS AND PROPOSALS

It results that the dispersion of pollutant emissions discharged into the atmosphere by tall chimneys leads to optimal sizing of flues and represents a major opportunity to maintain air quality by industrial operators. In this approach, a very important role is play by environmental protection authorities too, which must ensure permanent compliance by industrial polluters concerning all environmental requirements, in accordance with guidelines and the recommendations from European reference documents (guides and BATs), so as the environment and the health to be protected in order to achieve acceptable concentrations of pollutants, below standards, in all areas close to the emission sources.

The methodology for calculating the height of the chimney dispersion shown in this example can be generalized by using the same calculation as in European environmental recommendations. Environmental challenges facing industrial sites have significant consequences for human health, for the quality of life of urban citizens and for their economic performance.

Pollution size depends on the fuel used to produce electricity and heat and the combustion technology. From this point of view, eco-systems advanced combustion technology are particularly important and can lead to reducing environmental pollution by reducing approx. 30% of gaseous emissions (CO, CO_2, NO_x, SO_x).

REFERENCES

Ebertsch, G., STE (2005), “Calculating chimney height based on the example set by a lignite power plant and establishing the assessment domain and analysis of immissions”, State Administration Bavaria, Workshop “,Development of Action Plants for Implementation of the LCP Directive”, EU – Twinning Project RO 2002/IB/EN – 02, (in Romanian), Bucharest.

German Engineers Union Directive, (2002), VDI 3781, part 2.

Lăzăroiu, Gh. (2006), *Dispersion of polluting particles* (in Romanian), AGIR, Bucharest.

Nicolae, M. et al. (2002), *Analysis procedures in ecometallurgic management* (in Romanian), Fair Partners, Bucharest.

***, *Handbook on Applying Directive IPPC (96/61/EC) - Integrated pollution prevention and control – in Romania* (2006), Twinning Project RO 2004/IB/EN – 09, Implementation and Enforcement of the Environmental Acquis at National Level and Coordination of the Regional Twinning Project, Bucharest.

***, *Council Directive 2001/80/CE on the limitation of emissions of certain pollutants into the air from large combustion plants* (Directive LCP).

*** (2001), *Reference Document on Best Available Techniques in the Large Combustion Plants*, European Commission Directorate General JRC Joint Research Centre, Institute for Prospective Technological Studies, Sevilla – Spain, http://eippcb.jrc.es.

*** (2002), “*NEUE TA LUFT*” - New German Technical Guide for Air Quality Control (24 July 2002), Annex 3, 209.

INDEX OF AUTHORS

PARTNERS:

UNIVERSITY
OF BUCHAREST,
ROMANIA

LEATHER ENGINEERING
DEPARTMENT
EGE UNIVERSITY,
TURKEY

“GH. ASACHI”
TECHNICAL
UNIVERSITY
OF IASI,
ROMANIA

“POLITEHNICA”
UNIVERSITY
BUCHAREST,
ROMANIA

ITA TEXCONF
ROMANIAN
ENTITY WITHIN
INNOVATION &
LEATHER
TECHNOLOGICAL
TRANSFER

CONFEDERATION OF NATIONAL ASSOCIATIONS
OF TANNERS AND DRESSERS
OF THE EUROPEAN COMMUNITY

ROMANIAN LEATHER & FUR
PRODUCERS ASSOCIATION

ISSN: 2068-0783